Ocean-transported pumice in the North Atlantic

Anthony Newton

PhD

University of Edinburgh

1999

Declaration

I, Anthony Newton hereby declare that the work contained herein is my own and has not previously been presented for examination. Any contributions by others is acknowledged in the text.

September 1999

For Keith Newton

1930-1984

"Some days we would pass through pumice lying in ridges, each piece uniformly the size and appearance of a bath sponge, then again we should pass through perfect fields of small yellow pumice spread evenly over the surface just for all the world like a green field of grass covered all over with buttercups, and the undulation of the swell of the trade wind produced an indescribably pretty appearance."

(Reeves, 1884).

Abstract

The overall aims of this study are to identify the sources of the widespread Holocene pumice deposits found along the coasts of the North Atlantic region and establish the ages of the source eruptions. In order to tackle this, it is necessary to determine whether it is possible to "fingerprint" the pumice of individual eruptions and link ocean-transported material with the established tephrochronological framework based on the stratigraphy of airfall deposits. Over 1500 electron probe microanalyses and over 200 Secondary Ion Mass Spectrometry analyses have been undertaken on pumice and tephra samples. These are the first high quality grain specific analyses carried out on ocean-transported pumice in the North Atlantic.

Current knowledge of the extent of pumice distribution in the North Atlantic region is assessed for both shoreline (natural) and archaeological contexts. Pumice pieces have been recovered from Holocene raised shorelines of north-west Iceland for the first time. Further original fieldwork in Norway has confirmed the presence of multiple levels of brown, black and grey pumice on mid-Holocene Norwegian raised beaches and white pumice on early-Holocene shorelines. Archaeological pumice, donated by collaborators, from sites in the British Isles has also been analysed. The number of archaeological sites where pumice has been recorded has been doubled to 150.

All of the analysed pumice can be correlated to volcanic activity in Iceland. These analyses establish that the majority of the mid- to late-Holocene pumice found in the North Atlantic area is dacitic and produced from Katla. A collaborative project identified 17 silicic tephra layers (SILK layers) produced by the Katla, ten of which are linked to pumice production between c. 6600 and 1626 ^{14}C years BP. Geochemically different and older pumice also occurs in Mesolithic archaeological sites in Scotland and this was also produced by Katla. Some of this older Mesolithic pumice was probably erupted by Katla c. 7000 ^{14}C years BP. The remainder of the pumice was erupted by early Holocene activity at Katla, which also deposited pumice on the flanks of the volcano. In addition, early Holocene activity from Öræfajökull produced pumice found on a raised shoreline in Norway. The 1362 AD eruption of the same volcano produced the white pumice found in three medieval archaeological sites in Scotland. The pumice found on raised shoreline in Svalbard was produced by eruptions from both Katla and the island of Jan Mayen.

Crucially, the most prolific Icelandic producer of distal tephra layers, Hekla, is not the source of any of the pumice found around the North Atlantic. It is suggested that this could be because of the fragile nature of the Hekla pumice. This work shows that high quality geochemical data is essential if correlations are to be made between pumice deposits and sources, and highlights both the potential and limitations of the use of pumice as a tephrochronological tool.

Acknowledgements

Without the help of many friends, colleagues and strangers it would have been impossible to finish this thesis.

Many thanks to my supervisors Dr Andrew Dugmore and Prof. David Sugden for their encouragement and support over the years.

Guðrún Larsen has often provided invaluable information, support and samples, which would have been impossible to obtain from any other source. Without her collaboration this thesis and much of the other research I have been involved in would not have been completed. Thank you.

Prof. Paul Buckland has always been enthusiastic about my work and has been a constant supplier of pumice of all shapes and sizes from virtually everywhere. No piece of pumice is too small.

Particular thanks must go to the many people who have assisted me in the field. Andrew Dugmore has helped on many fieldtrips and has always been there with his infectious enthusiasm. Malcolm Murray provided invaluable help, surveying skills and that crucial extra pairs of eyes during the Norwegian fieldwork. Rob Rolph provided the same enthusiastic support in Strandir and a calm head during a crisis. Hreggviður Norðdahl also accompanied me to Strandir on a less dramatic trip and provided and translated Icelandic tide tables. Many thanks also to Jane Boygle, Sukhvir Parmar and Richard Corrigan for their help on my first quick visit to Strandir. Also to Fiona Foley who helped with fieldwork in Norway. Stienar Nilsen identified several pumice sites in Hitra, Norway and donated some of the pumice he had collected over the years. Prof. Sven Jakobsson kindly allowed me to search the collections of the Náttúrugripasafnið (Museum of Natural History) in Reykjavík and remove some of the pumice. Acknowledgement must also be made to the trusty old Lada which provided interesting, but surprisingly reliable transport in Norway and on one visit to Strandir. Toyota must be thanked for building their vehicles strong and the Icelanders for having very soft bogs. Also many thanks to the kind people who run the Hotel Djúpavík, Strandir. Gillian Boniface kindly provided accommodation for Malcolm and myself in Bergen and Guðriður and Hafliði have done the same on countless occasions in Reykjavík. Mary made and Bob christened the whale which was the star of the Norwegian fieldwork, thanks.

This thesis would not have been possible without the generous donations of pumice by archaeologists and other researchers. These people also kindly supplied much supplementary information often from unpublished work. So thank you in alphabetical order: Dr Torbin Ballin, Dr Beverley Ballin-Smith, Jerry Biglow, Prof. Paul Buckland, Dr. Ann Clarke, Dr Ciara Clarke, Dr Claire Cotter, Trevor Cowie, Dr Barbara Crawford, Iain Crawford, Dr Anne Crone, Dr Bill Finlayson, Dr Ewan Mackay, Dr Ann MacSween, Dr Rod McCullagh, Dr Steve Mithen, Prof. Ian Ralston and Melanie Smith. Thanks also to Trevor Cowie and Alison Sheridan for running the pumice searches on the NMS databases.

All of the geochemical analyses were undertaken at the Department of Geology at the University of Edinburgh. Electron probe microanalyses were carried out with the kind assistance of Dr Peter Hill, Dr Stuart Kearns and Simon Burgess. Ion probe analyses and scanning electron microscope work were supervised by Dr John Craven. X-ray Fluorescence analyses were undertaken by Dr Dodie James.

Instrument time for the ion probe analyses was provided by NERC Scientific Services and funding for fieldwork in Norway and Iceland was provided by two generous grants from the Carnegie Trust for the Universities of Scotland.

I am particularly grateful to Malcolm who read the whole text and Maeve who read Chapter 1. They both suggested essential changes and supplied encouragement when it was needed most. Any mistakes in this work, however, are my own. Maeve and Sarah also helped me piece the final versions of my thesis together, thank you. Also many thanks to my friends in Geography and elsewhere for the laughs and friendships which have kept me going and helped me finish this thesis.

I am also grateful to Dr Bill Phillips and Prof. David Gilbertson for taking the time to carefully read my thesis and suggest many constructive comments.

I would like to finally thank my Mum for all her love, help and support over the years.

List of Contents

List of Figures

List of Tables

Chapter

1

Pumice: production, transportation and deposition

1.1 Aims

The overall aims of this thesis are to identify the sources and the age of the eruptions which have produced widespread Holocene deposits of ocean-transported pumice which are found along the coasts of the North Atlantic region. More specifically this research aims:

1. to determine the origin of the ocean-transported pumice deposits and the age of the eruptions that produced them
    - to use high precision geochemical techniques to geochemically fingerprint the ocean-transported pumice.
    - to use the same techniques to correlate the pumice with tephra layers and pumice in the source areas.
2. to assess the scale of the deposits and their possible environmental significance
    - to identify the extent of the deposits and possible transport routes
    - to assess their use as a dating tool
3. to assess the wider significance of the ocean-transported pumice and associated tephra layers
    - to archaeological research.
    - to volcanological research.

1.2 Importance

Pumice deposits around the shores of the North Atlantic have been investigated before (Chapter 2), but recent developments in volcanological knowledge and analytical techniques now enable a thorough geographical assessment to be undertaken. For the first time a

combination of geological, volcanological, tephrochronological, geographical and archaeological techniques permits an integrated assessment of an unusual group of deposits which have a known distribution over the North Atlantic region of 5000 km east-west and 3000 km N-S and through at least 5000 years of the Holocene.

1.2.1 Volcanological

The principal volcanological contribution of this study is to identify the volcano or volcanoes which produced this pumice. It is now nearly 30 years since the last attempt was made to identify the source of the dacitic pumice found around the shores of the North Atlantic. Up to now, no volcano has been identified conclusively and it has only been possible to say that Iceland is the most likely source. The last 20-30 years have seen a huge increase in knowledge about volcanic activity in Iceland and elsewhere and many processes are now better understood. Despite this, however, the several silicic eruptions which produced pumice have not been identified. This thesis aims to identify those eruptions.

Tephrochronology has also grown during this time and it is now established in volcanological and palaeoenvironmental research. Tephrochronology relies on the successful integration of several techniques. These include mapping, stratigraphy, dating and geochemistry. The use of major and trace element geochemistry, in particular, has enabled spatially separated deposits to be correlated back to their source areas. By carrying out field mapping of pumice deposits on raised beaches in Norway and Iceland and collecting pumice from archaeological sites in the British Isles, this study will expand our knowledge of the distribution of pumice around the North Atlantic. The geochemical characteristics of the pumice will then be established and compared. In parallel, tephra layers from Iceland will be analysed to establish the likely source volcano and the eruptions or eruption responsible for producing the pumice.

It is not currently feasible to date the Holocene pumice directly. Dating of relatively young tephra layers is now possible with $^{40}Ar/^{39}Ar$ dating, with tephra as young as 2000 years old being dated (Renne *et al.*, 1997). These developments, however, are new and experimental and can only be undertaken on certain types of material and are not considered further in this thesis. Whilst dating organic material associated with pumice can be useful, it does not provide a date for the eruption of the pumice, let alone the time when the pumice was deposited. The pumice may have been deposited on a site almost immediately after an eruption or it may have been reworked from an older deposit.. For these reasons it is

important to try and identify the volcano and eruptions responsible for producing the pumice. It is far simpler to date a proximal tephra or pumice layer, than a pumice deposit washed up on a raised beach. This is only possible, however, if good quality geochemical data are available for both the proximal and distal deposits. This study, therefore, aims to date the eruptions responsible for producing the pumice by linking the pumice to dated proximal tephra deposits, not the ocean-transported pumice.

Finally, the scale of the eruptions that produced the pumice will be established. This is important, as at present there are no published data on eruptions in the North Atlantic region that have produced widely distributed pumice. This contrasts strongly with the situation in the Southern Hemisphere, where a considerable literature has been able to link pumice rafts and deposit to particular eruptions.

1.2.2 Archaeological/Environmental

As well as providing valuable volcanological information, the multidisciplinary nature of this study will also produce data of value to archaeological and palaeoenvironmental research.

As Chapter 2 will show, distinctive pumice deposits on raised beaches in Norway and Svalbard have been used to correlate raised beach sequences. The lack of data on the origin of this pumice means that erroneous correlations are possible. It may be that problems of reworking and geochemical homogeneity mean that pumice should not be used as a correlative tool.

As well as helping to date palaeoenvironmental sites, such as raised beaches, the presence of pumice in archaeological contexts, could provide a means of dating, if the individual eruptions can be identified. It is only possible, however, to provide minimum dates as pumice used by humans could have been picked up from old or reworked deposits, not just from pumice washed ashore immediately after an eruption.

1.3 Introduction

Before beginning the investigation of pumice in the North Atlantic, it is first necessary to establish the processes that produce pumice and the mechanisms by which it can be transported across the world's oceans. This chapter will now investigate the production,

transportation and deposition of pumice on a global scale. Firstly, pumice itself is defined and its relationship to other particulate products produced during a volcanic eruption is discussed. Next, the volcanic processes that produce pumice are described. Once pumice has been produced during a volcanic eruption it can be transported by a variety of processes including those directly associated with the eruption and independent oceanographic, geomorphological and anthropogenic mechanisms. These processes are assessed using various examples. In particular, contemporary reports of ocean-transported pumice rafts are studied in some detail. The last 100 years has provided good quality contemporary records which describe pumice rafts and give an indication of their physical characteristics, such as grain size and composition, as well as rate of drift and depositional processes. These modern analogues provide a means of interpreting older pumice deposits. Pumice deposits, both proximal and distal are discussed next, including the processes which can lead to reworking and redeposition of primary deposits of pumice.

1.4 The nature of pumice and tephra

The word *pumice* is often used interchangeably with the term *tephra*, and sometimes used to describe virtually all particulate material erupted from a volcano, from volcanic bombs to sub-micron glass shards. Although Whitham and Sparks (1986) point out that it is not possible to provide a precise definition of pumice, as it forms a continuum in both composition and vesicularity, Fisher and Schmincke (1984) define *pumice* as being composed of highly vesicular volcanic glass foam the composition of which may vary from basaltic to silicic. Though there are no precise limits to the density of pumice, it is often less than 1 g cm^{-3} (the density of water) and may drop as low as 0.19 g cm^{-3} (Whitham and Sparks, 1986). Pumice is a term, however, that is frequently applied to deposits and particles which have a density more than 1 g cm^{-3}. As this thesis is concerned with ocean-transported pumice, the word *pumice,* in this study, will refer to the material as defined by Fisher and Schmincke (1984), i.e. pumice which normally floats. Other vesicular volcanic rocks which are composed of fine-grained mineral matrix, not glass, always have a density greater than 1 g cm^{-3}. These do not float and are therefore not considered any further.

The volcanic glass, of which pumice is composed, can be assumed to have an average density of 2.3 to 2.8 g cm^{-3} (Allen, 1980). The density of a piece of pumice will be less and

is wholly dependent on its vesicularity, which is defined as the percentage of void. In a floatation experiment, Whitham and Sparks (1986 see 1.4.3) measured Minoan plinian[1] pumice pieces with vesicularities of 85 - 92 % (which corresponds to densities of between 0.32 to 0.19 g cm^{-3}) and in their study Thomas *et al.* (1994) used pumice with vesicularities between 64 and 81 %. Houghton and Wilson (1989) found that basaltic pumice from the 1959 eruption of Kilauea Ika, in Hawaii had a vesicularity range of between 51 and 93 %, whilst more silicic plinian deposits, erupted under dry conditions without the influence of external water, tended to have a narrower range of 71 - 81 %. A comprehensive study of pumice from the island of Ischia in the Bay of Naples, produced during a small (DRE[2] <0.02 km^3) sub-plinian trachytic[3] eruption in about 1860 ^{14}C years BP, showed a range in vesicularity of 63 - 77% (Orsi *et al.*, 1992).

The terms *tephra* and *tephrochronology* were originally proposed by Sigurður Thórarinsson in 1944 (Thórarinsson, 1944). At first, Thórarinsson intended the term tephra to define any volcanoclastic material transported through the air, as opposed to molten, flowing lava (Thórarinsson, 1954), but after experience of working on ignimbrites and other pyroclastic flows, he redefined tephra as:

> "a collective term for all airborne pyroclasts, including both air-fall and flow pyroclastic material" (Thórarinsson, 1974).

This is the definition of tephra which will be used throughout this thesis. This fits well with the use of the term *pumice*, which is a type of tephra. Tephrochronology, when used in this thesis, is as defined by Thórarinsson (1944) namely the production of a chronology based upon the measurement, correlation and dating of tephra layers. For this to be successful it is necessary that a tephra layer can be identified in separate locations, using one or more techniques, which may include geochemistry, mineralogy, stratigraphy, mapping and dating control.

---

[1] A plinian eruption is a violent eruption of volatile-rich fragmented magma which forms a column of gas and tephra. The mixing of atmospheric air provides buoyancy which enables the column to reach altitudes of up to 50 km. The airfall deposits tend to be well sorted.

[2] Dense rock equivalent (DRE) is the volume of the tephra layer if it were to be compressed to form solid rock with few pore spaces. This is roughly equivalent to the volume of magma from which the tephra was produced.

[3] The products of trachytic eruptions are over-saturated in silica, alkaline and of intermediate composition.

Unless stated otherwise uncalibrated ^{14}C dates are used throughout this thesis, except for the last 1100 years where dates are generally given in years AD. This is in order to allow the temporal correlation of pumice deposits with the historical Icelandic tephrochronological record.

1.5 Pumice formation

Having defined pumice, the next step is to consider how it is formed. It is important to understand the formation of vesicles and fragmentation[4] of magma which leads to the formation of pumice. If the magma is completely fragmented, no substantial pumice pieces will be produced; instead there are only fine-grained fragments. This section is divided into three parts: the first part deals with the general principles behind the fragmentation of magma and the formation of vesicles in pumice under *dry* (subaerial) conditions; the second deals with the consequences of external water interaction with magma under *wet* conditions; finally, the role of sub-glacial activity in Iceland is discussed.

1.5.1 Dry pumice formation

As pointed out by Mainski and Jaupart (1997) conduit width and flow play a crucial part in the fragmentation and vesiculation process. Wilson *et al.* (1980), in a seminal paper on plinian eruptions, established that fragmentation of magma occurs at shallow depths, in the order of several hundred metres. Gas velocities between 200 and 600 m s^{-1} occur near the vent, with pressures of several tens of bars being created in the conduit, but reducing to 1 bar at the vent. The transition to supersonic speeds (greater than 90 to 200 m s^{-1}) occurs at narrowest point of the vent, which can range in diameter between 5-100 metres. If the exit pressure remains about 1 bar, the eruption velocities are dependent mainly on the exsolved magma gas and less so on the vent and conduit diameter. For example, if H_2O is assumed to be the main volatile, velocities of 400 to 600 m s^{-1} are associated with 4 to 8 % H_2O by weight (Wilson, 1976). High discharge rates from lower viscosity magmas produce similar highly vesicular clasts but with greater variation. As discharge rates fall there is an increase in the amount of dense degassed clasts.

---

[4] Fragmentation is the process by which magma is broken apart by the expansion of volatiles to form pyroclasts.

Having established that magma can depressurise without the pumice clasts being completely fragmented, the next stage is to establish the processes that produce vesicles. The studies of Sparks and Brazier (1982) and Whitham and Sparks (1986) present a common three stage process by which vesicles are produced, whilst Thomas *et al.* (1994) suggest a slightly different model.

The study by Sparks and Brazier (1982) found three modal peaks in vesicle diameter. The largest peak had diameters greater than 60 μm, the next between 50 and 5 μm and smallest between 5 and 0.5 μm. Sparks and Brazier (1982) interpreted the largest vesicles as having originally formed in a magma chamber oversaturated with volatiles which formed bubbles. Although the percentage of oversaturated volatiles may be small, the long period the bubbles have to grow (up to several years) mean that they can grow large. As the magma rises to the surface at discharge rates of 10^3-10^5 m^3 s^{-1}, the medium-sized vesicles form. The magma decompresses from a few kilobars to a few tens of bars in a matter of minutes to hours as it rises up the conduit. Despite rapid decompression, viscosity will increase as H_2O escapes and, therefore, bubble growth rate will drop. As the bubbles already formed continue to grow, the difference in size between the two groups is maintained. Finally, the small vesicles are formed as the magma is erupted from the vent at velocities of 300-600 m s^{-1} and the final decompression from a few tens of bars to atmospheric pressure occurs. The lava fragments solidify (are quenched) as cold air is mixed with the hot eruption column.

Whitham and Sparks (1986) carried out a more detailed study of vesicle formation in pumices. They employed three techniques. Firstly, they impregnated pumice with resin, to study pore-size connectivity. The pumice was impregnated with resin under a vacuum and then sectioned. All of the vesicles in the pumice were filled with resin, showing that all the vesicles are interconnected. Next they used BET nitrogen absorption techniques[5] to measure surface area of the pumice. Three pumice samples from the Mount St Helens plinian deposit, Minoan pumice and pumice from the plinian deposit of the 1875 Askja eruption produced surface areas of 0.421, 0.489 and 0.513 $m^2 g^{-1}$ respectively. Whitham and

---

[5] A mixture of nitrogen and helium is forced through the pumice at 77 K in a vacuum. The nitrogen molecules are absorbed onto the surfaces. Helium is then passed through the pumice until equilibrium is reached, the absorbed nitrogen is released, as helium replaces the nitrogen sites on surfaces, and the volume of nitrogen is measured. This is repeated at various pressures and the BET function is used to plot the volume of nitrogen against pressure. The surface area can then be calculated as the area occupied by a single nitrogen molecule is known (Whitham and Sparks, 1986).

Sparks (1986) point out that these values are not high compared with many industrially produced materials and conclude that the pumice cannot contain many sub-micron pores. Finally, they used mercury porosimetry on 20 pumice samples which showed that there is a polymodal distribution of pore size with two or three peaks. This last result compares favourably with the earlier results of Sparks and Brazier (1982).

Whitham and Sparks (1986) found that the previous assumption that pumice pores are simple cylinders appeared to be wrong. The porosimetry method suggested that there were many sub-micron sized vesicles whilst scanning electron microscope (SEM), thin section, and BET studies suggested that this was not the case. The BET method showed an average surface area of 0.5 $m^2 g^{-1}$ whereas the porosimetry surface area was 17.35 $m^2 g^{-1}$. This is caused by pores having narrow openings but large volumes. The porosimetry method is actually measuring the diameter of the opening, not the diameter of the pore itself. Despite this, they were convinced that their results showed the same three-fold degassing history as Sparks and Brazier (1982), although the smallest vesicles may have originally been unconnected and were only joined by cracking during cooling.

Considering the pressure changes which occur, Whitham and Sparks (1986) expressed surprise that pumice survives at all, and is not simply blown apart to form fine-grained tephra. They suggested that this may be because the magma destined to become pumice already contains a high proportion of interconnected vesicles as it degasses to atmospheric pressure. Other magma may contain more closed vesicles and as it degasses it is blown apart to form fine-grained tephra. Alternatively, interconnectedness may be a result of later cracking of bubble walls as the pumice cools (Whitham and Sparks, 1986). This last hypothesis, however, does not explain why pumice is not blown apart. Wilson *et al.* (1980) concluded that as most pumice appears to have a void volume of between 70 and 85 %, fragmentation of the magma to form fine-grained tephra occurs as the void space reaches this level.

In a more recent study, Thomas *et al.* (1994) do not agree that vesicles are interconnected at the time of eruption. They propose that magma fragments expand after fragmentation, as

reticulites[6] and bread-crust pumices demonstrate that expansion occurs late in an eruption, and that variations in vesicularity are determined by the rate at which bubbles can expand and are related to the viscosity of the melt, not the fragmentation process.

A three-stage evolution of lava fragmention is also proposed by Thomas *et al.* (1994): the first stage occurs in the volcanic conduit between the fragmentation point and the vent; the second stage is in the column and the third occurs when the fragments fall and form a deposit. During the first stage little heat is lost to the country rock. The velocities involved are high and the heat loss between gas and liquid is low because of the small amount of gas involved. Fragment evolution occurs in an isothermal state. In the second stage, temperature drops rapidly because of the inclusion of cold atmospheric air. Adiabatic cooling occurs as the fragments expand. This eventually stops when the magma is quenched (solidifies). As temperature drops by an average 100°C every second after leaving the vent, the viscosity of the magma increases and the bubble expansion rate drops (Kaminski and Jaupart, 1997; Thomas *et al.*, 1994). Thomas *et al.* (1994) claim that differences in vesicularity between pumice deposits from different eruptions can be explained by differences in viscosity, as they regard this as being the primary factor controlling bubble growth. Within a deposit, vesicularity changes are explained by changes in magma composition. Finally, changes in vesicularity within a stratigraphic unit in a deposit, can be explained by the different trajectories taken by the fragment. Different fragments travelling in various trajectories undergo different decompression rates and hence expand by varying amounts. Distance from the vent does not affect vesicularity as quenching occurs early in their evolution and fragments stop expanding early in their trajectory. Differences in cooling rates actually vary between 20 and 120 °C s^{-1}, which according to Kaminski and Jaupart (1997) explains the big differences in vesicularity between various deposits.

As a consequence of their research, Thomas *et al.* (1994) are able to suggest that the reason for the change from a plinian to pyroclastic flow stages[7] in the Taupo and Minoan eruptions was not caused by magmatic composition changes. Instead, an increase in vent size caused

---

[6] Reticulites are a form of basaltic pumice formed from fire-fountains. Although they can have a porosity of up to 98 or 99 %, the open networks are formed by very thin non-vesicular triangular glass rods and sink quickly (Fisher and Schmincke, 1984).

[7] From a self sustaining eruption to column to a collapse of the column and the creation of pyroclastic flow deposits.

the change, as the vesicularity of both the plinian and the pyroclastic phases are the same. This agrees with Orsi *et al.* (1992), who found no significant systematic variation in vesicularity (63-77%) during the eruption. This also matches the lack of any geochemical variation. From laboratory experiments using solutions saturated with CO_2, Zhang (1998) concluded that vesicularity in pumice may be partly governed by the smoothness of conduit walls. Pumice with high vesicularity might be produced by a relatively smooth conduit, which varies in diameter only gradually with depth. Lower vesicularity pumice may be produced by uneven (i.e. rough or big changes in diameter) conduit.

Whilst vesiculation of magma reduces as viscosity increases, Houghton and Wilson (1989) suggest that vesiculation is halted by one of three possible events, which may act independently or together, whilst the research of Kaminski and Jaupart (1997) adds a fourth:

- *non-explosive degassing*: which is caused by the streaming of bubbles through a magma at a shallow depth or the collapse of vesiculation at depth
- *fragmentation by rupturing of vesicles*: a dry eruption driven by the exsolution of magmatic volatiles
- *interaction with external water*: which chills and fragments the magma, causing a phreatomagmatic eruption (see 1.5.2).
- development of a rind around the pumice clast which slows and eventually stops expansion.

This section has covered the processes, which are far from clearly understood, that affect the formation of vesicles in magma. It appears that several processes act in parallel to influence vesicularity of the erupting magma. Despite large pressure changes, from several kilobars, to several tens of bars to 1 bar during an eurption, the pumice pieces are not completely fragmented. Whitham and Sparks (1986), Sparks and Brazier (1982) and Thomas *et al.* (1994) all present a three-stage process towards fragmentation and vesiculation, although they disagree on the actual processes. It appears that changes in vesicularity can be explained by composition differences and the trajectory taken by the pumice fragments.

1.5.2 Wet pumice formation

When considering pumice found in deposits around the North Atlantic region, the possibility of the pumice being produced in a subaqueous environment has to be explored. The most likely sources for the pumice being investigated in this study are in Iceland or from an

eruption of a submarine volcano. A Holocene pumice producing eruption from Iceland could have involved sub-glacial activity and Section 1.5.3 will deal with subglacial volcanic activity. This section describes the type of deposits produced by *phreatomagmatic*[8] eruptions and the type of pyroclastic deposits produced during-submarine volcanic activity.

Self and Sparks (1978) carried out a study on the origin of pyroclastic deposits, which had only recently been identified as being formed from subaqueous volcanic activity. Their work concentrated on silicic volcanic activity, which in a subaerial environment would be expected to form typical plinian tephra fall deposits. They noted that deposits from what they termed phreatomagmatic eruptions were just as widespread as typical plinian deposits. This implies that the eruption cloud must have reached similar column heights to that of a plinian eruption. They also noted that terrestrial silicic phreatomagmatic deposits are generally fine-grained, even near to the source, frequently contain near source base-surges, are well bedded and often contain accretionary lapilli. Generally, plinian deposits show a decrease in grainsize from source, from very coarse proximal deposits to fine distal ones. Terrestrial phreatomagmatic airfall tephra deposits are invariably fine-grained and show no change in grainsize with distance from source. They explained that *fuel-coolant interactions* occurred when the waters comes into contact with magma. A water to magma ratio of about 0.25 is required for this to occur. The gases released by the water contributes to fragmentation, explaining the fairly uniform fine-grainsize of the deposits. It also explains the two sizes of vesicles seen in phreatomagmatic tephra, as the expansion of magmatic gases forms the coarse vesicles and the reaction with the water produces the smaller ones. Heat is transferred to the air, which becomes entrained in the column and sustains the column height and the more fragmented (the greater the surface area) the tephra the more efficient the energy transfer. Despite the fact that the conversion of water to steam uses up energy, the fragmented nature of the tephra means that heat transfer is very efficient.

The explosive potential of the interaction between magma and water was spectacularly illustrated by the eruption in 1973 on Heimaey, Vestmannæyjar, when an attempt to blow up an advancing lava flow, which threatened to close off the harbour was abandoned. It was realised that the high pressure steam produced by the violent fragmentation of the lava might

---

[8] An explosive eruption caused by the interaction between magma and external water.

result in the lava flow exchanging all of its heat with the surrounding seawater and releasing several megatons of energy (Colgate and Sigurgeisson, 1973).

Kokelaar (1986) carried out a review of magma-water interactions of basaltic magma mainly using examples of submarine basaltic deposits from eruptions such as the Surtsey (Iceland, 1963) and Taal (Philippines, 1965). Kokelaar identified the processes which influence magma-water interactions in basaltic eruptions. These processes are explained below and their influence on silicic pumice formation are discussed in the light of subsequent research.

In subaqueous environments, Kokelaar (1986) noted that at high pressures the exsolution of magmatic volatiles is limited, fragmentation does not occur and dense lavas are produced. The water depth at which volatiles are able to fragment lava is called the volatile fragmentation depth (VFD), which varies for different magmas (Table 1.1). This potentially defines a limit to the depth that pumice can be produced. It would be expected that silicic magma with a greater volatile content would be able to produce pumice at a greater depth than basaltic magma. This is demonstrated by the findings of deep-sea silicic pumice deposits erupted from nearby submarine cones. Pumice, produced from nearby submarine cones, has been found at depths of over 1500 m near Tonga (Fouquet *et al.*, 1991) and at over 2250 m west of the Izu-Ogasawara (Cashman and Fiske, 1991).

Type of magma	volatile content	VFD
tholeiitic	0.5%	100-200 m or shallower
alkalic	1-1.5%	780 m
silicic	> 2-3%	1500 – 2250 m

Table 1.1: Variation of VFD with volatile (Cashman and Fiske, 1991; Fouquet *et al.*, 1991; Kokelaar, 1986).

The nature of the fragmentation that occurs varies from extremely violent to virtually none, as seen when pillow lavas are produced. Kokelaar (1986) states that a water to magma ratio of about 0.36 is required for the maximum explosive force, a similar figure to the 0.25 for silicic activity described by Self and Sparks (1978) and the 0.3 - 0.4 ratio identified by Wohletz (1986). When magma comes into contact with water, steam bubbles form a thin film along the contact surface, this is called film boiling (Kokelaar, 1986). These films are very unstable and collapse and reform on a micro to millisecond timescale. This causes the magma to fragment finely and mix with the water. The mixture can explode if the water is superheated to its *spontaneous vapour nucleation temperature* (homogeneous boiling), or if a pressure wave causes collapse or disruption of the steam films, so that heat is rapidly exchanged and steam is instantly produced, which produces *thermal detonation*. This does

not always occur, however, as steam films around pillow lavas appear to insulate the lava from the surrounding water. During the eruption of Surtsey, slow moving lava lobes were covered by surf, which instantly turned black and as the black sand was washed off them they became incandescent again (Wohletz, 1983). This produced angular glass fragments, *hyaloclastite*. Faster moving flows crossed the surf zone into the sea, although they were affected by steam explosions and hyaloclastite actions. From low velocity contact, e.g. lava flows, it appears that vigorous dynamic contact of magma and water is needed for explosive fragmentation (Kokelaar, 1986). This type of activity that causes the magma to form very fine fragments (hyaloclastite) is unlikely to produce pumice deposits.

Bulk interaction steam explosivity occurs when relatively small amounts of water are converted into steam by lava or magma, e.g. when lava flows over a bog (Kokelaar, 1986). The resultant steam occupies a volume several times that of water and the pressure build up causes the magma to be blown apart. In shallow water this expansion can be of the order of several thousand times. Again this type of activity is more likely to form fine-grained hyaloclastite rather than larger pumice pieces. Cooling-contraction granulation occurs when a cooling droplet of lava forms a skin of rigid solidified crust which cannot cope with further cooling of the interior of the droplet, leading to cracking or granulation (Kokelaar, 1986). Again these types of activity are more likely to form fine-grained hyaloclastite rather than larger pumice pieces.

Studies of the Surtsey eruption have suggested that a cupola or shell of steam formed around the submerged eruption column of Surtla, so that the tephra inside did not come into contact with water until after it had settled (Kokelaar and Durant, 1983). This is important, as some types of phreatomagmatic eruptions can produce tephra with subaerial characteristics. At high eruption rates at shallow depths, the water mass can be displaced and it is possible for the interior of the submerged eruption column to be insulated from the effects of the water (Cas and Wright, 1991). Kokelaar and Busby (1992) in their study of the Vandever Mountain Tuff, Sierra Nevada, California, also identified a similar process in silicic submarine eruptions. Here the high discharge rates and steam films can insulate both the submerged eruption column and pyroclastic flows from wholesale mixing with seawater. Experiments by Cashman and Fiske (1991) also confirm that the environment that hot pumice erupts into is vitally important as to whether the pumice is deposited locally to form distinctive bimodal submarine deposits or is transported further away from the eruption site by ocean currents.

This last process has significant implications for the production of pumice. As stated by Whitham and Sparks (1986), hot pumice which comes into contact with water will sink immediately as the gas in the vesicles cools, contracts, creates a partial vacuum and sucks in water. The formation of a protective cupola, inside which the pumice can be erupted without coming into contact with the surrounding water, could provide time for the pumice to cool before encountering the seawater. This cooled, buoyant pumice could then float to the surface, to be dispersed by ocean currents (Figure 1.1).

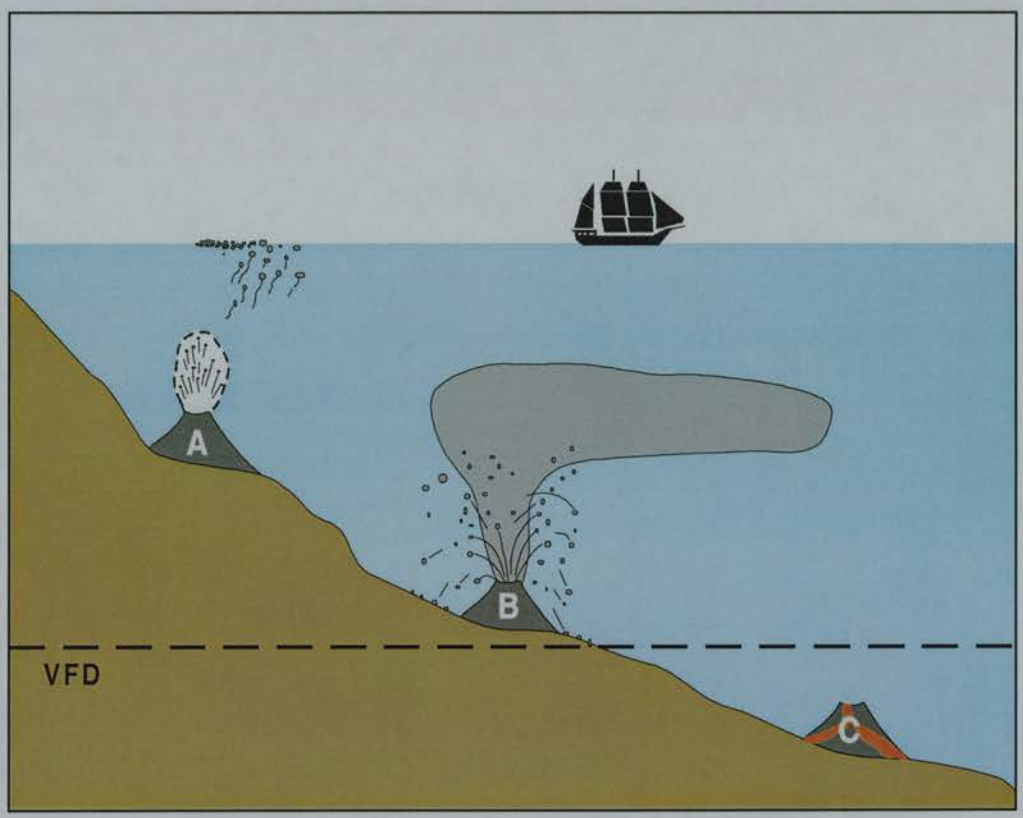

Figure 1.1: A schematic diagram to show the effects of water depth and plume type on pumice production. VFD is the volatile fragmentation depth, below which fragmentation by the release of volatiles is less likely, therefore forming lava flows (C). Volcano (B) illustrates that if hot pumice comes into contact with seawater; it quickly becomes waterlogged and sinks. Volcano (A) has an eruption column enclosed within a cupola. This isolates the pumice from the surrounding water, the pumice cools and remains buoyant once it encounters the seawater and floats to the surface.

From this section three important conclusions can be drawn. Firstly, although sub-aerial phreatomagmatic eruptions can produce widespread deposits on the same scale as plinian eruptions, the interaction between water and magma results in generally fine-grained deposits. For this reason, it would seem unlikely that subaerial phreatomagmatic eruptions would produce large pieces of pumice. Secondly, submarine activity can only produce

pyroclastic material above a depth where volatiles within the magma can escape. This depth, the VFD, varies according to the volatile content of the magma. There is, therefore, a depth below which it is unlikely that pumice will be produced. Thirdly, for floating pumice rafts to be produced from submarine eruptions, the pumice needs to have time to cool before it comes into contact with the water. Freshly erupted pumice which comes into contact with seawater will sink almost immediately. Pumice erupted inside of a protective cupola will have time to cool before contact with water.

1.5.3 Subglacial pumice formation

Any study of pumice found around the shores of the North Atlantic must regard Iceland as the most likely source, along with submarine eruptions along the Mid-Atlantic Ridge. During much of the Pleistocene large areas of the Earth have been covered in thick ice sheets. Inevitably this lead to many subglacial volcanic eruptions. Many fine examples of subglacial activity can be found in British Columbia and Iceland. In British Columbia, table mountains formed by basaltic eruptions beneath ice-caps and ice-sheets are called *tuyas*, whilst in Iceland they are termed *stapar*. Simkin *et al.* (1994) state that 83 % of identified Holocene sub-glacial eruptions have occurred in Iceland. Steep sided stapar are typically, but not always, composed of a basal unit of basaltic pillow lavas, overlain by semi-consolidated sideromelane[9] tuff, which forms the bulk of the mountain. The mountain is then capped with bedded sideromelane tuff with pillow fragments and sometimes a cap-rock of sub-aerially erupted basalt (Allen *et al.*, 1982). Allen (1980) demonstrated that the erupted basalt lava liberates enough heat to melt several times its own volume of ice before it cools. Ice is melted faster than lava is being produced. Pressure, i.e. depth below the surface of the ice-cap, has a big influence on the type of volcanic activity. This is the equivalent of the VFD in submarine activity. In sub-glacial basaltic eruptions in Iceland this appears to be at the equivalent depth of between 100-200 metres (Allen, 1980). The glass shards produced by explosive volcanic activity are themselves capable of melting over nine times their volume of ice (Allen *et al.*, 1982).

As well as relatively small stapar, another form of sub-glacial volcanic activity is common in Iceland. Most of the island's large central volcanoes are at present covered by glaciers

---

[9] Sideromelane is transparent volcanic glass, which usually indicates that the magma has been quenched by external water (Fisher and Schmincke, 1984).

and ice-caps (Figure 1.2). The Vatnajökull ice-cap, at 8,000 km^2 the largest in Europe, covers several active centres, including Gjálp (active in 1996), Grímsvötn (active in 1998) and Kverkfjöll (Figure 1.2). Öræfajökull (Iceland's highest volcano), which is found to the south of Vatnajökull, is also covered by an ice-cap. Langjökull, Hofsjökull, Eyjafjallajökull and Snæfellsjökull cover volcanoes with the same name. The large caldera of Katla is filled by Mýrdalsjökull. Small ice-caps are found at the summits of Tindfjallajökull and Torfajökull and even Hekla has a permanent snow field. Until the present study there appears to have been relatively little written about more silicic sub-glacial volcanic eruptions, with the exception of Lacasse *et al.* (1995) and Ólafsson *et al.* (1984).

Not only does overlying ice affect the type of volcanic activity, the melting of ice and the resultant floods provide a very efficient mechanism for transporting any pumice produced (see 1.6.2). The presence of ice-caps also has a large influence on the type of volcanic activity. Much of the Katla Volcanic System is beneath the Mýrdalsjökull ice-cap. This volcano plays a crucial part in this study and has had three distinct types of volcanic activity during the Holocene (Chapter 5). The most common type is basaltic, which have produced the many black tephra layers seen in the soil profiles in the area; the second type are large comparatively rare subaerial basaltic fissure eruptions; and the third is dacitic activity. Basaltic activity usually results in relatively "quiet" eruptions with fluid lava flows, fire fountains and little in the way of widespread tephra layers. For Katla, however, this type of activity is characterised by explosive eruptions, as the erupting lava interacts with melting ice. This phreatomagmatic activity has produced numerous relatively widespread coarse to fine-grained black/grey tephra layers. The basaltic and dacitic volcanic activity at Katla will be dealt with in more detail in Chapter 5.

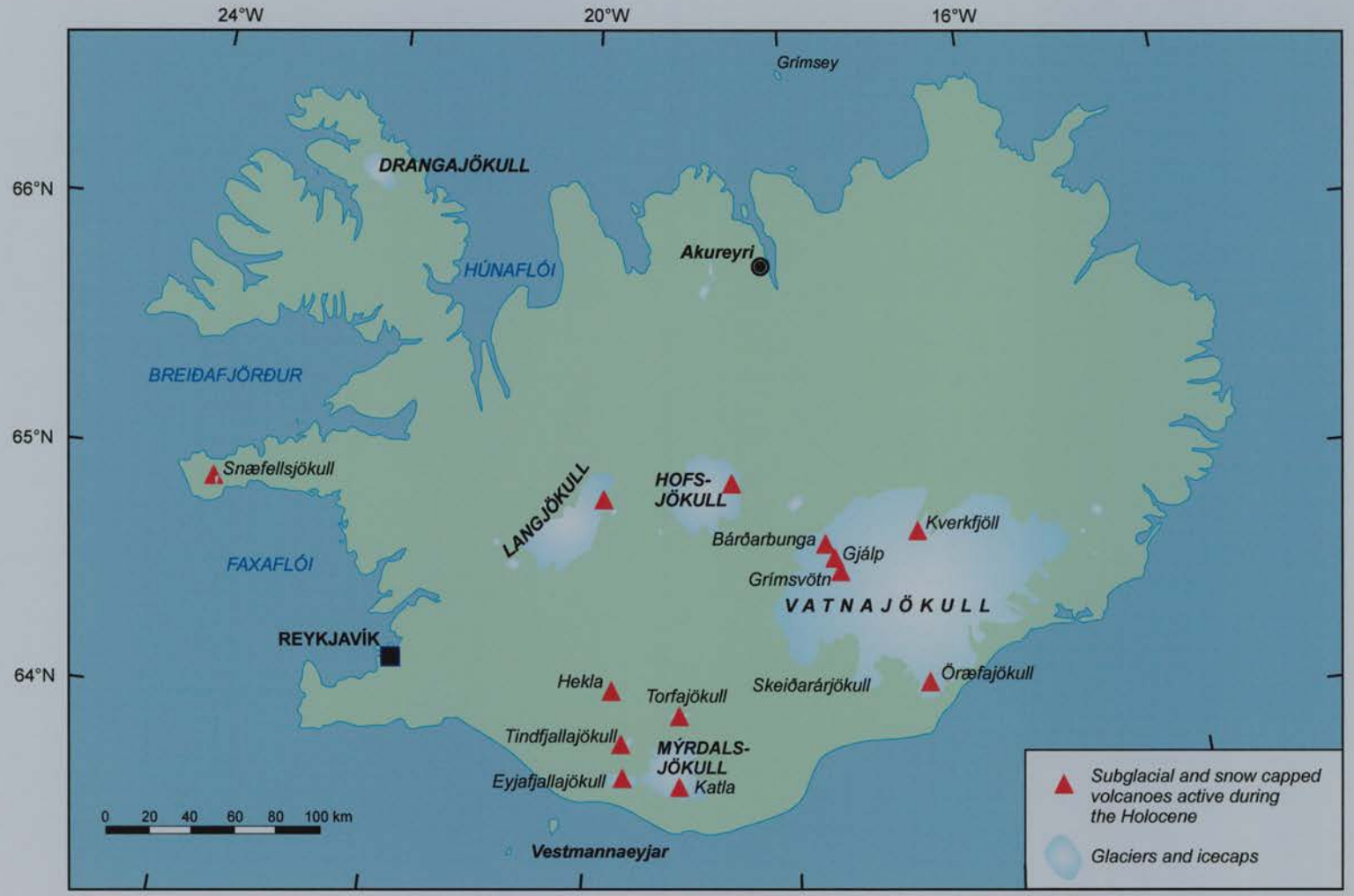

Figure 1.2: Map to show Icelandic volcanoes which are either sub-glacial or semi-permanent snow fields.

1.6 Transportation of pumice

Once the pumice has been erupted, there are a number of mechanisms by which it reaches its final resting place. Ocean-rafted pumice erupted from subaerial eruptions may have entered the sea via direct airfall, pyroclastic flows, rivers or floods. A submarine eruption may produce pumice, which can either sink immediately to form a local deposit or float for a period of time. The volcano therefore, must be situated on the coast, beneath the sea or in a position where pyroclastic flows, rivers or floods are able to flow into the sea. Once the floating rafts of pumice have formed, they are transported by a combination of ocean surface currents and winds until they either sink or are deposited on a shoreline. Whether ocean-transported pumice forms a deposit on a distant shore depends entirely on the ability of the pumice to stay afloat long enough. Although various flotation experiments have taken place, for example Whitham and Sparks (1986) and Manville *et al.* (1998), these confirm the results of direct observations of actual pumice rafts.

Section 1.6.1 describes various laboratory experiments which help explain how vesicularity, temperature and grain size can affect the ability of pumice to remain afloat for long periods. Section 1.6.2 examines the near source processes by which pumice produced during subaerial, submarine and subglacial eruptions enters the sea. Finally section 1.6.3 discusses contemporary observations of four recent pumice rafts which were tracked crossing oceans and washed up on shorelines thousands of kilometres from their source volcanoes.

1.6.1 Waterlogging of pumice

Waterlogging of pumice is the process by which water slowly replaces the air in the vesicles until the density of the pumice exceeds 1 g cm^{-3} and it sinks. In cold pumice, after an initial period of rapid absorption of water, there then follows a more gradual intake, which may last years (Whitham and Sparks, 1986) The exact processes by which water replaces air are not fully understood, but probably include capillary action and diffusional loss of air into the penetrating water (Manville *et al.*, 1998). As discussed in section 1.5.2, the temperature of the pumice when it comes into contact with water plays a crucial part in whether the pumice will sink or float. Whitham and Sparks (1986) demonstrated that at high temperatures (up to 700°C) steam is produced which rapidly speeds up the expulsion of gas and the intake of water. When the steam condenses, it creates a partial vacuum, which sucks in water. Pumice which absorbed water gradually for over a year at ambient temperatures, sank

almost instantaneously at these high temperatures. They also established that at temperatures below 100°C pumice behaved as if it was cold. As demonstrated in section 1.5.2, if it is to form a raft, pumice erupted in submarine environments must not come into immediate contact with seawater, it must be protected by a cupola.

Grain size also has an important influence on the length of time pumice remains afloat. Manville *et al.* (1998) developed a mathematical model that demonstrated that the length of time a piece of pumice takes to become saturated and sink is proportional to the square of its radius. Basically, larger pieces of pumice float for longer than smaller ones. This has important implications. In lacustrine environments, this will produce reverse graded volcanoclastic pumice deposits. Their model predicts that it would take 5 years for 50% of pumice with a 128 mm diameter to sink. Only 10% of pumice with a 256 mm diameter can be expected to sink in the same period. Furthermore, Manville *et al.* (1998) carried out experiments on pumice which showed that pieces less than 1-2 mm in diameter sank almost immediately. Although both grainsize and temperature will have a major influence on the distance that pumice can be transported by ocean currents, there is probably a more complex relationship between these two conditions.

1.6.2 Near source processes

As pointed out by Fisher and Schmincke (1984), subaqueous deposits, including pumice, are produced from two processes; either from underwater eruptions or from subaerial eruptions, where material is transported to the water. This section discusses the near source transportation processes associated with subaerial and subglacial volcanic activity.

Subaerial activity

The simplest method by which pumice can travel from a subaerial eruption to the sea is through the air. For this to occur the volcano needs to be fairly close to the sea for large (> several cm) diameter pumice pieces to be deposited. After the August 26 1883 eruption of Krakatau there were reports of pumice pieces as large as 10 cm across landing on ships 25 km from the eruption (Self and Rampino, 1981). As the pumice travels through the air it has the chance to cool to below the 100°C threshold. Thomas and Sparks (1992) in their study of cooling tephra from eruption columns, used models to calculate the effect of grain size, eruption height and distance from vent on the temperature of airfall deposits. They concluded that large pyroclasts erupted from a plinian eruption with diameters greater than

25 cm lose very little heat whilst falling from an eruption column. Clasts between 1.6 and 25 cm in diameter lose heat at an increasing rate with a decrease in grainsize, until those below 1.6 cm are always deposited cold. For example, within a radius of 2 km from the vent, temperatures of pumice clasts on deposition from a 25 km high eruption column can be over 585°C, whilst at nearly 6 km from the source temperatures can be still be as high 200°C (Thomas and Sparks, 1992). The hottest pumice is deposited from the base of a high eruption column. These studies demonstrate that small pieces of pumice which land close to the vent are cold and are therefore likely to float. Small pieces of pumice, however, sink faster than larger pieces. Larger pieces of pumice which are likely to float for a considerable time therefore, must be deposited at a suitable distance from the vent, which allows their temperature to drop below the threshold at which they would immediately become waterlogged and sink.

The second method by which pumice from a subaerial eruption can be transported to the sea is via pyroclastic flows, avalanches and lahars. Pyroclastic flows from volcanoes close to the coast have been known to travel for tens of kilometres across the surface of the ocean. This appears to have occurred at Krakatau where some of the pyroclastic flows travelled across the surface of the sea for up to 50 km, before hitting the coast of Sumatra (Sigurdsson *et al.*, 1991). Cas and Wright (1991) suggest that pumiceous pyroclasts entering water will often travel across the surface for considerable differences, as it is theoretically impossible for the expanded gas-supported low density pumice flow to enter the water unless it does so very slowly at a steep angle. This mechanism allows pumice bearing pyroclastic flows to transport pumice far out to sea and favours long distance transport.

Pyroclastic flows which travel over land can also transport pumice to the sea. These can travel several tens of kilometres and cross substantial topographic highs, meaning that volcanoes with no apparent direct connections to the sea need to be considered as possible sources for ocean-rafted pumice. For example, Vólcan de Colima, a stratovolcano in western central Mexico has in the past produced pyroclastic flows which have travelled over 50 km to the sea, aided in their journey by river channels. Despite this, Vólcan de Colima is sufficiently far from the coast to be easily ignored when considering sources for ocean-rafted pumice in the Pacific Ocean.

Floods caused by the melting of overlying ice and snow at the summit of a volcano or the condensation of moisture from the eruption column can also transport pumice large distances along river valleys to the sea (Vilmundardóttir and Hjartarson, 1985). Hekla, in

southern Iceland, provides a good example of this and is dealt with in more detail in Chapter 5.

Subglacial activity

There are several mechanisms by which the pumice from a subglacial eruption could reach the sea. The first is by a jökulhlaup, a flood resulting from the catastrophic melting of part of the icecap by volcanic activity or hydrothermal activity. These jökulhlaups regularly occur from at least six subglacial geothermal areas in Iceland, with probably over 80 having occurred since the settlement of Iceland in the late ninth century AD (Björnsson, 1992). For example, Björnsson (1992) shows that jökulhaups have occurred at 4-6 yearly intervals from Grímsvötn since the 1940s. These jökulhlaups are not caused by volcanic eruptions, but by the melting of the overlying ice by the heat produced in the geothermal areas. This creates a subglacial ice-dammed lake. Once a critical lake level has been reached, the ice dam is breached by the pressure of the water and the lake drains catastrophically. The October 1996 Gjálp subglacial eruption (Figure 1.2) melted an estimated 3 km^3 of ice, which drained into the Grímsvötn subglacial lake (Gudmundsson *et al.*, 1997). After five weeks, this water drained out of the lake and emerged as a jökulhlaup out of Skeiðarárjökull and flowed across Skeiðarársandur (Figure 1.2).

Jökulhlaups, produced either from geothermal melting or volcanic eruptions, provide a mechanism for transporting pumice to the sea. They occur frequently around Mýrdalsjökull[10], southern Iceland (Figure 1.2), the last three being in July 1999, 1955 (Thórarinsson and Rist, 1955), and with the eruption of Katla in 1918. The largest floods from Katla have a peak discharge of some 100-300,000 $m^3 s^{-1}$, a duration of 3-5 days and a total volume of about 1 km^3 (Björnsson, 1992). Lesser floods, such as the 1999 event, are much smaller and are probably not associated with eruptions. The 1999 flood reached a maximum flow of 2000-3000 $m^3 s^{-1}$ and only lasted for a few hours (Larsen, pers. comm.). Floods during historic times, however, have only deposited gravel sized pumice, rather than the larger pieces found around the North Atlantic coasts. Despite this, it seems that

[10] Jökulhlaups produced by the volcanic activity of Katla, beneath Mýrdalsjökull are called Kötluhlaups.

jökulhlaups remain the most likely transport mechanism by which pumice from sub-glacial eruptions reaches the sea.

1.6.3 Oceanographic processes

Once pumice has reached the sea it will be transported by a combination of ocean-currents and winds. The amount of time the pumice remains afloat depends on the speed with which the air trapped inside vesicles in the pumice is replaced by water causing it to sink and the distance of any coastlines suitable for deposition. Section 1.6.1 considered the process of waterlogging of pumice showing that contemporary reports of pumice rafts provide important information which can benefit studies of pre-historic deposits and eruptions. This section contains details of the behaviour and characteristics of pumice produced by four eruptions or eruptive episodes in the southern hemisphere during the last 120 years. These reports are important as they give information on both the size of pumice drifts and individual pumice pieces, the rate of drift, the speed with which pumice can be become waterlogged and sink and subsequent deposition and reworking.

Krakatau 1883

The eruption of Krakatau in 1883 is probably one of the most famous historical eruptions. Prior to 1883, the area around Krakatau contained three main islands, Krakatau itself (the largest), Sertung and Panjang. Krakatau consisted of three overlapping cones (Sigurdsson *et al.*, 1991) and is situated in the Sunda Straits, which separated the islands of Sumatra and Java (Figure 1.3). Although in their abstract Self and Rampino (1981) describe the 1883 eruption of Krakatau as a "modest ignimbrite event", its devastating impact on the environment and people living near to the island, the short-term climatic perturbations and dramatic sunsets observed around the world, ensured that the eruption has become one of the most famous and studied on Earth. The eruption is also particularly important to any study of ocean transported pumice. Floating pumice rafts produced during the eruption, crossed the Indian Ocean and were deposited on the shores of Africa, whilst others reached Melanesia and were still floating two years later (Simkin and Fiske, 1983). One of the most important works produced immediately after the eruption was "Krakatau" published in Dutch by R.D.M. Verbeek in 1885. Only the abstracts of Verbeek's work were produced in English in the journal *Nature* in 1884 and 1886. To rectify this, Simkin and Fiske (1983) published large parts of Verbeek's monograph translated into English for the first time. It includes numerous observations of floating pumice from the crews and passengers of ships

in the Indian Ocean and elsewhere and provides a valuable insight into the properties of pumice rafts. All of the references to Verbeek (1885) in this section are based on the translation in Simkin and Fiske (1983). Figure 1.3 shows the major reported positions of the Krakatau pumice and the location where it is was washed ashore.

Activity began with an explosive eruption on the 20th May 1883. There followed several months of minor explosive activity until the paroxysmal eruption which began on 26th August 1883 (Self and Rampino, 1981). By 20:00 on the 20th May pumice produced during the initial eruption was spotted by the ship the *Sunda,* some 32 km west of Krakatau and by 05:35 on 22nd May, both the *Sunda* and the *Archer* encountered pumice 63 km west of Krakatau (Verbeek, 1885). On the same day, pumice reached the shores of south-east Sumatra at Vlakken Hoek, over 80 km to the west-north-west of Krakatau. On July 9th, the *Quetta* took three days to steam through the floating pumice produced by the eruption on 20th May. By the evening of the 12th July the *Quetta* encountered pumice 1274 km west of Krakatau, despite a current flowing towards the Sunda Straits. The *Idomene*, encountered the pumice on August 11th and 12th, 1870 km west of Krakatau (Figure 1.3). By August 28th, the pumice produced by the 20th May eruption was some 2000 km west of Krakatau and was drifting westward at 23 km/day (Simkin and Fiske, 1983).

At 13:00 on 26th August the highly explosive phase of the eruption began. The eruptions of the 26th and 27th August produced a 26 km high eruption column. Ships up to 20 km from the volcano reported heavy tephra fall, with pumice pieces up to 10 cm in diameter (Judd in Symons, 1888). Pumice from the airfall part of the eruption could have entered the sea to be carried by ocean currents. More pumice was produced by ignimbrites, formed by the collapse of the eruption column at about 06:30 on the 27th August (Sigurdsson *et al.*, 1991). Pyroclastic flows travelled over the sea surface for up to 50 km and hit the coast of Sumatra. Of a total bulk volume of up to 21 km^3 (10 km^3 DRE), between 12 and 13 km^3 was produced by the pyroclastic flows and 8.5 km^3 from co-ignimbrite activity (Self and Rampino, 1981; Sigurdsson *et al.*, 1991). The immediate local effect of the pumice was to block many bays and ports (Simkin and Fiske, 1983). Pumice blocked Lampoeng Bay, to the north of Krakatau during the first few days of the eruption. The bay was finally opened up by NW-W winds in December 1883 (Verbeek 1885).

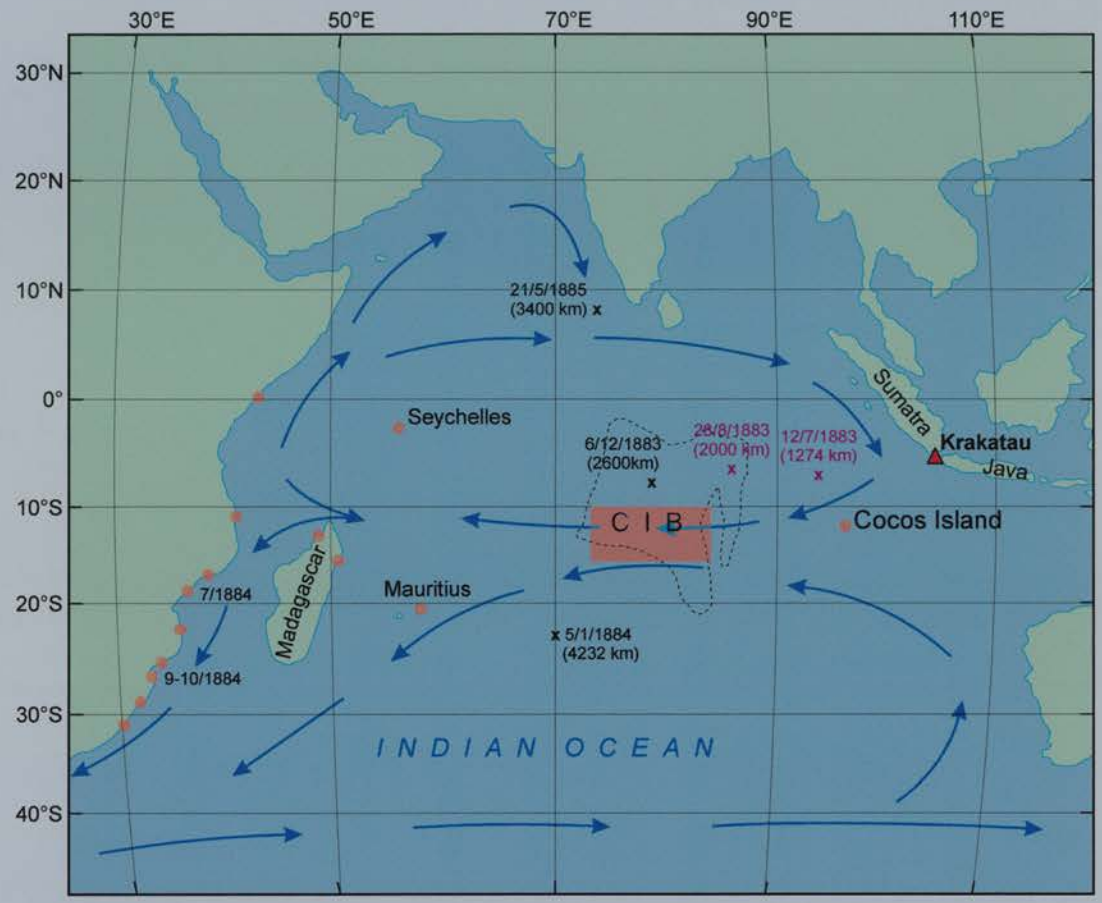

Figure 1.3: The location of Krakatau; the Central Indian Basin (CIB) and deep-sea ocean finds (coloured box); the pumice sightings from ships, shown by x and the date and position of these sightings (see text), and ocean currents which carried the pumice from Krakatau. The red dates and distances show the position of the pumice produced by the 20 May 1883 eruption and the black writing shows the position of the pumice produced by the 26 August 1883 eruption. Note that Krakatau pumice has also been found at four more western sites on in South African coast and in the Pacific Ocean (see text) which are not shown on this map. Data on this map is from Simkin and Fiske (1983), Frick and Kent (1984), Iyer and Karisiddaiah (1988), Iyer and Subhakar (1993) and Mudholkar and Fujii (1995).

This was probably the first time in history that the number of ships crossing the oceans made it possible to track pumice rafts. This lead to many ships reporting sightings of the pumice produced by the 1883 activity of Krakatau during the next couple of years. The *Bothwell Castle* encounted pumice on December 6th 1883 at 8°S 80°E. The vessel steamed through over 2000 km of pumice covered sea. The pumice was thick enough to support seamen (Simkin and Fiske, 1983). By 5th January 1884, pumice was sighted 4232 km west-south-west of Krakatau, by the *Umvoti* (Simkin and Fiske, 1983). Charles Reeves, the captain of the *Umvoti*, reported that the pumice formed ridges arranged in a south-easterly to north-westerly direction by the trade winds and covered at least 1170 geographical miles of latitude, but was not sure how much longitude it covered. The ship lost sight of the pumice 3320 km west of Krakatau. By August 1884, the *Umvoti* and Captain Reeves sighted pumice between 20 and 25°S and next between 10 and 5°S. The latter was the freshest looking:

> "Some days we would pass through pumice lying in ridges each piece uniformly the size and appearance of a bath sponge, then again we should pass through perfect fields of small yellow pumice spread evenly over the surface just for all the world like a green field of grass covered all over with buttercups, and undulation of the swell of the trade wind produced an indescribably pretty appearance." (Reeves, 1884 quoted in Simkin and Fiske, 1983).

The pumice which travelled to the west, across the Indian Ocean, finally reached the coast of Africa in the third week of July 1884, when pumice washed ashore on Mozambique. More pumice reached the shore of Natal in September and October 1884 (Simkin and Fiske, 1983). Krakatau pumice was also found stranded in a Sargasso Sea like feature, between Sri Lanka and the Maldives, over 21 months after the eruption by the *Umvoti*.

Not all of the pumice floated westward across the Indian Ocean (Simkin and Fiske, 1983). It appears that pumice from the 1883 eruptions of Krakatau was also carried into the Pacific Ocean. Pumice was spotted floating near to Batavia (Jakarta) in January 1884 (Rendall, 1884). About a year after the eruption pumice was also found washed ashore on the west of Strong's Island (now Kosrae) in the eastern Caroline Islands, 6500 km NE of Krakatau. Many pieces were between 30 and 40 cm in diameter and were covered in barnacles (Bishop, 1885). Along with the pumice, many trees, including mangroves, were also washed ashore, including species not found in Micronesia.

The trees washed ashore in Micronesia were not isolated occurrences of flora and fauna being transported across vast distances with and by the Krakatau pumice. The well travelled Captain Reeves and the *Umvoti* found that many small fishes were swimming beneath the pumice, along with crabs, barnacles and many other "... creeping things innumerable on each piece ...[and] ... also legions of crabs sculling from piece to piece ..." (Simkin and Fiske, 1983). The pumice washed ashore on Mozambique had a more gruesome cargo. Local mission school children found clean human skulls and bones lying along with the pumice (Simkin and Fiske, 1983). The pumice from Krakatau, therefore, transported fauna and flora across the Indian Ocean to the eastern coasts of Africa and east into the Pacific. Simkin and Fiske (1983) note that eruptions like this happen once or twice a century and they may be important transporters of biota around the world's oceans. Pumice locked into a bay has plenty of time to acquire passengers until it is broken up and distributed by ocean currents. Animals and plants can climb onto the pumice rafts and shallow water fish can be transported across deep oceans, beneath the protection of the pumice.

Although, this section of the thesis is concerned with historical accounts of pumice, it is worth considering the pumice found from the Krakatau eruption which did not reach land, but sank in the Indian Ocean. The presence of pumice on the seafloor provides physical evidence of the paths the pumice rafts travelled. The Central Indian Basin (CIB) is an area of about 5.7 million km^2 found between 0° and 20° S and 70° and 88° E, with an average depth of 5000 m (Figure 1.3). Pumice pieces have been found on the ocean floor between about 5° to 12° S and 70 ° to 84° E covering about 600,000 km^3 (Iyer and Karisiddaiah, 1988; Mudholkar and Fujii, 1995). The pumice is dacitic and clear glass is the dominate phase, forming about 90-92 % of the pumice with phenocrysts of orthopyroxenes, clinopyroxenes, feldspars and some spinal (Iyer and Karisiddaiah, 1988; Mudholkar and Fujii, 1995). The pumice varies in size from about 4 mm to 15 cm in diameter and is generally well-rounded (Iyer and Karisiddaiah, 1988; Mudholkar and Fujii, 1995). The pumice, which is either brown to brownish grey can be divided into two types, that which is covered by a ferromanganese coating and that which is not (Iyer and Karisiddaiah, 1988). Several authors believe that pumice pieces can be the nuclei for the formation of manganese nodules (Iyer and Sudhakar, 1993; Martin-Barajas *et al.*, 1991; Mudholkar and Fujii, 1995; von Stackelberg, 1987).

Iyer and Subhakar (1993) claim that the pumice was produced from relatively local activity from an unknown eruption near or within the CIB. This is based partly on the large size of many of the pumice clasts, though pumice up to 30 cm in diameter travelled over 12,000 km around the Southern Ocean, after an eruption from the South Sandwich Islands (see below). In addition, Iyer and Subhakar (1993) state that analyses published by Shapiro (1975) show that the pumice was not produced during the Krakatau eruption. These analyses, however, were not directly comparable with other geochemical data, as they were determined spectrometrically and complete analyses were not presented. Hedervari (1982) also attributes the pumice found in the CIB to a local submarine source. Finally, Iyer and Subhakar (1993) suggest that ocean circulation patterns would not allow the pumice from Krakatau to reach the CIB.

Mudholkar and Fujii (1995) disagree with Iyer and Subhakar (1993) and state that the fresh pumice (non-ferromanganese covered) found in the CIB was produced by the 1883 Krakatau eruption. Their evidence is mainly based on microprobe analyses of the glass and mineral phases of the pumice. These geochemical analyses are compared with analyses of Krakatau pumice. Although the glass chemistry shows some differences from the Krakatau pumice, Mudholkar and Fujii (1995) suggest that the CIB pumice may have been produced early in the eruption. In support of this, the mineralogical composition of the pumice also resembles that of Krakatau. Mudholkar and Fujii (1995) point out that the mid-ocean ridge type volcanism of the CIB is unlikely to produce highly silicic, vesicular pumice. There is also no evidence that the seamounts around the CIB have been active recently. Pumice has also been found as far west as 64° E, which suggests that they are not just a local CIB phenomena. Finally, Mudholkar and Fujii (1995) disagree that the ocean circulation pattern in the Indian Ocean does not allow pumice to float from Krakatau to the CIB. During August there are generally westerly currents and winds which would transport the pumice towards the CIB. The evidence of Frick and Kent (1984) also supports the case made by Mudholkar and Fujii (1995). Geochemical analyses of pumice from 26 locations including the Indian Ocean islands of the Seychelles, Mauritius, Cocos Islands and Madagascar, confirm the Krakatau eruption of 1883 as their origin.

The pumice from Krakatau provides an important record of the behaviour of ocean transported pumice. The reports from ships enable accurate determinations of the rate of drift, which average between 20 and 30/km day. Although most of this flow was with ocean currents, observations from passing ships suggest that some of the pumice was transported

against prevailing currents by wind action. The pumice which entered the sea by two mechanisms, direct airfall and pyroclastic flows, was also responsible for transporting shallow water biota across the Indian Ocean.

Isla San Benedicto 1952

One of the best documented examples of pumice being transported by ocean currents is found in Richards (1958). Volcán Bárcena, on Isla San Benedicto, situated over 550 kilometres off the western coast of Mexico (19.18° N 110.82 W: Figure 1.4) erupted on 1 August 1952. Most of the pumice which entered the sea was not produced directly from the eruption, but was mainly the result of the destruction of the nearby cone of Monticulo Cineritico. As Richards (1958) points out the location of the island close to the North Equatorial Current aided the transportation of the pumice. A series of reports from ships which passed through the pumice drifts provide valuable evidence for the speed of drift and the length of time pumice can stay afloat. Table 1.2 and Figure 1.4 show the position and dates of sightings of the Isla San Benedicto pumice and demonstrate that some of the some pumice remained afloat for over 18 months.

Location of pumice	Date collected	Days since eruption	Distance km	drift rate km/day	drift rate km/h
Eruption	02/08/1952	-	-	-	-
N of Isla San Benedicto	24/08/1952	22	193	8.8	0.4
SW of Isla San Benedicto	13/09/1952	42	593	14.1	0.6
Hawaii Island	10/04/1953	251	4820	19.2	0.8
Johnston Island	15/03/1953	225	6120	27.2	1.1
Wake Island	15/02/1954	562	8710	15.5	0.6
Ailinginaw Atoll	10/02/1954	557	8710	15.6	0.7
Palau Island*	01/10/1954	790	12000	15.2	0.6

Table 1.2: Drift rates of Isla San Benedicto pumice. * possible sighting of the pumice (Richards, 1958).

The following is a description of a pumice drift sited on 20 September 1952 by the S.S. *Virginia Lykes*:

> "... at ... 1730 GMT, we began passing through numerous patches of what appeared to be lava or volcanic ash. It was of various sizes, some as large as a man's head, but mostly the size of rough lava. It was light grey in colour. ... at 0330 GMT of Sept. 21 ... it had increased to huge patches surrounding the ship ... by 1530 GMT ... it had disappeared and no more was seen." (Cited in Richards, 1958).

All of the pumice found on beaches examined by Richards (1958) was rounded by abrasion. The largest pumice found on Wake Island, 8710 km from Isla San Benedicto (Table 1.2), was 19 cm in length, although the majority were smaller, only "... walnut to potato size ..." (Richards, 1958).

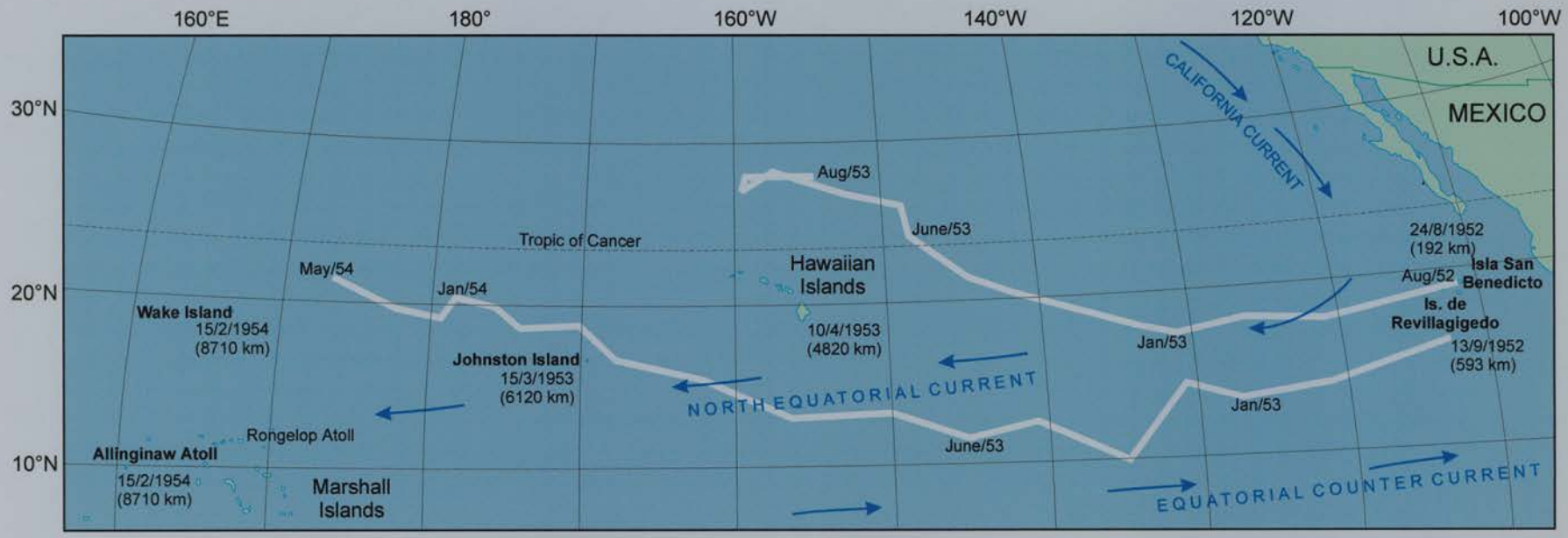

Figure 1.4: The location of Isla San Benedicto and the location of pumice sightings in the central Pacific. The white lines show the tracks of computed drift by the pumice as shown in Figure 1 of Richards (1958). Dates showing when pumice was collected and the distance of these sites from Isla San Benedicto are also shown.

Pumice from Isla San Benedicto provides several useful sources of information. Firstly, the pumice which enters the sea during an eruption does not have to have been produced by that particular eruption. Secondly, the rate of drift of the pumice, between generally between 15 and 27 km/day is comparable to that for the Krakatau pumice. Finally, the amount of pumice required to produce large long distance pumice rafts is relatively small. Richards (1958) estimates that only about 0.003 km^3 of pumice was deposited in the sea after the eruption, which produced widespread drifts that travelled across the Pacific.

South Sandwich Islands 1962

The South Sandwich Islands or Scotia Arc is an active volcanic island arc system about 800 km south-east of South Georgia in the Southern Ocean (Figure 1.5). Although little is known about eruptions prior to the islands' discovery in the 18th Century[11], there have been 18 recorded eruptions from volcanoes since 1823 (Simkin *et al.*, 1994). A large raft of both large and small pumice pieces was sighted by H.M.S. *Protector* on 14 March 1962. Only the aftermath of the eruption, the floating pumice, was spotted by H.M.S. *Protector*. The epicentre of an earthquake, the deduced origin of the floating pumice, and samples of pumice from the seafloor were used to identify the location of the submarine eruption. This was adjacent to a seamount in about 27 m of water, 56 km north-west of Zavodovski Island (55.9° S 28.1° W) on 5 March 1962 (Gass *et al.*, 1963).

The floating pumice investigated by H.M.S. *Protector* covered an area of nearly 5200 km^2 and consisted of individual rafts up to 100 metres in diameter and several hundred metres in length aligned in an east-west direction (Gass *et al.*, 1963). The size of the pumice ranged from very small (< 3 mm) suspended pumice (present in the water column to a depth of 4.5 m) to pumice between 15 and 45 cm in diameter (Gass *et al.*, 1963). Some of the largest pieces spotted were over 1.5 metres in diameter. Gass *et al.* (1963) estimate that the volume of pumice erupted was about 0.6 km^3.

Pumice from this eruption was transported by the West Wind Drift and washed ashore on parts of southern and western Australia and southern New Zealand, between two and three years later. The locations of this and the other sightings can be seen in Figure 1.5. The first

---

[11] The islands were first discovered during Captain Cook's 1772-1775 voyage (Simkin *et al.*, 1994)

recorded sightings of the pumice at Macquarie Island (54° S 158° E) occurred in June 1963 (Sutherland, 1965). This pumice drift covered the nearly 12,900 km from the South Sandwich Islands at a rate of almost 29 km/day. Sutherland (1965) suggests that this early pumice was wind assisted on its journey, whilst smaller pumice pieces which travelled at a slower drift rate of between 10 and 11 km/day, travelled at around the average speed of the West Wind Drift. This slower pumice may be the gravel-sized pumice spotted by H.M.N.Z.S *Pukaki* south of Macquarie Island in January 1964 (Coombs and Landis, 1966). The rates of drift produced here compare well with an estimate of the drift rate of the currents around the Sandwich Islands area of between 12 and 13 km/day in an easterly direction (Deacon, 1960). Major and trace element geochemical analyses were carried out by Frick and Kent (1984) on a piece of pumice collected by H.M.S. *Protector* and pumice pieces found on Bouvet Island and Marion Island in 1964 (South Atlantic Ocean and Indian Ocean respectively) and Kerguelen Island in the 1965 (Indian Ocean). Frick and Kent (1984) were able to geochemically correlate the pumice found on the islands with the pumice collected from near to Zavodovski Island by H.M.S. *Protector.*

The first Sandwich Islands pumice reached Australia around January or February 1964, when pumice was washed onto the shores of Tasmania (Sutherland, 1965). By April 1964 pumice was being washed ashore on Victoria and by January 1965 on the southern coast of Western Australia. Sutherland (1965) points out that the currents around Tasmania change according to the seasons. During the winter there is a dominant eastwards and southwards flow during the winter and westerly and northerly flow during the summer. The pumice would have been carried south of Tasmania probably during April or May 1963 and would not have been able to head north until the summer currents were established. The pumice was well-rounded and many pieces were larger than 30 cm in length. Sutherland (1965) correlated the pumice to the South Sandwich pumice eruption through petrology and geochemistry.

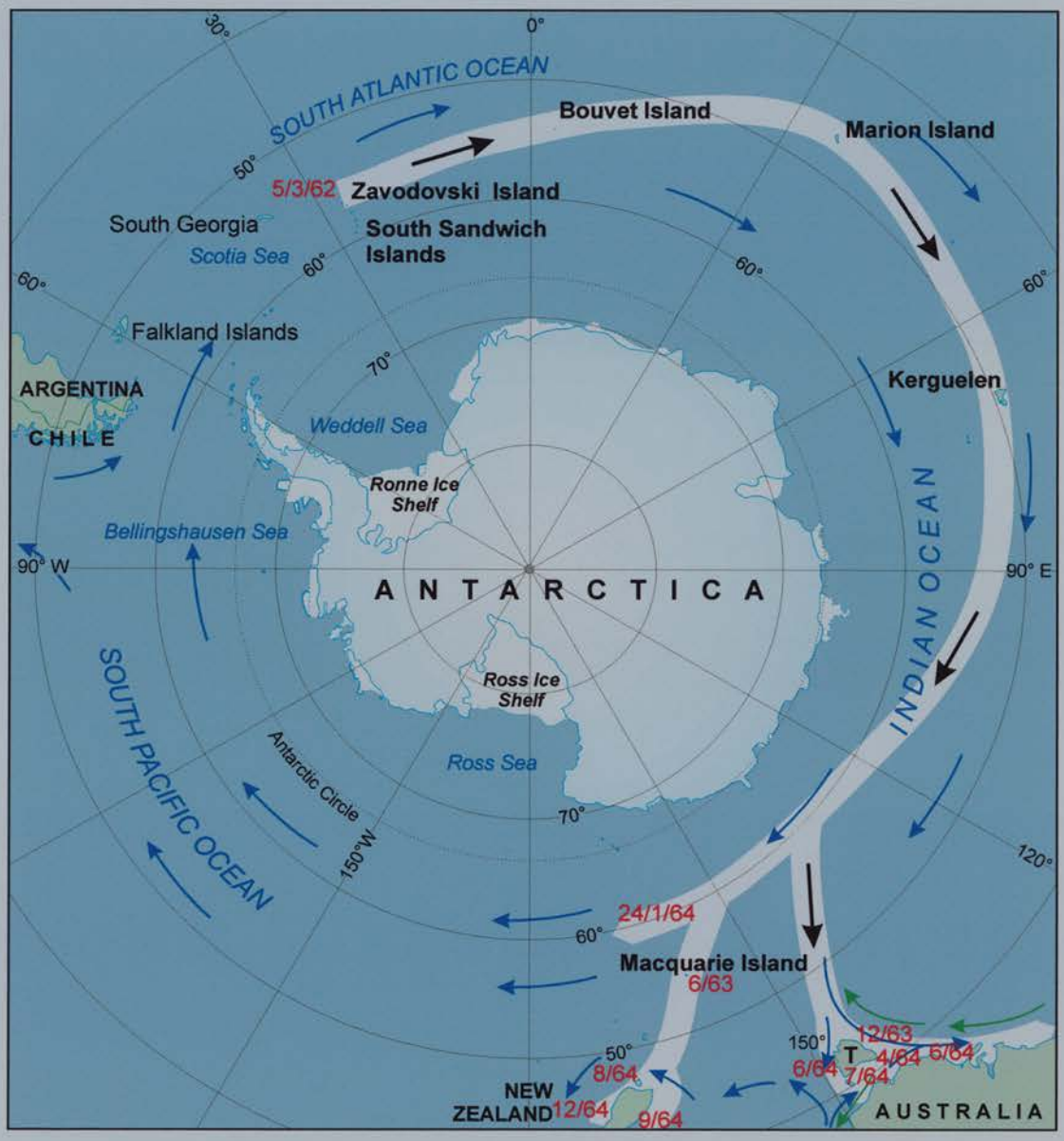

Figure 1.5: The position of the South Sandwich Islands and the deduced positions of pumice rafts produced from the 1962 eruption. Prevailing ocean circulation patterns are shown (blue arrows). The local winter surface currents around Tasmania (T) are shown by the green arrows.

By September 1964, pumice washed ashore on the west coast of the South Island of New Zealand and by December 1964 pumice was being found on both the west and east coasts of the South Island at beaches including those near Dunedin and Christchurch (Coombs and Landis, 1966). Pumice up to 45 cm in length was found at the western entrance to the Cook Strait, between the North and South Islands. Using Refractive Index and mineralogy Coombs and Landis (1966) were able to correlate the pumice with that was produced by the South Sandwich Islands eruption. They were also able to show that the pumice was not produced by any recent volcanic activity in North Island. The pumice travelled the 12,900 km to the Foveaux Strait, between the South Island and Stewart Island, in about 850 days, giving an average drift rate of about 15 km/day. The earliest pumice to reach the South Island did so at a rate of about 24 km/day.

Although far smaller in volume than the Krakatau eruption, the pumice produced from the South Sandwich Islands eruption travelled a vast distance. These drift rates are comparable with those of the Krakatau and San Benedicto pumice rafts. Interestingly, H.M.S. Protector encountered suspended fine-grained pumice, indicating that it may not always sink immediately as indicated by the experiments of Manville *et al.* (1998).

South Sea and Coral Sea Drift Pumice 1964-69

Between late 1964 and 1969, dacitic pumice was washed up on beaches on islands in the Great Barrier Reef, Fiji, Tonga and Cape Bret on North Island, New Zealand (Bryan, 1968; Bryan, 1970; Bryan, 1971) (Figure 1.6). Pumice was also collected from North-East Cay, 325 km west of Cairns, off the coast of Queensland, Australia and part of the Herald Cays Group in December 1964. After a cyclone in March 1965 similar pumice was washed up on the western Fiji Islands (Bryan, 1968). The exact date of the arrival of the pumice at North-East Cay is not known, but it is thought that it arrived after either a particular high tide or storm. Visually identical pumice was also found washed up on Eua Island, the southern most island of the Tonga group in early 1969 (Bryan, 1971). The pumice at Eua, which was stranded after a severe storm several metres above the usual limit of the beach, was visually similar to the pumice found at Fiji and the Great Barrier Reef.

The dacitic pumice from Herald Cays and One Tree Island (Great Barrier Reef), Fiji Islands and Eua all have indistinguishable refractive indices and microprobe analyses of both the glass and minerals showed that the pumice from these various deposits were from the same source and possibly the same eruption (Bryan, 1968; Bryan, 1971). The pumice on North-

East Cay and Fiji was between 1.8 - 3.8 cm in diameter, slightly rounded with at least one or more angular edges (Bryan, 1968), whilst that found on Eua was up to 5 cm in diameter and pumice from One Tree Island contained pieces as big as 10 cm across (Bryan, 1971).

After establishing that the pumice from Fiji, the Great Barrier Reef and Tonga appeared to be the same, Bryan (1971) tackles the problem of explaining the four year gap between the deposition of the pumice on beaches in Fiji and Herald Cays and the subsequent deposition of identical pumice four years later on Eua. After considering several convoluted routes the pumice drift could have taken, Bryan (1971) concludes that the pumice was probably erupted from a local submarine source, near to the Tonga group of islands on the Tonga-Kermadec ridge. This submarine volcano would have had to have produced geochemically identical pumice several times over a four year period.

There are in fact at least 10 active volcanoes in western Tonga, of which only three have emerged above sea-level during historical times (Melson *et al.*, 1970). Fonuafo'ou (Falcon Island), Tonga, was active between 1885-1894 and 1927-1936 and during these periods the volcano produced dacitic pumice of a similar composition to the pumice found at Eua. Frick and Kent (1984) were able to identify clear geochemical differences between the dacitic eruptions of 1928 and 1964. They were also able to extend the distribution of sites where the pumice produced by the 1964 eruption travelled. Analyses of pumice found at Brisbane in Australia (1968) and Réunion Island (1965) in the Indian Ocean also geochemically correlate with pumice produced by the 1964 eruption. A piece of pumice found at Jogensfotein, near Cape Town, South Africa was also from the same eruption. Bryan (1968; 1971) believes that for the pumice to have travelled to the places where it was finally deposited, requires the influence of cyclones. Common to most of the strandings, these cyclones would have carried the pumice across prevailing currents, or even temporary altered the currents.

Pumice erupted from the Tonga region is an important transporter of coral from this area to the Great Barrier Reef (Jokiel, 1990). Pelagic coral larvae only have a lifespan of about a month and therefore, can not normally live long enough to cover the thousands of kilometres to the Great Barrier Reef. Colonies of coral are often found on pieces of pumice washed ashore on the Great Barrier Reef. These colonies become established by either sinking with the pumice in shallow water, become detached from the pumice and sinking or by reaching

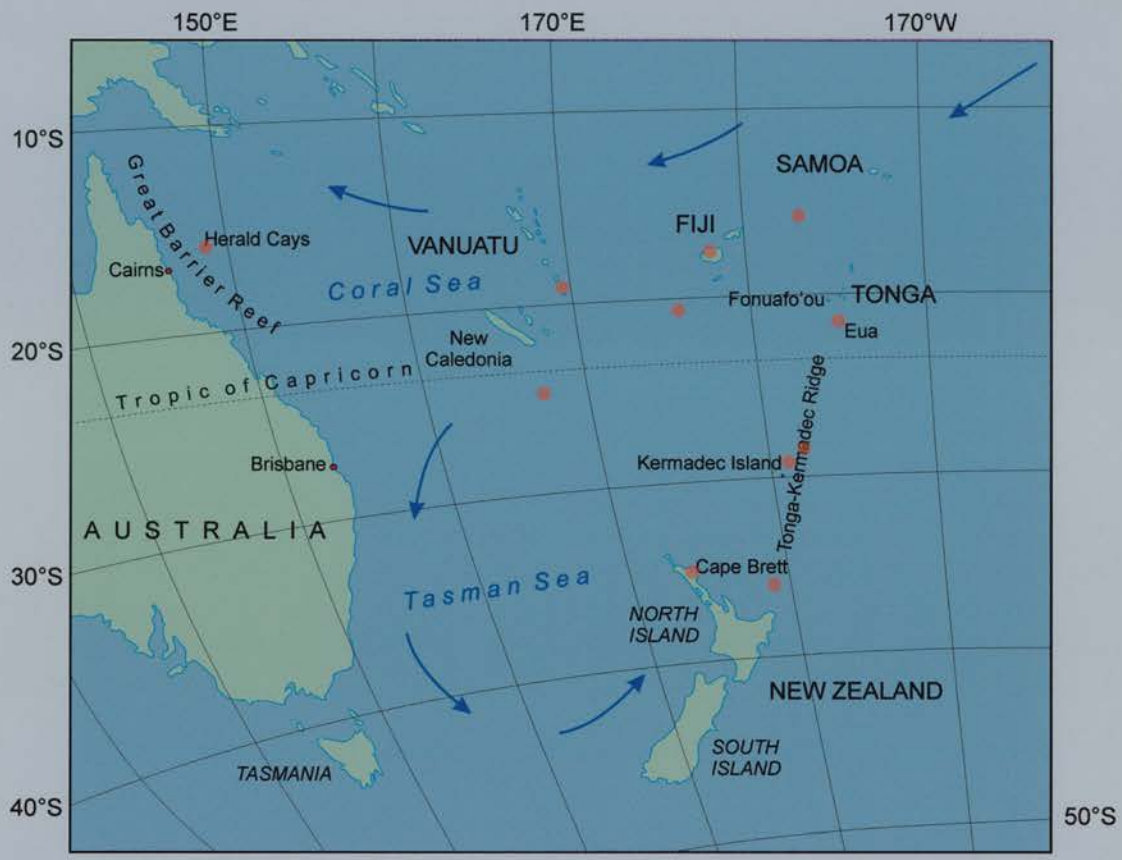

Figure 1.6: The sites mention in text where the South Sea and Coral Sea Drift pumice were found between 1964-69. Sites where pumice was either collect or sited (red dots) and ocean surface currents (blue arrows) are shown. Map based on Bryan (1968; 1971).

reproductive age on the pumice and producing larvae which colonise shallow areas (Jokiel, 1990).

As with the eruptions from San Benedicto and the South Sandwich Islands, the relatively small eruptions near Tonga produced widely travelled pumice rafts. Unlike the two earlier eruptions, the pumice from near Tonga appears to have been produced by several eruptions over a four year period. Again the pumice from Tonga had an important role to play in the transportation of shallow water marine biota across relatively large stretches of deep ocean.

1.6.4 Summary of pumice transportation

This section has demonstrated that if pumice enters the ocean at a low enough temperature it is capable of being transported long distances. Even relatively small volumes of pumice can produce extensive pumice rafts. The majority of the case studies in this chapter involved dacitic pumice. There are few reports of large drifts of basaltic pumice and even highly silicic pumice appears not to form large long distance transported rafts. Frick and Kent (1984) believe that only intermediate and rhyolitic eruptions produce pumice which is capable of floating on water, which is contrary to other evidence. What is clear, is that intermediate pumice is capable of being transported long distances. This may, of course, be a function of the morphology of the pumice rather than its geochemical composition. It is also possible that rhyolitic pumice is more fragile than intermediate pumice and is more likely to be eroded and broken down as it travels in its raft. Whilst most pumice is transported by ocean currents and its drift rate is approximately the same as the speed of the current there are exceptions. Some of the pumice from the South Sandwich Islands eruption was wind assisted on its journey to New Zealand and Australia, whilst some of the rafts from the Krakatau eruption appeared to travel against prevailing currents. Some of the Tongs pumice also appears to have travelled contrary to the current patterns and this has been attributed to local weather conditions. These descriptions of contemporary pumice rafts will be discussed in light of the findings of this study in Chapter 5.

1.7 Deposition and reworking of pumice deposits

Little research has been carried out specifically on the deposition and reworking of pumice deposits. There are several processes which will influence whether a pumice deposit

becomes part of the geological record and if it is reworked at a later date. These are considered below.

1.7.1 Deposition and reworking of pumice

For a pumice deposit to become part of the geological record it must washed high enough up a beach to be out of the reach of normal tides. Bryan (1971) noted that the heaviest concentrations of the Coral Sea pumice on Eua form storm ridges between 15 and 20 cm high along the whole of the beach. The upper edge of the beach was 3 m above the normal high water mark. Further research around the island showed that the local conditions, such as off-shore islands, reefs, local currents and the nature of beach, appear to influence the location of pumice deposition. Bryan (1971) considered it unlikely that the pumice had been eroded from local deposits by the same storm that deposited it, as there would be a time-lag between the erosion and deposition.

This example highlights the two processes which determine whether pumice pieces are preserved in the geological record. The pumice first needs to be washed ashore. This requires a beach which is capable of collecting the pumice. The presence of off-shore islands, for example, will reduce the chances of pumice washing ashore. Local surface currents may discourage or encourage the concentration of pumice onto a beach. Once on the beach the pumice may be reworked by subsequent high tides or storms. The pumice on Eua, for example, was deposited after a storm and formed beach ridges well above the usual high tide line. This pumice may in time become covered by other deposits and preserved. Pumice deposited on the main beach, however, will continue to be refloated and deposited until it is eroded away. These conditions mean that a particular stretch of coastline will probably have a discontinuous record of any one pumice raft.

It is also possible that pumice deposits, that are incorporated into the geological record, can be eroded by subsequent rises in relative sea-level and some of this pumice may be refloated. This refloated pumice may be redeposited either higher up the beach or moved along the coast to a new site. If pumice is going to be used as a correlative tool, the potential for reworking needs to be considered.

1.7.2 Human activity

Human activity can also release otherwise stable pumice deposits into the environment and, if these are near the coast into the sea. Pumice is used in the fashion industry for the

manufacture of stone-washed jeans, for example, as well as in the building industry. In 1989, 60,000 tons of pumice from central and eastern Anatolia, Turkey was imported into the United Kingdom. The Mediterranean is a major source of pumice with over 800,000 tons a year being quarried from the small Greek island of Yali (Wood, 1990). Iceland also has its own pumice industry and the Hekla 1104, Hekla 3 and Hekla 4 pumice deposits are now being quarried, with waste pumice appearing on the south coast of Iceland after being washed into rivers.

1.8 Summary of Chapter 1

This chapter has discussed the processes by which pumice is produced and transported across the world's oceans. For pumice to form rafts, certain conditions must be met. The pumice produced by subaerial eruptions must be transported to the sea by either direct airfall, pyroclastic flows, floods or rivers. Submarine activity deposits the pumice directly into the sea, but the pumice must have cooled to below a threshold temperature if it is not to immediately sink on contact with water. The studies of behaviour of pumice rafts show that even relatively small scale eruptions can produce pumice which is capable of being transported thousands of km across oceans. Pumice ranging in size from a few mm to several metres in diameter is capable of being transported these distances, but it appears that dacitic pumice is the most likely to survive the journey. For the pumice to become part of the geological record it must be deposited above the normal reach of tides and storms. If not the pumice will be reworked and eventually eroded away.

The next chapter reviews the spatial and temporal distribution of pumice finds around the North Atlantic and reviews the previous research.

Chapter

2

North Atlantic Pumice: A critical review

Chapter 1 defined pumice and tephra and described the processes involved in the formation and transportation of pumice around oceans. This chapter reviews the previous research undertaken on pumice deposits around the North Atlantic, before Chapters 3 and 4 present new data.

2.1 Introduction

The aims of this chapter are to synthesise present knowledge of the distribution of pumice deposits in the North Atlantic region critically, review past research and assess previous theories on its age and origin. Since the work of Binns carried out nearly 30 years ago (1967a; 1967b; 1971; 1972a; 1972b; 1972c; 1972d), there have been no major studies of the pumice around the North Atlantic region, but many site specific records have accumulated, particularly in the archaeological literature. The first section of this chapter discusses current knowledge of the spatial and temporal distribution of pumice around the North Atlantic region. The previous theories on the origin of the pumice are discussed next, including the probable source volcanoes and possible transport routes.

2.2 Spatial and temporal distribution of pumice

This section discusses previous research on the spatial and temporal distribution of the pumice in the North Atlantic region. Pumice is found around the shores of much of the northern North Atlantic region (Figure 2.1). It can be found in either natural contexts, such as raised beaches or present day beaches and archaeological sites. All of the sites where pumice has been found are either mapped or described in this section.

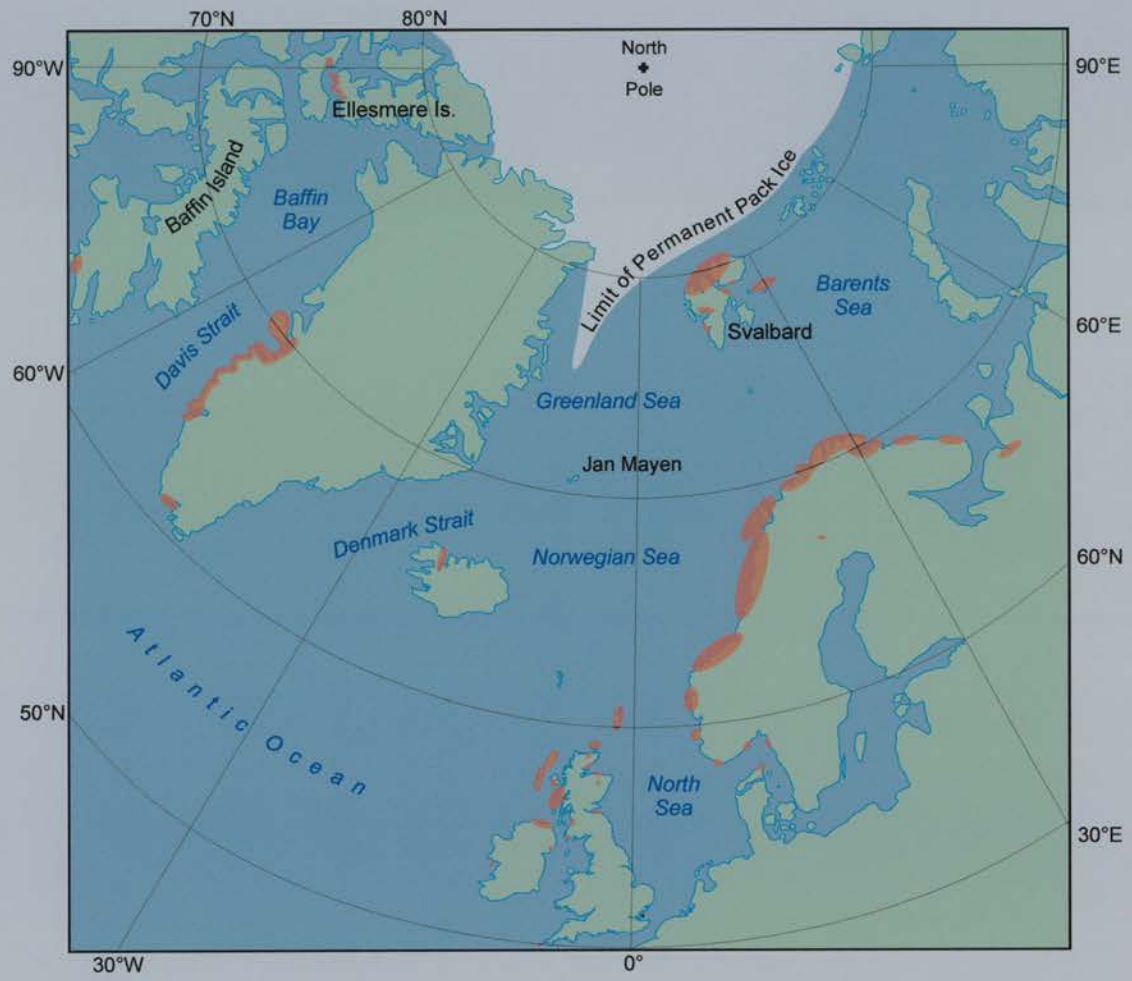

Figure 2.1: Map to show the distribution of published pumice finds around the North Atlantic region.

Raised shorelines preserve a record of pumice deposition which can be mapped spatially on regional scales. A particular deposit or horizon may be the result of some mixing of sources or reworking, but this will not operate over a long period of time. A pumice deposit from an archaeological site, however, may be comprised of material collected over thousands of years by different cultural groups exploiting changing landscapes and mixed often within a poorly dated stratigraphy. Different dating methods ranging from radiocarbon to cultural dates (e.g. Bronze Age) are applied to archaeological contexts with radically differing accuracy and precision. Despite this, archaeological pumice is important as it preserves a record of pumice deposition in areas where the primary deposits have been lost through erosion or subsidence. The pumice may also provide archaeologists with a potentially powerful dating tool. The challenge is to interpret the pumice record found in archaeological sites. As a result different approaches are necessary to investigate archaeological and natural contexts. The key aspects of the shoreline record are location, altitude and age. These are dealt with in the first part of this section, which is generally concerned with pumice found on raised shorelines. The second more lengthy part discusses the finds of mainly archaeological pumice in the British Isles. The detailed discussion of the types of sites and their dating is necessary because of the potentially wide ranging routes by which pumice has come to rest in archaeological sites. It is also necessary to critically assess the varying dating controls on the contexts in which the pumice has been found. This also highlights possible cultural differences in the exploitation of pumice from the Mesolithic to modern times (7000 years).

2.2.1 Canada and Greenland

There is limited recent information about the pumice found in Arctic Canada and Greenland with virtually all of the work summarised by Blake (1970; 1975). Blake (1970) describes brown pumice from Arctic Canada (Figure 2.2) which occurs on raised beaches at six localities around Jones Sound, four on south Ellesmere Island and two on Devon Island. Pumice also occurs on archaeological sites on Baffin Island. These sites vary in altitude from 16.5 metres at South Cape Fiord, Ellesmere Island, to 24 metres at Colin Archer Peninsula, Devon Island, a distance of 130 km. Blake (1975) was able to show from radiocarbon dates of 5020 ± 50, 5100 ± 50 and 5040 ± 60 ^{14}C years BP that these deposits were of the same age. The archaeological sites on Baffin Island which contain pumice are slightly younger, with dates of between 3300 and 4500 ^{14}C years BP (Blake, 1970).

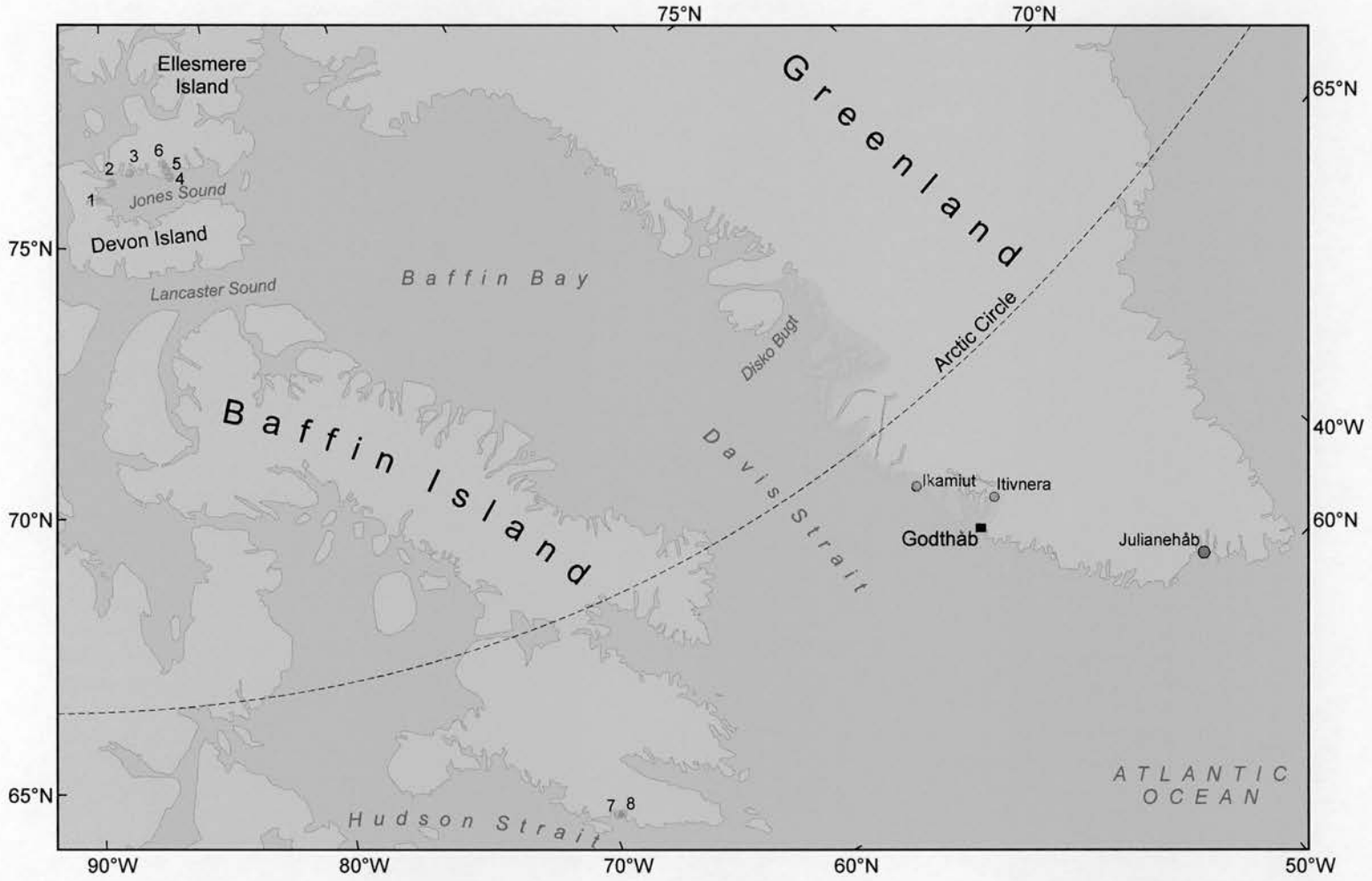

Figure 2.2: Map to show the distribution of pumice in Arctic Canada and Greenland. 1 = Boat Point; 2 = Cape Hawes; 3 = Cape Storm; 4 = South Cape; 5 and 6 South Cape Fiord; 7 and 8 = Cape Tanfield. The shaded west coast of Greenland shows the area where pumice has been found (based on Blake, 1970).

Blake (1970) states that as the pumice deposits occur over a very limited vertical range and are not embedded in the beach shingle but lie on top, it is most probable that they were washed ashore and concentrated by the highest tides, not thrown up by storms. It appears that in this region the logs from which dates are obtained have not been extensively reworked. Observations and dating of modern logs (Blake, 1975) indicates that the maximum height to which they are reworked is only 2 metres, and usually much less.

Pumice has been found along the west coast of Greenland (Figure 2.2) at numerous locations on modern beaches between Godthåb Fjord and Disko Bugt and at 8 Sarqaq Inuit sites, these are summarised by Blake (1970). Noe-Nygaard (1944) found andesitic pumice further south, at or near the present day beach at Julianehåb. Radiocarbon ages for archaeological sites are 3200±120 and 3140±120 ^{14}C years BP (Fredskild, 1967 quoted in Blake 1970; Tauber, 1968). A further radiocarbon date from a raised beach associated with pumice, gives an age of 4590±110 ^{14}C years BP (Weidick, 1968, quoted in Blake 1970). At least one archaeological site in Godthåb Fjord shows evidence that the pumice has been used for sharpening implements (Blake, 1970). Blake quotes from evidence that suggests that the primary deposit, from which the Inuit found the pumice, is now at an altitude of about 20 to 26 m.

Based on Blake's work it appears that a single level of pumice can be found in Arctic Canada, which can be dated to about 5000 ^{14}C years BP and this horizon may also exist in Greenland, but there is need for more detailed study. Inuit in both Arctic Canada and Greenland used the pumice, which they either retrieved from contemporary or raised beaches.

2.2.2 Svalbard

The Arctic islands of Svalbard are found 800 km north of Norway (Figure 2.1and Figure 2.3) have a long record of ocean- and ice-rafted material washing up on their shores. Driftwood has been deposited on the beaches of Svalbard for much of the Holocene. The sources of this driftwood are Russia, Alaska and Canada, where northward flowing rivers deliver wood felled by natural processes and now human logging to the Arctic Ocean (Eggertsson, 1994). This wood is then transported by Arctic Ocean currents. For this wood to reach places such as Svalbard it must first become entrapped within or on sea-ice, as otherwise it will sink long before reaching any shorelines. The presence or absence of driftwood on shorelines in Svalbard has been used as a proxy record of sea ice conditions (e.g. Häggblom, 1982).

Along with driftwood, pumice also occurs on many raised shorelines and the following section describes these deposits.

Northern Spitsbergen and Nordaustlandet

Figure 2.3 shows that pumice has been found in many areas of Svalbard. Since the second half of the nineteenth century, pumice has been recovered from the raised and present day beaches of Svalbard (a summary of these early finds can be found in Binns, 1971). Pumice was found on beaches at scattered sites around Isfjorden and north-west Nordaustlandet in particular. Donner and West (1957), working in north-east Spitsbergen and north-west Nordaustlandet, were the first to map the distribution of pumice levels and use them to correlate raised beach sequences across large areas. They found two levels of pumice at Brageneset, where pumice was particularly concentrated. The upper level was at an altitude of 13.8 metres above sea-level and lower one at 6.4 metres. As they traced these levels north and west, the height of the upper pumice level decreased and they were able to use this distinctive pumice to map the tilt of raised beaches in the area. At Mosselbukta, the altitude of the upper pumice level is only 3.0 metres above sea-level. Blake (1961) was able to trace the upper pumice deposit along most of the north coast of Nordaustlandet and extend the mapping of the tilted raised beaches. The altitude of the upper pumice level rises to 20 metres above sea-level at Finn Malmgrenfjorden. The main upper pumice level on the island of Wilhelmøya is found at 28 metres above sea-level. Blake (1961) obtained several radiocarbon dates on the upper pumice level around Kinnvika and Wilhelmøya. All of these dates ranged between 6200 and 7000 ^{14}C years BP. Combining this data with pumice finds in the southern part of Wijdefjorden, Schytt *et al.* (1968) were able to construct an isobase map for the 6500 ^{14}C BP pumice strandline. This demonstrated that the area of greatest post-glacial uplift lay to the south-east of Svalbard and that this was the result of a large late-Pleistocene ice-sheet, centred over at least the northern part of the Barents Sea.

Blake (1970) examined the dating of pumice-bearing raised beaches.. Logs associated with the pumice on beaches previously dated at between 6200-7000 ^{14}C years BP (Blake, 1961), had themselves since been dated at between 7000 and 7500 ^{14}C years BP. Younger logs had also been found with dates between 4800 and 6000 ^{14}C years BP. Blake (1970) attributes these confusing dates to a transgression which carried younger logs to beaches containing older logs and refloated older logs from areas of slow uplift, for example Siberia.

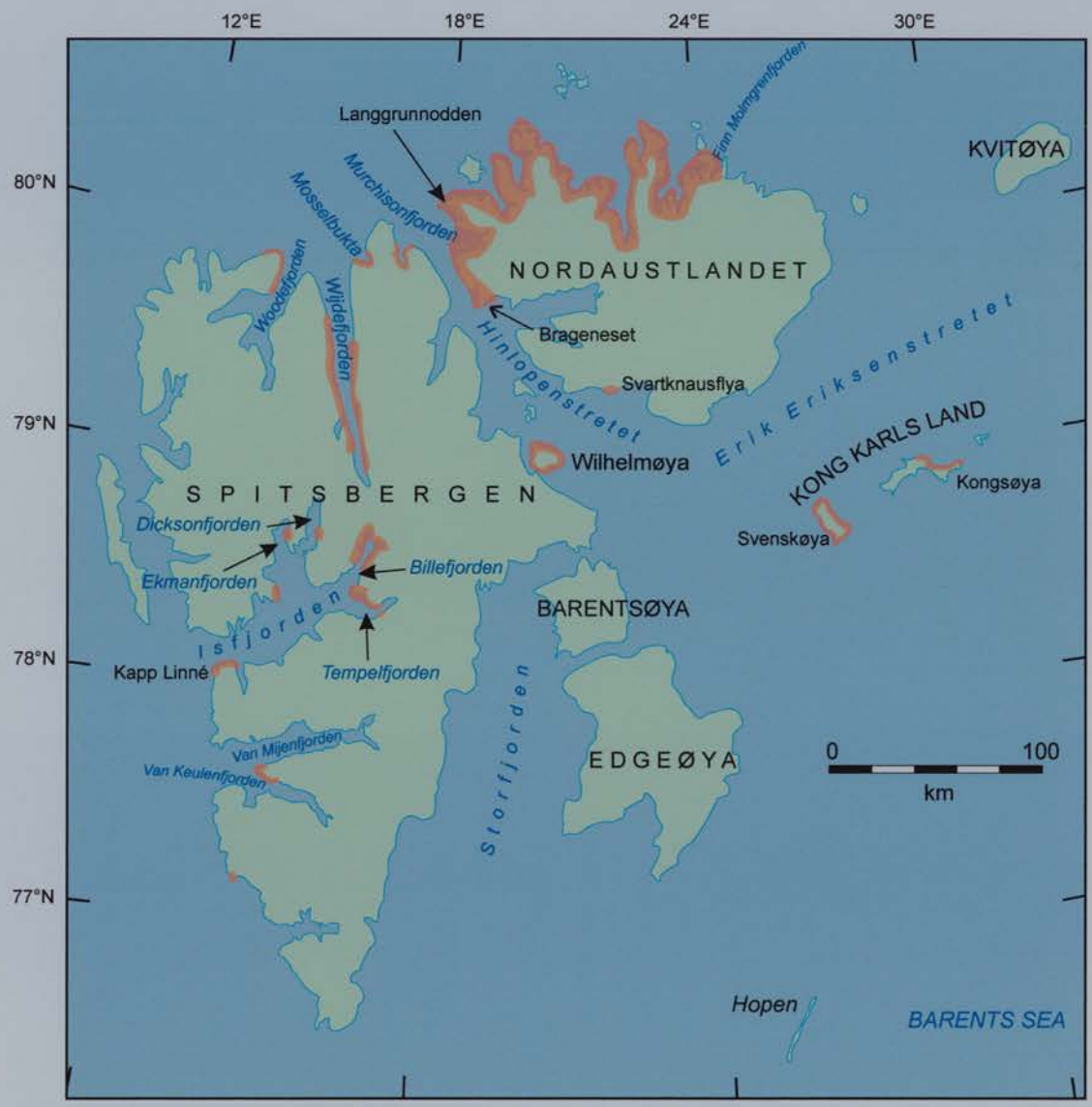

Figure 2.3: Map to show the distribution of pumice finds (red shading) in Svalbard and place names mentioned in the text. The references on which this map are based are included in the text.

Boulton and Rhodes (1974) carried out further research in the north-eastern part of Spitsbergen and far north-western Nordaustlandet. They were able to identify and date four pumice levels, with the upper one again having the largest concentration of pumice. Unfortunately, limited details are given about the radiocarbon dates, though they do apparently use some of the dates published by Schytt *et al.* (1968). At least one of the dates is on driftwood (a date of 6420 ^{14}C years BP on the uppermost layer) and others are on shells, marine algae and whalebone. When using radiocarbon dates from marine sources (marine mammal bones, shells, corals, fish etc), it is important to take into effect the reservoir effect of the oceans and correct this when stating the radiocarbon age. Marine dates from around Svalbard should have about 440 years subtracted from their age (Mangerud and Gulliksen, 1975; Olsson, 1980). It is not possible to do this with the dates produced by Boulton and Rhodes (1974). Bearing this in mind, they dated their upper horizon (Horizon A, red, brown and black pumice, up to 10 cm in diameter) to 6500 ^{14}C years BP; the next (Horizon B, mainly brown pumice, 2-5 cm in diameter) to 6200 ^{14}C years BP; the next (Horizon C, black with some white pieces, some up to 25 cm in diameter) to 4100 ^{14}C years BP; and the youngest one (Horizon D, black with some white pieces, some up to 25 cm in diameter) to 2200 ^{14}C years BP. Horizons A and C have the highest concentrations of pumice and are regarded as being primary deposits, whilst B and D may be primary or reworked (Boulton and Rhodes, 1974).

Salvigsen and Österholm (Salvigsen and Österholm, 1982) also found pumice further to the west along the north coast of Spitsbergen, around the Woodfjorden area. The presence of substantial amounts of pumice either in the surf zone (northern Reinsdryflya) or with the flotsam and jetsam (outer Woodfjorden), lead them to the conclusion that if this was the 6500 ^{14}C BP pumice, there had been no uplift in this area for the last 6500 ^{14}C years BP.

Southern Nordaustlandet and Kong Karls Land

Until 1978, no pumice deposits had been found along the south coast of Nordaustlandet. Salvigsen (1978), however, found pumice in the Svartknausflya area of south-west Nordaustlandet. The largest amount of black/grey black pumice (100 pieces) was found between 15.5 and 16 metres above sea-level and dated to between 4500 and 4600 ^{14}C years BP (4560 ± 80 ^{14}C years BP and 4650 ± 90 ^{14}C years BP). Salvigsen (1978) does not correlate his 4500 ^{14}C years BP pumice level with any of the four levels of Boulton and Rhodes (1974), but correlates it instead with the youngest level first identified by Donner and West (1957). Boulton and Rhodes (1974) correlate Donner and West's lowest pumice

deposits with their level C (4100 ^{14}C years BP). Although individual pieces of pumice were found at higher altitudes, some at heights with an age of about 8000 ^{14}C years BP, no pumice, driftwood or whalebones dating between 7500 ^{14}C and 6300 ^{14}C years BP were found at Svartknausflya. Salvigsen (1978) suggests that this may be because of different current or sea ice conditions at the time.

The distribution of pumice in Svalbard was extended further south by Salvigsen (1981), when pumice was found on Kong Karls Land, a group of islands to the south-east of Nordaustlandet. Two levels of black/grey pumice were found on the eastern coast of Kongsøya. The upper level (32 metres above sea-level) was dated to 5240 ± 70 ^{14}C years BP and the lower one (17 metres above sea-level) to 3110 ± 80 ^{14}C years BP. The single layer of pumice found on Svenskøya (14 metres above sea-level) was dated to 3240 ± 190 ^{14}C years BP. These two pumice levels cannot be correlated with any other pumice deposits found in Svalbard Salvigsen (1981). Several single pieces of pumice were found on Svenskøya, possibly including one at about 6500 ^{14}C years BP.

West coast of Spitsbergen

In contrast to the extensive pumice finds along the north coasts of both Spitsbergen and Nordaustlandet, there have been few records of any pumice deposits on the west coast of Spitsbergen. In fact, apart from the 19th Century finds reported by Binns (1971), there are only two published records (Salvigsen, 1984a; Salvigsen, 1984b) and Boulton and Rhodes show a pumice find in Billefjorden on a map (Figure 1 in 1974), but do not describe the height of the find.

Salvigsen (1984b) found pumice at two sites on the outer part of Isfjorden. Between Kapp Linné and Russekeila, pumice can be found at an altitude of between 8.9 and 9.9 metres above sea-level. At Van Keulenhamna, Salvigsen (1984b) found pumice at three levels, the highest level (10.2 and 11.5 metres) had the largest concentration of pumice, whilst other pumice deposits were found at 9.7-7.7 metres and 4.5 metres. Salvigsen (1984b) correlates the pumice between Kapp Linné and Russekeila and the highest level at Van Keulenhamna with the 6500 ^{14}C years BP pumice found elsewhere in Svalbard.

At least four pumice levels (a, b, c and d) can be found in the inner most part of Isfjorden (Figure 2.3), at 10 sites (Salvigsen, 1984a). All of the pumice is greyish black, with some brown and is usually less than 8 cm in diameter, with one piece over 15 cm across. This pumice is physically similar to most of the other pumice found in Svalbard (Salvigsen,

1984a). The highest pumice level (a), which varies in altitude between 20.5 and 9.8 metres, was radiocarbon dated to 6440 ± 80 ^{14}C years BP. Salvigsen (1984a) concludes that a maximum age for this pumice deposit is 6500 ^{14}C years BP. It was not possible to date the lower levels, but Salvigsen (1984a) estimates that the second oldest layer (b) is several hundred years younger than the oldest (a), and probably dates from about 6000 ^{14}C years ago. This would seem to correlate with Horizon B of Boulton and Rhodes (1974). Pumice level (c) has the highest concentration of pumice after (a) and Salvigsen (1984a) correlates this with either the 4100 ^{14}C years BP Horizon C of Boulton and Rhodes (1974) or the 4500 ^{14}C years BP from Svartknausflya (Salvigsen, 1978). Level (d) is correlated with the 3100 ^{14}C years BP pumice deposit found on Kong Karls Land by Salvigsen (1981).

Summary of Svalbard pumice

Table 2.1 shows a summary of the possible pumice levels found in Svalbard. Between six and seven pumice levels exist, with pumice pieces scattered shorelines older than 6500 ^{14}C years BP Salvigsen (1981). Unfortunately, these correlations between the various pumice deposits must be treated with some care. Blake (1970) highlighted the problems of dating when logs from the same beach give widely different dates. It should also be noted that not only can the material being dated (the logs) be moved by a transgression, but the pumice itself can be reworked (Chapter 1). Despite this, it is clear that Svalbard has had multiple episodes of ocean-rafted pumice deposition during the Holocene. Interestingly the c. 5240 ^{14}C years BP pumice deposits on Kong Karls Land can be temporally correlated with the Arctic Canadian pumice.

Age (^{14}C years BP)	Location	References
c. 6500	N Spitsbergen, N. Nordaustlandet, Isfjorden	1, 2, 3, 4, 7
c. 6200	NE Spitsbergen, N. Nordaustlandet, Isfjorden	3
c. 5240	Kong Karls Land	6
c. 4500*	Svartknausflya, Isfjorden	5, 7
c. 4100*	NE Spitsbergen, N. Nordaustlandet, Isfjorden	3
c. 3200	Kong Karls Land, Isfjorden	6, 7
c. 2200	NE Spitsbergen, N. Nordaustlandet	3

Table 2.1: Table to show the ages of the various pumice levels found in Svalbard. * these two levels are possible the same. Reference are: 1 = Blake (1961); 2 = Schytt *et al.* (1968); 3 = Boulton and Rhodes (1974); 4 = Salvigsen and Österholm (1982); 5 = Salvigsen (1978); 6 = Salvigsen (1981); 7 = Salvigsen (1984b).

2.2.3 Iceland

Although Iceland is the most probable source of the dacitic pumice found around the North Atlantic Region, up until the time of this study there have been no published finds of any

brown/black/grey dacitic pumice on Icelandic raised beaches. Although Binns (1971) carried out a thorough survey of pumice around the North Atlantic Region, he does not mention a single find on the raised shorelines of Iceland. The south coast of Iceland does not provide an ideal environment for the development of raised beach sequences. Although the coastline has undergone isostatic recovery during the Holocene, there are very few raised beach sequences. The early part of the Holocene saw a rapid fall in relative sea-level caused by isostatic rebound, followed by a slower rise to present levels (Thors and Helgadóttir, 1991). The south coast of Iceland has been buried beneath hundreds of metres of sandur plain, produced from a combination of catastrophic jökulhlaups and fluvioglacial activity. Jökulhlaups are catastrophic floods from glaciers that may be caused by the drainage of an ice dammed or subglacial lake, landslides, surging glaciers or as a result of volcanic or geothermal activity melting large volumes of ice. The largest floods, caused by volcanic activity can exceed 10.5 $m^3 s^{-1}$, have large sediment loads and usually only last for between 24-36 hours (Maizels, 1991). These have covered any raised beaches (Maizels, 1991). Relic, buried, former sea cliffs, stacks and islands can be seen along the south coast, especially to the south of Eyjafjallajökull. Large fissure eruptions, such as those from Eldgjá and Skafta Fires eruptions, have also covered hundreds of square kilometres of coastal lowlands. Raised beach sequences, however, are found on the east and north coasts, the Snæfellsnes Peninsular and Reykjarnes Peninsular. Despite research on these raised beaches, there are no published records of brown/grey pumice being found. In fact, a study of a raised beach ridge by Bárðarson (1910) at Bær, on the east coast of Hrútafjörður, fails to mention the large amount of pumice present at the site and described in detail in Chapter 3. The more recent work of Eiríksson *et al.* (1998), however, has produced dates of 5160 ± 100 ^{14}C years BP from a shell from the base of the ridge and 5390 ± 90 ^{14}C years BP from a shell from within the ridge at Bær. They also report the pumice deposits found there.

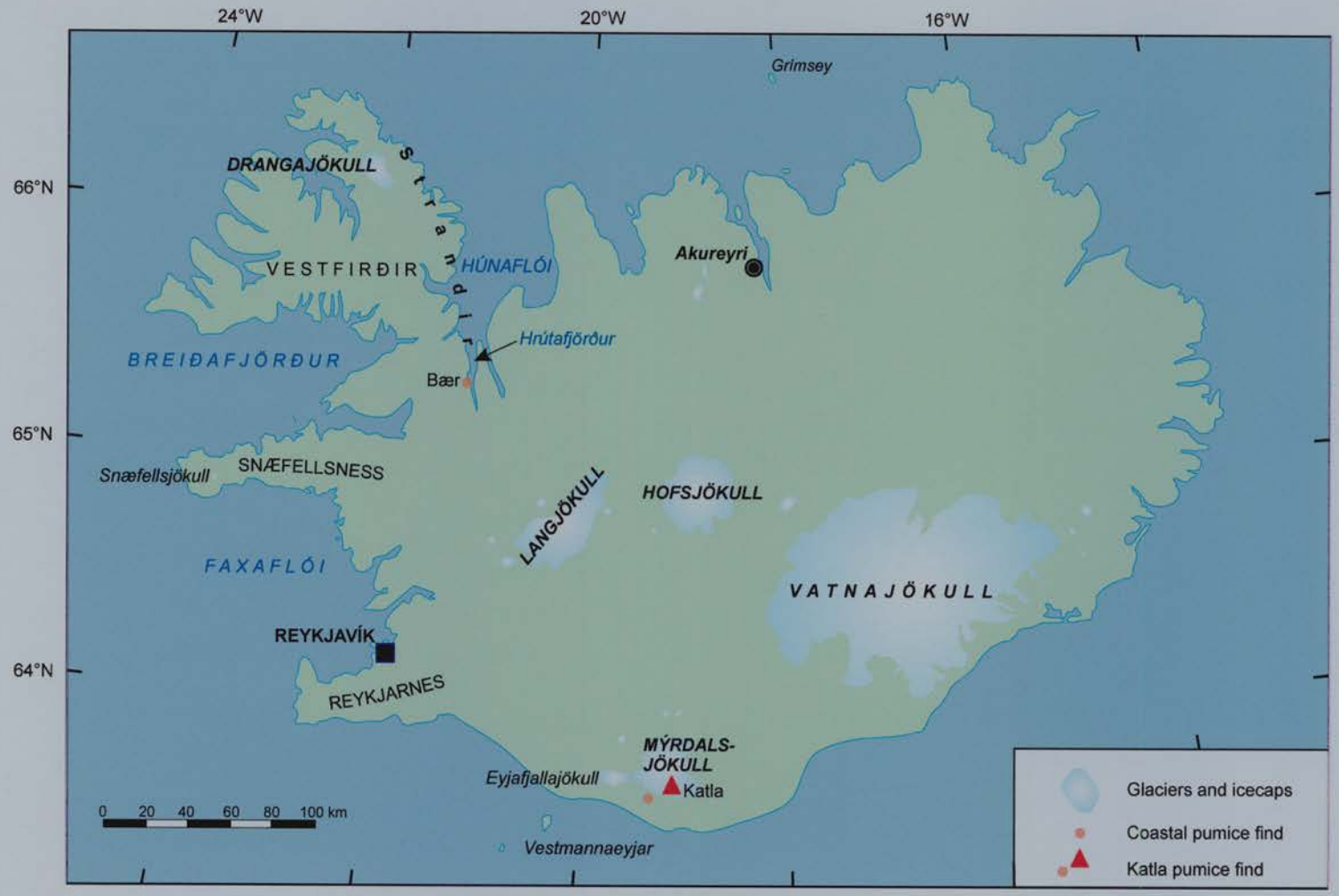

Figure 2.4: Map to show the location of sites where pumice has been found in Iceland. These are along the Strandir coast of Vestfirðir and on the southern slopes of Katla.

Pumice finds from this study have all occurred along Strandir on the eastern coast of Vestfirðir (North-West Peninsula, Figure 2.4). All of these finds are either on raised or present day beaches. Pumice finds from the Strandir coast are described in detail in Chapter 3. Pumice has also been found on the upper slopes of Katla on the south coast of Iceland (Larsen and Dugmore, pers comm. 1990; Lacasse *et al.*, 1995). These sites and the pumice found at them are described in more detail in Chapter 5.

The lack of specific records of pumice finds in Iceland may be simply due to the volcanic nature of the island and that pieces of pumice found on raised beaches lack the novelty of pumice on Svalbard, for example. As a result investigations of beach pumice have probably not seemed an important area of research. Chapter 3 does show, however, that pumice pieces have been collected and stored in museums, even if no research has been carried out on them. Iceland, therefore, does have a record of Holocene dacitic pumice deposits, although there are few references in the literature to them.

2.2.4 Scandinavia

Figure 2.5 shows that pumice deposits can be found along virtually the whole of the western coast of the Norway, with individual sites in south-west Sweden and Denmark. Noe-Nygaard (1951) points out that the presence of pumice on raised beaches was noted as far back as the 18th century by a clergyman from west Norway (Strøm, 1762). The last major reviews of pumice finds in the Scandinavia were provided by Binns (1971; 1972a) and Blake (1970). The work of Binns (1971) is crucial, as it contains a thorough review of the Scandinavian literature which refer to pumice up until 1971. Most of these references are in Norwegian and are not readily accessible to the non-Norwegian researcher. In recent years, more research has been published in international English language journals. For this reason most of the references to pre-1970 sources are quoted from Binns (1971), with the exception of English language publications, such as Undås (1942) and Noe-Nygaard (1951).

The works of Binns (1971; 1972a; 1972c) are still quoted as the standard references for the spatial and temporal distribution of pumice in Norway. Whilst his research produced a comprehensive and probably accurate description of the spatial distribution of pumice, the dating of these pumice deposits must be treated with care. Binns relied heavily on the radiocarbon dating of shorelines by Marthinussen (1962) and used his four-fold division of the mid-Holocene Tapes transgression (Tapes I, II, III, and IV).

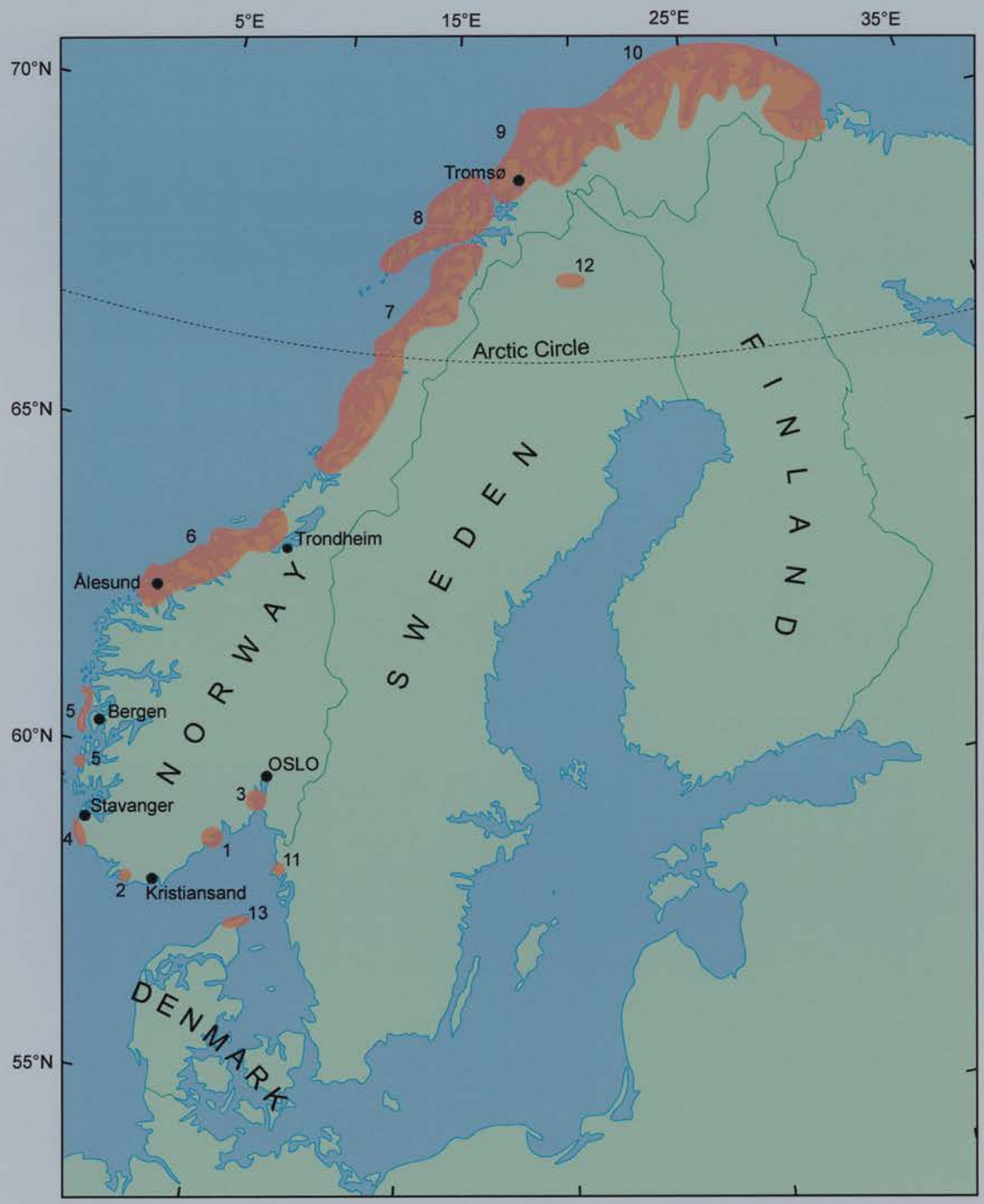

Figure 2.5: Map to show the distribution of pumice finds around Scandinavia. The numbers are referred to in the text.

Both Undås (1938; 1942; 1945) and Marthinussen (1960; 1962) relied on pumice deposits to correlate raised shorelines. Recently though, both the complexity and dating of the Tapes transgression has been reinterpreted along the whole of the Norwegian coast. The use of isolation basins has revolutionised the construction of sea-level curves, especially in central western Norway (Kaland *et al.*, 1984; Svendsen and Mangerud, 1987; Svendsen and Mangerud, 1990). Finally, the deposits previously identified as evidence of a gradual marine transgression have recently been reinterpreted as having been formed by the 7200 ^{14}C years BP Storegga tsunami (Bondevik *et al.* 1997a; 1997b; 1998). This progress means that the dating of Norwegian pumice deposits needs to be reassessed if their correct age is to be determined. Without firm chronological control it will not be possible to correlate the pumice deposits to tephra layers in Iceland and identify the eruptions which produced the pumice.

Geographical Distribution

This section summarises the spatial distribution of pumice in Scandinavia, including details about the height of the various pumice deposits above sea-level. The following section will deal with the dating of these levels.

Norway

Figure 2.5 shows that pumice occurs along the whole of the western coast of Norway, but despite a comprehensive search of the literature, Binns (1971) was only able to find evidence of scattered pumice deposits on the well studied raised beaches of south-eastern and southern Norway. Binns (1971) reports a pumice find at Jomfruland, near Kragerø[1], Telemark, on the Tapes transgression midway between Kristiansand and Oslo, in the south-east of Norway (area 1 on Figure 2.5), which is described in Hansen (1915; 1918). There are no other published records of pumice being found on natural sites in this part of Norway.

Pumice, however, been found in many archaeological sites in southern Norway. Excavations at seven sites around the town of Farsund (area 2 on Figure 2.5), southern Norway, produced at total of 96 pieces of pumice from mainly Mesolithic or Neolithic contexts. The largest single pumice find was at Engøy, Vest Agder (near Kristiansand), where 574 pieces of

---

[1] Note that the characters "ø" and "ö" are used interchangeably on Norwegian maps, in this thesis the "ø" is used.

pumice were found in a Late Neolithic/early Bronze Age site. Other pumice finds have been made at Eg, also in Vest Agder (near Kristiansand); Sluppan, Telemark, close to Kragerø (area 1 on Figure 2.5); Gjølstad, near Oslo; an Early-Middle Neolithic site, Auve at Sandefjord (area 3 on Figure 2.5); and Vindenes and Austvik. There are also reports of pumice being found in several archaeological sites in Rogaland (area 4 in Figure 2.5; Binns, 1971).

Further north, pumice finds on the island of Bømlo (area 5 in Figure 2.5) were first reported by Fægri (1944). He found two levels at Djupadal the highest at about 11 metres, whilst Kaland (1984) finds a single level of pumice at 11.4 metres at the same site. There are no other published records of pumice finds in this area. Further north, the next area with published finds of pumice are from the islands to the west of Bergen (area 6 on Figure 2.5). Bäckström (1890) reported finding black pumice, whilst Undås (1945) found pumice at three levels. The highest of these levels is at about 12 metres and the lowest 5.7 metres above sea-level on the island of Blomøy (quoted in Noe-Nygaard, 1951).

The regions of Møre and Trøndelag provide perhaps the most detailed record of pumice deposits in Norway (area 7 in Figure 2.5). This is mainly due to the work of Isak Undås, who in 1942 published a detailed survey of the raised shorelines in this area and recorded the elevations of pumice finds. The correlation of pumice levels he found were a fundamental part of his reconstruction of shorelines in the region. This detailed record is unique and Table 2.2 includes details of all of the sites and the elevation of the pumice finds, whilst Figure 2.6 includes the location of these sites. Table 2.2 shows that there are between two and three pumice levels at each site and invariably, where stated, the uppermost level is composed of brown pumice and the lowest is mainly black. The three pumice levels found are all associated with the Tapes transgression according to Undås (1942). This region was visited for this study and sites where pumice was found were resurveyed and pumice samples were taken for possible geochemical analysis. Details of these sites and their pumice deposits are discussed in detail in Chapter 3.

No.	Name of site	Level	Colour	M.A.S.L.	
				Lower	Upper
	Nordfjord				
	Ervik, Stad	1	?		5
	islands of northern Sunnmøre - Ålesund area				
1	Kvalvika, Haramsøy*	1	Black	5.9	7.6
		2	Brown	7.5	10.5
2	Brimnes, Vigra*	1	Black	5.1	5.8
		2	Brown	7.5	9.1
3	Rønstadhelleren, Lepsøy	1	black	5.7	
4	Gjøsund, Valderøy*	1	black	5.3	
		2	brown	9.6	
		3		c.10?	
5	Kvernbekken, Harøy	1	black	5.6	
		2	brown	10.4	11.6
	Romsdal-Nordmøre – near Molde				
6	Gulberget, Bud*	1	black	5.2	
		2	?	11.8	13.9
		3	?	25.2	
7	Kalsvik-Gulberget, Bud*	1		12.5	
8	Stavik-Breiskarrem	1	black	6.0	7.1
		2	brown	9.9	10.5
	Nordmøre - near Kristiansund				
9	Kvitsund (Kobbvika in Figure 2.6)*	1	black	7.0	
		2	brown	12.6	
		3	brown	16.0	17.3
10	Brandsvik, Tustna*	1	black	7.0	8.5
		2	?	13.9	
		3	brown	19.9	23.3
	Hitra-Frøya-Hemne				
11	Sandvik, Frøya	1	black	7.3	8.1
		2	brown	14.2	15.0
		2	brown	17.0	19.0
12	Hernes, Hitra*	1	?	?	
13	Småge west, Hitra*	1	black	8.0	
		2	brown	14.0	16.2
		3	brown	19.7	21.0
14	Myra, Dolmøy*	1	?	21.1	23.3
15	Grønsletta, Dolmøy*	1	?	20.1	22.1
16	Hjertåsen, Dolmøy*	1	?	11.0	
		2	?	25.0	
		3	?	29.0	
17	Vingvågen	1	?	12.0	
		2	?	21.0	
	Trondheimsfjord				
18	Linesøy, opp Harsvik	1	?	c. 34	
19	Mølnbukt, opp. Brekstad	1	?	c.33	
20	Agdenes, SW of Mølnbukt	1	?	c 13	
		2	?	c 25	
		3	?	c 38	
21	Brettingsfjell, NE Brekstad	1	?	c. 13	
		2	?	c. 39	
	southern part of Nord-Trøndelag				
22	Linesøy 1	1	?	c. 32	
23	Linesøy 2	1	?	c. 10	
24	Strand at Osen	1	black	13.7	14.5
		2	brown	22.0	23.0
		3	masses	33.4	40.8

Table 2.2: Sites where pumice is found in Møre and Trøndelag. All sites from Undås (1942). * indicates sites visited or sampled for this study. ? = colour of pumice not stated.

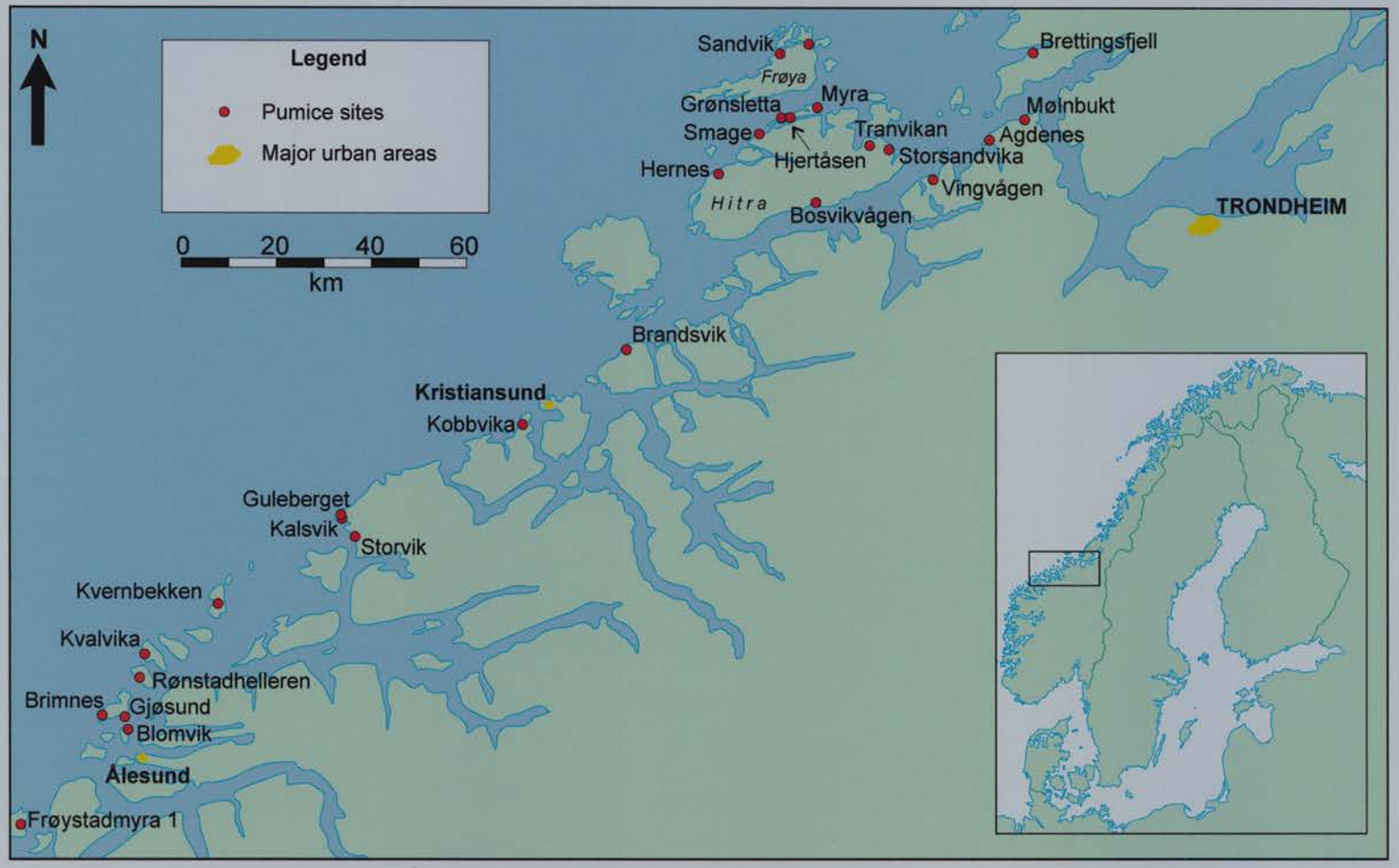

Figure 2.6: Map to show the location of the sites in Undås (1942) where pumice was found. Kobbvika is referred to as Kvitsund by Undås and Frøystadmyra, Blomvik, Storvik, Bosvikvågen, Sorsandvika and Trandvikan are additional sites not mentioned in his report.

Pumice has also been found near Frøystadmyra on the island of Lenøy, to the south-west of Ålesund, at an altitude of about 6.45 metres above sea-level (Bondevik *et al.*, 1998).

As well as the typical brown or black pumice, Binns (1971) also reports the finding of light grey/white pumice in Romsdalsfjorden by Kaldhol (1922). This piece was found at an altitude of about 50 metres, some 30 metres above the Tapes pumice described by Undås (1942). White pumice is also found at relatively high altitudes on the island of Hitra at Trandvikan (Stienar Nilsen, pers. comm., 1993; Møllenhus, 1977). This pumice is discussed in detail in Chapter 3. Black pumice has also been found at an altitude of between 20-25 metres at Storsandvika on island of Hitra, by Stienar Nilsen (pers comm., 1993).

Pumice also occurs on raised beaches in Nordland (area 7 on Figure 2.5) and Binns (1971) mentions reports of pumice in Bäckström (1890) and Marthinussen (1960).

Several authors earlier this century found pumice at numerous locations in Lofoten and Vesterålen [area 8 on Figure 2.5; Binns, 1971), including Undås (1938). Kulvika (Coal Bay) on the island of Vestvågøy, the central island of the Lofoten group, is named after the large amounts of black pumice found on the raised shoreline there (Binns, 1971). Petvik beach, on the southern coastline of Vestvågøy, has brown pumice between 2 and 5 cm in diameter on a raised beach at an altitude of about 2 metres above sea-level (Peulvast and Dejou, 1982). Binns (1971) found pumice deposits at a dozen locations on Andøya, northern Vesterålen. Near Nordmjule (west Andøya), Binns (1971) found mainly brown pumice on and buried within the Tapes complex, suggesting reworking of the deposit. Binns (1971) also reports that pale grey/white pumice has been found at several places in the Lofoten-Vesterålen area. As in the Møre and Trøndelag area, these sites are usually at higher altitudes than the pumice associated with the Tapes transgressions. But he did find white/grey pumice, along with brown pumice at an altitude of 5 metres at Bleik on Andøya. Buckland (pers comm., 1998) found brown and black pumice (between 4 to 5 cm in diameter) at an altitude of about 2 meters above sea-level at Ramså on Andøya.

Several authors earlier this century found pumice at numerous locations in Lofoten and Vesterålen (area 8 on Figure 2.5; Binns, 1971), including Undås (1938). Kulvika (Coal Bay) on the island of Vestvågøy, the central island of the Lofoten group, is named after the large amounts of black pumice found on the raised shoreline there (Binns, 1971). Petvik beach, on the southern coastline of Vestvågøy, has brown pumice between 2 and 5 cm in diameter on a raised beach at an altitude of about 2 metres above sea-level (Peulvast and

Dejou, 1982). Binns (1971) found pumice deposits at a dozen locations on Andøya, northern Vesterålen. Near Nordmjule (west Andøya), Binns (1971) found mainly brown pumice on and buried within the Tapes complex, suggesting reworking of the deposit. Binns (1971) also reports that pale grey/white pumice has been found at several places in the Lofoten-Vesterålen area. As in the Møre and Trøndelag area, these sites are usually at higher altitudes than the pumice associated with the Tapes transgressions. But he did find white/grey pumice, along with brown pumice at an altitude of 5 metres at Bleik on Andøya. Buckland (pers comm., 1998) found brown and black pumice (between 4 to 5 cm in diameter) at an altitude of about 2 meters above sea-level at Ramså on Andøya.

The Troms area (area 9 on Figure 2.5) also has several reports of pumice findings, although Binns (1971), suggests that pumice deposits are not as common as further north in Finnmark (area 10 on Figure 2.5). Black pumice is found on the Tapes shoreline at Lyforden on Kvaløya, west of Tromsø, at an altitude of between 13-14 metres above sea-level (Hald and Vorren, 1983). Pumice has also been found at Ersfjord, to the south-west of Tromsø at an altitude of about 10 metres above sea-level (Møller, pers comm., 1998; Møller, 1995).

Binns (1971) reports many finds of pumice along the coasts of East and West Finnmark (area 10 on Figure 2.5), with more sites in the latter (Marthinussen, 1945). Several sites, including Girsavaguoppe and Revsbotn, to the north and west of Hammerfest have up to 8 levels of pumice (Binns, 1971).

Sweden

Strömstad (area 11 in Figure 2.5) is the only natural site in Sweden where pumice has been found (Bäckström, 1890; Binns, 1971; Undås, 1952). This pumice is brown and was found at two levels, 22.2 metres and 43-45 metres. Pumice also occurs in archaeological sites in south-west Sweden (Binns, 1971). Medieval inland archaeological sites in northern Sweden also have produced pumice pieces, presumably carried in from the north coast of Scandinavia (Binns,1971; Caraplain, pers comm., 1992; area 12 in Figure 2.5).

Denmark

Pumice has been found at three sites in the Vendsyssel area of north Denmark (13 in Figure 2.5; Noe-Nygaard, 1951). All of the pumice was brown and was found at a height of 10-11 metres at Sovkrog and between 7.6-9.1 metres above sea-level at Kandestederne. Noe-Nygaard (1951) also mentions the possibility of scattered pumice finds in the northern part of Jutland.

Summary of Scandinavian pumice distribution

From these results it is clear that pumice is a common feature on the Holocene raised shorelines along the west and northern Norwegian coasts, with only a handful of sites in the south of Norway. Binns (1972a), concludes that there are probably two main primary drifts of pumice that formed the upper brown layer and the lower mainly black pumice level and that the subsequent reworking of the deposits by transgressions produced the multiple layers seen in several places, especially in Finnmark. Unlike the pumice deposits found in Canada, Greenland and Svalbard white pumice is found on some of the older beaches in central Norway and on younger ones further north.

Dating of pumice levels

Binns (1972a; 1972c) dated the two "primary" pumice deposits to ca. 6700 ^{14}C years BP (the upper brown deposit) and ca. 4000 ^{14}C BP (the lower mainly black horizon). This was based largely on the occurrence of the pumice levels on six strandlines labelled Tapes I, II, III, IV, N5 and N4 by Marthinussen (1945; 1960; 1962).

Chronology	Approximate Age ^{14}C BP*	Colour of pumice
Tapes I	7000-6700	brown
Tapes II	6450-6200	brown
Tapes III	5700-5500	brown
Tapes IV	5000-4700	brown
N_5	4400-4300	brown
N_4	4100-3900	black, with some brown

Table 2.3: The dating of pumice levels in Norway from Binns (1971; 1972a). Tapes I and N4 were identified as primary deposits by Binns (1971; 1972a).

As stated above, the use of Marthinussen's chronology must now be reassessed in the light of recent research into Holocene sea-level changes in Norway. Before radiocarbon dating, researchers had to rely on correlating marine terraces, beach ridges and pumice deposits to produce sea-level curves for particular sites (Kaland *et al.*, 1984). Radiocarbon dating of raised beach deposits, however, can also cause problems. Shells can be reworked, for

example Blake (1989) found that a bulk date on shells from a raised shoreline in Svalbard produced an age of 17,700 ±200 ^{14}C years BP, but individual AMS dates on the same shells produced three dates of older than 40,000 ^{14}C years BP and one of 29,865 ^{14}C years BP. Driftwood can also obviously be reworked. In order to get around these problems, isolation basins have largely been used in Norway to produce sea-level curves.

Kjemperud (1981), Kaland (1984) and Svendsen and Mangerud (1987) provide useful summaries of the methods involved in the construction of sea-level curves using isolation basins. For example, at Fonnes, south of Bergen, eight basins are found with thresholds[2] between 2.4 and 9.4 metres (Kaland *et al.*, 1984). With the input of seawater, lithostratigraphical, biostratigraphical and chronological methods can be employed to date the change. Variations in salinity can result in major changes in the colour and structure of sediments within the lake basin. These lithostratigraphic changes are one means of establishing the isolation or connection of a basin to the sea. Aquatic life will also be affected by changes in salinity. Diatom species, for example will change with the transition from a lacustrine to marine environment and vice-versa. Kjemperud (1981) found that diatom zone boundaries are often coincident with lithostratigraphic changes. Sometimes it is possible to identify only two zones (marine/freshwater), but often three zones are present (marine/brackish/freshwater). Although the specific diatoms present in zones varies from lake basin to lake basin certain patterns can be observed. For example, Kjemperud (1981) found that the freshwater zone always begins with a peak in total diatoms and an increase in alkaliphilous taxa and circumneutral types. Other indicators such as aquatic pollen and foraminifera can also be used. Dating of these changes will give the date that the threshold either became lower than sea-level or isolated from the sea. By looking at several different lakes in the same area at different altitudes, sea-level changes during the Holocene can be dated. Lacustrine, rather than marine sediments are often dated, to remove the problems associated with dating marine deposits (the reservoir affect).

These changes are liable to be more gradual during a regression, than a transgression. It was thought that the ingress of seawater was responsible for the erosion of sediment, whilst the transition to brackish and freshwater during a regression was gradual. It is now clear,

---

[2] Thresholds are the elevation of the bedrock through which sea-water can enter and leave the basin. If sea-level reaches the altitude of the threshold, seawater will enter the lake basin. When sea-level drops below the threshold, the salinity of the water in the lake will become brackish and eventually fresh. A bedrock threshold is preferred over one made of unconsolidated material, such as a moraine.

however, that this erosion of sediment was not caused by the Tapes transgression, but by a tsunami, associated with the c. 7000 ^{14}C years BP Storegga Slide event (Bondevik *et al.*, 1997a; Bondevik *et al.*, 1997b; Bondevik *et al.*, 1998).

It is possible to estimate the age of some of the Scandinavian pumice deposits based on recent research. Much of the dating of the raised shorelines has been calculated by using the sea-level change program developed by Møller and Holmeslet (1998). This program consists of a map with isobase lines for the Tapes transgression (dated to around 6000 ^{14}C years BP, as suggested by Bondevik *et al.*, 1998). By clicking on this map a Holocene sea-level curve is drawn for that point, which enables comparison between sites and gives a useful estimate of the age of pumice at each site. Where appropriate direct dating evidence has been used and all of the dates have be considered in the light of the Storegga Slide event and other published research in the area.

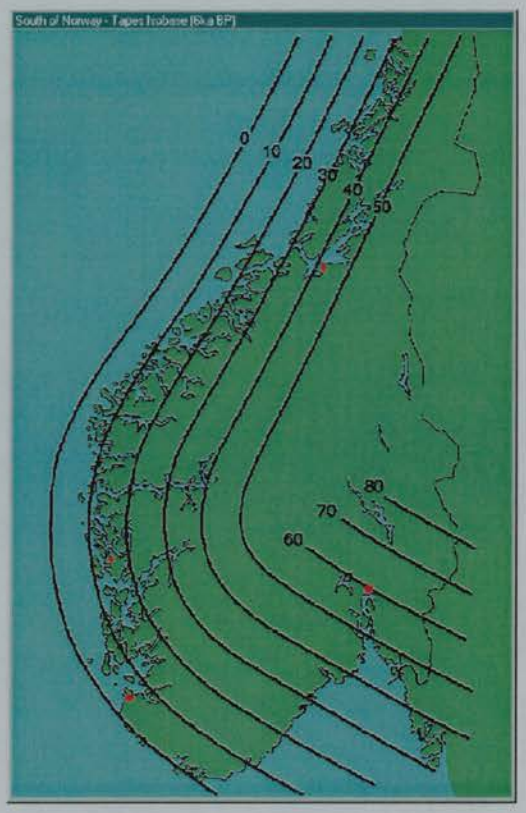

Figure 2.7: Isobase map from Møller and Holmeslet (1998). The isolines on this map show the relative height of sea-level at the time of the maximum Tapes transgression (c. 6000 ^{14}C years BP). At any point on the 10 metre line, for example, relative sea-level was 10 metres higher 6000 years ^{14}C ago compared to the present day.

The ages of the archaeological pumice contexts in southern Norway can be seen in Table 2.4. The table shows that there is a concentration of finds in Mesolithic and Neolithic contexts. Some of the Mesolithic pumice can be dated to between about 8400 and 6500 ^{14}C years BP and there are also deposits dated to 6190-4925 and 5030 ^{14}C years BP. Pumice is also found in Bronze Age and Iron Age contexts.

Site	Location	Context/Age
Lundevågen R17	near Farsund, Vest Agder	Mesolithic (c. 7770 ^{14}C years BP)
Lundevågen R21/22	near Farsund, Vest Agder	Mesolithic (c. 8400-7500 ^{14}C years BP)
Lundevågen R24	near Farsund, Vest Agder	Mesolithic–Neolithic (c. 6190-4625 ^{14}C years BP)
Lundevågen R6	near Farsund, Vest Agder	Mesolithic-Neolithic, Iron Age
Lundevågen R3	near Farsund, Vest Agder	Mesolithic-Neolithic, Iron Age
Lundevågen R3-TN	near Farsund, Vest Agder	Early Neolithic
Lundevågen R18	near Farsund, Vest Agder	Late Mesolithic-Neolithic
Lundevågen R5	near Farsund, Vest Agder	Late Mesolithic
Engøy R3	Vest Agder	Late middle Neolithic
Eg	Vest Agder	Late middle Neolithic
Gjølstad R33	near Oslo, near Akerhus	Late Mesolithic
Auve	Sandefjord, Vestfold	Early to Middle Neolithic
Sluppan	near Kragerø, Telemark	Late Neolithic
Vindenes		Middle to late Mesolithic (c. 8400-6650 ^{14}C years BP)
Austvik III		Early Neolithic (c. 5030 ^{14}C years BP)

Table 2.4: Archaeological sites in southern Norway with pumice artefacts. Information from Østmo (pers comm. 1999), Ballin Smith (pers. comm. 1996; 1999), Ballin (1995).

The sea-level curve produced by Kaland (1984), suggests that the Tapes maximum pumice deposit at Djupedal, Bømlo, should be dated to around 6500 ^{14}C years BP. The sea-level curve produced by Møller and Holmeslet (1998) and the information provided by Bondevik (1998), however, dated the Tapes maximum to about 6000 ^{14}C years BP. The two pumice deposits on Blomøy are dated to around 6000 and 3300 ^{14}C years BP. Virtually all of the upper pumice deposits found in the Møre and Trøndelag (Table 2.2) coincide with the Tapes maximum transgression and so are dated to about 6000 ^{14}C years BP, as are the single horizons at Kalsvik-Gulberget, Myra, Grønsletta, Storsandvika, Linesøy and Mølnbukt. Table 2.2 shows that several sites have multiple pumice horizons and the dates of these deposits varies, probably due to inaccuracies in the sea-level curves. Many of lowermost pumice horizons can be dated to between about 3500 and 3000 ^{14}C years BP. The lower pumice deposits at Kvalvik, and the middle horizon at Kobbvika, Frøya and Småge are dated to between 4000-5000 ^{14}C years BP. There are also some older pumice deposits in the north of this region, with the upper horizons at Hjertåsen, Brettingsfjell and Osen dating between 8000-8500 ^{14}C years BP. The 50 metre pumice reported from Romsdalsfjorden is difficult to

date as the exact location of the find is not known, but its altitude suggest that it must be dated to near 9000 ^{14}C years BP.

The dating of pumice deposits in the Lofoten and Vesterålen islands is mainly based on the research of Møller (1984; 1985; 1986; 1989; 1992) and Vorren (1986). Multiple Tapes transgressions were identified by Marthinussen (1962). Møller (1984), however, only finds a single transgression which peaks at about 6000 ^{14}C years BP, with a smaller transgression at about 4500 ^{14}C years BP which interrupts the general fall in relative sea-level. Using this new data it is possible to date the pumice deposits found in this area. The uppermost pumice deposit found in the area, such as the one found embedded in the Tapes complex on the west coast of Andøya can be dated to between around 6000 ^{14}C years BP. This pumice, however, could have deposited within the beach during the transgression and may be a few hundred years older. It is also possible that some was deposited during the regression and may be slightly younger. The mean age for this deposit is therefore around 6000 ^{14}C years BP, although there may be a large error on this date. The lower pumice deposit found at Bleik on the west coast of Andøya, is probably related to the 4500 ^{14}C years BP transgression. The pumice found at an altitude of about 2 metres at Petvik and Ramså probably dates from about 1700-1800 ^{14}C years BP. This suggests that the pumice deposits in the area can be dated to around 6000 ^{14}C years BP, 4500 ^{14}C years BP and 1700 ^{14}C years BP. Binns (1971) also identified some pumice deposits which were slightly older than the Tapes transgression.

Some of the pumice from the Troms area can also be dated by the recent work of Møller (pers comm., 1998) and Møller, 1995). The two shells from the raised shoreline where the pumice from Ersfjord was found have been dated to 6470±90 ^{14}C years BP (Møller, 1995). The black pumice from Kvaløya is associated with the Tapes maximum, which is again dated to around 6000 ^{14}C years BP (Hald and Vorren, 1983).

This reassessment of the ages of the Norwegian pumice horizons (Table 2.5) has highlighted several differences to those produced by Binns (1971; 1972a; Table 2.3). The oldest pumice horizon appears to date from between c. 8500 and 8000 ^{14}C years BP and pumice of this age is found in the southern Mesolithic archaeological sites and northern Møre and Trøndelag. The single pumice finds from Romsdalsfjorden and Trandvikan are older, however, and probably date from around 9000 ^{14}C years BP. The main upper pumice horizon, dated by Binns (1971; 1972a) to about 6700 ^{14}C years BP, appears to be younger and the upper deposit at many sites is found on ridge formed by the maximum Tapes transgression at about 6000 ^{14}C years BP. Sites in Møre and Trøndelag and Lofoten and Vesterålen also

show evidence of a horizon dated to between about 4000 and 5000 ^{14}C years BP. The youngest horizon at many sites is dated to between about 3000 and 3300 ^{14}C years BP. The youngest pumice is the c. 1700 ^{14}C years pumice found at Ramså and Petvik in Lofoten and Vesterålen.

Location	Age (^{14}C years BP)
Southern archaeological sites	Mesolithic (8400 and 6500) Neolithic Bronze Age Iron Age
Bømlo	c. 6000
Blomøy	c. 6000 c. 3300
Møre and Trøndelag	c. 9000 c. 8000-8500 c. 6000 c. 4000-5000 c. 3000-3300
Lofoten and Vesterålen	c. 6000 c. 4500 c. 1700
Troms area	c. 6500-6000

Table 2.5: The location and age of Norwegian pumice horizons. There is also evidence of older white pumice in the Troms area and several pumice levels in Finnmark, although the precise height of these is not known

The dating of the pumice from Sweden and Denmark is less clear. By extrapolating the isobase lines from Norway, the upper pumice layer at Strömstad (Sweden) dates from between about 7000-6000 ^{14}C years BP, whilst the lower horizon dates from about 4000 ^{14}C years BP. The Danish pumice probably dates from about 4000-3000 ^{14}C years BP.

The dating of raised shorelines only dates the minimum age of the eruption which produced the pumice. These results suggest that the there was at least one eruption in the early Holocene, which produced white/grey pumice, represented by single pumice pieces found at Romsdalsfjorden and Trandvikan on Hitra. This eruption is probably older than 9000 ^{14}C years BP. Some of the Mesolithic archaeological pumice and the 8000-8500 ^{14}C years BP from Møre and Trøndelag were produced by an eruption older than 8000 ^{14}C years BP. The widespread upper pumice horizon at many sites was produced by an eruption older than about 6000 ^{14}C years BP. The maximum altitude reached by the Tapes transgression may contain a concentration of pumice pieces, some of which have been reworked from older deposits. This emphasises the limitations of the dating potential of pumice, it can only ever provide a minimum date for an eruption. Other eruptions older than 4000, 3000 and 1700 ^{14}C years BP produced the younger horizons. It seems highly unlikely that the widespread pumice horizons of the same age can have been produced by reworking of older pumice

deposits. This older pumice if eroded by a storm may form a new younger local deposit, although it is difficult to understand how a new horizon stretching across hundreds of kilometres of coastline could have been produced. Unlike Binns (1971; 1972a), it now seems likely that most of the pumice finds along the coast of Norway were produced by contemporary eruptions and any reworking of material would have localised.

2.2.5 British Isles

Figure 2.8 shows that pumice has been found at sites throughout the British Isles, with a major concentration in Scotland. There are 150 sites where there are documented occurrences of pumice pieces, of which one site is in England, two sites in Ireland, five sites in Northern Ireland, 141 sites in Scotland and one site in Wales. This builds on the earlier work of Binns (1971), who described 80 sites in the British Isles. Due to the large number of sites, the sites identified by the numbers in Figure 2.8 and Figure 2.9 are listed in full in Appendix 1. Details, including location, context of pumice find, ages of deposits and references are presented in Appendix 1. This includes both archaeological and natural sites.

Although Figure 2.8 and Appendix 1 contain 68 more sites than were listed in Binns (1971), it confirms the pattern of the findings of Binns, who found that the vast majority of reported pumice finds in the British Isles have been from archaeological sites, not from natural contexts, as in Norway. Table 2.6 shows that 88% of sites where pumice has been found are archaeological ones, with only 8% being from raised or present day beaches, i.e. natural sites.

	Binns (1971)	%	This study	%
Archaeological sites	68	85.0%	136	90.7%
Natural contexts	12	15.0%	14	9.3%
Total sites	80		150	

Table 2.6: The distribution of sites within the British Isles in archaeological and natural contexts. The Unknown category refers to those sites where the records do not state where the pumice was found.

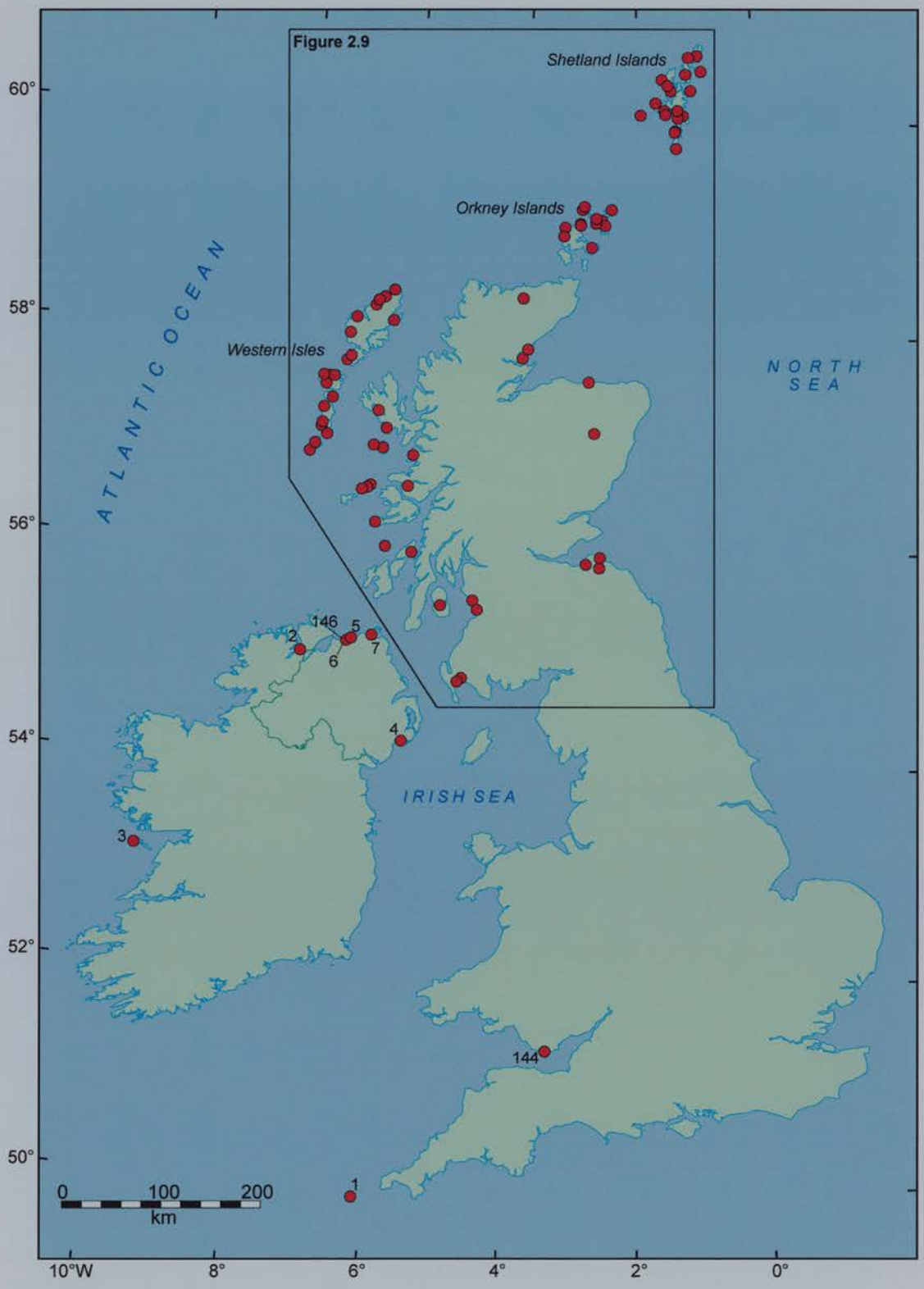

Figure 2.8: Map to show the distribution of pumice finds around the British Isles. Full details about the numbered sites can be found in Appendix 1 and a more detailed map of the Scottish sites is shown in Figure 2.9.

Binns (1971) found only three, late 19th century references to pumice on raised beaches unrelated to any archaeology (Praeger, 1895; Reade, 1896; Smith, 1896). These are on the coasts of Ayrshire (south-east Scotland) and Antrim (Northern Ireland). An extensive search of raised beaches by Binns failed to produce more than a few pieces of pumice at several sites. He attributed this to relatively poorly developed raised beaches in the British Isles compared to Norway and Svalbard. This has been confirmed by this study, and only three new natural sites have been found, although a rationalisation of site classification means that the total number of natural sites is just two more than that found by Binns (1971). In contrast, the number of archaeological sites has exactly doubled.

Binns (1971) found records of a total of 650 pieces of pumice in 80 sites in the British Isles. Searches of post-1971 archaeological literature, information and material kindly donated by archaeologists and details obtained from computerised records at the National Museums of Scotland (QUIXIS Collections Management System) and the Royal Commission of Ancient and Historical Monuments of Scotland's (RCAHMS) CANMORE[3] online database have boosted the number of sites to 150 and the total number of pumice pieces to 2358. The exact number of pumice pieces recovered is not known for several reasons. Firstly, pumice is sometimes confused with other porous material such as industrial or cremation slag, also known as cramp (Newton, 1995, see Chapter 4). Despite this, the vast majority of the hundreds of pieces of pumice supplied by archaeologists have been correctly identified. Secondly, the precise number of pieces of pumice found in archaeological sites is often not stated. Appendix 1, which contains full details about all of the sites in the British Isles where pumice has been found, lists many entries such as *pumice* or *many pieces* or *several pieces*. The National Museum of Scotland also has a large backlog of finds which need to be entered into the QUIXIS Collections Management System (Cowie, pers. comm., 1999). The importance of the reported number of pieces found at a site has to be questioned. Often pumice pieces in archaeological sites are fragments of larger pieces that have either been burnt, broken in use or broken after being discarded. The number of pieces of pumice found at a site, does not therefore, necessarily indicate the amount of pumice which was available to the local population. Table 2.7 shows the distribution of pumice finds from the various parts of the British Isles.

---

[3] The CANMORE database hold records of all of the sites that have been surveyed and recorded by the RCAHMS and is available on the World Wide Web at http://www.rcahms.gov.uk/

	England	Wales	Northern Ireland	Ireland	Scotland	Total
Total Pumice sites	1	1	5	2	141	150
% pumice sites	0.7%	0.7%	3.3%	1.3%	94.0%	100%
Archaeological Sites	1	0	3	1	131	136
Natural Sites	0	1	2	1	10	14
Pumice pieces*	1	2	3	179	2173	2358
% of pumice pieces*	0. 04%	0.08%	0.13%	7.59%	92.15%	100%

Table 2.7: The distribution of pumice sites and types of site in the British Isles. *The number of pumice pieces found is dependant on the reporting of the number of pieces of pumice being reported in the literature (see above), hence there are less reported pumice pieces than sites in Northern Ireland.

England and Wales

Only two sites in southern Britain have produced pumice finds. The only reported site in the England where pumice has been found is in the Isles of Scilly (Figure 2.8; Scott, 1932; Hencken, 1932; Binns, 1971). One piece of small brown pumice was found in a Bronze Age Passage Grave[4] (Appendix 1). Since the work of Binns (1971), there appear to have been no more finds of pumice either in archaeological or natural sites in England. There appear to have been no reports of pumice finds in Wales, apart from two pieces of grey pumice found on a storm beach on the small island of Sully off the south coast of Wales by Binns (1971).

The lack of pumice finds in England and Wales is in sharp contrast to the large number of sites in Scotland (Table 2.6). Southern Britain has been dominated by subsidence during the Holocene, with the current hinge line between areas of uplift in the north and the subsiding south running through north Wales, Lancashire and Yorkshire (Shennan, 1989). In a review of over 400 sea-level index points, Shennan (1989) was able to show that during the last 8000 ^{14}C years BP the south-east England, East Anglia, the Bristol Channel and Cardigan Bay have all been affected by subsidence. There are no raised shorelines in these areas. Pumice is unlikely to be found here, except on archaeological sites, or on modern beaches. If pumice was washed ashore in the past, it is likely that the inhabitants of England and Wales would have used it, as they did in Scotland. Although not an important tool, pumice could have proved a useful addition to their collection of tools. There is however, no evidence that this was the case, as pumice does not occur in coastal archaeological sites in England and

[4] A passage grave is a type of chambered cairn which forms a round structure covering a burial chamber with a narrow entrance passage (Bray and Trump, 1982).

Wales, with the exception of a single site in the Isles of Scilly. From this it can be concluded that pumice was not washed upon the shores of England or Wales in any great quantities.

Ireland and Northern Ireland

Pumice is not common on the island of Ireland either, and has only been found at seven sites (Figure 2.8). Pumice has been found at four sites in Northern Ireland, along the north coast and in the east at Dundrum Bay (Site 4; Figure 2.8). These sites were first summarised by Binns (1971) and since then no more reports of pumice finds have come to light. The earliest finds were published by Smith (1896) who found many pieces of pumice on at least two raised beaches at the mouth of the River Bann. Binns (1971) estimated the ages of these beaches to be ca. 5600 ^{14}C years BP and between 4100-2400 ^{14}C years BP, although the work of Carter (1982) suggests that a date of around 6500 ^{14}C years is more likely. Pumice also occurs rarely in Early Bronze Age Sandhill sites on raised beaches along the north and east coasts of Northern Ireland (Binns, 1971; Cleland and Evans, 1942; Knowles, 1889; May, 1948). These sites are probably on the 6500 ^{14}C years BP raised shoreline, the date of the occupation of the sites is about 3450 ^{14}C years BP. Fieldwork in Northern Ireland in 1990 failed to find any pumice along the Antrim coast or Dundrum Bay

There are only two sites in Ireland where pumice finds have been reported (Figure 2.8). Pumice was found on a raised shoreline at Portstewart, Innshowen in Donegal, by Praeger (1895) and Binns dates this to between 5700-5500 ^{14}C years BP (Binns, 1971). Again the evidence of Carter (1982), means that this date should probably be pushed back to around 6400 ^{14}C years BP.

The other site is on the Aran Islands off the coast of Galway, where 179 pieces of pumice were found at the archaeological site Dún Aonghasa, on the island of Inis Mór (Clarke and Newton, in press). Dún Aonghasa is the largest of seven large stone forts found on the Aran Islands and one of four on Inis Mór (Cotter, 1993). All of the pumice pieces are brown and generally have small vesicles and many show evidence of having been worked, with grooves (Clarke and Newton, in press). The pumice is found in Late Bronze Age deposits, which are dated to between approximately 2900-2600 ^{14}C years BP. No finds of pumice have been reported from any other archaeological sites in the area and for this reason Clarke and Newton (in press) suggest that the pumice was a local deposit and not imported. Pumice from this site is dealt with in more detail in Chapter 4.

The relative scarcity of pumice in Ireland could be for three reasons. Firstly, it is there, but has not been found. This seems unlikely, since if it had been used by people in the past in any quantities, evidence would have shown up at archaeological sites. The second possible reason is that Ireland, as much of England and Wales, has generally been subsiding during the Holocene and there were few raised beaches on which pumice could have been preserved, although this generalisation hides a complex picture of localised changes (Carter *et al.*, 1989). Holocene sea-level changes in the south of Ireland, generally show a decelerating rise over the last 8000 years (Carter *et al.*, 1989), with present-day levels existing for the last 4000 years. Those in the north are more complex with significant east-west variations. For example, there appears to have been a transgression, with a peak about 6500 ^{14}C BP in Northern Ireland (Carter, 1982). This peak was only about 2 metres above present sea-level. Farther to the west in Donegal, there is no evidence for a transgression and Shaw and Carter (1994) suggest that this was because mid-Holocene sea-levels peaked below present day sea-level. This picture of sea-level change means pumice deposits are unlikely to have formed and if so, they are now buried. The third reason why pumice is rare in Ireland could be that ocean currents carrying the pumice did not generally encounter the Irish coast. This is dealt with in more detail in section 2.3.3. It is important to note that shore processes in Ireland can operate up to 15 metres above mean sea-level (Carter *et al.*, 1989). This means that it is highly probable that there is considerable reworking of material, including any pumice deposits. Although ages are estimated for the following finds of pumice in natural locations, the possible reworking of such deposits should be borne in mind.

Scotland

Figure 2.8 and Table 2.7 show that the vast majority of pumice finds in the British Isles are in Scotland, with particular concentrations in the Western Isles, Orkney and Shetland. The map of Scotland presented in Figure 2.9 shows the distribution of sites in Scotland in more detail. For this reason the description of the distribution of pumice in Scotland has been divided into five sections each describing the regions shown in Table 2.8. Full details about the pumice finds, their age and publications can be found in Appendix 1. The description of sites in the five regions below only includes details of selected sites.

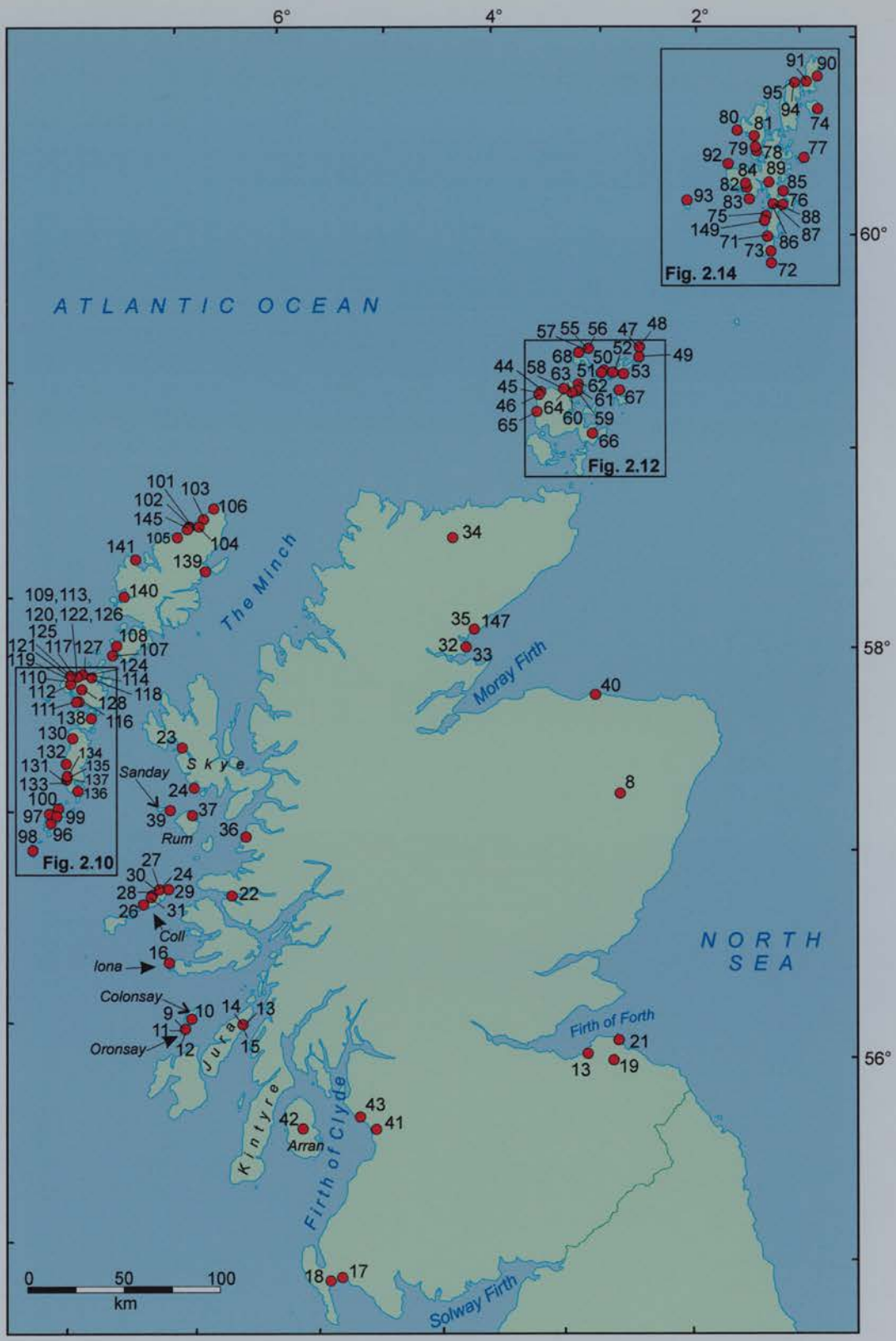

Figure 2.9: Map to show the distribution of pumice sites around Scotland. The numbered sites refer to the list of sites in Appendix 1 and the boxes to detailed maps of the southern Western Isles (Figure 2.10), Orkney (Figure 2.12) and Shetland (Figure 2.14).

	Scotland	Western Isles	Orkney	Shetland	Inner Islands	Mainland Scotland
Total Pumice sites	141*	47	27	26	22	17
% pumice sites	100%	33.3%	19.1%	18.4%	15.6%	12.1%
Archaeological Sites	131	46	26	25	22	10
Natural Sites	9	1	1	1	0	7
Pumice pieces	2173	783	634	267	155	32
% of pumice pieces	100%%	36.0%	29.2%	26.1%	7.1%	1.5%

Table 2.8: The distribution of pumice sites in Scotland. The percentage figures refer to the % of pumice in Scotland. *The location of two sites is unknown.

Table 2.9 shows the archaeological ages and the calibrated (BC/AD) and uncalibrated (^{14}C years BP) ages which will be used in this thesis. These divisions are based on technological changes and the boundaries are, therefore, blurred and the dates can only ever be approximate. The dates used for the archaeological sites are often from unrelated literature which only give an estimate of the age of the site. Where possible, however, direct ^{14}C dates of related deposits is given, but there are many sites which are just culturally dated for example as being Neolithic or Bronze Age.

Archaeological Age	BC/AD Calibrated Age	^{14}C years BP
Mesolithic	older than c. 4000 BC	older than c. 5200 BP
Neolithic	c. 4000 – 2500 BC	c. 5200 – 4000 BP
Bronze Age	c. 2500 – 700 BC	c. 4000 – 2500 BP
Iron Age	c. 700 BC – 900 AD	c. 2500 – 1200 BP
Early Christian	c. late 6th Century -	younger than c.1500 BP
Norse	c. 800 AD – 1400 AD	-
Medieval	- c. 1500 AD	-
Modern (post-medieval)	younger than 1500 AD	-

Table 2.9: British archaeological ages and their calibrated calendar dates and uncalibrated radiocarbon dates (the pre-Medieval dates are based on dates suggested in Edwards and Ralston, 1997). The Norse period is of varying duration in different parts of Scotland. The Medieval period can encompass both Early Christian and Norse Periods.

Western Isles

47 sites, comprising 33% of the sites in the British Isles, are found in the Western Isles (Table 2.8; Figure 2.10). Of these, nearly half (21) are found in North Uist and all but one are archaeological sites. Roisinish, on Benbecula (site 138), is an unstratified site, although it is probably also associated with archaeology.

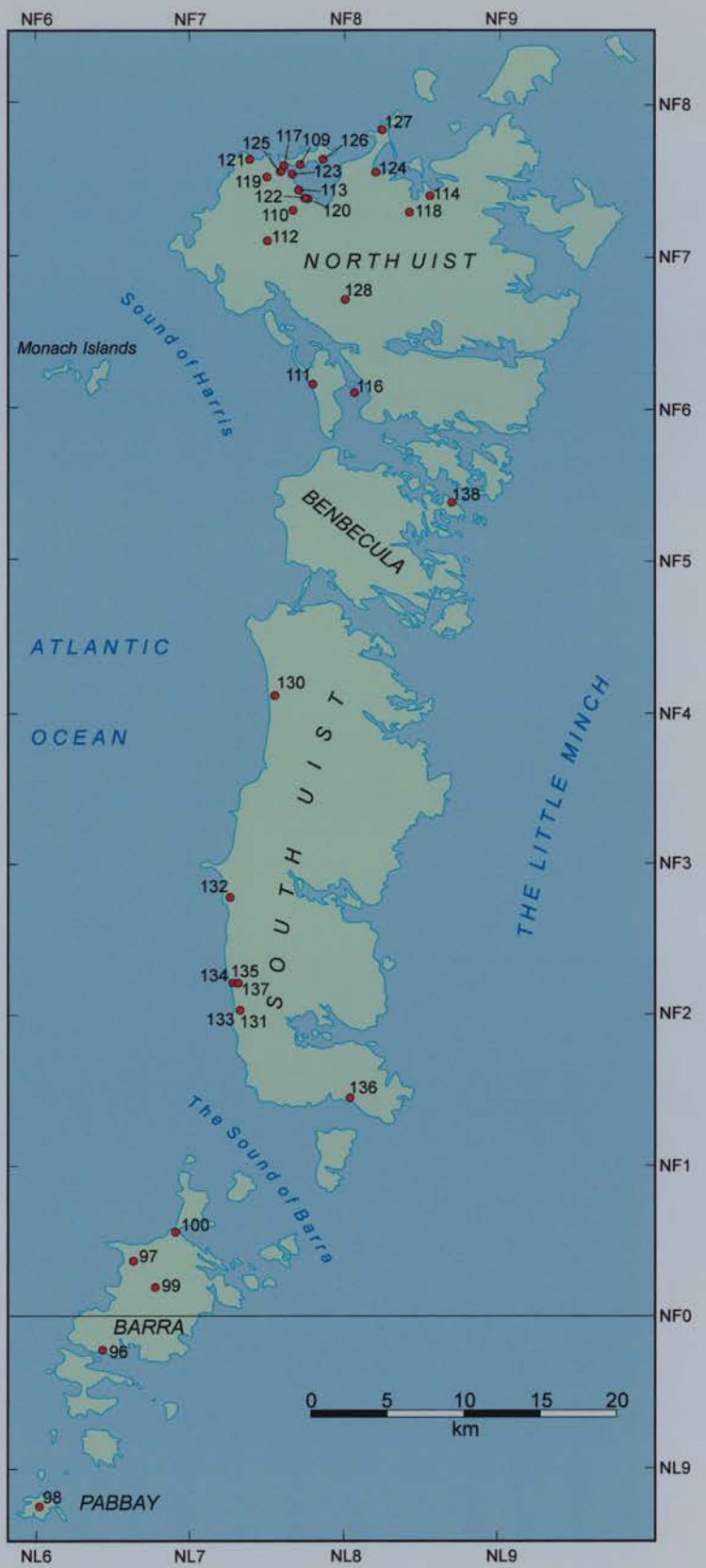

Figure 2.10: Map to show the distribution of pumice sites in the southern Western Isles. Site numbers refer to the site list in Appendix 1. The coordinates are Ordnance Survey grid references.

The cluster of 14 sites along the north coast of North Uist is particularly interesting. Of these 14 sites, 10 are Iron Age or early Christian (2500 - 950 ^{14}C years BP), two are Neolithic (5200-4100 ^{14}C years BP) and one, The Udal (site 127), is a multi-occupation site, with 138 pumice pieces found in all levels from the pre-Neolithic (older than 4500 ^{14}C years BP) to modern (Newton, Forthcoming-a). Eilean Domhnuill (site 119), a Neolithic site, produced 119 pieces of black pumice, of which just over 50% show evidence of having been worked (Smith, Forthcoming-c). 50 pumice pieces have been found at Caerdach Rudh on Baleshare in Bronze Age to Iron Age contexts (c. 3400 to 2050 14C years BP; Newton and Dugmore, Forthcoming). Where details about colour are available, most of the pumice found in North Uist is brown (see above) and many pieces show signs of having been worked (Appendix 1). Pumice from the archaeological sites at Udal and Caerdach Rudh are dealt with in greater detail in Chapter 4.

A further eight pumice sites are found on South Uist, with a concentration on the south-western coast. Details on the type of pumice found at several of these sites is not available and indeed details about the age and type of the some of the archaeological sites is vague. Cill Donain III (site 132), is a mainly late Iron Age midden, but there are also Bronze Age artefacts from this site (Gilbertson *et al.*, 1999). The site produced 41 pumice pieces, which were mainly brown with some black and light brown pieces, some of the pumice pieces have been smoothed. Drimore A'Cheardach Mhor (Drimore, site 130 on Figure 2.10) is an Iron Age wheelhouse[5] (c. 2200-1800 ^{14}C years BP) and 28 pieces of pumice have been found, several of which show evidence of having been worked (Young and Richardson, 1960). A single piece of pumice was recovered from Cille Pheadair (Kilpheder, site 133), an Iron Age wheelhouse. Further details on the geochemistry of pumice from Cill Donain and Cille Pheadair are presented in Chapter 4.

To the south of South Uist are found several islands, including Barra and Pabbay, where 5 sites have pumice finds. The largest number of pieces were recovered from Allt Chrisal (Tangaval, site 96 on Figure 2.10), Barra, another multi-occupation site. Brown pumice was found in contexts older than 4470 ± 60 ^{14}C years BP right through to 18th and 19th Century

[5] Wheelhouses are late Iron Age circular houses with partition walls resembling the spokes of a wheel and most date from the late first millennium to about the second century AD (Armit, 1996).

AD levels, although most of the pumice is found in Neolithic and Beaker[6] contexts (Branigan *et al.*, 1995; Newton and Dugmore, 1995). Under half of the pumice showed traces of wear. In contrast to Allt Chrisal, the other sites on Barra, a Bronze Age hearth (Vaslain, site 100); Dùn Cuier (site 97) which was originally thought to be an early Christian 4-7th Century dun[7] (Young, 1956), but reinterpreted as a multi-period site from the first millennium BC to pre-Norse roundhouse (Armit, 1988); and an Iron Age longhouse (Tigh Talamhanta, site 99) have only produced a few pumice pieces.

There are ten archaeological sites in Lewis where pumice has been found (Figure 2.9; Table 2.6). These are all Bronze Age or younger, with the youngest being a Norse site (Barvas Machair 2, site 102) which dates from about 11th-12th centuries AD (Cowie, unpublished), although the age of three sites is not known. Most pieces, 36, were found at a Late Bronze Age/Early Iron Age (ca. 3000-2500 ^{14}C years BP) site called Barvas Machair 2 (site 101, Cowie, unpublished). Three pieces of pumice from the late Iron Age wheelhouse site (c. 2000-1850 ^{14}C years BP) at Cnip, Lewis (site 141) are dealt with in more detail in Chapter 4. The "island" of Harris, to the south of Lewis, has one site at Northton (site 108), where 180 pieces of mainly brown pumice were found in Neolithic, Beaker and Iron Age middens (Binns, 1971; Simpson, 1976). Pumice has also been found in a beaker midden on the nearby island of Ensay (site 107).

Pumice occurs mainly along the western coasts of the Western Isles (Figure 2.9) and is found in archaeological sites from the Neolithic to modern times (younger than 5200 ^{14}C years BP). Much of the Atlantic coast of the Western Isles is calcareous sand dunes and meadows which form the fertile *machair* (Owen *et al.*, 1996). This important habitat began forming as early as 7900 ^{14}C years BP (Gilbertson *et al.*, 1999). The machair has supported agriculture for some 5000 years and have ensured that the Western Isles have a long history of human settlement. This may help explain the concentration of pumice sites on the west coast. Whilst the pumice would appear more likely to be washed ashore on the west coast, the concentration of archaeological sites in this area would also favour the finding of more pumice in numerous archaeological sites. This coastline is, however, under threat from

---

[6] Beaker culture is identified in the early the Bronze Age, about 2000 BC (3650 ^{14}C years BP) with the appearance of "fine, fairly small drinking cups profusely decorated with a series of recurring motifs ... {which} ... were often placed with the dead ..." (Armit, 1996).

[7] Duns are fortified dwellings found in western Scotland and Ireland and dating from the late Iron Age to Medieval times (Bray and Trump, 1982).

overgrazing, rabbits, new farming techniques and coastal erosion (Gilbertson *et al.*, 1996; Owen *et al.*, 1996). This not only leads to the destruction of archaeological sites, but could erode pumice, for example from middens. This is already happening at Caerdach Rudh.

Figure 2.11 shows that the highest concentration of finds has been in Iron Age contexts. Of all the dated finds, the Bronze Age and Early Christian periods have the highest concentrations of pumice finds, although the large number of finds with an unknown age (11) account for the second highest proportion of finds. No settlements dating from the later second millennium and first half of the first millennium BC (c. 3000-2500 ^{14}C years BP) have been found in the Western Isles, although there is some evidence of human occupation (Armit, 1996). The problems of dating archaeological sites, the lack of sealed contexts and the arbitrary nature of the periods means that Figure 2.11 and similar subsequent histograms in this chapter should only be regarded as rough but useful guides. The relatively large number of undated pumice finds only emphasises this fact. The pumice found at archaeological sites in the Western Isles is mainly brown with some black pieces. Although pumice has been found at many sites, only a few Western Isles domestic sites have so far been archaeologically excavated and published, only six by 1995 (Foster, 1995). Pumice has been found at all of these sites and it seems likely that more pumice finds will be made as more sites are investigated.

Finlayson and Edwards (1997) state that it is possible that records of fire on the Western Isles indicate human impact during the Mesolithic (Edwards *et al.*, 1995), but there are no artefactual records to confirm this. It has been suggested that any evidence has been buried beneath coastal deposits of peat and sand as Holocene sea-levels rose (Edwards, 1996). For example, it is estimated that the rise in relative Holocene sea-levels in the southern part of the Western Isles, means that any Mesolithic coastal settlements on the island of Barra would now be located 3 km out to sea (Foster, 1995).

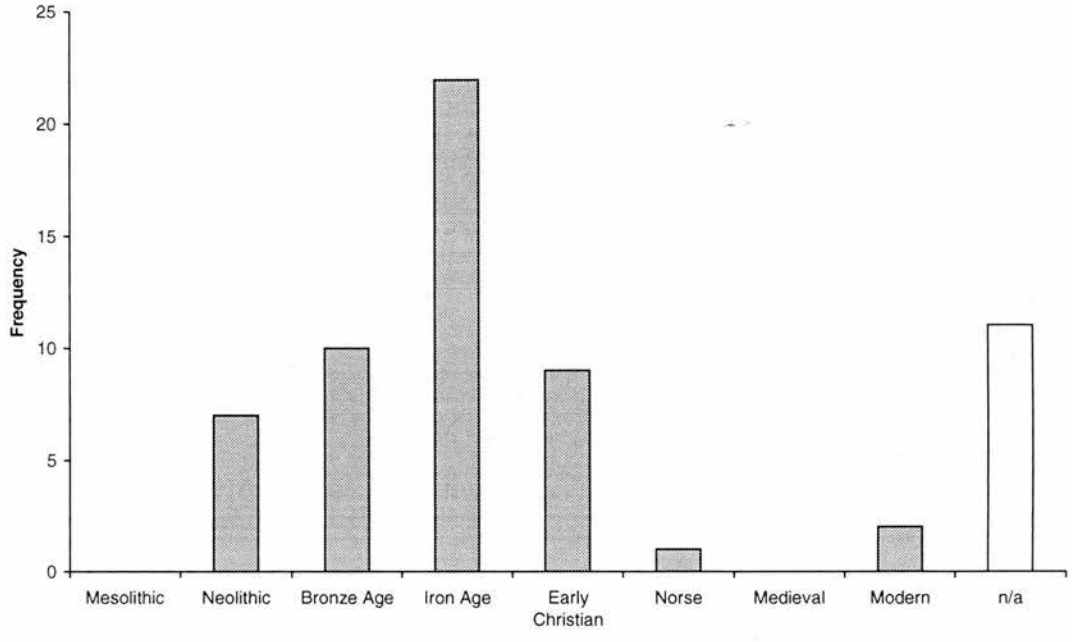

Figure 2.11: The age of pumice finds in archaeological sites in the Western Isles. In this and the graphs which follow where pumice was found in a context of more than one age at a site, each age is given a value. Similarly, if a context spans two or more ages, e.g. Iron Age/E. Christian, a value is given to each class.

Orkney

The Orkney Islands have the second highest concentration of both sites (27 sites) and recorded pumice pieces (634 pieces) in the British Isles after the Western Isles (Table 2.8). These finds are concentrated in the northern islands and the north of Mainland (Figure 2.12). Five archaeological sites with pumice finds are found on Mainland. These are all concentrated on the western coast, with the exception of a piece found in a burnt mound at Hawell (site 66). The oldest site on Mainland where pumice occurs is the famous Neolithic village of Skara Brae (site 65), where over 70 pieces of pumice have been found. The remaining three sites are Early Christian to Norse in age (sites 44, 45, 46). The most interesting find was made by Cursiter (1886), when he found a piece of pumice in an early Christian age (post 6th Century) leather worker's tool box buried in a peat bog (site 46) and now on display in the National Museum of Scotland.

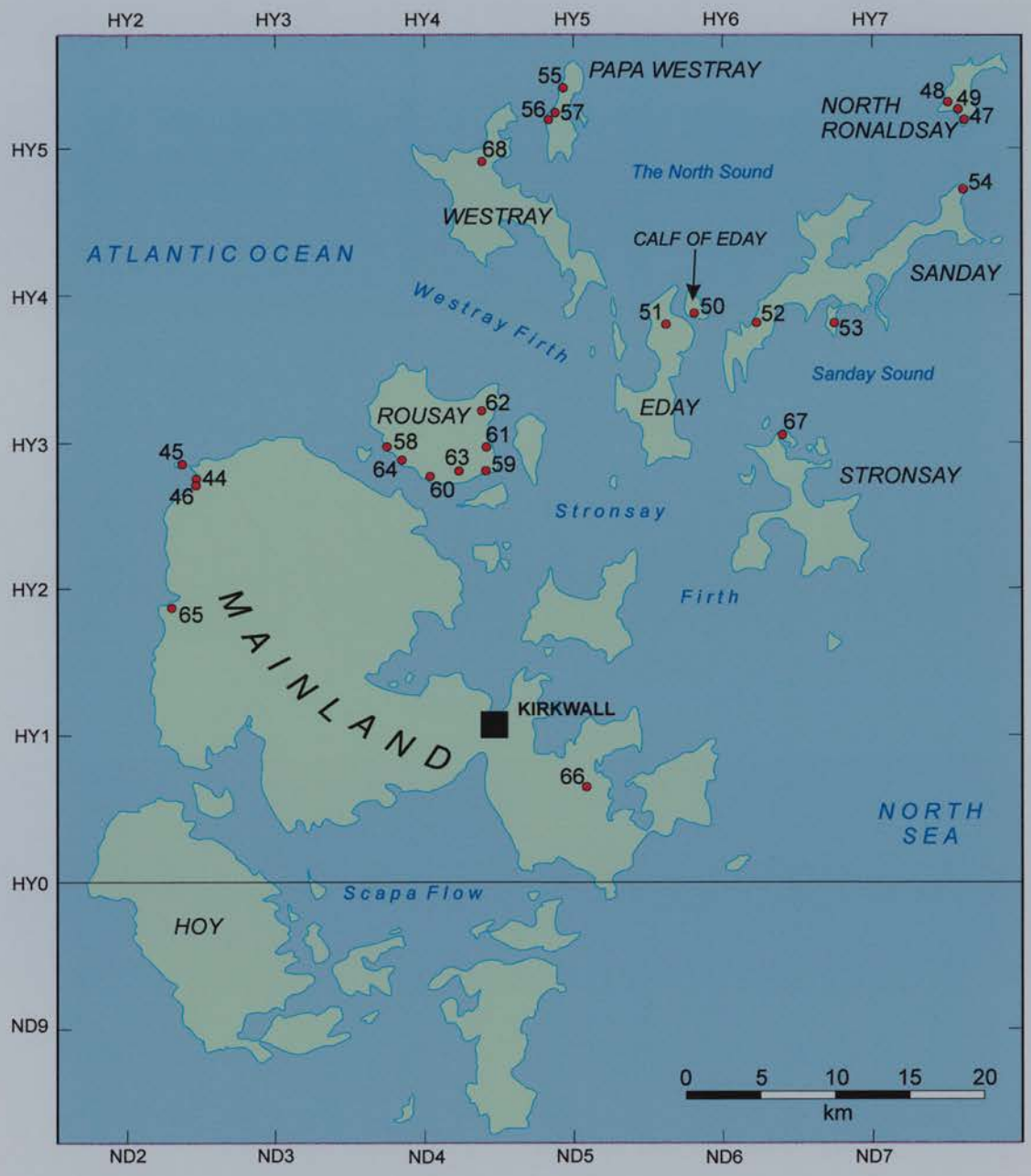

Figure 2.12: Map to show the distribution of pumice sites in the Orkney Islands. Site numbers refer to the site list in Appendix 1. The coordinates are Ordnance Survey grid references.

Seven pumice sites occur around the southern and eastern coast of the island of Rousay, just to the north of Mainland. The site at the Bay of Moaness (site 58) is the only site in Orkney, and indeed in one of the few in the British Isles, where pumice has been found in a well-stratified completely natural setting (Buckland *et al.*, 1998). The 14 pumice pieces were found in two pits dug into inter-tidal deposits at –0.6 metres OD. Although work on this site is still being carried out, it is estimated that this pumice dates from before 5000 ^{14}C years BP (Buckland *et al.*, 1998). The archaeological sites on Rousay with pumice finds include two unstratified sites (sites 59 and 61, Appendix 1); a late Neolithic (c. 4100 ^{14}C years BP) site at Rinyo, where many pieces of worked pumice have been found (site 62; Childe and Grant, 1939; Childe and Grant, 1948); and an Iron Age souterrain[8] (site 60; Grant, 1939). Pumice from the Bay of Moaness is dealt with in more detail in Chapter 3.

35 pieces of pumice were found in an Iron Age (2450-1870 ^{14}C years BP) potter's workshop (site 50) on the Calf of Eday (Calder, 1937; Calder, 1939). Pumice has also been found at a Neolithic chambered cairn at Huntersquoy (site 51) on Eday. Seven pieces of pumice have been found in a late-Neolithic site on the island of Westray (site 68; Appendix 1; Sharples, 1984). Three archaeological sites on the small island of Papa Westray, to the north-east of Westray (Figure 2.12) have pumice finds. The Iron Age broch[9] at St Boniface (site 57) produced 22 pieces of pumice, of which one third are grooved (Clarke, 1991). Two pieces of brown and one black pumice were found at Howe (site 49), a Late-Bronze to Iron Age house (c. 2700-1800 14C years BP; Traill and Kirkness, 1937) and 13 pieces turned up at an undated site at the Knap of Hower (site 56).

---

[8] Souterrains are underground stone-built passages, which were probably used to store food (Bray and Trump, 1982).

[9] Brochs are fortified circular stone towers which can be up to 20 metres in diameter (Bray and Trump, 1982).

Just under half of all of the pumice pieces recorded in Orkney (256 pieces) were found at Tofts Ness on Sanday (site 54). These pumice pieces were found throughout the archaeological levels in the site. Evidence of wear was found on only 57 of these pieces (Smith, Forthcoming-b). Another large find of pumice was made at Pool (site 52), where 164 pieces were found in late Neolithic, Iron Age and Norse contexts (Smith, Forthcoming-a).

Two Iron Age sites, the Broch of Burrian (site 47) and Howmae (site 49), on North Ronaldsay (Callander, 1931; Traill, 1890a; Traill, 1890b) produced seven and nine pieces of pumice respectively. Pumice from the later site is recorded as being dark brown.

Pumice has not been found on the southern islands of Orkney and is relatively rare on Mainland. Unlike the Western Isles, there is not an obvious pattern of distribution of pumice sites on the western coasts of the islands. Figure 2.14 shows that of the dated pumice finds, an equal number occur in the Neolithic and Iron Age periods. As in the Western Isles, however, a significant number of the pumice finds are undated. Although Mesolithic artefacts have been found on Orkney (Finlayson and Edwards, 1997), no pumice has been found associated with them.

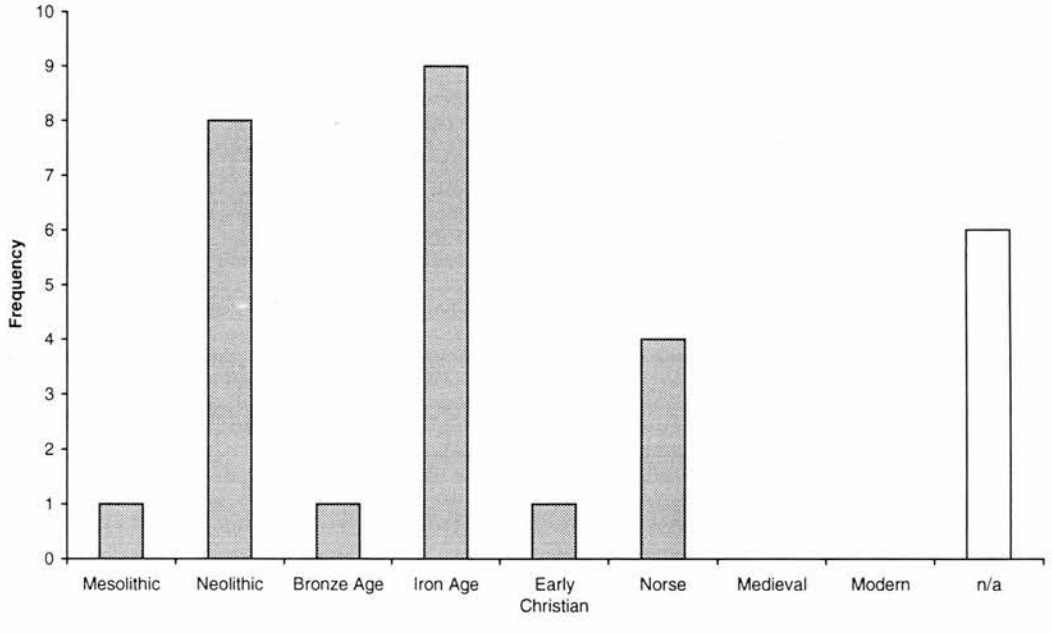

Figure 2.13: The age of pumice finds in archaeological sites in the Orkney Islands. The single Mesolithic pumice refers to the pumice pieces found in the inter-tidal deposits at the Bay of Moaness (site 58).

Shetland

Pumice has been found on archaeological sites on most of the large islands of Shetland, with 16 of the 26 sites found on Mainland, the largest island (Figure 2.14). The southernmost pumice find is at the famous site at Jarlshof on Mainland, a multi-occupation site, where mainly brown pumice has been found in Neolithic, Iron Age and Norse contexts (Curle, 1933; Curle, 1935; Curle, 1936a; Hamilton, 1956). The other two sites in southern Mainland with pumice finds are a Bronze Age house (site 73) and an Iron Age midden (site 71), with several pieces being found at each. There is a cluster of sites around the East Voe of Scalloway (sites 86, 87 and 88). An Iron Age broch at Scalloway (site 88) produced the largest number of pumice pieces from any archaeological site in the British Isles. 347 pieces were found at the site, which are dated to between 2030 ± 40 and 1330 ± 70 ^{14}C BP (Sharples, 1998). Pumice from this site is mainly brown, although there are also black and greyish pieces. A nearby site at Scalloway (site 87) has produced a couple of pieces of black pumice and a white piece from a Norse site (Dugmore and Newton, unpublished; Biglow, pers. comm.). North of Lerwick is the archaeological site of Kebister (site 85), where 60 pieces of pumice have been found (Clarke, 1999). The earliest pumice was found in Bronze Age contexts, but all except four pieces were found in Iron Age to post-medieval contexts and two thirds of the pumice show evidence of wear. Many pieces of mainly brown pumice were also found at the Iron Age broch, Clickhimin (site 76) in Lerwick (Hamilton, 1968). All of the other sites in Mainland have only produced a few pieces of pumice each (Appendix 1). These sites range in age from Neolithic chambered cairns, e.g. Stanydale (site 84), to Iron Age brochs, e.g. Sae Breck (site 80). Pumice from Upper Scalloway, Scalloway and Kebister will be dealt with in more detail in Chapter 4.

A single perforated piece of pumice has been found on the island of Foula, to the west of Mainland (Figure 2.14). An excavation at a medieval/Norse to modern site at Biggings on the island of Papa Stour (Figure 2.14) produced 21 pieces of pumice Ballin Smith (1999). The results of the excavations are presented in Crawford and Ballin Smith (1999). Most of this pumice is found in contexts ranging in age from the pre-11th to 19th centuries AD, as well as some pumice being in unstratified deposits. 15 of the pumice pieces are brown and resemble the brown pumice found elsewhere in Scotland, but six pieces are white/grey, with a low density (Newton, 1999). The oldest white pumice is found in contexts dated to the 13th Century, whilst the youngest is found in 19th Century contexts. Pumice from Papa Stour is studied in detail in Chapter 4.

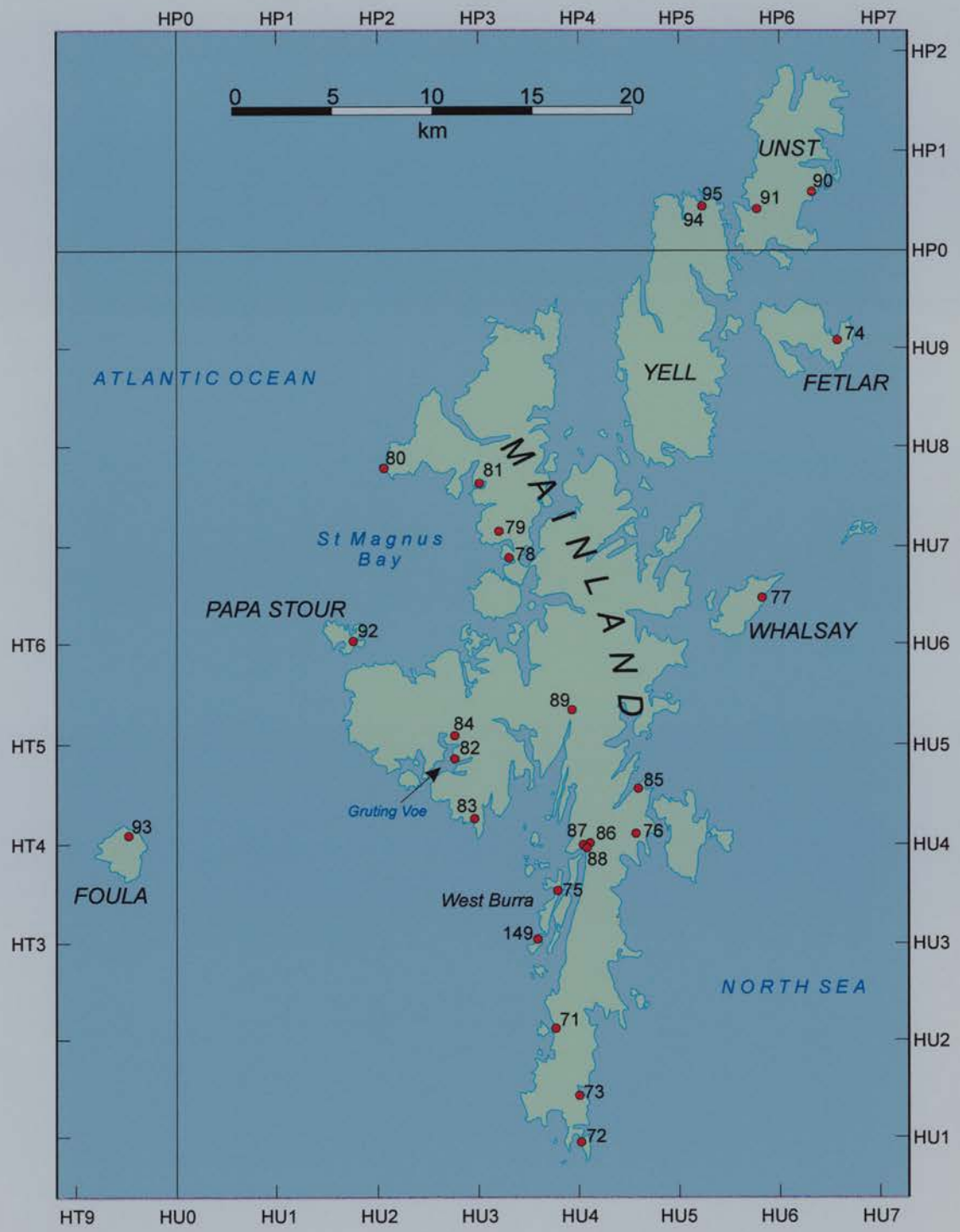

Figure 2.14: Map to show the distribution of pumice sites in the Shetland Islands. Site numbers refer to the site list in Appendix 1. The coordinates are Ordnance Survey grid references.

Dark brown pumice has been found at the Bennie Hoose, on the eastern island of Whalsay (site 77), at a site which dates between the late Neolithic and Iron Age (Calder, 1961; Henshall, 1961). The Breckon area of the island of Yell, to the north-east of Mainland, has produced over 95 pieces of pumice from archaeological sites eroding out of the sand dunes. A survey by Carter and Fraser (1996) revealed 75 small pumice pieces from unstratified deposits (site 95). Buckland (pers. comm., 1993) found 19 pieces of brown pumice and one white pieces, which resembles the white pumice at Scalloway and Papa Stour. Pumice from Breckon is dealt with in more detail in Chapter 4. Clugan (site 91), one of two sites on the island of Unst, contained many pieces of black pumice in Iron Age and Norse contexts (Small, 1967).

A single piece of dark grey angular pumice of non-archaeological pumice has been recovered from inter-tidal peat deposits from Clettnadal, West Burra (site 149). This pumice has been radiocarbon dated to 9170±45 ^{14}C years BP (Buckland and Hall, pers. comm.). This is the oldest recorded piece of pumice recovered from any site in the British Isles.

All, except three of the archaeological sites on Mainland where pumice has been found are situated on the west coast. This pattern is not, however, followed by the archaeological sites on the other islands (Figure 2.14). Most of the pumice found is brown, although some sites also have black and uniquely in Scotland white pumice. Of the dated pumice finds, most have been found in Iron Age contexts, with the Neolithic and Bronze Ages periods producing the next most numerous finds (Figure 2.15). There are, however, as many undated finds as there are Neolithic ones. As in the Western Isles, although there is no artefactual evidence of human occupation of the Shetland Islands, the palaeoenvironmental record contains evidence of possible human induced fires and of grazing by animals which may have been transported to the islands by people (Bennett *et al.*, 1992; Edwards, 1996; Finlayson and Edwards, 1997).

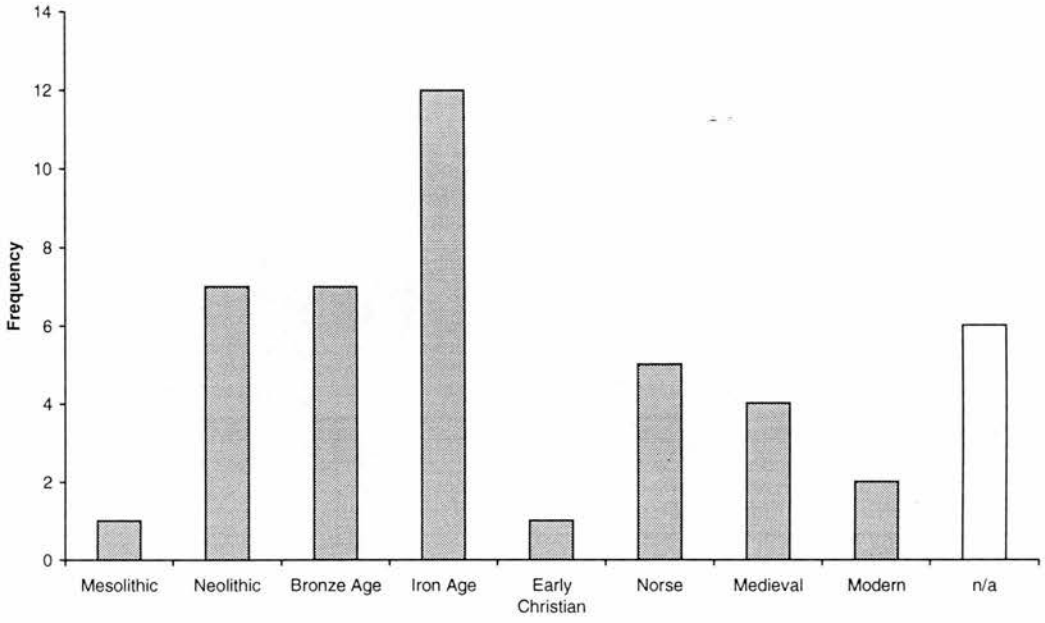

Figure 2.15: The age of pumice finds in archaeological sites in the Shetland Islands. The single Mesolithic count refers to the pumice found in the inter-tidal peat deposits at Clettnadal.

Inner Islands

The term the *Inner Islands* is used here to describe the islands off the west coast of Scotland but does not include the Western Isles. This separates these islands from the sites on the Scottish mainland and those on the Western Isles. The more common term *Inner Hebrides* was not used, as islands such as Arran do not belong to this group. A total of 22 sites with pumice finds have been found on ten islands, Arran, Canna, Coll, Colonsay, Iona, Jura, Oronsay, Rum, Skye and Tiree (Figure 2.9).

Only a single piece of worked pumice has been found on the southernmost island, Arran (Appendix 1). Several pieces of pumice have been found on the Lussa River area, on the east coast of Jura (Figure 2.9; Appendix 1). These include pumice from a Mesolithic context, where a dark grey piece is dated to around 7414±80 ^{14}C years BP (Mercer, 1972) and a younger early Neolithic site (4700-4400 ^{14}C years BP), where a single piece of dark brown pumice was found (Mercer, 1970). Binns (1971) also reports another 24 pieces of pumice, although it is not clear exactly where these were found. To the west of Jura, the island of Colonsay has yielded more pumice from a Mesolithic site where 23 pieces of pumice were found at Staosnaig (site 10) in a pit radiocarbon dated to between 7900-7000 ^{14}C years BP. There are two distinct types, a light brown and a black denser variety

(Newton, Forthcoming-b). Pumice from Staosnaig is dealt with in more detail in Chapter 4. The island of Oronsay, to the south-east of Colonsay has produced pumice from three sites, one of which Cnoc Sligeach (site 9) has been dated to 5426±159 ^{14}C years BP (Mellars, 1987). The exact location of the other two is unfortunately not known, but they probably date from the same period.

Recent research on Coll has found 105 pumice pieces at seven sandhills sites around the coast of the island (Crawford, 1997). Unfortunately, the finds are from eroding surface deposits and most of the material has been reworked and mixed. For example, the site at Sorisdale (site 29) contains 65 pumice pieces amongst a mixture of Mesolithic, Late Neolithic and Bronze Age artefacts (Crawford, 1997). It seems that pumice from these seven sites ranges in age from Mesolithic to Norse. Eleven pieces of pumice were recovered from Kinloch Farm, a Mesolithic archaeological site on the island of Rum (site 36). Two types of pumice were recovered from contexts dating from the Mesolithic (grey pumice) to the Neolithic (brown pumice) (Clarke and Dugmore, 1990). The earliest pumice was found in deposits dated to 8590 ± 50 ^{14}C years BP, whilst the youngest was recovered from material dated to 3890 ± 65 ^{14}C years BP. Pumice from Kinloch is dealt with in more detail in Chapter 4. The three sites on Skye which have produced pumice finds are a cave containing Beaker-late Neolithic artefacts and two pieces of pumice and two late Iron Age brochs where at least four pieces of pumice have been found (Sites 23, 24, 151).

Significant differences can be seen between the pumice found in the Inner Islands and those in the other Scottish islands. The major difference is the occurrence of older Mesolithic pumice, which does not occur in any other locality in Scotland. The pumice at Staosnaig is physically different to the pumice found at younger archaeological sites in the rest of Scotland. This difference will be examined further in Chapter 4. The large number of undated pumice finds in Figure 2.16 is the result of the mixed surface finds on Coll (Crawford, 1997), although many of these finds included Mesolithic artefacts.

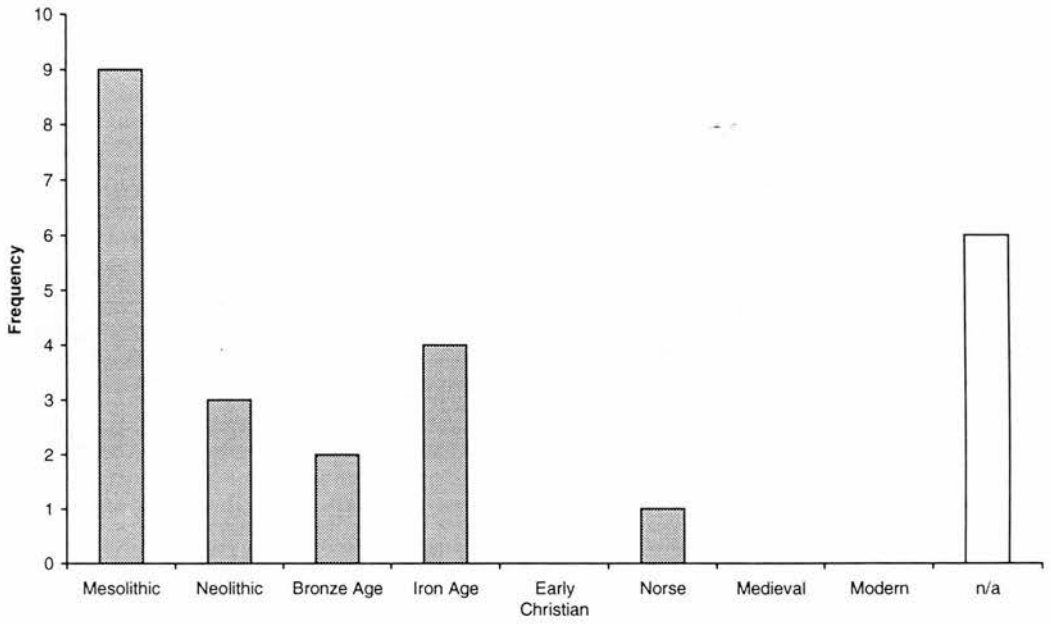

Figure 2.16: The age of pumice finds in archaeological sites in the Inner Islands.

Scottish Mainland

Figure 2.9 shows that pumice finds have been relatively rare on the Scottish mainland. Of the 17 sites, ten are from archaeological and seven from natural sites (Table 2.8). Binns (1971) carried out a thorough survey of several areas of Scotland where raised shorelines are found and reported the pumice finds. These sites are comparatively rare (Figure 2.9), but pumice was first found at some of them at the end of the nineteenth century. Smith (1896) found pumice on raised shorelines at Ardeer (site 43), at 4.6-7.6 metres above sea-level, and Shewalton Moor (site 41), at 12.2 metres above sea-level, both on the North Ayrshire coast. Binns (1971) found at least 30 small brown pumice pieces at Shewalton Moor, but was unable to find any at Ardeer, as the lower shoreline is now built upon. The older beach at Shewalton is dated by Binns (1971) to 5700-5500 ^{14}C years BP and the beach at Ardeer to about 4100-2400 ^{14}C years BP. The 12.2 metre beach at Shewalton Moor, however, appears to equate to the Main Postglacial Shoreline, which is dated to between 7200 and 6000 ^{14}C years BP (Ballantyne and Dawson, 1997; Firth, 1992). The precise age of the lower beach at Ardeer is not clear, but it may well fall within the range of dates suggested by Binns (1971). Further south, Binns (1971) found a black/dark pumice piece on sand dunes at Glen Luce (site 18) and there is also a record of a find on a modern beach (site 17). The only other finds along the west coast of mainland Scotland are from a Mesolithic midden on Risga in

Loch Sunart (site 22; Appendix 1) and nine pieces found at unstratified sites between Rubha'n Achaidh Mhóir and Beinn an Achaidh Mhóir in Morar (site 36).

There are as many sites on the eastern coast of Scotland, as on the west. A single piece of pumice, found somewhere in Strathnaver (site 34), was donated to the Royal Museum of Scotland (Appendix 1). Pumice has been found on both raised shorelines and archaeological sites at Embo (sites 147 and 35) and Golspie (sites 33 and 32). The raised shorelines are about 6 metres above sea-level and Binns (1971) found small brown pumice pieces at Embo. The 6 metre beaches are probably the Main Postglacial shoreline and can thus be dated to between 7200 and 6000 ^{14}C years BP (Ballantyne and Dawson, 1997; Firth, 1992). A search of the raised shoreline at Golspie in 1992 produced a further six small brown pieces of pumice lying on the surface near a rabbit burrow. A pumice pendant was found in an Iron Age/Dark Age cist[10] at Golspie (Woodham and Mackenzie, 1957) and a single piece was recovered from a late Neolithic chambered cairn (4500-4000 ^{14}C years BP) at Embo (Henshall and Wallace, 1963). Eight pieces of grey/brown pumice were found at an archaeological site at Green Castle, Portknockie, Moray (site 40). Unfortunately, these are from poorly constrained deposits, which range in age from Late Bronze Age to Pictish (2800-1200 ^{14}C years BP). Pumice from this site is dealt with in more detail in Chapter 4. An inland stone circle at Old Keig (site 8; late Neolithic-Bronze Age) also produced pumice pieces (Childe, 1934).

Three sites in East Lothian, south-east Scotland, have produced pumice pieces. Cree (1924) found pumice in Romano-British (1600-1900 ^{14}C years BP) deposits during excavations at Traprain Law (site 19), an inland site on top of a small hill. Pumice has also been found at an Iron Age site (site 21) near Seacliff (Callander, 1931) and Binns (1971) found several small brown pieces of pumice on a raised shoreline at 3-4 metres above sea-level at Longniddry (site 13), which Binns dates to between 4100 and 2400 ^{14}C years BP.

Figure 2.17 shows that the majority of pumice finds date from the Mesolithic to Iron Ages, although several of these finds are not from archaeological sites, they are included in this graph to allow comparison with the predominately archaeological finds elsewhere in Scotland. No pumice has been found in the Early Christian, Norse or Medieval periods.

---

[10] A cist is a rectangular stone slab lined grave, which is often covered with a large stone slab.

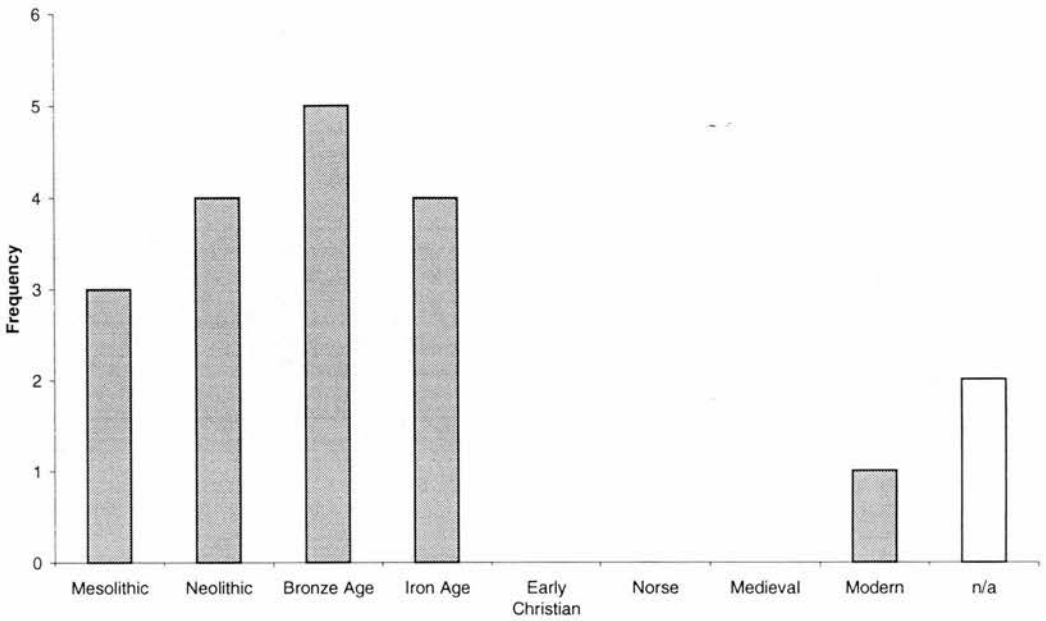

Figure 2.17: The age of pumice finds on sites on the Inner Scottish mainland. This also includes several raised beach deposits, which account for two of the Mesolithic and three of the Neolithic pumice finds.

Summary of Scottish pumice distribution

The most striking aspect of the distribution of pumice around Scotland is the rarity of finds on raised shorelines. Since the work of Binns (1971), hardly any new finds have been made and in the 100 years since pumice was first found in Scotland, pumice has only been found on ten sites which are raised shorelines. inter-tidal deposits or present day beaches. This contrasts strongly with the large number of archaeological sites with pumice deposits. The comment by Andrea Smith in Carter and Fraser (1996) that "*Pumice is found on most archaeological sites in the Northern and Western Isles from the Neolithic to the Norse periods.*" is probably an exaggeration, the lack of pumice finds from Mainland in Orkney being an example, pumice is extremely common in these islands and comparatively rare on the mainland of Scotland. There are no pumice finds in north-west Scotland and a conspicuous absence on Kintyre in south-west Scotland. Binns (1971) carried out a search of raised shorelines on Kintyre and found no pumice. Pumice on the Western Isles is mainly found along the west coast and the same is generally true on Mainland, Shetland, although this westerly distribution pattern is not reproduced in Orkney.

Figure 2.18 shows that pumice has been found most frequently in Iron Age sites, with Neolithic contexts being the next most common. The oldest pumice deposits are found in

the Inner Islands with several sites containing pumice in Mesolithic contexts dating between 8000 and 7000 ^{14}C years BP (Figure 2.11). In most other areas, pumice is found in archaeological sites dating from the Neolithic to Norse periods (5200-900 ^{14}C years BP), with the most finds in Iron Age (2500-1200 ^{14}C years BP). The youngest finds are from Orkney, where late-medieval and modern finds occur. The survey of the literature has demonstrated that many archaeological pumice finds are from poorly dated deposits. Many of these sites are only classed as belonging to a cultural or technological age, which means that the pumice can only be dated to within a broad age range. Over 30 sites are undated and these form the second most common class in Figure 2.11.

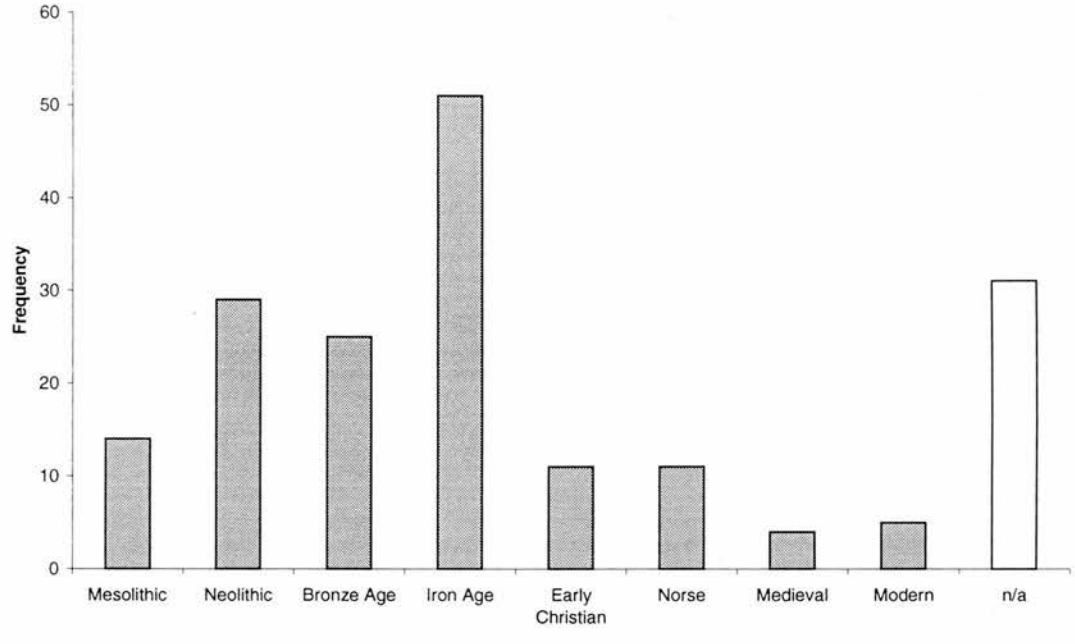

Figure 2.18: The age of pumice finds in archaeological sites in Scotland.

This study has highlighted some of the problems in describing the colour of the pumice pieces. Smith (Forthcoming) describes the colour of pumice from sites around the Atlantic coast of Scotland as being black and does not describe the colour of the pumice from the sites she has studied. From this it can be assumed that this pumice was also regarded as being black. In this study, a differentiation is made between brown and black pieces, although this is often a subjective choice. Most other authors have found that brown pumice predominates in Scottish archaeological sites, therefore Smith's claim of finding just black pumice seems unlikely. Although colour should not be used as a distinguishing characteristic (Chapters 3 and 4), the work of Smith (Forthcoming) on the colour of pumice does not agree with previous and current finds. Most of the pumice has been described by

authors as brown, grey or black. There appears to be a gradual range of colours, although some pieces are obviously black or brown. Pumice which has been buried within an archaeological site will probably whether at a slower rate, than pumice left exposed on the surface. This will lead inevitably to colour changes, with fresh black pumice, for example, becoming more grey with age. This process also means that the colour of the pumice should not be used when using pumice to correlate deposits. There is no evidence of any banding in any of the pumice described in the literature or obtained for this study. Some of the oldest pumice appears to be a different colour (light brown) to the majority brown/grey/black pumice pieces found at younger sites. Some of the Norse sites in Shetland have also produced white/grey pumice.

The distribution of pumice finds in archaeological and natural sites around the British Isles suggest that there were probably several pumice drifts. The oldest of these pumice drifts deposited the pumice which was found at Clettnadal in Shetland. The eruption that produced this pumice must be older than 9000 ^{14}C years BP. The next oldest pumice is represented by the pumice found at the Mesolithic sites mainly in the Inner Isles. Many of these sites contain pumice older than 7000 ^{14}C years BP and some older than 8500 ^{14}C years BP. These dates produce minimum ages for the eruption which produced the pumice. As the Western and Northern Isles subsided during the Holocene it seems likely that people exploited pumice finds that were washed up on the beaches. This pumice could have either been eroded from an older deposit or more probably produced by a contemporary eruption. Some pumice was buried, as shown by the finds at Clettnadal and the Bay of Moaness. As relative sea-levels rose, however, it is likely that some of this was eroded, refloated and washed up on beaches. Many sites have only produced singular or a few pieces of pumice, which suggests that pumice in many areas was not a common find. The only large pumice find in Ireland is from the site in the Aran Islands, which suggests that at least one pumice drift was deposited here sometime before about 2900 ^{14}C years BP. The large number of Iron Age finds may reflect a significant pumice drift about 2000 ^{14}C years BP, or just the large number of Iron Age sites that have been excavated. The white pumice found in Norse and Medieval sites in Shetland appears to be significantly different to the pumice found elsewhere in the British Isles and may represent an eruption in the early second Millennium AD.

The presence of pumice mainly in archaeological sites in the British Isles means that it is difficult to date the pumice drifts. It is clear, however, that pumice has been washing onto

the British Isles for the last 9000 years. The next section summaries the results of this survey of pumice finds in the North Atlantic.

2.2.6 Summary of the spatial distribution and temporal of pumice in the North Atlantic

Pumice is found on raised shorelines and archaeological sites around the whole of the North Atlantic region. This review has for the first time brought together details of pumice finds which have occurred after the last major review undertaken by Binns (1967a; 1967b; 1971; 1972a; 1972b; 1972c; 1972d). Both the pumice finds in Svalbard and Norway suggest that there have been multiple pumice drifts which have left deposits on a series of raised beaches, the oldest of which dated by to about 9000 ^{14}C years BP. This early phase of pumice deposition is supported by pumice finds from archaeological sites in southern Norway and Scotland. Evidence from Svalbard and Scandinavia suggests that there appears to have been at least one major pumice eruption at around 6000 ^{14}C years BP., with other eruptions between 5000-4000 and 3200-3000 ^{14}C years BP. Several other pumice horizons are found and it is not clear whether some of these are due to eruptions or reworking of older pumice deposits. A pumice deposit has also been identified on a raised shoreline in north-west Iceland dating from about 5000 ^{14}C years BP. The pumice found in archaeological sites is harder to interpret, although the pattern of pumice finds suggests that several pumice drifts are responsible for the finds at sites ranging from the Mesolithic to Modern ages.

The errors which are inherent in both the dating of raised shorelines and archaeological sites mean that it is not possible to correlate pumice deposits simply on age. The next section discusses previous attempts to correlate pumice deposits by their geochemical characteristics and to identify the sources.

2.3 Origin of pumice

This section discusses the previous theories on the origin of the pumice. Research into the source of the pumice found around the North Atlantic region has progressed slowly. There has been no real advance in this work, since the early 1970s (Boulton and Rhodes, 1974). Again, Binns (Binns, 1971; Binns, 1972a) has produced the most detailed study to date into the origin of the pumice. The nearly 30 years that have passed since this work was published, however, has seen a huge increase in our knowledge of volcanic activity in the North Atlantic area and Iceland in particular. A comparison of the geochemical analyses of the pumice pieces with new data from source areas will be shown in the Chapter 5, this section only aims to summarise previous published work on the source of the pumice.

2.3.1 Geochemical data

Geochemical analyses of the pumice provides the best means of correlating geographically dispersed deposits and identifying the source volcanoes and eruptions, a technique now firmly established in tephrochronological research (Chapters 3, 4 and 5).

There is a surprising lack of good quality geochemical analyses of pumice from the North Atlantic area. A search of the literature has shown that there are only 40 complete major element analyses of pumice from the North Atlantic region and seven trace element analyses from Svalbard. Since the work of Binns (1971; 1972a) and until the present study, there have been only two papers published which contain geochemical data of the pumice (Boulton and Rhodes, 1974; Peulvast and Dejou, 1982). The geochemical data that is available is summarised in Table 2.10 and shown in full in Appendix 2.

a)

Location	Canada			Greenland	Svalbard A			Svalbard B		
Reference	1			2	1, 3, 4			1, 3		
	mean	1σ	n		mean	1σ	n	mean	1σ	n
SiO_2	61.21	0.77	8	63.53	64.39	0.85	10	53.21	0.54	2
TiO_2	1.20	0.03	8	1.05	1.26	0.58	10	2.42	1.19	2
Al_2O_3	15.94	1.42	8	13.72	15.11	0.97	10	19.18	1.73	2
FeO*	5.67	0.14	8	6.25	5.87	0.81	10	7.01	0.06	2
MnO	0.19	0.01	8	0.18	0.18	0.01	9	0.94	0.37	2
MgO	1.53	0.24	8	1.22	1.43	0.41	10	1.39	1.64	2
CaO	3.39	0.23	8	3.90	3.72	1.98	10	4.37	3.06	2
Na_2O	4.89	0.10	8	5.39	4.84	0.46	10	4.42	0.17	2
K_2O	2.59	0.04	8	2.35	2.67	0.29	10	3.14	0.06	2
Total	98.75	1.03	8	99.59	100.22	1.66	10	99.87	0.23	2

b)

Location	Scand. A			Scand. B	Scand. C	Scotland A			Scotland B
Reference	2, 3, 5			2	2	2			2
	mean	1σ	n			mean	1σ	n	
SiO_2	64.07	1.00	10	51.8	69.00	63.37	1.11	6	53.7
TiO_2	1.07	0.30	10	2.41	0.12	1.25	0.10	6	2.12
Al_2O_3	14.39	0.36	10	17.5	14.80	14.62	0.04	6	17.8
FeO*	5.55	0.82	10	8.18	1.96	5.97	0.13	6	4.02
MnO	0.18	0.03	10	0.22	0.08	0.19	0.01	6	0.21
MgO	0.99	0.54	6	3.79	0.27	1.41	0.03	4	2.94
CaO	2.99	0.80	10	6.41	1.44	3.30	0.22	6	6.48
Na_2O	5.13	0.44	10	4.16	4.40	4.81	0.28	6	3.90
K_2O	2.22	0.76	10	1.90	2.60	1.78	0.08	6	2.20
Total	97.29	1.95	10	97.81	95.04	97.09	1.32	6	94.42

c)

Svalbard	Rb	Sr	Y	Zr	Nb
Elvetangen D	65	265	65	655	80
Ausfjordness C	65	285	65	675	80
Valhallfonna C	65	275	70	750	95
Valhallfonna C	65	275	75	750	100
Polhem A	65	1000	35	435	125
Valhallfonna A	75	950	30	435	110
Elvetangen A	75	915	35	495	115

Table 2.10: Summary geochemical data of pumice from around the North Atlantic Region. Where more than one analysis is available, the mean, standard deviation and the number of analyses are shown. *All analyses have had Iron Oxide values converted to show total iron as FeO. Analyses are a mixture of wet chemical and XRF techniques. a) and b) show major element analyses only and c) shows the trace elements analyses published by Boulton and Rhodes (1974). All other analyses are from: 1 (Blake, 1970); 2 (Noe-Nygaard, 1944); 3 (Binns, 1971); 4 (Bäckström, 1890); 5 (Peulvast and Dejou, 1982). Full details of these analyses are available in Appendix 2.

Binns (1971; 1972a) recognised three main groups as defined by their geochemical composition. These groups are easily distinguished (Table 2.10) and are: dacites, with

weight % SiO_2 abundances around 64% (Greenland, Svalbard A, Scand. A and Scotland A in Table 2.10); the more silicic rhyodacites, with weight % SiO_2 abundances of 69% (Scand. C) and the trachyandesites, with weight % SiO_2 abundances between 51 and 54% (Svalbard B, Scand. B, Scotland B). The analyses of pumice from Canada, published by Blake (1970), however are significantly different from the dacitic pumice, with lower amounts of SiO_2 (Table 2.10). Binns (1972a) regards these analyses as inaccurate and believes that the Canadian pumice probably belongs to the same group as the dacites. Figure 2.19 and Table 2.10 show that despite having lower SiO_2 abundances, the Canadian pumice is very similar to the other dacitic pumice in all other oxides. This suggests that Binns's (1972a) interpretation of the differences being due to an error in the analyses, rather than a real difference in geochemical composition was correct. Other analyses, however are also probably of dubious quality. Appendix 2 shows that one of the trachyandesite analyses presented by Blake (1970) has 20.40 % Al_2O_3 (from Zordrargerfjorden). This is an unusually high amount of Al_2O_3 and more probably reflects some form of contamination caused by the bulk nature of the analysis. The analysis of pumice from Brageneset published by Binns (1971) total 103.84%, again this suggests a poor analysis.

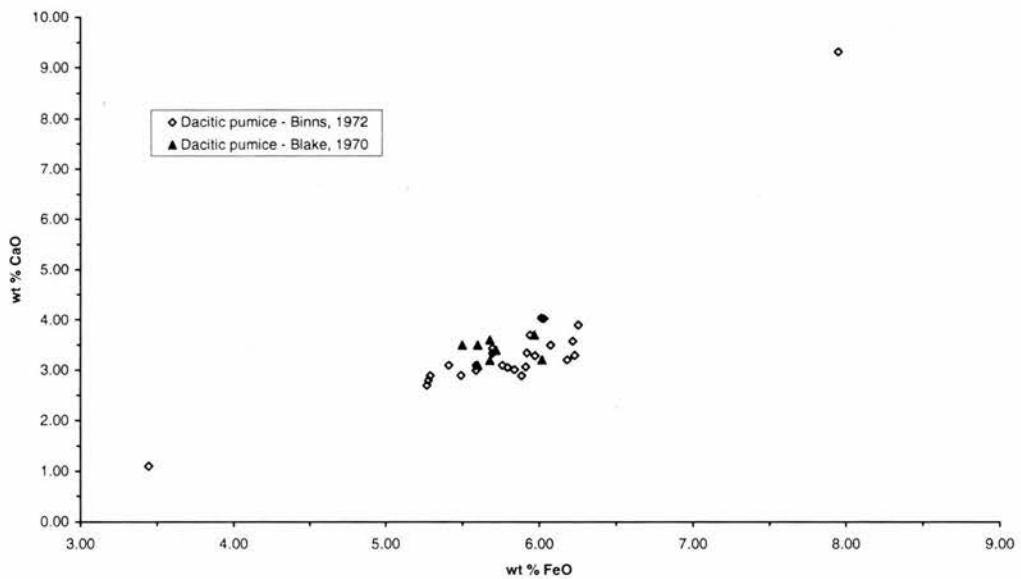

Figure 2.19: Geochemical analyses of dacitic pumice based on published data in Table 3.9. The open diamonds are analyses of dacites as defined by Binns (1972a) and the filled triangles are analyses of the Canadian pumice (Blake, 1970) and one analyses from Binns (1972a).

The homogeneity of the major element composition (Figure 2.19 and Table 2.10) suggests that most of the pumice is from same source. This is as, Binns (1972a) points out, despite the analysed pumice being from widely geographically separated sites and deposits covering a large age range (over 3000 years). Binns (1972a) also claims that the dacitic pumice found in Norway can be geochemically split into two groups. These two groups correspond to the brown older pumice found on Tapes 4 and the younger black pumice found on N4, which has slightly lower amounts of MgO and CaO (see 3.2.4). Unfortunately, most of the analyses are only partial and it is not possible to compare these results with the others.

The analyses presented by Boulton and Rhodes (1974) are unfortunately not comparable with any of the other published analyses either (Table 2.10). They only present selected trace element analyses in their paper. Two groups are immediately apparent, however, with the oldest pumice from horizon A having much high abundances of Sr and lower Y and Zr than pumice from horizons C and D.

Binns (1971; 1972a) also published refractive index and petrographic details on the pumice he analysed. The refractive index of the glass in the dacitic pumice is consistent with values of about 1.520, whilst the trachyandesites are about 1.540 and the rhyodacites are between 1.494-1.507. The consistency of the refractive index values of the dacitic pumice mirrors the geochemical homogeneity.

The quantity and quality of the geochemical data available makes it difficult to correlate the various pumice deposits. Analyses were carried out using a variety of techniques, by different workers and over some 90 years. All of these analyses were carried out on crushed large samples of pumice. The porous nature of the pumice means that it is very difficult to remove all extraneous material before the analysis, which can contaminate and bias the results. Also, as Binns (1972a) points out, it is preferable to analyse just the glass fraction of the pumice, but it is difficult to remove all of the minerals from within the glass before analysis. These problems and their solutions will be dealt with in more detail in chapters 3, 4 and 5.

2.3.2 Possible sources

Although the quality of the geochemical data available is far from ideal, several workers have attempted to attribute sources to the pumice deposits. Iceland has always been regarded as the most likely source for most of the pumice. Unfortunately at the time of much of the

research into the origin of the pumice (1950s to 1970s), only limited details were known about the volcanic history of Iceland and even less on the geochemical composition of the products produced by suitable Holocene eruptions.

Noe-Nygaard (1951) believed that Hekla, southern Iceland, was the most likely source of the pumice found in northern Denmark, Norway, Greenland and Svalbard. He includes a photograph of pumice rafts off the south coast of Iceland produced after the eruption of Hekla in 1947 (Figure 2 in Noe-Nygaard, 1951), showing that despite its inland position eruptions were capable of producing pumice which could reach the sea. At the same time of writing this paper, Sigurður Thórarinsson was developing the use of tephrochronologies and tephrastratigraphies (Thórarinsson, 1944). Although this work was outstanding, it was only just beginning and the ages of the tephra layers were not accurately known, as radiocarbon dating had yet to be developed. Equally, there were few geochemical analyses available on products from Hekla.

Both Binns (1971; 1972a) and Blake (1970) also thought that Iceland was the most likely source for most of the pumice. Binns (1971; 1972a) carried out a detailed study of possible source areas including Iceland, the Caribbean, Alaska and Japan, as well as submarine volcanic activity. By comparing whole rock analyses mainly from lavas, with those of the ocean-rafted pumice, Binns (1971; 1972a) concluded that Iceland was the most likely source of both the dacitic and rhyodacitic pumice. The origin of the trachyandesitic pumice was attributed to one or more of the smaller North Atlantic islands (Binns, 1971; 1972a). Peulvast and Dejou (1982) also agree that Iceland is the likely the source area and Hekla in particular, is the most probable origin of the pumice. Salvigsen (1984a) disagrees and believes that Hekla's inland position means that it is unlikely that an eruption would be able to supply the quantity of pumice found around the coastlines of the North Atlantic. The possibility of submarine eruptions from around Iceland are suggested as possible sources of the pumice. Boulton and Rhodes (1974) state that Jan Mayen is the most likely source of pumice found on the raised shorelines of Svalbard, although they produce no evidence to support their suggestion.

There is a consensus among authors that Iceland or the Iceland area is the probable source of most of the pumice found around the North Atlantic region. This seems to be a reasonable conclusion and the generalised geochemical data used by Binns (1971; 1972a) supports this. Up until the present study it has not been possible to positively identify which volcano, let alone which eruption produced the pumice. It is only recently that detailed geochemical data

and details on the dates of Iceland eruptions have been available (e.g. Dugmore *et al.*, 1995; Dugmore *et al.*, 1992; Larsen *et al.*, 1999; Larsen *et al.*, in press; Larsen and Thórarinsson, 1977) only now can a realistic attempt can be made to discover the sources of the pumice.

2.3.3 Transport routes

Chapter 1 discussed the possible mechanisms by which pumice can be transported from a volcano to the sea and then to a shoreline. For pumice to be transported to the sea from an eruption, the volcano must either be near the sea (to allow direct airfall, pyroclastic flows or jökulhlaups to carry pumice into the ocean) or by a river system which allows pumice to be carried to the sea. Both Blake (1970) and Binns (1971; 1972a; 1972d) realised that current circulation patterns in the North Atlantic allow pumice to be transported from Iceland to all of the sites around the North Atlantic where it is found, as shown in Figure 2.20. As stated above, Hekla was commonly regarded as the source of much of the pumice, although Salvigsen (1984a) thought its inland position discounted this possibility. Despite its inland position, Hekla is known to have produced pumice rafts which have become entrained in ocean currents around Iceland (Noe-Nygaard, 1951).

Binns (1972a) considered the amount of time it would take for pumice erupted in Iceland to reach the coasts where pumice has been found. He concludes that it would only take 2-3 months to reach Norway and between 7-9 months (via southern Greenland and then the North Atlantic Drift) to 21-27 months (via Norway, Svalbard, East Greenland, southern Greenland and then the North Atlantic Drift) to reach the British Isles. The latter route appears to be a rather improbably complicated one for pumice to reach the British Isles and it seems that most pumice would have probably arrived by the former, shorter route. As Chapter 1 showed, dacitic pumice is capable of remaining afloat for several years and it would appear that Iceland's position in the North Atlantic is an ideal location for the widespread distribution of any pumice which enters the sea. The ocean transportation of pumice, in the light of identified sources, is discussed in more detail in Chapter 5.

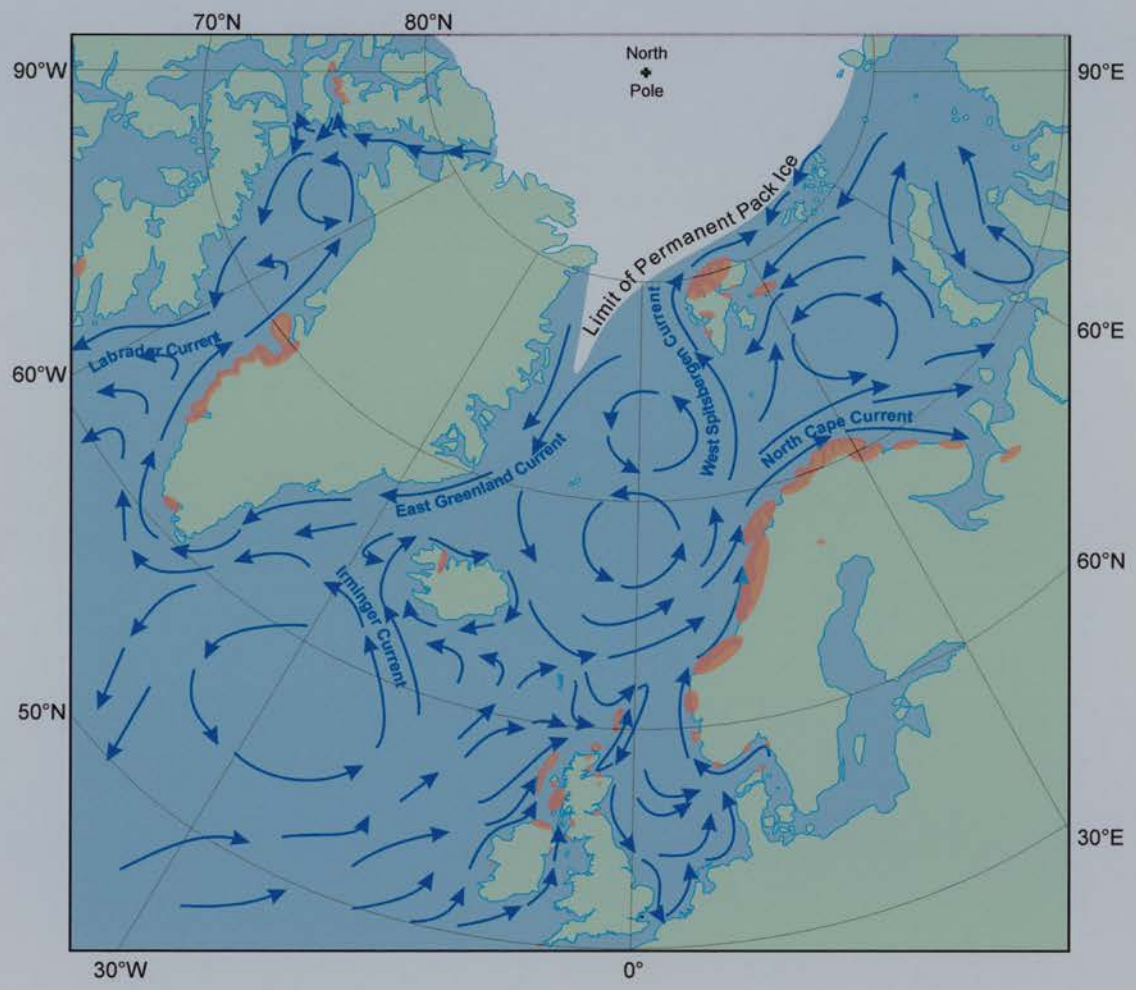

Figure 2.20: Map to show modern day circulation of ocean surface currents (arrows) in the North Atlantic region. Pumice finds shown in red. Ocean surface circulation based on Bearman (1989), Editor (1977), Eggertsson (1994), Herman (1974).

Summary of the origin of the pumice

Although the geochemical data available to previous workers has been limited, Iceland was identified as the most likely source of much of the ocean-transported pumice. Iceland was known to have a long active volcanic history and its mid Atlantic position means that ocean currents could transport pumice to all of the sites where pumice has been reported. Unfortunately, none of these studies have been able to confidently identify a source volcano. Hekla was chosen by several authors as a possible source, based mainly on the fact that it is known to have produced pumice in the recent past. There is little evidence, however, to support this and it is only in the last 10 years that substantial amounts of geochemical data on the Holocene activity of Icelandic volcanoes has been published.

2.4 Summary of Chapter 2

This chapter has reviewed the previous research undertaken on pumice finds around the North Atlantic. The review of the literature and information kindly supplied by archaeologists has greatly increased both the number of archaeological sites where pumice has been discovered and the total number of pumice pieces found. Pumice is found on shorelines ranging in age between 9000 ^{14}C years BP and the present day and archaeological pumice are found at sites with a similar timescale. Despite this extensive record, several previous attempts, have failed to satisfactorily identify the source of the eruptions, although Iceland and Jan Mayen have been identified as the most likely source areas.

Chapters 3 and 4 will provide new high quality geochemical data from pumice deposits in Iceland, Norway and Scotland. Chapter 5 compares these analyses with new and published data from source volcanoes in Iceland and Jan Mayen.

Chapter

Pumice from raised beaches: new data

3

The previous chapter described the spatial and temporal distribution of pumice finds around the North Atlantic and the limited amount of geochemical data available. This lack of good quality geochemical data means that so far, it has not been possible to satisfactorily correlate or differentiate between geographically or temporally separated deposits, or identify the source volcanoes and eruptions which produced the pumice. Chapter 2 also showed that since the work of Binns (1967a; 1967b; 1971; 1972a; 1972b; 1972c; 1972d), many new pumice finds have been reported, especially in Scotland and Svalbard, but little new geochemical data published.

This chapter presents new data on pumice finds from raised shorelines, whilst Chapter 4 will present details of pumice finds from archaeological sites. Both chapters will include details on the sites, the type of pumice found, the age of the deposits and any geochemical analyses undertaken. Results from the analyses of pumice from both types of site will be compared at the end of Chapter 4, before Chapter 5 presents new information on the possible sources of the pumice and correlates the pumice to particular volcanoes and eruptions.

3.1 Introduction

Pumice from natural sites forms the majority of the finds in the North Atlantic, except in the British Isles where archaeological sites have provided over 90% of samples. Pumice occurs along virtually the whole of the west coast of Norway and much of Svalbard, whilst there are also scattered deposits in the Canadian Arctic and western Greenland. Notably, there have been no published reports of finds in Iceland, the assumed source of much of the pumice.

To acquire pumice pieces for geochemical analyses it was decided to carry out fieldwork in selected areas of Norway and Iceland. The detailed work of Undås (1942) in Møre and Trøndelag provided an opportunity to collect samples from sites where pumice had already been identified, but no geochemical analyses were undertaken. In 1989, a feasibility study was undertaken in this area by Dr Andrew Dugmore and Prof. David Sugden which provided some samples for this work. For this thesis, further fieldwork on raised shorelines in central

west Norway was undertaken in 1993 and to the north-west of Iceland on several short visits between 1992 and 1995.

Section 3.2 provides details of the sites where the pumice was found in Norway, Iceland and Scotland. This includes details on the geomorphology of the sites and the physical properties of the pumice. The following section describes the geochemical techniques used to analyse pumice and tephra layers in this thesis. Both major and trace element analytical techniques will be discussed. Next, the geochemical properties of the pumice found on natural contexts will be described before section 3.4 compares the new results with the published data described in Chapter 2.

3.2 Pumice sites

Pumice was collected from three countries around the North Atlantic for use in this thesis. The aim of the fieldwork was to identify the type of pumice found and to collect samples for geochemical analyses. It is important to collect a representative sample of pumice pieces from a site for geochemical analysis. This is, however, a subjective process and limited time on the electron and ion microprobes (see section 3.4) mean that only a small proportion of pumice collected from any site can ever be analysed. The sites visited in Norway will be discussed first, followed by those in Iceland and finally the single site in Scotland.

3.2.1 Surveying techniques

Unless otherwise stated, the altitude of pumice finds was determined using an auto-set (engineers) level. This was deemed to be more accurate than using an altimeter, especially as many of the pumice deposits occur at a low altitude, i.e. a few metres above sea-level. In Norway sea-level was determined to be the upper boundary of the black algal staining on the present day beach and rocks, which sometimes, depending on the time of the survey, coincided with high tide. At most sites, the current height of the tide was also measured, as was the boundary between the beach and permanent vegetation. In Iceland, levelling was carried out from local sea-level and tide tables, kindly supplied and translated by Hreggviður Norðdahl. These were used to convert the local sea-level into a reference sea-level, at Reykjavík. This system allows the relative heights of pumice deposits in Iceland to be compared and eliminates the need to determine an arbitrary measure of mean sea-level. As the difference between high and low tide in the Strandir region is only about 1 metre, the height of the pumice above high tide will also be quoted. Some measurement uncertainty

exists, but the potential altitudinal errors are acceptable for reliable comparison between deposits.

A test of the relative altitudes of the levelling used in this study was obtained along the shore of Ófeigsfjörður in Vestfirðir (North-West Iceland). The current sea-level was measured along a 350 metre stretch of shoreline on a calm day over a period of a few minutes. The difference in height at either end of the survey line was 0.005 metres. This constrains probable measurement errors and shows they may be ignored.

All Norwegian grid coordinates are stated as *standard references* and were obtained from the 1:50000 topographic maps published by Statens Kartverk (The Norwegian Mapping Authority).

3.2.2 Norway

The coast between Ålesund and Trondheim, western central Norway was surveyed by Undås (1942), who found pumice at 21 sites. These sites are summarised in section 2.2.4. Ten of these sites were selected for resurvey and sampling and four new sites were added. One of the major problems encountered during this fieldwork was finding the precise locations of the pumice deposits as described by Undås (1942). Descriptions in the text can be fairly vague and often pumice was not found. Other reasons for pumice not being found could include revegetation covering deposits or the collapse of the eroding features. This mirrors the problems that Binns (1971) encountered when he attempted to find pumice on raised shorelines in Scotland and indeed the problems found when carrying out fieldwork in Northern Ireland in 1990. The pumice sites in this section will be described beginning with those in the south, near to Ålesund and ending with those in the north, on the island of Hitra (Figure 3.1). The dates of the pumice deposits will be determined using the same methods as described in Chapter 2.

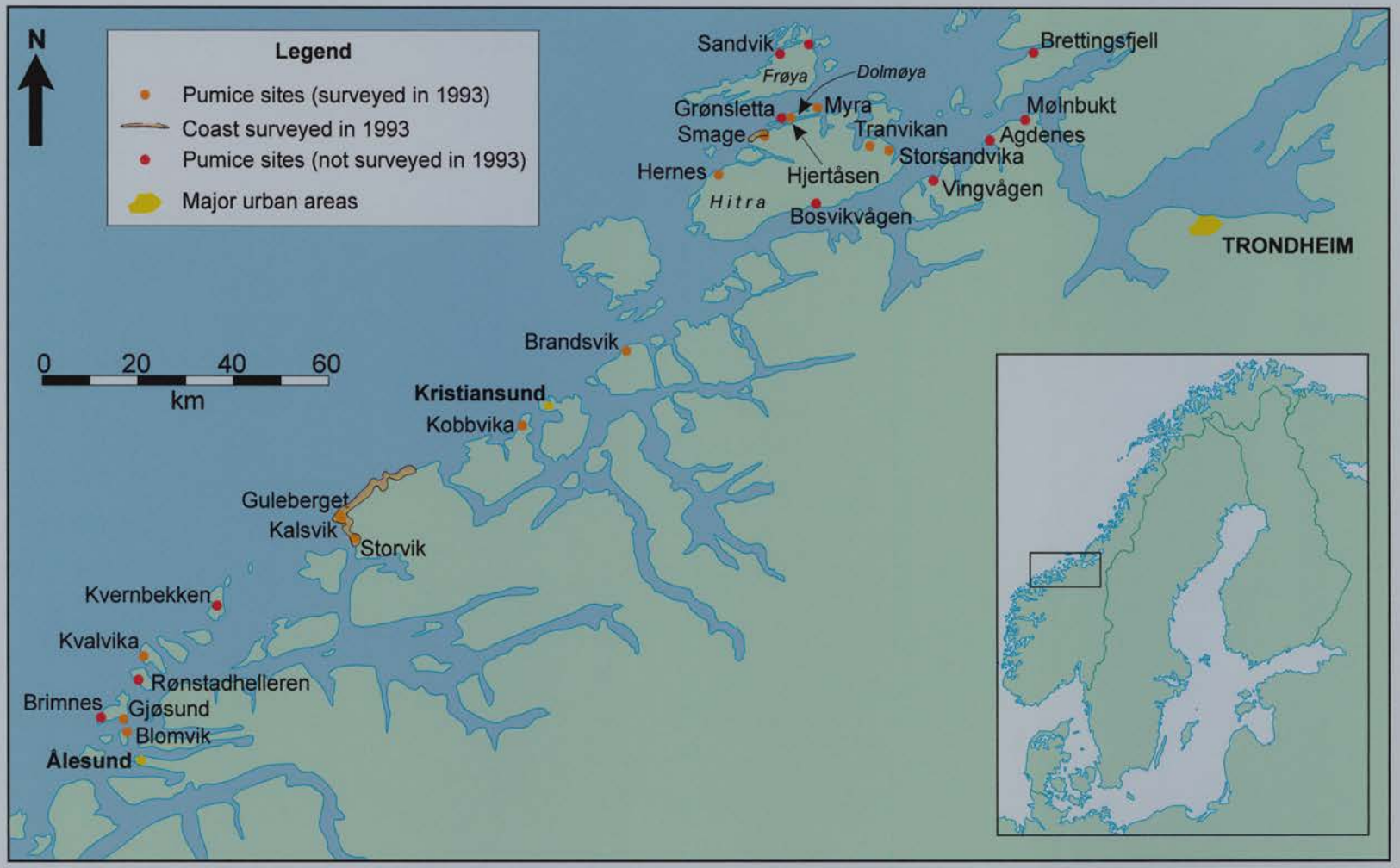

Figure 3.1: The distribution of pumice sites between Ålesund and Trondheim. This includes all of the sites visited (orange dots), areas of coastline searched and the sites in Undås (1942) which were not visited in 1993 (red dots).

Ålesund area

Undås (1942) found pumice at six sites on the islands to the north of Ålesund. These are Gjøsund and Brimsness on Vigra, Rønstadhelleren on Løvsøya, Kvalvika on Haramsøya and Kvernbekken on Harøy. The sites at Gjøsund and Kvalvika were revisited for this study.

A single piece of brown pumice was also found at an altitude of 3.3 metres above sea-level, near the settlement of Oksnes on the north-western part of the island of Valderøya. This site was called Blomvik (LQ 525 360), after the name of the bay. The raised beach had been exposed by road widening and it is possible that more pumice pieces were also removed during this process. A search of the surrounding area failed to find any more pumice, although the recent construction of houses in the area meant that most of the raised beach was now built upon and vegetated.

Pumice was found on the island of Vigra, immediately to the north of Valderøya, near the settlement of Gjøsund. It was not clear if the pumice was found at exactly the same locations as stated by Undås (1942). The highest level was found at LQ 517 378, in a drainage ditch running parallel to the side of the road (Figure 3.2). This site, named Gjøsund U (GJU), was estimated to be just over 1 metre lower than the nearby 12 metre trig. point, giving an elevation of just less than 11 metres above sea-level. It seems likely that this is the same as the upper pumice deposit found by Undås (1942), who found pumice at 9.3 metres. The error in the height could be due to differences in the techniques used to measure the altitude and the slightly different locations of the sites. Numerous pieces of mainly brown pumice up to 5 cm in diameter were found on both sites of the ditch (Figure 3.2). The lower pumice horizon, Gjøsund L (GJL), was found a few hundred metres further north (LQ 515 379). The pumice was found embedded in the sides of two parallel drainage ditches cut into the raised beach (Figure 3.3). Black and brown pieces of pumice (Figure 3.3) up to 10 cm in diameter were found at an altitude of 5.3 metres above sea-level, which exactly coincides with the altitude of the black pumice described by Undås (1942). A local man stated that the present day bay below the GJL pumice site was renowned locally for trapping lots of flotsam and jetsam. Chapter 2 showed that the age of the GJU horizon is about 6000 ^{14}C years BP, whilst the GJL pumice is about 3300 ^{14}C years BP.

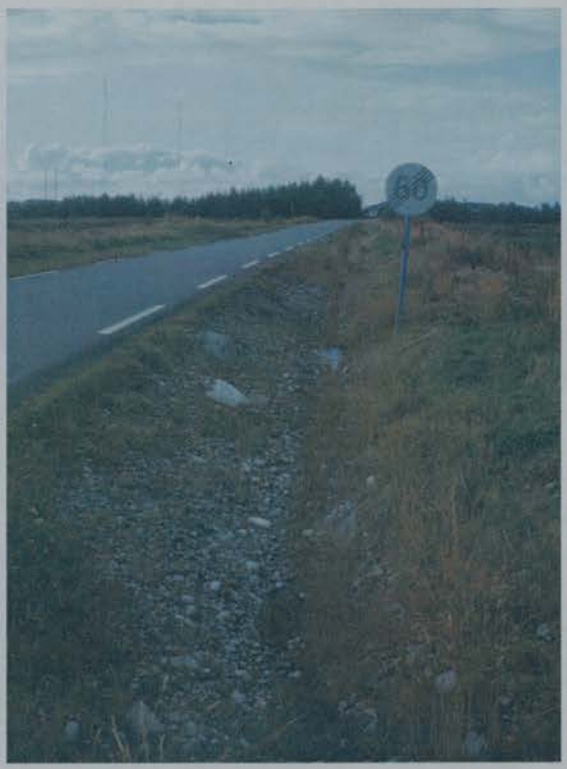

Figure 3.2: Photographs to show the raised shoreline and pumice at Gjøsund U (GJU). The upper photograph shows the road ditch which cuts through the shoreline and exposes pumice. The lower photograph shows the brown pumice found at this site.

Figure 3.3: Photographs to show the raised shoreline and pumice at Gjøsund L (GJL). The upper photograph shows one of the drainage ditches which cut through the shoreline and expose pumice. The lower photograph shows the mainly black pumice found at GJL, although the middle piece is brown.

Undås (1942) found three pumice horizons on beach ridges at Kvalvika (LQ 555 510) on the island of Haramsøya, 8.5 km to the north-east of Vigra. Although the beach ridges described by Undås are very prominent (Figure 3.4), the pumice deposits are not. Despite a thorough search of the area and the large number of unvegetated beach ridges, only a single piece of black pumice was found in situ, on what is probably the 10.5 metre *f-ridge* of Undås (1942). A small black piece of pumice was also found sitting on top of a wall.

Figure 3.4: A photograph to show an example of the beach ridges at Kvalvika.

Although the lack of pumice deposits associated with the beach ridges at Kvalvika was disappointing, finding pumice at approximately the same levels as described by Undås at Gjøsund was encouraging. The finds at Gjøsund, however, suggest that the lower 3300 ^{14}C years BP pumice horizon is a mixed deposit of black and brown pumice, not just black pumice as claimed by Undås (1942).

Gulberget area

There has been a cluster of pumice finds to the west and south of the small hill called Gulberget (LQ 958 773), near to the coastal town of Bud (Undås, 1942). Although the coast around Gulberget and Bud was searched, no pumice was found. Undås reports beach ridges below the 20 metres above sea-level moraine at Kalsvik, however, there was little evidence of them during the 1993 visit. The area had been ploughed and several drainage ditches, which could have provided sections through the raised shorelines, were either heavily overgrown or have been infilled.

Pumice was found, however, at Storvik (LQ 981 726), which is to the south of Stavika. The lowermost raised shoreline at Storvik (2.1 metres above sea-level), is the site of a small racecourse and numerous pieces of black and brown pumice were found inland of this at an altitude of 5.2 metres above sea-level. This deposit has been exposed by a stream which has cut through the beach ridge. A search upstream, to an altitude of about 10 metres, which should coincide with the Tapes transgression maximum, failed to reveal any more pumice finds. Although pumice was not found at a higher altitude, a local farmer stated that pumice pieces sometimes appear in low lying fields after they have been ploughed. A search along the coastline to the north-east of Bud, as far as the small village of Sandvik, also failed to turn up any more finds of pumice.

Pumice was only found at Storvik, and this equates to the 5.2-6 metre pumice horizon found by Undås (1942). Again this deposit was found to contain both black and brown pumice, not just the black pumice reported by Undås. The pumice at Storvik is at altitude which can be dated to between 3000-3300 ^{14}C years BP.

Kristiansund area

Pumice has been found at two sites to the north and south of Kristiansund, the first Brandsvik, on the island of Tustna and the second to the west of Kvitsund, which is really called Kobbvika (Undås, 1942). Dugmore and Sugden visited these sites in 1990 and confirmed the existence of three pumice horizons at each site at Kobbvika and at least one at Brandsvik. Although the Brandsvik site (MR 524 107) was revisited in 1993, on that occasion no pumice horizons were found. As a result, pumice samples, collected in 1990 were analysed, as shown in section 3.5. These pumice pieces are mainly brown and up to about 8 cm in diameter, although there are numerous smaller pieces about 2-5 cm across. Beach ridges were surveyed up to an altitude of 23 metres, but no pumice was found on any of these ridges. The pumice found at Brandsvik in 1990, was found on the main Tapes ridge, the site was heavily overgrown and was only exposed by construction work (Dugmore, pers. comm.).

The raised shorelines at Kobbvika are found in a narrow valley and a track exposes the beach material in which the pumice is found (Figure 3.5 and Figure 3.6). The uppermost pumice horizon (KVU), 15.5 to 16.4 metres above sea-level, consists of a mixture of brown and black pumice pieces up to 10 cm in diameter with many pieces about 2 cm across. This equates to the brown pumice horizon found by Undås at between 16 and 17.3 metres above

sea-level. This exposure is about 350 metres from the current high tide mark. The raised beach exposure is clearly visible on Figure 3.5. Many brown and black pumice pieces were found lying on the surface and within the raised beach material (Figure 3.7). Pumice was also found between 11.1 and 11.5 metres above sea-level (KVM), alongside the track (Figure 3.5), which is the 12.6 metre deposit of brown pumice described by Undås (1942). The pumice here was eroding out of the raised beach material and consisted of brown and black pumice. The lowermost horizon (KVL) was found at an altitude of between 6.3 and 6.4 metres above sea-level, thought to be the 7.0 metre horizon reported in Undås (1942). This deposit consisted of mainly black but also some brown pumice. The modern beach at Kobbvika, did not have noticeably large amounts of flotsam and jetsam.

The largest concentrations of pumice pieces in the Møre and Trøndelag area were observed in the uppermost horizon, which confirms the findings of Undås (1942) and the other references to the highest pumice horizon in Norway containing the largest concentration of pumice. The slight differences in altitude of the pumice horizons compared with those reported by Undås (1942) could be for two reasons: firstly, how the altitude of sea-level was determined and secondly, changes may be due to the erosion processes which have created the exposure. The boundaries of the pumice horizons will vary with time, as parts of the raised beach deposits become vegetated or degraded.

When relative sea-levels were higher, the Kobbvika site would have formed a narrow sheltered inlet (Figure 3.5 and Figure 3.6). These conditions would have reduced the risk of the uppermost deposits being eroded and removed by storms as relative sea-levels dropped. Chapter 2 demonstrated that the KVU pumice can be dated to about 6000 ^{14}C years BP, KVM to about 4000 ^{14}C years BP and KVL to approximately 3000 ^{14}C years BP.

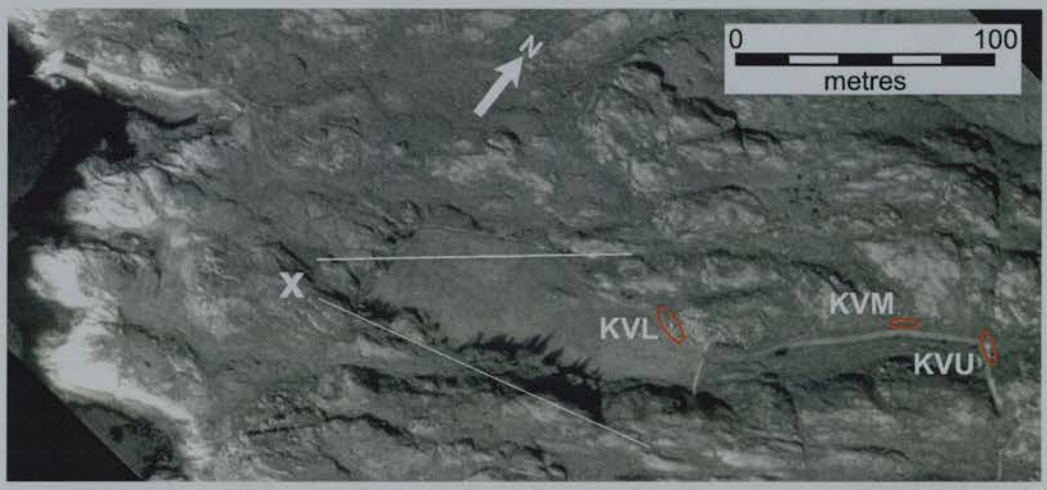

Figure 3.5: Aerial photograph of the Kobbvika, showing the location of the three pumice horizons. X marks the position where the photograph in Figure 3.5 was taken and the white lines show the orientation of the photograph. The red ellipses show the precise location of the pumice deposits. Those at KVL and KVU are visible as white marks on the photograph. © Fjellanger Widerøe AS.

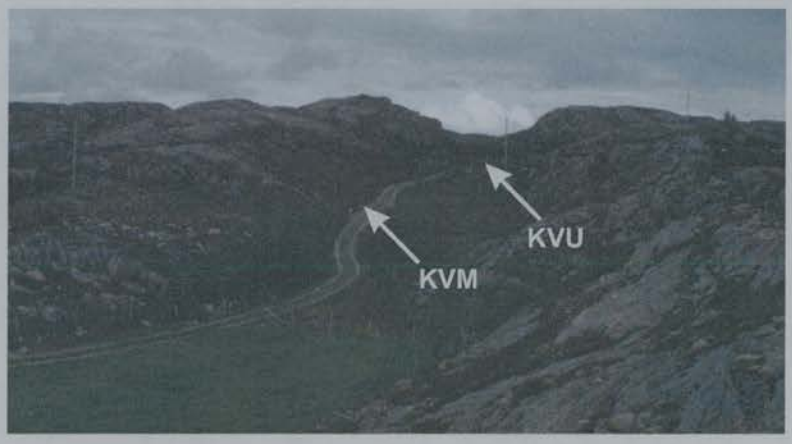

Figure 3.6: Photograph showing the positions of the pumice horizons KVM and KVU within the inlet.

Figure 3.7: Photographs to show the black and brown pumice found at KVU, Kobbvika. The upper photograph shows numerous pieces of black and brown pumice (the scale divisions are in cm). The lower picture shows more scattered smaller pieces reworked from those shown in the upper picture (the whale is 15 cm across).

Hitra and Dolmøya

Undås (1942) found pumice on the islands of Hitra (two sites), Dolmøya (three sites) and Frøya (two sites). All of the sites on Dolmøya and Hitra were visited during 1993, but no new finds of pumice were found. The site near Hjertåsen, on Dolmøya had recently been radically altered by the building of a new road and pipeline. Småge and Hernes were extensively vegetated and no exposures could be found cutting through the raised beach deposits at these two sites.

Over the last 20 years, finds of pumice have been made in this area by a local amateur geologist, Steinar Nilsen. Black pumice was found at an altitude of between 20-25 metres above sea-level at Storsandvika, on the east coast of Hitra. The area is now forested, with a thin peaty soil and no obvious ditches or streams cutting through to the raised beach material. Recently, Nilsson has returned to the site several times but also failed to find any more pumice pieces. The pumice at Storsandvika is dates from approximately 6000 ^{14}C years BP. Near Trandvikan, a single piece of white pumice was also found by Nilsen at an altitude of about 45 metres above sea-level, but in this study no new finds of pumice were made at this site. The site is close to a gate and the beach material has been exposed by erosion caused by cattle (Figure 3.8). The raised shoreline at Trandvikan dates to around 9000 ^{14}C years BP (Møller and Holmeslet, 1998) and has produced the oldest pumice piece found in Norway.

Figure 3.8: Photograph to show the 45 metre shoreline at Trandvikan. Small pieces of flint were also found at this site.

Summary of new pumice finds on Norwegian raised shorelines

Pumice was recovered from both sites described by Undås (1942) and new areas. The altitudes off occurrence described by Undås were confirmed, but the colour of the pumice found does not conform with the theory that the upper and middle pumice horizons are just composed simply of brown pumice and the lower only black. Although the lower level does seem to contain more black pieces of pumice than higher levels, there are also substantial amounts of brown pumice present. There are also black pumice pieces present in the two upper horizons. The pumice which will be analysed during this pumice comes from raised shorelines dated to c. 9000, 6000, 4000 and 3000-3300 ^{14}C years BP.

Several unsuccessful surveys of sites in Norway where pumice had previously been reported emphasise the problems in estimating the extent of pumice deposits along a coastline. A combination of one or more of the following conditions affect the chances of finding pumice at a particular site in an area where pumice is known to have been washed ashore:

- Pumice is more likely to be washed ashore in areas with favourable local currents. The site at Gjøsund, is typical of this kind of site.

- Pumice deposited during an extreme storm event, well above the normal high water mark, is less likely to be reworked. This idea is confirmed by the timings of pumice deposition along the coasts of Fiji during cyclones, as discussed in Chapter 1.

- Pumice deposits are likely to be preserved during periods of rapid relative sea-level fall, such as the end of the Tapes transgression.

- Pumice deposits are more likely to be preserved in sheltered parts of the coastline, such as the sites at Kobbvika and Brandsvik. In the past the narrow inlet at Kobbvika, probably formed a very sheltered environment suitable for the preservation of pumice deposits. No pumice was found, however, at the fairly open bay at Brandsvik, surveyed in 1993, where pronounced beach ridges occur; in contrast to the pumice found at the nearby sheltered valley by Undås (1942) and Dugmore and Sugden in 1989.

- The finding of pumice deposits is usually dependant on some form of erosion exposing the raised beach material. This could be the result of the construction of a road, track, or pipeline, drainage, or erosion caused by a stream or animals. Where the raised beach

sequences are covered in continuous vegetation or have been built upon, the pumice deposits can be concealed.

It now appears doubtful that the description of the three pumice horizons described by Undås (1942) are really divided into a lower black one and two older brown layers, although black pumice is found in greater concentrations at the lower levels. Black and brown pumice was found mixed at several sites, not only in the lower layer, but also at the highest horizon (e.g. Kobbvika). All of the pumice found, however, except for the much older white pumice from Trandvikan, was either black or brown. The white pumice is found at higher altitudes as mentioned by Binns (1971). These inconsistencies in the reported colour of pumice found in the field means that colour alone is not suitable for correlating pumice horizons.

3.2.3 Iceland

Chapter 2 has shown that whilst there are no published records of pumice being found on raised shorelines in Iceland, pumice finds are held by the Náttúrugripasafnið (Museum of Natural History) in Reykjavík. These pumice pieces were found when raised shorelines were being mapped along the Strandasýsla coastline (Strandir) of Vestfirðir (Figure 3.9). One sample was found by Trausti Einarsson (collection number 11235) at Bær on the coast of Hrútafjörður and the other by Hauker Jóhannesson (collection number 11894) at Eyvindarfjörður (Figure 3.9). Unfortunately, no further details about the locations of these finds are available. Eyvindarfjörður was too remote to be reached during this study, but Bær was revisited. Paul Buckland (pers. comm.) has also been found pumice on a beach at Ófeigsfjörður and at a recently abandoned farm site at Reykjarnes (Figure 3.9). Both of these sites were revisited. Recently, Icelandic researchers have worked on the raised shoreline at Bær, on Hrútafjörður, and have studied the pumice found there, although their work was primarily concerned with the *Nucella* ridge, not the pumice deposits (Eiríksson *et al.*, 1998). Shells were also taken for ^{14}C dating and yielded the ages quoted in chapters 1 and 2. This represents the only other work carried out on pumice deposits in this area.

Sheet 1 of the 1:250,000 geological map of Iceland (Náttúrufræðustifnun Íslands and Landmælingar Íslands), shows that much of the coastline shown in Figure 3.9 has been transgressed by the sea during the Holocene. The only areas where raised shorelines are not found, are cliffs. Although it was not possible check the whole coastline, many potential sites along the length of this coastline were visited between 1992 and 1995.

Hrútafjörður area

Hrútafjörður forms a north-south trending fjord, which Vestfirðir separates from the rest of northern Iceland (Figure 3.9). A few scattered small pieces of black and brown pumice were found at Reykjahver, where raised beach material had been disturbed by the construction of a pipeline. The precise height of the pumice deposit is not known, but the related ground surface was estimated to be about 2 metres above present sea-level. No other pumice was found in the surrounding area.

The site of Bær, on the west coast of Hrútafjörður (Figure 3.9) has been subject to several studies in the past, including Bárðarson (1910), Thórarinsson (1955) and John (1974). None of these authors reported finding any pumice. The finding of pumice from Bær in the Náttúrugripasafnið collection and the coincidental work of Eiríksson *et al.* (1998) prompted a visit to the area. The most distinctive raised shoreline feature at Bær is the *Nucella* ridge (Figure 3.10a), which was first studied in detail by Bárðarson (1910). The ridge is named after the shells of *Nucella* sp. which are found in abundance amongst the deposits that make up the ridge. This ridge, dated to around 4000 BP by John (1974) and between 5160 ± 100 and 5390 ± 90 ^{14}C years BP by Eiríksson *et al.* (1998), is about 4 metres above sea-level. Brown and black pieces of pumice are eroding out of the beach ridge into a small stream, the Bæjará. The in situ pumice forms a layer one piece thick, which sits on the seaward side of the ridge and is covered by turf (Figure 3.10b). All of the larger pumice pieces found in situ are brown, whilst most of the eroded pumice are smaller and a mixture of both brown and black pieces (Figure 3.10c). The top of the ridge was 3.1 metres above the reference sea-level, which equates to a height above the high tide of just under 4 metres. The pumice is found about 10 cm below the current top of the ridge. As at many of the pumice sites in Norway, the present day beach was covered with large amounts of flotsam and jetsam.

A search of area around Hvítahlíð (Figure 3.9), a site on Britufjörður, investigated by Hansom and Briggs (1991), failed to find any pumice pieces.

The site at Bær appears to be the only site in the Hrútafjörður area where pumice occurs in any great quantity. Scattered pieces are probably found elsewhere, such as at Reykjahver, although it is possible that the future erosion of a beach ridge by a stream or road may expose more pumice deposits.

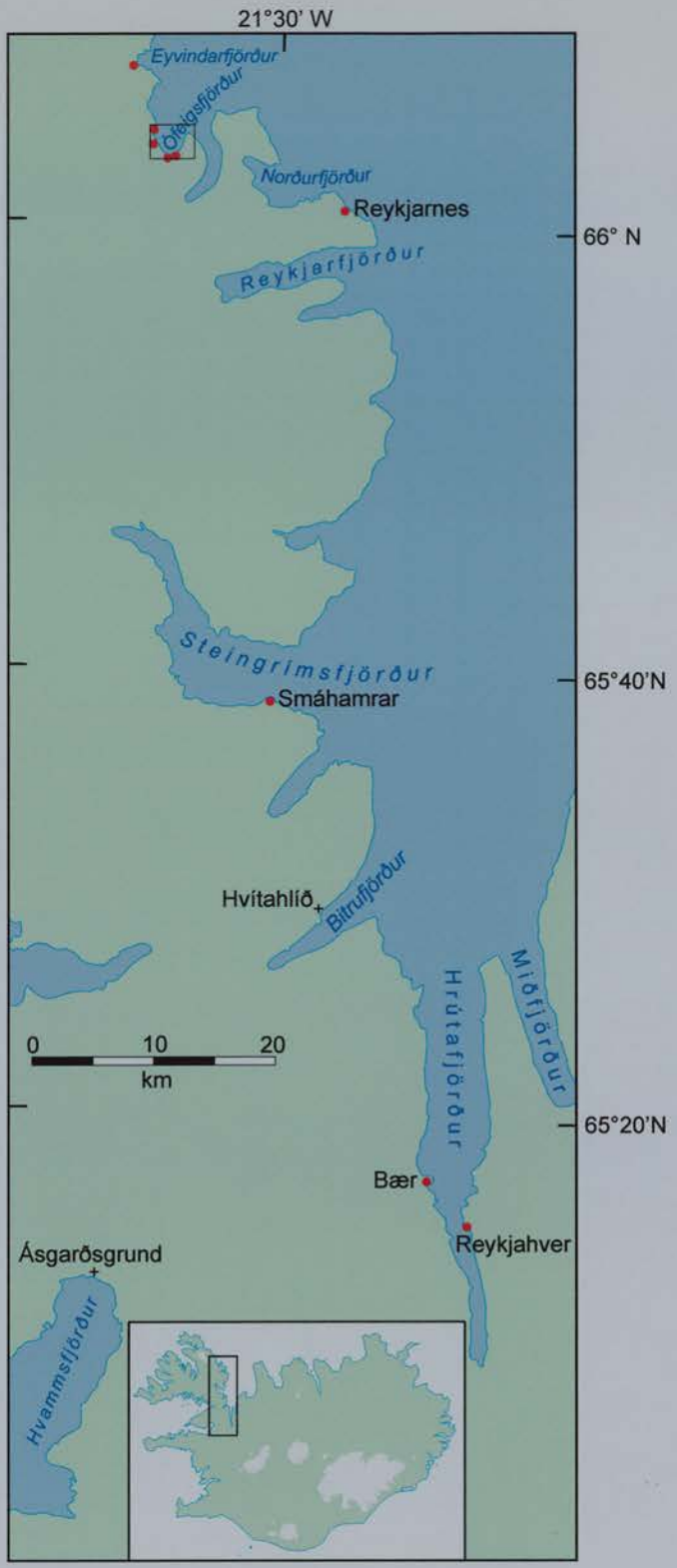

Figure 3.9: The Strandir coast of Vestfirðir and the location of pumice finds and other places mentioned in the text. The box in Ófeigsfjörður shows the location of Figure 3.12.

a)

b)

c)

Figure 3.10 Photographs to show the *Nucella* ridge and pumice at Bær. a) The *Nucella* ridge at Bær forms a distinctive ridge which is cut by several streams (the white arrow shows the location of the pumice deposit). b) shows the brown pumice found on the seaward side of the ridge. Virtually all of the large pebbles are pumice (the knife blade is about 3 cm across). c) shows the pumice being washed out of the banks of the Bæjará (the coin is about 2 cm across)..

Steingrímsfjörður – Norðurfjörður

Hansom and Briggs (1991) also investigated the raised beach sequence at Smáhamrar, where they describe 30 beach ridges between sea-level and an altitude of about 70 metres. The beach ridges, composed of gravel and shells, are separated by swales of peat. An investigation of the lower part of this sequence to an altitude of about 10 metres above sea-level, was aided by the recent construction of two parallel drainage ditches which are cut perpendicular to the beach ridges. Pumice was found associated with two beach ridges at altitudes of between 2.4 and 3.2 metres above reference sea-level (3.5-4.4 metres above high tide). Several very small black and brown pieces were found on these ridges. The direct relationship of these pumice pieces to the ridges is not clear, as the pumice had eroded out of the sides of the ditch and no pumice was found in situ. The small scattered pieces of pumice found at Smáhamrar are in contrast to the numerous larger pieces found at Bær.

Sheltered bays can be found along the coastline between Steingrímsfjörður and Norðurfjörður, but despite a thorough investigation of several of these no pumice was found. This lack of pumice was surprising, considering the amount of driftwood found on many of the present day beaches (Figure 3.11). Some of the raised shoreline were well vegetated, but even where streams cut through them no pumice was found. A single piece of pumice has been found at the recently abandoned farm site at Reykjarnes (Buckland pers. com.). This pumice appears to have been used as a fishing float and was not from a natural site. An impressive sequence of raised beach sequences occur at this site and reach an altitude of about 50 metres above sea-level. A search of both these raised beach ridges and the present day shoreline failed to produce any other pumice finds.

There appear to be few sites between Steingrímsfjörður and Norðurfjörður where pumice pieces can be found on raised shorelines. Smáhamrar, the only site where pumice has been found on raised shorelines only produced a few very small black and brown pieces. The small quantities of pumice found are in contrast to the large amounts of flotsam and jetsam, including driftwood, which occur on the beaches along this stretch of coast.

Figure 3.11: Photograph to show the large quantity of driftwood found on the beaches south of Reykjarfjörður.

Ófeigsfjörður area

The relatively small number of pumice finds along the Strandir coast, contrasts with the pumice which can be found on raised shorelines at Ófeigsfjörður. Figure 3.12 shows that pumice occurs on at least eight sites along the coast of Ófeigsfjörður.

The most striking modern day feature of Ófeigsfjörður is the amount of driftwood and other ocean-transported material found on the raised and present day shorelines (Figure 3.13). So much wood is washed onshore that a temporary (summer) sawmill has been established at the abandoned farm of Ófeigsfjörður. Fishing floats, buoys and plastic fish boxes are also collected and sold to fishermen.

Figure 3.12: Ófeigsfjörður and the location of sites where pumice has been found.

The highest pumice deposits were found at Saxavogur (Site 8), where brown/black pumice was concentrated on two levels, the lower one around 4.7-5.2 metres and the higher between 6.3-6.8 metres above reference sea-level. Black pumice pieces were found in a quarry at Ófriði-Stapavik (Site 1) scattered around the floor of the excavated beach gravel. The pumice was found between 3.2-4.1 metres above reference sea-level, although the possibility of this having been reworked when the quarry was in use, means that these heights should be regarded with caution. A couple of pieces of brown pumice were found at Site 3, close to the shore of Melgraseyrarvatn. The quantity of pumice found at all of the Strandir sites described so far, is tiny compared to the amount of pumice which is found between Site 6 and Site 7 on Hvaláreyrar. The vegetation and soil has been eroded off the raised shoreline between about 2.7 and 4.07 metres above reference sea-level (Figure 3.14). Sitting on the surface of this exposed raised beach are literally thousands of pieces of mainly brown, with some black, pumice (Figure 3.15 and Figure 3.16). Some of the pumice pieces are larger than 10 cm in diameter, whilst others are less than 3 cm. Scattered amongst the mainly brown pumice were also some red pieces. Many pieces are covered in moss and appeared to have been lying on the surface from some time. The lighter grey coloured pumice appears to have been weathered. Small pieces of white pumice occur just above the present day beach at Höfn (site 4), whilst two large (>20 cm) pieces were found in amongst the modern driftwood and on a stone wall.

The vast quantity of pumice found at Ófeigsfjörður is in stark contrast to the relatively small amounts found further south. It was not possible to see if there were similarly large deposits further north, although the find by Jóhannesson shows that some pumice does occur. There appears to be a large pumice horizon which can be found between 2.7-4.1 metres above reference sea-level. This is predominately of brown pumice, but as Figure 3.17 shows. a wide range of colours can be found, although most of these do not look like volcanic pumice. It is not clear whether the other pumice deposits found at about or above 4 metres above reference sea-level (sites 1, 3 and 5) are a continuation of the same deposit or a separate older one. Certainly black pumice pieces are in the majority at Site 1. The pumice at Site 8 appears to be older still. The youngest pumice is found either just on or above the present beach.

Figure 3.13: Photograph to show the driftwood and other material washed up on the shoreline of Ófeigsfjörður. The beach is close to Site 5.

Figure 3.14: Photograph to show the exposed raised shoreline at Site 6. A remnant of the original soil profile (rofbarð) can be seen in the centre of the photograph.

Figure 3.15: Photograph to show pumice scattered over the exposed raised beach at Site 6 (the stick is 1 metre long).

Figure 3.16: Photograph to show black and brown pumice found at Site 6.

Figure 3.17: Photograph to show non-typical coloured pumice found at Ófeigsfjörður. Most of this pumice is unlike any other pumice found on other raised shorelines.

Other areas

Another site, Ásgarðsgrund, studied by Hansom and Briggs (1991) was also visited (Figure 3.9). The *Nucella* ridge again occurs at about 4 metres above sea-level. No pumice was found at this site, or at several other fjords further to the west.

Summary of pumice distribution on Icelandic raised shorelines

Pumice forms a relatively rare deposit on the coast of Strandir, with the exception of Bær and Ófeigsfjörður. Despite this, more pumice has been found on raised beaches here than anywhere else in Iceland. Whilst brown and black pumice deposits predominate (as elsewhere in the North Atlantic), other types of pumice are also found at Ófeigsfjörður. These pieces are, however, comparatively rare, and their presence presumably reflects the relative nearness of potential source area in southern Iceland. Relatively little is known about the sea-level history of this part of Iceland, although the recent work of Eiríksson, Símonarson and Sveinbjörndóttir (1998) is beginning to change this. None of the raised beaches at Ófeigsfjörður have been dated, but Melgraseyrarvatn provides a good opportunity to study sea-level in the area and will be the site of a future study. Only one pumice deposit has been directly dated (Bær) where it appears to be associated with deposits dating from about 5200 ^{14}C years BP. The survey at Ófeigsfjörður was not detailed enough to establish the precise number of pumice deposits. The relative low lying position of the pumice deposits means that they are also susceptible to subsequent reworking during storm events.

3.2.4 Scotland

The only pumice pieces from a natural site in the British Isles analysed during this study are those found at the Bay of Moaness (site 58) on Rousay. As described in Chapter 2 (section 2.2.5) this pumice deposit was found in inter-tidal deposits (-0.6 OD), which although not directly dated, are probably older than 5000 ^{14}C years BP (Buckland *et al.*, 1998).

3.2.5 Summary of new finds from raised shorelines

Pumice pieces from raised shorelines dated to between 9000 and 1700 ^{14}C years BP have been selected for analysis. The majority of the pumice pieces to be analyses are from Norway, which reflects the large number of dated raised shorelines and the numerous pumice pieces found on them. Pumice from raised shorelines in Iceland and a single inter-

tidal site in Scotland will be analysed. The next section describes the geochemical analyses undertaken on the pumice.

3.3 Geochemical analyses: techniques

Geochemical analyses of pumice and associated tephra layers form the major analytical tool in this thesis. Three techniques are used in this study: electron probe microanalyses (EPMA), X-ray fluorescence (XRF) and secondary ion mass spectrometry (SIMS). All of these analyses were undertaken in the Department of Geology at the University of Edinburgh. This section describes the merits and problems of each technique, before section 3.5 presents the results of geochemical analyses of pumice from natural sites.

3.3.1 Electron Probe Microanalysis

The majority of the major element geochemical compositions of the pumice pieces and all of the major element abundances of the tephra layers (Chapter 5) were obtained by EPMA using a Cambridge Instruments Microscan V. One pumice piece, from Trandvikan (T1), was analysed on a Cameca Camebax.. Grain discrete major element EPMA of glass shards have proved invaluable in tephrochronological studies and are now firmly established as the standard technique for analysing the geochemical composition of tephra layers (Larsen, 1981; Westgate and Gorton, 1981). Dugmore et al. (1992) summarise the advantages of using this technique over others, such as analyses of the mineral fraction. The geochemical composition of the glass fraction of a tephra layer is generally representative of the bulk geochemistry of the magma, enabling tephra layers and pumice to be geochemically correlated over large distances (greater than 1000 km) independent of variations caused by grain size and distance from source. Measuring mineral abundances also provides a method of discriminating between different tephra layers (Kittleman, 1979). Relative mineral abundances, however, change with distance from the eruption source, as denser minerals selectively settle from the atmosphere first, leading to a concentration of these minerals in proximal areas (Juvigne and Porter, 1985). This means that correlations over large distance are difficult. Finally, many of the tephra layers studied here do not contain minerals, so that glass fraction analyses is the only option available (e.g. Larsen *et al.*, in press). Grain discrete EPMA analyses of the glass fraction is the most suitable method for analysing the tephra layers, it is also applicable for the analyses of pumice pieces, as they are mainly composed of glass.

EPMA measures the X-ray spectrum emitted by a solid sample, which is bombarded by a focussed beam of electrons to obtain a very localised chemical analysis (Reed, 1995). The major advantage of EPMA over bulk analytical techniques is the grain discrete nature of the analysis. The small diameter of the EPMA electron beam (approximately 8 μm) allows individual tephra layer glass shards to be chosen and analysed. This reduces the risk of contamination and negates the use of complex separation techniques, which are necessary if a pure glass sample is required for bulk analyses such as X-ray fluorescence. Pumice is also composed mainly of volcanic glass, with some mineral phenocrysts and microlites (Chapter 1), which is ideal for EPMA analyses. The presence of vesicles means that extraneous material often becomes trapped and could be incorporated in any bulk samples. EPMA enables clear pieces of glass to be chosen for analysis and areas of glass containing phenocrysts and microlites to be avoided.

As many of the pumice pieces are from archaeological sites and are artefacts showing evidence of use as tools, only small samples could be taken for analysis. A small hole was drilled in the pumice pieces and the pumice fragments were collected. For consistency, the same method was used on all of the pumice pieces. The glass shards produced by this method are often several hundred microns in diameter and allow easy analysis. Some of the tephra samples were sieved and where significant amounts of organic matter was present they were acid digested (Dugmore *et al.*, 1992). The glass shards from tephra layers or pumice were then incorporated into resin (araldite) on a frosted slide. The sample is then cured before being ground to a thickness of 75 μm and then polished with 6 μm and 1μm diamond pastes. This creates a smooth clean surface to be analysed. The reflected light microscope only shows the surface of the slide and cannot identify vesicles or minerals which may occur beneath the surface. The use of glass slides allows the use of transmitted light microscopy to identify areas of glass with no contamination for analysis. The polished slides are coated in a thin layer of carbon (approximately 20 nm; Reed, 1995), which provides a path for incident electrons to flow to ground.

A mixture of simple silicate minerals, pure metal standards and synthetic oxides are used to calibrate the instrument (Table 3.1). The samples were analysed using the wavelength dispersive method (WDS[1]), an accelerating voltage of 20 kV, beam current of 15 nA and a

---

[1] WDS is usually used for quantitative analyses, whilst the ED (energy dispersive) method is often used for qualitative analyses.

beam diameter of about 8 μm, in order to minimise the impact of the mobilisation of the alkalis, especially sodium. The use of a beam current of 15nA, rather than the usual 30nA, reduces alkali mobility and the electron beam was blanked each time the spectrometers moved to their next position. This latter technique reduces the total time the sample is exposed to the electron beam and so decreases the apparent loss of alkalis. The one sample analysed by the Cameca Camebax was analysed using WDS, an accelerating voltage of 20 kV and a beam current of 10 nA. As recommended by Hunt and Hill (1993), sodium and potassium are measured first, followed by silica, which again minimises the impact of alkali mobility on the abundances of other elements, especially silica. It is not possible to blank the beam on the Camebax, but the presence of four spectrometers, rather than two, halves the total analysis time.

Element	Standard material
K	Orthoclase ($KAlSi_3O_8$)
Ca	Wollastonite ($CaSiO_3$)
Ti	Rutile (TiO_2)
Mn	Pure Metal
Fe	Pure Metal
Na	Jadeite ($NaAlSi_2O_6$)
Mg	Periclase (MgO)
Al	Corundum (Al_2O_3)
Si	Wollastonite ($CaSiO_3$)

Table 3.1: The standards used to calibrate the electron microprobe.

Only analyses of pure glass with totals above 95 % and less than 100 % were accepted. Corrections were made for counter deadtime, atomic number effects, fluorescence and absorption using a ZAF correction programme based on Sweatman and Long (1969). A piece of homogeneous andradite (a garnet) was analysed at regular intervals[2], in order to establish the stability of the machine. A summary of the andradite analyses are shown in Table 3.2 and demonstrates that machine conditions remained stable. Only small variations were accepted. These results agree with Reed (1995), who states that microprobe analyses can be expected to achieve an overall analytical accuracy of around ±2%. A small reduction in the precision of the analyses during this study can be expected because of the lower beam current employed, as less X-ray counts are received by the spectrometers, which slightly increases any errors. Table 3.2 demonstrates, however, that despite this consistent results were obtained. The study by Hunt and Hill (1996) showed that both the Microscan V and the Camebax instruments produce comparable and consistent results. In an inter-laboratory

[2] Andradite analyses were carried out at least once an hour and if the results were not within acceptable limits all of the analyses between the last acceptable andradite analyses and the current one were discarded.

test, when analyses of an obsidian sample from several microprobes was compared to XRF and wet chemical analyses, both instruments produced highly reliable and repeatable results (Hunt and Hill, 1996).

Instrument		SiO_2	TiO_2	Al_2O_3	FeO	MnO	MgO	CaO	Total	n
Microscan V	Mean	35.57	0.05	1.73	27.20	0.44	0.09	32.48	97.56	221
	1σ	0.25	0.02	0.04	0.21	0.03	0.02	0.22	0.41	
	RE %	0.70	40.0	2.31	0.77	6.81	22.2	0.68	0.42	
Camebax	Mean	35.28	0.07	1.67	27.25	0.47	0.07	32.30	97.17	5
	1σ	0.20	0.02	0.04	0.08	0.06	0.02	0.10	0.27	
	RE %	0.57	28.57	2.40	0.29	12.77	28.57	0.31	0.28	

Table 3.2: Andradite analyses obtained between 1994-1999. The mean, standard deviation (1σ) and Relative Error (RE %) of analyses obtained during analyses of the pumice and tephra samples used for this study are shown. Note that only 5 analyses are presented for the Camebax. The andradite contains little, TiO_2 and MgO, which results in high relative errors.

Analyses of the glass fraction of tephra layers using the same microprobe conditions, as described above, have been used in several papers which have been published over the last seven years (Boygle, 1998; Dugmore *et al.*, 1995; Dugmore *et al.*, 1992; Dugmore and Newton, 1997; Dugmore *et al.*, 1996; Dugmore *et al.*, in press; Larsen *et al.*, 1999; Larsen *et al.*, in press; Newton and Dugmore, 1993; Newton and Dugmore, 1995; Newton and Metcalfe, 1999; Oldfield *et al.*, 1997; Ortega-Guerrero and Newton, 1998; Turney *et al.*, 1997). This consistency over the period of this project enables confident comparisons between analyses of Icelandic tephra layers from a variety of sources with the analyses of pumice. The results from the EPMA are presented as weight percentage weight (wt %) of an oxide in the sample.

3.3.2 X-ray Fluorescence Analysis

A limited number of X-ray Fluorescence (XRF) analyses are also presented here. Unlike the grain specific EPMA, this is a bulk geochemical analytical tool. Several grams of sample are required. This creates three problems when it comes to establishing the geochemical composition of pumice or tephra layers for correlating spatially separated deposits.

1. If the glass geochemistry of tephra layers is to be established, the glass fraction of the tephra layer has to be separated from any minerals or lithics associated with the tephra, or any contamination. This process is laborious and obtaining a completely pure glass fraction is difficult. It may also be difficult to obtain a large enough sample from a thin tephra layer. XRF analysis does, however, provide the opportunity to establish the

major, trace and rare earth composition of rock samples, including tephra layers and pumice. For this reason some XRF analyses were carried out on pumice pieces for this project. These analyses were only intended to be preliminary analyses and were carried out at the beginning of the project. Although the pumice is mainly composed of glass, there are mineral inclusions within this glass. Removing these inclusions from the pumice is more difficult than removing the minerals from a tephra layer. The pumice needs to be crushed and then the pure glass fragments separated from the rest for analyses. This technique also removes contamination from the pores of the pumice.

2. The bulk nature of the analysis, produces a mean geochemical composition for each pumice piece. There is no indication of the geochemical variability within the glass.

3. Finally, the bulk nature of the analyses means that the analysis is destructive. EPMA only requires a small sample, whilst XRF analysis often requires the destruction of a whole or part of a piece of pumice. This is an unacceptable method of analysing archaeological artefacts. Although some of the early analyses of archaeological pumice were by XRF, the destruction of the pumice pieces meant that this technique was considered unsuitable for most of this study.

For these reasons grain-specific analyses are preferred when correlations between spatially separated deposits have to be made.

For the limited analyses carried out here, the pumice was scrubbed clean in order to remove any loose sand and dirt from the pores of the pumice and was then placed in an ultrasound to dislodge more firmly ingrained contamination.

Pumice pieces were analysed for 10 major and 17 trace elements in the Department of Geology and Geophysics at Edinburgh University using the Philips PW1480 wavelength-dispersive, automatic, sequential X-ray fluorescence spectrometer fitted with a Rh anode side-window X-ray tube. The spectrometer was calibrated using international standard samples (Govindaraju, 1994) and monitors were used to correct the calibration for instrument drift before each batch of samples analysed. Major-element analysis was carried out on fused glass discs prepared by a method based on that of Norrish and Hutton (1969) and described by Fitton *et al.* (1998). Samples were prepared using a flux containing a heavy absorber (La_2O_3) to produce glass discs with a relatively constant matrix composition. The data were corrected for residual matrix effects using theoretical alpha factors (de Jongh, 1973). Pressed powder pellets were used for trace-element analysis. Line overlap

corrections were made using interference factors calculated from international standards and synthetic glass samples at the time of calibration. Data obtained from longer wavelength trace-element lines were corrected for matrix effects using theoretical alpha factors based on major-element concentrations measured on the pressed pellets at the same time. Other trace elements were corrected using the Rh Kalpha Compton scatter peak as an internal standard (Reynolds, 1963).

3.3.3 Secondary Ion Mass Spectrometry

Although EPMA of glass shards is usually sufficient to correlate a tephra layer (Larsen, 1981), enabling the construction of tephrochronological frameworks. there are, however, occasions when major elements are unable to differentiate between different tephra layers and trace element compositions are required. Traditionally this has involved bulk analysis by either XRF or Instrumental Neutron Activation Analysis (INAA). These methods unfortunately require relatively large amounts of material (over 0.5 g), which leads to the problem of separating the volcanic glass from other components of the tephra layer and any extraneous contamination. The need to have a grain discrete method of trace element analysis has been recognised in the last few years. Laser Ablation Inductively Coupled Plasma Mass Spectrometry (LA-ICPMS) has recently progressed from a technique that needed about 0.01 g of volcanic glass, 10-15 grains (Westgate, 1994) to a grain discrete method (Sylvester, 1997).

Another technique available to tephrochronologists is Secondary Ion Mass Spectrometry (SIMS). SIMS analyses are carried out using an ion microprobe, in which a focussed primary ion beam is fired at a sample. Secondary ions, produced by the bombardment of primary ones are extracted and measured in a mass spectrometer. Using SIMS it is possible to measure the abundances of isotopes, trace and ultra-light elements which cannot be analysed by other techniques such as EPMA (Hinton, 1995). Clift and Dixon (1994) established that trace element geochemical data could be obtained from basaltic glass shards using the ion microprobe. As with LA-ICPMS, this is a grain discrete method, allowing suitable glass shards to be chosen for analysis. This allows trace and rare-earth element data to be obtained from both crushed pumice samples and tephra layers. The same slides used for EPMA can be analysed by the ion microprobe, which further enhances the reliability of the method. Clift and Dixon (1994) established that even at low concentrations, good precision is attainable. For example, Nb abundances were obtained with a 5 % error for concentrations of less than 1 ppm. All the ion probe analyses in Clift and Dixon (1994) were

carried out on glass shards with less than 58 % SiO_2. Apart from the analyses published in Clift and Dixon (1994), the only other known SIMS analyses of tephra layers are those of Steve Morton (unpublished) using Quaternary tephra layers from the Southern Ocean. The results presented in this thesis are the first SIMS analyses of tephra layers and pumice from the north-east Atlantic region.

The SIMS analyses were carried out on a Cameca IMS 4f ion microprobe in the Department of Geology at the University of Edinburgh. Samples were prepared as for EPMA, with either pumice fragments or tephra being incorporated into resin on a glass slide. The resin is cured, before being ground to a thickness of 75 μm and then polished with 6 μm and 1μm diamond pastes. The slide is then ground to fit the circular sample holder of the ion probe and then gold coated in a sputter coater, which reduces the amount of charging by allowing ions to flow to ground. A beam of O^- primary ions with a current of 8nA, an accelerating voltage of 10kV and an offset energy of 78 ± 20 eV was employed to produce the secondary ions. The high energy offset reduces molecular interference and the effect of the matrix on the production of secondary ions. The beam diameter was about 25μm. Each analyses involved 10 counting cycles and the mean ratio was calculated as the value for each element. The SRM-610 glass standard was used to standardise the instrument which was then checked against the BCR glass standard. The abundance of all elements were calculated relative to a known concentration of Si, which was obtained by EPMA. Results from the SIMS analyses are presented in parts per million (ppm). The mean errors encountered during this study ranged from 1.15 % for Rb to 0.19 % for Ti.

3.3.4 Summary of geochemical analytical techniques

This section has summarised the various types of analysis which are available for the geochemical analysis of pumice and airfall tephra layers. The grain specific nature of EPMA and SIMS enables the most suitable areas of glass to be analysed. EPMA is now a well established tool for obtaining the major element geochemistry of tephra layers and the instruments used in this study are reliable and consistent. SIMS analysis of tephra layers is a relatively new technique, but it is ideally suited to the analysis of tephra glass shards and pumice fragments. These two techniques form the basis of all of the correlations made during this study. XRF analysis is well established, but the bulk nature of the sample makes it unsuitable for both the analysis of tephra and pumice. The next section describes the geochemical analyses of pumice from raised shorelines in Norway, Scotland and Iceland.

3.4 Geochemical analyses of pumice

Section 3.2 described the location and age of the analysed pumice pieces which were recovered from natural raised beaches, this section presents the results of the analyses. The new geochemical data are compared to existing published results in the next section. the results of the analyses of the pumice from archaeological sites are described in Section 4.4. In total, 388 EPMA were undertaken on 44 pieces of pumice from six Norwegian sites, 227 EPMA analyses on 24 pieces of pumice from Icelandic sites and 36 EPMA analyses of four pumice pieces from one Scottish site. Six XRF analyses were also carried out on pumice from two Norwegian sites. 39 SIMS analyses were undertaken on five pumice pieces from two Norwegian sites, seven SIMS analyses on a piece of pumice from a site in Iceland and 10 analyses from one piece from Scotland.

Many of the analysed pumice pieces from sites or countries are grouped together as an aid to describing their geochemical properties. These groups should only be seen as an aid to description and does not imply that the pumice is from a different eruption or source to the other pumice pieces.

3.4.1 Norway

As EPMA, XRF and SIMS analyses were undertaken on pumice from Norwegian raised shorelines, this section describes each type of analyses in turn. The first two parts describe the major element analyses acquired by EPMA and XRF, whilst the second discusses the trace and rare earth element analyses obtained by XRF and SIMS analysis.

Major Element EPMA Analyses

The vast majority of the analyses show that most of the pumice is silicic and calc-alkaline in composition (Figure 3.18). Although the main group is dacitic with mean SiO_2 abundances of around 65-66 % and mean K_2O of between 2.5 and 3 %, there are a number of analyses with higher and lower amounts of K_2O (Figure 3.18a). The third main group is more silicic (Figure 3.18b). Figure 3.18b shows that the same three groups can be identified on the calc-alkaline tectonic setting ternary diagram (Irvine and Baragar, 1971). A group formed by the majority of analyses, a second group mainly defined by particularly low values of MgO and the third by much higher abundances of MgO. The means and standard deviations of these analyses are presented in Tables 3.3, 3.4, 3.5 and 3.6 and the full analyses are available in Appendix 3.

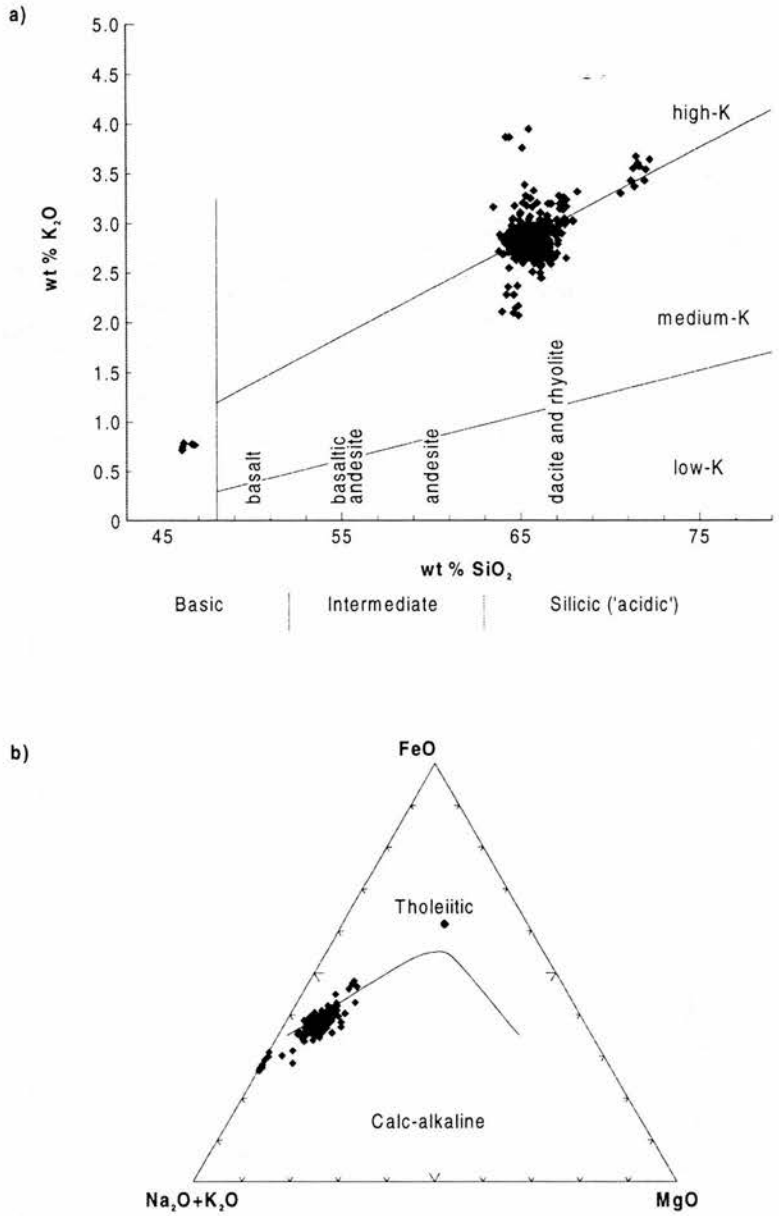

Figure 3.18: Graphs to show that: a) most of the pumice pieces analysed are silicic, with some basic analyses and can be split into at least three distinct groups (based on recommendations of Le Maitre, 1989). b) The majority of the pumice is calc-alkaline, with some tholeiitic analyses. At least three major groups can be identified (based on Irvine and Baragar, 1971). The term acidic has been replaced by silicic in this thesis, as recommended by Dugmore *et al.* (1995), in order to avoid confusion with volcanic aerosols.

Although three distinct groups are obvious from Figure 3.18, there is considerable geochemical variation around the main dacitic group. In order to examine this, the data will be split into each of its distinct groups, which will be discussed in turn. Figure 3.19 identifies the three distinct groups shown in Figure 3.18. A fourth group is also identified (Group 2b) as the scattered analyses around the main Group 2a. Each of these groups will now be discussed in turn.

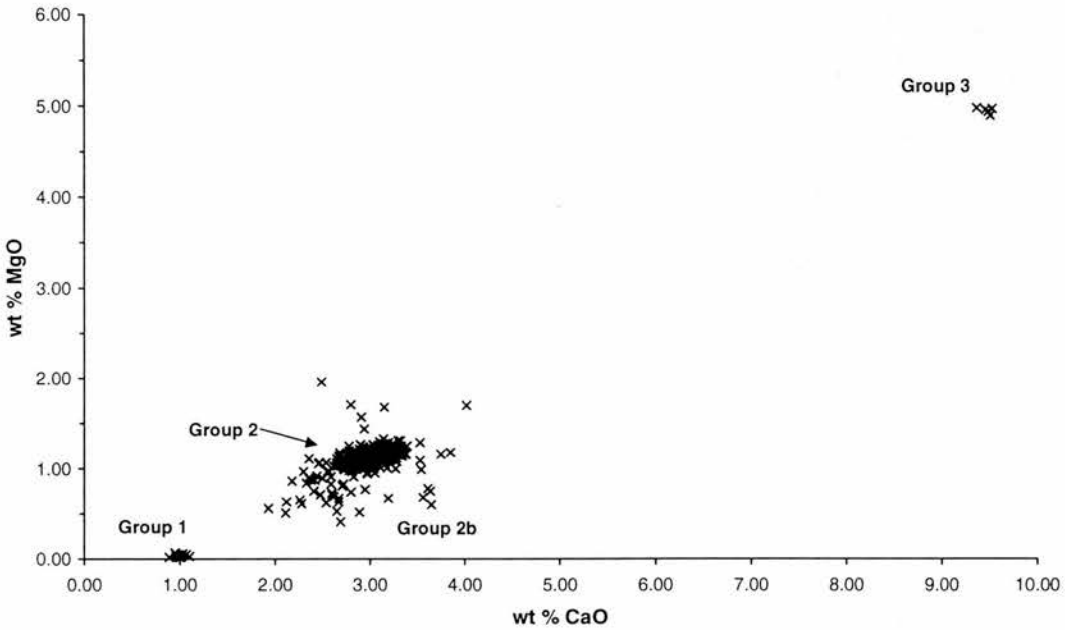

Figure 3.19: Graph (CaO/MgO) to show that at least three main groups can be identified. The first group (Group 1) is defined by low abundances of MgO (less than 0.1%) and CaO (around 1 %); the second most numerous group (Group 2a) is represented by a cluster of analyses around 3-3.3% CaO and just over 1% MgO; the third group (Group 3) is defined by MgO and CaO abundances of around 5% and about 9.5% respectively; a fourth group (Group 2b) is also added, representing the spread of analyses around Group 2a.

Group 1

Figures 3.5 and 3.6 identified a group of rhyolitic analyses with particularly low MgO and CaO abundances. All of these analyses are from the single piece of pumice found at c. 9000 ^{14}C years BP site at Trandvikan on the island of Hitra. Table 3.3 shows the results of the analyses. This piece of pumice is physically different from all of the other Norwegian pumice pieces as it is whitish grey (Figure 3.20), unlike the usual brown or black.

	SiO_2	TiO_2	Al_2O_3	FeO	MnO	MgO	CaO	Na_2O	K_2O	Total
	72.25	0.19	13.49	3.21	0.14	0.02	1.01	4.95	3.64	98.90
	72.03	0.27	13.68	3.21	0.10	0.04	0.97	5.28	3.54	99.12
	71.97	0.19	13.21	3.38	0.06	0.06	1.03	4.42	3.43	97.75
	71.67	0.22	13.52	3.27	0.13	0.07	0.95	5.08	3.57	98.48
	71.58	0.18	13.51	3.30	0.08	0.04	0.96	5.04	3.60	98.29
	71.48	0.23	13.29	3.40	0.08	0.02	1.00	3.86	3.67	97.03
	71.40	0.26	13.84	3.29	0.12	0.05	1.07	5.58	3.37	98.98
	71.33	0.16	13.16	3.18	0.13	0.03	1.10	4.71	3.55	97.35
	71.19	0.19	12.88	3.17	0.08	0.03	0.99	4.68	3.43	96.64
	70.63	0.18	13.03	3.39	0.13	0.02	0.89	4.91	3.30	96.48
Mean	71.55	0.21	13.36	3.28	0.11	0.04	1.00	4.85	3.51	97.90
1σ	0.47	0.04	0.30	0.09	0.03	0.02	0.06	0.48	0.12	0.99

Table 3.3: Analyses, including the mean and standard deviation (1σ) of the white pumice from the site at Trandvikan on Hitra.

Figure 3.20: Photograph of the whitish grey pumice from Trandvikan. The pumice is about 3.5 cm in diameter. The pumice is whiter than it appears on the photograph.

Group 2a

All but eight of the 44 pieces of analysed Norwegian pumice are from Group 2a as defined in Figures 3.5, 3.6 and Table 3.4. Table 3.4 shows that all of these pieces share similar major element geochemical properties. There is little variation between the individual pieces of pumice. Often there is as much variation within a single piece of pumice as between pumice pieces. The pumice from Group 2a typically has weight % abundances of about 65.5% SiO_2, 5.5 % FeO and 3% CaO. The analyses from Kobbvika and Gjøsund are particularly interesting as each site has stratigraphically separated deposits. The other analyses presented

in Table 3.4 are from single deposit sites. Although the EPMA results presented in Table 3.4 are similar there are some differences and these are displayed in CaO/MgO graphs in Figures 3.7, 3.8 and 3.9. Both the means of FeO and CaO show variations between deposits, the standard deviation (1σ) is generally smaller in CaO, which makes it a more suitable oxide to use when trying to identify differences between individual pumice pieces. These graphs only show the means and standard deviations (1σ) of the analyses of each piece of pumice. As a large number of samples are being compared graphically, the use of means and standard deviations allows easier interpretation. All of the Group 3 pumice displayed by the same method, to allow direct comparison. Appendix 3 shows the full analyses from which the mean and standard deviation are derived.

Figure 3.21a shows that all of the Group 2 pumice from c. 6000 ^{14}C year BP site at KVU, Kobbvika, are similar. The only exception being KVU 10, which has lower CaO and MgO, as well as lower TiO_2, FeO and higher SiO_2 (Table 3.4). Although there are some pumice pieces in the main group which do not overlap at 1σ (i.e. KVU 6 and KVU 11), there are other pieces which overlap both of these (e.g. KVU 7), which suggests that these differences represent natural geochemical variation within the deposit. Figure 3.21b shows that the pumice pieces from KVM (c. 4000-5000 ^{14}C years BP) and the single piece from KVL (3000-3300 ^{14}C years BP) generally have lower abundances of both CaO and MgO, although there is considerable overlap between the three deposits. These results suggest that either the two lower deposits are formed from reworking of material from the original upper pumice deposit or were erupted by separate eruptions which produced material with little geochemical variation.

Figure 3.22a compares analyses from the upper and lower deposits from Gjøsund. Most of the pumice pieces show very little variation in their mean values, whilst two from the upper deposit (GJU 2 and GJU 3) have slightly lower abundances of CaO and MgO. Although the differences are small, the analyses from Gjøsund are more similar to the KVU deposit, as they mostly have CaO values of between 3 and 3.2% (Figure 3.21a and Figure 3.22a). Despite this, even at 1σ there is considerable overlap between the pumice pieces between the lower deposits at Kobbvika and the Gjøsund pumice (Figure 3.21b and Figure 3.22a). The upper deposits at both Kobbvika and Gjøsund are both found on the main Tapes shoreline (c. 6000 ^{14}C years BP). Again this suggests that the pumice from the lower deposits is either reworked material from the upper ones or was produced by eruptions with few major element geochemical differences.

a)

Site	Pumice	SiO_2	1σ	TiO_2	1σ	Al_2O_3	1σ	FeO	1σ	MnO	1σ	MgO	1σ	CaO	1σ	Na_2O	1σ	K_2O	1σ	Total	1σ	n
Brandsvik	**BV 1**	65.48	0.81	1.16	0.07	13.90	0.30	5.31	0.19	0.16	0.05	1.08	0.09	2.83	0.12	4.58	0.14	2.89	0.13	97.39	1.21	10
	BV 2	65.30	0.97	1.13	0.06	13.92	0.13	5.05	0.23	0.15	0.03	1.08	0.06	2.87	0.15	4.64	0.10	2.91	0.12	97.06	1.09	10
	BV 3	65.27	0.78	1.14	0.06	13.87	0.23	5.27	0.18	0.14	0.04	1.11	0.08	3.03	0.15	4.65	0.13	2.84	0.09	97.32	1.07	10
	BV 4	65.32	0.44	1.15	0.07	13.95	0.17	5.26	0.29	0.15	0.03	1.15	0.05	3.06	0.09	4.51	0.19	2.87	0.09	97.42	0.48	10
Gjøsund	**GJU 1**	65.90	0.51	1.16	0.07	14.00	0.19	5.60	0.17	0.19	0.19	1.19	0.05	3.24	0.12	4.64	0.11	2.77	0.11	98.68	0.60	10
	GJU 2	65.32	0.39	1.12	0.06	13.96	0.26	5.32	0.19	0.19	0.19	1.08	0.03	2.92	0.15	4.59	0.14	3.01	0.16	97.50	0.63	9
	GJU 3	65.63	0.62	1.14	0.07	14.14	0.43	5.29	0.16	0.18	0.18	1.05	0.07	2.79	0.18	4.62	0.13	2.85	0.09	97.69	0.59	10
	GJU 4	65.10	0.46	1.11	0.09	14.02	0.37	5.61	0.14	0.17	0.17	1.14	0.03	3.12	0.13	4.74	0.15	2.78	0.08	97.78	0.58	9
	GJL 1	65.30	0.73	1.28	0.06	13.81	0.40	5.79	0.17	0.16	0.02	1.14	0.07	3.07	0.16	4.52	0.57	2.76	0.21	97.81	1.03	11
	GJL 2	64.75	0.29	1.25	0.09	13.65	0.12	5.74	0.12	0.18	0.02	1.13	0.04	3.09	0.06	4.36	0.68	2.79	0.08	96.94	0.65	10
	GJL 3	65.52	0.62	1.19	0.06	14.02	0.29	5.57	0.29	0.15	0.03	1.12	0.10	3.07	0.18	4.67	0.12	2.85	0.07	98.16	0.80	10
	GJL 4	65.42	0.55	1.22	0.07	13.99	0.19	5.53	0.27	0.16	0.04	1.15	0.05	3.04	0.21	4.71	0.21	3.02	0.35	98.22	0.66	22
Kobbvika	**KVL 2**	65.10	0.52	1.16	0.09	13.55	0.50	5.59	0.09	0.19	0.04	1.12	0.06	2.92	0.21	4.62	0.42	3.14	0.55	97.40	0.50	7
	KVM 1	65.96	0.12	1.31	0.10	13.72	0.14	5.74	0.29	0.24	0.03	1.16	0.06	2.79	0.16	4.22	0.65	2.83	0.09	97.96	0.58	10
	KVM 2	65.31	0.09	1.27	0.07	13.89	0.42	5.80	0.20	0.19	0.04	1.15	0.06	3.00	0.14	4.53	0.09	2.78	0.11	97.94	0.96	10
	KVM 3	65.53	0.06	1.24	0.07	13.61	0.22	5.70	0.18	0.19	0.02	1.10	0.05	2.95	0.08	4.55	0.13	2.78	0.14	97.65	0.55	10
	KVM 4	65.55	0.05	1.25	0.05	13.78	0.28	5.71	0.17	0.19	0.02	1.05	0.04	2.85	0.13	4.49	0.09	2.86	0.08	97.72	0.62	10
	KVM 5	65.82	0.64	1.20	0.04	13.90	0.15	5.58	0.18	0.19	0.03	1.17	0.05	3.20	0.25	4.35	0.17	2.77	0.06	98.18	0.73	10
	KVU 1	65.58	0.56	1.19	0.05	13.96	0.19	5.42	0.35	0.16	0.02	1.18	0.09	3.09	0.17	4.64	0.13	2.81	0.12	98.03	0.47	12
	KVU 2	65.07	0.38	1.25	0.05	13.99	0.19	5.51	0.26	0.20	0.03	1.23	0.07	3.21	0.09	4.52	0.13	2.78	0.11	97.73	0.39	10
	KVU 3	65.34	1.03	1.18	0.07	13.91	0.20	5.41	0.23	0.19	0.07	1.14	0.08	2.99	0.19	4.61	0.10	2.86	0.10	97.63	0.85	10
	KVU 4	65.17	0.36	1.21	0.05	13.99	0.14	5.51	0.20	0.17	0.03	1.19	0.05	3.09	0.10	4.60	0.10	2.77	0.09	97.70	0.41	10
	KVU 6	65.81	0.42	1.21	0.05	13.97	0.24	5.51	0.21	0.20	0.03	1.15	0.09	3.20	0.04	4.58	0.13	2.77	0.11	98.32	0.48	5
	KVU 7	65.92	0.41	1.27	0.04	13.78	0.11	5.47	0.18	0.17	0.01	1.17	0.04	3.17	0.10	4.59	0.14	2.83	0.11	98.36	0.36	5
	KVU 9	65.89	0.59	1.16	0.06	13.90	0.20	5.62	0.23	0.17	0.04	1.14	0.09	3.05	0.16	4.55	0.07	2.81	0.06	98.28	0.32	5
	KVU 10	66.38	0.63	1.08	0.05	13.80	0.07	5.10	0.19	0.14	0.06	1.00	0.01	2.83	0.08	4.64	0.13	2.82	0.07	97.79	0.65	3
	KVU 11	65.74	1.13	1.24	0.08	13.70	0.13	5.49	0.16	0.17	0.02	1.18	0.12	3.09	0.03	4.61	0.11	2.85	0.07	98.05	1.23	3
	KVU 12	65.40	1.07	1.23	0.03	13.74	0.20	5.61	0.30	0.19	0.03	1.13	0.16	3.19	0.13	4.60	0.11	2.87	0.09	97.94	1.11	3

Site	Pumice	SiO_2	1σ	TiO_2	1σ	Al_2O_3	1σ	FeO	1σ	MnO	1σ	MgO	1σ	CaO	1σ	Na_2O	1σ	K_2O	1σ	Total	1σ	n
	KVU 13	66.24	0.38	1.10	0.05	13.83	0.10	5.24	0.05	0.17	0.02	1.11	0.05	3.02	0.18	4.62	0.15	2.80	0.07	98.13	0.44	3
Ramså	**R 1**	66.24	0.42	1.18	0.06	14.07	0.18	5.40	0.09	0.17	0.03	1.11	0.04	2.97	0.12	5.14	0.16	2.75	0.13	99.03	0.47	10
	R 2	65.62	0.50	1.16	0.08	14.01	0.16	5.60	0.23	0.18	0.03	1.11	0.06	2.75	0.09	5.13	0.12	2.74	0.10	98.30	0.42	10
	R 3	65.45	0.49	1.17	0.06	14.05	0.17	5.60	0.23	0.19	0.03	1.15	0.06	2.96	0.14	4.68	0.15	2.74	0.09	97.99	0.60	10
	R 4	65.16	0.41	1.23	0.04	14.07	0.19	5.65	0.22	0.17	0.03	1.13	0.04	2.96	0.08	4.57	0.14	2.77	0.07	97.72	0.55	10
Storvik	**ST 2**	65.65	0.88	1.21	0.07	13.99	0.14	5.51	0.25	0.19	0.03	1.15	0.05	2.97	0.10	4.81	0.19	2.74	0.10	98.22	0.60	10
	ST 3	66.14	0.68	1.23	0.07	14.06	0.16	5.50	0.16	0.20	0.03	1.10	0.04	2.96	0.10	4.70	0.15	2.71	0.06	98.59	0.66	10
	ST 4	65.74	0.72	1.22	0.09	14.07	0.32	5.65	0.18	0.18	0.02	1.14	0.04	3.05	0.10	4.31	0.75	2.72	0.13	98.09	0.93	9

b)

		SiO_2	TiO_2	Al_2O_3	FeO	MnO	MgO	CaO	Na_2O	K_2O	Total	n
Group 2a	Mean	65.50	1.20	13.93	5.51	0.18	1.13	3.01	4.62	2.83	97.89	325
	1σ	0.67	0.08	0.26	0.27	0.04	0.07	0.18	0.31	0.18	0.82	

Table 3.4: a) shows the means and standard deviations (1σ) of the Group 2a pumice pieces from five raised beach sites in Norway. b) shows the means and standard deviations (1σ) of all 326 analyses. The number of analyses are also shown (n) and full details about these analyses are available in Appendix 3.

a)

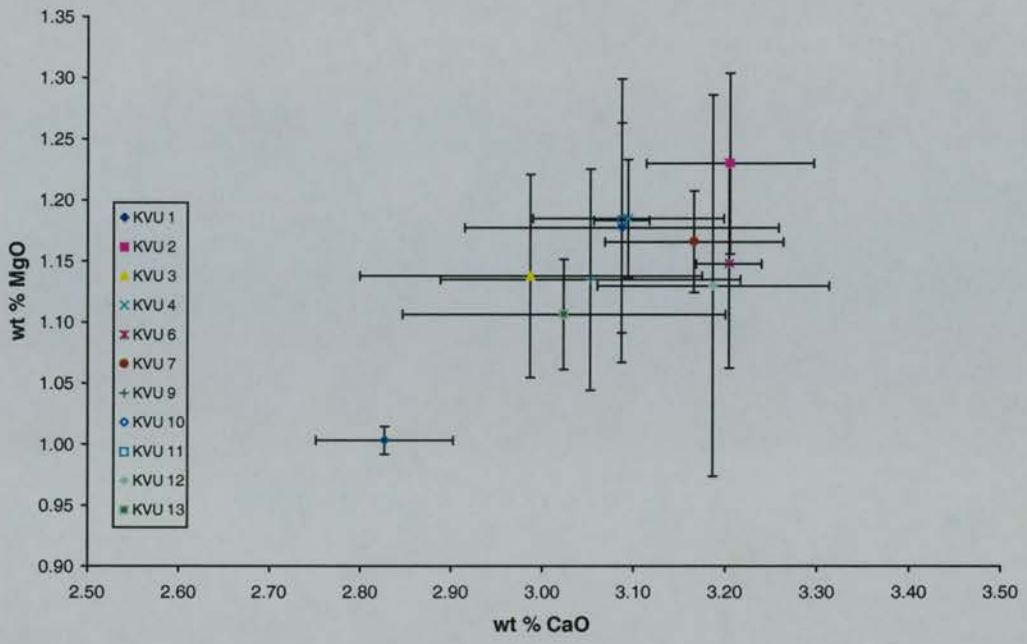

b)

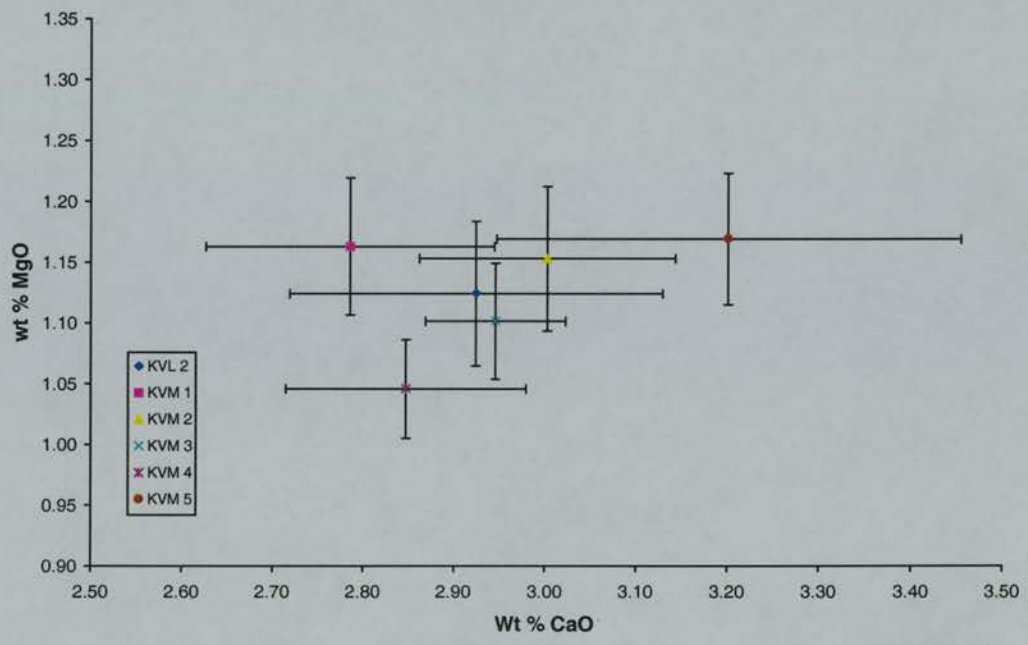

Figure 3.21: Graphs (CaO/MgO) to compare the analyses of the Group 2a pumice from Kobbvika. Pumice pieces from KVU (graph a) tends to have slightly higher abundances of CaO than the pumice from KVM and KVL (graph b). There is considerable overlap between the analyses in the two graphs. The points show means ± 1 standard deviation.

a)

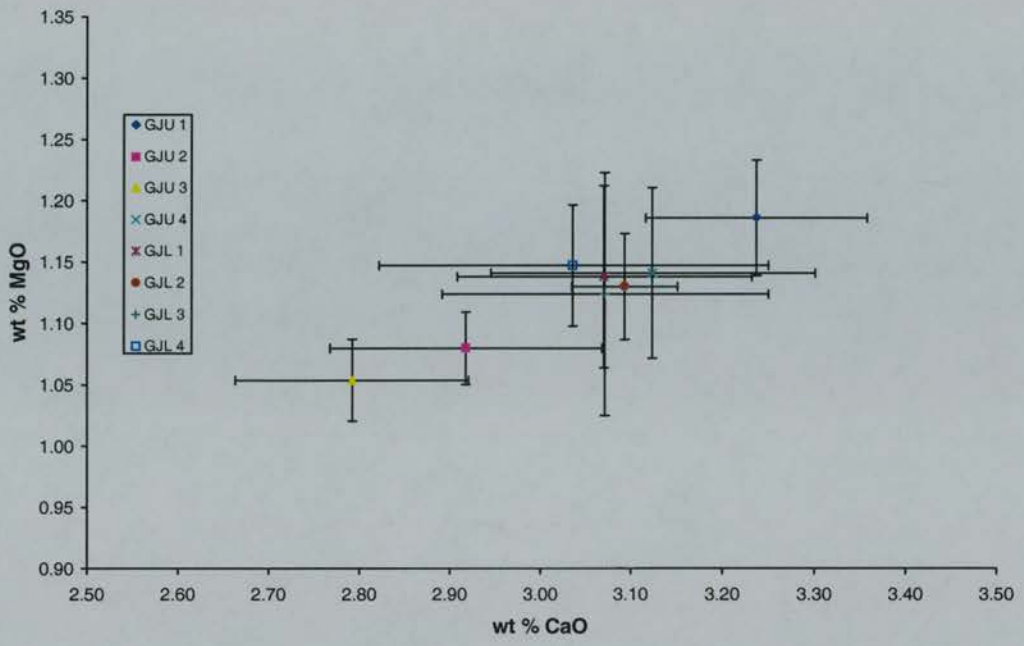

b)

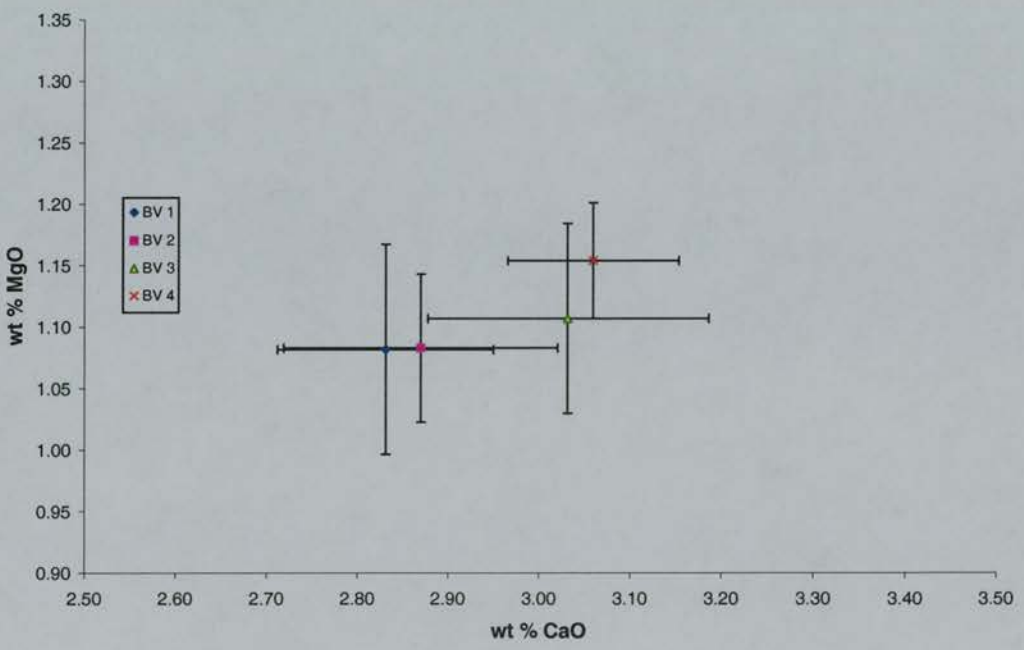

Figure 3.22: Graph (CaO/MgO) to compare the analyses of Group 2a pumice from the two deposits at Gjøsund (graph a) and Brandsvik (graph b). There is no significant difference between the analysed pumice pieces from the two deposits at Gjøsund (graph a). Similarly the Brandsvik pumice shows two groups, but these also overlap. The points show means ± 1 standard deviation.

a)

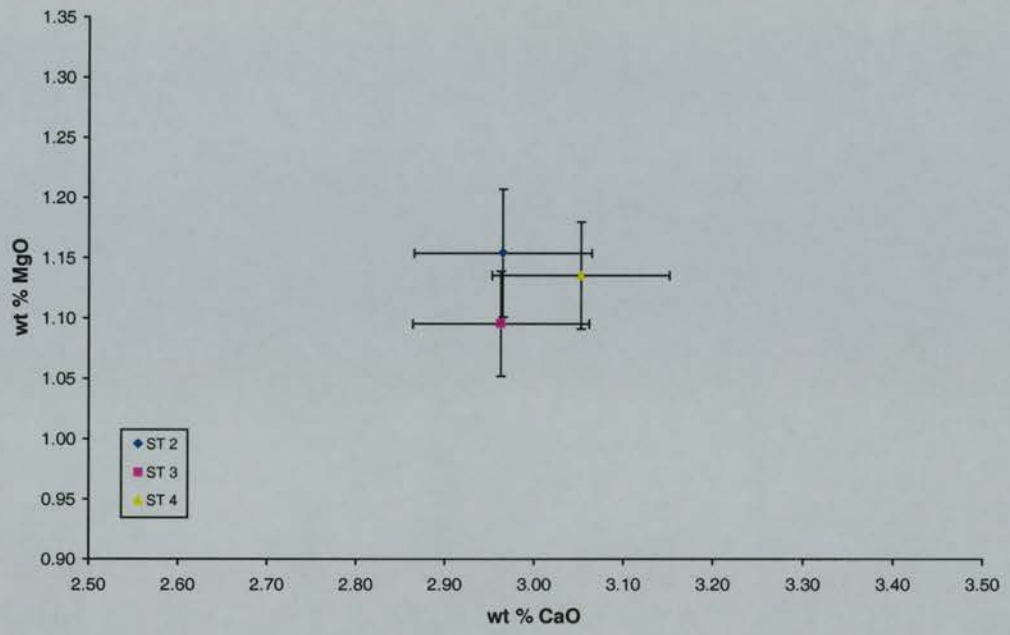

b)

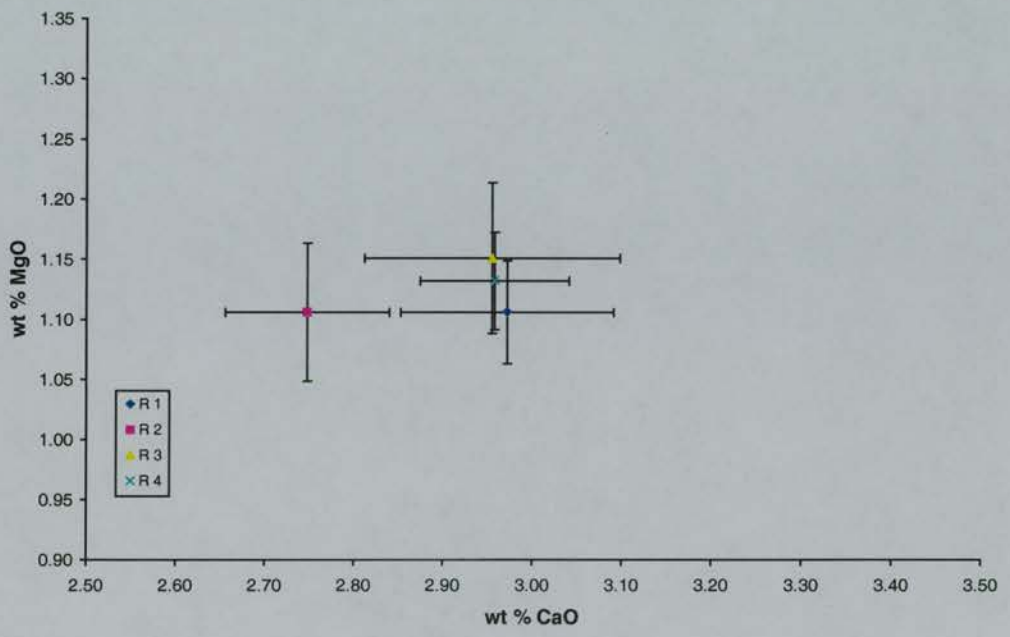

Figure 3.23: Graph (CaO/MgO) to compare the analyses of Group 2a pumice from Storvik (graph a) and Ramså (graph b). Both of these deposits have very similar pumice pieces, with the exception of a single piece from Ramså (R 2), which has slightly lower abundances of CaO. The points show means ± 1 standard deviation.

Figure 3.22b shows that the four pieces of pumice from Brandsvik form two groups, defined by variations in CaO, both of which overlap. BV 3 and BV 4, both of which have slightly higher CaO abundances, are most similar to the upper pumice deposit from Kobbvika. Again these correlations are not significant as there is considerable overlap between the various pumice pieces from the different deposits. The pumice from Brandsvik is of a similar age to that from the upper deposits at Kobbvika and Gjøsund.

The three pieces of pumice from Storvik, shown in Figure 3.23a show little geochemical variation. Figure 3.23b shows that three of the four pumice from Ramså are also very similar, whilst R 2 has lower abundances of CaO, although this is not shown in the other oxides (Table 3.4). The main group of pumice from Ramså is indistinguishable from the pumice from Storvik and is most similar to some of the analyses of pumice from the lower pumice deposits at Kobbvika. The Ramså pumice is from a shoreline about 1300 ^{14}C years younger than the pumice from Storvik and the lower deposits at Kobbvika and Gjøsund.

The EPMA of the Group 2a pumice show that it is not possible to identify consistent geochemical characteristics between the upper and lower deposits at Gjøsund and Kobbvika. The upper deposit at Kobbvika dominated by pumice with slightly higher abundances of CaO, whilst no such pattern can be identified in the upper Gjøsund pumice. It appears that the analysed pumice was either produced from the product of a single eruption, which has been subsequently reworked or that a series of eruptions produced the pumice, but major element geochemical variations are insufficient to enable these separate events to be identified.

Group 2b

Although the pumice in Group 2b is similar to Group 2a, it has a more variable geochemical composition. The Group 2b pumice is identified by generally lower mean FeO, MgO and CaO abundances compared to the dacitic pumice from Group 2a . With the exception of the pumice piece KVU 8, all of the pieces in Group 2b also have large standard deviations (Table 3.5). Figure 3.24 shows that there is little significant geochemical variation between the pumice in Group 2b, with the exception of KVU 8, which shows less geochemical variation and lower mean CaO (Table 3.5). The majority of the pumice pieces in Group 2b are from the lower (c. 3300-3000 ^{14}C years BP) pumice deposit at Kobbvika (KVL), with other two pieces from the similar age deposit at Storvik and the older KVU shoreline. The differences between the two groups (2a and 2b) is due to the phenocrysts found within the

glass. Figure 3.25 shows a light microscope image of these feldspar phenocrysts compared to phenocryst free glass. The presence of these phenocrysts means that it is nearly impossible to find clear areas to analyse. The resulting partial analysis of glass and mineral results in variable geochemical analyses which do not allow these pumice pieces to be correlated with other deposits. The most obvious result of this is apparently elevated Al_2O_3 abundances (Ortega-Guerrero and Newton, 1998). The presence of the phenocrysts is in itself interesting and may reflect a slower cooling history for this pumice compared to the majority of the pumice, which was quenched quickly and there was little time for large crystals to develop. Post-depositional alteration of the pumice glass seems unlikely, as these deposits are relatively young and previous evidence suggests that weathering of glass in northern European temperate climates is not an issue with Holocene deposits (Dugmore *et al.*, 1992).

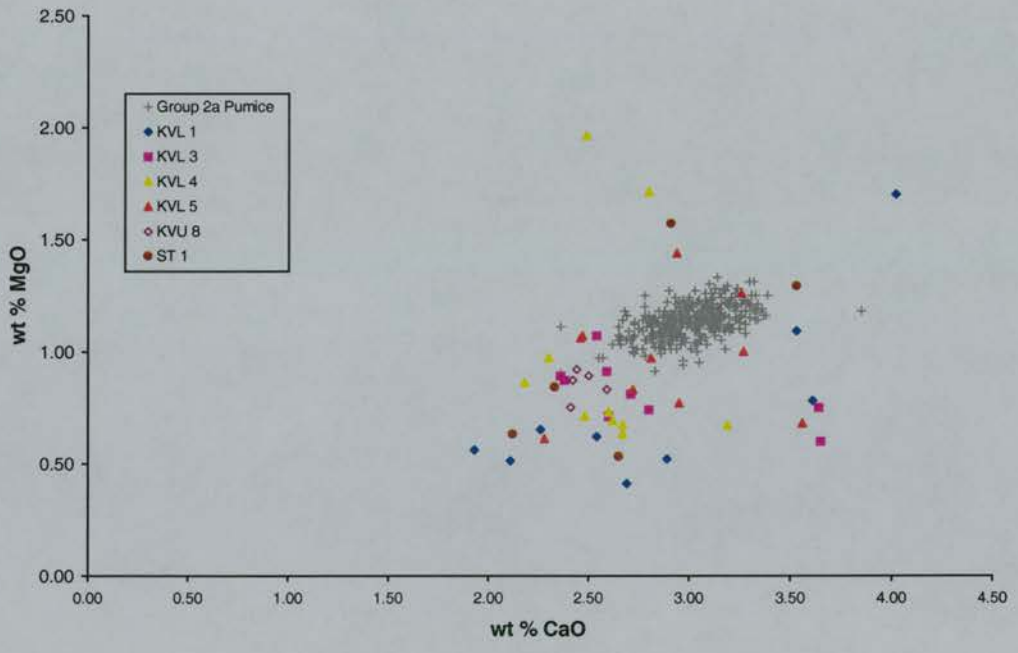

Figure 3.24: Graph (CaO/MgO) which illustrates the lower mean MgO and CaO abundances which distinguish the Group 2b from the Group 2a pumice. There is also considerable overlap between the two groups because of the large spread of most of the Group 2b analyses.

a)

Site	Pumice	SiO_2	1σ	TiO_2	1σ	Al_2O_3	1σ	FeO	1σ	MnO	1σ	MgO	1σ	CaO	1σ	Na_2O	1σ	K_2O	1σ	Total	1σ	n
Kobbvika	**KVL 1**	66.59	1.33	1.21	0.11	13.75	0.72	5.27	0.90	0.18	0.05	0.76	0.43	2.75	0.72	4.98	0.38	2.83	0.42	98.31	0.87	8
	KVL 3	66.09	1.09	1.16	0.19	14.01	1.47	5.03	0.65	0.20	0.04	0.82	0.14	2.81	0.49	4.84	0.47	2.77	0.38	97.73	0.63	9
	KVL 4	66.47	0.95	1.18	0.15	13.70	1.06	5.34	0.71	0.21	0.05	0.98	0.43	2.77	0.48	4.62	0.45	2.89	0.34	98.16	0.62	10
	KVL 5	65.99	1.09	1.13	0.13	13.73	1.20	5.14	0.52	0.20	0.04	0.97	0.26	2.87	0.41	4.60	0.31	2.89	0.20	97.55	0.99	10
	KVU 8	67.19	0.67	1.08	0.07	13.76	0.09	4.86	0.10	0.14	0.03	0.85	0.07	2.47	0.07	4.55	0.12	3.03	0.05	98.13	0.74	5
Storvik	**ST 1**	66.81	1.23	1.19	0.14	13.59	0.83	5.61	0.50	0.19	0.05	0.97	0.44	2.71	0.55	4.94	0.52	2.95	0.39	98.97	0.58	5

b)

		SiO_2	TiO_2	Al_2O_3	FeO	MnO	MgO	CaO	Na_2O	K_2O	Total	n
Group 2b	Mean	66.44	1.16	13.76	5.19	0.19	0.89	2.74	4.75	2.88	98.03	47
	1σ	1.09	0.15	1.06	0.69	0.05	0.33	0.47	0.45	0.33	0.83	

Table 3.5: a) shows the means and standard deviations (1σ) of the Group 2b pumice pieces from five raised beach sites in Norway. b) shows the means and standard deviations (1σ) of all 47 analyses. The number of analyses are also shown (n) and full details about these analyses are available in Appendix 3.

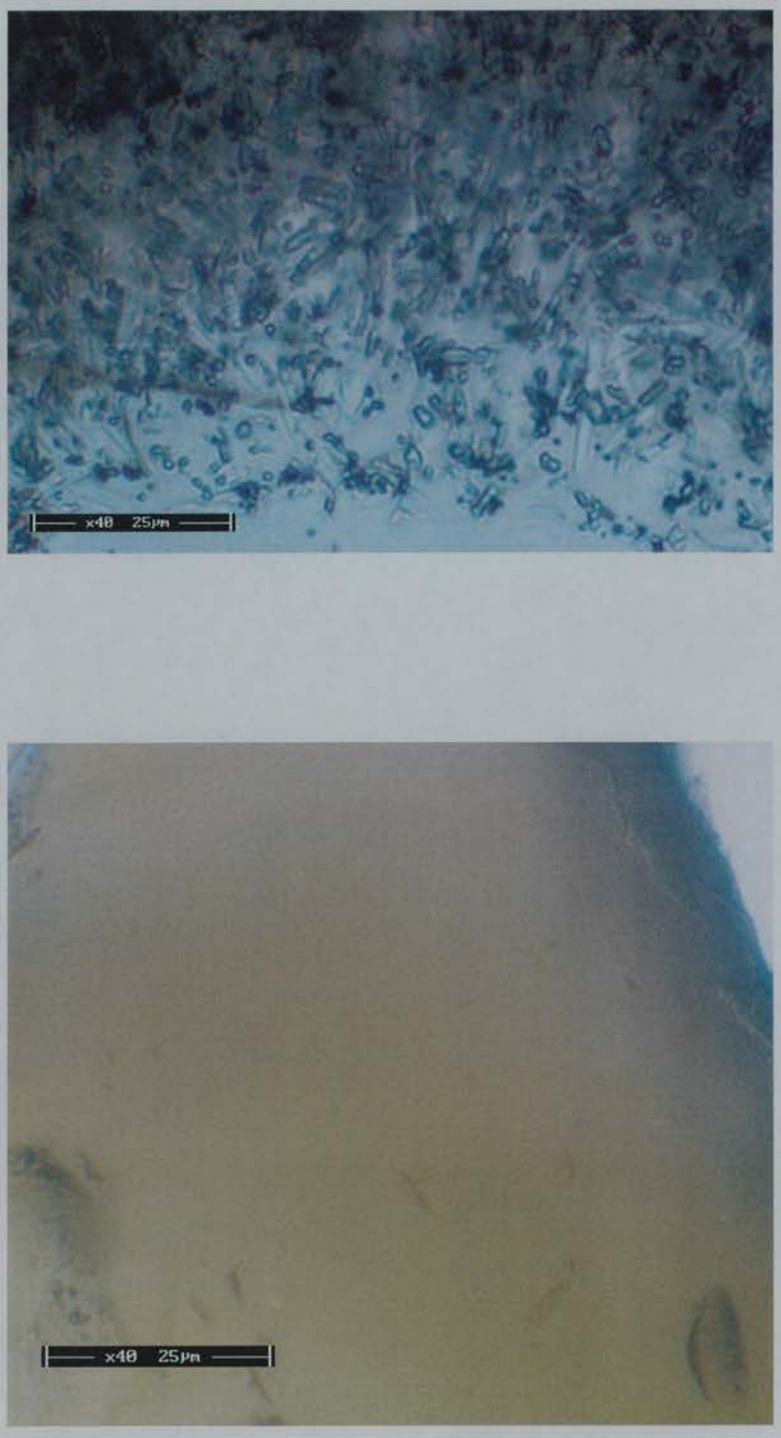

Figure 3.25: Light micrographs to show the difference between the phenocryst rich and poor pumice. a) shows a thin section of the KVL 1 and illustrates the large number of phenocrysts present. KVL 2 (Group 2a) is composed of virtually phenocryst free glass.

Group 3

Group 3 is represented by a single piece of black pumice from the c. 6000 ^{14}C years BP upper pumice deposit at Kobbvika. This piece of pumice is the only basaltic piece found in any of the pumice deposits during this study. This piece of pumice has particularly high TiO_2 abundances.

	SiO_2	TiO_2	Al_2O_3	FeO	MnO	MgO	CaO	Na_2O	K_2O	Total
	46.12	4.56	12.42	14.37	0.20	4.97	9.47	3.23	0.75	96.09
	46.19	4.77	12.40	14.53	0.22	4.98	9.54	3.21	0.79	96.63
	46.79	4.64	12.33	14.27	0.26	4.95	9.50	3.26	0.77	96.78
	46.09	4.63	12.47	14.38	0.23	4.99	9.38	3.29	0.72	96.20
	46.65	4.48	12.32	14.40	0.23	4.91	9.52	3.23	0.78	96.53
Mean	46.37	4.62	12.39	14.39	0.23	4.96	9.48	3.24	0.76	96.45
1σ	0.33	0.11	0.06	0.09	0.02	0.03	0.06	0.03	0.03	0.29

Table 3.6: The analyses of the basaltic black pumice piece, KVU 5, from Kobbvika.

Major Element XRF Analyses

Six XRF major element analyses were undertaken on pumice from Brandsvik and the upper two deposits at Kobbvika (Table 3.7). Table 3.7 shows that the XRF analyses are similar to the EPMA of Groups 2a and 2b, but unfortunately the bulk nature of XRF analyses means that they mask the heterogeneity revealed by the earlier EPM results.

a)

Site	Pumice	SiO_2	TiO_2	Al_2O_3	FeO*	MnO	MgO	CaO	Na_2O	K_2O	P_2O_5	Total
Kobvikka	**KVL 5**	65.66	1.25	13.98	5.43	0.18	1.14	3.03	4.76	2.62	0.26	98.31
	KVM 5	64.04	1.29	14.24	5.79	0.17	1.10	2.99	4.61	2.58	0.34	97.15
	KVU X1	64.37	1.21	14.22	5.60	0.17	1.09	3.06	4.88	2.79	0.31	97.70
Brandsvik	**BV 1**	63.54	1.38	13.87	7.24	0.34	1.25	3.15	4.60	2.57	0.30	98.24
	BV 2	64.88	1.30	14.00	6.07	0.21	1.20	3.18	4.71	2.61	0.29	98.45
	BV 4	64.53	1.29	13.93	6.33	0.24	1.18	3.14	4.64	2.62	0.30	98.20

b)

	SiO_2	TiO_2	Al_2O_3	FeO	MnO	MgO	CaO	Na_2O	K_2O	P_2O_5	Total	n
Mean	64.50	1.29	14.04	6.08	0.22	1.16	3.09	4.70	2.63	0.30	98.01	6
1σ	0.73	0.06	0.15	0.66	0.07	0.06	0.08	0.11	0.08	0.03	0.49	

Table 3.7: a) Major element XRF analyses of Norwegian pumice. FeO* is calculated from the original Fe_2O_3 in order to allow comparison with the EPMA (FeO = Fe_2O_3/1.1113). b) shows the means and standard deviations of the XRF analyses.

Five of the six analyses were carried out on pumice pieces which were also analysed by EPMA. These results are shown in Table 3.8. All of the XRF analyses have lower SiO_2 and K_2O compared to the EPMA. Abundances of TiO_2 and of FeO in particular are higher in the XRF analyses. The FeO abundances in the Brandsvik are significantly higher than the EPMA. This lack of consistency between the two types of analyses means that it is not possible to determine precise correlations using a combination of the techniques. Whilst the two types of analyses can used to decide if the pumice pieces are similar, any small differences will be hidden by the inherent differences between them. These differences are probably mainly due to minerals present within the glass of the pumice and contamination in the pores of the pumice. The comparison of XRF and EPMA major element analyses are discussed in more detail in Chapter 4.

a)

		SiO_2	1σ	TiO_2	1σ	Al_2O_3	1σ	FeO	1σ	MnO	1σ	MgO	1σ	CaO	1σ	Na_2O	1σ	K_2O	1σ	Total	1σ	n
KVL 5	EPMA	65.99	1.09	1.13	0.13	13.73	1.20	5.14	0.52	0.20	0.04	0.97	0.26	2.87	0.41	4.60	0.31	2.89	0.20	97.55	0.99	10
	XRF	65.66		1.25		13.98		5.43		0.18		1.14		3.03		4.76		2.62		98.31		
KVM 5	EPMA	65.82	0.64	1.20	0.04	13.90	0.15	5.58	0.18	0.19	0.03	1.17	0.05	3.20	0.25	4.35	0.17	2.77	0.06	98.18	0.73	10
	XRF	64.04		1.29		14.24		5.79		0.17		1.10		2.99		4.61		2.58		97.15		

b)

		SiO_2	1σ	TiO_2	1σ	Al_2O_3	1σ	FeO	1σ	MnO	1σ	MgO	1σ	CaO	1σ	Na_2O	1σ	K_2O	1σ	Total	1σ	n
BV 1	EPMA	65.48	0.81	1.16	0.07	13.90	0.30	5.31	0.19	0.16	0.05	1.08	0.09	2.83	0.12	4.58	0.14	2.89	0.13	97.39	1.21	10
	XRF	63.54		1.38		13.87		7.24		0.34		1.25		3.15		4.60		2.57		98.24		
BV 2	EPMA	65.30	0.97	1.13	0.06	13.92	0.13	5.05	0.23	0.15	0.03	1.08	0.06	2.87	0.15	4.64	0.10	2.91	0.12	97.06	1.09	10
	XRF	64.88		1.30		14.00		6.07		0.21		1.20		3.18		4.71		2.61		98.45		
BV 4	EPMA	65.32	0.44	1.15	0.07	13.95	0.17	5.26	0.29	0.15	0.03	1.15	0.05	3.06	0.09	4.51	0.19	2.87	0.09	97.42	0.48	10
	XRF	64.53		1.29		13.93		6.33		0.24		1.18		3.14		4.64		2.62		98.20		

Table 3.8: Comparison of pumice pieces from three sites which were analysed both by both EPMA and XRF. The means, standard deviations and the number of the EPMA are shown. a) Two pumice pieces from Kobbvika. b) Three pumice pieces from Brandsvik.

Trace and Rare Earth SIMS Analyses

39 SIMS analyses were carried out on three pumice pieces from Kobbvika and two pieces from Gjøsund (Table 3.9). Pumice from these two sites were chosen as the deposits are on stratigraphically separate levels. Table 3.9 shows that all of the analysed pumice have similar trace element compositions, although there are some significant differences. The most striking differences can be seen in the concentration of Ti in the samples. Ti was also measured as TiO_2 by EPMA (see above) and the SIMS analyses seem to show greater variations between pumice pieces (Figure 3.26). This allows differences between the pumice pieces to be identified. Both SIMS analyses and EPMA show that KVL 1 has a wide geochemical range and this is probably the result of the phenocrysts found in the glass as discussed above. Figure 3.26a shows that KVM 1 forms a distinct group and does not overlap with any of the other pieces. GJU 1 and KVU 3 are the most similar, although KVU 3 has slightly lower Ba than GJU 1 (Figure 3.26 and Table 3.9). Finally, the only major differences between GJU 1 and GJL2 are the higher Ti and Sr found in GJL 2.

These results confirm the conclusions obtained by studying the EPMA. All of the pumice is from the same source. The upper levels of pumice from Kobbvika and Gjøsund have similar geochemical characteristics. KVM 1, which has significantly lower CaO (Figure 3.21) also forms a separate group from the other pumice analysed by SIMS. The relationship of the lower pumice deposits from Kobbvika and Gjøsund is not clear, as GJL 2 does not have the spread of data of KVL 1 or the higher Ti abundances of KVM 1. From these results it is not possible to confirm that geochemical differences seen in the pumice at the two sites and different levels is the result of geochemical variation between different eruptions or within a single eruption. The consistent geochemical variation of KVL pumice suggests that this pumice was probably erupted from a separate event. Ideally it would have been preferable to have analysed more pumice pieces from each level by SIMS to investigate the trace and rare earth variations identified by these results. There does appear, however, to be less overlap between the analyses of the individual pumice pieces (Figure 3.26) analysed by SIMS.

	Tephra	Ti	1σ	Rb	1σ	Sr	1σ	Y	1σ	Zr	1σ	Nb	1σ	Ba	1σ	La	1σ	Ce	1σ	n
Kobbvika	**KVU 3**	5694	163	41	3.3	244	37.6	54	1.5	724	24.1	90	3.6	478	9.6	63	1.0	135	2.8	**7**
	KVM 1	6072	77	43	1.2	238	9.8	56	2.3	762	16.9	97	3.5	493	17.4	66	3.4	141	7.3	**6**
	KVL 1	6057	405	46	4.3	212	57.7	56	2.8	816	40.0	100	5.3	502	16.5	67	2.5	144	5.9	**10**
Gjøsund	**GJU 1**	5668	46	42	1.3	231	7.3	55	1.1	745	13.4	95	1.9	487	13.4	65	1.6	138	4.1	**7**
	GJL 2	5881	61	40	2.1	248	3.6	55	1.5	743	12.3	92	1.7	482	10.8	65	1.8	140	3.8	**9**

Table 3.9: Means and standard deviations (1σ) of the SIMS analyses of pumice from raised shorelines in Norway. Full analyses are available in Appendix 3.

a)

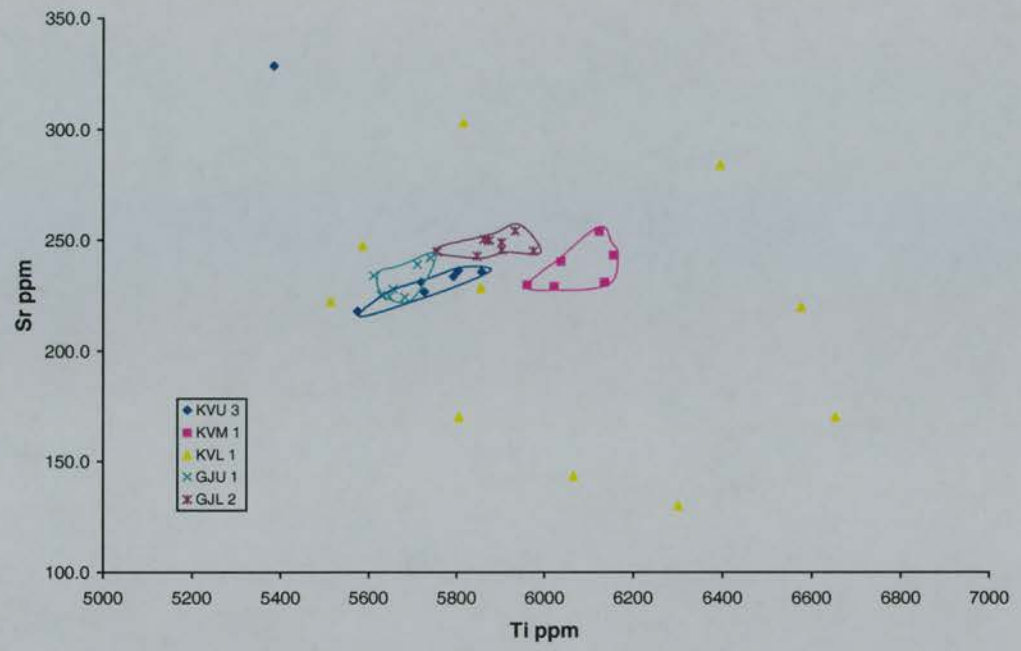

b)

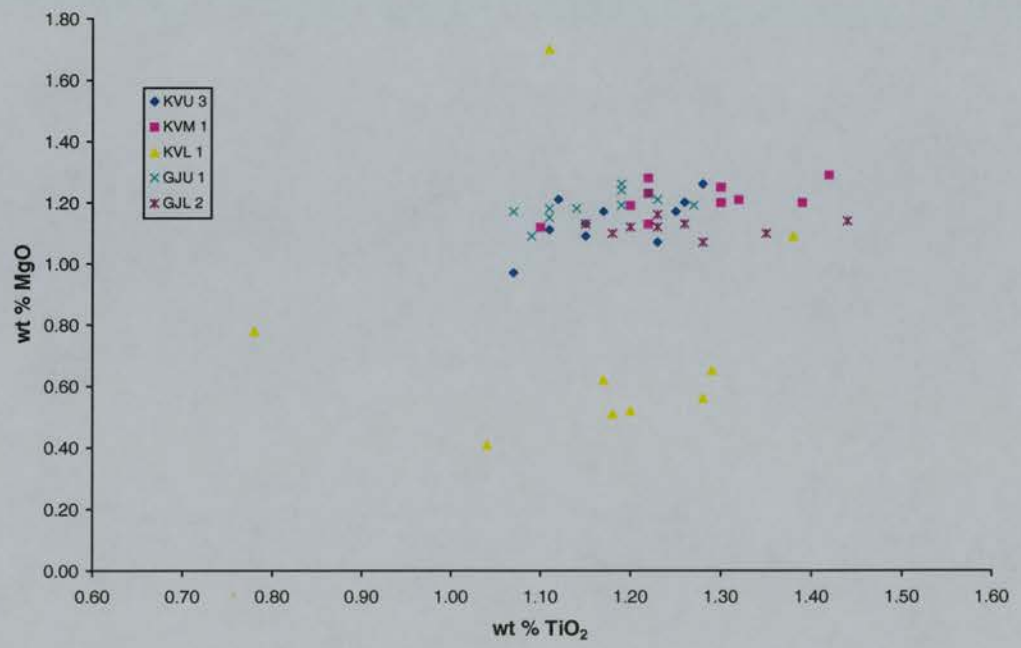

Figure 3.26: Graphs which compare the Ti and TiO_2 abundances produced by SIMS (a) and EPMA (b). The SIMS analyses "pull" the individual pumice pieces apart and enable differences between them to clearly identified. One extreme SIMS analysis of KVU 3 is not included in the main group and probably the results of the accidental analysis of part of a mineral inclusion.

Trace and Rare Earth XRF Analyses

Trace and rare earth XRF analyses were undertaken on six pumice pieces from Kobbvika and Brandsvik (Table 3.10a and b). These analyses were undertaken on the same pieces of pumice as the major element XRF analyses describe above. The lighter elements Sc, V and Cu show considerable variation between the pumice pieces (Table 3.10a). As with the major element XRF analyses, these analyses are bulk samples, one analysis per pumice piece, no indication is given on the homogeneity of the pumice. This problem of XRF analyses is a major drawback to their use as a correlative tool. It is possible to say that the all of the pumice pieces analysed are from the same source, as their trace and rare earth composition is similar and although the lighter elements show some variation, the heavier trace and rare earth elements show minimal variation.

What is particularly interesting are the differences between the XRF and SIMS analyses. The SIMS analyses, like the EPMA, are point analyses, where the best (non-contaminated) glass is chosen for analysis. Even with SIMS, the above discussion highlighted the problems of accidentally analysing inclusions within the glass. Table 3.10c shows the means and standard deviations (1σ) of the SIMS analyses and allows comparison of the two techniques. There are some significant differences between the two techniques, which questions the validity of comparing trace element data of pumice acquired by SIMS and XRF. Particularly striking is the higher Rb, Sr, La, Ce found in the XRF analyses compared to the SIMS analyses (Table 3.9 and Table 3.10). Other elements, however, such as Zr, Ba and Nd show little or no significant variations between the two types of analyses. The conclusion has to be drawn that in this particular case it is not possible to use the SIMS and XRF data together to correlate pumice deposits. A comparison of XRF and SIMS analyses of archaeological pumice will be discussed in Chapter 4.

a)

Site	Pumice	Sc	V	Ni	Cu	Zn	Rb	Sr	Y	Zr	Nb	Ba	La	Ce	Nd	Pb	Th
Kobbvika	KVL 5	9.4	13.7	2.6	2.9	153.6	61.5	318.8	80.9	784.3	103.1	474.5	72.2	162.1	82.4	9.4	8.5
	KVM 5	5.2	23.8	3.0	7.4	155.4	61.6	321.4	76.3	742.3	101.6	513.0	73.1	176.8	84.3	21.1	10.3
	KVU X1	4.0	27.6	3.0	4.4	149.3	65.1	312.2	76.1	733.4	97.3	573.2	77.0	166.8	83.9	10.5	8.1
Brandsvik	BV 1	7.3	51.7	2.7	6.4	160.2	60.7	318.0	78.1	750.9	112.4	505.8	79.0	171.1	75.6	11.6	9.4
	BV 2	6.9	38.1	3.0	6.9	152.3	62.9	305.9	79.8	764.1	105.9	472.1	63.9	164.6	78.5	7.7	9.4
	BV 4	6.9	39.0	2.7	3.8	152.9	60.8	303.4	79.3	755.3	106.1	490.6	74.0	158.4	81.1	10.2	8.8

b)

	Sc	V	Ni	Cu	Zn	Rb	Sr	Y	Zr	Nb	Ba	La	Ce	Nd	Pb	Th
Mean	6.6	32.3	2.8	5.3	153.9	62.1	313.3	78.4	755.0	104.4	504.9	73.2	166.6	81.0	11.8	9.1
1σ	1.9	13.4	0.2	1.8	3.7	1.7	7.4	1.9	17.8	5.1	37.2	5.2	6.6	3.4	4.8	0.8

c)

	Ti	Rb	Sr	Y	Zr	Nb	Ba	La	Ce	n
Mean	5884	42.6	233	55.2	761	94.9	489	65.5	139.6	39
1σ	271	3.51	35.14	2.13	41.65	5.15	15.96	2.47	5.63	

Table 3.10: a) Trace and rare earth element XRF analyses of Norwegian pumice. b) shows the means and standard deviations (1σ) of the XRF analyses. c) shows the means and standard deviations (1σ) of the Norwegian SIMS analyses (full analyses can be found in Table 3.9).

3.4.2 Iceland

Major Element EMPA

All of the analysed Icelandic pumice found on raised shorelines in the Strandir had its major element geochemistry determined by EPMA. The means and standard deviations of these analyses are presented in Table 3.11. Most of the analysed pumice is dacitic and calc-alkaline in composition, with four more rhyolitic analyses (Figure 3.27). Two groups can be clearly distinguished in Table 3.11 and Figure 3.27, with the majority of the pumice pieces being dacitic and one piece, OF8L 1, being more rhyolitic. Unfortunately, several of the deposits are only represented by single pumice finds and it is possible that greater variation, for example shown in the pumice from Ófeigsfjörður would be apparent with larger samples sizes[3].

Group 1

Pumice sample OF8L 1 from the Site 8 at Ófeigsfjörður is can be easily distinguished from the other pumice pieces by having higher SiO_2, Al_2O_3, MgO and K_2O and lower FeO, CaO and Na_2O abundances (Table 3.11). This pumice piece also varied from the other analysed pieces by being light grey in colour.

[3] The single finds were included in this thesis as pumice finds along the Strandir coast are relatively rare and they provide a valuable record of geographical extent of pumice deposition along this stretch of Icelandic coast.

a)

Site	Pumice	SiO_2	1σ	TiO_2	1σ	Al_2O_3	1σ	FeO	1σ	MnO	1σ	MgO	1σ	CaO	1σ	Na_2O	1σ	K_2O	1σ	Total	1σ	n
Bær	BR 1	66.21	1.01	1.15	0.07	14.07	0.13	5.21	0.24	0.17	0.06	1.01	0.07	2.68	0.16	5.04	0.12	2.87	0.11	98.42	0.96	10
	BR 2	66.34	0.50	1.19	0.05	14.23	0.18	5.40	0.22	0.17	0.03	1.16	0.04	2.92	0.09	5.03	0.14	2.73	0.09	99.17	0.46	10
	BR 3	65.74	0.54	1.17	0.05	13.98	0.22	5.34	0.22	0.14	0.03	1.07	0.04	2.74	0.10	4.39	0.64	2.95	0.10	97.51	0.98	10
	BR 4	66.01	0.58	1.13	0.07	13.98	0.22	5.19	0.25	0.17	0.04	0.97	0.07	2.60	0.11	4.64	0.09	2.94	0.15	97.62	0.64	10
Eyvindarfjörður	E 1	65.85	0.83	1.23	0.05	14.07	0.27	5.53	0.17	0.17	0.03	1.20	0.07	3.25	0.11	4.69	0.18	2.93	0.08	99.04	0.86	11
Hrútafjörður	HF 1	66.52	0.97	1.18	0.09	14.01	0.24	5.29	0.33	0.18	0.04	1.08	0.07	2.91	0.15	4.93	0.02	2.91	0.08	99.00	0.62	4
Ófeigs. (Site 6)	OF6C 1	66.24	0.46	1.26	0.04	14.00	0.19	5.74	0.26	0.18	0.04	1.13	0.07	3.08	0.09	4.64	0.18	2.82	0.06	99.10	0.46	10
	OF6C 2	66.31	0.75	1.22	0.06	13.93	0.15	5.46	0.35	0.20	0.04	1.11	0.08	3.00	0.18	4.64	0.32	3.09	0.40	98.95	0.61	10
	OF6C 3	66.46	0.52	1.19	0.06	13.90	0.13	5.54	0.18	0.16	0.04	1.10	0.05	3.04	0.08	4.75	0.08	2.85	0.11	98.99	0.55	10
	OF6C 4	66.34	0.27	1.21	0.05	13.74	0.14	5.45	0.31	0.19	0.02	1.10	0.04	3.18	0.40	5.11	0.87	2.64	1.05	98.95	0.57	10
	OF6D 1	66.56	0.51	1.17	0.06	13.94	0.18	5.29	0.24	0.21	0.02	0.87	0.08	2.53	0.14	4.69	0.11	2.96	0.13	98.21	0.79	10
	OF6D 2	66.18	0.62	1.11	0.07	13.93	0.18	5.47	0.18	0.16	0.03	1.15	0.05	3.05	0.09	4.76	0.07	2.85	0.09	98.65	0.70	10
	OF6D 3	66.40	0.49	1.28	0.23	14.05	0.16	5.41	0.22	0.18	0.02	1.14	0.07	2.94	0.16	4.48	0.15	2.83	0.13	98.70	0.41	10
	OF6D 4	66.25	0.48	1.20	0.10	13.88	0.17	5.48	0.18	0.16	0.03	1.09	0.05	2.87	0.10	4.33	0.72	3.09	0.30	98.34	0.56	10
	OF6D 5	67.02	0.32	1.23	0.05	13.70	0.11	5.30	0.44	0.16	0.02	0.98	0.05	2.70	0.14	4.54	0.10	3.00	0.15	98.61	0.55	9
Ófeigs. (Site 8)	OF8L 1	71.31	0.85	1.11	0.34	16.15	0.79	2.36	0.36	0.12	0.18	1.75	0.12	0.32	0.04	1.42	0.08	4.27	0.18	98.80	0.85	4
	OF8L 2	65.86	0.90	1.21	0.08	13.87	0.18	5.66	0.14	0.17	0.03	1.12	0.03	3.04	0.10	4.66	0.12	2.82	0.08	98.40	1.10	9
	OF8L 3	66.26	0.62	1.20	0.11	14.01	0.15	5.63	0.24	0.18	0.04	1.12	0.04	2.99	0.11	4.62	0.16	2.86	0.10	98.86	0.61	10
	OF8L 4	65.73	0.19	1.22	0.08	13.87	0.37	5.40	0.21	0.19	0.02	1.14	0.09	3.18	0.23	4.71	0.60	2.90	0.92	98.34	0.38	10
	OF8U 1	65.21	0.70	1.24	0.09	13.99	0.22	5.51	0.17	0.16	0.03	1.15	0.05	3.07	0.10	4.81	0.15	2.78	0.11	97.93	0.94	9
	OF8U 2	65.89	0.41	1.20	0.07	13.80	0.09	5.71	0.17	0.19	0.02	1.13	0.07	3.06	0.10	4.50	0.11	2.77	0.09	98.25	0.46	10
	OF8U 3	65.87	0.58	1.21	0.05	13.81	0.21	5.65	0.16	0.18	0.04	1.15	0.06	3.02	0.09	4.54	0.11	3.01	0.15	98.44	0.78	10
	OF8U 4	66.07	0.41	1.21	0.06	13.88	0.07	5.62	0.23	0.18	0.03	1.14	0.04	3.05	0.09	4.79	0.13	2.80	0.07	98.73	0.37	10
Reykjarnes	RJ 1	64.21	0.73	1.23	0.08	13.64	0.20	5.60	0.16	0.19	0.03	1.12	0.05	2.94	0.13	4.99	0.21	3.02	0.11	96.94	0.76	10

b)

	SiO_2	TiO_2	Al_2O_3	FeO	MnO	MgO	CaO	Na_2O	K_2O	Total	n
Mean	66.15	1.20	13.96	5.42	0.17	1.11	2.90	4.65	2.91	98.48	227
1σ	1.05	0.10	0.38	0.49	0.04	0.13	0.42	0.57	0.38	0.86	

Table 3.11: a) shows the means and standard deviations (1σ) of the Icelandic pumice pieces from six raised beach sites in Iceland. b) shows the means and standard deviations (1σ) of all 227 analyses. The number of analyses are also shown (n) and full details about these analyses are available in Appendix 3.

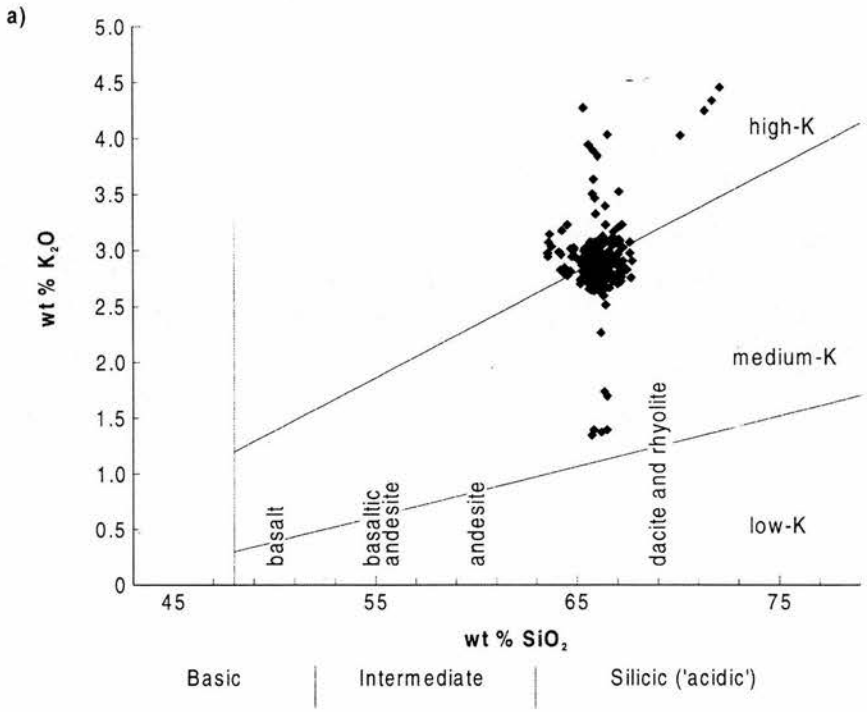

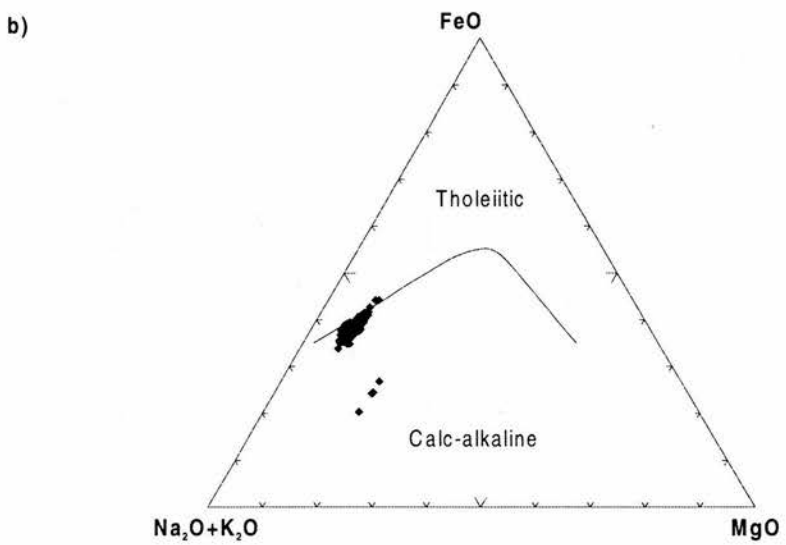

Figure 3.27: Graphs which show that: a) all of the pumice pieces analysed are silicic, based on recommendations of Le Maitre (1989); b) all of the analysed pumice is calc-alkaline, with the group of 4 separate analyses being from OF8L 1, based on Irvine and Baragar (1971).

Group 2a

The remainder of the analysed pumice is composed of dacitic pumice. There are, however some differences and this main group is divided into two subgroups. The majority of the analysed pumice pieces are found within Group 2a. This group contains all of the pumice from Ófeigsfjörður Site 8 (except for OF8L 1), Ófeigsfjörður Site 6 (except for OF6D 1 and OF5D 5), Bær pumice pieces BR 2 and BR 3, Eyvindarfjörður E 1, Hrútafjörður HF 1 and Reykjarnes RJ 1. The Group 2a Ófeigsfjörður Site 8 pumice pieces are indistinguishable on their major element geochemistry (Table 3.11). There is also considerable overlap between the Group 2a pumice pieces from Ófeigsfjörður Site 6, although OF6C 4 has a couple of analyses with higher CaO, as well as four analyses with much higher abundances of Na_2O. These anomalous Na_2O totals are reflected in the high mean Na_2O of 5.11 wt % and the larger standard deviation of 0.87 (1σ) shown in Table 3.11. Figure 3.28 shows that the Site 8 pumice has less geochemical variation than the Site 6 pumice. There appears to be no significant difference between the upper and lower pumice deposits at Site 8 or the spatially separated deposits at Site 6. Whilst BR 2, HF 1 and RJ 1 overlap with both the Ófeigsfjörður pumice pieces, the BR 3 pumice only overlaps with the lower CaO and MgO analyses from Ófeigsfjörður Site 6 pumice (Figure 3.28). The single piece of pumice from Eyvindarfjörður overlaps with some pumice pieces from Ófeigsfjörður sites 6 and 8, but not with pumice from Bær, Hrútafjörður and Reykjarnes (Figure 3.28).

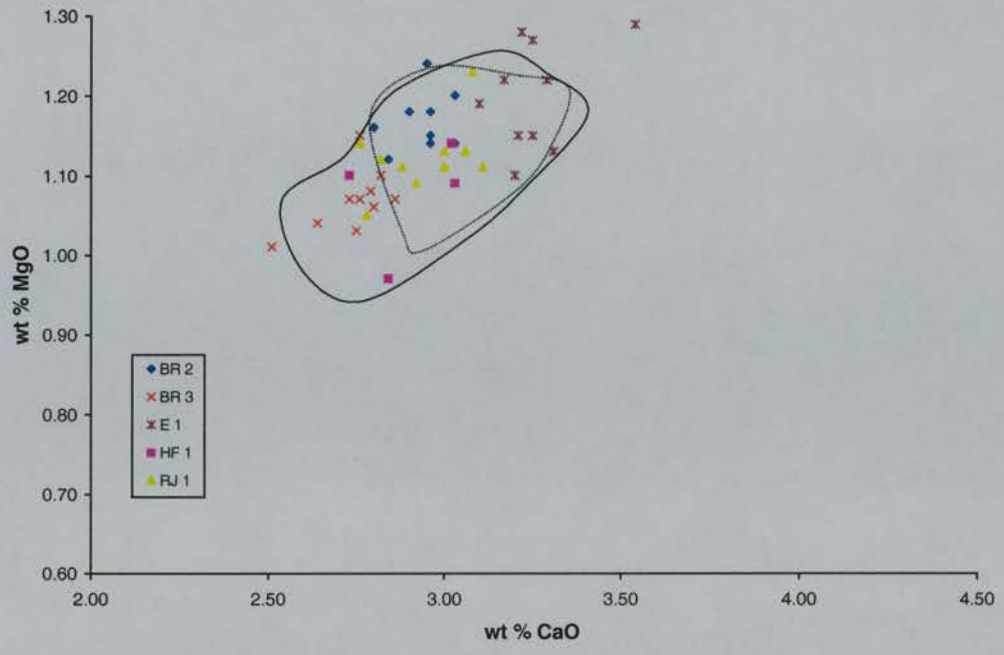

Figure 3.28: Graph (CaO/MgO) which shows the geochemical properties of the Group 2a pumice from the Strandir coast. The dotted field defines the pumice from Ófeigsfjörður Site 8 and the solid field Ófeigsfjörður Site 6.

Group 2b

The Group 3 pumice has less CaO and generally less MgO than the Group 2a Norwegian pumice pieces, although there is some overlap between the two groups, with the brown pumice OF6D 1 having the lowest abundances of CaO and MgO. (Figure 3.29). This overlap highlights the similarities and suggests that although there is no overlap between some of the extreme members of the Group 2b and Group 2a pumice they are all probably from the same source. In fact all of the Group 2a and Group 2b pumice analyses form a linear trend in CaO/MgO, which suggests that they were either produced by several eruptions from a volcano with an evolving magma chamber, or they were produced by a single eruption from a fractionated magma chamber. The pumice from Bær shows differences between the individual pumice samples. For example, BR 2 (Group 2a) shows a clear difference from BR 4 . Despite this it is not possible to say that these pumice pieces are from different eruptions. There is considerable overlap between most of the pieces and even BR 2 could be just an end point of a linear geochemical trend from the same eruption.

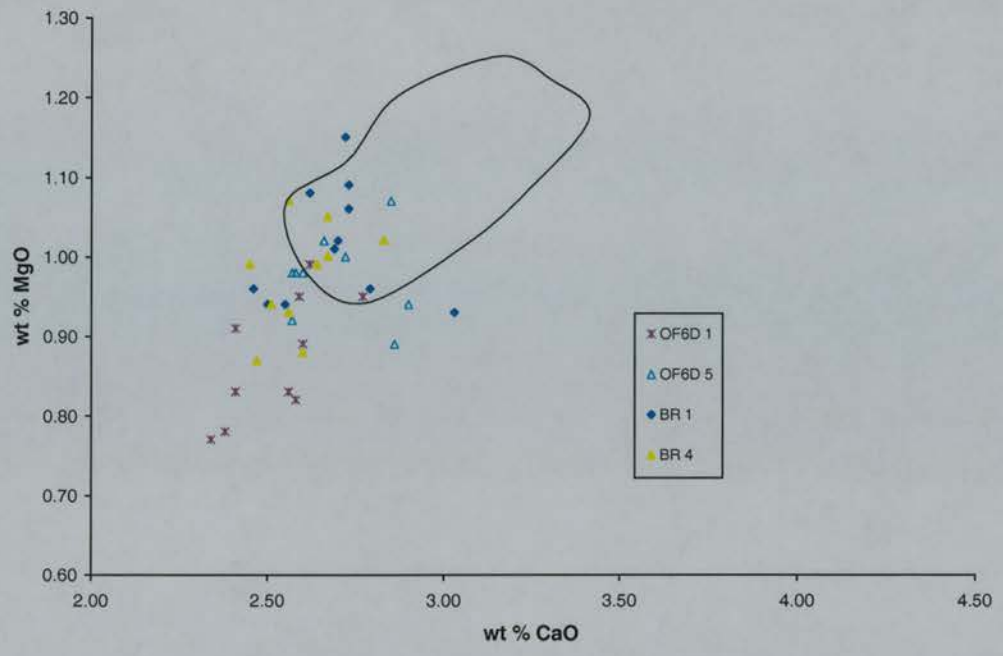

Figure 3.29: Graph (CaO/MgO) which compares Group 2b pumice from Strandir to the Group 2a pumice as defined by the solid field.

With the exception of the grey pumice OF8L 1, the EPMAs suggest that all of the other analysed pumice from the raised shorelines of Strandir appear to have been erupted from the same source. Whilst the Group 2b pumice is slightly different to the Group 2a pumice, both appear to have been erupted from the same source, if not the same eruption.

Trace and Rare Earth SIMS Analyses

SIMS analyses were carried out on a single piece of pumice from Bær (BR 1), as this site is the only relatively well-dated raised shoreline along the Strandir coast and will allow comparison to other pumice deposits of a similar age found elsewhere in around the North Atlantic. The EPMA of BR 1 showed that it had slightly different geochemical properties than the majority of the pumice from Strandir, although it was clear that it had been erupted from the same source. The SIMS analyses are summarised in Table 3.12. Although the Ti concentrations are similar to KVU 3, Sr is much lower and Nb and Ba higher in BR 1.

		Ti	Rb	Sr	Y	Zr	Nb	Ba	La	Ce	n
BR 1	Mean	5723	44	215	56	785	100	500	67	143	**10**
	1σ	126	1.4	13.3	1.4	18.2	2.2	-13.3	2.0	4.7	

Table 3.12: Means and standard deviations (1σ) of the SIMS analyses of the BR 1 pumice piece from Bær. Full analysis details are available in Appendix 3.

3.4.3 Scotland

Pumice from the Bay of Moaness was the only pumice analysed from a natural raised beach site in the British Isles. EPMA and SIMS analyses were undertaken on pumice from this site.

Major Element EMPA

The means and standard deviations of these EPMA analyses of pumice from the Bay of Moaness are presented in Table 3.13 and Figure 3.30 shows that the pumice is dacitic and calc-alkaline in composition.

Figure 3.31 shows that BM 1 and BM2 are very similar and Table 3.13a shows that there are also very small differences in the other oxides. BM 3 overlaps with two analyses from BM4, but BM 4 has several analyses with lower CaO and MgO. There is also evidence of a linear trend in the analyses shown in Figure 3.31.

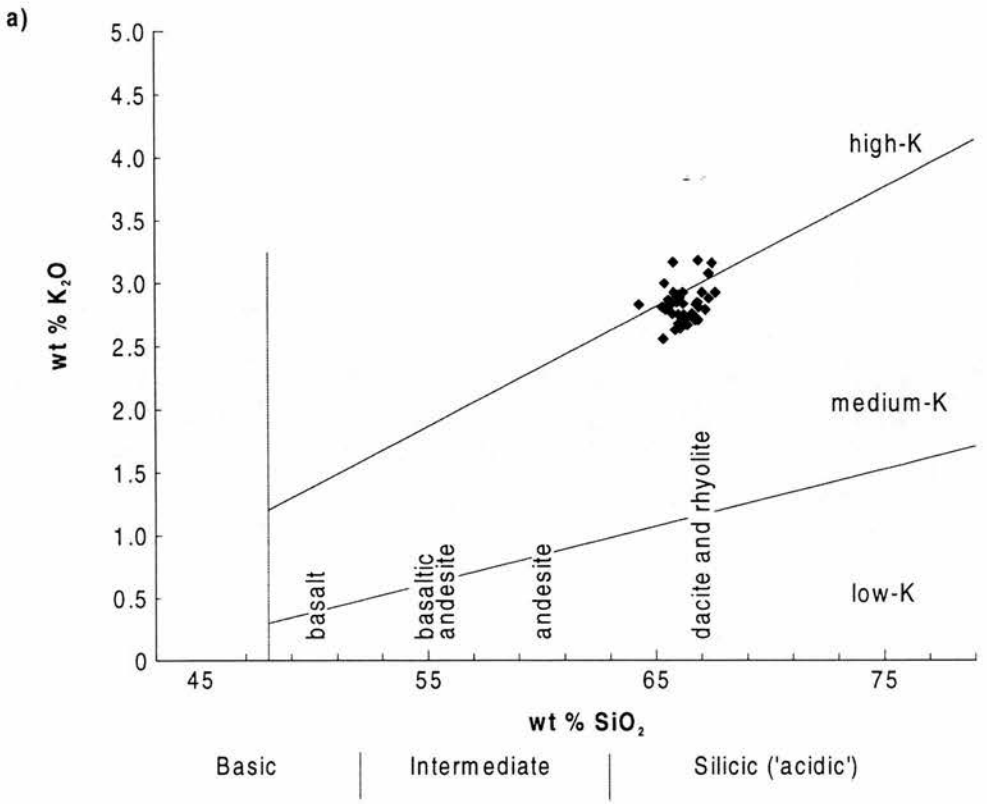

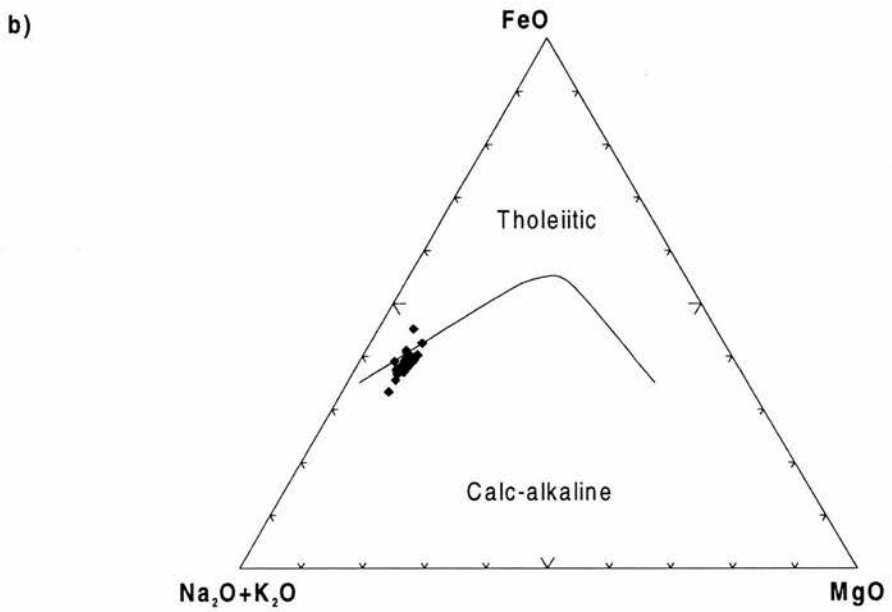

Figure 3.30: Graph which show that: a) all of the pumice pieces analysed are silicic based on recommendations of Le Maitre (1989). b) with the exception of a couple of analyses all of the pumice is calc-alkaline, based on Irvine and Baragar (1971)

a)

Pumice	SiO_2	1σ	TiO_2	1σ	Al_2O_3	1σ	FeO	1σ	MnO	1σ	MgO	1σ	CaO	1σ	Na_2O	1σ	K_2O	1σ	Total	1σ	n
BM 1	66.09	0.55	1.19	0.05	13.72	0.38	5.63	0.14	0.19	0.03	1.16	0.07	3.00	0.13	4.78	0.13	2.71	0.09	98.47	0.79	10
BM 2	65.69	0.56	1.16	0.07	13.81	0.24	5.54	0.21	0.20	0.03	1.13	0.07	3.07	0.14	4.76	0.14	2.84	0.07	98.19	0.89	10
BM 3	66.70	0.64	1.09	0.08	13.77	0.18	5.22	0.19	0.21	0.04	1.04	0.06	2.78	0.10	4.64	0.57	2.86	0.10	98.32	0.95	10
BM 4	66.79	0.72	1.21	0.13	13.03	0.47	5.58	0.68	0.21	0.01	0.92	0.10	2.58	0.22	4.56	0.44	3.02	0.20	97.90	0.87	6

b)

	SiO_2	TiO_2	Al_2O_3	FeO	MnO	MgO	CaO	Na_2O	K_2O	Total	n
Mean	66.26	1.16	13.65	5.48	0.20	1.08	2.89	4.70	2.84	98.26	36
1σ	0.74	0.09	0.41	0.35	0.03	0.11	0.23	0.36	0.15	0.86	

Table 3.13: a) shows the means and standard deviations (1σ) of the Bay of Moaness pumice. b) shows the means and standard deviations (1σ) of all 38 analyses. The number of analyses are also shown (n) and full details about these analyses are available in Appendix 3.

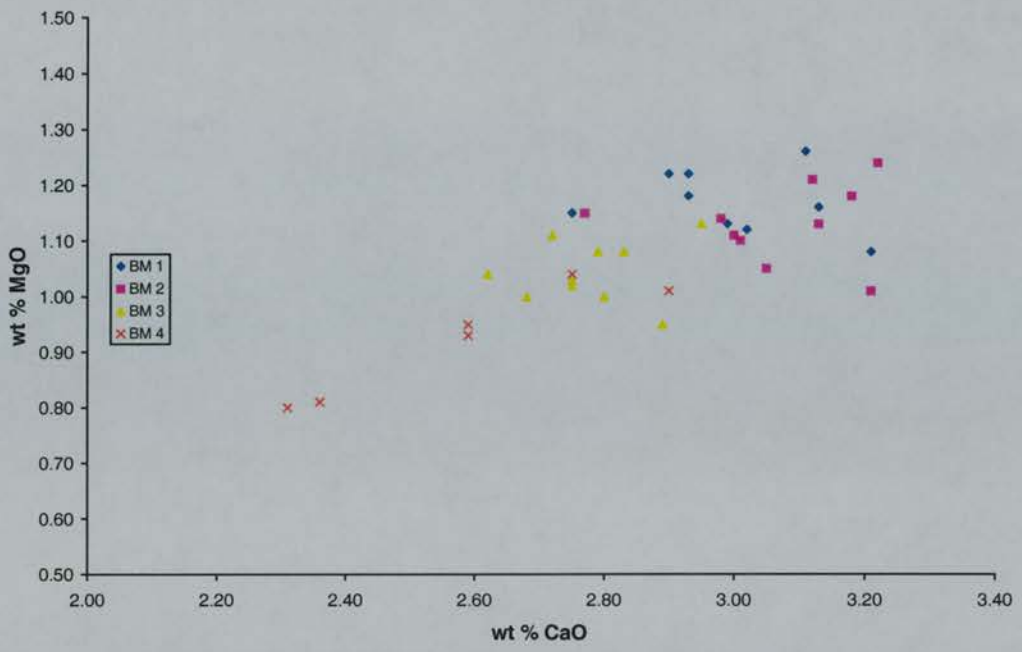

Figure 3.31: This graph (CaO/MgO) shows that there is evidence of a positive linear trend with BM 1 and BM 2 being very similar and BM 3 and especially BM4 having generally lower CaO values.

Trace and Rare Earth SIMS Analyses

Trace and rare earth SIMS analyses were undertaken on a single piece of pumice (BM 4) from the Bay of Moaness (Table 3.14). Again the analyses show that the pumice from the Bay of Moaness is similar to the other dacitic pumice found elsewhere in the North Atlantic, although there are some small differences. The large standard deviation in Ti is caused by only two analyses with Ti concentrations of 6118 and 6478 ppm. Again, this is probably the result of the partial analysis of mineral inclusions, as these values are so different to the others and are indeed perpendicular to the general trend seen in Figure 3.32.

		Ti	Rb	Sr	Y	Zr	Nb	Ba	La	Ce	n
BM 4	Mean	5921	45.0	220.8	56.2	806.3	100.9	503.2	66.6	141.3	**7**
	1σ	288	2.0	38.3	1.9	29.7	4.0	8.3	1.6	3.8	

Table 3.14: Means and standard deviations (1σ) of the SIMS analyses of the BM 4 pumice from the Bay of Moaness. Full analysis details are available in Appendix 3.

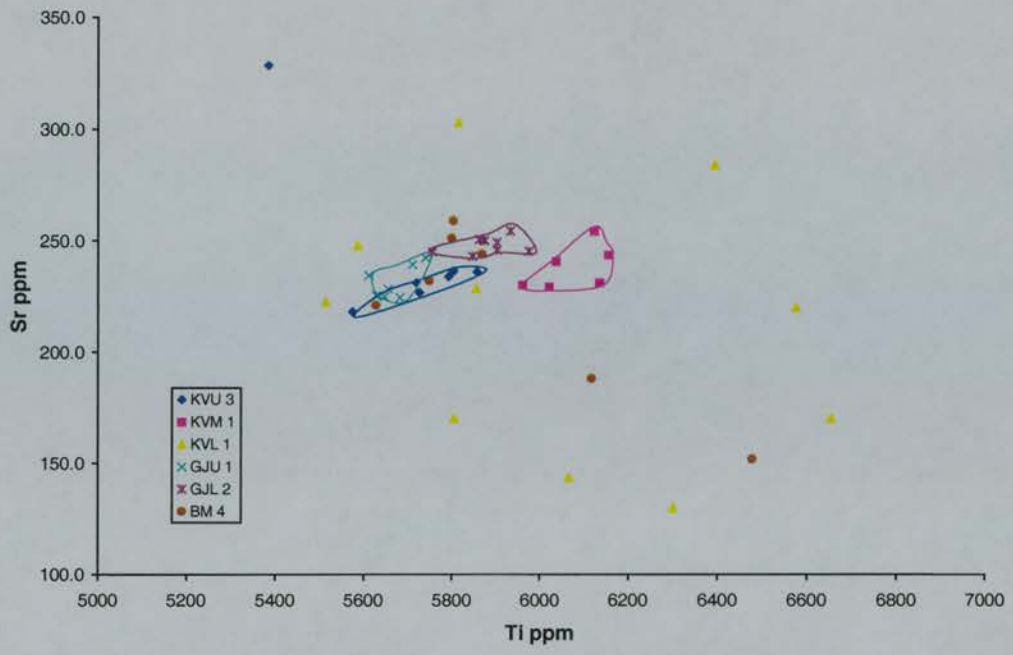

Figure 3.32: Graph (Ti/Sr) to compare the SIMS analyses of the Bay of Moaness pumice with the Norwegian pumice.

As can be seen in Figure 3.32 most of the analyses of the Bay of Moaness pumice are most similar to the KVU 3 and GJL 2 pumice pieces. These leads to contradictory conclusions. Whilst the overlap between these two pumice pieces suggests that the geochemical variations seen and the distinct groups produced on the graphs could be the result of geochemical variation during a single event, it is possible that multiple eruptions from the same source could also result in the same pattern.

3.4.4 Summary of the new geochemical data

The new geochemical data has established that the majority of the pumice pieces found on raised shorelines in central Norway, north-west Iceland and the single site in Scotland are dacitic. This dacitic pumice varies in colour from brown to black/grey and is found on raised shorelines ranging in age between about 6000 ^{14}C years BP to 1700 ^{14}C years BP. SIMS analyses confirmed the geochemical homogeneity of this group, but small differences between individual pieces were identified. The pumice Scottish pumice deposit at the Bay of Moaness can also be correlated with the Icelandic and Norwegian Groups 2a. Whilst this large group has relatively clear glass with only scattered phenocrysts, the smaller Norwegian Group 2b pumice has many phenocrysts within its glass resulting in less homogeneous analyses. This group, which also has lower CaO, MgO and FeO compared to Group 2a, dominates the lower Kobbvika pumice level. Icelandic Group 2b also has lower CaO, MgO

and FeO compared to Icelandic and Norwegian Groups 2a but lacks the phenocrysts and therefore the geochemical homogeneity seen in Norwegian Group 2b. A single piece of white rhyolitic pumice was found on the early Holocene raised shoreline at Trandvikan, Norway and a grey piece of rhyolitic pumice found at a lower pumice level at Ófeigsfjörður. A single of piece of basaltic pumice was also found at the upper pumice level at Kobbvika, Norway.

The Scottish pumice and Icelandic and Norwegian Groups 2a were produced by the same source and can be geochemically correlated. What is not clear is the number of eruptions which produced these pumice deposits. Major element variations between the majority of the pumice pieces and deposits is small and are either the result of a single event, or multiple eruptions from a volcano with a slowly or non-evolving magma chamber. The pumice from Icelandic and Norwegian Groups 2b, although geochemically slightly different to the main group, was most probably erupted from the same source. What is not clear is whether the low CaO/MgO/FeO group was erupted by the same event that produced the main group. Differences between the groups could either be caused to variation within an eruption, as suggested by the presence of the low CaO/MgO/FeO pumice amongst the main pumice group, or separate eruptions, as the lower pumice level at Kobbvika suggests. The two rhyolitic pumice pieces are geochemically different and only one basaltic pumice piece has been found.

3.5 Comparison with published data

Although this chapter has highlighted the problems of using the published data for correlation, it is worth comparing the published data against the results presented above. Figure 3.33 and Figure 3.34 show that some of the published data has close geochemical similarities to the new geochemical data presented in this chapter. In particular, the analyses of some the pumice from Svalbard (the Svalbard A Group) and Scandinavia (Scand A) have similar geochemical characteristics to the new main dacitic analyses. The other published analyses are obviously similar, but do not overlap with the main field, although some do overlap with the Norwegian Group 2b analyses. It must be remembered, however, that the Norwegian Group 2b analyses are grain specific and the means of these analyses do fall within the main EPMA/XRF field. The Canadian analyses presented by Blake (1970) have already been discussed in Chapter 2, and it is not surprising that although the pumice is similar it does not correlate with the new results.

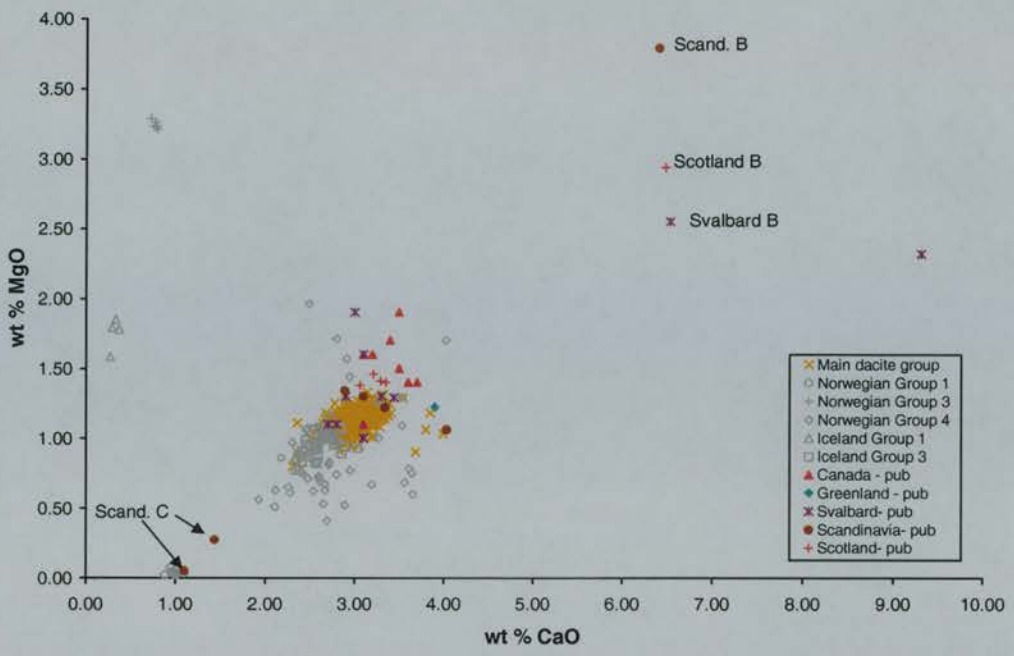

Figure 3.33: A comparison of the published geochemical data (see Chapter 2) with the new data presented in this chapter. Some individual published analyses are identified. All new data is defined by suffix *Group* and published data by suffix *pub*.

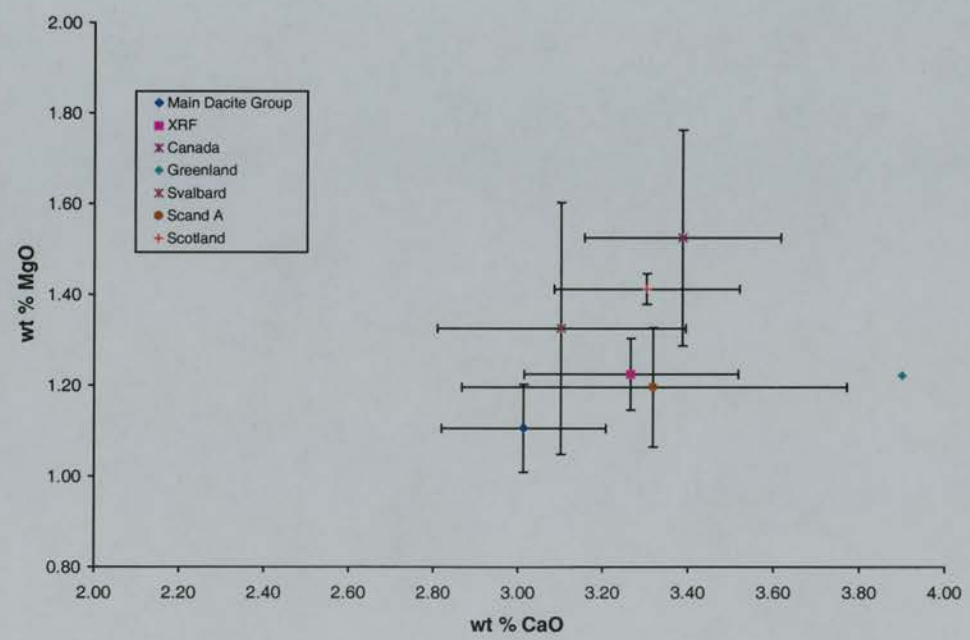

Figure 3.34: The means and standard deviations (1σ) of the main dacitic pumice and the published data showing that the Scandinavian and Svalbard analyses are the most similar to the new results.

a

		SiO_2	TiO_2	Al_2O_3	FeO	MnO	MgO	CaO	Na_2O	K_2O	Total	n
Main Dacite	**mean**	65.71	1.20	13.91	5.51	0.18	1.13	3.00	4.65	2.84	98.13	544
	1σ	0.75	0.09	0.27	0.26	0.04	0.07	0.19	0.35	0.25	0.88	
XRF	**mean**	64.50	1.29	14.04	6.08	0.22	1.16	3.09	4.70	2.63	98.01	6
	1σ	0.73	0.06	0.15	0.66	0.07	0.06	0.08	0.11	0.08	0.49	
Svalbard	**mean**	64.58	1.09	15.27	5.64	0.18	1.33	3.10	4.95	2.63	99.82	9/8*
	1σ	0.64	0.22	0.86	0.36	0.00	0.28	0.29	0.29	0.28	1.13	
Scand A	**mean**	63.85	1.13	14.42	5.83	0.18	1.20	3.32	5.09	2.04	97.87	9/5*
	1σ	0.96	0.15	0.30	0.24	0.02	0.13	0.45	0.35	0.39	1.75	
Canada	**mean**	61.21	1.20	15.94	5.67	0.19	1.53	3.39	4.89	2.59	98.75	8
	1σ	0.77	0.03	1.42	0.14	0.01	0.24	0.23	0.10	0.04	1.03	
Greenland		63.53	1.05	13.72	6.25	0.18	1.22	3.90	5.39	2.35	99.59	
Scotland	**mean**	63.37	1.25	14.62	5.97	0.19	1.41	3.30	4.81	1.78	97.09	6
	1σ	1.11	0.10	0.04	0.13	0.01	0.03	0.22	0.28	0.08	1.32	

b

		SiO_2	TiO_2	Al_2O_3	FeO	MnO	MgO	CaO	Na_2O	K_2O	Total	n
Nor Grp 1	**mean**	71.55	0.21	13.36	3.28	0.11	0.04	1.00	4.85	3.51	97.90	10
	1σ	0.47	0.04	0.30	0.09	0.03	0.02	0.06	0.48	0.12	0.99	
Scand C		69.00	0.12	14.80	1.96	0.08	0.27	1.44	4.40	2.60	95.04	1
		65.10	0.33	13.60	3.45	0.11	0.05	1.10	6.00	4.00	94.42	1

Table 3.15: Comparison of the new geochemical data with that published sources (see Chapter 2). a) compares the EPMA and XRF analyses of the main dacitic group to similar published analyses. * indicates that the mean was calculated from incomplete analyses, at least one element was not measured in all the analyses. The high CaO Svalbard analysis is excluded from the mean totals. b) compares the more silicic Norwegian pumice with two published analyses of Norwegian pumice.

Figure 3.33 also shows that two of the published analyses from Scandinavia share some geochemical properties with the silicic pumice from Trandvikan (Norwegian Group 1), although there are also several significant differences as shown in Table 3.15 and the two published pieces cannot be correlated to the Trandvikan pumice. Finally, the published analyses known as Scan A, Scotland B and Svalbard B cannot be correlated to any of the new analyses.

The analyses presented by Boulton and Rhodes (1974) are also worth comparing to the new geochemical data. Boulton and Rhodes (1974) published seven analyses of pumice from Svalbard which are presented in Table 2.10. The analysed pumice can be split into two groups. The pumice from the c. 6500 ^{14}C years BP level has Sr abundances of between 915-1000 ppm, Y of 30-35 ppm and Zr of 435 ppm. This compares to the other pumice found on the lower 4100 and 2200 ^{14}C years BP beaches which have Sr abundances of between 265-285 ppm, Y of 65-75 ppm and Zr if between 655-650 ppm. Figure 3.35 shows that although

the pumice from the younger Svalbard beaches has similar geochemical properties to the pumice analysed by XRF and SIMS, the Svalbard pumice from the older must have been produced by a different volcano.

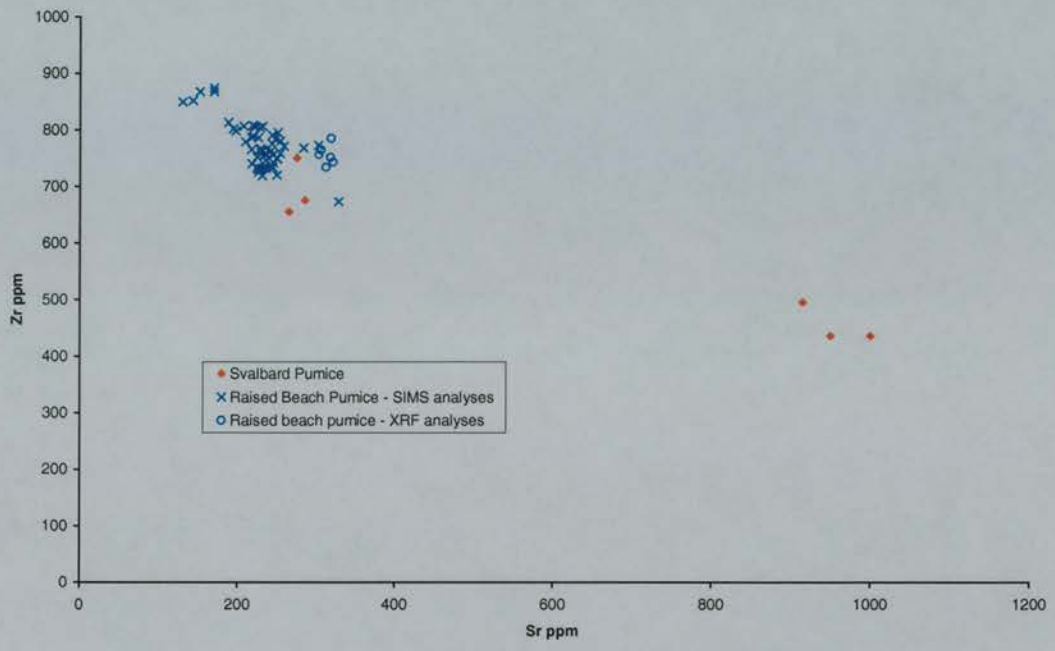

Figure 3.35: Graph to show the relationship of the analyses of Svalbard pumice published by Boulton and Rhodes (1974) with the new data from raised shorelines. Both XRF and SIMS analyses are shown.

The results of the analysis of archaeological pumice will be compared to the published data in Chapter 4 (section 4.4) and the final conclusions on the quality of the published data will be discussed.

3.6 Summary of Chapter 3

Original fieldwork has confirmed the presence of multiple levels of mainly brown and black dacitic pumice along the coastline of central Norway. The lower pumice levels are mainly composed of black pumice, but brown pumice pieces also occur. A single piece of black basaltic pumice was found on a mid-Holocene beach and a rhyolitic piece on an early Holocene one. The presence of scattered Holocene pumice deposits on raised shorelines in north-west Iceland was also established. This chapter has also shown that high quality geochemical analyses are essential if the geochemical properties of the pumice is be established. These data established that the majority of the pumice are geochemically similar and appear to have been erupted by the same volcano. It is not clear on these data

alone, however, how many eruptions were responsible. It is not possible to correlate the analysed pumice with older published data. This is probably the result of different and relatively poor quality analytical techniques.

The next chapter discusses pumice finds from archaeological sites and presents new geochemical data before comparing it with the results presented in this chapter.

Proposed additions to SSSIs on Islay

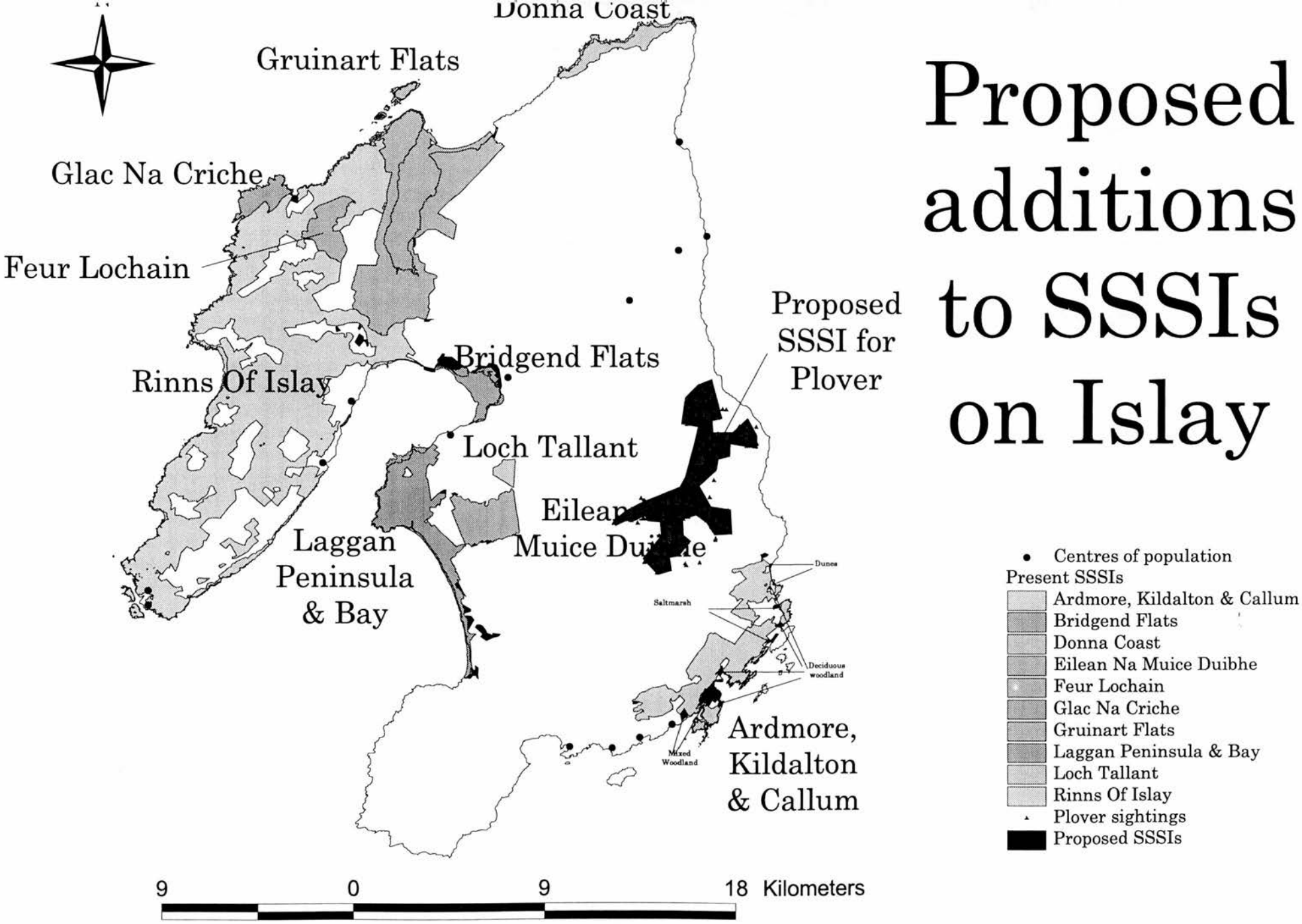

Chapter

4

Pumice from archaeological sites: new data

This chapter presents the results of the geochemical analysis of pumice found in archaeological sites.

4.1 Introduction

As shown in Chapter 2, the vast majority of the pumice finds from the British Isles have been from archaeological sites. This chapter investigates pumice from 16 archaeological sites in the British Isles. All of the pumice studied in this chapter has been kindly supplied by archaeologists. A varying amount of post-excavation research has been carried out on the pumice by archaeologists. This work includes investigations of the wear on the pumice, i.e. evidence of pumice being used as a tool. All of the geochemical work, except for some analyses by Andrew Dugmore, has been carried out by myself. Many of the results of the archaeological pumice research have been written up as reports to be included in the final excavations reports on the archaeological sites. The majority of these have yet to be published, even though the work on the pumice was completed several years ago. Where this is the case, the reports will be referred to as "Forthcoming".

The first part of this chapter describes Scottish and Irish archaeological sites where pumice was found and analysed for this study. It was hoped to analyse pumice from several Mesolithic Norwegian archaeological sites, but unfortunately the material did not arrive in time to be included in this work. The geochemical analyses are presented and discussed next. The geochemical analyses are compared to previously published data, then with the analyses of the pumice from raised shorelines presented in Chapter 3. The chapter ends with a summary of the pumice from both natural and archaeological sites.

4.2 Site and pumice descriptions

Pumice finds are recorded from 150 sites in the British Isles, of which 136 are archaeological ones (Chapter 2). This section describes the pumice found at 14 archaeological sites in the British Isles. Each site is concisely described, with details of the age of the deposits the pumice has been found in and the physical characteristics of the pumice. All of the pumice was recovered during archaeological excavations and the descriptions of the sites are based on either published reports or unpublished information kindly supplied by the archaeologists.

4.2.1 Scotland

Figure 4.1 shows the location of the archaeological sites in the British Isles where pumice has been analysed for this study. Unfortunately no pumice pieces from archaeological sites in Orkney were analysed. This is a pity, as Orkney has one of the highest number of pumice sites in Scotland. The only site is from an inter-tidal peat deposit (site 58) at Bay of Moaness which is described in detail in Chapter 3. Cremation slag (cramp[1]) from Midskaill, Egilsay, and Linga Fiold, Sandwick was analysed. This had been misinterpreted as pumice and the results of this work can be found in Newton (1995). In this section, Scotland is divided into the same regions as in Chapter 2.

---

[1] Cramp, vitrified cremation material, from the two sites was composed of three types of glass. The first type was vesicular and was largely composed of Si (70%), Al, and K; the second type was also composed of Si, Al, and K, but also varying amounts of Na, Mg, P, Ca, Ti and Fe; the third type was non-vesicular and the major components were Al and Ca, less Si than 1 and 2, with S, Ti, Mg and some Na. The differences in composition and colour were probably due to both differences in local soils and bedrock and the temperatures reached during the cremation (Newton, 1995).

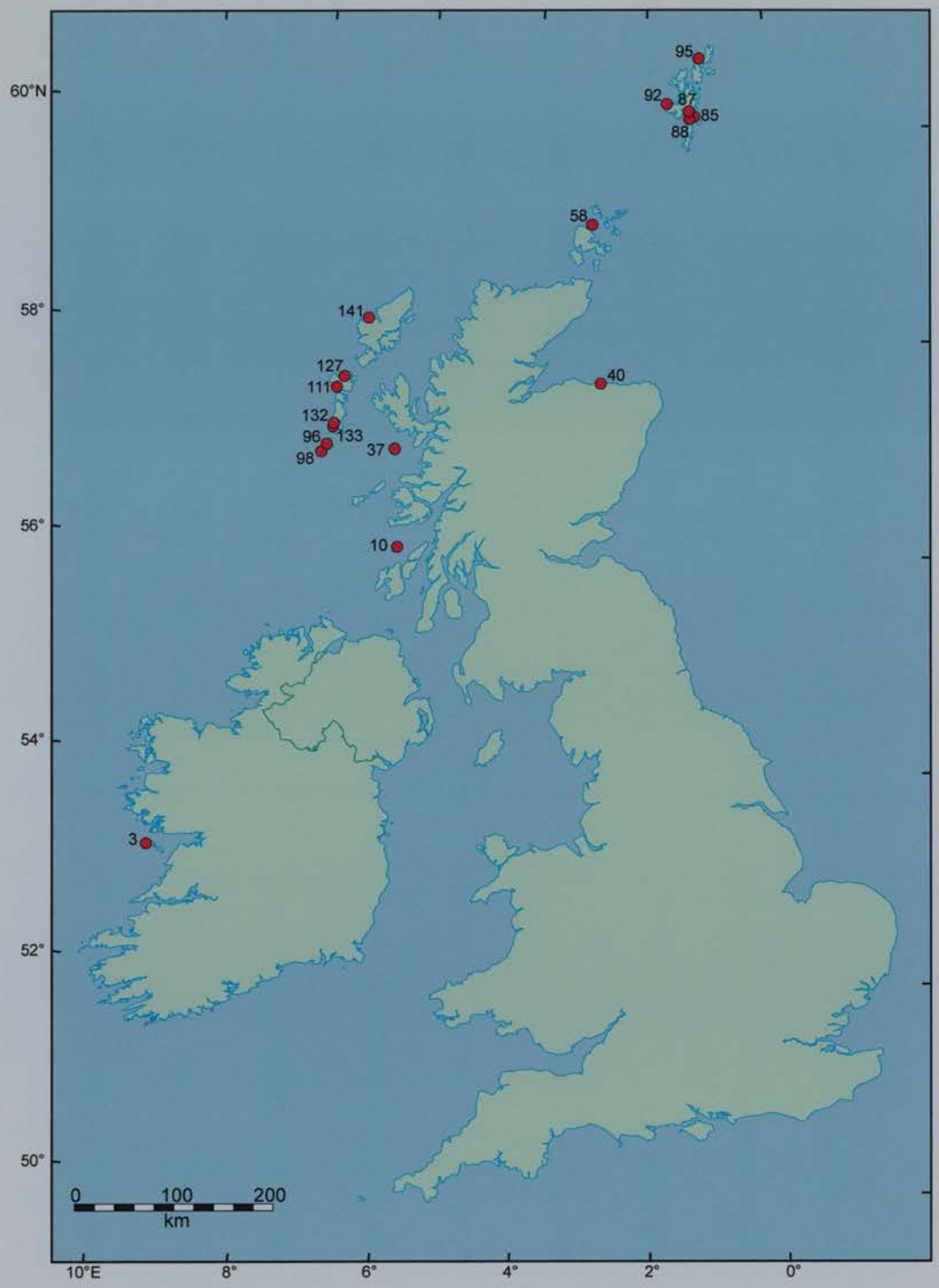

Figure 4.1: Map to show the location of archaeological sites in the British Isles from which pumice was analysed. Site 58 is included to show its location in relation to the archaeological sites.

Western Isles

The Western Isles contain the highest number of archaeological sites where pumice has been found in Scotland (Chapter 2). Pumice pieces from six of the 47 sites have been analysed for this study.

Allt Chrisal, Barra

The results of the excavations by The Department of Archaeology and Prehistory at The University of Sheffield, at Allt Chrisal, on the south of coast of Barra (site 96), are described in Foster (1995). The results of the analysis of the pumice are presented in the same volume (Branigan *et al.*, 1995; Newton and Dugmore, 1995). Allt Chrisal is the name of a small stream which flows into the Sound of Vatersay and the adjacent area shows evidence of intermittent human occupation, by small communities, over a period of some 4000 years. Early Neolithic settlers were the first to occupy the site, but there is no evidence of occupation during the Bronze Age, the early to middle Iron Age, the early to late Medieval or the early post-Medieval periods. Most of the evidence points to occupation of the site during Neolithic-Beaker, Iron Age and Modern (post 18th Century) times.

A total of 57 pieces of brown pumice were found at site T26, which consists of an 18th Century blockhouse built on top of a prehistoric platform. All of the pumice was found in contexts ranging from the 18th Century floor to beneath the 4470 ± 60 ^{14}C years BP occupation platform. There appears to be no pattern to the distribution of pumice deposits, with finds occurring in both stratigraphic contexts and spoil heaps (middens).

The largest piece found weighed 190 grams. The morphology of the pumice is fairly consistent with the vast majority having small to medium (1-2 mm) sized non-glassy vesicles and 21 pieces show evidence of having been used as tools (Branigan *et al.*, 1995). These can be divided into three categories: those which have one or more faces rubbed flat (13 pieces); those with concave rubbed surfaces (4 pieces); those with abrasion marks from twine or string (4 pieces). Branigan *et al.* (1995) suggest that the pumice with the abrasion marks could have been used as fishing floats.

As the pumice from T26 showed little physical variation, electron microprobe analyses were carried out on just four pieces of pumice which were considered typical of the pumice found on the site (Table 4.1). XRF analysis was also undertaken on a single piece of pumice.

Code	Location	Colour	Age
AC 1	Layer 18	light brown	Post abandonment layer in 18th century blockhouse
AC 2	Layer 23	light brown	Redeposited Neolithic soil in 18th ditch
AC 3	Layer 18	light/dark brown	Redeposited Neolithic soil in 18th ditch
AC 4	Layer 73	light brown	Neolithic soil under floor of 18th century blockhouse

Table 4.1: The colour and age of the analysed pumice from Allt Chrisal (data from Newton and Dugmore, 1995). Code refers to the sample number used throughout this chapter.

Cille Pheadair (Kilpheder), South Uist

A single of piece of pumice (CP 1 - 01/24U) found at the Iron Age wheelhouse at Cill Pheadair was analysed by both EPMA and XRF. The results of this excavation have not been published (Mike Parker Perarson, pers. comm., 1999).

Cill Donain (Kildonan), South Uist

Cill Donain III is the largest of three closely spaced middens, which forms a 230 m long ridge. Unfortunately details about this site have yet to be published, although it seems to date from the late Iron Age (Gilbertson *et al.*, 1999) and 41 pieces of brown, light brown and black pumice pieces have been recovered. A total of 8 pumice pieces were analysed by EPMA and the colour of these pumice pieces is shown in Table 4.2. A further two pieces were analysed by XRF. The results of this excavation have not been published.

Code	Colour	Age
CD 1	brown	Late Iron Age
CD 2	black	Late Iron Age
CD 3	brown/black	Late Iron Age
CD 4	light brown/grey	Late Iron Age
CD 5	light brown/grey	Late Iron Age
CD 6	light brown/grey	Late Iron Age
CD 7	brown/black	Late Iron Age
CD 8	brown/black	Late Iron Age

Table 4.2: The colour and age of pumice analysed from Cill Donain. Code refers to the sample number used throughout this chapter.

Ceardach Rudh, Baleshare (Baile Sear), North Uist

The archaeological site at Ceardach Rudh is found on the island of Baleshare, situated about 0.5 km to the west of North Uist (site 111 on Figure 4.1). The site's most obvious archaeological structure is a 48 metre long exposed midden, from which material including pumice, is eroded on to the beach (Melanie Smith, pers. comm., 1993;Gilbertson *et al.*, 1999). Although excavations have been carried out by AOC (Scotland) Ltd, partly under their previous name of the Central Excavations Unit, the final excavation report has yet to be

published. The results of the pumice analyses from Ceardach Rudh will be included in the final excavation report (Newton and Dugmore, Forthcoming-a).

The excavations at Ceardach Rudh produced 44 pieces of brown and black pumice weighing a total of nearly 300 grams (Table 4.3). The 44 pumice pieces were recovered from 12 blocks, as shown in Table 4.3. The pumice was found in a variety of contexts ranging from middens, cultivated deposits to wind blown sand. Many of the pieces show signs of having been carved (Barber, Forthcoming). Only one block contained just black pumice, with two producing black and brown pumice and the rest just brown. Although black is a fair description of the colour of the "black pumice", brown may not be as accurate in describing the "brown pumice". The "brown pumice" may appear brown but may also have a more greyish brown colour. Despite this there appears no reason to differentiate any more sub-groupings of colour. Morphological differences between the black and brown pumice are mainly shown by the vesicles which appear far more glassy in the black pumice than the brown. Vesicles in the black pumice also appear to be better developed. The brown pumice at Ceardach Rudh is similar in appearance to the pumice found at Allt Chrisal.

Codes	Block	No. pieces	Colour	Weight (grams)	Age of block (^{14}C years BP)
-	2	4	Brown	27.6	2240 ± 50 2260 ± 80
-	3	2	Brown	9.6	-
CR 1	12*	2	Brown	20.3	-
CR 2	15*	4	Brown	18.4	2375 ± 55
CR 3/4	16*	14	Brown	109.4	older than block 15
	18	2	-	11.7	2900 ± 140
CR 5	22*	2	Black	12.8	3360 ± 80
CR 6	23*	3	Brown/black	18.7	3030 ± 50
	24	1	-	2.7	2057 ± 50
CR 8	25*	1	-	10.3	younger than block 26
CR 7	26*	7	Black/brown	37.5	2815 ± 50 2900 ± 140
CR 9	27*	2	-	20.2	2910 ± 50
	Total	**44**		**299.2**	

Table 4.3: The number, age, weight and age of pumice deposits at Ceardach Rudh. * indicates blocks[2] from which pumice samples were analysed (Newton and Dugmore, Forthcoming-a). Code refers to the sample number used throughout this chapter. CR1-7 were analysed by both EPMA and XRF, whilst CR 8 and 9 were only analysed by XRF. Dates are from Barber (Forthcoming).

Table 4.3 also shows some dates for the blocks containing pumice. These dates are given in uncalibrated radiocarbon years and the relative age of blocks 16 and 25 are shown where no

[2] The use of blocks is a method by which archaeological sites are divided into coherent deposits. For example, a block could be a hearth, or floor or a stratigraphic unit within a midden.

dates were obtained. Two groupings of dates can be seen in Table 4.3. The older group consisting of blocks 18, 22, 23, 26, and the younger one of 2, 15 and 24. The two dates for blocks 2 and 26 represent the two dates from each block. Brown pumice is found in both the old group and the younger group, whilst black pumice is found in only the older group.

The Udal, North Uist

The Udal, a site of archaeological excavations for the last 36 years, is found on the Aird a'Bhorrain peninsular in North Uist, Western Isles (site 127). The site has been occupied since the early Neolithic, with Bronze Age, Iron Age, Gaelic, Norse, Medieval, and post-Medieval to 19th Century structures (Selkirk and Selkirk, 1996). This long period of occupation and the well stratified nature of the site means that this is one of the most important archaeological sites in the Western Isles. Wind blown sand has buried and sealed successive periods of occupation. Unfortunately, little research from the site has been published.

A total of 138 pieces of pumice were found at site RUX6 at the Udal. This pumice was found in all phases of the site, ranging from the early to pre Neolithic Phase E to the proto-Bronze Age to Modern Phase A (Crawford, unpublished). The highest concentrations of pumice were found in the Neolithic (52 pieces) and Early Bronze (60 pieces) deposits. All of the pumice found at the Udal was brown varying only between light and brown. The oldest pumice was found in Phase E (6 pieces), which is older than 4500 ^{14}C years BP (Crawford, pers. comm. 1997). The precise age of this pumice is unknown, as the results of radiocarbon dates are awaited, although Crawford (pers. comm.) believes that this non-anthropogenic context stretches into the early Holocene. There is also evidence that later Neolithic artefacts have also penetrated into Phase E. This pumice is physically similar to the other brown pumice found in the Western Isles and the rest of Scotland (Figure 4.2).

Figure 4.2: Photograph to show the oldest pumice piece U24007 (U 1) from The Udal. This is physically a typical piece of brown dacitic pumice. The hole in the pumice was created by sampling for EPMA.

Table 4.4 shows details about analysed pumice pieces from Udal. All of the pieces, apart from U 5, are from the older deposits, whilst most of the other Western Isles pumice analysed has been from younger Bronze or Iron Age deposits. The results of the analyses of the Udal pumice have been submitted in a report (Newton, Forthcoming-b).

Code	Sample	Colour	Phase	Approximate Age*
U 1	U24007*	light brown	E	> 4500 ^{14}C years BP
U 2	U26890	light brown	D	c. 4500 ^{14}C years BP
U 3	U23751	brown	D	c. 4200 ^{14}C years BP
U 4	U23814	brown	D	c. 4200 ^{14}C years BP
U 5	U23788	dark brown	A	unclear

Table 4.4: The colour and age (*Crawford pers comm., 1997) of the analysed pumice from the Udal. Code refers to the sample number used throughout this chapter. U24007 is the stratigraphically the oldest of the Phase E pumice.

Cnip, Lewis

Cnip, on the west coast of Lewis, the Western Isles (site 127 on Figure 4.1) is an Iron Age settlement. The early structures at the site consist of two wheelhouses which probably date from 4-7th centuries BC. These structures were occupied until about the 1st Century AD. Evidence of two younger phases are provided by cellular structures which were occupied between the mid-late 1st Century BC and abandonment in the 3rd Century AD (Armit, 1988b quoted in Armit, 1996).

Only three pieces of pumice were found at Cnip 88 in contexts 266/233 (C 1), 153/89 (C 2), and 85/61 (C 3). All have flattened faces, suggesting that they have been worked. The pumice varies in size between 4 and 6 cm and is dark brown/grey in colour. All of the pumice was found in Phase 2 contexts which suggests an age of around the 1st or 2nd Century

AD (2000-1850 ^{14}C years BP). Although only three pieces have been found, this site is important as it is the only site in Lewis where pumice has been analysed. The results of these analyses have been included in the final excavation report (Newton, Forthcoming-c).

Shetland

Pumice has been found at 27 archaeological sites in Shetland, which account for 17% of pumice sites and 23% of pumice pieces found in the British Isles. Pumice from five archaeological sites was geochemically analysed for this project.

Kebister, Mainland

Kebister, north of Lerwick, has been the site of human occupation for much of the last 4000 years and the results of recent excavations are published in Owen and Lowe (1999). The site is divided into four phases: pre-Iron Age (older than 2440 ^{14}C years BP), Iron Age (2440-1580 ^{14}C years BP), Medieval (500 AD to 1500 AD) and post-Medieval (1500-1820 AD). The oldest pumice is found in Bronze Age contexts (3 pieces), but the largest concentration is in the Iron Age deposits, where 28 pieces were recovered (Clarke, 1999). The pieces range in weight between 4 and 230 grams and two thirds of them have evidence of wear, of which 17 have grooves. The pumice is especially common in redeposited contexts. A single piece of pumice (K 1) was analysed by EPMA and the analyses of this and the tephra layers found at the site are published in Dugmore and Newton (1999a; 1999b). Six pieces (AJD 5-9 and XRF 19) were also analysed by XRF.

Scalloway, Mainland

Two pieces of pumice were analysed from this site, one brown, S 1 (SW MU3 11/7/80 #4b SU3 224/807) and one white, S 2 (SWA H3 231/799 3201 2978). This is a Norse site (Biglow, pers. comm.), further details about this site are unfortunately not available

Upper Scalloway, Mainland

Chapter 2 described that the late Iron Age broch at Scalloway (site 88, termed Upper Scalloway here to differentiate it from Scalloway above) has produced 347 pieces of mainly brown pumice. The results of the excavations are published in Sharples (1998). 25% of the pumice was found in contexts associated with the construction and occupation of the broch between the 2nd and 5th centuries AD (Campbell *et al.*, 1998; Clarke, 1998a). 50 % of the

pumice occurs in the secondary occupation of the broch, dated to between 5th/6th Century to the 8th Century AD. A few pumice pieces are also found in the older contexts, which date to the late Bronze Age. 98 of these pieces show signs of wear, ranging from grooves to flattened and smoothed faces (Clarke, 1998b).

Two pieces of brown pumice were analysed from the site at Upper Scalloway, US 1 and US 2 (F13/4070).

The Biggings, Papa Stour

The Biggings is a Norse to 19th Century site found on the island of Papa Stour (site 127 on Figure 4.1). This site has contexts ranging from early Norse (11th-12th centuries) to mid 19th Century contexts and was continuously inhabited during this period (Crawford and Ballin Smith, 1999). The 12th to 14th Century contexts appear to be a high status "royal" Norwegian farm and 21 pieces of pumice were found in most phases of the site, although the majority were found in the mixed Phase 7 (Ballin Smith, 1999). This consists of disturbed mixed deposits which incorporate artefacts from all phases. Interestingly the pumice consists of both brown and white/grey pieces (Newton, 1999). The brown pumice is similar to the pumice found elsewhere in Scotland, whilst the five white pieces are rare. The only other similar pieces are found at sites in Yell and Scalloway, also in Shetland.

Figure 4.3: Photograph to show an example of the white/grey pumice found at The Biggings. Although the surface of the pumice looks brown, it is white/grey beneath. This pumice is less dense and more fragile than the brown dacitic pumice. This pumice piece, SF274 (NB 2), is 7.5 cm in diameter.

The youngest piece of white pumice, sample SF441, was found in deposits tentatively dated to the 13th Century AD, whilst the oldest, SF617, was found amongst 19th Century deposits. Several pieces show obvious signs of wear. One of the largest pieces (SF 273, 118 grams), has four flattened faces, formed by rubbing against a substance, perhaps leather or wood. Four pieces of white pumice were analysed for this project (Table 4.5).

Code	Sample	Colour	Age
TB 1	SF 188	white	18-19th Century
TB 2	SF 274	white	unstratified
TB 3	SF 441	white	11-13th Century
TB 4	SF 616	white	16-18th Century

Table 4.5: The age and colour of analysed pumice from The Biggings. Code refers to the sample number used throughout this chapter.

Sands of Breckon, Yell

The Sands of Breckon, have produced pumice in two separate surveys. The survey by Carter and Fraser (1996) found 75 pieces of pumice, whilst that of Buckland (pers. comm.) recovered 19 brown and one white piece of pumice. All of the pumice was found around settlement sites, being exposed by the erosion of overlying sand dunes. This lack of secure context means that it was not possible to date any of the pumice. There is evidence, however, of Iron Age to Medieval settlements at the site (Carter and Fraser, 1996). EPMA were undertaken on one piece of white/grey (SB 1) and on one brown pumice (SB 2). The only other sites where the white/grey type of pumice has been found are both on Shetland, The Biggings and Scalloway. SB 2 was also analysed by XRF.

Inner Isles

During this study pumice from Staosnaig on Colonsay was the only site in the Inner Islands where pumice was analysed. Details are included about Kinloch Farm on Rum, as this pumice was analysed by Dugmore (Clarke and Dugmore, 1990) under the same conditions as some of the other XRF analyses described in this chapter.

Kinloch Farm, Rum

Kinloch Farm, on the island of Rum (site 37 on Figure 4.1), is found at the head of Loch Scresort. The site's importance is based on the early dates for occupation. The Mesolithic settlement of the site has been dated to between 8685 and 7520 ^{14}C years BP (Wickham-Jones, 1990). This early Holocene date is the oldest evidence of human settlement in Scotland. The most numerous finds from the site are lithic fragments and there is evidence

of the construction of shelters with racks and frames (Wickham-Jones, 1990). The eleven pieces of pumice found at the site were examined by Clarke and Dugmore (1990). Five of the pieces show signs of use, with some of the pumice having grooves. Clarke and Dugmore (1990) analysed three pieces of pumice by XRF and decided that the two Mesolithic pieces were probably artificial, the result of a high temperature fire. The Neolithic (3890±65 ^{14}C years BP) brown pumice piece is included in the discussion about XRF analyses.

Staosnaig, Colonsay

Staosnaig is a Mesolithic archaeological site on the east coast of Colonsay (site 10 on Figure 4.1). The site was discovered in 1989 in a field and was the focus of a major excavation during the early 1990s (Mithen, Forthcoming). Although it has been difficult to interpret the structures found at Staosnaig, it is possible that the main feature (F14) a large circular pit, could be the remains of a hut built by the Mesolithic hunter-gathers. ^{14}C dating of charred hazelnut shells suggest that the hut was used as a refuse dump, probably between about 7900 and 7000 ^{14}C years BP.

A total of nine pumice samples (23 individual pieces) were found in F24 which varied in diameter between 0.5 and 7 cm (Newton, Forthcoming-a). All of the larger, unbroken pumice pieces were rounded and showed no signs of having been burnt. Morphologically two types of pumice can be readily identified (Figure 4.4). The first type has a very low density, is light brown in colour and has elongated vesicles. The second type, which is slightly denser, is black with more rounded vesicles. Both types of pumice appear in the same samples. The light brown pumice appears to be morphologically different to virtually all of the dacitic pumice found both in archaeological and natural sites in the British Isles. The darker, black pumice appears to be morphologically similar to other dacitic pumice deposits. Two pieces of black and two pieces of light brown pumice were analysed (Table 4.6).

Figure 4.4: Photographs to show the two types of pumice found at Staosnaig. The upper photograph is an example of the light brown pumice (5.5 cm across). The lower photograph is typical of the black pumice (5 cm across).

Code	Sample	Colour	Age
SG 1	52064	light brown	7000-7900 ^{14}C years BP
SG 2	51007	black	7000-7900 ^{14}C years BP
SG 3	53031/1	black	7000-7900 ^{14}C years BP
SG 4	53031/2	light brown	7000-7900 ^{14}C years BP

Table 4.6: The colour and age of analysed pumice pieces from Staosnaig. Code refers to the sample number used throughout this chapter.

The Staosnaig pumice is an important deposit: it is amongst the oldest pumice deposit found in any archaeological site in the British Isles and is amongst the oldest Holocene pumice deposits studied in detail anywhere. Some of the pumice appears to be physically different to pumice found at the younger (Neolithic or more recent) archaeological sites elsewhere in Scotland. The results of the analyses of the Staosnaig pumice have been included in the final excavation report (Newton, Forthcoming-a).

Mainland Scotland

Green Castle, to the east of Aberdeen, was the site of the only pumice analysed from mainland Scotland.

Green Castle, Portknockie, Moray

Green Castle, found on the north coast of Moray (site 40 on Figure 4.1), is unfortunately a poorly stratified site (Ralston, Forthcoming). It is only possible to date the deposits in the archaeological site between the Late Bronze Age to Pictish times (2800-1200 ^{14}C years BP), from the first millennium BC to the first millennium AD . The eight pieces of pumice found at Green Castle are light to dark grey in colour, although SF2290 has darker almost black areas. The vesicles are generally small, 1 mm or less in diameter. All of the pumice has a non-glassy appearance, except for SF2290 which has some glassy areas, corresponding to the darker areas and a few vesicles up to 1.5 cm in diameter. The colour and appearance of the pumice is most similar to the brown pumice found elsewhere. One of the pumice pieces has a hole drilled in it and may have been used as a fishing float (Figure 4.5). The black pumice has larger vesicles which have a more glassy appearance than the brown pumice. Six of the eight pieces of pumice were analysed (Table 4.7)

Figure 4.5: Photograph to show an example of a worked piece of pumice from Green Castle. A hole has been drilled through the pumice and it may have been used as fishing float. The pumice is just over 4 cm in diameter.

Code	Sample	Colour	Age
GC 1	SF49	light/dark grey	Late Bronze Age-Pictish
GC 2	SF1717	light/dark grey	Late Bronze Age-Pictish
GC 3	SF2078	light/dark grey	Late Bronze Age-Pictish
GC 4	SF2290	light/dark grey	Late Bronze Age-Pictish
GC 5	SF2340	light/dark grey	Late Bronze Age-Pictish

Table 4.7: The colour and age of analysed pumice pieces from Green Castle. Code refers to the sample number used throughout this chapter.

Despite the imprecise dating of the pumice found at Green Castle, this site is important, as finds from the mainland of Scotland are comparatively rare (Chapter 2) and these analyses are the only Scottish mainland pumice studied in this thesis. The results of these analyses are included in the final excavation report (Newton and Dugmore, Forthcoming-b).

4.2.2 Ireland

The only Irish site from which pumice was analysed is Dún Aonghasa, which is found on the Aran Islands, off Ireland's west coast.

Dún Aonghasa

Dún Aonghasa, a Late Bronze Age hillfort, is found on the island of Inis Mór, part of the Aran Islands, located off the coast of County Galway, Ireland (site 3 on Figure 4.1). The results of the analysis of the pumice from Dún Aonghasa are presented in a report which has

yet to be published (Clarke and Newton, 2001). The site was excavated by a team of archaeologists from The Discovery Programme (Ar Thóir Na Sean) based in Dublin. Although dating at the site is not too precise, it appears that the pumice assemblage is associated with Late Bronze Age deposits (2900-2600 ^{14}C years BP). There are no reports of any pumice finds from the later post AD 500 occupation of the site. All of the 179 pieces of pumice found at the site are brown with small non-glassy vesicles. A total of 93 pieces have worn faces, five have worn faces and grooves and seven have only grooves. The remainder of the pumice consists of either angular (33) or rounded pieces (41). The grooved pumice was probably used for sharpening bone points or wooden shafts. whilst the flattened pumice was probably used for smoothing large flat areas, such as leather, although MacGregor (1974) also suggest that they could also have been used to smooth or burnish leather hard pottery before firing. Three pumice pieces were analysed from this site (Table 4.8).

Code	Sample	Colour	Age
D 1	334	brown	L. Bronze Age (2900-2600 14C years BP)
D 2	F.42/198	brown	L. Bronze Age (2900-2600 14C years BP)
D 3	333	brown	L. Bronze Age (2900-2600 14C years BP)

Table 4.8: The colour and age of analysed pumice pieces from Dún Aonghasa. Code refers to the sample number used throughout this chapter.

4.2.3 Summary of pumice selected for analysis

Three types of pumice have been selected for analyses. The most numerous are the brown/black/brown variety of pumice, whose presence is common in archaeological sites throughout western and northern Scotland (Chapter 2). The second type is the white pumice found at three sites in Shetland and the third is the light brown pumice which comprise about half of the pumice found at the Mesolithic finds at Staosnaig. The pumice chosen for analysis ranges in age from the Mesolithic (older than about 7000 ^{14}C years BP) to the 19th Century AD. The next section describes the geochemical analyses undertaken on the pumice.

4.3 Geochemical analyses of pumice

Whilst section 3.4 discussed the results of the geochemical analyses of pumice pieces from raised shorelines, this section describes the results of the analyses of pumice pieces from archaeological sites in Scotland and Ireland.

4.3.1 Introduction

Three types of geochemical analyses were carried out on the archaeological pumice as well as the pumice from natural sites discussed in Chapter 3. The standard and most numerous were electron probe microanalyses (EPMA). In total: 436 EPMA were undertaken on 50 pieces of pumice from 14 archaeological sites in Scotland and Ireland (section 4.2); 20 XRF analyses were carried out on selected pumice pieces from seven Scottish archaeological sites; 39 SIMS analyses on pumice from four Scottish archaeological sites. Details about these three techniques can be found in Chapter 3 (section 3.3).

The analyses from the Scottish and Irish archaeological pumice will be discussed first. Sections 4.4 and 4.5 compare these results with published data and the data acquired from pumice from natural contexts.

4.3.2 Scotland and Ireland

Major Element EPMA Analyses

All of the Scottish and Irish archaeological pumice analysed by EPMA for this study is silicic and mainly calc-alkaline in composition (Figure 4.6). Figure 4.6a shows that all of the pumice is either high medium-K or high-K and ranges from dacitic to rhyolitic (Le Maitre, 1989). Two distinct groups are formed, the largest group has lower abundances of SiO_2 and K_2O relative to the small more silicic group. Figure 4.6b also shows that all of the analyses are typical of those from a calc-alkaline tectonic setting (Irvine and Baragar, 1971) and can again be split into two distinct groups. The smaller group being identified mainly by much lower abundances of MgO. The means and standard deviation of the EPMA are presented in Tables 4.3, 4.4, 4.5 and 4.6 and full details showing each analysis are shown in Appendix 3.

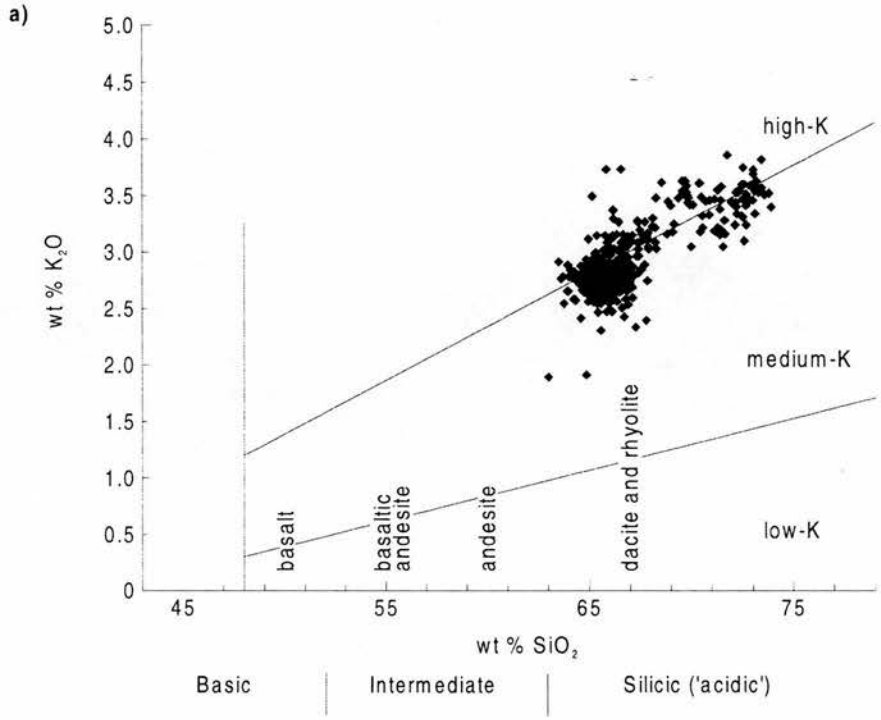

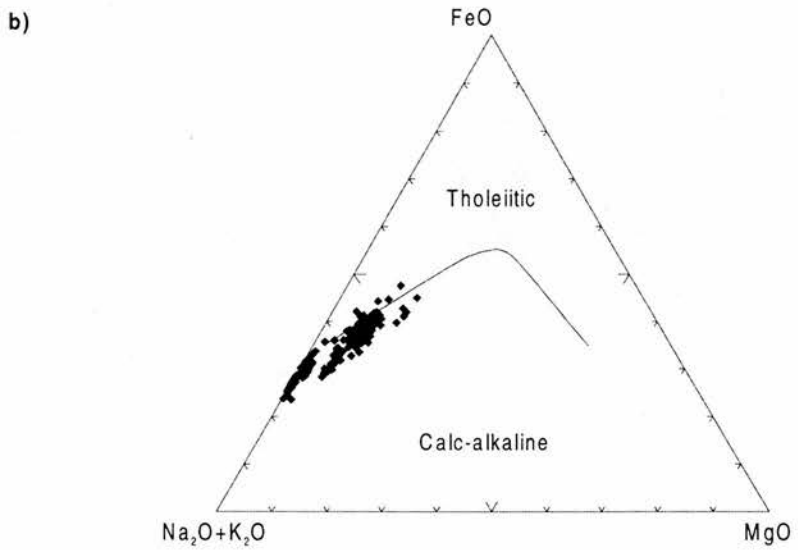

Figure 4.6: Graphs to show that: a) all of the analysed pumice pieces are silicic in composition and can be split into two distinct groups, based on recommendations of Le Maitre (1989). b) All of the pumice is calc-alkaline, with the exception of a few analyses and can again be split into two groups, based on Irvine and Baragar (1971).

Despite the groupings shown in Figure 4.6, as with the analyses of pumice presented in section 3.4, there is still considerable spread of some data points. In order to examine these data in a systematic manner, the data will be split into distinct groups and each of these groups studied in turn. As in section 3.4, the separate groups do not in themselves imply different eruptions or sources. Finally, the major element properties of all of the pumice will be summarised.

Figure 4.6 showed that the data as a whole can be broadly divided into two groups, mainly on the abundances of SiO_2 (a) and K_2O (b). These differences are highlighted in Table 4.9. The four groups identified in Figure 4.7, show that the pumice found in archaeological sites in the British Isles is of at least four types.

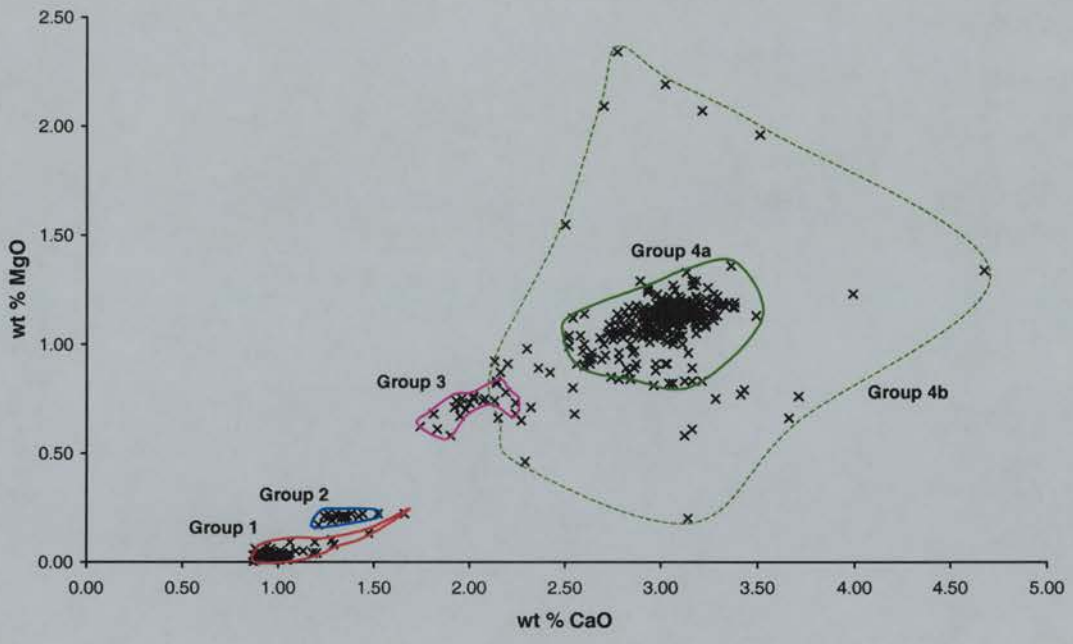

Figure 4.7: Graph (CaO/MgO) to show that at least four main groups of analyses can be seen. Two groups (Groups 1 and 2) have low CaO (0.87-1.66%) and MgO (0.0-0.22%) abundances. A third group is centred with CaO abundances of around 2% and MgO of 0.75%. The fourth and most numerous group is centred around about 3% CaO and 1.2% MgO. A number of analyses (Group 4b) do not fit these groups and are scattered around these groups.

Groups 1 and 2

Figure 4.6 and Figure 4.7 picked out two distinct groups of rhyolitic pumice with particularly low values of MgO and relatively low abundances of CaO. These are from the archaeological sites at The Biggings, the Sands of Breckon and Scalloway in Shetland and

Staosnaig on Colonsay. These sites range in age from Mesolithic (Staosnaig) to Medieval (The Biggings, Scalloway and Sands of Breckon). The pumice with the lowest MgO abundances, Group 1, is the white pumice found at The Biggings, Scalloway and the Sands of Breckon (Table 4.9; Figure 4.8). This pumice, as noted above, is physically different from that found elsewhere in archaeological sites in the British Isles, distinctive because of its high vesicularity and white colour (Figure 4.9). Figure 4.8 shows that the pumice from these three sites is fairly homogeneous, with the notable exception of TB 1. The data presented in Table 4.9 and Figure 4.8 suggest that the white pumice found at the medieval sites of The Biggings, Scalloway and the Sands of Breckon was erupted from the same source, if not necessarily the same eruption. The geochemistry of TB 1 is slightly different, with a definite trend existing: a decrease in SiO_2 being accompanied by a rise in the abundance of FeO, MgO and CaO (Figure 4.8; Table 4.9; Appendix 3). The lower CaO and MgO analyses are similar to those of the other white pumice pieces (Figure 4.8) and it is likely that this pumice was produced by the same eruption that produced the other white pumice. TB 1, however, is slightly different but it appears to have erupted by the same source as the other white pumice. The trend seen in the analyses of TB 1 are common in tephra layers produced by Iceland volcanoes, for example Hekla (Dugmore *et al.*, 1995).

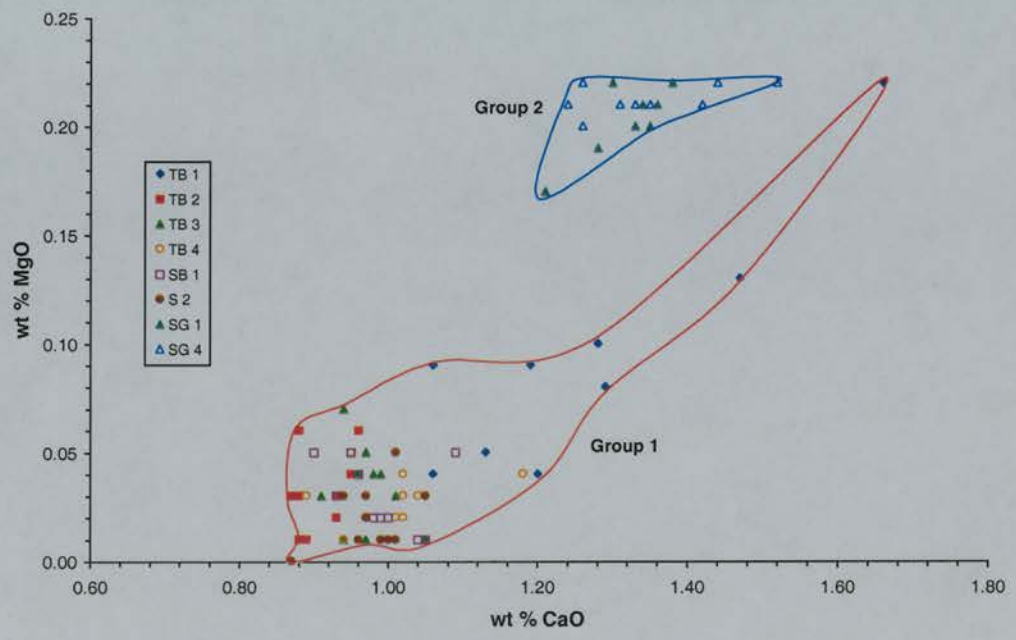

Figure 4.8: This graph (CaO/MgO) shows the that two distinct groups exist, with the pumice from The Biggings (TB), Scalloway (S) and the Sands of Breckon (SB) having much lower MgO abundances than the two pieces from Staosnaig (SG), with the exception of TB 1 from The Biggings.

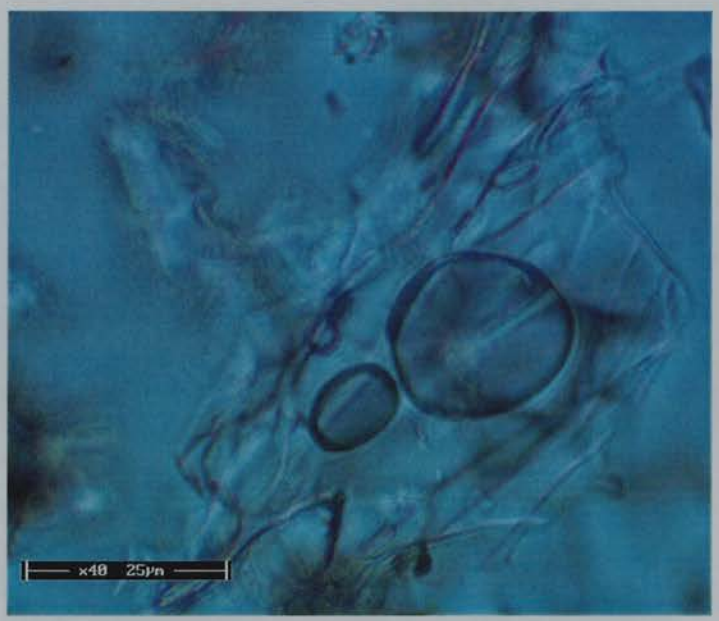

Figure 4.9: Light micrograph to show an example of the clear colourless glass which makes up the Group 1 pumice. The glass is virtually phenocryst free. This example is SB 1.

The light brown pumice from Staosnaig (SG 1 and SG 2) forms the second distinct part of the low-MgO group, Group 2. There is little difference between these two pieces of pumice, as shown in Table 4.9 and Figure 4.8. These two pieces, which form part of the pumice deposit at Staosnaig, are morphologically and geochemically distinct from any other pumice pieces found in the British Isles.

a)

Site	Pumice	SiO_2	1σ	TiO_2	1σ	Al_2O_3	1σ	FeO	1σ	MnO	1σ	MgO	1σ	CaO	1σ	Na_2O	1σ	K_2O	1σ	Total	1σ	n
N. Biggings	TB 1	71.52	*0.85*	0.32	*0.07*	13.29	*0.32*	3.68	*0.40*	0.11	*0.04*	0.09	*0.06*	1.23	*0.21*	4.70	*0.17*	3.20	*0.09*	98.13	*0.98*	10
	TB 2	71.76	*0.91*	0.25	*0.03*	12.79	*0.37*	3.06	*0.12*	0.10	*0.03*	0.03	*0.02*	0.90	*0.03*	5.08	*0.42*	3.49	*0.26*	97.45	*1.31*	10
	TB 3	72.25	*0.81*	0.23	*0.03*	13.25	*0.17*	3.17	*0.09*	0.09	*0.03*	0.03	*0.02*	0.97	*0.04*	4.86	*0.46*	3.55	*0.14*	98.40	*1.14*	10
	TB 4	72.69	*0.93*	0.22	*0.04*	13.14	*0.25*	3.23	*0.06*	0.10	*0.03*	0.03	*0.01*	1.01	*0.08*	4.78	*0.18*	3.43	*0.12*	98.63	*1.16*	10
S. of Breckon	SB 1	71.28	*0.71*	0.21	*0.03*	13.24	*0.25*	3.14	*0.11*	0.11	*0.04*	0.03	*0.02*	0.99	*0.06*	5.48	*0.15*	3.41	*0.14*	97.89	*1.11*	10
Scalloway	S 2	72.82	*0.41*	0.24	*0.04*	13.23	*0.11*	3.29	*0.04*	0.08	*0.02*	0.02	*0.01*	0.98	*0.05*	4.97	*0.23*	3.50	*0.06*	99.12	*0.45*	10
Staosnaig	SG 1	69.48	*0.51*	0.27	*0.03*	13.11	*0.11*	3.78	*0.14*	0.13	*0.03*	0.20	*0.01*	1.33	*0.05*	5.34	*0.05*	3.49	*0.14*	97.12	*0.48*	10
	SG 4	70.02	*0.58*	0.27	*0.06*	12.93	*0.29*	3.78	*0.16*	0.14	*0.03*	0.21	*0.01*	1.35	*0.09*	5.31	*0.18*	3.52	*0.07*	97.51	*0.52*	9

b)

		SiO_2	TiO_2	Al_2O_3	FeO	MnO	MgO	CaO	Na_2O	K_2O	Total	n
Group 1	Mean	72.05	0.24	13.15	3.26	0.10	0.04	1.01	4.98	3.43	98.27	60
	1σ	0.96	0.05	0.30	0.27	0.03	0.03	0.14	0.38	0.18	1.15	
Group 2	Mean	69.74	0.27	13.02	3.78	0.13	0.21	1.34	5.33	3.50	97.31	19
	1σ	0.60	0.05	0.23	0.15	0.03	0.01	0.07	0.13	0.11	0.53	

Table 4.9: a) shows the means and standard deviations (1σ) of the rhyolitic pumice pieces with low MgO abundances. b) shows the means and standard deviations (1σ) of the two groups and illustrates the differences between them, Group 1 has lower MgO and CaO and higher SiO_2 than Group 2. The number of analyses are also shown (n) and full details about these analyses are available in Appendix 3.

Group 3

The third homogeneous group is defined by the analyses of two black dacitic pumice pieces from the Mesolithic site at Staosnaig on Colonsay. The geochemical properties of the light brown pumice found at the same site have already been discussed. The black pumice differs from the light brown pumice by having higher CaO and especially TiO_2 and MgO. Figure 4.10 compares the two types of pumice found at Staosnaig and illustrates the differences between them. Both SG 2 and SG 3 have very similar geochemical properties, as shown in Table 4.10. The physical and geochemical properties of the pumice show that the pieces found at the Mesolithic site were produced by two separate eruptions.

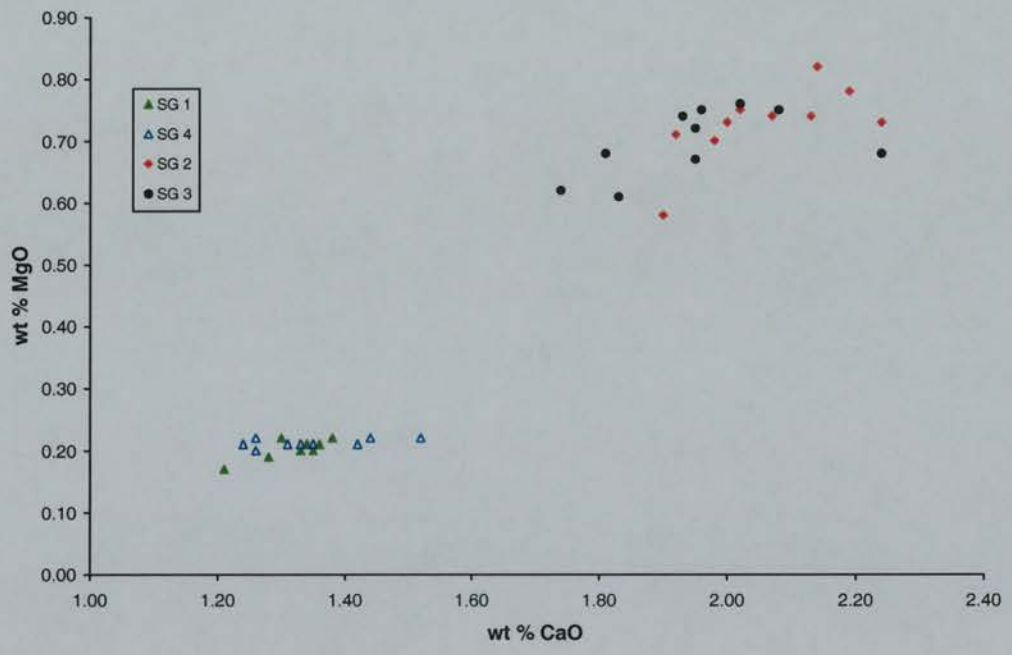

Figure 4.10: Graph (CaO/MgO) to show the differences between the two types of pumice found at Staosnaig.

Group 4a

The largest concentration of analyses in Figure 4.7 is composed of pumice pieces with an average abundance of CaO of about 3% and MgO of around 1.1%. Table 4.11a shows that this group represents 302 analyses of 36 pieces of pumice from nine archaeological sites. Other characteristic features of this group is the average SiO_2 abundance of between 65 and 66%, mean TiO_2 abundances of around 1.2%, mean FeO of about 5.5% and mean K_2O of 2.8% (Table 4.11b).

Pumice	SiO_2	1σ	TiO_2	1σ	Al_2O_3	1σ	FeO	1σ	MnO	1σ	MgO	1σ	CaO	1σ	Na_2O	1σ	K_2O	1σ	Total	1σ	n
SG 2	67.43	*0.52*	0.83	*0.06*	13.62	*0.19*	4.13	*0.20*	0.12	*0.02*	0.73	*0.06*	2.06	*0.11*	5.20	*0.11*	3.14	*0.08*	97.27	*0.76*	10
SG 3	68.06	*0.78*	0.83	*0.06*	13.59	*0.18*	3.93	*0.24*	0.14	*0.04*	0.70	*0.05*	1.95	*0.14*	5.01	*0.21*	3.15	*0.10*	97.37	*0.76*	10

Table 4.10: The means and standard deviations (1σ) of the Group 3 pumice found at Staosnaig. There is little variation between the analyses of these two pumice pieces. The number of analyses are also shown (n) and full details about these analyses are available in Appendix 3.

Figure 4.11 and Table 4.11a illustrate that although the majority of pumice pieces from Allt Chrisal, Caerdach Rudh, Green Castle and The Udal have overlapping major element geochemical characteristics, as do the other five sites, there are some exceptions. All of the light brown pumice pieces from Allt Chrisal have similar geochemical characteristics, although the Neolithic AC 4 has consistently higher SiO_2 and lower TiO_2, FeO, MgO and CaO abundances compared to the other three pumice pieces (Figure 4.11a and Table 4.11a).

Five of the seven pumice pieces analysed from Caerdach Rudh show little variation, but CR 4, as AC 4, has slightly higher percentages of SiO_2 and lower TiO_2, FeO, MgO and CaO than the rest (Figure 4.11b and Table 4.11). CR7 has similar amounts of MgO and CaO to CR 4, but has slightly higher amounts of TiO_2 and K_2O (Figure 4.11b and Table 4.11a). There seems to be little correlation to age, with the AC 3 and AC 4, for example, having slightly different geochemistries, but are both from the same context.

All of the analyses of pumice from Green Castle have similar geochemical properties, except for GC 3, which has lower abundances of MgO, although there are only two analyses from this pumice piece, which means that only limited conclusions can be drawn (Figure 4.11c and Table 4.11a).

Finally, the dated U 5, one of the five pumice pieces analysed from The Udal, also has relatively low amounts of MgO and TiO_2 and U 1 (older than 6500 ^{14}C years BP) has lower MgO, although most of the other oxides are very similar to the other three.(Figure 4.11d and Table 4.11a). U 5 does not fit the pattern shown by the pumice pieces in the other graphs. The other graphs show a weak positive linear trend in the proportion of CaO to MgO, as does the Udal pumice, except for U 5.

The weak positive trend seen in Figure 4.11 suggests that most of these pumice pieces were either produced during a single event, or from several eruptions which produced tephra and pumice with little geochemical variation. The major element geochemistry of the Group 4a pumice suggests that all of the pumice is from the same source. Table 4.11 shows that there is relatively little variation between the majority of the pumice pieces and that there is as much variation in the geochemistry of a single pumice piece as there is between the majority of pieces. The exceptions are individual pumice pieces from Allt Chrisal, Caerdach Rudh, Green Castle and The Udal where relatively low abundances of MgO and to a lesser extent TiO_2 are accompanied by a rise in SiO_2. The significance of these variations will be discussed later in this chapter and in Chapter 5.

a)

Site	Pumice	SiO_2	1σ	TiO_2	1σ	Al_2O_3	1σ	FeO	1σ	MnO	1σ	MgO	1σ	CaO	1σ	Na_2O	1σ	K_2O	1σ	Total	1σ	n
Allt Chrisal	AC 1	66.32	*0.75*	1.10	*0.03*	13.82	*0.08*	4.78	*0.22*	0.21	*0.02*	0.97	*0.06*	2.67	*0.14*	4.65	*0.11*	2.95	*0.10*	97.45	*0.63*	8
	AC 2	65.16	*0.78*	1.21	*0.06*	13.68	*0.14*	5.33	*0.30*	0.20	*0.03*	1.13	*0.05*	3.03	*0.09*	4.39	*0.07*	2.75	*0.08*	96.87	*0.53*	5
	AC 3	65.12	*0.84*	1.23	*0.06*	13.74	*0.35*	5.40	*0.32*	0.19	*0.05*	1.14	*0.12*	3.03	*0.16*	4.62	*0.05*	2.81	*0.12*	97.28	*0.96*	5
	AC 4	64.33	*0.65*	1.19	*0.05*	13.61	*0.28*	5.35	*0.27*	0.15	*0.03*	1.13	*0.11*	3.09	*0.18*	4.62	*0.09*	2.82	*0.06*	96.29	*0.84*	7
C. Rudh	CR 1	65.15	*0.76*	1.22	*0.05*	13.97	*0.18*	5.81	*0.18*	0.19	*0.04*	1.17	*0.02*	3.08	*0.10*	4.95	*0.14*	2.69	*0.08*	98.26	*0.87*	5
	CR 2	65.59	*0.99*	1.22	*0.06*	14.05	*0.14*	5.70	*0.21*	0.18	*0.03*	1.11	*0.04*	3.09	*0.12*	4.71	*0.15*	2.70	*0.09*	98.28	*1.21*	10
	CR 3	65.09	*0.68*	1.23	*0.07*	13.99	*0.19*	5.83	*0.27*	0.22	*0.05*	1.16	*0.03*	3.15	*0.22*	4.77	*0.07*	2.65	*0.13*	98.11	*0.78*	5
	CR 4	66.60	*0.63*	1.07	*0.05*	13.94	*0.32*	4.98	*0.37*	0.14	*0.02*	0.96	*0.09*	2.81	*0.14*	4.76	*0.13*	2.91	*0.16*	98.17	*0.79*	9
	CR 5	65.94	*0.60*	1.19	*0.09*	14.13	*0.18*	5.42	*0.12*	0.16	*0.03*	1.13	*0.04*	3.14	*0.11*	4.50	*0.51*	2.65	*0.08*	98.26	*0.84*	9
	CR 6	65.16	*0.59*	1.20	*0.01*	13.85	*0.12*	5.76	*0.20*	0.19	*0.04*	1.17	*0.07*	3.02	*0.11*	5.02	*0.17*	2.77	*0.05*	98.11	*0.56*	5
	CR 7	65.55	*0.66*	1.18	*0.02*	13.86	*0.20*	5.48	*0.37*	0.16	*0.05*	0.98	*0.06*	2.67	*0.27*	4.83	*0.51*	3.15	*0.77*	97.86	*1.21*	5
Cill Donain	CD 1	65.46	*0.69*	1.18	*0.05*	14.10	*0.13*	5.51	*0.22*	0.18	*0.03*	1.16	*0.07*	2.99	*0.18*	4.51	*0.16*	2.76	*0.06*	97.85	*0.76*	12
	CD 2	65.49	*0.62*	1.22	*0.06*	14.01	*0.19*	5.72	*0.30*	0.18	*0.03*	1.11	*0.05*	2.97	*0.09*	4.55	*0.12*	2.76	*0.07*	98.02	*0.72*	13
	CD 3	65.52	*0.65*	1.20	*0.06*	14.17	*0.21*	5.46	*0.13*	0.18	*0.03*	1.15	*0.04*	3.07	*0.15*	4.30	*0.63*	2.72	*0.08*	97.75	*0.50*	13
	CD 4	65.61	*0.61*	1.24	*0.07*	14.15	*0.25*	5.47	*0.25*	0.19	*0.04*	1.16	*0.06*	3.07	*0.17*	4.42	*0.19*	2.68	*0.14*	97.99	*0.58*	12
	CD 5	65.72	*0.64*	1.14	*0.09*	14.01	*0.24*	5.36	*0.15*	0.17	*0.04*	1.12	*0.04*	3.08	*0.10*	4.42	*0.11*	2.79	*0.11*	97.80	*0.73*	13
	CD 6	65.78	*0.74*	1.17	*0.09*	14.04	*0.16*	5.39	*0.19*	0.18	*0.04*	1.11	*0.05*	3.02	*0.12*	4.45	*0.21*	2.78	*0.09*	97.90	*0.70*	13
	CD 7	65.35	*1.04*	1.14	*0.08*	14.03	*0.13*	5.33	*0.16*	0.18	*0.04*	1.12	*0.09*	3.01	*0.13*	4.49	*0.23*	2.79	*0.12*	97.44	*1.20*	13
	CD 8	66.33	*0.92*	1.21	*0.06*	14.10	*0.10*	5.37	*0.42*	0.17	*0.03*	1.11	*0.08*	2.94	*0.21*	4.61	*0.13*	2.76	*0.12*	98.60	*0.50*	13
Cnip	C1	65.72	*0.36*	1.23	*0.06*	14.11	*0.15*	5.78	*0.10*	0.19	*0.04*	1.16	*0.04*	3.06	*0.04*	4.85	*0.09*	2.68	*0.10*	98.77	*0.47*	10
	C2	65.81	*0.39*	1.23	*0.07*	14.05	*0.15*	5.74	*0.15*	0.18	*0.04*	1.14	*0.04*	3.09	*0.08*	4.67	*0.07*	2.79	*0.09*	98.69	*0.45*	10
	C3	66.44	*0.59*	1.21	*0.18*	13.39	*1.25*	5.45	*1.14*	0.16	*0.06*	1.09	*0.58*	2.86	*0.47*	4.89	*0.60*	2.86	*0.33*	98.36	*0.74*	10
D. Aonghasa	D 1	65.73	*0.83*	1.20	*0.08*	13.92	*0.11*	5.49	*0.34*	0.16	*0.04*	1.18	*0.06*	3.21	*0.08*	4.74	*0.13*	2.70	*0.09*	98.33	*0.81*	10
	D 2	66.22	*0.58*	1.20	*0.03*	13.82	*0.12*	5.30	*0.20*	0.18	*0.03*	1.05	*0.05*	2.92	*0.25*	4.70	*0.10*	2.74	*0.06*	98.20	*0.56*	10
Green Castle	GC 1	65.51	*0.47*	1.21	*0.04*	13.98	*0.18*	5.56	*0.16*	0.22	*0.02*	1.12	*0.07*	3.00	*0.17*	4.80	*0.14*	2.82	*0.06*	98.22	*0.44*	5
	GC 2	65.67	*0.62*	1.22	*0.06*	13.99	*0.11*	5.54	*0.17*	0.19	*0.02*	1.10	*0.07*	2.93	*0.06*	4.79	*0.10*	2.79	*0.11*	98.21	*0.68*	8
	GC 3	65.53	*2.14*	1.20	*0.15*	12.49	*0.57*	5.93	*0.55*	0.25	*0.11*	0.79	*0.18*	2.93	*1.03*	4.92	*0.40*	2.99	*0.21*	97.01	*1.16*	2
	GC 4	66.44	*0.27*	1.15	*0.09*	14.19	*0.23*	5.50	*0.14*	0.19	*0.03*	1.14	*0.04*	2.93	*0.11*	4.75	*0.26*	2.83	*0.22*	99.09	*0.46*	4

Site	Pumice	SiO_2	1σ	TiO_2	1σ	Al_2O_3	1σ	FeO	1σ	MnO	1σ	MgO	1σ	CaO	1σ	Na_2O	1σ	K_2O	1σ	Total	1σ	n
	GC 5	66.02	*0.66*	1.18	*0.07*	14.13	*0.29*	5.44	*0.22*	0.19	*0.03*	1.10	*0.09*	2.96	*0.10*	4.86	*0.14*	2.77	*0.20*	98.65	*0.85*	12
Kebister	K 1	65.67	*0.66*	1.18	*0.09*	13.75	*0.19*	5.52	*0.26*	0.16	*0.03*	1.15	*0.06*	3.07	*0.15*	4.97	*0.10*	2.73	*0.12*	98.09	*0.78*	10
Scalloway	S 1	65.31	*0.49*	1.26	*0.04*	13.96	*0.21*	5.57	*0.18*	0.16	*0.04*	1.11	*0.06*	2.99	*0.08*	4.72	*0.13*	2.99	*0.18*	98.08	*0.66*	10
The Udal	U 1	66.35	*0.45*	1.21	*0.07*	14.16	*0.60*	5.22	*0.19*	0.18	*0.01*	0.91	*0.05*	2.75	*0.33*	4.64	*0.20*	2.87	*0.14*	98.28	*0.44*	5
	U 2	65.92	*0.47*	1.24	*0.06*	14.25	*0.14*	5.36	*0.15*	0.22	*0.04*	1.05	*0.06*	2.85	*0.11*	4.75	*0.20*	2.84	*0.13*	98.46	*0.48*	5
	U 3	65.68	*0.96*	1.26	*0.09*	14.11	*0.17*	5.36	*0.36*	0.19	*0.04*	1.12	*0.12*	3.07	*0.27*	4.87	*0.06*	2.91	*0.11*	98.58	*0.49*	5
	U 4	66.05	*0.40*	1.25	*0.05*	14.34	*0.09*	5.43	*0.16*	0.23	*0.04*	1.14	*0.06*	3.09	*0.11*	4.73	*0.13*	2.76	*0.08*	99.03	*0.46*	5
	U 5	64.62	*0.46*	1.15	*0.07*	13.68	*0.11*	5.49	*0.17*	0.20	*0.03*	0.85	*0.05*	3.10	*0.16*	4.54	*0.18*	2.74	*0.09*	96.37	*0.66*	7

b)

		SiO_2	TiO_2	Al_2O_3	FeO	MnO	MgO	CaO	Na_2O	K_2O	Total	n
Group 4a	Mean	65.68	1.20	13.99	5.46	0.18	1.10	3.01	4.65	2.78	98.05	302
	1σ	0.79	0.08	0.27	0.31	0.04	0.10	0.19	0.27	0.16	0.90	

Table 4.11: a) shows the means and standard deviations (1σ) of the Group 4a pumice pieces from nine archaeological sites in the British Isles. b) shows the means and standard deviations (1σ) of all 302 analyses. The number of analyses are also shown (n) and full details about these analyses are available in Appendix 3.

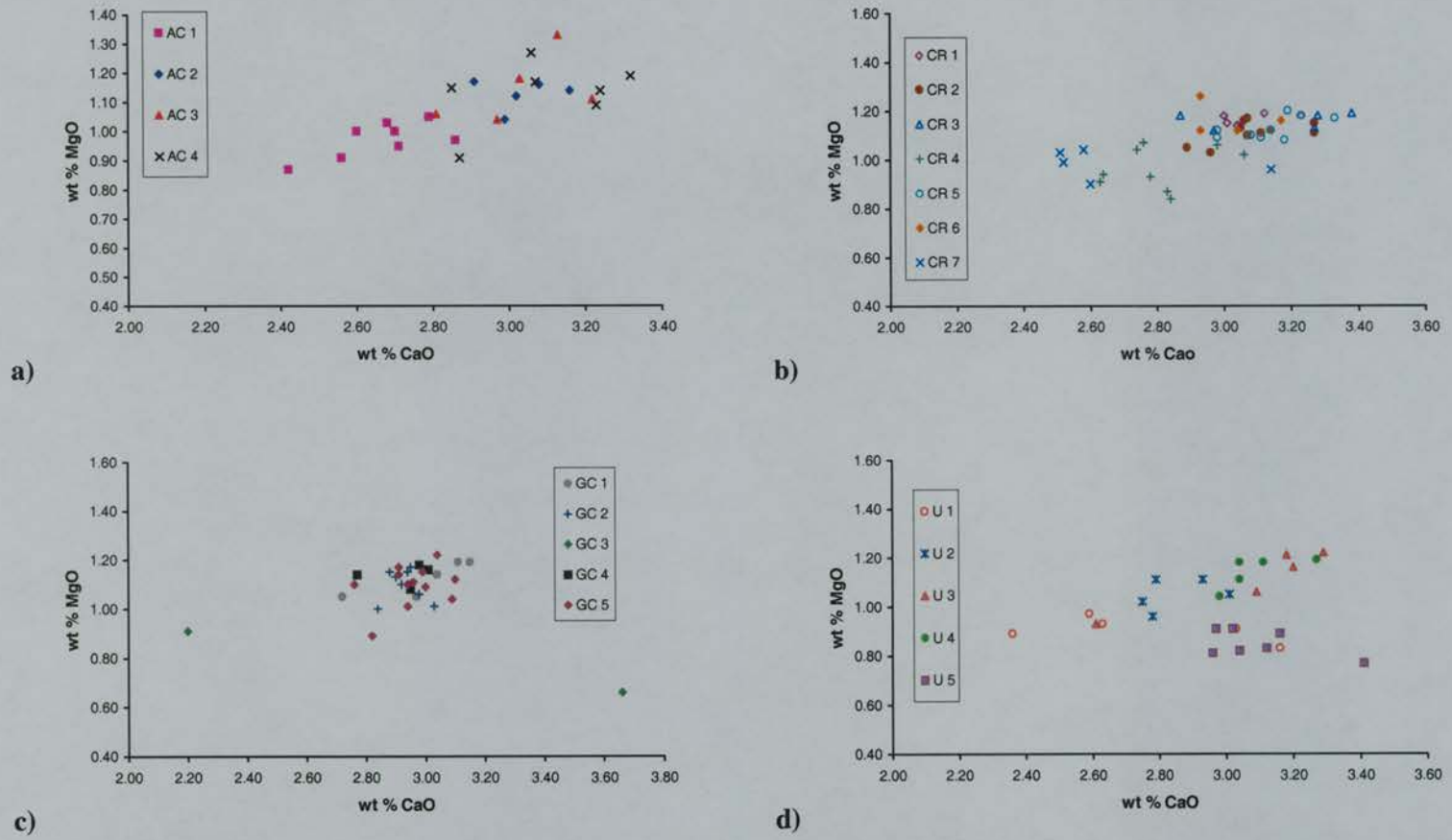

Figure 4.11: Graphs to show the geochemical variation of pumice from Scottish archaeological sites: a) Allt Chrisal; b) Caerdach Rudh; c) Green Castle; d) The Udal.

Group 4b

The remainder of the analysed pumice pieces archaeological sites in the British Isles fall into a fifth group which share many properties Group 4a pumice, but show much greater variability. Figure 4.12 shows that all of the Group 4b, with the exception of US 1, overlap with Group 4a. This pattern is shown in other oxides (Table 4.12), such as the much higher abundances of Al_2O_3, CaO and Na_2O and lower SiO_2 and FeO in US 2 compared with the other pumice pieces in Group 4a and Group 4b. The mean values of the Group 4b pumice are very similar to the mean values of major elements in the Group 4a pumice. The greater geochemical range in the Group 4b pumice, is most probably due to the presence of phenocrysts. As described in Chapter 3, the most likely explanation for the presence of these phenocrysts is a slower cooling history for this pumice compared to the majority of the pumice. For these reasons it is most probable that the Group 4b pumice are from the same source as the Group 4a pumice. Interestingly, most of the pumice pieces from Group 4b are from Iron Age contexts, although the small number of pumice pieces analysed from the sites means that it is not clear how significant this is.

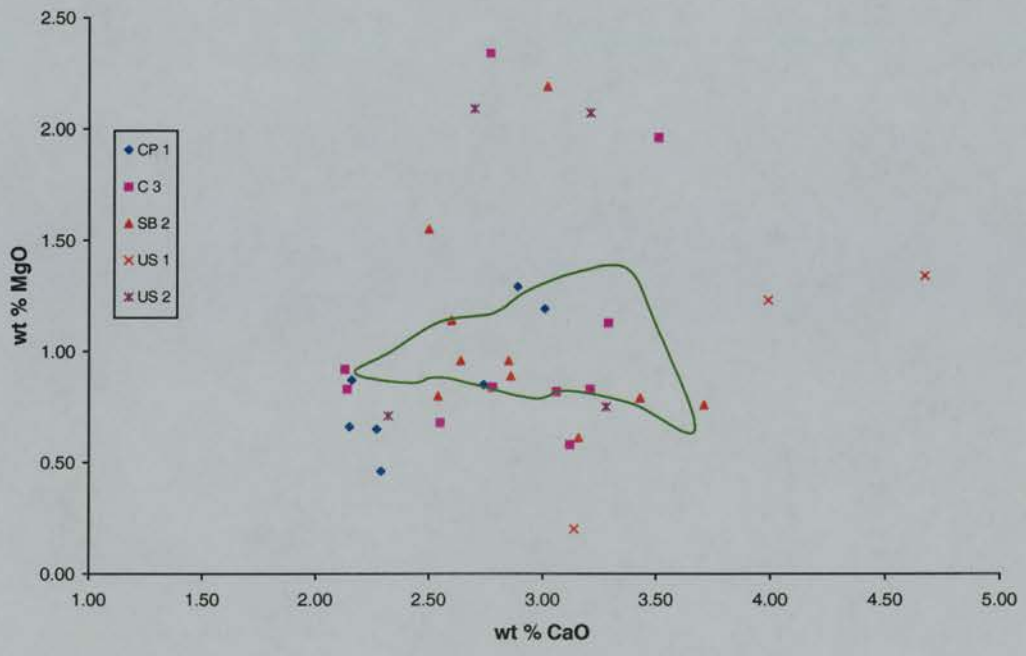

Figure 4.12: Graph (CaO/MgO to show that the Group 4b pumice has greater geochemical variability compared with the Group 4a pumice. The green field on the graph is defined by the 302 analyses of the Group 4a pumice.

a)

Site	Pumice	SiO_2	1σ	TiO_2	1σ	Al_2O_3	1σ	FeO	1σ	MnO	1σ	MgO	1σ	CaO	1σ	Na_2O	1σ	K_2O	1σ	Total	1σ	n
C.Pheadair	CP 1	67.29	*1.01*	1.33	*0.14*	13.10	*0.53*	5.32	*0.36*	0.19	*0.04*	0.83	*0.29*	2.46	*0.36*	4.94	*0.30*	3.11	*0.25*	98.56	*0.58*	8
Cnip	C 3	66.44	*0.59*	1.21	*0.18*	13.39	*1.25*	5.45	*1.14*	0.16	*0.06*	1.09	*0.58*	2.86	*0.47*	4.89	*0.60*	2.86	*0.33*	98.36	*0.74*	10
S. of Breckon	SB 2	66.00	*0.51*	1.20	*0.15*	13.61	*1.11*	5.43	*0.76*	0.21	*0.06*	1.07	*0.47*	2.93	*0.40*	5.00	*0.45*	2.85	*0.26*	98.19	*0.50*	10
U. Scalloway	US 1	64.44	*1.49*	0.90	*0.09*	16.12	*0.67*	4.05	*1.19*	0.16	*0.08*	0.92	*0.63*	3.93	*0.77*	5.65	*0.34*	2.28	*0.34*	98.45	*1.14*	3
	US 2	66.80	*0.89*	1.17	*0.05*	13.43	*1.61*	5.62	*1.08*	0.22	*0.11*	1.41	*0.78*	2.88	*0.45*	4.65	*0.53*	2.85	*0.35*	99.02	*1.13*	4

b)

		SiO_2	TiO_2	Al_2O_3	FeO	MnO	MgO	CaO	Na_2O	K_2O	Total	n
Group 4b all	Mean	66.35	1.20	13.65	5.31	0.19	1.06	2.90	4.96	2.86	98.44	35
	1σ	1.07	0.17	1.31	0.95	0.06	0.52	0.56	0.51	0.35	0.74	

c)

		SiO_2	TiO_2	Al_2O_3	FeO	MnO	MgO	CaO	Na_2O	K_2O	Total	n
Group 4b	Mean	66.53	1.22	13.41	5.43	0.19	1.07	2.80	4.90	2.91	98.44	32
except US1	1σ	0.85	0.15	1.09	0.85	0.06	0.52	0.44	0.48	0.30	0.72	

Table 4.12: a) shows the means and standard deviations (1σ) of the individual Group 4b pumice pieces. b) shows the mean and standard deviation (1σ) of the Group 4b pumice as a whole. c) shows the mean and standard deviation (1σ) of all of the Group 4b pumice pieces, except for US1. Note the much lower 1σ values of SiO_2, Al_2O_3, FeO and CaO when US1 in c). The number of analyses are also shown (n) and full details about these analyses are available in Appendix 3.

Major Element XRF Analyses

Major element geochemistry of some of the pumice from Scottish archaeological sites was determined by a series of XRF analyses. Most of the XRF analyses of the Scottish pumice were undertaken by Dugmore (unpublished), before the work for this thesis began. The XRF analysis of one piece of pumice from Kinloch Farm, Rum, published in Clarke and Dugmore (1990) is also included. The analysis of this pumice was undertaken by Dugmore at the same time as those presented in Table 4.13.

Table 4.13 shows that all of the pumice analysed by XRF is similar to the Group 4a pumice identified by the EPMA (Table 4.11). The major differences are that the wt % SiO_2 abundances of the XRF data tends to be lower and the wt % FeO and MgO higher than the EPMA analyses. None of the pumice analysed can be correlated with any of the other groups identified by the EPMA analyses. Group 4b, for example, was identified by the geochemical heterogeneity of the pumice pieces, which cannot be obtained by XRF analysis. Direct comparison between the EPMA and XRF data is available as nine pumice pieces were analysed by XRF and EPMA. Table 4.14 shows that analyses of pumice from Caerdach Rudh, Cille Pheadair and Sands of Breckon produce variable results. Of the seven pumice pieces from Caerdach Rudh the closest match is between the EPMA and XRF analyses of CR 1. Other close matches exist between the two types of analyses of CR 2, CR 3 and CR 6. The XRF analysis of CR 4 has much lower SiO_2 and higher TiO_2, FeO and CaO than the EPMA. CR 5 is similar except for higher FeO suggested by the XRF analyses and CR7 has significantly higher MgO and MgO in the XRF analyses. The XRF analyses of the pumice pieces from Cille Pheadair and the Sands of Breckon have consistently lower abundances of SiO_2 and higher FeO, MgO and CaO compared to the EPMA.

The differences between the EPMA and XRF analyses is probably due to the presence of mineral inclusions in the glass and contamination in the pores of the pumice. Despite the excellent correlation of some of the pumice, e.g. CR 1 and CR 6, the inconsistency of this means that major element XRF analyses are unsuitable for correlating pumice deposits. This confirms that data obtained by different analytical techniques is difficult to correlate.

a)

Site	Pumice	SiO_2	TiO_2	Al_2O_3	FeO*	MnO	MgO	CaO	Na_2O	K_2O	P_2O_5	Total
Allt Chrisal	**XRF 14**	64.36	1.23	14.23	6.32	0.20	1.21	3.13	4.68	2.54	0.46	98.36
Cille Pheadair	**CP 1**†	64.58	1.22	13.95	5.87	0.19	1.21	3.61	4.99	2.60	0.34	98.56
C. Rudh	**CR 1**†	65.39	1.21	14.02	5.79	0.19	1.12	3.08	4.95	2.68	0.35	98.78
	CR 2†	65.60	1.20	13.90	5.74	0.19	1.21	3.09	4.95	2.66	0.32	98.86
	CR 3†	64.83	1.28	13.98	6.00	0.19	1.29	3.34	4.84	2.59	0.33	98.67
	CR 4†	63.94	1.23	14.17	6.13	0.19	1.25	3.43	4.77	2.56	0.49	98.16
	CR 5†	64.11	1.21	13.96	5.74	0.19	1.18	3.20	4.87	2.64	0.31	97.41
	CR 6†	65.44	1.21	14.01	5.86	0.19	1.19	3.11	4.89	2.66	0.31	98.87
	CR 7†	64.92	1.17	13.94	5.67	0.18	1.25	3.27	4.98	2.70	0.32	98.40
	CR 8†	64.85	1.27	13.88	5.90	0.20	1.26	3.35	4.92	2.59	0.34	98.56
	CR 9†	64.89	1.26	13.91	5.91	0.19	1.23	3.30	4.91	2.58	0.33	98.51
Kebister	**AJD 5**†	62.40	1.33	14.17	6.03	0.21	1.24	3.53	4.65	2.41	0.54	96.51
	AJD 6†	62.46	1.52	13.56	6.85	0.21	1.42	3.34	4.51	2.49	0.73	97.09
	AJD 7†	64.53	1.21	13.95	5.90	0.19	1.06	3.01	4.70	2.65	0.51	97.71
	AJD 8†	64.47	1.21	13.88	6.19	0.19	1.15	2.97	4.84	2.62	0.55	98.07
	AJD 9†	64.85	1.20	13.88	6.01	0.18	1.15	2.95	4.67	2.65	0.53	98.07
	XRF 19	64.83	1.25	13.96	6.15	0.21	1.30	3.09	4.53	2.56	0.44	98.32
Cill Donain	**XRF 13**	64.23	1.24	14.11	5.70	0.17	1.26	3.99	4.79	2.59	0.48	98.56
	XRF 16	63.54	1.23	14.21	6.32	0.20	1.18	3.12	4.87	2.56	0.48	97.71
Kinloch Farm	**KF 1**†	64.76	1.23	14.21	5.57	0.18	1.23	3.18	4.82	2.58	0.33	98.09
S. of Breckon	**SB 2**	63.11	1.34	13.83	6.51	0.20	1.33	3.42	4.78	2.51	0.42	97.45

b)

	SiO_2	TiO_2	Al_2O_3	FeO	MnO	MgO	CaO	Na_2O	K_2O	P_2O_5	Total	n
Mean	64.39	1.25	13.99	6.01	0.19	1.22	3.26	4.81	2.59	0.42	98.13	21
1σ	0.88	0.07	0.16	0.31	0.01	0.08	0.25	0.14	0.07	0.11	0.62	

Table 4.13: a) Major element XRF analyses of Scottish archaeological pumice. FeO* is calculated from the original Fe_2O_3 in order to allow comparison with the EPMA (FeO = Fe_2O_3/1.1113). † denotes analyses undertaken by Dugmore (unpublished). The KF 1 data was originally published in Clarke and Dugmore (1990). b) shows the means and standard deviations of the archaeological XRF analyses.

a)

		SiO_2	1σ	TiO_2	1σ	Al_2O_3	1σ	FeO	1σ	MnO	1σ	MgO	1σ	CaO	1σ	Na_2O	1σ	K_2O	1σ	Total	1σ	n
CR 1	EPMA	65.15	*0.76*	1.22	*0.05*	13.97	*0.18*	5.81	*0.18*	0.19	*0.04*	1.17	*0.02*	3.08	*0.10*	4.95	*0.14*	2.69	*0.08*	98.26	*0.87*	5
	XRF	65.39		1.21		14.02		5.79		0.19		1.12		3.08		4.95		2.68		98.78		
CR 2	EPMA	65.59	*0.99*	1.22	*0.06*	14.05	*0.14*	5.70	*0.21*	0.18	*0.03*	1.11	*0.04*	3.09	*0.12*	4.71	*0.15*	2.70	*0.09*	98.28	*1.21*	10
	XRF	65.60		1.20		13.90		5.74		0.19		1.21		3.09		4.95		2.66		98.86		
CR 3	EPMA	65.09	*0.68*	1.23	*0.07*	13.99	*0.19*	5.83	*0.27*	0.22	*0.05*	1.16	*0.03*	3.15	*0.22*	4.77	*0.07*	2.65	*0.13*	98.11	*0.78*	5
	XRF	64.83		1.28		13.98		6.00		0.19		1.29		3.34		4.84		2.59		98.67		
CR 4	EPMA	66.60	*0.63*	1.07	*0.05*	13.94	*0.32*	4.98	*0.37*	0.14	*0.02*	0.96	*0.09*	2.81	*0.14*	4.76	*0.13*	2.91	*0.16*	98.17	*0.79*	9
	XRF	63.94		1.23		14.17		6.13		0.19		1.25		3.43		4.77		2.56		98.16		
CR 5	EPMA	65.94	*0.60*	1.19	*0.09*	14.13	*0.18*	5.42	*0.12*	0.16	*0.03*	1.13	*0.04*	3.14	*0.11*	4.50	*0.51*	2.65	*0.08*	98.26	*0.84*	9
	XRF	64.11		1.21		13.96		5.74		0.19		1.18		3.20		4.87		2.64		97.41		
CR 6	EPMA	65.16	*0.59*	1.20	*0.01*	13.85	*0.12*	5.76	*0.20*	0.19	*0.04*	1.17	*0.07*	3.02	*0.11*	5.02	*0.17*	2.77	*0.05*	98.11	*0.56*	5
	XRF	65.44		1.21		14.01		5.86		0.19		1.19		3.11		4.89		2.66		98.87		
CR 7	EPMA	65.55	*0.66*	1.18	*0.02*	13.86	*0.20*	5.48	*0.37*	0.16	*0.05*	0.98	*0.06*	2.67	*0.27*	4.83	*0.51*	3.15	*0.77*	97.86	*1.21*	5
	XRF	64.92		1.17		13.94		5.67		0.18		1.25		3.27		4.98		2.70		98.40		

b)

		SiO_2	1σ	TiO_2	1σ	Al_2O_3	1σ	FeO	1σ	MnO	1σ	MgO	1σ	CaO	1σ	Na_2O	1σ	K_2O	1σ	Total	1σ	n
CP 1	EPMA	67.29	*1.01*	1.33	*0.14*	13.10	*0.53*	5.32	*0.36*	0.19	*0.04*	0.83	*0.29*	2.46	*0.36*	4.94	*0.30*	3.11	*0.25*	98.56	*0.58*	8
	XRF	64.58		1.22		13.95		5.87		0.19		1.21		3.61		4.99		2.60		98.56		

c)

		SiO_2	1σ	TiO_2	1σ	Al_2O_3	1σ	FeO	1σ	MnO	1σ	MgO	1σ	CaO	1σ	Na_2O	1σ	K_2O	1σ	Total	1σ	n
SB 2	EPMA	66.00	*0.51*	1.20	*0.15*	13.61	*1.11*	5.43	*0.76*	0.21	*0.06*	1.07	*0.47*	2.93	*0.40*	5.00	*0.45*	2.85	*0.26*	98.19	*0.50*	10
	XRF	63.11		1.34		13.83		6.51		0.20		1.33		3.42		4.78		2.51		97.45		

Table 4.14: Comparison of pumice pieces from three sites which were analysed both by EPMA and XRF. The means, standard deviations and the number of the EPMA are shown. a) Seven pumice pieces from Caerdach Rudh. b) Pumice piece from Cille Pheadair. c) Pumice piece from the Sands of Breckon.

Trace Element SIMS Analyses

A total of 39 SIMS analyses were undertaken on pumice from three Scottish archaeological sites (Table 4.15). These analyses can be readily divided into three or possibly four groups. The Mesolithic two pumice pieces from Staosnaig form two separate groups. SG 1 has the lowest concentration of Ti and Sr and significantly higher abundances of Ba, Y and Zr compared to SG 2 and the other pumice (Table 4.15 and Figure 4.13). Figure 4.13 and Table 4.15 also show that CR 2 (2375±55 ^{14}C years BP) and CR 5 (3360±80 ^{14}C years BP) have no significant geochemical variation, which confirms the results of the EPMA. This demonstrates that pumice pieces from the same archaeological site, although there is thousand years between the two contexts, can have virtually identical major, trace and rare earth element composition. It is possible to say that CR 2 and CR 5 were produced by the same eruption. Finally, U 1, the oldest pumice piece from The Udal, is significantly different geochemically to CR 2 and CR 5, with lower Ti and Sr.

The SIMS analyses of Scottish archaeological pumice has shown a similar pattern to the EPMA. The pumice pieces from Staosnaig are significantly different to all of the other analysed pumice and can be divided into two types. The two pumice pieces from Caerdach Rudh are typical of the common dacitic pumice. SIMS analyses confirm the difference between this type of pumice and the U 1 pumice from the Udal.

Site	Pumice	Ti	1σ	Rb	1σ	Sr	1σ	Y	1σ	Zr	1σ	Nb	1σ	Ba	1σ	La	1σ	Ce	1σ	n
Staosnaig	**SG 1**	1415	54	56	2.4	100	3.3	64	2.3	902	46.2	115	6.4	593	22.5	75	2.0	154	6.6	**5**
	SG 2	4023	48	48	2.1	170	6.1	56	1.7	825	10.5	105	3.2	531	13.8	68	2.7	143	5.6	**10**
The Udal	**U 1**	5444	133	44	1.6	203	29.7	54	2.1	761	19.3	95	4.1	480	22.2	64	3.3	135	7.7	**8**
C. Rudh	**CR 2**	5922	61	41	0.7	251	6.0	55	0.7	753	10.0	92	1.9	493	12.9	65	1.5	140	3.8	**8**
	CR 5	5902	62	42	0.9	254	3.7	55	0.9	754	12.5	92	1.5	495	11.9	66	1.8	140	3.7	**8**

Table 4.15: Means and standard deviations (1σ) of the SIMS analyses of archaeological pumice from sites in Scotland. Full analysis details are available in Appendix 3.

a)

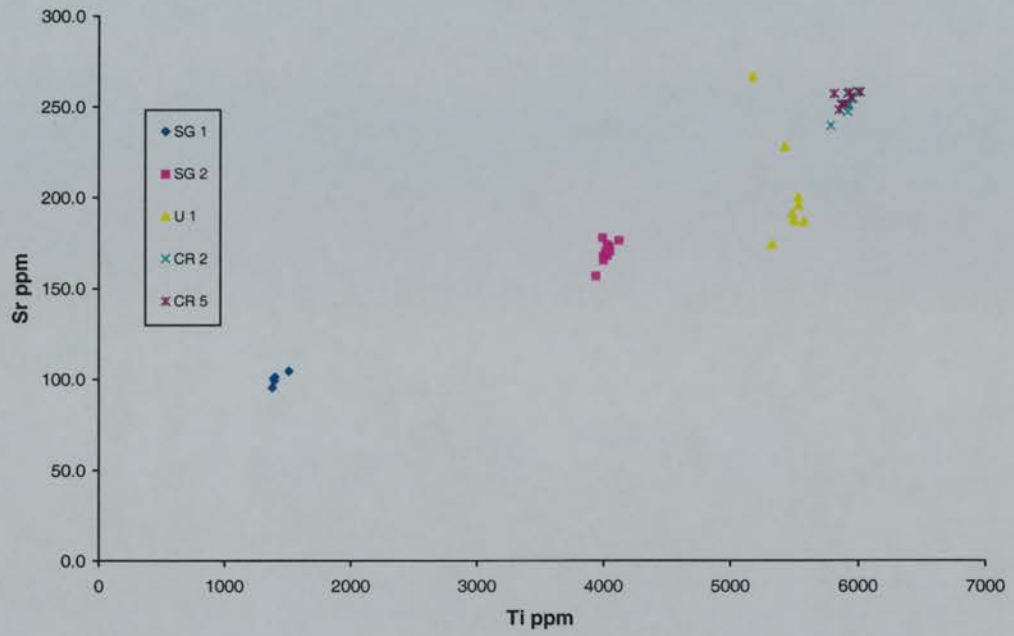

b)

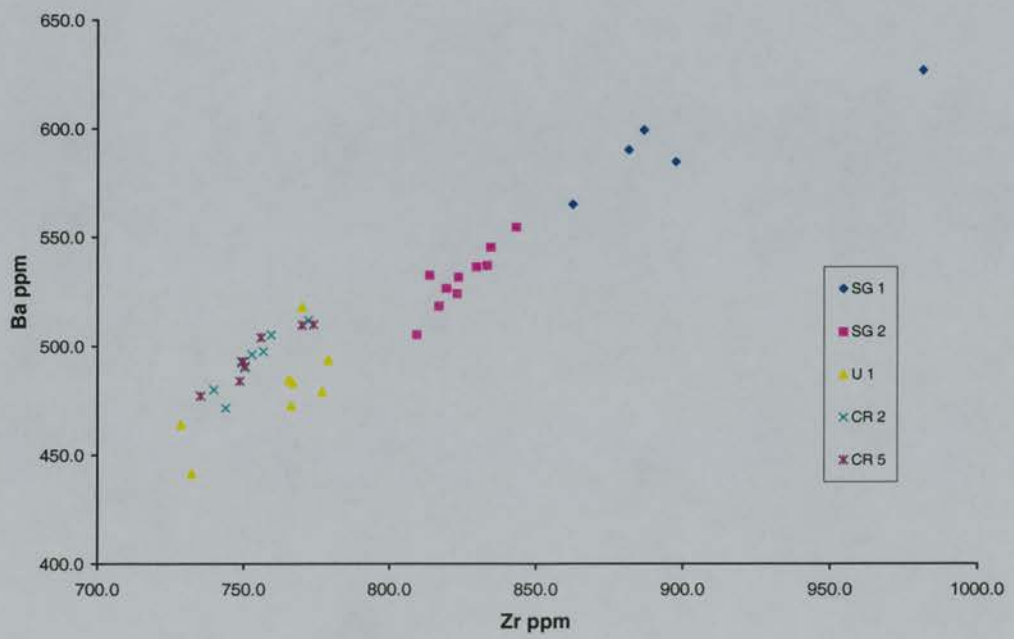

Figure 4.13: Graphs (Ti/Sr and Zr/Ba) to show the differences between the archaeological pumice analysed by SIMS.

Trace Element XRF Analyses

The major element XRF analyses of Scottish archaeological pumice have already been discussed above. Trace and rare earth element analyses were also carried out on the same pumice pieces. These analyses are presented in Table 4.16 and a comparison with the SIMS analyses of two pieces of pumice from Caerdach Rudh is shown in Table 4.17. Although all of the pumice pieces are similar, some differences are apparent. Whilst the pumice from Caerdach Rudh shows little geochemical variation, except for Zr, there is more variability between the pumice pieces from Kebister. The pumice from Allt Chrisal, Cille Pheadair and the Sands of Breckon have lower Ba than the others, as does XRF 19 from Kebister.

Table 4.17 compares directly the SIMS analyses of the CR 2 and CR 5 pumice pieces from Caerdach Rudh. With the exception of Zr, both sets of analyses show the same consistent pattern of homogeneity between the two pumice pieces. The two SIMS analyses are virtually identical, which confirms that this type of analysis is capable of producing consistent and repeatable accurate analyses. The XRF analyses of the two also show the same geochemical homogeneity, although the Zr concentration of CR 5 is much higher. The two types of analyses, however, produce differing concentrations of elements (Table 4.17). The XRF analyses have higher Rb, Sr, Y, Zr, Ba, La and Ce. The only element which shows no significant variation between the two types of analyses is Nb. This is a similar pattern as described in section 3.4.1, where analyses of Norwegian pumice using both techniques resulted in conflicting concentrations of elements.

It is not clear why the XRF analyses of pumice have proved to be so inconsistent. XRF analyses do not form the major focus of this study, as it was decided early on that the point specific non-destructive EPMA and later SIMS analyses provide the most reliable method of producing accurate and precise analyses. Both accuracy and precision are required to allow the comparison of both tephra and pumice. This point is important. It is difficult to carry out XRF analyses of the glass fraction of tephra layers, as the separation of glass from the mineral and lithic fractions is both time consuming and not 100% reliable. Together with the rather inconsistent results produced on the pumice, XRF data will not be used to correlate pumice deposits in this study, although they will mentioned briefly when comparing the new data to the limited published data.

a)

Site	Pumice	Sc	V	Ni	Cu	Zn	Rb	Sr	Y	Zr	Nb	Ba	La	Ce	Nd	Pb	Th
Allt Chrisal	**XRF 14**	6.8	20.5	4.7	5.0	158.8	56.2	302.3	74.0	711.5	93.1	481.4	77.4	163.0	75.6	6.6	8.7
Cille Pheadair	**CP 1**†	4.8	16.7	3.2	2.7	155.9	60.1	339.5	78.7	776.8	97.6	477.3	72.9	158.9	76.8	7.5	9.1
Caerdach Rudh	**CR 1**†	10.3	16.9	4.0	0.3	169.1	58.7	309.9	75.9	805.5	93.4	587.7	81.6	180.0	84.6	7.6	11.1
	CR 2†	7.9	16.8	3.5	0.2	168.4	58.0	308.7	75.7	797.4	93.0	559.9	79.5	178.4	85.1	6.9	9.8
	CR 3†	7.5	21.2	5.3	-0.8	167.4	56.7	318.1	75.1	781.1	92.0	558.3	80.3	174.8	85.0	7.2	10.8
	CR 4†	5.9	27.2	3.6	2.8	162.3	60.7	300.2	79.2	824.0	96.2	593.1	84.9	186.7	87.3	6.2	10.9
	CR 5†	10.5	17.8	4.4	-0.9	168.2	58.5	307.9	75.3	842.7	92.4	583.7	81.3	183.7	83.4	7.2	10.3
	CR 6†	7.5	19.8	3.8	-0.5	169.9	58.9	307.4	75.0	803.3	93.3	597.6	79.1	184.9	88.9	6.9	11.0
	CR 7†	7.8	24.5	4.3	0.8	162.1	55.0	333.4	72.0	770.3	88.6	581.3	77.8	170.3	82.3	6.8	10.5
	CR 8†	6.8	20.9	3.5	0.8	166.9	56.5	316.8	74.5	790.0	90.7	573.3	73.8	180.0	84.5	8.2	9.8
	CR 9†	9.6	22.3	4.9	1.2	166.4	55.8	313.3	73.9	781.0	90.2	548.2	77.7	184.7	82.3	6.8	9.8
Kebister	**AJD 5**†	10.7	40.1	7.4	2.4	151.1	53.5	319.8	71.9	686.3	90.1	533.4	80.1	182.6	82.9	7.1	10.1
	AJD 6†	8.7	32.6	3.9	2.9	167.7	54.8	312.6	71.4	754.6	89.5	578.0	75.4	167.0	76.6	10.1	9.3
	AJD 7†	8.2	17.5	5.7	1.4	171.6	57.2	302.2	75.4	801.6	93.5	555.4	78.0	185.0	84.9	11.3	9.8
	AJD 8†	12.3	20.1	3.9	-1.4	166.8	57.4	300.3	74.4	796.9	92.8	569.5	80.9	185.1	84.4	9.2	10.6
	AJD 9†	10.1	19.1	5.2	0.5	168.0	58.4	302.4	73.9	794.5	92.2	547.6	80.2	178.4	81.3	12.8	10.7
	XRF 19	9.2	28.4	4.1	4.1	155.6	58.4	345.5	75.8	729.7	93.9	495.0	76.6	169.3	79.6	7.8	9.0
Cill Donain	**XRF 13**	6.8	28.4	6.1	6.3	157.6	57.2	334.5	76.9	737.5	94.2	507.3	72.5	169.8	82.2	6.9	8.2
	XRF 16	8.7	22.6	8.7	7.5	186.4	59.5	319.4	79.1	752.0	96.6	508.5	75.3	164.1	83.4	7.6	8.7
Kinloch Farm	**KF 1**†	9.3	19.3	5.5	0.2	161.5	56.3	313.8	74.8	782.2	93.1	575.6	82.0	185.0	85.1	8.2	9.8
Sands of Breckon	**SB 2**	10.3	24.2	3.6	4.3	172.2	59.1	328.3	78.2	728.0	92.0	480.1	74.4	164.1	71.8	12.8	7.3

b)

	Sc	V	Ni	Cu	Zn	Rb	Sr	Y	Zr	Nb	Ba	La	Ce	Nd	Pb	Th
Mean	6.6	32.3	2.8	5.3	153.9	62.1	313.3	78.4	755.0	104.4	504.9	73.2	166.6	81.0	11.8	9.1
1σ	1.9	13.4	0.2	1.8	3.7	1.7	7.4	1.9	17.8	5.1	37.2	5.2	6.6	3.4	4.8	0.8

Table 4.16: a) Trace and rare earth element XRF analyses of Scottish archaeological pumice. † denotes analyses undertaken by Dugmore (unpublished). b) shows the means and standard deviations (1σ) of the XRF analyses.

		Rb	1σ	Sr	1σ	Y	1σ	Zr	1σ	Nb	1σ	Ba	1σ	La	1σ	Ce	1σ	n
CR 2	EPMA	41	0.7	251	6.0	55	0.7	753	10.0	92	1.9	493	12.9	65	1.5	140	3.8	8
	XRF	58		308		75		797		93		559		79		178		
CR 5	EPMA	42	0.9	254	3.7	55	0.9	754	12.5	92	1.5	495	11.9	66	1.8	140	3.7	8
	XRF	58		307		75		842		92		583		81		183		

Table 4.17: Table to compare the SIMS and XRF analyses of two pieces of pumice from Caerdach Rudh.

4.3.3 Summary of geochemical analyses on archaeological pumice

This study has demonstrated that grain specific geochemical analyses provide the most accurate and precise method of obtaining good quality major, trace and rare earth analyses from pumice pieces. Four distinct geochemical groups of pumice have been identified. Most of the pumice is dacitic and belongs to Group 4, although this group can be divided into two subgroups, with a the smaller one, Group 4b, having much greater geochemical variation. Group 4 has pumice ranging in age from the Neolithic to the Iron Age, with Group 4b is composed of mainly Iron Age pumice. The white Medieval pumice from Shetland form Group 1 and the two types of Mesolithic pumice from Colonsay forms Groups 2 and 3. The next section compares the new analyses of archaeological pumice with the published data.

4.4 Comparison with published data

The new data from natural sites was compared with the published data in Chapter 3 (section 3.5). Table 4.18 compares the results of the new EPMA and XRF analyses of the main archaeological dacitic pumice (Group 4a) with the published data. Together with Figure 4.14 and Figure 4.15, Table 4.18 supports the conclusions reached in section 3.5. Most of the published analyses are similar to the main dacitic pumice (Group 4a). The published Scandinavian and Svalbard analyses are most similar to the Group 4a pumice (Figure 4.14 and Figure 4.15). Figure 4.14 shows that the Scand C pumice is similar to the Group 1 and 2 pumice, Table 4.18b shows that the piece that resembles Group 1 on Figure 4.14 has much lower SiO_2 and higher Na_2O. Although the pumice piece which resembles the Group 2 pumice on Figure 4.14 has similar abundances of SiO_2, it has lower FeO, lower Na_2O and K_2O.

a)

		SiO_2	TiO_2	Al_2O_3	FeO	MnO	MgO	CaO	Na_2O	K_2O	Total	n
Main Dacite	**mean**	65.68	1.20	13.99	5.46	0.18	1.10	3.01	4.65	2.78	98.05	302
	1σ	0.79	0.08	0.27	0.31	0.04	0.10	0.19	0.27	0.16	0.90	
XRF	**mean**	64.37	1.25	13.97	6.03	0.19	1.22	3.27	4.80	2.59	98.13	20
	1σ	0.90	0.08	0.15	0.30	0.01	0.08	0.25	0.14	0.07	0.64	
Svalbard	**mean**	64.58	1.09	15.27	5.64	0.18	1.33	3.10	4.95	2.63	99.82	9/8*
	1σ	0.64	0.22	0.86	0.36	0.00	0.28	0.29	0.29	0.28	1.13	
Scand A	**mean**	63.85	1.13	14.42	5.83	0.18	1.20	3.32	5.09	2.04	97.87	9/5*
	1σ	0.96	0.15	0.30	0.24	0.02	0.13	0.45	0.35	0.39	1.75	
Canada	**mean**	61.21	1.20	15.94	5.67	0.19	1.53	3.39	4.89	2.59	98.75	8
	1σ	0.77	0.03	1.42	0.14	0.01	0.24	0.23	0.10	0.04	1.03	
Greenland		63.53	1.05	13.72	6.25	0.18	1.22	3.90	5.39	2.35	99.59	
Scotland	**mean**	63.37	1.25	14.62	5.97	0.19	1.41	3.30	4.81	1.78	97.09	6
	1σ	1.11	0.10	0.04	0.13	0.01	0.03	0.22	0.28	0.08	1.32	

b)

		SiO_2	TiO_2	Al_2O_3	FeO	MnO	MgO	CaO	Na_2O	K_2O	Total	n
Group 1	**mean**	72.05	0.24	13.15	3.26	0.10	0.04	1.01	4.98	3.43	98.27	60
	1σ	0.96	0.05	0.30	0.27	0.03	0.03	0.14	0.38	0.18	1.15	
Scand C		65.10	0.33	13.60	3.45	0.11	0.05	1.10	6.00	4.00	94.42	1
Group 2	**mean**	69.74	0.27	13.02	3.78	0.13	0.21	1.34	5.33	3.50	97.31	19
	1σ	0.60	0.05	0.23	0.15	0.03	0.01	0.07	0.13	0.11	0.53	
Scand C		69.00	0.12	14.80	1.96	0.08	0.27	1.44	4.40	2.60	95.04	1

Table 4.18: Comparison of the new geochemical data with that published sources (see Chapter 2). a) compares the EPMA and XRF analyses of the main dacitic group to similar published analyses. * indicates that the mean was calculated from incomplete analyses, at least one element was not measured in all the analyses. b) compares the Groups 1 and 2 archaeological pumice with two published analyses of Norwegian pumice.

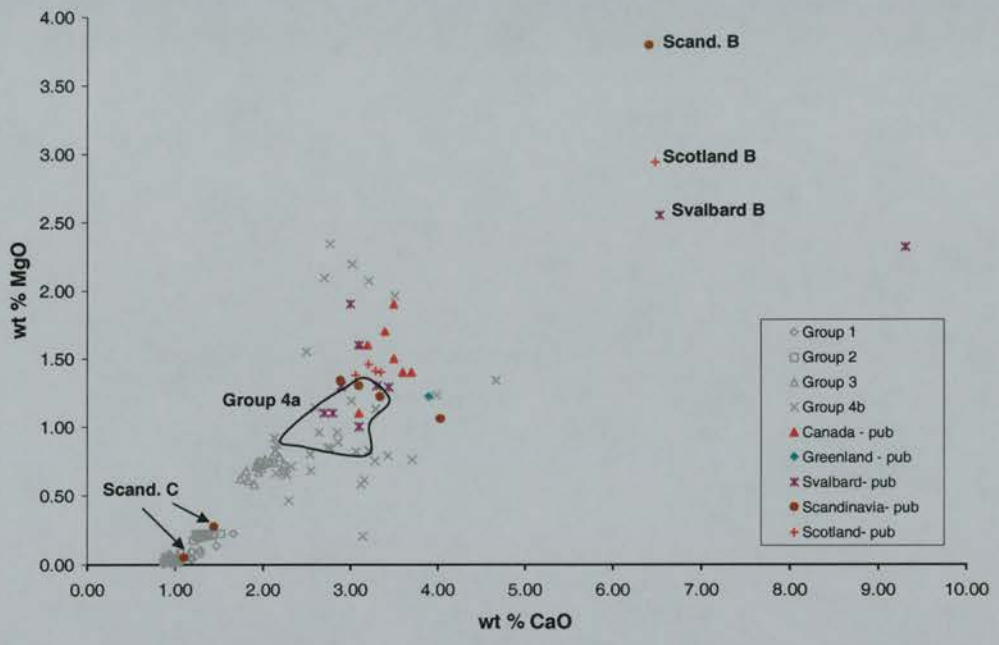

Figure 4.14: Graph (CaO/MgO) to compare the published geochemical data (see Chapter 2) with the new data presented in this chapter. The field is defined by the 298 analyses which comprise Group 4a archaeological pumice from Ireland and Scotland (four analyses outside the main group are excluded. Some individual published analyses are identified. The high CaO Svalbard analysis is excluded from the mean totals in Table 4.17. All new data is labelled by the suffix *Group* and published data by *pub*.

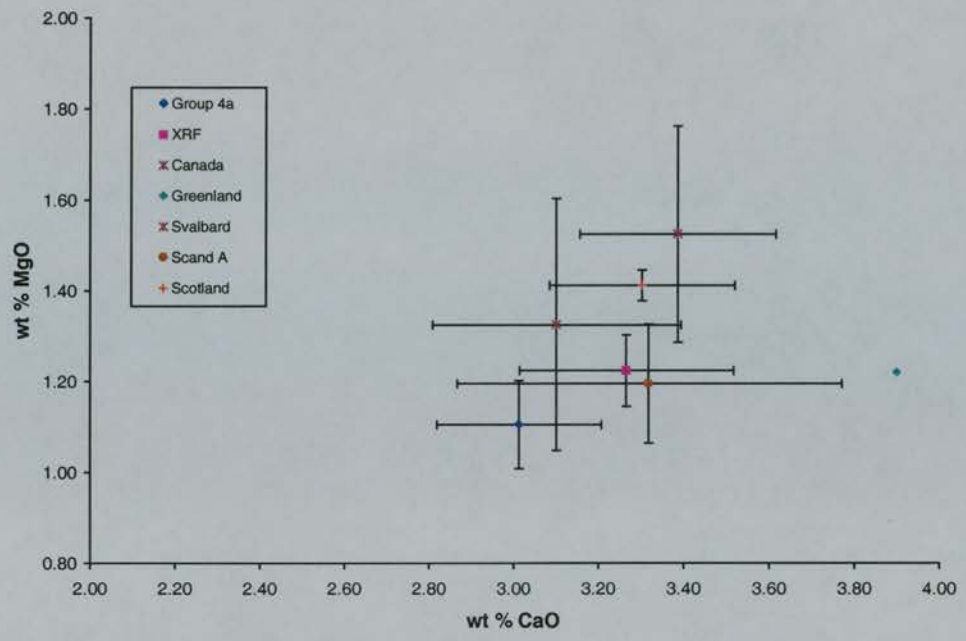

Figure 4.15: Graph (CaO/MgO) to plot the means and standard deviations (1σ) of the main dacitic pumice and the published data. It shows that the Scandinavian and Svalbard analyses are the most similar to the new results. This also highlights the differences between the XRF and EPMA analyses.

Figure 4.16 shows that as with the pumice from natural sites, half of the pumice data published by Boulton and Rhodes (1974) can be loosely correlated with the main dacitic archaeological pumice. This supports the view that the pumice from the 6500 ^{14}C years BP Svalbard shoreline is from a different source to the main dacitic pumice found elsewhere.

The rather poor quality of the published geochemical data on North Atlantic pumice means that it is not possible to produce confident correlations with the new geochemical analyses. A comparison of the limited geochemical data on pumice from Svalbard, suggests that at least two different sources are responsible for the deposits there. The older pumice from the 6500 ^{14}C years BP shoreline was not produced from the same volcano as the pumice found on the younger beaches or any of the other analysed pumice from the North Atlantic region. As pointed out in Chapter 2, the published geochemical data has been gathered over a long period, using a variety of techniques and all of the analyses have been carried out on bulk samples. This section has highlighted the advantages of using grain specific analyses and it would be impossible to use the published data to correlate the pumice to a particular volcanic event.

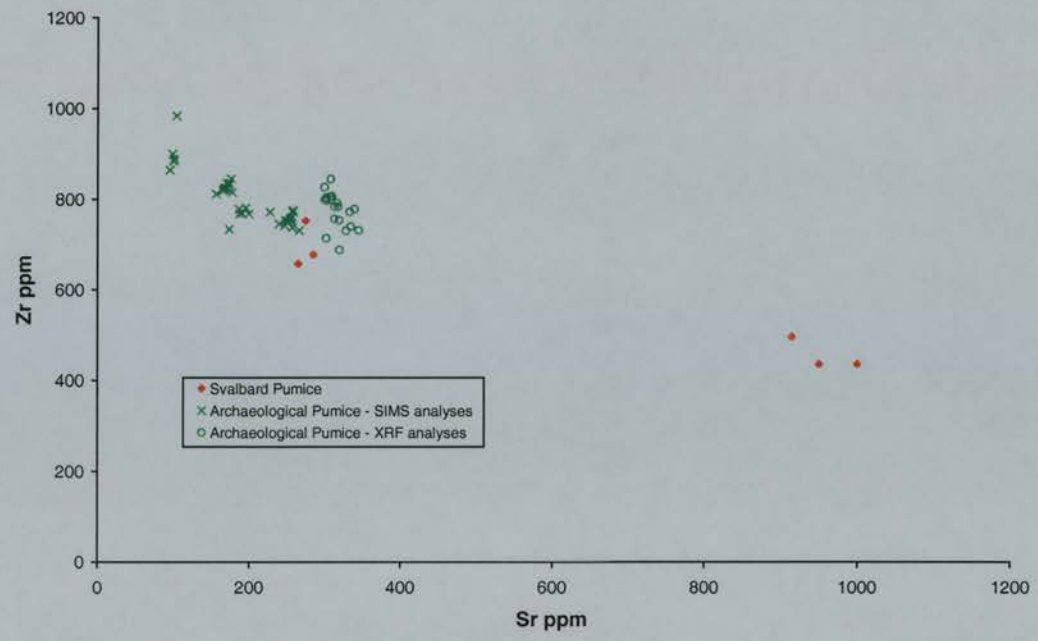

Figure 4.16: Graph (Sr/Zr) to plot the relationship of the analyses of Svalbard pumice published by Boulton and Rhodes (1974) with the new data from Scottish archaeological sites. Both XRF and SIMS analyses are shown.

4.5 Comparison with natural sites

Sections 3.4 and 4.3 present new geochemical data of pumice from both natural and archaeological sites in Norway, the British Isles and Iceland. This section compares and contrasts these analyses and builds a more complete picture of the geochemical composition of pumice found throughout the North Atlantic region.

The analyses of pumice from the two types of environment produced two main conclusions. The first was that the EPMA demonstrated that the vast majority of all the analysed pumice was dacitic. This dacitic pumice, with a few exceptions, is geochemically homogeneous and is presumed to have been produced by either a single eruption or by several eruptions from the same volcano, where the magma composition did not alter significantly between events. Table 4.19 shows that the main dacitic groups from both these types of sites has very similar geochemical properties. Both the means and standard deviations of the two groups show no consistent variation. Figure 4.17 illustrates this similarity between the two types of deposits. With the exception of some of the pumice from The Udal, the scatter of analyses outside the main group is the results of individual analyses of pumice, where the majority of the analyses of that piece fall in the main group. This is probably the result of the accidental analysis of inclusions within the glass.

		SiO_2	TiO_2	Al_2O_3	FeO	MnO	MgO	CaO	Na_2O	K_2O	Total	n
Natural Sites	**mean**	65.71	1.20	13.91	5.51	0.18	1.13	3.00	4.65	2.84	98.13	544
	1σ	0.75	0.09	0.27	0.26	0.04	0.07	0.19	0.35	0.25	0.88	
Archaeological	**mean**	65.68	1.20	13.99	5.46	0.18	1.10	3.01	4.65	2.78	98.05	301
Sites	**1σ**	0.79	0.08	0.27	0.31	0.04	0.10	0.19	0.27	0.16	0.90	

Table 4.19: Comparison of the means and standard deviations (1σ) of the EPMA of the main dacitic groups from the natural sites (Group 2a from Norway, Group 2 from Iceland and the Bay of Moaness pumice) and the Scottish and Irish archaeological sites (Group 4a).

From these results it can be concluded that the majority of pumice found on mid-Holocene or younger raised shorelines in Iceland, Norway, Scotland and on Neolithic and younger archaeological sites in the British Isles is of a similar type. This pumice is dacitic, has a fairly homogeneous geochemical composition and can vary in colour between brown and black/grey. This pumice was produced by either a single eruption or more probably by a series of eruptions from the same volcano, which has a slowly or non-evolving magma source. The only pumice which differs significantly from this is some of The Udal pumice. The oldest pumice pieces are from the upper pumice deposits at Kobbvika, Gjøsund, Brandsvik and the oldest pumice from The Udal and must have been produced by one or more eruptions which occurred over 6000 ^{14}C years ago. The youngest deposits are from Iron Age archaeological sites and the 1700 ^{14}C years old shoreline on Ramså, Norway. From this it can be concluded that the eruptions that produced the majority of the dacitic pumice must have occurred at least 6000 ^{14}C years ago, with the possibility that there have been similar activity to at least 1700 ^{14}C years BP.

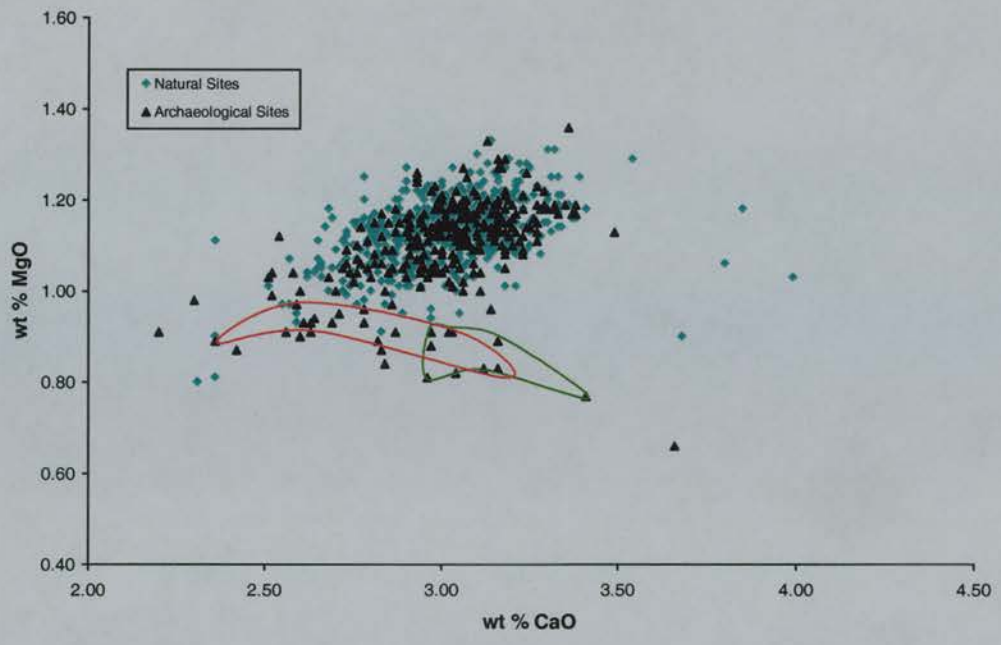

Figure 4.17: Graph (CaO/MgO) to show the similarity between the main dacitic pumice groups from natural and archaeological sites. The majority of the analyses with low MgO are represented by pumice from The Udal archaeological site. The red field defines the analyses of U 1 and the green of Udal 5.

Although most of the dacitic pumice is found in the main pumice group described above, a number of other dacitic pumice pieces were also analysed. The pumice in Group 2b from Norway and Group 4b from mainly Iron Age to Medieval archaeological sites in the British Isles, have similar geochemical properties to the main pumice, but are less homogeneous (Table 4.20). The major differences between this pumice and the main group are the higher SiO_2 abundances, lower FeO, MgO and CaO and the greater geochemical variability (Figure 4.18). The Group 3 Icelandic pumice pieces have less geochemical variability, but consistently lower CaO and MgO than the main pumice group. Whilst the Group 2b and 4b pumice tends to be from younger deposits in Scotland and Norway, the lower Norwegian pumice is some 2000-1300 years older than the archaeological pumice.

		SiO_2	TiO_2	Al_2O_3	FeO	MnO	MgO	CaO	Na_2O	K_2O	Total	n
Norway	**mean**	66.44	1.16	13.76	5.19	0.19	0.89	2.74	4.75	2.88	98.03	48
Group 2a	**1σ**	1.09	0.15	1.06	0.69	0.05	0.33	0.47	0.45	0.33	0.83	
Archaeological	**mean**	66.35	1.20	13.65	5.31	0.19	1.06	2.90	4.96	2.86	98.44	34
Group 4b	**1σ**	1.07	0.17	1.31	0.95	0.06	0.52	0.56	0.51	0.35	0.74	
Iceland	**mean**	66.43	1.17	13.93	5.25	0.18	0.96	2.63	4.74	2.94	98.21	40
Group 3	**1σ**	0.75	0.07	0.21	0.29	0.04	0.09	0.15	0.22	0.14	0.82	

Table 4.20: Comparison of the means and standard deviations (1σ) of the EPMA of the other dacitic pumice not found in the main group.

The majority of the other dacitic pumice was probably produced by the same eruption or eruptions which produced the other pumice pieces. The greater geochemical variability is probably the result of the phenocrysts found within the glass. This could be because this pumice was not quenched as rapidly as the majority. The Icelandic Group 3 pumice does appear to be slightly different to the other pumice, although large phenocrysts are not present. This may have been produced by a different eruption, or by an earlier phase in an eruption which also produced the other pumice. The pumice containing the large phenocrysts may have cooled more slowly than the other pumice, allowing time for the microlites found in most other pumice pieces to grow into large phenocrysts. Therefore, it is possible that these pumice pieces were produced by the same eruptions which produced the other pumice but were cooled at a different rate. Despite this, it is clear that all of the dacitic pumice was produced by the same source. All of the dacitic pumice is from either mid-Holocene raised shorelines (younger than about 6000 ^{14}C years BP) or Neolithic (generally younger than about 5000 ^{14}C years BP) or younger archaeological sites. From this it can be concluded that the eruptions that produced the majority of the dacitic pumice must have occurred at least 6000 ^{14}C years ago, with the possibility that there have been similar activity to at least 1700 ^{14}C years BP.

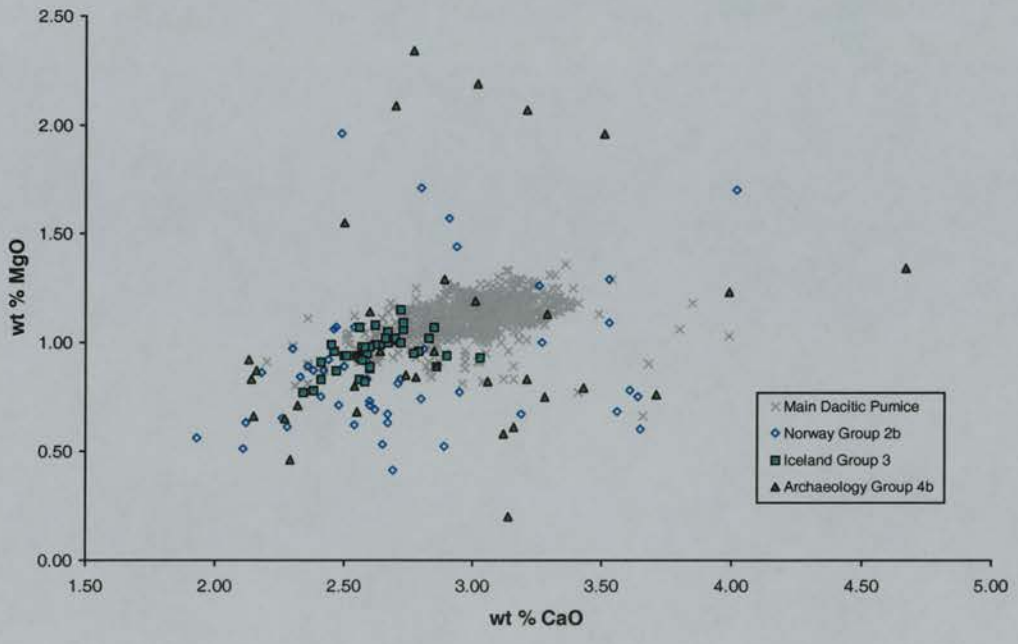

Figure 4.18: Graph (CaO/MgO) to compare the other less homogeneous dacitic pumice analyses with the main dacitic pumice group.

The Scottish Group 1 pumice has similar geochemical properties to the Trandvikan pumice (Table 4.21 and Figure 4.19) . It is unlikely that the Scottish pumice and the Trandvikan pumice were produced by the same eruption, although they were produced by the same volcano. The Trandvikan pumice was found on an early Holocene raised shoreline in western Norway dated to around 9000 ^{14}C years BP, whilst the Group 1 pumice only occurs in Medieval archaeological sites in Shetland. This suggests that that the Group 1 pumice was probably erupted during Medieval times, i.e. post 10 or 11th Centuries, as it is absent from any of the younger archaeological sites in Shetland. The volcano that produced the Trandvikan and Group 1 archaeological pumice appears to have erupted on at least two occasions separated by at least 8000 years producing pumice with virtually identical major element compositions.

		SiO_2	TiO_2	Al_2O_3	FeO	MnO	MgO	CaO	Na_2O	K_2O	Total	n
Archaeological	**mean**	72.05	0.24	13.15	3.26	0.10	0.04	1.01	4.98	3.43	98.27	60
Group 1	**1σ**	0.96	0.05	0.30	0.27	0.03	0.03	0.14	0.38	0.18	1.15	
Archaeological	**mean**	69.74	0.27	13.02	3.78	0.13	0.21	1.34	5.33	3.50	97.31	19
Group 2	**1σ**	0.60	0.05	0.23	0.15	0.03	0.01	0.07	0.13	0.11	0.53	
Archaeological	**mean**	67.74	0.83	13.60	4.03	0.13	0.71	2.01	5.11	3.15	97.32	20
Group 3	**1σ**	0.72	0.06	0.18	0.24	0.03	0.06	0.14	0.19	0.09	0.74	
Trandvikan	**mean**	71.55	0.21	13.36	3.28	0.11	0.04	1.00	4.85	3.51	97.90	10
	1σ	0.47	0.04	0.30	0.09	0.03	0.02	0.06	0.48	0.12	0.99	

Table 4.21: Comparison of the means and standard deviations (1σ) of the EPMA of the more silicic pumice.

None of the other analyses of pumice from Iceland and Norway match the archaeological Group 2 and 3 pumice pieces. This pumice from Staosnaig is from a Mesolithic (7900-7000 ^{14}C years BP) archaeological site and, except for the Trandvikan pumice, is the oldest pumice analysed. It is possible that other Mesolithic archaeological sites, such as those in Norway, have similar pumice pieces present.

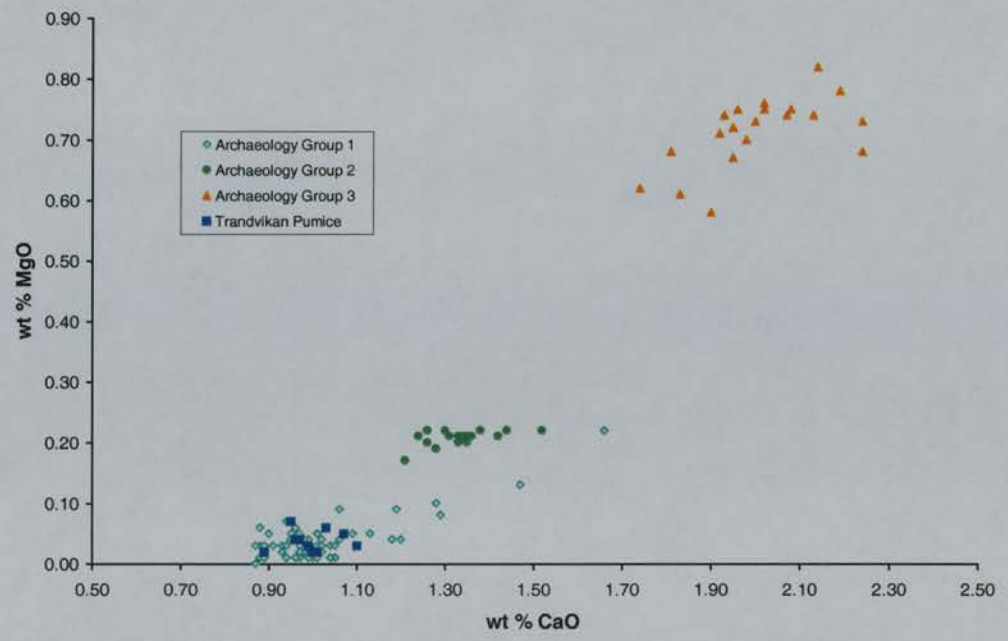

Figure 4.19: Graph (CO/MgO) to compare the more silicic pumice pieces found in Norway and Scotland.

The SIMS analyses provide another method by which the pumice from natural and archaeological sites can be compared, although only a limited number of analyses are available. Figure 4.20a shows that none of the analyses from the natural sites is similar to the two types of pumice found at Staosnaig. These results confirm the EPMA analyses presented above.

The Udal pumice has slightly different trace and rare earth element geochemistry to most of the other pumice pieces, although there is some overlap with the Bær pumice (Figure 4.20b). It is clear from the EPMA and SIMS analyses that the older U 1 pumice pieces appears to have slightly different geochemical properties to the majority of the pumice. What is not certain, however, is whether this variation is the result of the variation within an eruption or between eruptions.

a)

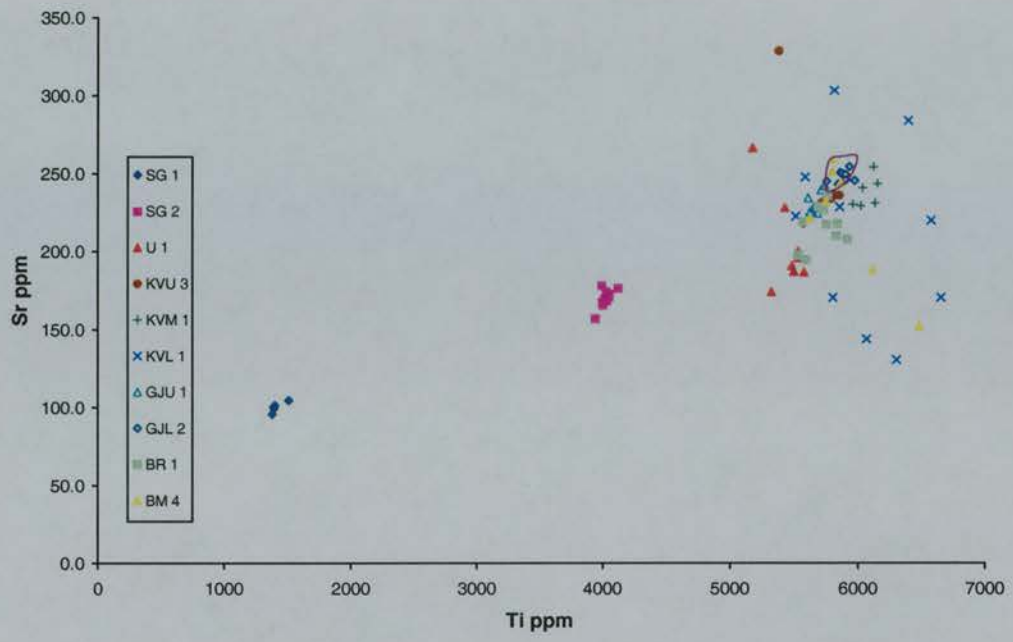

b)

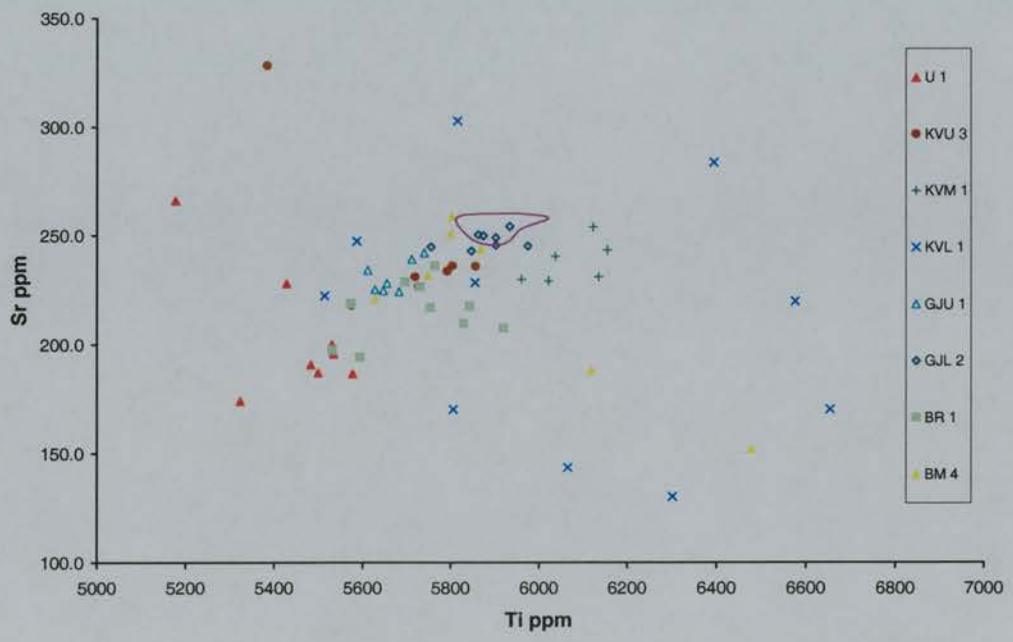

Figure 4.20: Graphs (Ti/Sr) to compare the natural and archaeological pumice analysed by SIMS. The purple fields represent the analyses of the pumice from Caerdach Rudh (CR 2 and CR 5). The other archaeological pumice analyses are SG 1, SG 2 (Staosnaig) and U 1 (The Udal).

The SIMS analyses show that the Caerdach Rudh pumice, is most similar to the GJL 2 (Figure 4.20b). This is a similar pattern as seen in the EPMA analyses (Figure 4.21). Although as section 4.3 shows, as there is considerable overlap with other pumice pieces at the site. The GJL pumice is dated to about 3300-3000 ^{14}C years BP and CR 2 and CR 5 are from deposits ranging in age between c. 3300-2375 ^{14}C years BP.

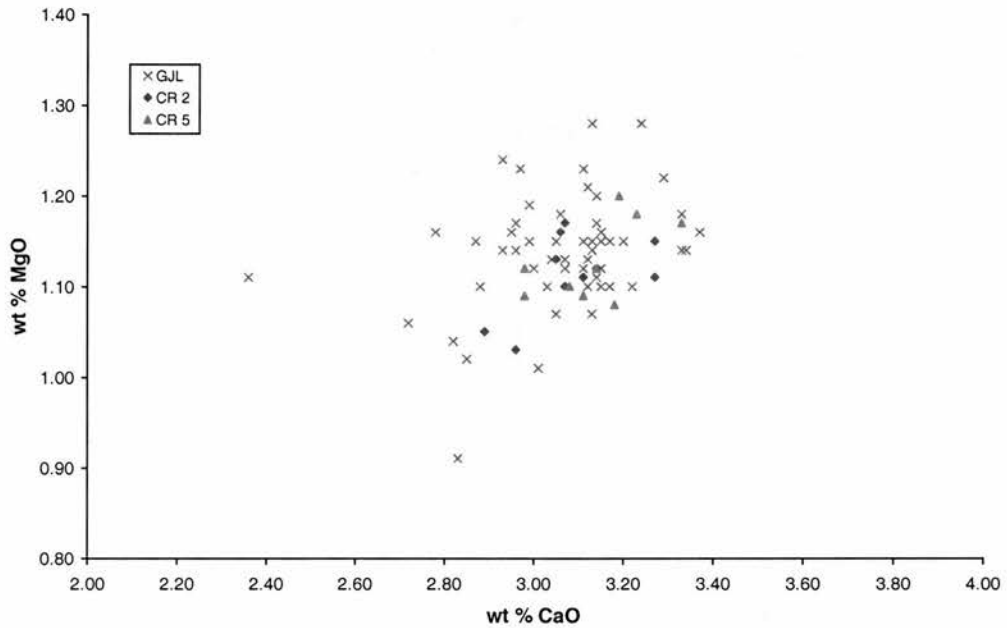

Figure 4.21: Graph (CaO/MgO) to compare the EPMA of the GJL and Caerdach Rudh pumice pieces CR 2 and 5.

4.6 Summary of Chapter 4

The geochemical analyses of the archaeological pumice have confirmed that the majority of the pumice found in the North Atlantic region is dacitic and was erupted from the same source. This pumice was first produced by an eruption sometime before 6000 ^{14}C years BP and evidence from Norway suggests that the last eruption may have occurred sometime around or before 1700 ^{14}C years BP. More silicic pumice is also present on raised shorelines ranging from a 9000 ^{14}C years beach in Norway to Mesolithic and Medieval sites in Scotland. The 9000 year old and Medieval pumice appears to have been produced by the same source, a different volcano to that which produced the dacitic pumice, whilst the Mesolithic pumice appears to have been produced by at least two separate eruptions from an unidentified source.

Both the major and trace element analyses have shown that the main dacitic pumice is geochemically homogeneous and suggests that the pumice was either produced by a single eruption, or more likely by several eruptions from a volcano with a slowly or non-evolving magma chamber. Some of the younger pumice from archaeological sites in Scotland and raised shorelines in Norway appears to be slightly different, but it is not clear whether this is the result of variation within or between eruptions. Chapters 3 and4 have demonstrated that grain specific geochemical analyses of pumice produce more consistent data than bulk XRF analyses.

The next chapter discusses possible sources for the pumice and presents new geochemical data from Iceland, before correlating the ocean-transported pumice to particular volcanoes and sources.

Chapter

The sources of the pumice

5

5.1 Introduction

The potential sources of pumice in the North Atlantic Region are the islands associated with the Mid-Atlantic Ridge (MAR). The largest and most of important of these is Iceland. Chapter 2 established Iceland as the most likely source area for pumice production in the North Atlantic. Section 5.2 discusses the likely Icelandic volcanoes which could have produced pumice during the Holocene. There is no published evidence of submarine activity producing dacitic pumice and therefore this type of activity will not be discussed. The second most important northern North Atlantic volcanic island is Jan Mayen. This island is ideally placed to produce pumice which could be easily transported to Svalbard. This possibility is discussed in the third part of this chapter before the results are summarised.

5.2 Iceland

Iceland is 102,843 km^2 and is nearly entirely composed of volcanic rocks. The oldest rocks formed during the Miocene and plateau basalts in Vestfirðir are around 15 million years old (Saemundsson, 1979). The island is unique as it is positioned astride the MAR, but is also coincident with a mantle plume. This has resulted in the development of a large topographic high associated with a much thicker crust. Various estimates have been made to the size of this plume, with the latest identifying a relatively narrow 400 km high by 150 km wide plume located at a depth of 125 km (Wolfe *et al.*, 1997). The result of this constant supply of mantle material to the crust is that Iceland forms the largest surface expression of a spreading ocean ridge system in the world. The presence of the mantle plume, which is believed to be centred under the north-east of Vatnajökull [Figure 5.1; Wolfe *et al.*, 1997), has lead to an offset of the MAR, as it passes through Iceland. The offset active volcanic zones are connected to the MAR by rifting which is centred in the South Iceland Seismic Zone (SISZ) and the Tjörnes Fracture Zone (TFZ) in the north.

Volcanic Systems

The currently active volcanic areas of Iceland can be divided into four major geographic zones: the Snæfellsness Volcanic Zone, the Reykjanes-Langjökull Volcanic Zone, the Northern Volcanic Zone and the Eastern Volcanic Zone (EVZ). Öræfajökull in south-east Iceland, however, lies outside these zones and its activity is probably directly related to the presence of the mantle plume, rather than the MOR. Late-Quaternary activity has occurred within 29 discrete volcanic systems which Jakobsson (1979) defines as a "*spatial grouping of eruption sites in a certain period of time, with particular characteristics of tectonics, petrography and geochemistry*". According to Jakobsson (1979) this definition indicates the magma from each volcanic system must be derived independently from the mantle, which then evolves as it rises through the crust. This implies that each volcanic system can be considered as a closed petrological system evolving its own typical rock suite. Volcanic systems also appear to have produced products with relatively stable geochemical compositions during the Holocene, whilst maintaining their differences from other systems. This has important implications for tephrochronological research, suggesting that it is usually possible to correlate distal tephra layers or pumice to particular volcanic systems using geochemistry or petrology (Larsen, 1981). The volcanic centres in the Snæfellsnes zone and Vestmannaeyjar are alkalic[1]; Hekla, Vatnafjöll, Torfajökull, Eyjafjallajökull, Katla and Öræfajökull are transitional alkalis; and the rest are tholeiitic[2] (Jakobsson, 1979). The EVZ volcanic centres are tholeiitic in the north, but more alkaline further south.

---

[1] Alkalic magma has a high proportion of alkalis (Na_2O and K_2O) and is undersaturated in SiO_2 (Kearey, 1996).

[2] Tholeiites are silica oversaturated basalts which are the most abundant basalt group (Kearey, 1996).

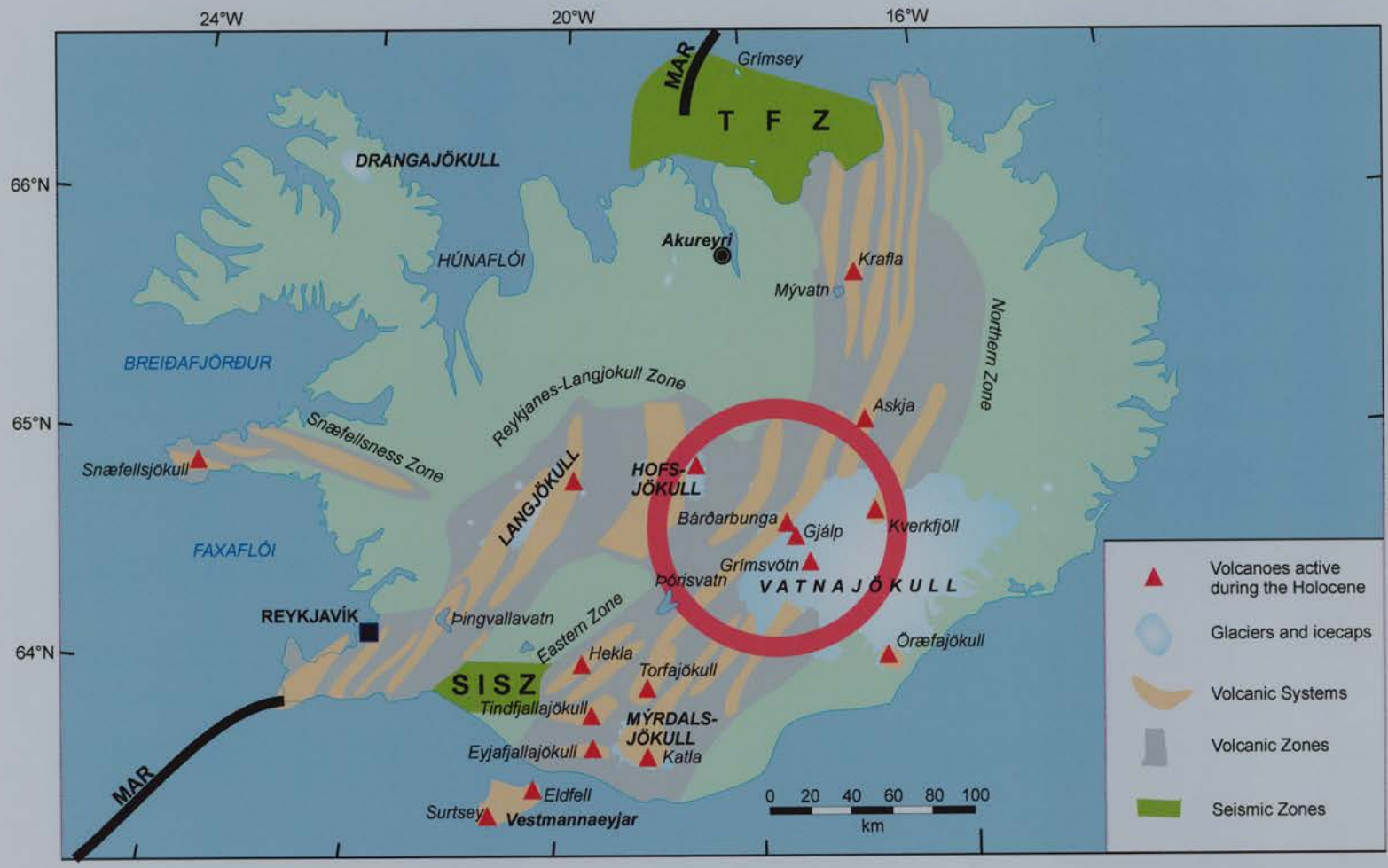

Figure 5.1: Map to show the location of Icelandic volcanic zones, volcanic systems, recently active volcanoes, fracture zones and mantle plume. The position of the mantle plume is indicated by the red circle. MAR = Mid-Atlantic Ridge, SISZ = South Iceland Seismic Zone, TFZ = Tjörnes Fracture Zone. Based on information in Jakobsson (1979), Wolfe (1997), Larsen *et al.* (1998).

According to Jakobsson (1979), volcanic systems generally begin as fissure swarms producing effusively erupted basaltic rocks, examples of which are the eruptions from Krafla (1974-1984 AD), Veidivötn, Eldgjá (see below) and Lakagígar (1783 AD). In time, more evolved rocks are erupted and activity often becomes concentrated in one area. This results in the formation of a central volcano that usually develops a caldera. Silicic rocks are erupted from the central volcano, whilst basaltic rocks may continue to be erupted from the surrounding area. Eyjafjallajökull, Öræfajökull, Tindfjallajökull and Torfajökull are examples of large central volcanoes which dominate their volcanic systems. Finally, a high temperature geothermal field develops in the remains of the caldera with Torfajökull being a typical example of this. Systems generally have a life of between 300,000 and 500,000 years, but central volcanoes may reach an age of over 2 million years.

Possible sources

The most probable Icelandic sources of any Holocene ocean-rafted dacitic or rhyolitic pumice are the volcanic systems in the southern part of the Eastern Volcanic Zone which are known to have produced silicic products during the Holocene; the Dyngjuföll volcanic system, which has the Askja central volcano; Snæfellsjökull part of the Snæfellsnes volcanic system and Öræfajökull, in south-east Iceland (Figure 5.1). Several of these possible sources can be dismissed as unlikely. Askja, the central volcano in the Dyngjuföll volcanic system, is an unlikely source as it is over 125 km from the sea, has no overlying icecap to generate a suitable flood for transport and no direct drainage to the coast.

The 1446 metre high stratovolcano Snæfellsjökull is found at the westerly edge of the Iceland's westernmost volcanic system, Snæfellsnes. The volcanic zone is about 30 km long and Holocene basaltic lava flows and cinder cones are also found around the base of Snæfellsjökull (Jóhannesson *et al.*, 1981). Jóhannesson *et al.* (1981) carried out a detailed tephrochronological study of the Snæfellsnes peninsula and published the results of 91 stratigraphic sections. Simkin *et al.* (1994) find evidence of at least nine Holocene eruptions, of which three are from the central crater and the others are flank eruptions, whilst Jóhannesson *et al.* (1981) report evidence of at least 20 individual post-glacial lava flows, although it is not clear how many individual eruptions are responsible for these. The cones near the summit of Snæfellsjökull tend to produce acid or intermediate lavas, whilst the ones lower down produce more basic lava flows. The tephrochronological studies of Jóhannesson *et al.* (1981) provide evidence of at least three Holocene silicic eruptions.

These eruptions were dated to 1750±150, 3960±100 and between 7000-9000 ^{14}C years BP. During fieldwork in 1990, Dugmore and Hulton (pers. comm.) sampled four silicic tephra layers from soil profiles on the Snæfellsnes peninsula. These tephras were analysed and although they are dacites, like most of the ocean-rafted pumice, they cannot be correlated to the pumice as they tend to have higher Al_2O_3, lower SiO_2, higher FeO and also a much wider general geochemical range.

The Eastern Volcanic Zone (EVZ) consists of nine volcanic systems, Eyjafjallajökull (Eyjafjöll), Grímsvötn, Hekla, Katla, Tindfjallajökull, Torfajökull, Vatnafjöll, Veidivötn and Vestmannaeyjar. According to Jakobsson (1979), there is little evidence that Grimsvötn, Vatnafjöll and Veidivötn have produced any significant amounts of silicic material during the Holocene. Jakobsson (1979) states that all of the 75 eruptive units associated with Veidivötn are basaltic. A minor component of the c. 870 AD Landnám Tephra is silicic (Larsen *et al.*, 1999), but this was only produced from the southern end of the active fissure and was a result of the interaction with the Torfajökull volcano (Larsen, 1984)

Although Eyjafjallajökull may have produced as many as 17 intermediate lava flows during the Holocene, the geochemistry of the last eruption, 1821-1823 (one of two historic eruptions), suggests that the tephra and pumice produced by this system are geochemically different to the dacitic and rhyolitic pumice. For example, SiO_2 and Na_2O abundances are much higher, and TiO_2 is much lower than in the dacitic ocean-rafted pumice (Larsen *et al.*, 1999). Pumice is found on the terminal moraine of Gígjökull (a small outlet glacier from the central crater) and the 1821 jökulhlaup deposit, which forms a small fan outside the end moraine. This pumice is grey with 1-2 mm long white phenocrysts. Significantly, this pumice is dense and sinks in water. Jökulhlaups from Eyjafjallajökull, therefore, produce pumice but the relatively high density and geochemistry means that this volcano is not the source of the ocean-rafted pumice.

Tindfjallajökull, probably the oldest volcanic system in the EVZ, has not been very active during the Holocene, with only some activity at the very beginning of this period. This lack of activity means that Tindfjallajökull is an unlikely source of widespread mid-Holocene pumice deposits. During the Holocene, the Vatnafjöll volcanic system has only produced basalts Jakobsson (1979).

The Torfajökull volcanic system contains the largest area of silicic extrusive rocks in Iceland and the volcano covers an area of 450 km^3 (McGarvie, 1984). During the Holocene there have been at least 11 post-glacial eruptions, all of which were rhyolitic, but show evidence of basaltic magma mixing with the rhyolitic magma (MacDonald *et al.*, 1990; McGarvie, 1984; McGarvie *et al.*, 1990). At least one tephra layer from an eruption of Torfajökull has reached north-west Europe. The Hoy tephra, found in Orkney, was correlated to the Torfajökull volcanic system and dated to 5560±90 ^{14}C years BP (Dugmore *et al.*, 1995a). Although this volcano has produced rocks with a similar wt % SiO_2 to the dacitic pumice, other major differences exist, with the Torfajökull rocks having lower FeO and TiO_2 and higher MgO and Al_2O_3 compared to the dacitic pumice.

Given the elimination of Askja, Eyjafjallajökull, Grimsvötn, Snæfellsjökull, Tindfjallajökull Torfajökull, Vatnafjöll and Veidivötn only the Holocene activity of Hekla, Katla and the outlying Öræfajökull will be considered further in the rest of this chapter. These three volcanoes are known to have produced silicic tephra layers and pumice during the Holocene and there are realistic mechanisms to transport pumice from the volcanoes to the coast.

5.2.1 Hekla Volcanic System

The first volcanic system to be discussed in detail is the Hekla volcanic system, which is situated on the western border of the Eastern Volcanic Zone (EVZ). The Hekla system is about 40 km long and 7 km in width and reaches a topographic high on the central volcano of Hekla at an altitude of 1491 metres above sea-level. Hyaloclastite mountains and ridges, belonging to the upper Pleistocene "Moberg formation" are exposed in several places (Jakobsson, 1979). The central volcano of Hekla forms a ridge and most major eruptions are centred on the 5.5 km long summit crater and its extensions to the south-west and north-east. Some 6.7 km^3 of acidic rocks and 12 km^3 of intermediate rocks have been produced by the system in the last 6000 years (Jakobsson, 1979). Basaltic rocks are also found in the south-eastern part of the system. During the last 6000 years there have been several large silicic eruptions which have produced tephra layers which form the cornerstone of Icelandic tephrochronology: Hekla 1 (1104 AD), Hekla 3, Hekla-S, Hekla 4, Hekla 5 and Hekla Y.

Hekla is the origin of several widespread silicic distal tephra deposits found in north-west Europe. The pioneering work of Persson (1966; 1967; 1968; 1971) tentatively identified several tephra layers from peat bogs in Norway, Sweden and the Faroe Islands as being erupted by Hekla. Although tephra fall from the 1947 eruption of Hekla was identified by

Salmi (1948), it was not until EPMA were carried out glass shards from the north of Scotland by Dugmore (1989a) that the presence of Hekla tephra layers in the geological record was confirmed. Since then, Hekla tephra layers have been identified throughout Scotland (Blackford *et al.*, 1992; Dugmore *et al.*, 1995a; Dugmore *et al.*, 1992; Dugmore and Newton, 1992; Dugmore *et al.*, 1996; Dugmore *et al.*, 1995b), northern England (Pilcher and Hall, 1996), the island of Ireland (Hall *et al.*, 1994a; Hall *et al.*, 1994b; Hall *et al.*, 1993; Hall *et al.*, 1994c; Pilcher and Hall, 1992; Pilcher *et al.*, 1995; Pilcher *et al.*, 1996), Faroe Islands (Dugmore and Newton, 1997), Sweden (Boygle, 1998) and northern Germany (van den Bogaard *et al.*, 1994). Many tephra layers from Hekla have a distinctive geochemical range, with Hekla 4 for example having a SiO_2 content that varies from 76% to less than 56% (Larsen *et al.*, 1995; 1999; Tephrabase[3]). This is the result of the chemically zoned magma chamber which exists beneath Hekla.

Hekla has also been known to have produced pumice flows, some of which have been transported to the sea. The 1947 eruption of Hekla produced a large raft of pumice which was swept out to sea (Noe-Nygaard, 1951). This raft of pumice was transported by currents around the west coast of Iceland and was spotted off the north coast (Thórarinsson, 1967). There are no records of this pumice, however, being washed on to the shores of north-west Europe (Chapter 1).

Pumice flows from Hekla are termed *vikurhlaups* and the Hekla 3 (2879 ± 34 ^{14}C years BP; Dugmore *et al.*, 1995b), Hekla-S[4] (3515 ± ^{14}C years BP, Larsen, *et al.*, in prep), and Hekla 4 (3826 ± 11 14C years BP; Dugmore *et al.*, 1995b) eruptions are known to have produced large and extensive floods. Vikurhlaups have been produced as the result of the temporary damming of neighbouring river systems of the Ytri-Rangá, Þjórsá, Stóra-Laxá and the Hvítá (Vilmundardóttir and Hjartarson, 1985). Thick layers of waterlain pumice from the Hekla 3 eruption are found over 50 km to the south-west of Hekla and both Hekla 4 and Hekla 3 pumice form 2 metre thick deposits 39 km from the volcano (Vilmundardóttir and Hjartarson, 1985). The pumice in these floods was originally airfall material and so can be defined by analyses on airfall tephra layers.

---

[3] A search of Tephrabase (www.geo.ed.ac.uk/tephra/) produced 520 analyses of Hekla 4 from Iceland and the British Isles.

[4] Hekla-S was originally designated Hekla-2, but its stratigraphic position was realised to be between Hekla-3 and Hekla 4 (Larsen and Thórarinsson, 1977).

The flood deposits from the Hekla-S eruption, which are designated HSv (or the Selsund pumice) in order to distinguish it from the airfall tephra, were produced in a slightly different manner. It appears that only a limited amount of the tephra and pumice became airborne and the rest flowed down the sides of the volcano engulfing surrounding birch forests as the eruption column collapsed (Vilmundardóttir and Hjartarson, 1985; Larsen et al., in prep). Analyses of both the airfall part of the eruption (H-S) and the Selsund pumice show that there is a distinct difference between the two. The flood deposit was produced by more generally evolved magma, i.e. magma with higher wt % SiO_2 and corresponding lower abundances of other oxides (Figure 5.2), compared to the airfall tephra which produced the tephra layer KAL-X at Kálfafell (Dugmore *et al.*, 1992), although both KAL-X and the Selsund Pumice both have some basic analyses. Table 5.1 shows a summary of the analyses of four pieces of the Selsund pumice. As the means and standard deviations partly hide the large range in the geochemical composition of the pumice pieces, the maximum and minimum values are also included and full details of the analyses are available in Appendix 3. A thorough report of the Hekla-S eruption is being prepared (Larsen *et al.*, in prep).

Figure 5.2 shows that the main dacitic pumice group, the two groups of pumice from Staosnaig and OF8L1 from Ófeigsfjörður were not produced by known Holocene eruptions from Hekla. The medieval white pumice from Shetland (Group 1 archaeological pumice) and the white early Holocene pumice from Trandvikan, Norway have similar CaO and MgO to Hekla 4, although Figure 5.3 shows that they were not produced by the same eruption as Hekla 4. One possibility is that although Hekla has produced substantial amounts of pumice during the Holocene none, or little, of this has been successfully transported by ocean currents to the shores of the North Atlantic. It is difficult to understand why this should be the case. It is possible, however that pumice from these eruptions was transported by ocean currents but has failed to survive in the geological record. The Selsund Pumice, Hekla 3 and Hekla 4 pumice pieces found in Iceland are composed of very vesicular, low density pumice (Figure 5.4). Attrition between such pumice pieces in a pumice raft would quickly lead to this fragile type of pumice being broken down before being washed ashore and further destruction due to surf zone erosion after deposition.

a)

Pumice		SiO_2	1σ	TiO_2	1σ	Al_2O_3	1σ	FeO	1σ	MnO	1σ	MgO	1σ	CaO	1σ	Na_2O	1σ	K_2O	1σ	Total	1σ	n
HSv 1		66.17	7.43	0.82	0.79	13.39	0.35	5.27	3.51	0.16	0.11	0.89	0.96	3.15	1.92	4.37	0.24	2.21	0.55	96.44	1.07	**9**
	max	75.74		2.03		13.74		10.29		0.35		2.21		6.17		4.62		2.82		98.31		
	min	56.07		0.11		12.55		1.24		0.07		0.05		1.11		4.02		1.45		95.11		
HSv 2		63.45	8.16	1.06	0.98	13.39	0.62	6.83	4.15	0.23	0.10	1.24	1.20	3.73	1.99	4.36	0.29	1.93	0.54	96.21	0.98	**9**
	max	75.04		2.13		14.44		11.26		0.42		2.71		5.93		4.85		2.70		98.08		
	min	54.57		0.08		12.57		1.81		0.13		0.04		1.30		4.06		1.29		95.12		
HSv 3		72.32	0.70	0.20	0.03	13.80	0.08	2.94	0.14	0.12	0.03	0.18	0.02	1.90	0.08	4.72	0.16	2.58	0.07	98.76	0.73	**10**
	max	73.17		0.23		13.90		3.24		0.16		0.21		2.01		5.00		2.69		99.90		
	min	70.88		0.16		13.65		2.78		0.08		0.16		1.75		4.48		2.44		97.51		
HSv 4		61.71	6.07	1.25	0.85	13.88	0.83	8.06	3.38	0.30	0.14	1.60	1.12	4.59	1.50	4.19	0.37	1.77	0.45	97.34	0.90	**10**
	max	69.63		2.28		14.90		11.50		0.61		2.79		6.01		4.94		2.41		98.32		
	min	55.38		0.14		12.34		3.07		0.16		0.17		2.51		3.70		1.36		95.47		

b)

	SiO_2	TiO_2	Al_2O_3	FeO	MnO	MgO	CaO	Na_2O	K_2O	Total	n
Mean	65.97	0.83	13.63	5.76	0.20	0.97	3.33	4.41	2.12	97.23	38
1σ	7.26	0.83	0.58	3.62	0.12	1.05	1.80	0.33	0.53	1.35	
max	75.74	2.28	14.90	11.50	0.61	2.79	6.17	5.00	2.82	99.90	
min	54.57	0.08	12.34	1.24	0.07	0.04	1.11	3.70	1.29	95.11	

Table 5.1: a) shows the means and standard deviations (1σ) of the HSv (Selsund) pumice pieces. The maximum and minimum values for each pumice piece are also included. b) shows the means and standard deviations (1σ) of all 39 analyses. The maximum and minimum values for the HSv pumice pieces are also included. The number of analyses are also shown (n) and full details about these analyses are available in Appendix 3.

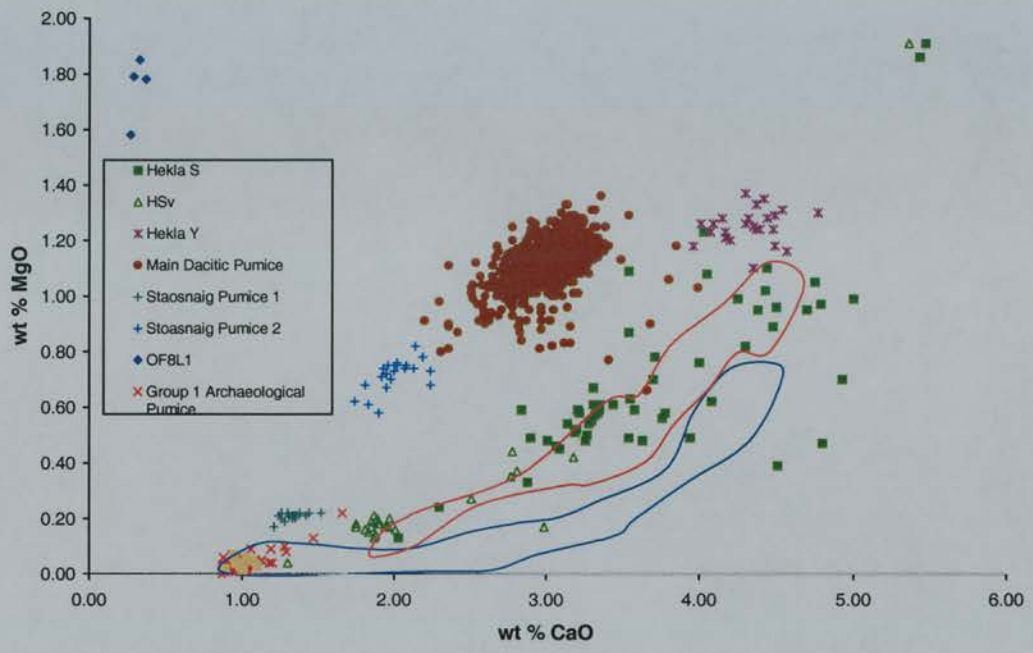

Figure 5.2: Graph (CaO/MgO) to show comparison of the silicic ocean-rafted pumice to several possible Hekla eruptions. Hekla 4 is defined by the blue field (520 analyses retrieved from Tephrabase[5]), Hekla 3 is defined by the red field (75 analyses retrieved from Tephrabase[6]), Hekla Y data is unpublished (Newton, Dugmore and Larsen, unpublished), Hekla S data is KAL-X in Dugmore *et al.* (1992).

[5] Hekla 4 data are from Boygle (1994) and Boygle (1999), Dugmore *et al.* (1995a), Dugmore *et al.* (1992), Dugmore and Newton (1992), Pilcher and Hall (1996), Pilcher *et al.* (1995) and Pilcher *et al.* (1996).

[6] Hekla 3 data are from Boygle (1994) and Boygle (1999).

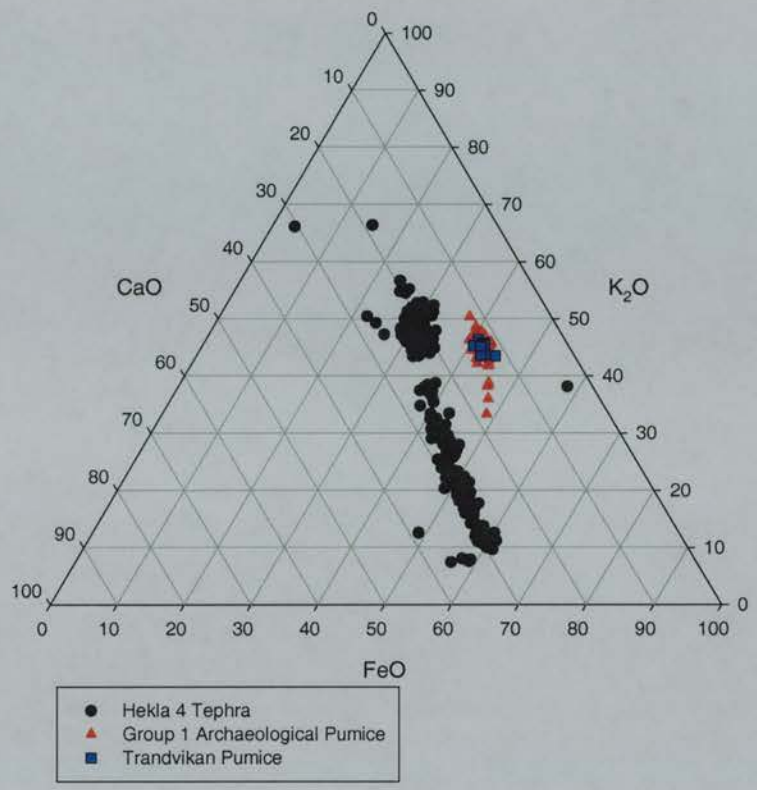

Figure 5.3: Ternary graph ($FeO/K_2O/CaO$) which demonstrates that the Group 1 Archaeological and the Trandvikan pumice are not from the same eruption as Hekla 4.

Figure 5.4: Photograph to show a piece of Hekla 3 pumice from Þórsárdalur, about 15 km west of Hekla. The pumice piece is about 17 cm across and is composed of friable and fibrous glass.

From these results it is clear that although Hekla is the most important source of distal tephra layers found in north-western Europe and indeed forms the backbone of Iceland's tephrochronological framework, it is not the source of any of the analysed ocean-rafted pumice deposits found around the North Atlantic region. The conclusions by Noe-Nygaard (1951), Binns (1972) and Peulvast (1982) that Hekla is the source of much of the ocean-rafted pumice, therefore, can be discounted.

5.2.2 Katla Volcanic System

Introduction

The Katla Volcanic System, as defined by Jakobsson (1979) is found in the southern part of the Eastern Volcanic Zone, southern Iceland (Figure 5.6). This south-west to north-east trending system is about 30 km wide at its south-west part, narrowing gradually to the north-east and reaches a length of 78 km. The most prominent feature of the system is the hyaloclastite central volcano of Katla (1437 m), partly covered by Mýrdalsjökull (595 km^2), which reaches an altitude of 1512 metres above sea-level (Figure 5.5). The icecap fills the 14 km wide, 110km^2, 200-700 metre deep caldera found at the summit of Katla (Björnsson *et al.*, 1993). The 54 km long Eldgjá fissure swarm represents the north-easterly extension of the system (Miller, 1989). Recent research has shown that seismic activity within the Katla caldera is concentrated in two areas (Einarsson, 1991) and these are thought to be connected with the shallow (3 km) sub-caldera magma chamber identified by Gudmundsson *et al.* (1994). Katla last erupted in 1918 and their have been two jökulhlaups, possibly associated with minor activity, in 1955 and July 1999.

Figure 5.5: Photograph of the western side of Mýrdalsjökull taken from Gígjökull.

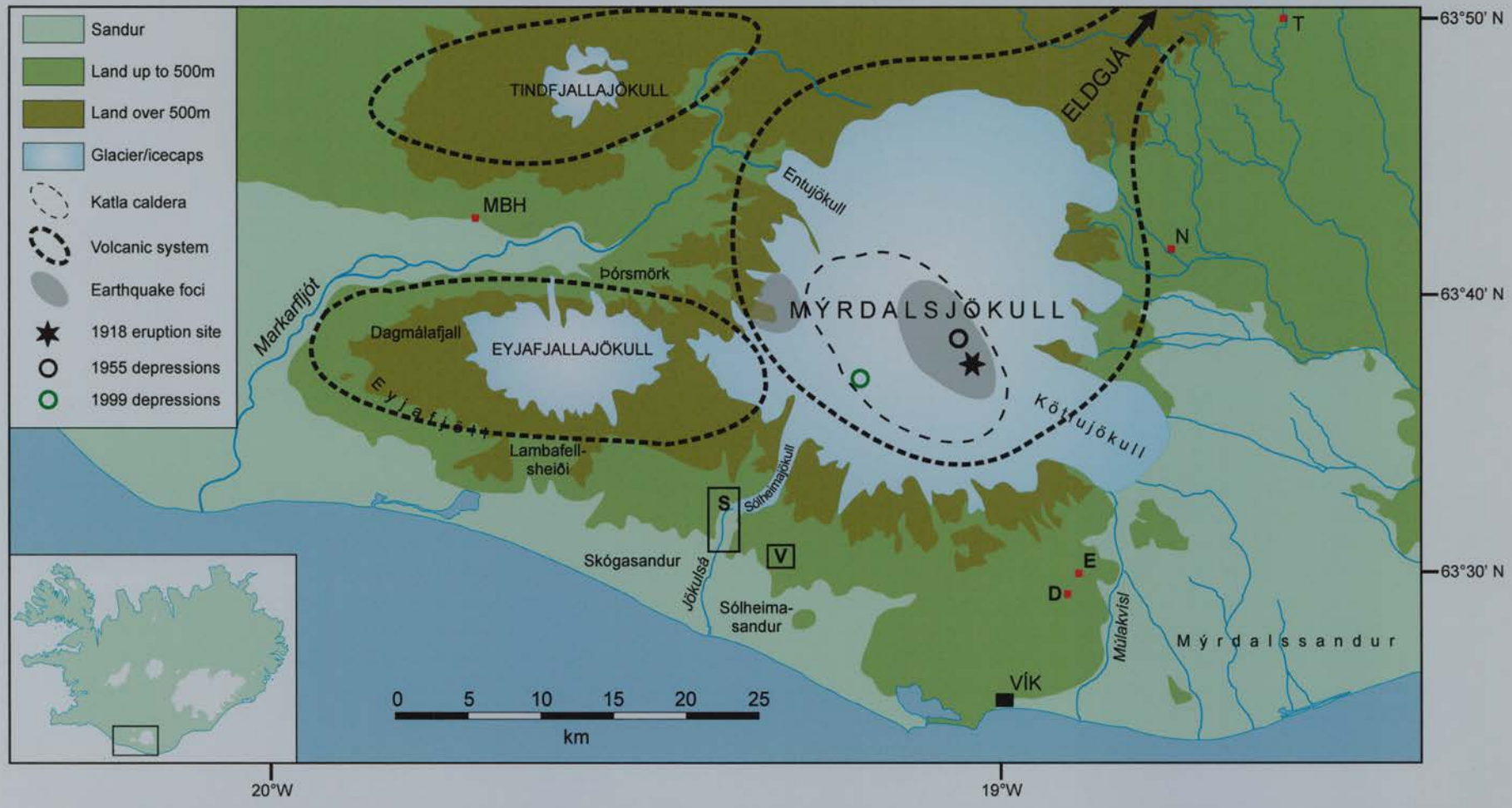

Figure 5.6: Map to show southern part of the Katla volcanic system. The Eldgjá fissure swarm extends to the north-east of Mýrdalsjökull. The locations of the caldera, present earthquake foci, the 1918 eruption and the depressions in the ice-cap associated with the 1955 and 1999 jökulhlaups are shown. The red squares indicate the location of sites where tephra layers have been analysed: D = Dimmagil, E = Engimýri and N = Needle Gully. The TYN site is located 10 km north of T. S = location of Figure 5.12 and V = location of Figure 5.14. Information from Larsen *et al.* (in press); Jakobsson (1979); Einarsson (1991).

Whilst the system has generally produced transitional alkali basalts (Jakobsson, 1979; Meier *et al.*, 1985), Katla has also been identified as the source of the basaltic high-Ti and silicic components of the late-glacial North Atlantic Ash Zone One (Lacasse *et al.*, 1995) and the associated terrestrial tephra layers: the Skógar tephra in northern Iceland (Norddahl and Haflidason, 1992) and the Vedde tephra in Scandinavia and Scotland (Mangerud *et al.*, 1984; Turney *et al.*, 1997). Larsen (1994) also identified that silicic activity has been a regular feature of Holocene activity. Three types of Holocene volcanic activity can be identified from the Katla volcanic system (Larsen, 1994; Larsen *et al.*, in press):

1. Hydromagmatic basaltic eruptions focussed on small fissures beneath the ice-cap, have probably occurred over 150 times during the Holocene, with the last eruption occurring in 1918. Evidence of these eruptions can be found in soil profiles in southern Iceland, where they are represented by black basaltic tephra layers. The largest Holocene tephra layers were produced by an eruption of Katla in 1755 AD (1.5 km^3 uncompressed). Tephra from this eruption and at least two others was reported falling on ships, and on Shetland and Norway during the 17^{th} and 18^{th} centuries (Thórarinsson, 1980; Thórarinsson, 1981). All of the tephra layers produced by this type of activity are basaltic, unlike the vast majority of the pumice, which is either dacitic or rhyolitic. The single piece of basaltic pumice from Norway, KVU5, however is basaltic. Hydromagmatic basaltic activity can be eliminated as the source of virtually all of the North Atlantic pumice with the exception of KVU 5. This type of activity will be discussed briefly in the next section.

2. The second type of activity is typified by mainly effusive basaltic eruptions, which occur either on the outer parts of the Katla central volcano, but mainly on the north-east trending fissure swarm. Although the activity is mainly effusive there is usually an explosive component, represented by coarse grained tephra layers. Although this type of activity is rare, with only two major events during the Holocene, the size of these eruptions means that they form an important part of the system's activity. Two large effusive eruptions occurred about 6800 ^{14}C years BP, the Hólmsá Fires, and around 938 ± 4 AD (Zielinski *et al.*, 1995), Eldgjá. The latter produced the largest outpouring of lava (14 km^3) in recorded history (Miller, 1989) and tephra produced by this eruption is present within the Greenland ice cores (Zielinski *et al.*, 1995). Although these eruptions do not produce pumice and the lavas and tephras are basaltic, their immense size has

resulted in other effects on subsequent volcanic activity at Katla, including putative pumice-forming events, and will be discussed later

3. The third type of activity is represented by explosive dacitic eruptions from within the Katla caldera. Silicic tephra layers from this type of activity are also found in the soil profiles around southern Iceland. Larsen *et al.* (in press), abbreviated these layers as SILK, as opposed to the K usually used for basaltic Katla tephra layers. This type of activity is comparatively rare and until the present study, little was known about these eruptions, with no geochemical data available. Jökulhlaups from Katla, as described in Chapter 1, are often associated with volcanic activity within the Katla caldera. The geochemistry of the SILK tephras is very similar to the main dacitic pumice and effective routeways and transport mechanisms exist. This makes Katla the prime candidate for the source of the majority of the ocean-rafted pumice and will it be discussed in detail below.

This section first describes the possible correlation of the single piece of basaltic pumice KVU 5 with basaltic Katla activity. Next, the mapping, stratigraphy and dating of the Holocene silicic tephra layers produced by the Katla volcanic system will be described. Then pumice deposits found on the southern slopes of Katla will be described. The geochemical properties of both the silicic Katla tephra layers and the Katla pumice deposits will be discussed next. These results will then be compared to the analyses of the ocean-transported pumice deposits and correlations made. Finally, possible transport routes from the Katla caldera to the sea are discussed.

Basaltic Katla activity and KVU 5

Only one piece of basaltic pumice (KVU 5) was found on a raised shoreline during this study. This suggests that basaltic pumice is relatively uncommon part of the deposits found around the North Atlantic. Basaltic pumice, however, does occur on the sandur plains south of Mýrdalsjökull and Vatnajökull. These pumice deposits are formed by jökulhlaups which flow across Mýrdalssandur and Skeiðarársandur. The most likely sources of basaltic pumice are the Katla and Grímsvötn volcanic systems. The potential for volcanic activity at Katla to cause substantial floods has already been discussed, but eruptions at Grímsvötn are also associated with jökulhlaups. This is a very active volcanic centre and has probably erupted over 50 times since 1200 AD (Larsen *et al.*, 1998). Despite the possibility of both of these systems being potential producers of ocean-transported pumice, the geochemical signatures

are distinct, with basalts from Katla having much higher FeO and particularly TiO_2 abundances than those from Grímsvötn (Figure 5.7; Larsen, 1982). Figure 5.7 shows that the five analyses of KVU 5 pumice are most similar to the Katla basalts and are unlike any other of the basalt producer volcanic systems. The slight differences between the field and the analyses can be accounted for by different analytical conditions and the fact that the field are defined by bulk analyses of lavas and those of the pumice are just of the volcanic glass. Unpublished geochemical analyses by Dugmore and Larsen suggest that basaltic eruptions from Katla are geochemically identical and it is not possible to identify individual events. This evidence shows that KVU 5 was produced by a volcanic eruption from the Katla Volcanic System sometime before 6000 ^{14}C years BP.

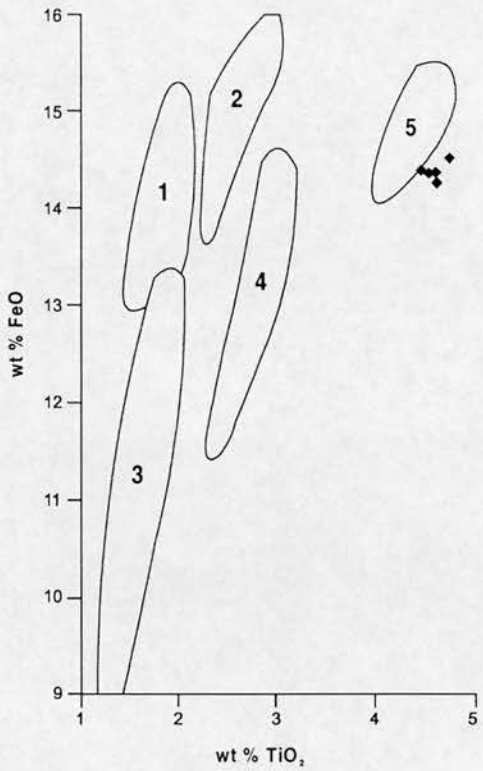

Figure 5.7: This graph (TiO_2/FeO) shows fields defined by analyses of basalts from Krafla (1); Dyngjufjöll (2); Dyngjuháls, Dyngjufjöll and Veiðivötn (3); Kverkfjöll and Grímsvötn (4); Katla (5). The diamonds are analyses of the KVU 5 pumice. This graph is based on Larsen (1982).

Mapping, stratigraphy, dating of Holocene silicic tephra layers

The study of the Holocene SILK tephra layers produced by the Katla volcanic system has been part of a joint project with researchers in Iceland and Edinburgh. Whilst there have been a number of publications about both the explosive and effusive Katla eruptions (e.g. Einarsson *et al.*, 1980; Jakobsson, 1979; Larsen, 1979; Larsen, 1996; Miller, 1989;

Thórarinsson, 1957; Thórarinsson, 1975; Thórarinsson, 1981; Zielinski *et al.*, 1995), until the present study there have only been two publications on silicic Holocene activity (Larsen, 1994; Ólafsson *et al.*, 1984).

Larsen et al (in press) report the results of a study of over 600 stratigraphic sections, through which a detailed tephrastratigraphy of the area has been established. This research has been carried out as a parallel project to the search for the origin of the dacitic ocean-rafted pumice. The vast majority of this fieldwork was undertaken by Guðrún Larsen. Although the majority of the sections were only logged, tephra samples of silicic tephra layers were also taken from several key sections by Larsen, Dugmore and Newton, so that their geochemical characteristics could be established. The location of these sites is shown in Figure 5.6 A second parallel project was undertaken during this period, which investigated the variations in the apparent ^{14}C ages of various fractions of peat. Much of the fieldwork for this project was located to the south of Mýrdalsjökull. These results have been published in a series of papers (Dugmore *et al.*, in press; Dugmore *et al.*, 1994; Dugmore *et al.*, 1995b; Shore *et al.*, 1995) and these dates, as well as some of those from the earlier work of Dugmore (1987), are used in this thesis to date the SILK layers and the other tephra layers in the profiles where the SILK layers are found. ^{14}C dates are shown in Table 5.2 and the ages and approximate ^{14}C ages of the SILK layers are shown in Table 5.3. A composite profile showing a regional tephrastratigraphy, including radiocarbon dates, is shown in Figure 5.8. Figure 5.9 shows the profiles from Engimýri, from which the peat was obtained for dating SILK-MN.

Tephra Dated	^{14}C Age BP	$\delta^{13}C$	Lab No.	Sample	Ref.
SILK-YN	1676±12*	-26.9‰	n/a	Peat	1
SILK-UN	2660±60	-29.6‰	SSR-2805	Peat	2
SILK-MN	2975±12^{+}	n/a	n/a	Peat	3
SILK-LN	3139±40	-28.6‰	GU-7019	Peat	4
Hekla-S	3515±55		U-6291	Wood	5
Hekla-4	3826±12$^{\#}$	n/a	n/a	Peat	6
above SILK-A8	6305±70				4
A-13	7630±42$^{@}$	n/a	n/a		7

Table 5.2: Dates of tephra layers and associated layers shown in Figure 5.8. * weighted mean derived from 19 ^{14}C dates from a profile in southern Iceland. $^{+}$ weighted mean derived from 16 ^{14}C dates from a profile at Engimýri. $^{\#}$ weighted mean derived from 35 ^{14}C dates from 15 profiles in Iceland and Scotland. All means were calculated using the University of Washington, Quaternary Isotope Laboratory, radiocarbon calibration program 3.0.3c 1993 (Stuiver and Reimer, 1993). References: 1 = Dugmore *et al.* (in press); 2 = Dugmore and Buckland (1991); 3 = Shore *et al.* (1995); 4 = Larsen *et al.* (in press); 5 = Larsen (unpublished); 6 Dugmore *et al.* (1995b); 7 = Dugmore (1987).

Tephra Layer	Age
SILK-YN	1676±12 ^{14}C years BP
SILK-UN	2660±50 ^{14}C years BP
SILK-MN	2975±12 ^{14}C years BP
SILK-LN	3139±40 ^{14}C years BP
SILK-N4	c. 3600 ^{14}C years BP
SILK-N3	c. 3700 ^{14}C years BP
SILK-N2	c. 4000 ^{14}C years BP
SILK-N1	c. 4400 ^{14}C years BP
SILK-A1	c. 4600 ^{14}C years BP
SILK-A2	c. 5000 ^{14}C years BP
SILK-A3	c. 5500 ^{14}C years BP
SILK-A5	c. 6150 ^{14}C years BP
SILK-A7	c. 6200 ^{14}C years BP
SILK-A8	c. 6400 ^{14}C years BP
SILK-A9	c. 6600 ^{14}C years BP
SILK-A11	c. 7000 ^{14}C years BP
SILK-A12	c. 7200 ^{14}C years BP

Table 5.3: Ages and approximate ages of Holocene silicic Katla tephra layers. The estimated ages are based on extrapolations of ^{14}C tephra layers (Table 5.2 and Figure 5.8). Although the estimates of SILK–N1, SILK-A1, SILK-A2, SILK-A3 are weak, due to the temporal gap between ^{14}C dates, the relative sequence is firm and work elsewhere (e.g. Dugmore, 1989b) has shown that Icelandic soil accumulation rates in prehistory produce effective estimates of age.

Larsen *et al.* (in press) report at least 12 SILK layers which have been identified in the soil profiles in southern Iceland. Table 5.3 and Figure 5.8 indicate that there are in fact at least 17 post-glacial silicic eruptions from Katla. The extra tephra layers have not been mapped to Katla yet, but continuing work suggests that Katla is the source for all 17 layers (Larsen, pers. comm.). A study of 148 soil profiles in the Eyjafjallajökull- Sólheimajökull area indicates that there appear to be no soil profiles in southern Iceland which are older than about 8000 ^{14}C years BP (Dugmore, 1987; Dugmore, 1989b) and the 7630 ^{14}C years BP age of A-13 is the oldest radiocarbon age from a soil profile in the area. Soil formation in this part of Iceland is post-8000 ^{14}C years BP. This has important implications. This lack of soil indicates that the area was not ice-free until sometime probably just before 8000 ^{14}C years BP and that southern Iceland's impressive tephrochronological record is only available for the last 8000 ^{14}C years and before this there is no evidence of the production of tephra from Katla found close to source. For earlier activity it is necessary to investigate more distal areas, such as northern Iceland, the marine sediment record or other terrestrial records in places such as Europe. This late-glacial/early Holocene record will be discussed in more detail in the next section.

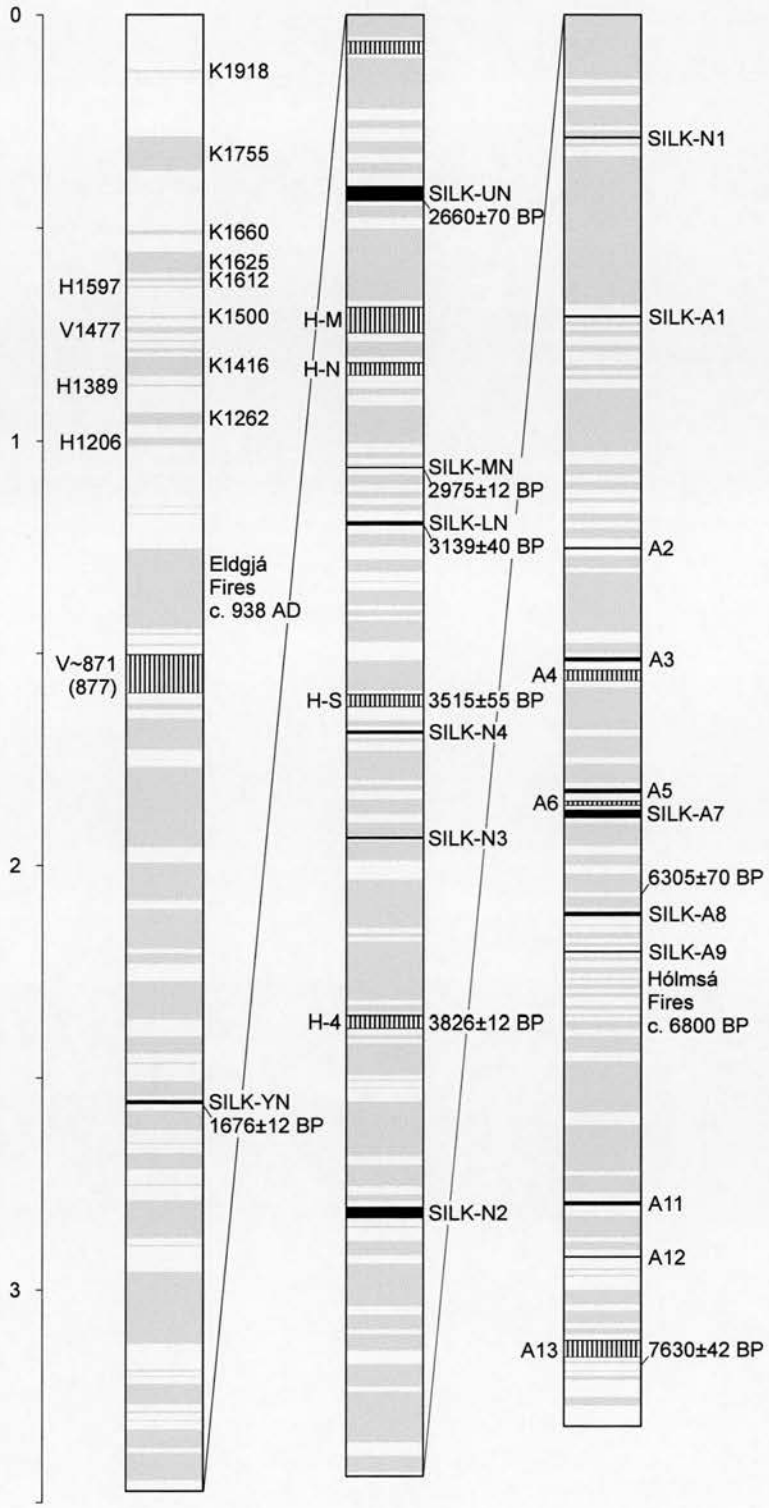

Figure 5.8: An 11 m composite Holocene profile from the south-east of Mýrdalsjökull showing the overall tephrastratigraphy and the stratigraphic positions of the SILK layers. All Katla tephras are to the right of the profile and others to the left. Basaltic tephra layers are light grey, silicic tephras have vertical lines and the SILK layers are black. The ^{14}C dates are presented in Table 5.2 and approximate ages of all SILK layers are shown in Table 5.3. H = Hekla, K = Katla and V = Veidivötn. The vertical scale is in metres. Based on Larsen *et al.* (in press).

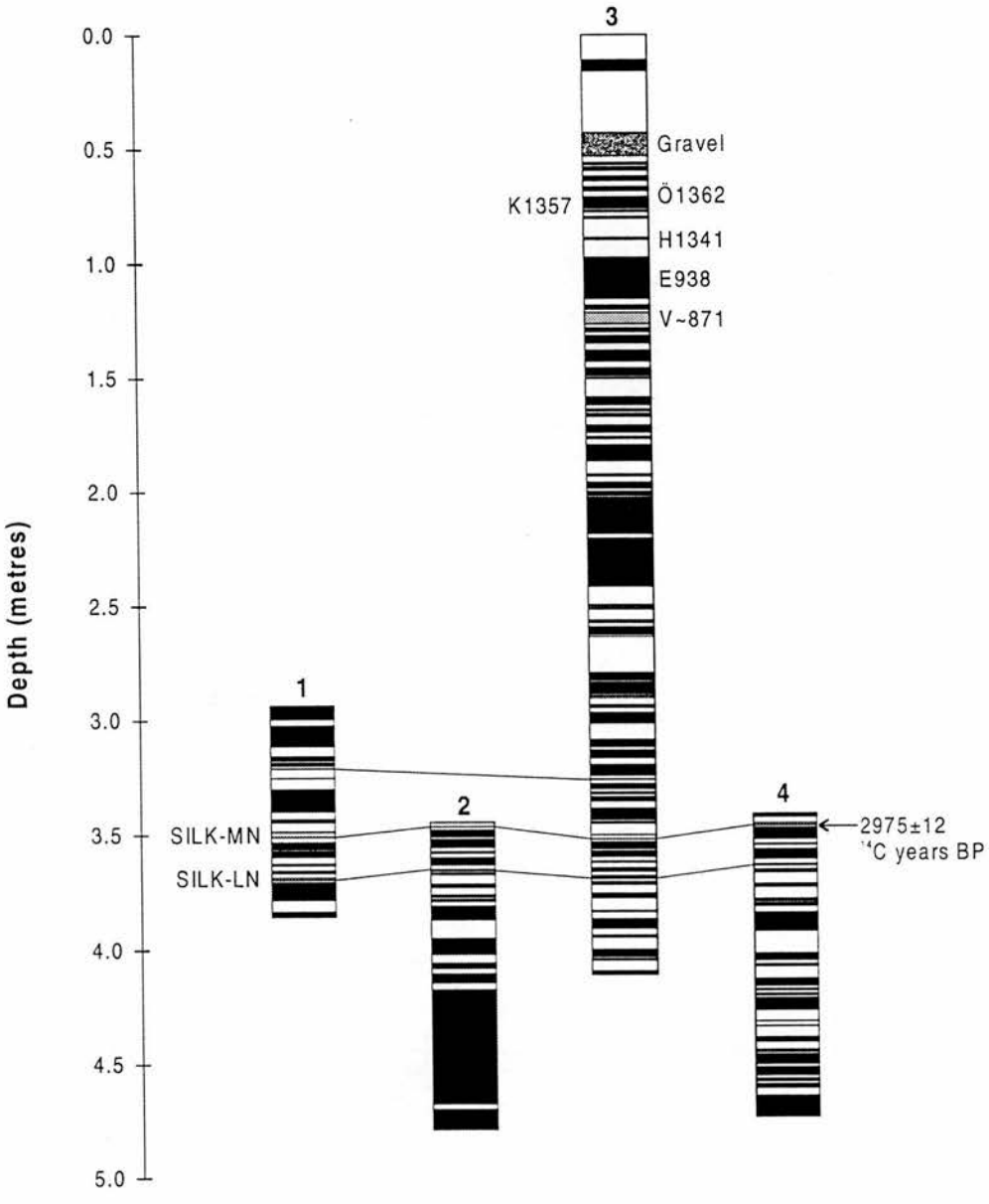

Figure 5.9: Diagram to show the upper part of the four profiles at Engimýri (E on Figure 5.6). Peat for dating SILK-MN was collected from below this tephra layer and the basaltic layer beneath from each profile and then homogenised. Geochemical analyses were undertaken on SILK-MN and SILK-LN from Profiles 1 and 3. H = Hekla, K = Katla, Ö = Öræfajökull, E = Eldgjá and V = Veidivötn.

The SILK layers are comparatively small, with the largest SILK-UN, having a compacted volume of only 0.16 km^3 within the 0.1 cm isopach. Table 5.4 shows the volumes of the six largest SILK layers and the volumes of the remaining smaller ones is estimated to be < 0.01 km^3. The isopach maps in Figure 5.10 demonstrate the different fallout patterns of the SILK layers. Except for SILK-UN, the isopach maps presented in Larsen *et al.* (in press), suggest that most the eruptions which produced the SILK layers were comparatively short-lived, as the frequently changing wind direction would have created a more complex pattern of fallout if the eruptions had lasted for several days (Figure 5.10). Larsen *et al.* (in press) also show the eruptive vents which produced the SILK layers are located beneath Mýrdalsjökull, within the Katla caldera, but to the west or north-west of the area active during the 1918 eruption (Figure 5.6). The relatively small size of the SILK layers could be due to the subglacial nature of the activity. The eruptions probably reached their peak intensity during the early stages of the eruption. During this early stage the activity may have been totally subglacial, not enough ice having been melted to enable a traditional eruption column to form. Any tephra or pumice produced during this stage of activity will be deposited in the rapidly expanding subglacial lake. The eruption may not have broken through the ice until the eruption was waning. Larsen *et al.* (in press) believe that some silicic Katla eruptions may have never broken through the ice, and those that did left a minimum record of their activity in the soil profiles around Mýrdalsjökull.

a) SILK-YN

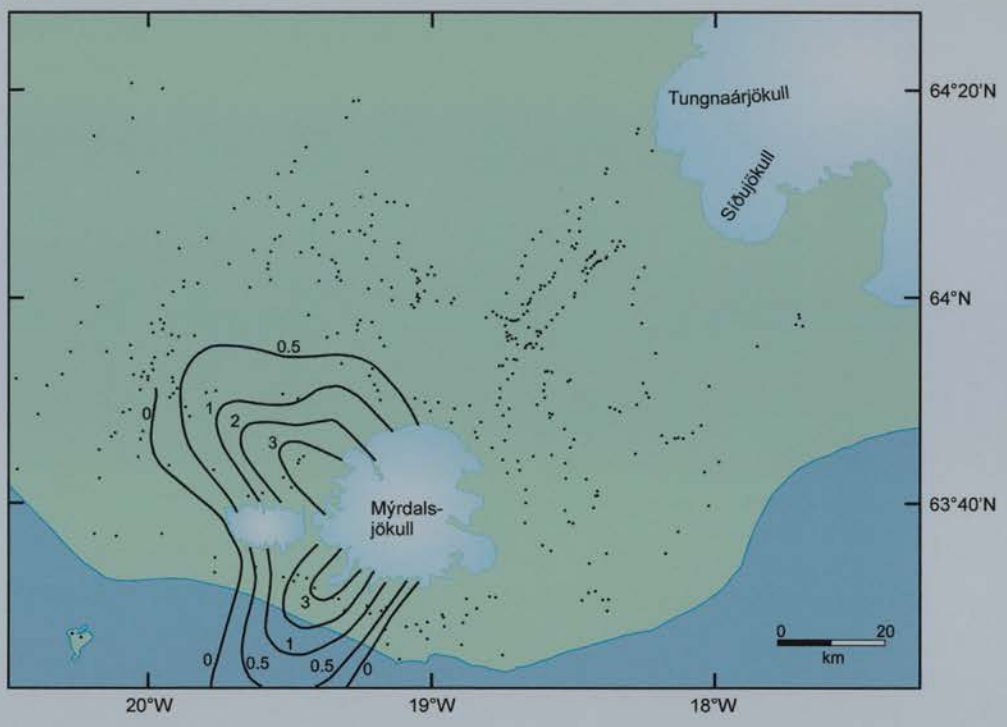

b) SILK-UN

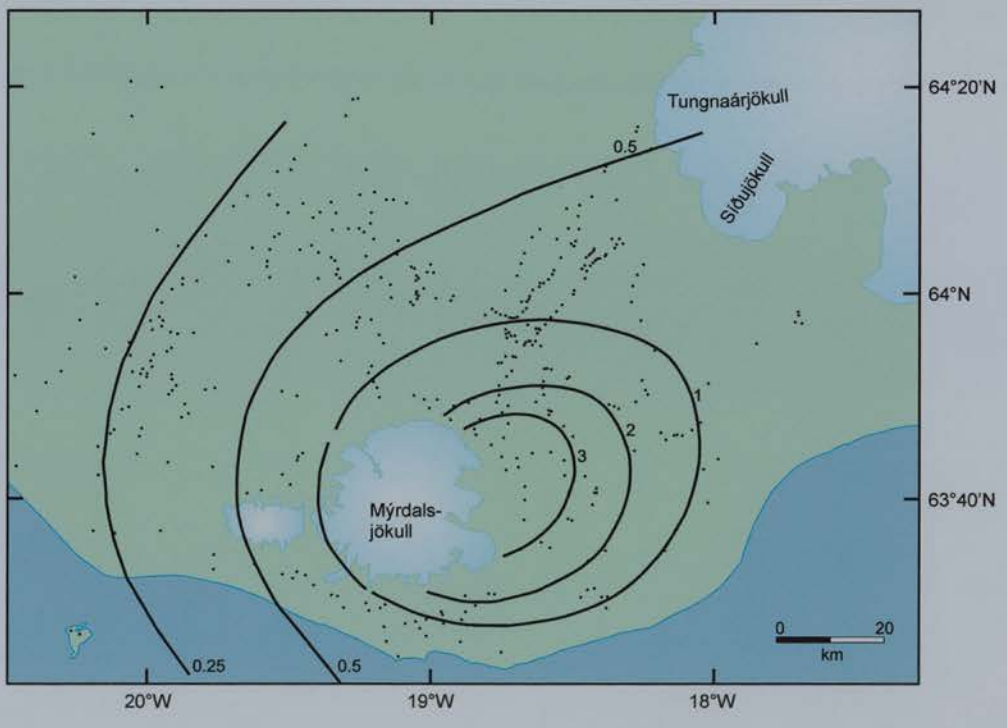

c) SILK-LN

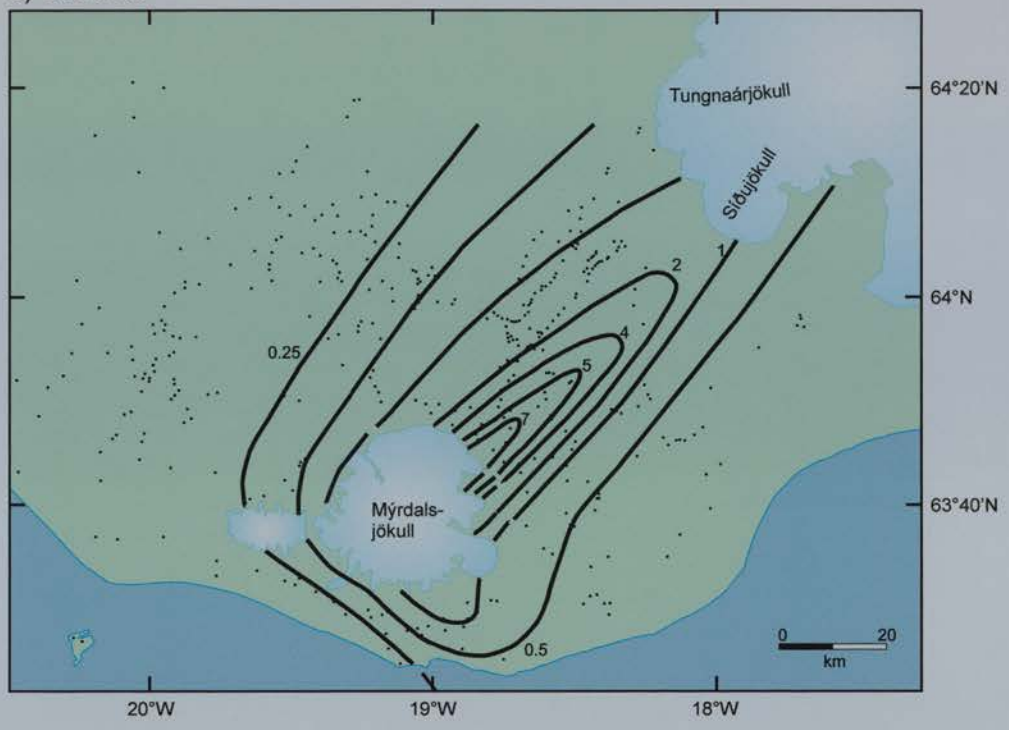

d) SILK-N4

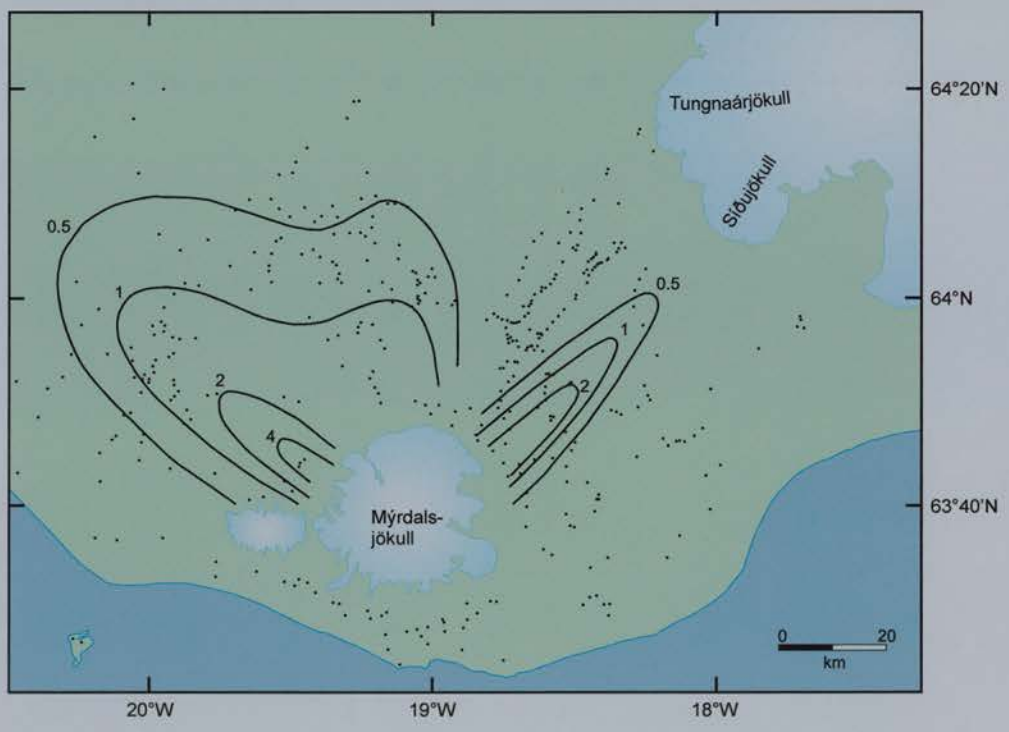

Figure 5.10: Isopach maps to show the fallout patterns of four of the SILK layers. The numbers refer to the thickness of the tephra layer in cm. The dots show the stratigraphic sections measured. Maps redrawn from Larsen *et al.* (in press).

Tephra	Volume on land $10^6 m^3$		Outermost isopach (cm)	Volume (UCP) within 0.1cm $10^6 m^3$
	CP	UCP		
SILK-YN	44	75	0.5	85
SILK-UN	160	265	0.2	290
SILK-MN	30	50	0.1	65
SILK-LN	120	200	0.1	220
SILK-N4	67	110	0.5	130
SILK-N2	36	60	0.5	75

Table 5.4: Volumes of six of the SILK layers. CP = compacted tephra volume and UCP = uncompacted tephra volume. This table is modified from Larsen *et al.* (in press).

The SILK layers, along with the silicic Hekla tephra layers, form distinctive marker horizons in the soil profiles of southern Iceland. In the field, the SILK layers can easily be identified by their distinctive grey-green to olive green colour. The most distinctive feature of many of courser fractions of these layers are the long thin glass rods and finer pele's hair needles. Elongated highly vesicular glass shards are also common in several of the layers, as well as other more rounded non-vesicular shards (Ólafsson *et al.*, 1984). No lithic fragments and few minerals have been found in the tephra layers. Although these "needle grains" are seen in many of the layers in the field, three layers, SILK-UN, SILK-MN and SILK-LN have particularly distinctive needle grains which allow easy field identification. Some layers such as SILK-A5 and SILK-N1 have less needle and elongate and more blocky grains. Figure 5.11 shows examples of the types of grains which are found in the SILK layers. The needle grains found in the SILK are unique amongst Icelandic silicic tephra layers.

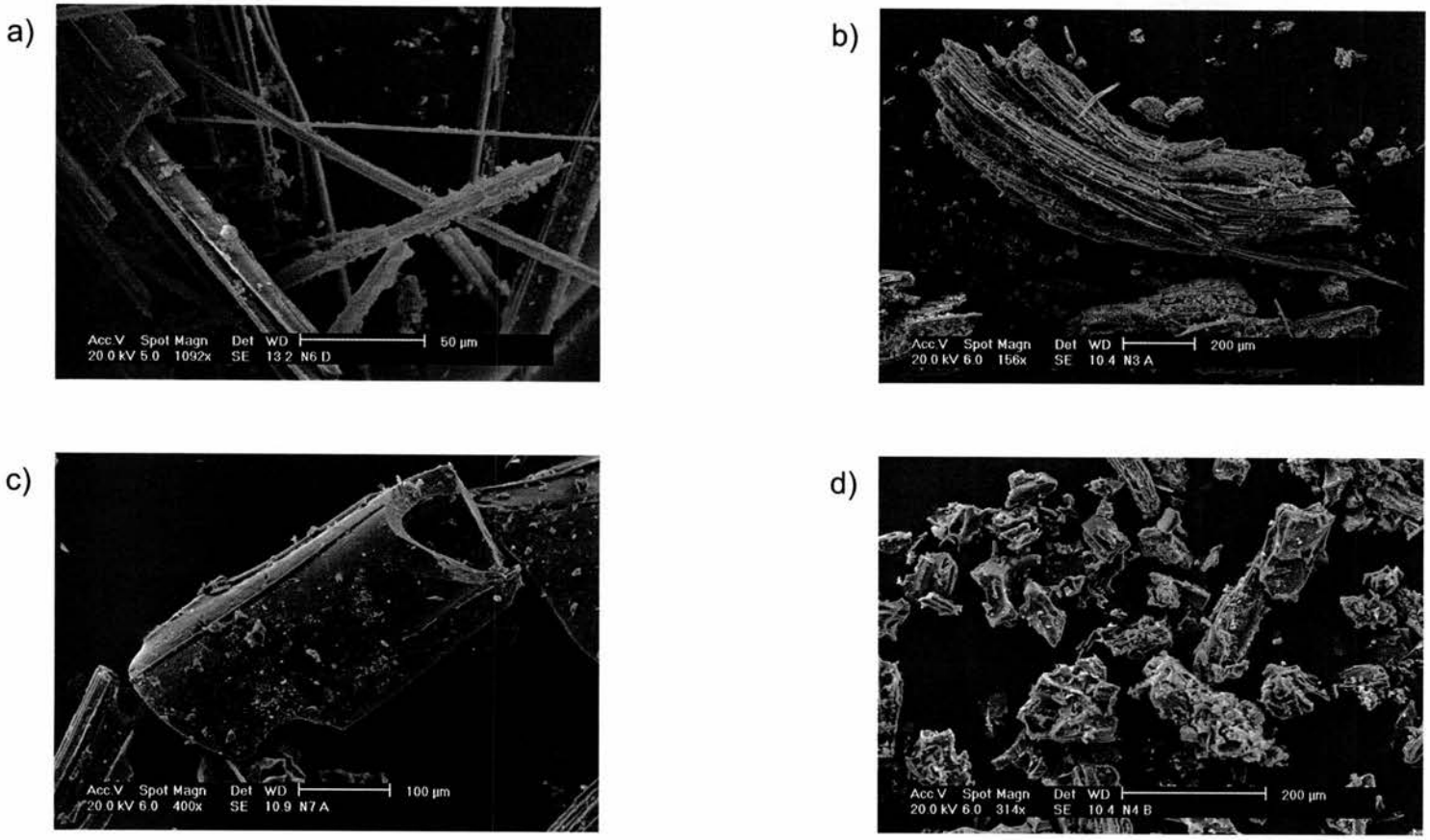

Figure 5.11: SEM micrographs of the types of grains which are found in some of the SILK layers. a) glass rods and needle grains (SILK-MN). These range in diameter from 1-2 µm to larger flattened and elongate shards 50-100 µm across and more than 1 µm in length b) a large elongate vesicular grain, which is splitting into thin long glass pelé's hair-like rods (SILK-N3). c) fragment of a large glass pipe with thick, 20 µm, walls (SILK-UN). d) vesicular tephra grains, with little or no evidence of elongate needles or glass tubes (SILK-N4).

Silicic pumice deposits and late-glacial activity

Due to the lack of any soil profiles in the area around Katla, there are no preserved tephra layers older than about 8000 ^{14}C years BP, yet there is still evidence of late-glacial to early Holocene volcanic activity on the slopes of Katla. Lacasse *et al.* (1995) suggest that the Sólheimar Ignimbrite, found on Skógaheiði (Figure 5.12), is associated with North Atlantic Ash Zone One (NAAZO), the tephra complex which is also associated with the widespread Younger Dryas tephra layer, the Vedde Tephra. This tephra layer, which has been found in the north of Iceland as well as in marine cores and lacustrine sequences in Europe (see above), has been recently dated to 10,310 ± 50 ^{14}C years BP by Birks *et al.* (1996). The ignimbrite is cut by three north-south trending meltwater channels, and a southerly facing break of slope that trends parallel to the main valley of the Jökulsá, which drains Sólheimajökull. Pumice is found on and within this welded ignimbrite.

Lacasse *et al.* (1995) acknowledge that for the ignimbrite to have been deposited, the area must have been ice-free during the Younger Dryas and this contradicts current theories on the deglaciation in Iceland (Hjort *et al.*, 1985; Ingólfsson, 1991; Ingólfsson and Norddahl, 1994). A Younger Dryas date for the Sólheimar Ignimbrite is further undermined by the fragmentary nature of the ignimbrite deposit and the morphological glacial features found on it (Figure 5.13). This is strong evidence that it has been repeatedly glaciated. Lacasse *et al.* (1995) dismiss "previous reports" of a tillite found on top of the ignimbrite and claim it was actually deposited by a lahar or jökulhlaup. Dugmore, Newton and Norðdahl (in prep) still regard this deposit as being a diamicton (tillite) and that this proves that the deposit has been glaciated. This suggests an age before the last glacial maximum c. 20,000 BP as Sólheimajökull has not advanced over the Sólheimar ignimbrite during the Holocene, with Holocene maximum glacial extent of Sólheimajökull (the Drangagil Stage, Figure 5.12) only reaching an altitude of just less than 300 metres (Dugmore, 1987; Dugmore, 1989b; Dugmore, Newton and Norðdahl, in prep). Dugmore, Newton and Norðdahl (in prep) suggest that the ignimbrite was emplaced during a warm period, with conditions similar to the present Holocene, and then subjected to full glacial conditions, which lead to only a small glaciated fragment of the ignimbrite surviving. The retreat of the ice left a diamicton and Holocene meltwater channels which further eroded the deposit, creating the record seen today.

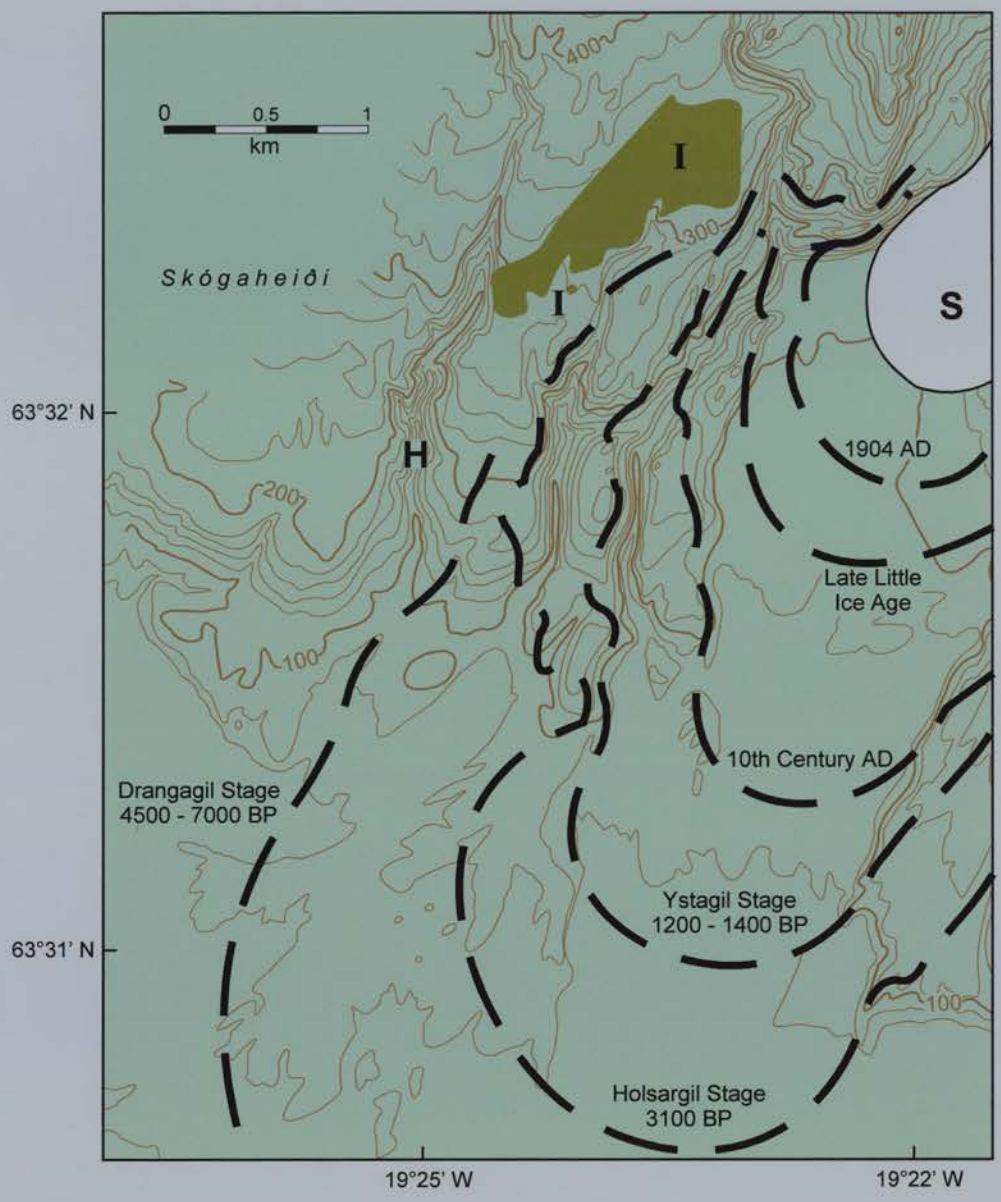

Figure 5.12: Map to show the location of the Sólheimar ignimbrite. The dashed lines indicate Holocene ice limits. I = Sólheimar Ignimbrite, H = Hofsárgil and S = Sólheimajökull. Redrawn from Dugmore (1987).

Figure 5.13: Photograph to show the glaciated streamlined form of the Sólheimar Ignimbrite deposit. The ignimbrite shows typical roche moutonnée features, stream-lined forms and fluting.

Lacasse (1995) also suggest that the pumice at Vikurhóll[7], 6 km metres to the south-west of the Sólheimar Ignimbrite, is part of the same deposit. Vikurhóll is found between the between the Rjúpnagil and Húsárgil rivers at between 400 and 300 metres above sea-level (Figure 5.14). The largest of a series of small hills which form a ridge of pumice is called Vikurhóll (Figure 5.15a). There is no soil cover in this area and the surface of Vikurhóll and the ridge is covered in mainly unconsolidated highly vesicular yellowish grey pumice which varies in size from about 1 cm to over 20 cm (Figure 5.15b). The deposit also contains obsidian and red scoria, which tend to be smaller than the pumice, usually less than 1 cm in diameter. There is no evidence of pumice deposits between Vikurhóll and the current ice-limit of Mýrdalsjökull. Although pumice is concentrated on the small hills and ridge it is scattered over a wide area and there is a concentration of pumice in a dry valley to the south of the main deposit. This presumably has been concentrated by rain fed floods. The amount of pumice slowly decreases down slope of the main deposit, indicating reworking of material. There is no evidence of pumice deposits between Vikurhóll and the current ice-limit of Mýrdalsjökull. The unconsolidated pumice deposit at Vikurhóll must be post-glacial and therefore, cannot be the same deposit as the pre-last glacial Sólheimar Ignimbrite. It seems that the pumice was emplaced by a jökulhlaup when the ice limit was at a substantially lower altitude. An ice-limit close to the upper boundary of the Vikurhóll deposit would account for the lack of any pumice in this area.

---

[7] Vikurhóll is Icelandic for "Pumice Hill"

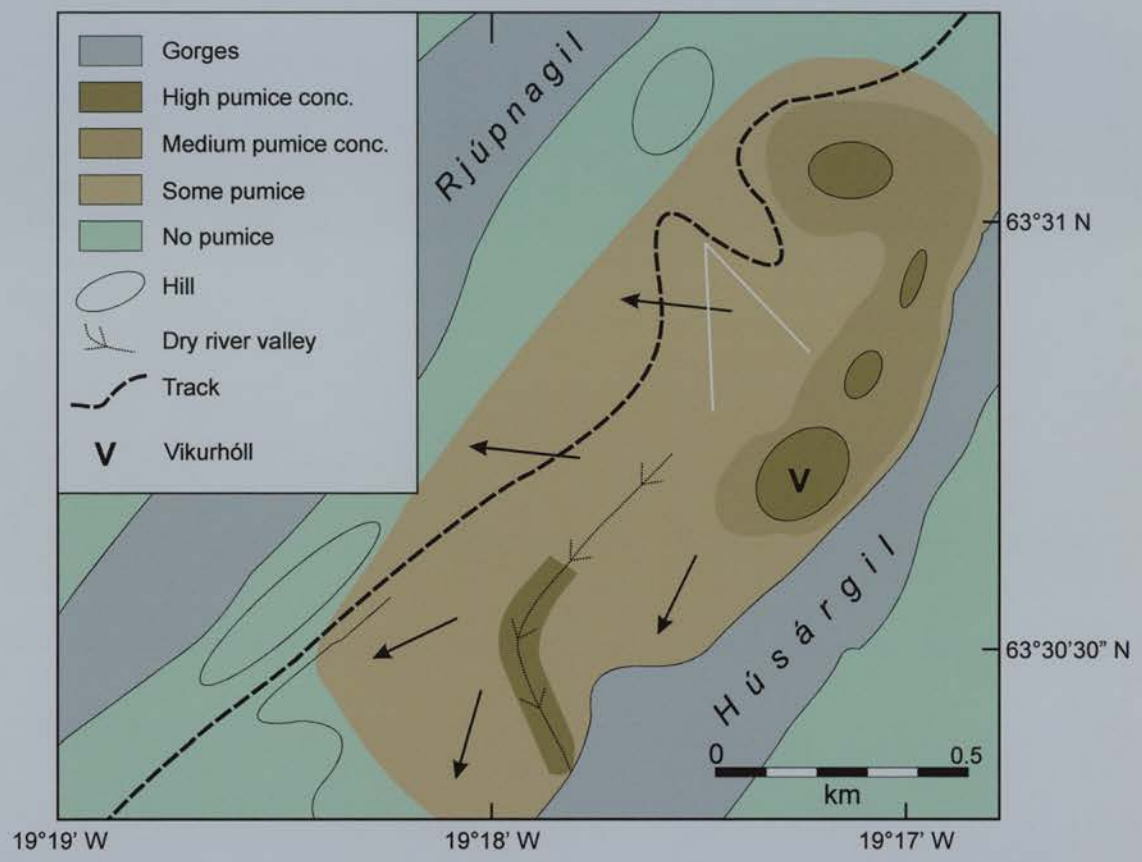

Figure 5.14: Map of the Vikurhóll area. The high pumice concentrations are along the ridge close to the edge of Húsárgil, with highest concentrations on the small hills, including Vikurhóll, and the dry river valley. The amount of pumice decrease away from the ridge, as indicated by the arrows. The whole of the area covered by the map is devoid of vegetation. The white lines indicate the field of view of Figure 5.15a. The location of this map is shown in Figure 5.6.

Figure 5.15: Photographs showing Vikurhóll and the pumice found on the surface. The upper photograph shows the prominent hill of Vikurhóll. The lack of vegetation and soil means that the pumice is constantly being reworked, as demonstrated by the rills on the sides of the hill. The lower photograph shows the ground surface of Vikurhóll. The light brown material is the pumice, which is found amongst vesicular and non-vesicular basalt. The ruler is 20 cm long.

The Vikurhóll pumice deposit is significant as it is the only unconsolidated pumice deposit found on the slopes of Mýrdalsjökull. It is also the only undisputed late-glacial to early Holocene silicic proximal deposit. This suggests that subsequent jökulhlaups which occurred after the ice had retreated further have taken different routes to the sea (see Transport section). The Vikurhóll pumice rests on diamicton and there are no organic materials which can be used for radiocarbon dating. The age of this deposit, therefore, cannot be firmly established. It must have formed after substantial deglaciation had begun and the ice had retreated to above about 400 metres above sea-level and before the formation of soils. This evidence suggest a date for the deposit to sometime after about 10,000 ^{14}C years BP and before about 8000 ^{14}C years BP.

Geochemical properties of Katla silicic tephras and pumice

Although the Holocene silicic activity has been known for some time and SILK tephras have been used to establish a detailed record of glacier fluctuations in southern Iceland (Dugmore, 1987; Dugmore, 1989b; Dugmore and Sugden, 1991), no geochemical data on the SILK layers has been published until this study and no connection to the North Atlantic pumice has been made. Bulk geochemical analyses of pumice from the Sólheimar Ignimbrite and Vikurhóll have been published by Lacasse (1995). EPMA major element analyses and SIMS trace and rare earth element analyses have been undertaken on the pumice from pumice at Sólheimar and Vikurhóll and the SILK layers in order to compare with analyses of the ocean rafted pumice.

EPMA SILK tephra geochemistry

A total of 243 EPMA analyses were carried out on the SILK tephra layers. Figure 5.16 shows that the SILK tephra layers are all silicic with the majority of analyses being calc-alkaline with some tholeiitic ones. These dacitic tephra layers can be divided into distinct groups (Figure 5.16b and Table 5.5), with the larger group being defined by the post-Hólmsá Fires SILK layers and the second one by the older SILK-A11 and SILK-A12 tephras. The second group is clearly identified by the having higher abundances of SiO_2 and K_2O and lower TiO_2, FeO, MgO and CaO than the larger younger group. These differences are clearly shown in Figure 5.17.

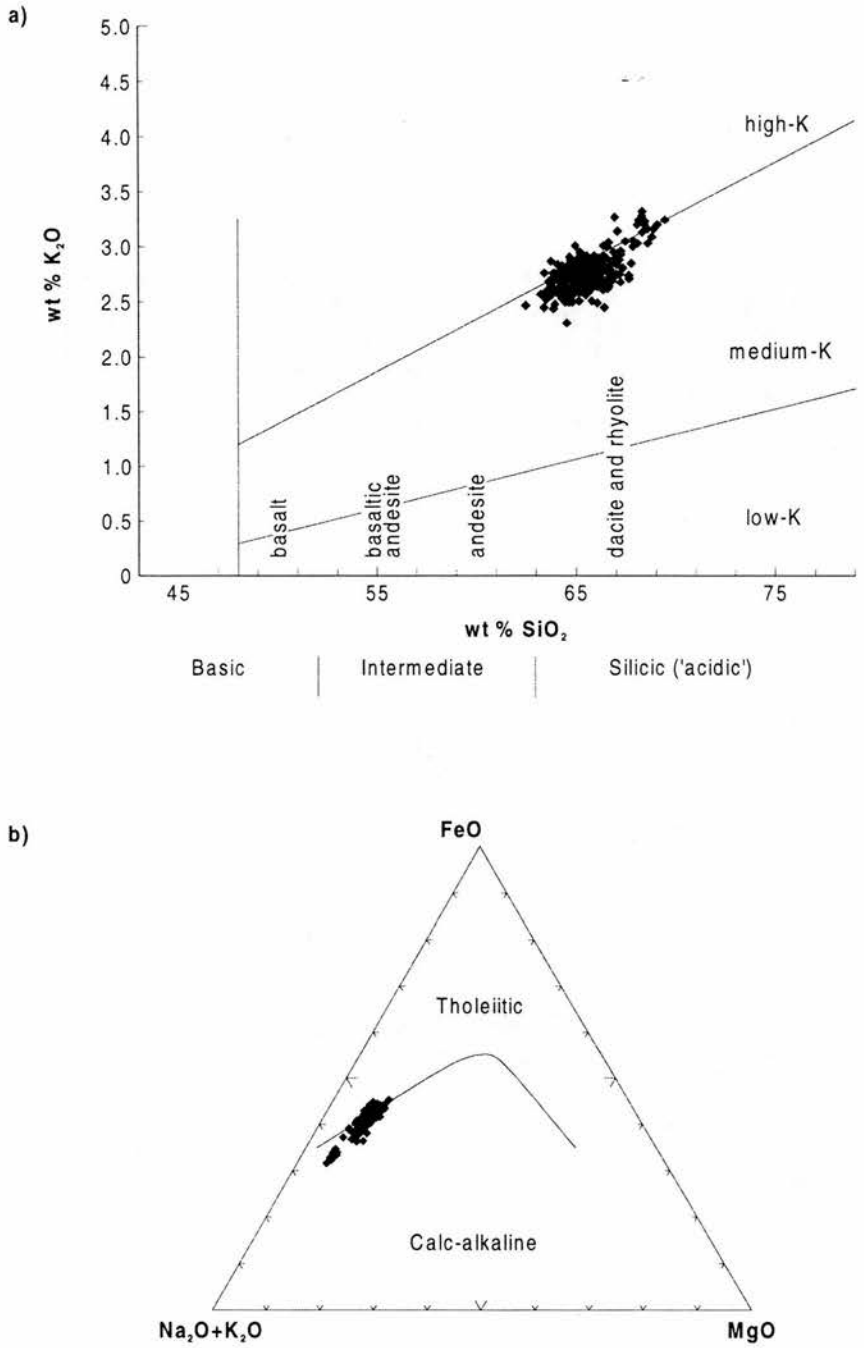

Figure 5.16: Graphs to show that: a) all of the analysed SILK layers are silicic, based on recommendations of Le Maitre (1989). b) The SILK layers can clearly be split into two groups with the smaller group being wholly calc-alkaline and the larger group straddling the tholeiitic/calc-alkaline boundary, based on Irvine and Baragar (1971).

a)

Tephra	Site	SiO_2	1σ	TiO_2	1σ	Al_2O_3	1σ	FeO	1σ	MnO	1σ	MgO	1σ	CaO	1σ	Na_2O	1σ	K_2O	1σ	Total	1σ	n
SILK-YN	**N. Gully (N8)**	65.31	0.64	1.19	0.10	14.15	0.18	6.04	0.23	0.19	0.03	1.06	0.10	2.94	0.22	4.55	0.21	2.70	0.13	98.12	0.48	**10**
SILK-YN	**Solheim.**	65.44	0.94	1.13	0.09	13.96	0.15	5.89	0.28	0.19	0.03	1.05	0.10	3.03	0.19	4.19	0.23	2.74	0.11	97.62	0.84	**19**
SILK-UN	**N. Gully (N7)**	64.16	0.41	1.33	0.06	13.95	0.24	5.94	0.31	0.20	0.03	1.36	0.08	3.40	0.13	4.37	0.20	2.59	0.11	97.30	0.54	**10**
SILK-MN	**N. Gully (N6)**	65.39	0.58	1.19	0.07	14.21	0.19	5.54	0.14	0.21	0.03	1.13	0.06	2.96	0.09	4.22	0.21	2.63	0.14	97.48	0.63	**8**
SILK-MN	**Dimmagil**	66.29	0.92	1.20	0.06	14.09	0.23	5.59	0.18	0.18	0.03	1.13	0.05	3.01	0.15	4.35	0.25	2.82	0.13	98.65	1.01	**10**
SILK-MN	**Engimýri (1/10)**	67.10	0.58	1.23	0.05	14.14	0.22	5.57	0.15	0.17	0.02	1.09	0.08	2.99	0.07	4.41	0.13	2.75	0.09	99.48	0.64	**9**
SILK-MN	**Engimýri (3/48)**	65.87	0.71	1.26	0.07	14.12	0.19	5.64	0.09	0.20	0.03	1.13	0.03	2.98	0.08	4.35	0.14	2.71	0.08	98.26	0.76	**10**
SILK-LN	**N. Gully (N5)**	65.18	0.63	1.22	0.05	14.21	0.17	5.60	0.17	0.19	0.04	1.12	0.04	3.00	0.10	4.37	0.22	2.74	0.11	97.63	1.09	**10**
SILK-LN	**Dimmagil**	66.11	0.83	1.22	0.04	13.85	0.40	5.67	0.08	0.18	0.03	1.11	0.04	3.00	0.06	4.58	0.20	2.69	0.07	98.43	1.17	**11**
SILK-LN	**Engimýri (1/15)**	66.64	0.54	1.20	0.04	14.11	0.24	5.79	0.12	0.19	0.03	1.09	0.04	3.03	0.08	4.52	0.18	2.79	0.08	99.34	0.47	**7**
SILK-LN	**Engimýri (3/53)**	66.05	0.57	1.20	0.05	14.40	0.26	5.63	0.25	0.16	0.03	1.15	0.07	3.02	0.12	4.18	0.32	2.73	0.09	98.53	0.68	**10**
SILK-N4	**N. Gully (N4)**	66.19	0.54	1.23	0.06	14.10	0.11	5.57	0.29	0.18	0.03	1.14	0.11	2.90	0.12	4.50	0.17	2.80	0.08	98.61	0.51	**10**
SILK-N3	**N. Gully (N3)**	64.69	0.62	1.48	0.08	14.15	0.15	5.96	0.48	0.20	0.04	1.35	0.04	3.35	0.10	4.25	0.15	2.60	0.07	98.02	0.72	**10**
SILK-N2	**N. Gully (N2)**	63.59	0.53	1.52	0.08	13.94	0.14	6.35	0.17	0.21	0.03	1.44	0.08	3.60	0.13	4.32	0.21	2.53	0.08	97.49	0.68	**10**
SILK-N1	**N. Gully (N1)**	65.32	0.44	1.37	0.04	13.67	0.21	5.78	0.26	0.19	0.04	1.19	0.06	3.03	0.20	4.52	0.21	2.78	0.11	97.83	0.53	**10**
SILK-A1	**TYN9**	65.02	0.60	1.38	0.06	13.49	0.17	5.91	0.24	0.19	0.03	1.17	0.07	2.98	0.11	4.27	0.24	2.76	0.11	97.17	0.70	**20**
SILK-A5	**MBH-3**	64.49	0.40	1.34	0.08	14.01	0.17	6.05	0.20	0.19	0.02	1.31	0.06	3.40	0.09	4.30	0.16	2.66	0.10	97.75	0.47	**10**
SILK-A7	**TYN3**	64.44	0.87	1.25	0.11	14.00	0.25	5.78	0.25	0.17	0.03	1.23	0.11	3.34	0.24	4.61	0.12	2.65	0.13	97.46	0.53	**10**
SILK-A7	**MBH-2**	64.83	0.51	1.27	0.09	13.94	0.14	5.52	0.27	0.19	0.02	1.20	0.07	3.27	0.14	4.48	0.11	2.75	0.11	97.44	0.44	**10**
SILK-A8	**MBH-1**	65.07	0.26	1.18	0.04	13.89	0.12	5.38	0.24	0.16	0.03	1.12	0.04	3.13	0.12	4.43	0.09	2.77	0.07	97.12	0.35	**10**
SILK-A9	**TYN-2**	64.88	0.63	1.14	0.06	13.99	0.19	5.45	0.12	0.17	0.03	1.14	0.03	3.10	0.14	4.60	0.15	2.70	0.06	97.17	0.79	**9**

b)

Tephra	Site	SiO_2	1σ	TiO_2	1σ	Al_2O_3	1σ	FeO	1σ	MnO	1σ	MgO	1σ	CaO	1σ	Na_2O	1σ	K_2O	1σ	Total	1σ	n
A11	**A-Site**	68.37	0.81	0.90	0.05	13.74	0.12	4.14	0.17	0.15	0.03	0.73	0.04	2.02	0.10	4.35	0.21	3.17	0.07	97.56	1.10	**10**
A12	**A-Site**	68.00	0.60	0.87	0.05	13.75	0.18	4.21	0.16	0.15	0.02	0.74	0.04	2.15	0.11	4.53	0.14	3.12	0.11	97.51	0.52	**10**

Table 5.5: a) shows the means and standard deviations (1σ) of the SILK tephra layers which post-date the Hólmsá Fires eruption. b) shows the means and standard deviations (1σ) the older A11 and A12 SILK layers. The number of analyses are also shown (n) and full details about these analyses are available in Appendix 4.

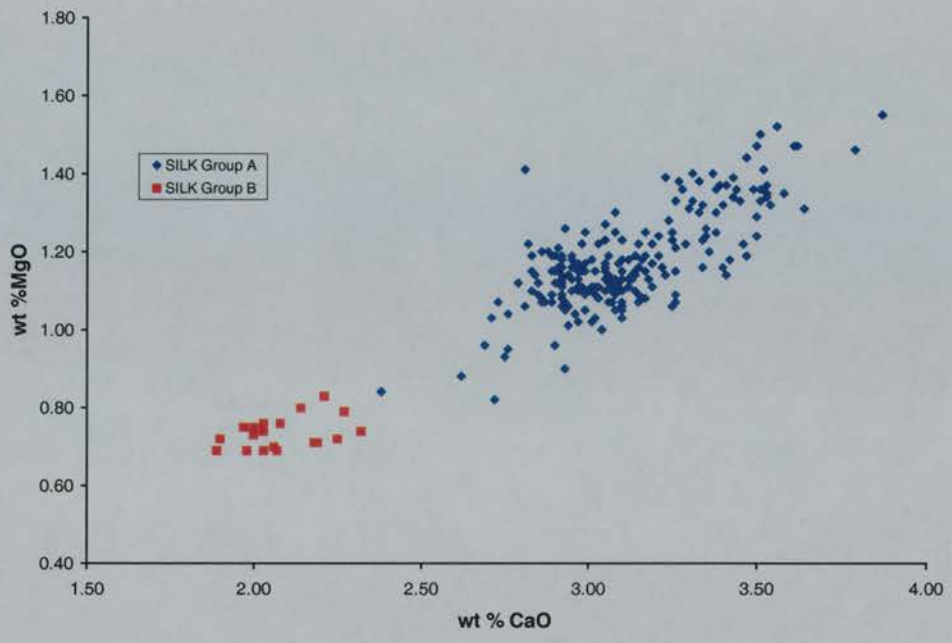

Figure 5.17: SILK Group A tephras have higher abundances of FeO and generally higher MgO values than Group B (SILK-A11 and SILK-A12).

The collaborative research with Guðrún Larsen has enabled analyses of most of the SILK layers from several profiles around the Katla Volcanic System. SILK-YN and SILK-A7 are both represented by analyses of the same tephra layer from two sites, whilst SILK-MN and SILK-LN are represented by analyses of the same tephra from four locations, although the two locations at Engimýri are only a few metres apart. These extra analyses give an estimate of the spatial geochemical variation of the same tephra layers, albeit over a relatively small distances of a few tens of kilometres. The oxide which shows the most variation is SiO_2 even at the closely spaced samples from Engimýri (e.g. 1/10 and 62/48 in Table 5.5a). Table 5.5a also shows that there is no significant differences between the other oxides between 1/10 and 62/48. This variability means that SiO_2 should not be used to correlate tephra samples, although the relatively small differences mean that it can be used for classification purposes. There is no significant variation in the oxides of the other multiple tephra samples and further discussion will only refer to the SILK tephra name not the individual sample or site name.

The tephra analyses shown in Table 5.5a are arranged in chronological order, with the youngest tephra, SILK-YN at the top. Table 5.5a shows that although all of the tephra layers

show similar geochemical properties, there are some significant differences between some of them and at least two and perhaps three subgroups can be identified. Furthermore, these subgroups are independent of both the chronological position of the tephra layer or the length of repose between eruptions (Larsen *et al.*, in press).

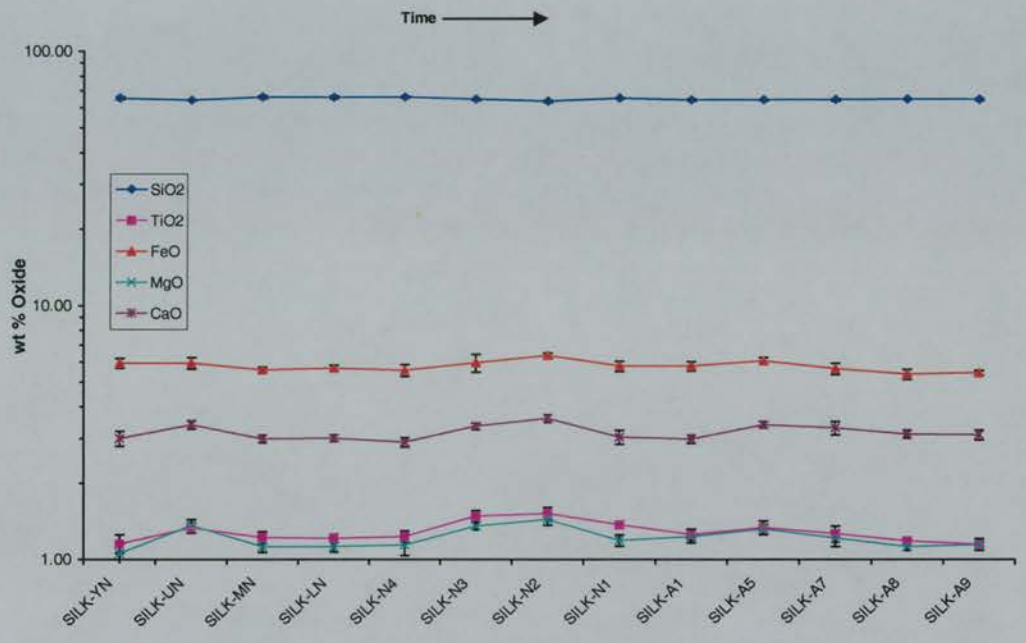

Figure 5.18: Graph to show that through time there has been little significant or systematic change in the geochemistry of the SILK the layers. Variations can be seen, such as the increased FeO, CaO, TiO_2 and MgO centred on SILK-N2, but these changes are not progressive. The error bars show standard deviation to 1σ.

Three subgroups of SILK Group A are shown in Table 5.6. Group A1 typically has CaO abundances of around 3.00 % and MgO of about 0.12, compared to the higher CaO and MgO abundances of Group A2. A further group (A3) is identified by having intermediate properties between the two main groups.

Figure 5.19 shows that Group A1 and Group A2 can be identified by differences in their position on the gradient and the analyses from the two groups are on a trend suggesting that they are both produced from the same magma source. The Group A1 SILK tephras, however, are products of slightly more evolved magma, as is shown by the slightly higher abundances of SiO_2 and lower amounts of TiO_2, FeO, MgO and CaO. This evolution did not occur over time and it appears that different parts of the magma were tapped at different times.

		SiO_2	TiO_2	Al_2O_3	FeO	MnO	MgO	CaO	Na_2O	K_2O	Total
Group A1	**SILK-YN**	65.39	1.15	14.03	5.94	0.19	1.05	3.00	4.32	2.73	97.79
	SILK-MN	66.18	1.22	14.13	5.59	0.19	1.12	2.99	4.34	2.73	98.49
	SILK-LN	65.95	1.21	14.14	5.66	0.18	1.12	3.01	4.41	2.73	98.42
	SILK-N4	66.19	1.23	14.10	5.57	0.18	1.14	2.90	4.50	2.80	98.61
	SILK-N1	65.32	1.37	13.67	5.78	0.19	1.19	3.03	4.52	2.78	97.83
	SILK-A1	64.44	1.25	14.00	5.78	0.17	1.23	2.98	4.61	2.65	97.46
	SILK-A9	64.88	1.14	13.99	5.45	0.17	1.14	3.10	4.60	2.70	97.17
	mean	65.69	1.23	13.99	5.72	0.18	1.12	3.00	4.38	2.74	98.05
	stdev	0.90	0.10	0.33	0.26	0.03	0.08	0.14	0.25	0.11	1.01
Group A2	**SILK-UN**	64.16	1.33	13.95	5.94	0.20	1.36	3.40	4.37	2.59	97.30
	SILK-N3	64.69	1.48	14.15	5.96	0.20	1.35	3.35	4.25	2.60	98.02
	SILK-N2	63.59	1.52	13.94	6.35	0.21	1.44	3.60	4.32	2.53	97.49
	SILK-A5	64.49	1.34	14.01	6.05	0.19	1.31	3.40	4.30	2.66	97.75
	mean	64.23	1.42	14.01	6.08	0.20	1.36	3.43	4.31	2.60	97.64
	stdev	0.64	0.11	0.19	0.35	0.03	0.08	0.15	0.18	0.10	0.65
Group A3	**SILK-A7**	64.63	1.26	13.97	5.65	0.18	1.21	3.31	4.54	2.70	97.45
	SILK-A8	65.07	1.18	13.89	5.38	0.16	1.12	3.13	4.43	2.77	97.12
	mean	64.78	1.23	13.94	5.56	0.17	1.18	3.25	4.50	2.72	97.34
	stdev	0.64	0.09	0.18	0.30	0.03	0.09	0.19	0.13	0.12	0.46

Table 5.6: Group A1 and A2 are clearly identified by Group A1 having lower CaO and MgO than A2. Group A3 appears to have intermediate properties between the two main groups. All standard deviations are to 1σ.

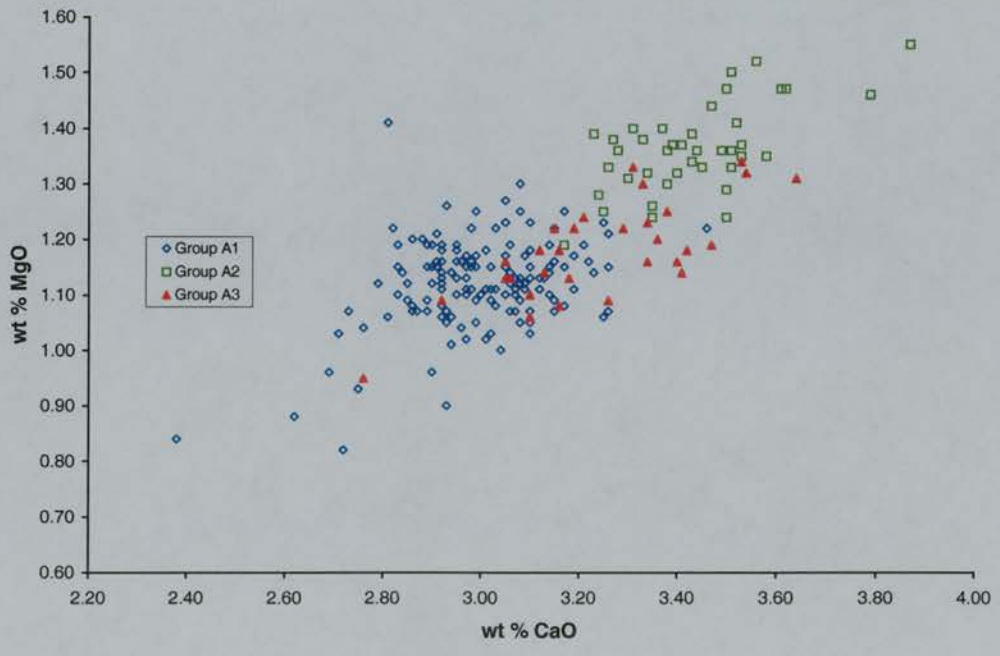

Figure 5.19: Graph (CaO/MgO) that shows two distinct groups can be identified in the post-Hólmsá Fires SILK tephras with a third intermediate group.

Although Figure 5.17 and Figure 5.19 identify Groups A1, A2, A3 and B, it is worth applying statistical analysis to these groups to see if they are significant. Figure 5.20 shows that Principal Component Analysis (PCA) of all of the SIMS EPMA data produces three main groups (A1, A2 and B) identified above. Although Al_2O_3 and Na_2O are closely associated with the first axis, usually implying the most important differences, this is not the case in Figure 5.20. In this PCA graph, samples show a greater dispersion along Axis 2, defined by high CaO, FeO, MgO and TiO_2 and low SiO_2 and K_2O. Axis 1 in PCA often picks out small differences. The fourth group, A3, overlaps with A1 and A2. The principal components of variations are, therefore, MgO, CaO and FeO, with SiO_2, K_2O and TiO_2 also being important. The least important oxides are Al_2O_3 and Na_2O.

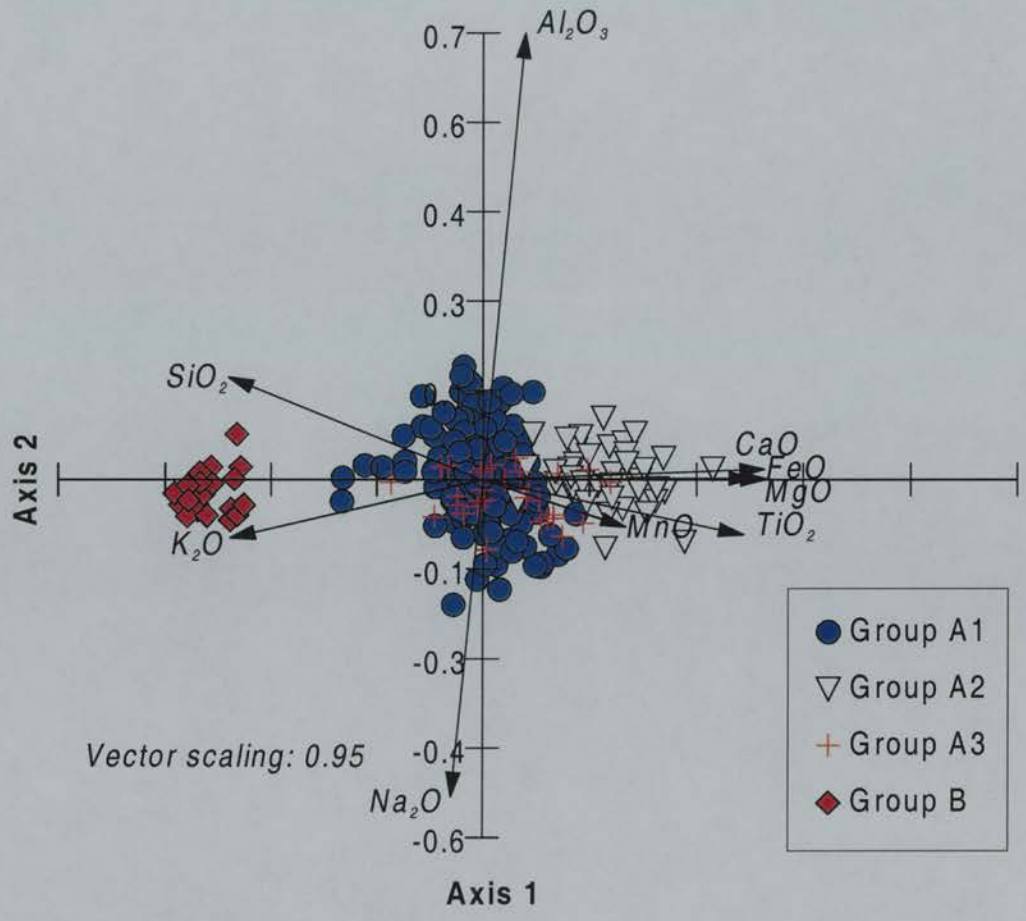

Figure 5.20: PCA graph to show which of the oxides best differentiate the groups. The groups can be clearly discerned and CaO, FeO and MgO are the principal components of variation, with TiO_2, K_2O and SiO_2 are also important. Na_2O and Al_2O_3 are the least important.

The PCA confirms that the three main groups identified correspond to "real world" groupings and it is reasonable to use these when correlating pumice to the SILK layers.

Having identified the principal components of variation identified in Figure 5.20, Table 5.7 shows the results of discriminant analyses using TiO_2, FeO, MgO and CaO. The addition of K_2O made no difference to the accuracy of the analysis and SiO_2 made it worse. All of Group B were placed correctly and most of A1 and A2. Figure 5.19 shows some overlap between these groups, which accounts for the misplaced analyses.

		True Group			
	Group	**A1**	**A2**	**A3**	**B**
Predicted	**A1**	133	0	3	0
	A2	1	35	5	0
	A3	18	5	22	0
	B	1	0	0	20
	Total N	153	40	30	20
	N Correct	133	35	22	20
	Proportion	0.869	0.875	0.733	1.000

Table 5.7: Discriminant analysis of the Groups A1, A2, A3 and B identified in Figure 5.17 and Figure 5.19 using only TiO_2, FeO, MgO and CaO. The total proportion of analyses placed in the True Group is 0.864.

The dendrogram in Figure 5.21 is able to identify the three main groups, A1, A2 and B. Statistically there is a highly significant difference between the Group A analyses and those from Group B. There is also a significant difference between the two groups in Group A, with only four analyses from Group A2 being included in Group A1 and one analyses from Group A1 placed in Group A2.

The statistical results show that the groups identified by the means, standard deviations and biplots are real. The dendrogram in Figure 5.21 shows that there is little statistical variation between the individual analyses of the SILK layers within their groups.

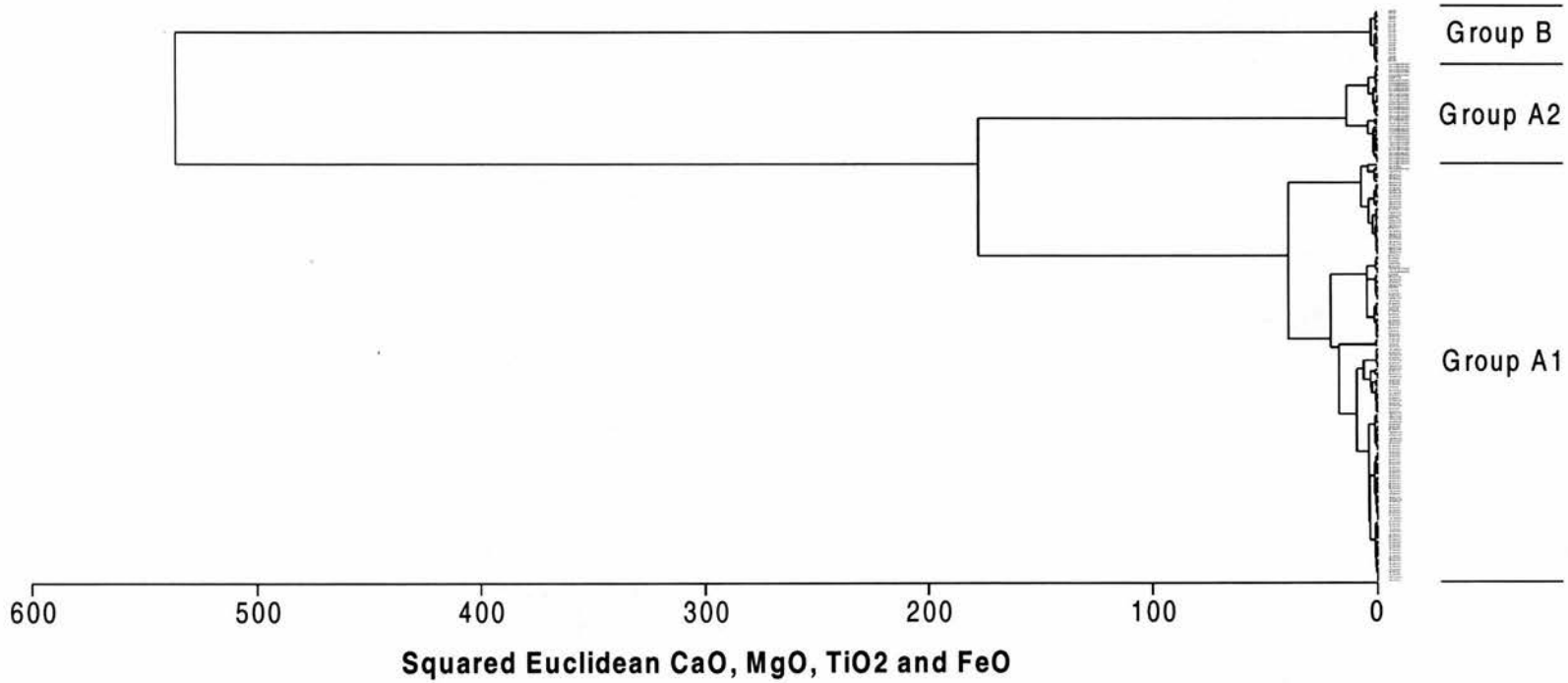

Figure 5.21: Dendrogram using minimum variance to group the EPMA analyses of the SILK layers. The marks on the right hand side identify the analyses: red = Group B; green = Group A2; blue = Group A1.

A detailed look at the three Group A tephras show that there is remarkable homogeneity within the groups. Figure 5.22 and Table 5.6 show that the Group A1 SILK layers are similar and that the only distinctive layer is the youngest SILK-YN. This layer shows an obvious trend in CaO/MgO compositions which is not seen in the other layers. The individual SILK-YN analyses are shown on Figure 5.22 to illustrate this.

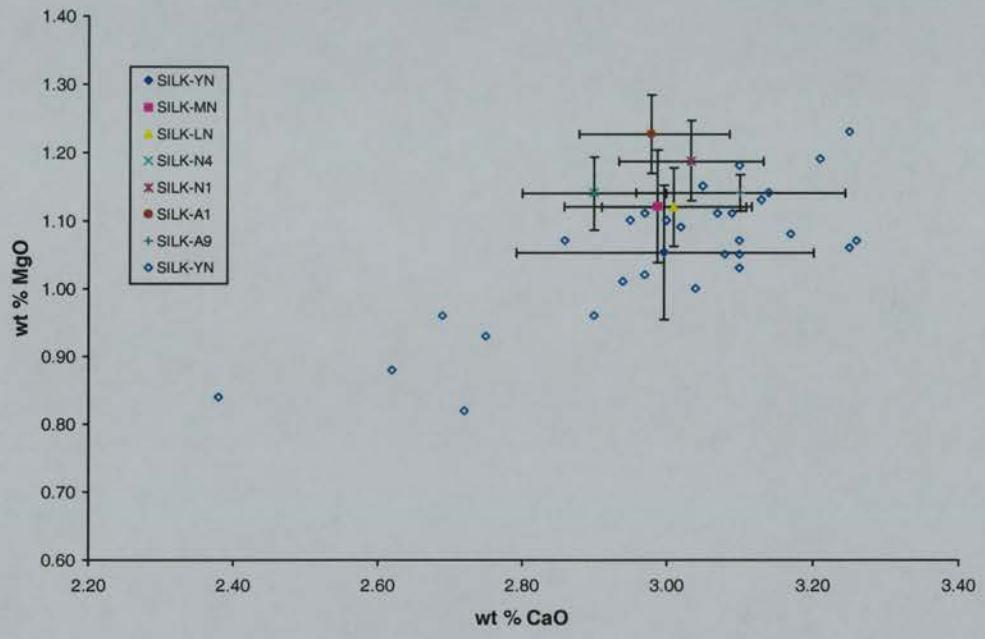

Figure 5.22: Comparison of the Group A1 SILK tephras. The means and standard deviations (1σ) are shown to simplify the graph. The open diamonds show all the analyses of the SILK-YN layer.

Group A2 SILK layers are shown in Figure 5.23, which demonstrates that SILK-UN, SILK-N3 and SILK-A5 have similar geochemical properties. SILK-N2 has slightly higher abundances of FeO, MgO and CaO and correspondingly lower SiO_2 compared to the rest the Group A2 tephras (Table 5.6 and Figure 5.23).

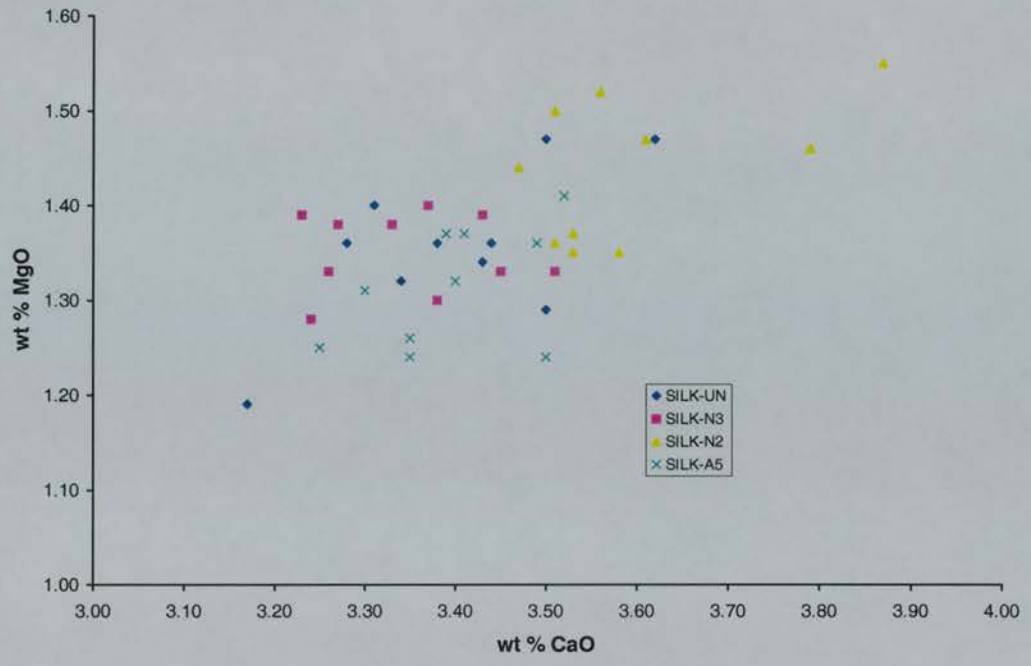

Figure 5.23: Graph (CaO) to show the geochemical properties of the Group A2 SILK tephra layers.

SILK Group A3 is composed of SILK-A7 and A8. These two tephra layers, which overlap with groups A1 and A2 (Figure 5.19) show some slight differences. SILK-A7 has higher abundances of CaO and MgO compared to SILK-A8, although some of the glass shards in SILK-A7 do have lower concentrations of these elements (Figure 5.24). SILK-A7 also has slightly higher abundances of TiO_2 and FeO and lower SiO_2 compared to SILK-A8 (Table 5.6).

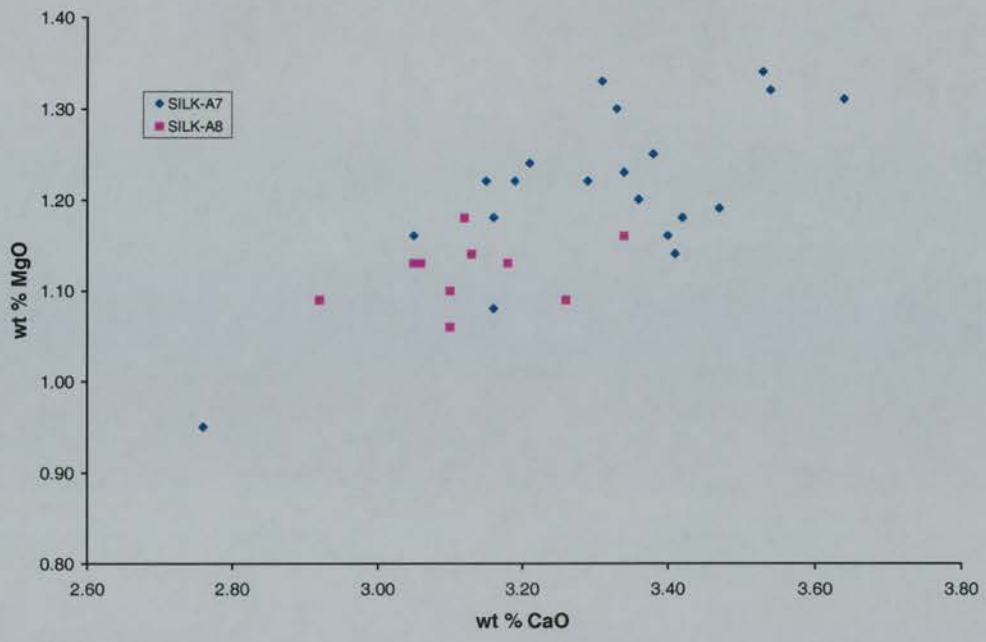

Figure 5.24: Graph (CaO/MgO) to show the geochemical properties of the Group 1C SILK tephras.

The pre-Hólmsá Fires tephras SILK-A11 and SILK-A12 have been identified as Group B in Figure 5.16 and Table 5.5. These two older tephra layers (7000-7200 ^{14}C years BP) are the oldest proximal Katla tephra layers found during this study. Both of these layers are similar, with SILK-A12 having slightly higher abundances of CaO and FeO than SILK-A11 (Figure 5.25 and Table 5.5). A two sample T-Test of the CaO abundances showed that the means of A11 and A12 are significantly different (P=0.015) at 2σ and could not have been drawn from the same populations. T-Tests of the other major discriminatory oxides failed to identify any other significant differences.

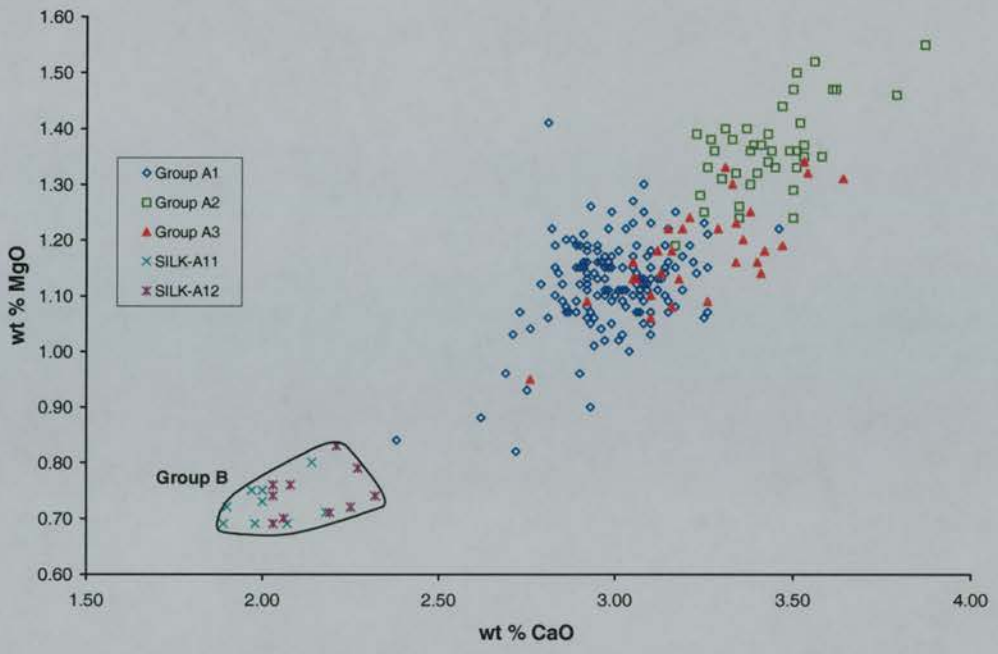

Figure 5.25: SILK-A11 and SILK-A12 (Group B) have lower CaO and MgO than the Group A tephra layers.

SILK-A11 and SILK-A12 (Group B) were produced from more evolved magma than the Group A tephra layers. Interestingly the youngest SILK layer, SILK-YN has the closest analyses to the Group B tephras.

The EPMA analyses of the Holocene SILK layers has established the presence of two distinct groups. The oldest is composed of SILK-A11 and A12, which predate the Hólmsá Fires fissure eruption. The post-Hólmsá Fires SILK were produced by less evolved magma. This group can itself be split into at least two and possibly three groups, the third group having common properties to the two main groups. There is little geochemical variation within the groups, although some differences are seen as demonstrated by SILK-YN. Both the Hólmsá Fires and the Eldgjá Fires eruptions appear to have had a profound impact on the plumbing of Katla. These were predominately basaltic eruptions, but it is possible that the scale of these events affected the presumably separate silicic magma chamber (Larsen *et al.*, in press). The Hólmsá Fires eruption separates the more silicic SILK-A11 and A12 tephras from the other SILK layers, whilst the Eldgjá Fires eruption precedes the longest silicic repose period in over 7000 years.

SIMS tephra geochemistry

As well as EPMA analyses, a series of SIMS analyses were also undertaken on selected SILK layers (Chapter 3). The EPMA analyses reveal that within the groups identified above, there is little geochemical variation between the SILK layers. As in the SIMS analyses undertaken on the pumice pieces, it was hoped that the trace and rare earth compositions would, in conjunction with the EPMA, identify geochemical differences between the SILK layers. The means and standard deviations of these analyses are listed in Table 5.8. Two obvious groups can be seen, which also reflect the two groups identified by the EPMA and are illustrated in Figure 5.26 and Figure 5.27. The Group B SILK layers identified by EPMA, SILK-A11 and A12, both have Zr and lower Ti and Sr values compared to the Group A tephras.

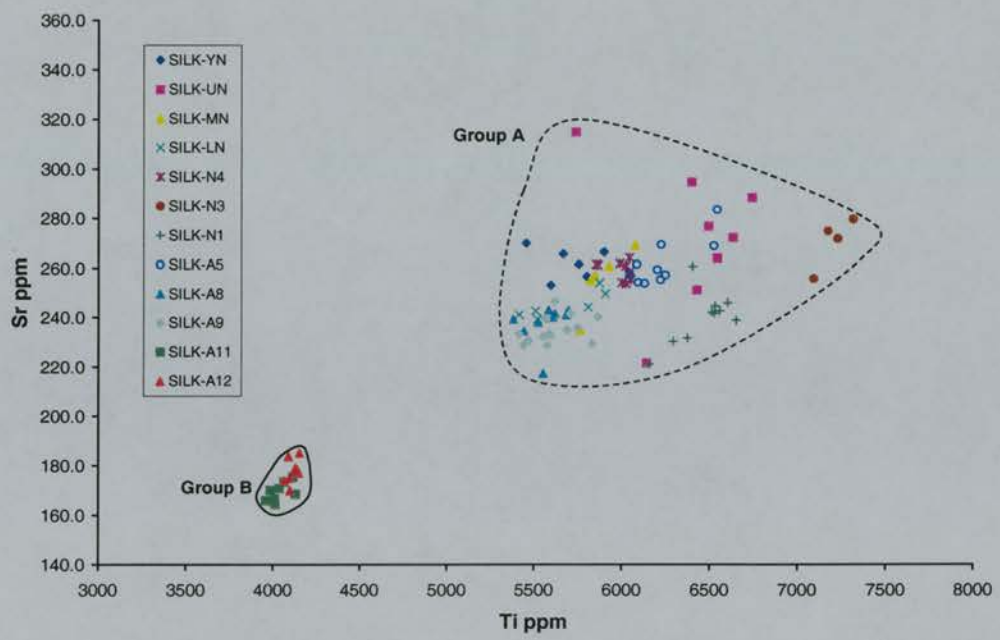

Figure 5.26: Graph (Ti/Sr) to show the variations in the trace element composition of the analysed SILK layers.

SILK-A11 and A12 show a similar variation in their trace and rare earth composition to the major element geochemistry discussed earlier, with A-12 having slightly higher Sr and Zr as well as Ti compared to A-11 (Figure 5.26 and Figure 5.27). Two sample T-Tests showed that the difference in the means of the Ti ($P = 0.0026$) and Sr ($P = 0.0002$) abundances is significant. This confirms the results of the significant difference identified by the T-Test of

CaO. It should be emphasised that the difference between these two tephra layers is small and it is possible that pumice produced could have overlapping geochemical characteristics. There is, however a major difference between the Group B tephras and those from Group A, the post-Hólmsá Fires SILK layers. Despite the differences, there are several consistencies with the Y, La and Ba abundances showing little significant variation between all of the analysed SILK layers.

The Group A, post-Hólmsá Fires tephra layers, show several distinct differences, which were not identified by the EPMA. For example, SILK-N1 forms a distinct group in Figure 5.26 and Figure 5.27a, whilst SILK-YN forms a distinct group in Figure 5.26. SILK-A9 overlaps with SILK-A8 and SILK-LN in Figure 5.26, but SILK-A8 does not overlap with SILK-A9 in Figure 5.27b. SILK-N4 forms a relatively tight cluster in Figure 5.26 and Figure 5.27a, although a couple of analyses are outside the main group.

Three of the Group A2 tephras were analysed by SIMS. SILK-UN can be easily separated from the other two A2 tephras by Ti (Figure 5.26) and SILK-N3 and SILK-A5 can be separated into two groups in Figure 5.27.

Both Figure 5.26 and Figure 5.27 show that several of the SILK layers analyses lie outside of the main groups, for example SILK-A8, N1 and UN in Figure 5.26. These outliers are probably the result of the inadvertent analysis of small unidentified inclusions within the glass. Although every care was taken to analyse clear, microlite free glass, small inclusions were probably sometimes analysed. Despite this, it appears that the SIMS analyses of the glass shards show greater differentiation between the SILK layers than can be seen in the major element EPMA. These small but significant differences help identify likely source eruptions for the ocean-transported pumice later in this chapter.

Tephra	Ti	1σ	Rb	1σ	Sr	1σ	Y	1σ	Zr	1σ	Nb	1σ	Ba	1σ	La	1σ	Ce	1σ	n
SILK-YN (N8)	5697	159	44	1.4	262	6.4	55	1.8	775	17.3	92	2.3	524	11.4	66	2.3	140	5.2	6
SILK-UN (N7)	6393	317	46	4.1	273	28.4	55	2.6	752	19.6	93	2.0	517	19.4	65	6.8	140	14.7	8
SILK-MN (N6)	5889	122	44	4.6	255	12.6	59	7.8	765	33.0	95	5.5	506	54.2	65	5.2	141	9.6	5
SILK-LN (N5)	5674	215	48	2.1	245	5.6	55	1.0	780	18.9	98	2.8	538	15.8	68	1.6	144	4.1	6
SILK-N4	5995	74	45	1.4	259	3.6	56	0.6	764	14.0	101	3.6	515	21.6	68	1.2	145	2.2	10
SILK-N3	7205	95	44	1.2	270	10.3	56	2.0	745	19.0	95	2.7	508	17.8	67	2.8	144	5.9	4
SILK-N1	6463	153	47	1.8	240	10.6	58	1.9	795	21.4	101	2.8	544	16.9	70	2.5	148	5.8	10
SILK-A5 (MBH3)	6235	173	45	1.8	262	9.3	55	1.2	735	25.4	94	4.6	515	19.0	65	2.7	140	5.0	10
SILK-A8 (MBH1)	5566	104	47	1.1	237	8.0	56	1.0	757	13.4	98	1.7	530	8.1	67	1.1	144	3.2	9
SILK-A9 (TYN2)	5619	136	44	1.4	235	5.3	56	1.2	743	19.7	98	4.3	498	14.5	67	1.8	144	4.6	14
SILK-A11	4037	57	50	1.4	169	3.8	55	1.2	811	18.8	106	2.6	539	15.4	68	2.5	144	6.2	9
SILK-A12	4119	29	48	2.4	178	4.5	57	0.6	822	6.2	105	2.5	542	8.9	70	1.5	145	3.6	10

Table 5.8: SIMS analyses of the SILK tephra layers, showing the means, the standard deviations (1σ) and number of analyses (n). Full details of these analyses are available in Appendix 4.

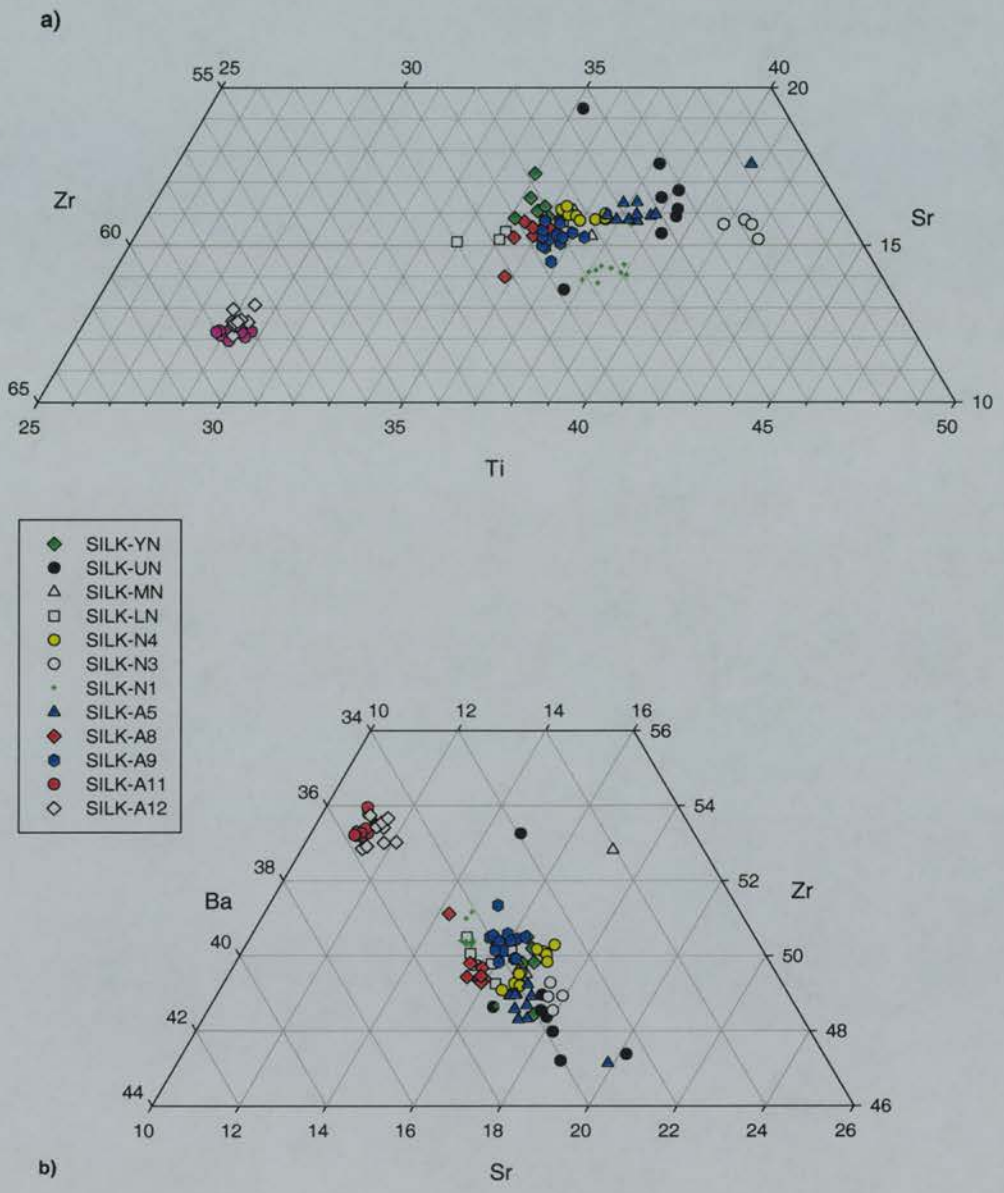

Figure 5.27: Two ternary graphs (Ti/Sr/Zr and Sr/Zr/Ba) which further illustrate the trace element variation in the SILK layers.

Katla pumice geochemistry

64 EPMA analyses were also undertaken on the pumice deposits from the Sólheimar Ignimbrite and Vikurhóll. These are the only silicic pumice deposits which occur close to Katla. The pumice from both sites is silicic and calc-alkaline in composition (Figure 5.29). The pumice from Vikurhóll, although very similar in appearance and composition to the Sólheimar Ignimbrite pumice, has slightly higher abundances of SiO_2, although there is a range between 68 and 70 or 71 wt % in all three pieces . These slight differences are shown in Figure 5.28, where the slightly lower concentrations of CaO and higher MgO in the Vikurhóll pumice are illustrated. Two sample T-Test of the CaO and MgO abundances showed that the means of the Vikurhóll and Sólheimar Ignimbrite pumice pieces are significantly different (CaO P=0.0000 and MgO P = 0.0007) at 2σ and could not have been drawn from the same populations.

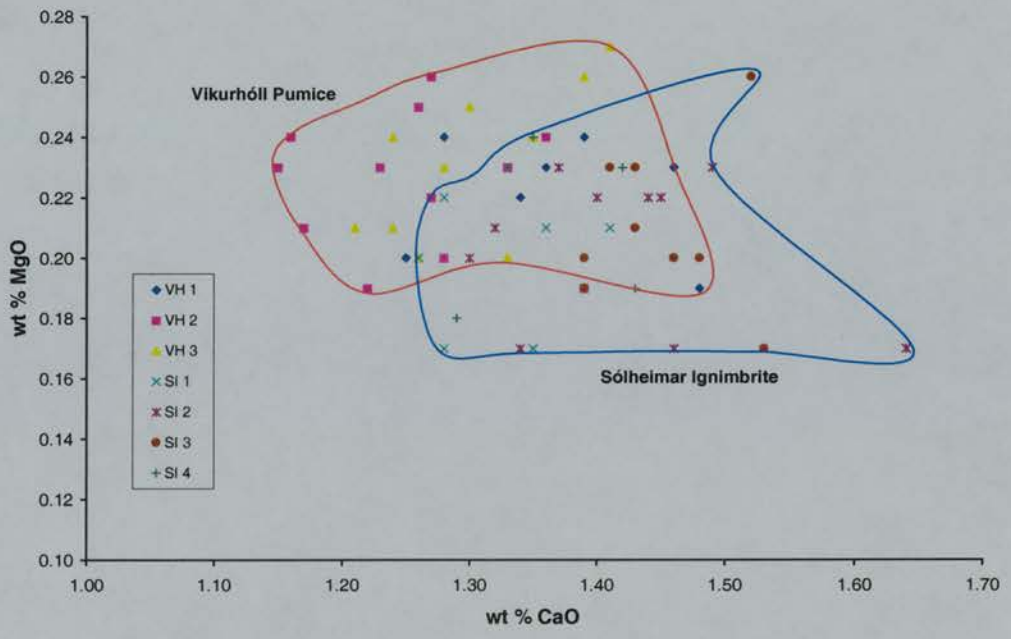

Figure 5.28: Graph (CaO/MgO) to show the slight variation between the Vikurhóll and Sólheimar Pumice.

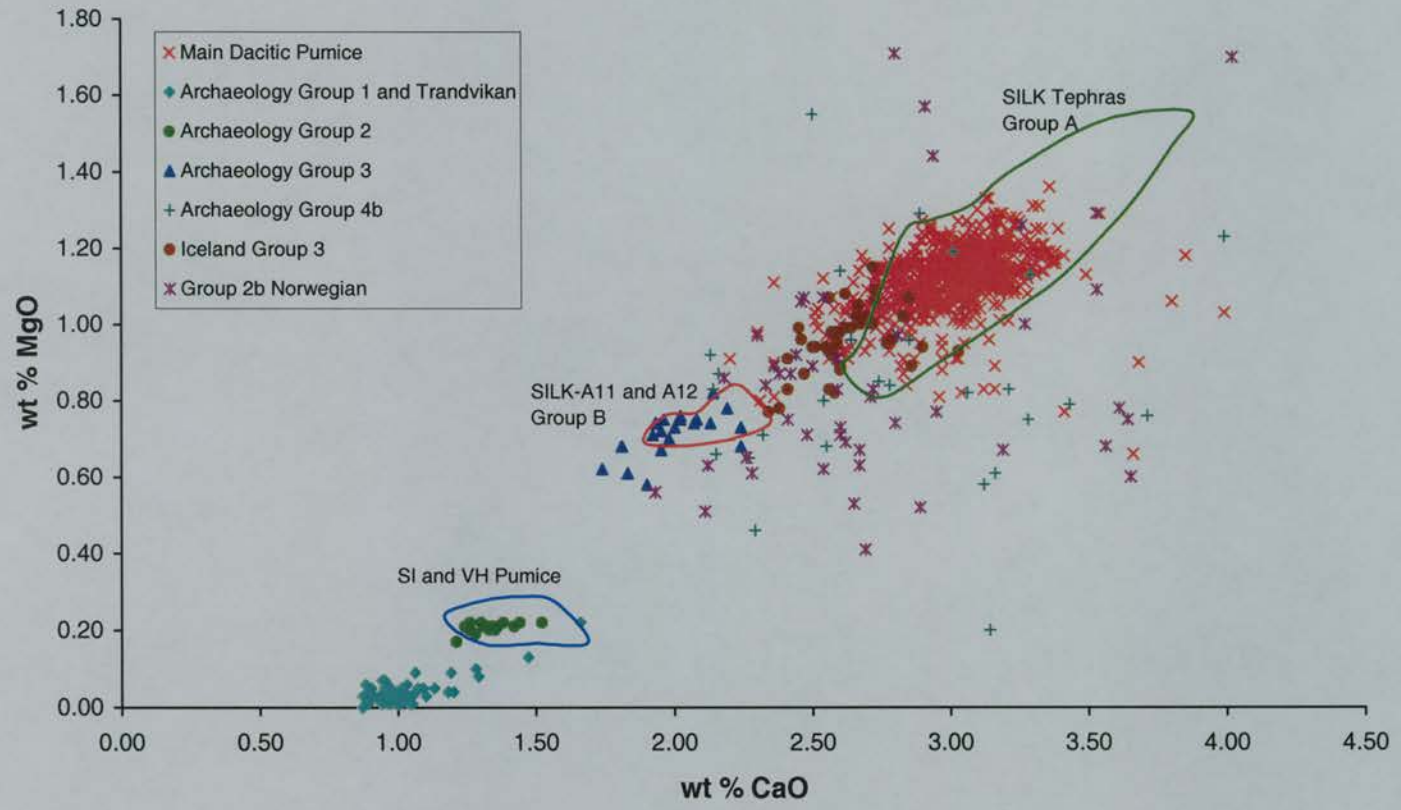

Figure 5.30: Graph to compare the ocean-rafted pumice with the SILK layers and silicic Katla Pumice.

a)

Site	Pumice	SiO_2	1σ	TiO_2	1σ	Al_2O_3	1σ	FeO	1σ	MnO	1σ	MgO	1σ	CaO	1σ	Na_2O	1σ	K_2O	1σ	Total	1σ	n
Vikurhóll	VH 1	69.82	0.65	0.32	0.03	13.37	0.24	3.77	0.09	0.14	0.03	0.22	0.02	1.36	0.08	5.24	0.21	3.49	0.12	97.72	0.69	**10**
	VH 2	70.26	1.23	0.29	0.02	13.11	0.14	3.74	0.15	0.16	0.04	0.23	0.02	1.25	0.07	5.18	0.11	3.43	0.14	97.65	1.27	**11**
	VH 3	69.21	0.71	0.31	0.02	13.33	0.17	3.71	0.14	0.15	0.04	0.23	0.03	1.30	0.07	5.22	0.14	3.49	0.12	96.94	0.70	**10**
Sólheimar	SI 1	68.72	0.71	0.31	0.04	13.15	0.26	3.74	0.16	0.14	0.03	0.20	0.02	1.34	0.06	4.83	0.15	3.48	0.08	95.90	0.78	**8**
	SI 2	69.02	0.78	0.31	0.04	13.20	0.16	3.67	0.13	0.14	0.03	0.20	0.03	1.42	0.10	4.74	0.12	3.47	0.11	96.18	0.81	**10**
	SI 3	68.97	0.33	0.27	0.04	13.28	0.18	3.76	0.11	0.12	0.02	0.21	0.03	1.44	0.05	4.98	0.11	3.53	0.09	96.56	0.59	**10**
	SI 4	68.95	0.51	0.28	0.01	13.35	0.10	3.78	0.15	0.14	0.04	0.21	0.03	1.36	0.06	5.00	0.10	3.41	0.09	96.48	0.67	**5**

b)

		SiO_2	TiO_2	Al_2O_3	FeO	MnO	MgO	CaO	Na_2O	K_2O	Total	n
Vikurhóll	Mean	69.78	0.31	13.26	3.74	0.15	0.23	1.30	5.21	3.47	97.45	31
	1σ	0.99	0.02	0.21	0.13	0.04	0.02	0.08	0.16	0.12	0.98	
Sólheimar	Mean	68.92	0.29	13.23	3.73	0.13	0.21	1.40	4.87	3.48	96.27	33
	1σ	0.60	0.04	0.19	0.13	0.03	0.02	0.08	0.16	0.10	0.74	

c)

Site	Anal.	SiO_2	1σ	TiO_2	1σ	Al_2O_3	1σ	FeO	1σ	MnO	1σ	MgO	1σ	CaO	1σ	Na_2O	1σ	K_2O	1σ	Total	n
Vikurhóll	8	70.76	0.36	0.30	0.04	13.19	0.11	3.94	0.19	0.15	0.09	0.21	0.03	1.30	0.05	5.36	0.23	3.61	0.04	98.82	**10**
Sólheimar	10	70.21	0.49	0.27	0.04	13.17	0.12	3.68	0.16	0.13	0.05	0.20	0.02	1.36	0.04	5.67	0.27	3.43	0.07	98.11	**11**
	11	70.34	0.30	0.28	0.04	13.35	0.12	3.67	0.21	0.10	0.06	0.20	0.02	1.26	0.15	5.58	0.29	3.47	0.07	98.24	**10**

Table 5.9: Tables to show the major element geochemistry of the silicic Katla pumice a) shows the means and standard deviations (1σ) of the Katla silicic pumice. b) shows the means and standard deviations (1σ) of all 64 analyses. The number of analyses are also shown (n) and full details about these analyses are available in Appendix 3. c) shows three EPMA analyses from Lacasse *et al.* (1995): 8 is a piece of obsidian from Vikurhóll and 10 and 11 are from the Sólheimar Ignimbrite.

Although the EPMA of the pumice pieces from Vikurhóll and Sólheimar has illustrated some small scale differences between them, the relatively small number of analyses of pumice pieces means that it is not possible to conclude how important these are. The T-Tests suggest that there are significant geochemical differences between the two deposits. If these two deposits were produced at different times, then Katla erupted geochemically similar deposits at various times during the late Pleistocene, as it has continued to do during the Holocene.

Table 5.9c shows three EPMA analyses of silicic Katla pumice published by Lacasse *et al.* (1995). These results are very similar to the analyses produced for this thesis. Lacasse *et al.* (1995) also published analyses from other rhyolitic deposits, such as nunataks rising above Mýrdalsjökull. Although Lacasse *et al.* (1995) believe that these represent the products of a single event, it is also seems possible that Katla is capable of producing products with similar geochemical products over long periods of time (Dugmore, Newton and Norðdahl, in prep).

The silicic pumice cannot be correlated to the proximal SILK tephras. The most silicic and oldest of the SILK layers have higher concentrations of CaO and MgO, for example (Table 5.5), which appears to reinforce the view that Katla's silicic activity has become less silicic with time. The post-glacial activity that produced the Vikurhóll pumice was more silicic (the magma was more evolved) than that which produced SILK-A11 and SILK-A12 and the post-Hólmsá Fires SILK layer were produced by less evolved magma than SILK-A11 and SILK-A12.

13 SIMS analyses were also undertaken on the VH 2 pumice and the results are presented in Table 5.10. As confirmed by the SIMS analyses these analyses are different from all of the other SIMS analyses of the SILK layers (Table 5.10 and Table 5.8).

		Ti	Rb	Sr	Y	Zr	Nb	Ba	La	Ce	n
VH 2	Mean	1421	58	103	66	913	120	608	79	164	13
	1σ	17	2.6	2.6	1.8	27.7	5.4	18.8	2.7	6.8	

Table 5.10: Means and standard deviations (1σ) of the SIMS analyses of the SI 2 pumice from Vikurhóll. The full analyses can be found in Appendix 3.

Lacasse *et al.* (1995) also published XRF trace element data from a piece of obsidian and pumice from Vikurhóll and Sólheimar. Although similar, this data does not appear to be directly comparable to the SIMS analyses, with for example, Sr values of around 140 ppm,

Rb of 72-77 ppm and Ba of 652-688 ppm. This may reflect the use of different analytical techniques and the small sample numbers.

Summary of the SILK and Katla pumice geochemistry

The geochemical analyses of the SILK layers has shown that Katla's silicic activity has become less silicic during the late Quaternary. The large fissure eruptions of the Hólmsá Fires and Eldgjá Fires lead to major changes in Katla's plumbing which resulted in significant changes in the geochemistry of the erupted silicic products. Before the Hólmsá Fires the tephrochronological record is incomplete, but the activity which produced SILK-A11 and A12 was more silicic than later activity. The Hólmsá Fires coincided with the beginning of several thousand years of activity which produced geochemically similar tephra layers (SILK-A9 to SILK-YN). During this period there appears to have been little or no evolution in the magma erupted. The Eldgjá Fires eruptions appears to have coincided with a halt in this type of activity. The analyses of the silicic pumice deposits allow investigation of Katla's silicic activity before soil formation preserved tephra layers. There appear to be small geochemical differences between the Sólheimar Ignimbrite and Vikurhóll pumice deposit. This and the identification of other silicic rocks with similar geochemical characteristics by Lacasse *et al.* (1995), suggest that Katla's silicic activity extends back into the Late Pleistocene. The geomorphology and geochemical data produced for this thesis points towards multiple late-glacial and earlier silicic eruptions. This is the subject of continuing research (Dugmore, Newton and Nordðahl, in prep).

Having geochemically characterised the SILK layers and the proximal pumice deposits, the next section establishes the extent to which Katla's silicic tephra and the ocean-transported pumice deposits are similar.

Correlation of distal pumice to Katla

This study has resulted in a transformation of our knowledge of the Holocene activity of the Katla Volcanic System. This activity is now known to include a large number of silicic eruptions which have produced small scale tephra layers close to the volcano and pumice deposits on the southern flanks of the volcano. All of the ocean-rafted pumice analyses, except for the basaltic pumice, are compared to the SILK layers and silicic Katla pumice pieces in Figure 5.30. This shows that most of the ocean-rafted pumice can be correlated with the silicic Katla products.

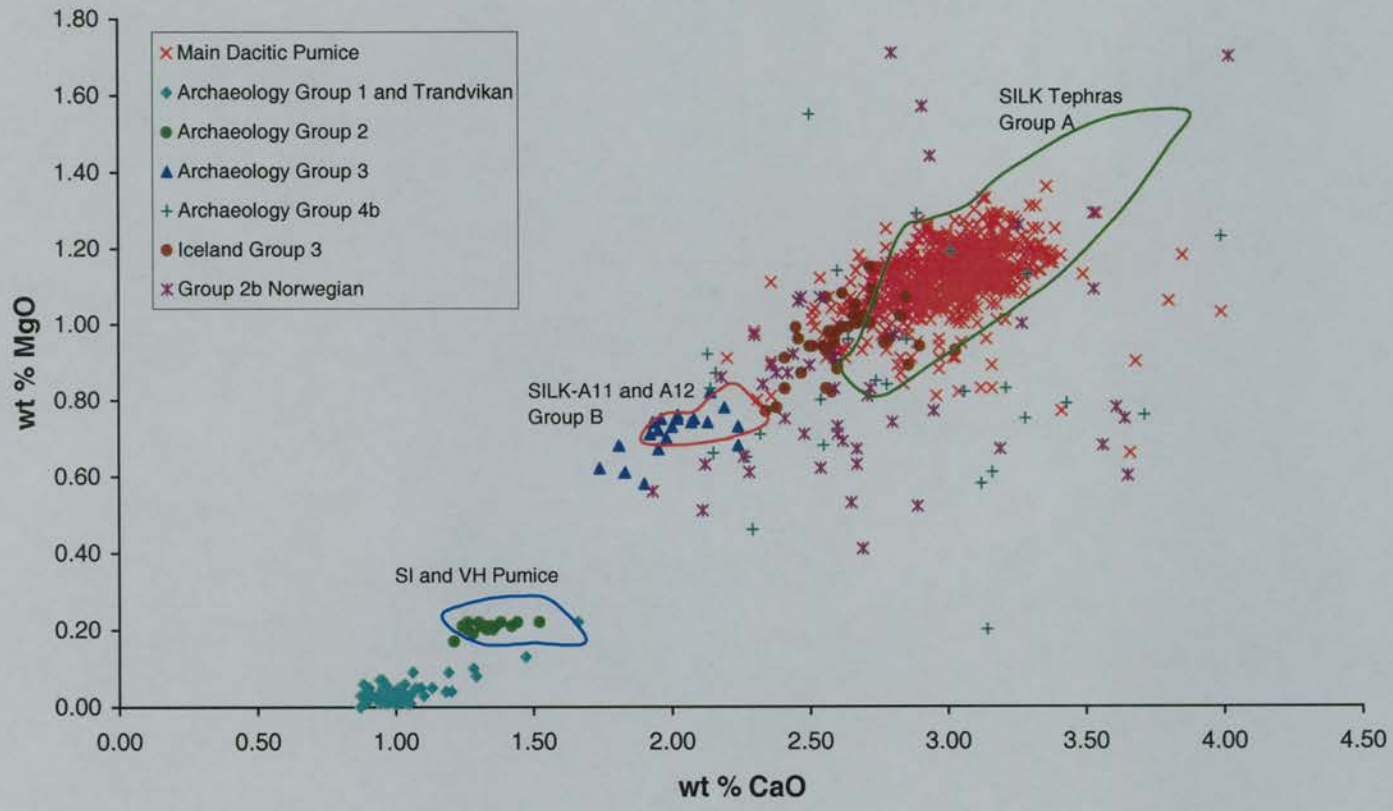

Figure 5.30: Graph to compare the ocean-rafted pumice with the SILK layers and silicic Katla Pumice.

The archaeology Group 1 from Shetland and the Norwegian Trandvikan pumice, however, cannot be correlated with any known Katla products and was, therefore, probably not erupted from this volcano. Section 5.2.3 compares these analyses with the tephra produced by Öræfajökull. The OF8L 1 pumice from Ófeigsfjörður forms a unique group (Chapter 3). It has Al_2O_3 abundances of over 15%, CaO of less than 0.37% and MgO of more than 1.58%. These values are unlike anything produced by the Katla Volcanic system and this pumice piece cannot be geochemically correlated to the silicic Katla pumice or tephras. The archaeology Group 2 pumice from Staosnaig can be correlated with the Sólheimar Ignimbrite and Vikurhóll pumice deposits. The archaeology Group 3 pumice from Staosnaig can be correlated with the Group B SILK tephras, A11 and A12. Finally, the main dacitic pumice can be correlated with the Group A SILK tephras. These correlations will now be discussed in more detail.

Group 2 archaeological pumice and the Sólheimar and Vikurhóll deposits

Figure 5.30 shows that the light brown Group 2 archaeological pumice can be correlated with the Sólheimar and Vikurhóll pumice. Section 5.2.2 concluded that although the Sólheimar and Vikurhóll pumice have very similar geochemical properties, it is unlikely that both deposits were erupted at the same time. It is suggested that the whilst the Vikurhóll pumice is an early Holocene deposit, the Sólheimar Ignimbrite was probably erupted before the Last Glacial Maximum. Figure 5.31 shows that there is considerable overlap between the two Katla pumice deposits and the Group 2 pumice overlaps with both of these. Table 5.11 shows that both the Sólheimar Ignimbrite and the Vikurhóll pumice also share similar geochemical properties with the Group 2 pumice when all the other oxides are examined. The two sample T-Tests undertaken only illustrate the similarities between the Group 2 pumice and both the Sólheimar Ignimbrite and the Vikurhóll pumice. The CaO test (P=0.0059) suggested that mean of the Group 2 pumice could not be derived from same population as the Sólheimar Ignimbrite. The MgO test, however, suggested that the Group 2 pumice could not be drawn from the same population as the Vikurhóll pumice (P=0.0003) at 2σ, whilst there was no significant difference between the MgO means of the Sólheimar Ignimbrite and Group 2 pumice (P=0.78). These conflicting results mean that it is not possible to identify whether the Sólheimar Ignimbrite or the Vikurhóll pumice can be correlated to the Group 2 pumice on major element geochemistry alone.

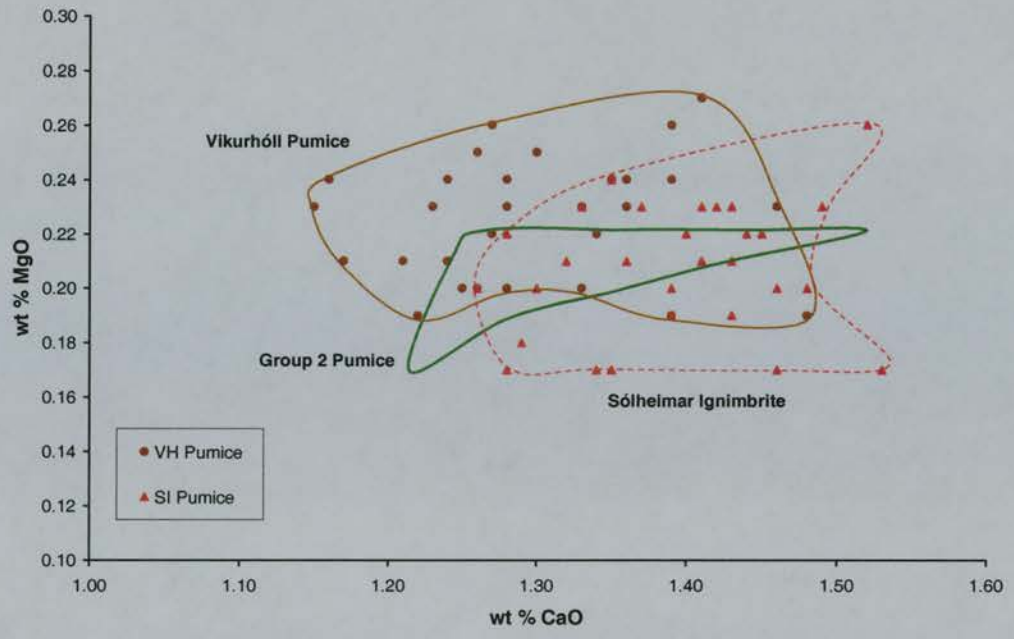

Figure 5.31: Graph (CaO/MgO) to compare the Group 2 archaeological pumice with the Vikurhóll and Sólheimar Ignimbrite pumice.

		SiO_2	TiO_2	Al_2O_3	FeO	MnO	MgO	CaO	Na_2O	K_2O	Total	n
Archaeological	**mean**	69.74	0.27	13.02	3.78	0.13	0.21	1.34	5.33	3.50	97.31	19
Group 2	**1σ**	0.60	0.05	0.23	0.15	0.03	0.01	0.07	0.13	0.11	0.53	
Vikurhóll	**Mean**	69.78	0.31	13.26	3.74	0.15	0.23	1.30	5.21	3.47	97.45	31
	1σ	0.99	0.02	0.21	0.13	0.04	0.02	0.08	0.16	0.12	0.98	
Sólheimar	**Mean**	68.92	0.29	13.23	3.73	0.13	0.21	1.40	4.87	3.48	96.27	33
	1σ	0.60	0.04	0.19	0.13	0.03	0.02	0.08	0.16	0.10	0.74	

Table 5.11: Table to compare the EPMA of the Group 2 pumice with the Vikurhóll and Sólheimar Ignimbrite pumice.

SIMS analyses were undertaken on a piece of Group 2 pumice from Staosnaig and a pumice piece from Vikurhóll. These results are summarised in Table 5.12. Unfortunately, there are no SIMS analyses of any pumice from the Sólheimar Ignimbrite and only five analyses from the SG 1 pumice. Despite this, it can be seen that even the trace and rare earth element geochemistry of the two pumice pieces is similar.

		Ti	Rb	Sr	Y	Zr	Nb	Ba	La	Ce	n
VH 2	**Mean**	1421	58	103	66	913	120	608	79	164	13
	1σ	17	2.6	2.6	1.8	27.7	5.4	18.8	2.7	6.8	
SG 1	**Mean**	1415	56	100	64	902	115	593	75	154	5
	1σ	54	2.4	3.3	2.3	46.2	6.4	22.5	2.0	6.6	

Table 5.12: Table to compare the SIMS analyses of the Vikurhóll and Staosnaig pumice.

The Group 2 pumice from Staosnaig can be geochemically correlated to the Sólheimar Ignimbrite and Vikurhóll pumice deposits on the southern flanks of Katla. If these two deposits are not contemporaneous and the Vikurhóll deposit is post-glacial, then this is the most likely correlation. These results emphasise the fact that Katla is capable of producing geochemically identical tephra and pumice over considerable time periods. To summarise, the Group 2 pumice was most likely erupted by the same or related eruption early Holocene, which produced the Vikurhóll pumice deposit. This eruption did not leave any record in the soil profiles as it predates soil formation. The age of the archaeological contexts that the Group 2 pumice was found in is between about 7900 and 7000 ^{14}C years BP. This suggests that the eruption which produced the Vikurhóll and Staosnaig pumice occurred more than about 8000 ^{14}C years ago.

Group 3 archaeological pumice and the Group B SILK Tephras

From Figure 5.30 a strong correlation can be seen between the SILK-A11 and A12 tephras and the black Group 3 archaeological pumice from Staosnaig. Table 5.13 showed that there are no large major element differences between the two Group 2 pumice pieces and SILK-A11 and A12, although the T-Tests suggested that the two layers could be discriminated on their CaO abundances. Both the pumice pieces have higher mean Na_2O abundances compared to the SILK layers, but Na_2O is not a reliable oxide to use for correlative purposes, due to its potential mobility under analysis (Chapter 3). The SG 2 pumice has slightly lower SiO_2, but this oxide again is not usually used as a correlative tool (Chapter 3). Other oxides are similar except for FeO and CaO, which are slightly lower in SG 3 compared to A11 and A12. These differences are, however, small and FeO consistently has a relatively large standard deviation throughout all the analyses undertaken during this study, making it an unsuitable oxide to use for correlation, where only small geochemical differences between different deposits and events are found. Figure 5.32 shows that the mean CaO abundances of SG 2 are slightly higher, there is really no significant difference between the two pumice pieces and that it is not possible to correlate either piece to a particular tephra. Two sample T-Tests comparing SG 2 and SG 3 to SILK-A11 and A-12, however, suggest that the SILK-A11 is the most likely correlation. As discussed in Chapter 4 it is not clear how much variation there would have been between the pumice pieces produced by the eruptions which produced SILK-A11 and A12. So it is not clear whether the differences identified by the T-Tests of major element geochemistry reflect real differences and similarities within or between eruptions.

		SiO_2	TiO_2	Al_2O_3	FeO	MnO	MgO	CaO	Na_2O	K_2O	Total	n
SG 2 Group 3	**mean**	67.43	0.83	13.62	4.13	0.12	0.73	2.06	5.20	3.14	97.27	10
	1σ	*0.52*	*0.06*	*0.19*	*0.20*	*0.02*	*0.06*	*0.11*	*0.11*	*0.08*	*0.76*	
SG 3 Group 3	**mean**	68.06	0.83	13.59	3.93	0.14	0.70	1.95	5.01	3.15	97.37	10
	1σ	*0.78*	*0.06*	*0.18*	*0.24*	*0.04*	*0.05*	*0.14*	*0.21*	*0.10*	*0.76*	
SILK-A11	**Mean**	68.37	0.90	13.74	4.14	0.15	0.73	2.02	4.35	3.17	97.56	10
	1σ	0.81	0.05	0.12	0.17	0.03	0.04	0.10	0.21	0.07	1.10	
SILK-A12	**Mean**	68.00	0.87	13.75	4.21	0.15	0.74	2.15	4.53	3.12	97.51	10
	1σ	0.60	0.05	0.18	0.16	0.02	0.04	0.11	0.14	0.11	0.52	

Table 5.13: Table to compare the EPMA of the two Group 3 pumice pieces with SILK-A11 and A12.

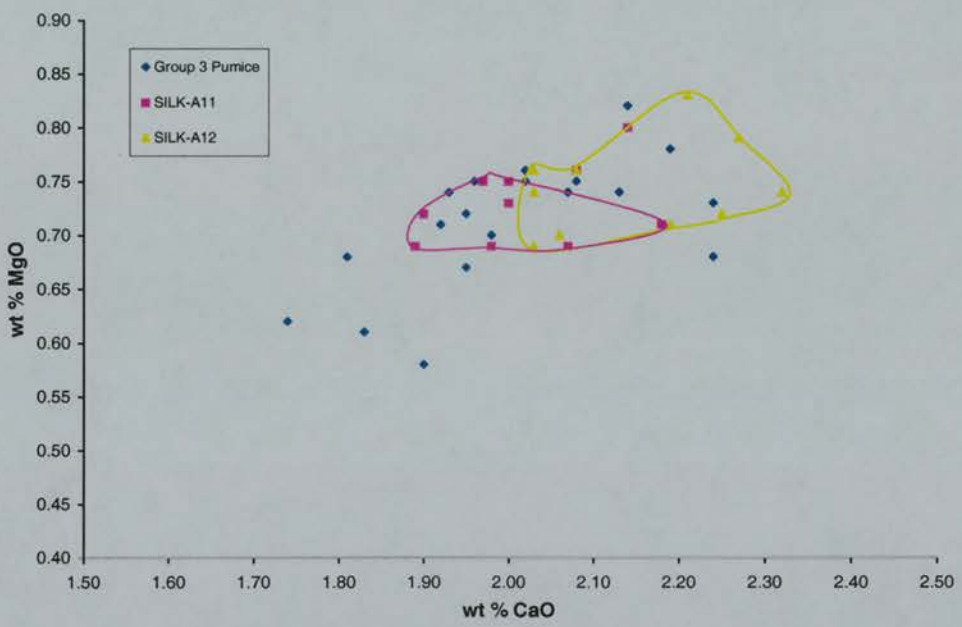

Figure 5.32: Graph (CaO/MgO) to compare the Group 3 archaeological pumice with SILK-A11 and A12 using EPMA analyses.

SIMS analyses were also undertaken on SILK-A11 and A12 and on SG 3 pumice piece from Staosnaig. The results of these analyses can be compared in Table 5.14 and Figure 5.33. The SIMS analyses suggest that the SG 3 pumice has most in common with the SILK-A11 tephra, the youngest of the two. For example, in Figure 5.33 only one analyses overlaps with the field defined by the SILK-A12 tephra. A two sample T-Test suggests that these differences are significant. There is no significant difference between SG 3 and the SILK-A11, but significant differences can be found between the Ti ($P = 0.0001$) and Sr ($P = 0.0043$) means of SG 3 and SILK A-12. This suggests that the SIMS analyses are capable of improved discrimination between tephra and pumice deposits than EPMA.

		Ti	Rb	Sr	Y	Zr	Nb	Ba	La	Ce	n
SG 3	**Mean**	4023	48	170	56	825	105	531	68	143	10
	1σ	48	2.1	6.1	1.7	10.5	3.2	13.8	2.7	5.6	
SILK-A11	**Mean**	4037	50	169	55	811	106	539	68	144	9
	1σ	57	1.4	3.8	1.2	18.8	2.6	15.4	2.5	6.2	
SILK-A12	**Mean**	4119	48	178	57	822	105	542	70	145	10
	1σ	29	2.4	4.5	0.6	6.2	2.5	8.9	1.5	3.6	

Table 5.14: Table to compare the SIMS analyses of SG 3 and SILK-A11 and A12.

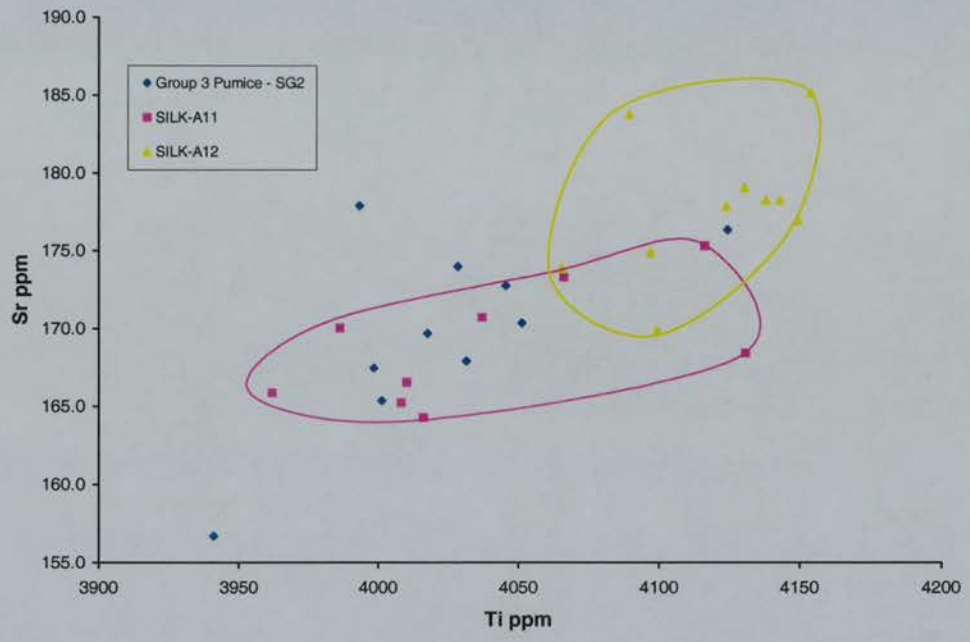

Figure 5.33: Graph (Ti/Sr) to compare the SG 3 pumice with SILK-A11 and A12 using SIMS analyses.

These results show that the Group 3 archaeological pumice from Staosnaig was produced by one or more eruptions from the Katla Volcanic System between about 7000 and 7500 ^{14}C years BP. These eruptions also produced the SILK-A11 and A12 tephra layers. The SIMS analyses of SG 3 and the T-Tests on SG 2 and SG 3 pumice suggest that they were erupted by the same eruption which produced the SILK-A11 layer about 7000 ^{14}C years BP. The SIMS analyses on SG 3 produced a more confident correlation than the EPMA. Unfortunately, it is not possible to have the same confidence about the remainder of the Group 3 pumice without further SIMS analyses. This conclusion is compatible with the age of the context the pumice was found in, which is between 7900 and 7000 ^{14}C years BP.

The pumice deposits at Staosnaig, therefore, consist of two types. The first was erupted by Katla sometime before 8000 ^{14}C years BP and consists of brown highly vesicular pumice. A second series of eruptions associated with the SILK-A11 and A12 layers, between about 7500 and 7000 ^{14}C years BP, but most probably about 7000 ^{14}C years BP (SILK-A11), produced the black pumice.

Main dacitic ocean-rafted pumice and the Group A SILK tephras

Figure 5.30 shows that the main dacitic ocean-rafted pumice can be correlated with the Group A SILK tephra layers, i.e. those post-dating the Hólmsá Fires eruption. Interestingly, the analysed dacitic pumice is found on beaches younger than about 6000 ^{14}C years BP and older than 1700 ^{14}C years BP. This coincides with the post-Hólmsá Fires silicic activity. The eruptions which produced this pumice must have occurred at least 6000 ^{14}C years ago. The dates of the SILK layer have been established by both direct ^{14}C dating and estimates from soil accumulation rates. These give relatively precise dates. The dates of the raised shorelines and archaeological sites the pumice has been found on is less precise. The dating of raised shorelines is problematic and the ages presented in Chapters 2 and 3 are estimates from data that are constantly being reassessed. Despite this, the ages provide a minimum age for any pumice producing eruption and this will be used along with the geochemical data to identify possible correlations with SILK layers. Although some of the archaeological pumice is ^{14}C dated, many pieces just belong to archaeological ages (e.g. Iron Age) or have ^{14}C dates with large ranges. Where pumice is only dated to an archaeological age, the end of this age will be used as the minimum age for an eruption which could have produced any pumice found within that context. This cautious approach will inevitably result in more SILK layers being considered for a correlation, but the dating of pumice deposits does not allow a more precise method and to suggest so would be misleading. The combination of temporal and geochemical data, however provide powerful dating tools.

Although the correlation in Figure 5.30 is clear, it is also apparent that several of the Group A SILK tephra layers are not associated with the pumice producing eruptions. The EPMA analyses of the SILK tephra layers demonstrated two distinct groups (A1 and A2) and an overlapping group (A3). Figure 5.34 shows that the Group A2 SILK tephra layers are significantly different to the EPMA analyses of the main dacitic pumice group. This means that the ocean-rafted pumice was not erupted by the same eruptions which produced the SILK-UN (the largest SILK layer), SILK-N3, SILK-N2 and SILK-A5 tephra layers. The Group A3 tephra, SILK-A7 is also unlikely to be associated with an ocean-rafted pumice

eruption as this is most similar to the Group A2 tephra layers. The most likely tephra layers to be associated with the eruptions that produced the dacitic pumice are SILK-YN, SILK-MN, SILK-LN, SILK-N4, SILK-N1, SILK-A1, SILK-A8 and SILK-A9.

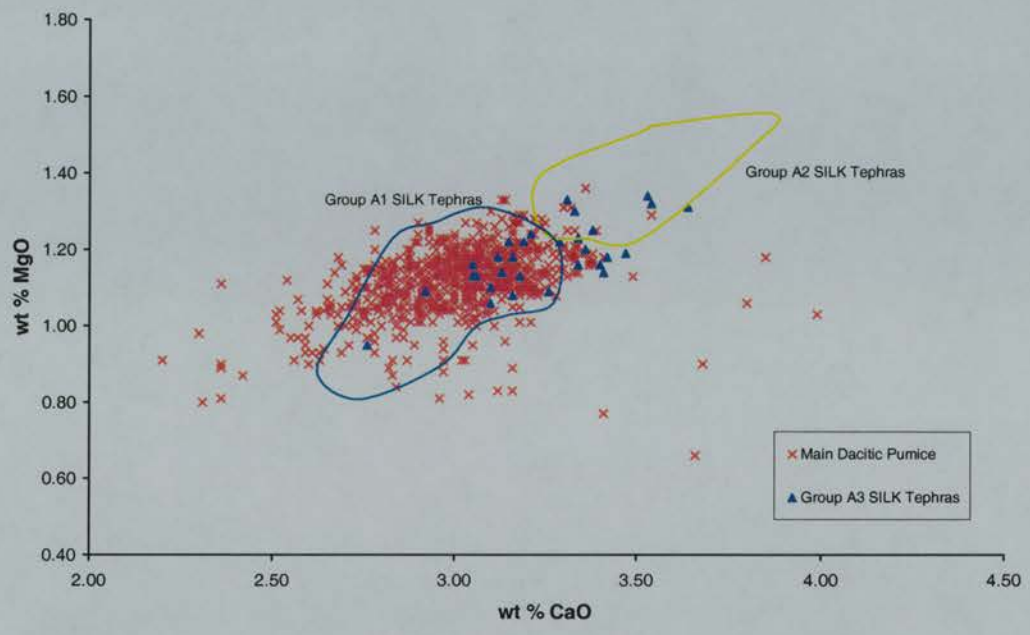

Figure 5.34: Graph to show the differences between the SILK Group A1, A2 and A3 tephra layers and the correlation of the A1 SILK layers with the main ocean-rafted pumice. The blue field is defined by 153 analyses of the Group A1 tephras (3 extreme analyses are excluded) and the yellow field is defined by 40 analyses of the Group A2 tephras.

It has already been demonstrated that there are no significant differences between the Group A1 SILK tephra layers. The only identifiable difference being the trend in the analyses of the youngest SILK tephra, SILK-YN. This means that it is not possible to identify the individual eruptions which were responsible for producing the main group of ocean-rafted dacitic pumice by EPMA alone. It is possible, however, to state that the earliest identified eruption which could have produced the oldest deposit of the main dacitic pumice occurred about 6600 ^{14}C years ago and the youngest is dated to 1676±12 ^{14}C years BP. This produces a possible age range of 5000 years for the eruptions or eruption responsible for the youngest pumice deposits. This suggests that the pumice pieces from the upper deposits at Kobbvika and Gjøsund and the pumice from Brandsvik can only have been produced by eruptions associated with SILK-A8 or SILK-A9. Table 5.15 shows all of the pumice deposits and their possible correlations with SILK layers. It is likely that much of the younger pumice was produced by younger SILK eruptions, but there is the possibility that some of this pumice could have been reworked from older deposits.

Pumice	Age (^{14}C years BP)	Possible SILK correlations
KVU	>6000	**A8, A9**
GJU	>6000	**A8, A9**
BV	>6000	**A8, A9**
BM	>5000	**A2, A3**, *A8, A9*
BR	>5000	**A2, A3**, *A8, A9*
KVM	>4000	**N1, A1**, *A2, A3, A8, A9*
AC 2-4	>4000	**N1, A1**, *A2, A3, A8, A9*
U 1-4	>4000	**N1, A1**, *A2, A3, A8, A9*
CR 5	>3360	**LN, N4**, *N1, A1, A2, A3, A8, A9*
KVL	>3000	**MN, LN**, *N4, N1, A1, A2, A3, A8, A9*
ST	>3000	**MN, LN**, *N4, N1, A1, A2, A3, A8, A9*
GJL	>3000	**MN, LN**, *N4, N1, A1, A2, A3, A8, A9*
CR 6	>3000	**MN, LN**, *N4, N1, A1, A2, A3, A8, A9*
CR 7	>2800	**MN, LN**, *N4, N1, A1, A2, A3, A8, A9*
CR 9	>2900	**MN, LN**, *N4, N1, A1, A2, A3, A8, A9*
D	>2600	**MN, LN**, *N4, N1, A1, A2, A3, A8, A9*
CR 2,3,4	>2375	**MN, LN**, *N4, N1, A1, A2, A3, A8, A9*
C	>2000	**MN, LN**, *N4, N1, A1, A2, A3, A8, A9*
CR 8	<2800	*YN*, **MN, LN**, *N4, N1, A1, A2, A3, A8, A9*
R	>1700	**YN**, *MN, LN, N4, N1, A1, A2, A3, A8, A9*
US	>1300	**YN**, *MN, LN, N4, N1, A1, A2, A3, A8, A9*
GC	>1200	**YN**, *MN, LN, N4, N1, A1, A2, A3, A8, A9*
SB 2	>1200	**YN**, *MN, LN, N4, N1, A1, A2, A3, A8, A9*
S 1	>500	**YN**, *MN, LN, N4, N1, A1, A2, A3, A8, A9*
OF6-8	?	YN, MN, LN, N4, N1, A1, A2, A3, A8, A9
E	?	YN, MN, LN, N4, N1, A1, A2, A3, A8, A9
HF	?	YN, MN, LN, N4, N1, A1, A2, A3, A8, A9
RJ	?	YN, MN, LN, N4, N1, A1, A2, A3, A8, A9
K	?	YN, MN, LN, N4, N1, A1, A2, A3, A8, A9
CD	?	YN, MN, LN, N4, N1, A1, A2, A3, A8, A9
CP	?	YN, MN, LN, N4, N1, A1, A2, A3, A8, A9
CR 1	?	YN, MN, LN, N4, N1, A1, A2, A3, A8, A9
AC 1	?	YN, MN, LN, N4, N1, A1, A2, A3, A8, A9
U 5	?	YN, MN, LN, N4, N1, A1, A2, A3, A8, A9

Table 5.15: Table to show the minimum ages of the dacitic pumice deposits and the possible correlations to the SILK tephras. Blue text indicates pumice found on raised shorelines. The possible correlations include all of the geochemically similar SILK layers which are older than the deposit where the pumice was found. Bold text, however, indicates the SILK layers nearest in age to the pumice deposits, whilst the italicised text indicates other SILK layers with which correlations are possible. ? = pumice deposits which are not dated.

Most of the SIMS tephra layers and some of the main dacitic pumice also had their trace and rare earth element compositions determined by SIMS and it is possible these will identify and date possible source eruptions. SIMS analyses were undertaken on SILK-UN, SILK-N3 and SILK-A5 and as these tephra layers have already been eliminated as being erupted by pumice producing eruptions, they will not be considered further.

Figure 5.35 shows that there is some considerable variation between the various pumice pieces, and KVM 1 cannot be correlated with any of the SILK layers on SIMS trace and rare earth geochemistry alone. The EPMAs, however, show that KVM 1 can be geochemically

correlated with the Group A SILK tephra layers on major element geochemistry. Interestingly, both the upper pumice deposits from Kobbvika (KVU 3) and Gjøsund (GJU 1) appear to be similar to the oldest Group A SILK layer SILK-A9.

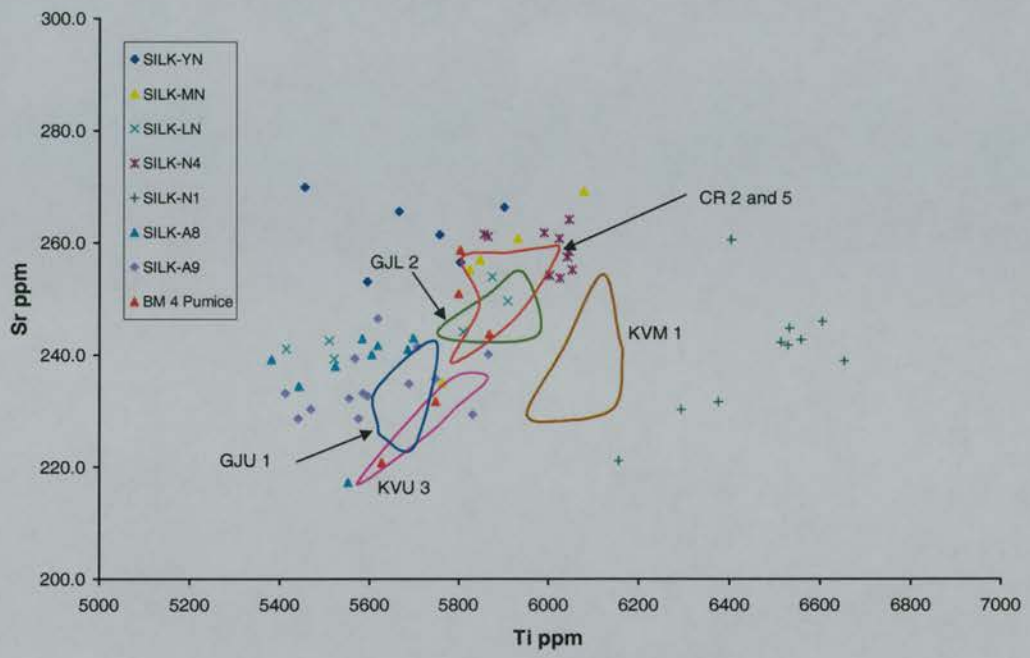

Figure 5.35: Graph (Ti/Sr) to compare the SIMS analyses of the SILK tephra layers with the main dacitic pumice group.

SILK-A8 also has similar geochemical properties to SILK-A9, although SILK-A8's mean Ba values are higher and cannot be correlated with the other pumice pieces. Chapter 4 showed that both the EPMA and SIMS analyses suggested that GJL2, CR 2 and CR 5 (Caerdach Rudh) pumice pieces have similar geochemical properties. Both of these pumice pieces also overlap with some of the SILK layers, such as SILK-N4, SILK-LN, and SILK-MN. These correlations, however, are weak and it is not possible to produce a confident correlation. The pumice from the Bay of Moaness has a fairly large geochemical range, especially in Ti, and overlaps with several of the SILK layers. The SILK-N1 tephra layer cannot be correlated with any of the analysed main dacitic group pumice.

To summarise, these results confirm that there is relatively little geochemical variation in the Group A1 SILK layers and the differences identified using the SIMS analyses are small. Similar small geochemical variations can be seen in the main dacitic pumice group, although the geochemistry of the pumice is more variable than the SILK layers. This greater geochemical variability means that it is difficult to geochemically correlate the pumice to

individual SILK layers. It is does appear, however, that two pumice pieces analysed by SIMS from the upper deposits at Kobbvika (KVU) and Gjøsund (GJU) appear to have similar geochemical properties to the c. 6600 ^{14}C years BP SILK-A9 layer. Table 5.15 shows that KVU and GJU could have been produced by the eruptions which produced either the SILK-A8 or SILK-A9 layers. The Caerdach Rudh and GJL 1 pumice also share similar geochemical properties and Table 5.15 shows that they could have been produced by the same SILK layers. The SIMS analyses suggest that SILK-MN, LN and N4 may be associated with these pumice deposits. If this is the case, the eruption that produced this pumice occurred sometime between about 3600 and 2975 ^{14}C years BP.

The KVM 1 pumice piece cannot be correlated with any of the SILK layers on the basis of the SIMS analyses. Whilst these correlations are only possible with the SIMS analyses, it must be pointed out that these are only based on the analysis of a single piece of pumice from each site, with the exception of the Caerdach Rudh pumice. It is possible that the geochemical variation within pumice pieces is always greater than that found within tephra layers produced from the same eruption. This would make the correlation of the pumice to particular tephra layer difficult. To test this, it would be necessary to find a SILK layer and its associated pumice deposit, which has yet to be found.

Other Pumice Groups

The above descriptions have accounted for all of the ocean-rafted pumice with the exception of the small number of pumice pieces which are either similar to the main dacitic group but show a much greater geochemical variation or have slightly different geochemical properties. These are the Norwegian Group 2b and the archaeological Group 4b, which show the former properties and the Icelandic Group 3 which demonstrates the latter.

The Norwegian Group 4 and archaeological Group 5 pumice pieces all have hetrogeneous major element geochemical compositions which although similar to the SILK layers have higher mean SiO_2 and lower CaO and MgO (Table 5.16 and Figure 5.36). The Iceland Group 3 pumice also has lower CaO and MgO but is far more geochemically homogeneous compared to the other two pumice groups. Unlike the Norwegian and archaeological pumice the Icelandic Group 3 pumice does not have large phenocrysts present in the glass. This accounts for their homogeneity. The major element geochemical differences between these pumice groups and the SILK layers and the main dacitic pumice appears to be real. What is not clear, however, is if this means that they were erupted by different eruptions.

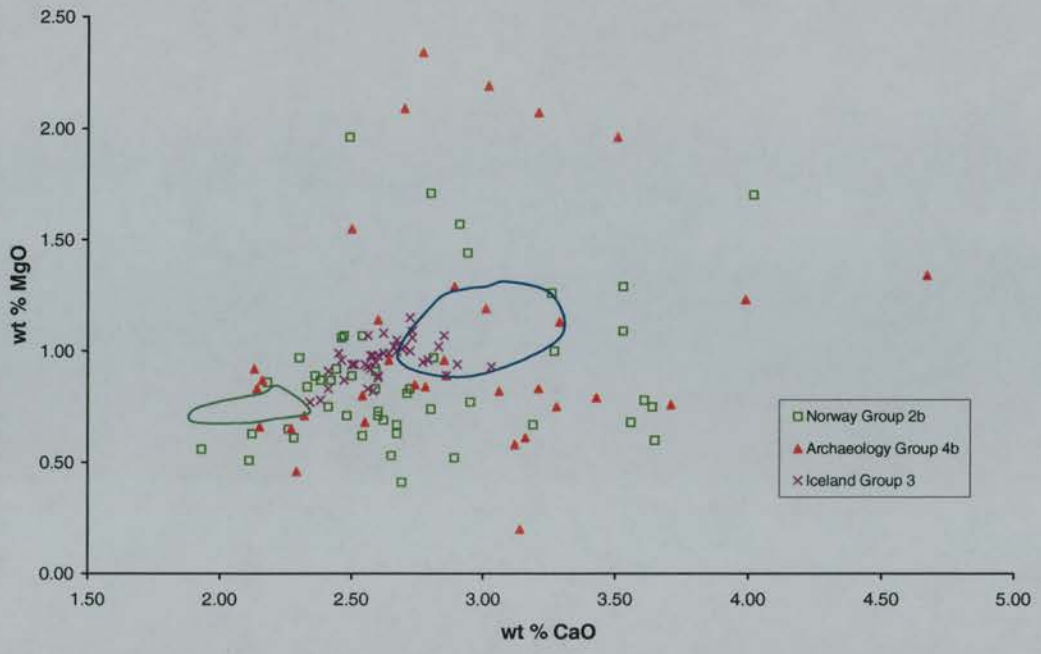

Figure 5.36: Graph (Ca/MgO) to compare the Norwegian Group 4, archaeology Group 5 and Iceland Group 3 pumice to the SILK tephra Group A1 (blue field) and Group B (green field).

		SiO_2	TiO_2	Al_2O_3	FeO	MnO	MgO	CaO	Na_2O	K_2O	Total	n
SILK Group A1	**mean**	65.69	1.23	13.99	5.72	0.18	1.12	3.00	4.38	2.74	98.05	153
	1σ	0.90	0.10	0.33	0.26	0.03	0.08	0.14	0.25	0.11	1.01	
Norway Grp. 4	**mean**	66.44	1.16	13.76	5.19	0.19	0.89	2.74	4.75	2.88	98.03	48
	1σ	1.09	0.15	1.06	0.69	0.05	0.33	0.47	0.45	0.33	0.83	
Arch. Grp. 5	**Mean**	66.35	1.20	13.65	5.31	0.19	1.06	2.90	4.96	2.86	98.44	34
	1σ	1.07	0.17	1.31	0.95	0.06	0.52	0.56	0.51	0.35	0.74	
Iceland Grp. 3	**Mean**	66.43	1.17	13.93	5.25	0.18	0.96	2.63	4.74	2.94	98.21	40
	1σ	0.75	0.07	0.21	0.29	0.04	0.09	0.15	0.22	0.14	0.82	

Table 5.16: Table to compare the EPMA of the Norwegian Group 4, archaeology Group 5 and Iceland Group 3 pumice to the SILK tephra Group A1.

SIMS analyses were undertaken on the KVL 1 (Kobbvika) and BR 1 (Bær) pumice pieces. Although these two analyses are not necessarily representative samples of these slightly different pumice deposits, they do corroborate the EPMA results. The KVL 1 pumice has a large geochemical spread, typical of the KVL pumice, which overlaps with several of the SILK layers, although there are more low Sr analyses. The BR 1 pumice does not overlap with any of the SILK layers, suggesting that it was not produced by any of the eruptions responsible for the analysed SILK layers.

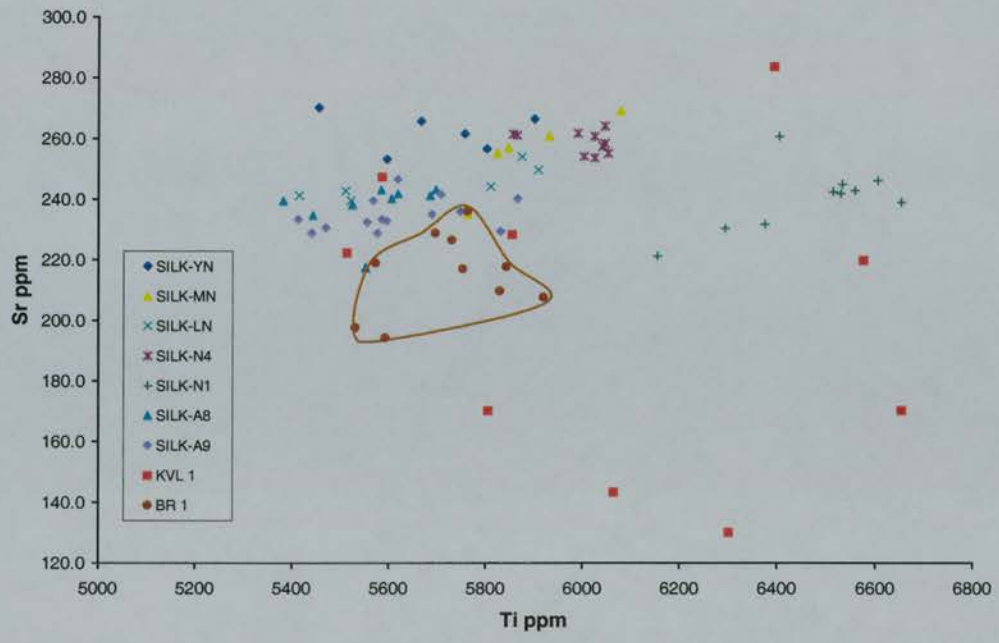

Figure 5.37: Graph (Ti/Sr) to compare the SIMS analyses of the KVL 1 and BR 1 with the SILK tephras.

These results may suggest that the Group 4 Norwegian and Group 5 archaeological pumice and the Group 3 Icelandic pumice may have been produced by an unidentified eruption of Katla. It is also possible that they were produced by a phase of an eruption of Katla which did not produce tephra. For example, if an eruption took some time to break through Mýrdalsjökull and subglacial pumice was produced, but no airfall tephra. There is also the possibility that the pumice was produced by a SILK eruption but that the subglacial pumice produced was geochemically slightly different to the tephra erupted later in the eruption when the column broke the glacial surface. As suggested in Chapter 4 the presence of phenocrysts in the Group 4 and Group 5 pumice may also represent a different cooling history to other pumice produced by the same eruption.

Summary

These results paint a slightly confusing picture because of the geochemical homogeneity of the SILK layers and the geochemical characteristics of the dacitic pumice pieces. Although Table 5.15 showed that most of the pumice can be correlated with the majority of the SILK layers, it is probable that the majority of the pumice deposits on raised shorelines were produced from contemporary eruptions (Chapter 2). The raised beach pumice deposits dated to around or older than 6000, 5000, 4000 and 3000 ^{14}C years BP (Table 5.15) were probably produced by contemporary eruptions. The geochemical evidence supports the fact

that the 6000 ^{14}C years BP pumice was produced by either SILK-A8 or SILK-A9 eruptions. The Bay of Moaness and Bær pumice are probably the same age (older than 5000 ^{14}C years BP) and the lower pumice horizons from Kobbvika and Gjøsund and the Storvik pumice also date from the same period (older than 3000 ^{14}C years BP). This correlation is also supported by the raised beaches at both Storvik and KVL having pumice with phenocrysts. Table 5.17 shows the possible correlations and dates of likely eruptions based on these conclusions.

Some of the archaeological pumice retrieved from contemporary beaches, will probably have included pumice from a recent eruption (Chapter 2). Although it is also possible that some pumice was found in older archaeological sites or had been eroded from older deposits on subsiding shorelines (Chapter 2). This and poor dating control is likely to result in more mixed pumice finds at archaeological sites than on natural raised shorelines, especially as often only one or two pieces of pumice are often found. All of the dated and analysed archaeological pumice is included in Table 5.17, although the caveats noted above should be considered. The mixed age of archaeological pumice is shown in Table 5.17 where pumice from Allt Chrisal (AC), The Udal and (Caerdach Rudh) CR have multiple dates and therefore possible source eruptions. A large number of pumice finds are too poorly dated to be correlated with any specific SILK layers (Table 5.15), although they have similar geochemical properties and must have been erupted sometime between 6600 and 1676 ^{14}C years BP.

^{14}C years BP	Pumice	SILK Layer	Pumice
6600	KVU, GJU, BV	**SILK-A9**	
6400		**SILK-A8**	
5500	BM, BR	**SILK-A3**	
5000		**SILK-A2**	
4600	KVM, AC 2-4, U1, 2	**SILK-A1**	
4400		**SILK-N1**	
3600	CR5	**SILK-N4**	
3139		**SILK-LN**	KVL, ST, GJL, CR 2,3,4,6,7,8,9
2975		**SILK-MN**	
1676	R, US, GC, SB 2, S1	**SILK-YN**	

Table 5.17: Table to show possible correlations between the dacitic pumice and the SILK layers. The mean age of the ^{14}C dated SILK layers is shown in the first column.

The EPMA and SIMS analyses have identified Katla as the source of the majority of the ocean-rafted pumice found around the North Atlantic region, although precise correlations with individual SILK layers is difficult. The next section describes the possible transport routes that the pumice took from eruption to entry into the Atlantic.

Transport routes

This chapter has shown that the geochemical data has identified Katla Volcanic System as the source of the majority of the ocean-transported pumice. As demonstrated in Chapter 1, Katla also possesses an efficient transport mechanism for moving large quantities of pumice to the coast, as eruptions are nearly always accompanied by jökulhlaups. Figure 5.38 shows identified historical and potential jökulhlaup routes which could transport pumice to the ocean. The jökulhlaups of 1823, 1860 and 1918 all flowed across Mýrdalssandur from Kötlujökull, whilst until the 14th Century AD floods emerged from Sólheimajökull (Dugmore, 1987; Larsen, 1993). There is also a potential flood route out of Entujökull and along the Markarfljót valley. It is not clear, however, if the deposits found on Markarfljót Sandur are the results of the drainage of an ice-dammed lake or a volcanic eruption (Haraldsson, 1981). Evidence of major floods along this route include a gorge cut into basalt lava flows. A breech in the Katla caldera creates a plausible route for a jökulhlaup, if the centre of activity for the eruption of SILK was to the north-west of the 1918 eruption site as suggested by Larsen *et al.* (in press).

Although jökulhlaups associated with drainage of subglacial lakes, perhaps triggered by increased geothermal activity such as those in 1955 and 1999, produce flows of around 2000-3000 $m^3 s^{-1}$, the larger floods created by volcanic activity can be greater than 150,000 $m^3 s^{-1}$ (Larsen, pers. com., 1999; Larsen, 1993; Maizels, 1991).

The precise route any particular jökulhlaup would have taken would depend on the size and thickness of the icecap. Although it is likely that there has been a significant icecap present for all of the Holocene, there have been significant fluctuations in the position of the outlet glaciers, such as Sólheimajökull, which probably reflects large changes in the size and thickness of Mýrdalsjökull itself (Dugmore, 1989b; Dugmore and Sugden, 1991; Larsen *et al.*, in press). As this early Holocene pumice deposit is found on the southern flanks of Katla and not in an obvious valley, the floods that deposited the Vikurhóll pumice must have taken a different route.

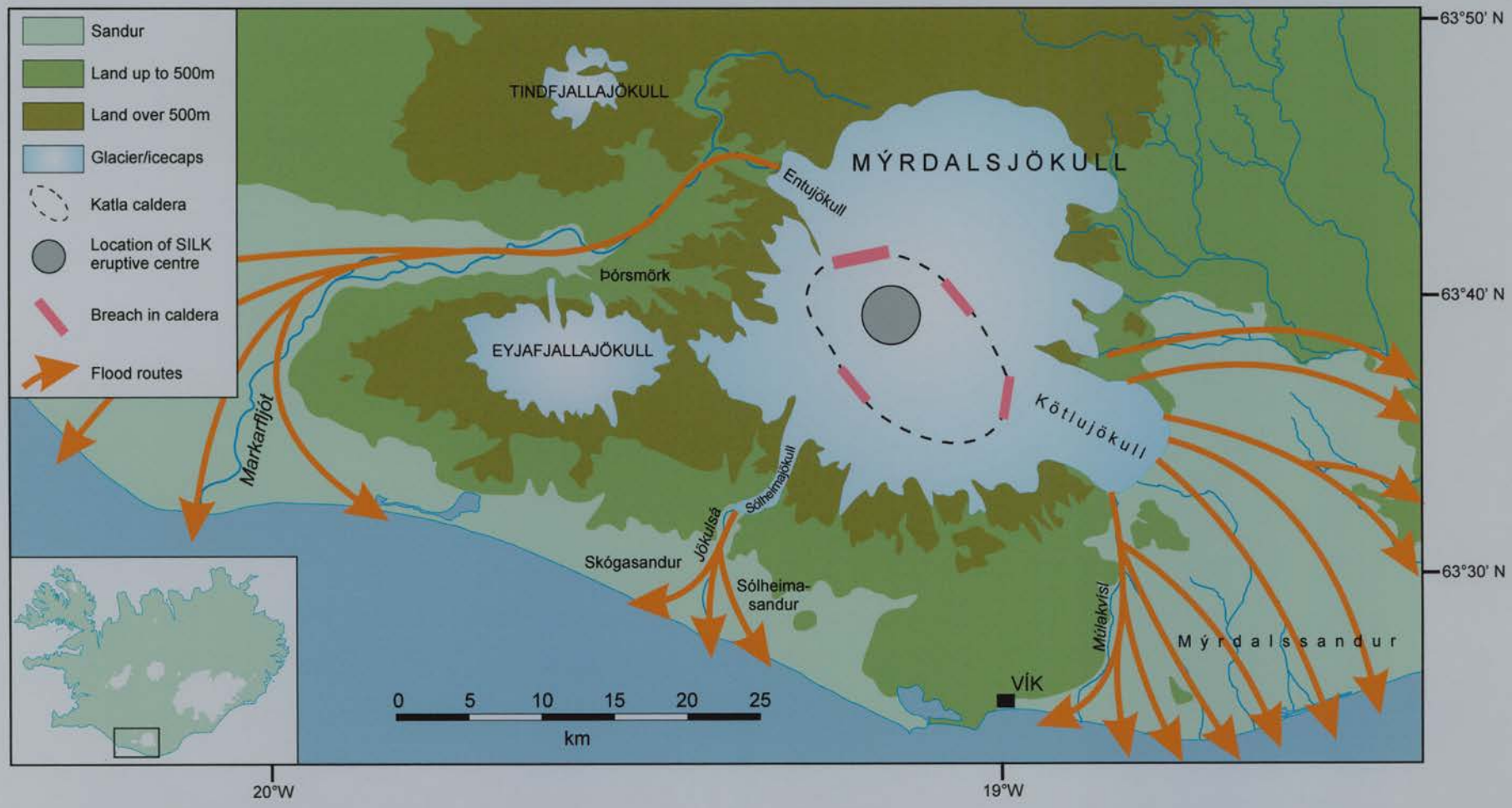

Figure 5.38: Map to show the potential flood routes based upon historical jökulhlaups, field mapping and evidence of breaches in the caldera from ice-radar studies. This map is based on current ice limits and flood routes would vary depending on the position of the ice margin and the location of the eruption. Map based on flood routes identified by Dugmore (1987), Haraldsson (1981), Larsen (1993) Larsen *et al.* (in press) and the ice radar study of Björnsson *et al.* (1993). The location of the SILK eruptive centre is from Larsen *et al.* (in press).

It is not thought that the jökulhlaups produced by the SILK eruptions would necessarily be any larger than those which have occurred during historical times (Larsen *et al.*, in press). The volume of pumice produced by the basaltic eruption of 1918 and deposited either on Mýrdalssandur or offshore has been estimated to be 0.64 km^3 (Larsen and Ásbjörnsson, 1995). Of this about 0.25 km^3 reached the sea, most of which sank rapidly to form a submerged spit, which extend the coastline by 4 km (Maizels, 1991). The less dense dacitic pumice would not have sunk and would have been quickly transported by ocean currents. The relatively small quantities of pumice is consistent with the observations of contemporary pumice rafts described in Chapter 1. The estimated volume of the Isla San Benedicto pumice was only 0.0003 km^3, whilst the South Sandwich Island pumice was about 0.6 km^3. From these records it is clear that it is not necessary to have large quantities of pumice to form a raft which can be transported thousands of kilometres and form extensive deposits on distant shorelines. The transport of the pumice by ocean currents to the shores of the North Atlantic are discussed in section 5.4.

Summary: establishing connection between the pumice, SILK tephras and Katla

This section has shown that all of the dacitic pumice, as well as the older more silicic pumice from Staosnaig, was produced by the Katla Volcanic System. Pumice on the flanks of Katla can be correlated with some of the Staosnaig pumice, whilst the SILK layers are associated with eruptions that produced the other dacitic pumice. It is difficult to correlate the pumice to precise eruptions, mainly due to the remarkable homogeneity of Katla's silicic activity. It appears that dacitic pumice produced by Katla is more geochemically hetrogeneous than the SILK tephra layers. Despite this, it is possible to attempt to correlate by combining geochemical data and the dates of the pumice deposits and SILK layers (Table 5.17). It is also possible, however, that some eruptions may have produced pumice, but no accompanying tephra layer.

The next section describes the volcanic activity Öræfajökull Volcanic System and attempts correlate this with the white rhyolitic pumice.

5.2.3 Öræfajökull Volcanic System

Öræfajökull is the highest volcano in Iceland at 2119 metres above sea-level and is found to the south of Vatnajökull, south-eastern Iceland (Figure 5.1). It is the only currently active

volcano in Iceland which lies outside the volcanic zones. This stratovolcano is composed of mainly basic and silicic rocks (Prestvik, 1980). The basic rocks are mainly tholeiitic, whilst the rarer intermediate and silicic ones are calc-alkaline in composition (Prestvik, 1980).

There have been two historical (post 870 AD) eruptions of Öræfajökull, in mid June 1362 and early August 1727 (Thórarinsson, 1958). The 1363 AD eruption of Öræfajökull was, according to Thórarinsson (1958) the largest historical eruption in Iceland, producing at least 10 km^3 of tephra (uncompacted volume), which was mainly carried in a south-easterly direction. Tephra from this eruption has been found in Ireland (Pilcher *et al.*, 1995). The lowest part of the proximal tephra is very fined grained, which may represent a phreatomagmatic phase, whilst the coarser upper part may be indicative of the plinian phase Larsen *et al.* (1999).

Little research has been carried out on the pre-historic record volcanic activity of Öræfajökull. It is known, however, that there have been several other silicic eruptions which have produced white tephra layers. Thórarinsson (1958) refers to two of these as Ö2 and Ö3. The geochemistry of these layers, although not studied in detail is believed to be similar to that of Öræfajökull 1362.

Although relatively little is known about the pre-historic activity of Öræfajökull, good quality geochemical analyses are now available for the Öræfajökull 1362 and 1727 tephra layers (Larsen *et al.*, 1999). These tephra layers were sampled from a detailed reference profile at Svínafell, which is about 10 km to the west of the summit of Öræfajökull. Details about this reference profile will be published elsewhere. Table 5.18 and Figure 5.39 show that both the white archaeological Group 1 pumice and the Trandvikan pumice are geochemically similar to the Öræfajökull 1362 tephra. The major differences being the lower Na_2O of both pumice types and the trend seen in the Group 1 pumice. The trend in the Group 1 pumice is wholly due to NB 1, which appears to be slightly different to the other pumice pieces from the same site. Chapter 4 concluded that this pumice could have been produced by the same eruption, but it is possible that this pumice piece is actually from an earlier eruption from Öræfajökull. The difference in Na_2O may be due to sodium mobility, as the same differences can be seen when analysing other tephra samples with high Na_2O abundances. This again emphasises the unsuitability of using Na_2O as a discriminatory oxide. The two sample T-Tests were unable to identify any significant differences between the Group 1 and Trandvikan pumice and the Öræfajökull 1362 tephra.

These results show that both the white pumice from Norway and Scotland appears to have been produced by Öræfajökull.

		SiO_2	TiO_2	Al_2O_3	FeO	MnO	MgO	CaO	Na_2O	K_2O	Total	n
Ö1362 Tephra	**mean**	71.36	0.22	13.14	3.12	0.10	0.03	0.98	5.55	3.38	97.89	15
	1σ	0.69	0.02	0.26	0.09	0.03	0.02	0.06	0.14	0.12	0.95	
Arch. Grp. 1	**mean**	72.05	0.24	13.15	3.26	0.10	0.04	1.01	4.98	3.43	98.27	60
	1σ	0.96	0.05	0.30	0.27	0.03	0.03	0.14	0.38	0.18	1.15	
Trandvikan	**Mean**	71.55	0.21	13.36	3.28	0.11	0.04	1.00	4.85	3.51	97.90	10
	1σ	0.47	0.04	0.30	0.09	0.03	0.02	0.06	0.48	0.12	0.99	

Table 5.18: Table to show that the Öræfajökull 1362 eruption is geochemically similar to the archaeological Group 1 and Trandvikan pumice.

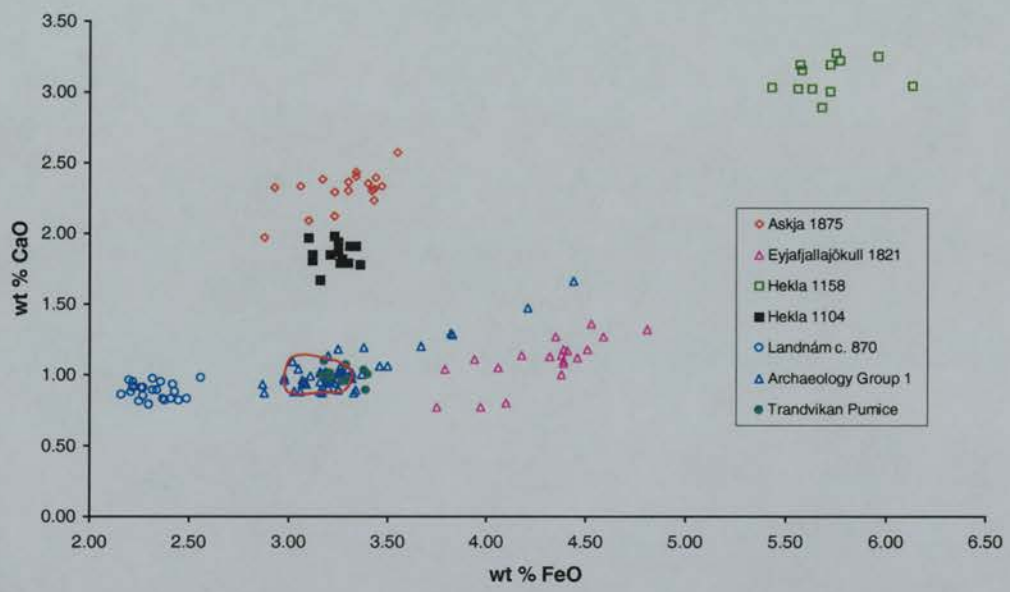

Figure 5.39: Graph (FeO/CaO) to compare the white Archaeological Group 1 and Trandvikan pumice with Öræfajökull 1362 and several other silicic historical tephra layers. Tephra data from Larsen *et al.* (1999) and also available in full at http://www.geo.ed.ac.uk/tephra/.

The Trandvikan pumice was found on an early Holocene raised shoreline in Norway, 40 metres above sea-level. This pumice most probably was erupted by an unidentified early Holocene eruption of Öræfajökull, which had similar geochemical properties to the 1362 AD eruption. The other, less likely, possibility is that this single piece of pumice was somehow transported to the raised shoreline, either by a bird or humans, and was actually erupted during the 1362 AD eruption.

The Group 1 archaeological pumice is only found in medieval archaeological sites in Shetland (Chapter 4). Pumice is a common archaeological artefact in Shetland and is found

at most sites of all ages, but the white pumice only occurs in Late Medieval ones. These dates are compatible with the white pumice having been erupted by the 1362 AD eruption of Öræfajökull and not one of the pre-870 AD eruptions.

The geochemical composition of the tephra from the 1727 AD has a SiO_2 range of between 59.98 and 56.92 % and FeO of 11.75 - 14.13 % (Larsen *et al.*, 1999) and can, therefore, be discounted as a possible source of any of the analysed pumice.

Transport

The research of Thórarinsson (1958) showed that the jökulhlaups from the 1362 eruption flowed out from Rótarfjallsjökull and Falljökull across Skeiðarársandur to the west of the Öræfajökull. These jökulhlaups would have provided an efficient method of transporting the pumice to the sea. Thórarinsson also points out that the close proximity of the volcano to the coast means that direct airfall into the sea would have transported a large proportion of the pumice. He also quotes from a contemporary Icelandic Annal produced in Skáholt, which states that:

> "pumice might be seen floating off the west coast in such masses that ships could hardly make way through".

From this it can be seen that pumice from this large eruption was transported either through the air or by floods into the sea. It was then transported by ocean currents along the south coast of Iceland, from where it travelled north along the west coast. Despite this, pumice from this eruption is a relatively rare find at proximal sites.

It is possible that some of the pumice found in Shetland did not float there by ocean currents. By the 14th Century, Iceland had been settled for over 400 years and Shetland was part of the Norse world. The pumice may have been transported from Iceland to Shetland by people. It is only after the settlement of Iceland in about 870 AD that this would have been possible. This may explain the lack of Öræfajökull pumice from older eruptions at sites in the British Isles. The rhyolitic Öræfajökull pumice, like the Hekla pumice, may too fragile to survive a journey across the Atlantic and the only way it reached Shetland was by ship. There is no direct evidence for this and it is possible that the pumice was still transported by ocean currents.

The smaller 1727 AD eruption also produced jökulhlaups and Thórarinsson (1958) concludes that these smaller floods probably followed the same course as the 1362 ones emerging out of Rótarfjallsjökull and Falljökull and flowing across Skeiðarársandur.

The transport of the pumice by ocean currents to the shores of the North Atlantic are discussed in section 5.4.

Summary: Öræfajökull and the North Atlantic pumice

The 1362 AD eruption of Öræfajökull produced white rhyolitic pumice found in Norse and Medieval contexts in Shetland. It appears that a similar eruption from Öræfajökull also produced the pumice found on the 9000 ^{14}C years BP shoreline at Trandvikan in Norway. This suggests that Öræfajökull is also capable of producing geochemically identical products over thousands of years. This type of pumice is, however, rare and it would seem that despite the large quantities produced in the 1362 eruption only a handful of pieces survived the journey across the North Atlantic.

The next section describes the volcanic activity at Jan Mayen and compares published analyses with the Svalbard pumice analysed by Boulton and Rhodes (1974).

5.3 Jan Mayen

Boulton and Rhodes (1974) suggest that the island of Jan Mayen, 650 km north of Iceland could be the source of the pumice they describe on Svalbard. The analyses of pumice from Svalbard in Chapter 3 shows more than one source produced the pumice, allowing the possibility of origins in Jan Mayen, as well as Iceland. This section considers Holocene volcanic activity on Jan Mayen and compares the published analyses of the Svalbard pumice with published analyses from Jan Mayen.

5.3.1 Introduction

Jan Mayen is a small island (380 km^2) 650 km north of Iceland (Figure 2.1; 71° N, 8° W) and is the northernmost volcanic island in the world. It is dominated by the large stratovolcano of Beerenberg (2277 m) and is located just to the south of Jan Mayen Fracture Zone and the Mohns Ridge (Imsland, 1986). It is not clear whether the island is the result of a mantle plume, as suggested by Wilson (1973) or associated with the high thermal gradient of the Mohns ridge as suggested by Imsland (1978). The island is entirely volcanic and the

oldest rocks are less than 0.7 million years old (Imsland, 1986). Sailors, scientists and settlers intermittently visited the island between 1600 and 1921, when a permanent meteorological and navigational station was established (Havskov and Atakan, 1991).

5.3.2 Volcanic activity

The island has risen about 5000 metres from the seafloor during the last million years. Beerenberg occupies the whole of the northern part of Jan Mayen, the summit of which contains Sentralkrateret, a one kilometre diameter crater from which a glacier emerges and flows to join Weyprechtbreen, Jan Mayen's largest glacier (Imsland, 1986). In contrast, the south of the island is dominated by a mountainous ridge, which is composed of lavas, submarine hyaloclastites and scoria cones (Imsland, 1986). The north of the island is mainly composed of ankaramites[8] and Mg-rich basalts, whilst the prominent rocks in the south are tristanites[9] and trachytes (Imsland, 1986). These volcanic rock types led Imsland (1984) to note that the volume of silicic rocks decreases from the north-east to the south-west of Jan Mayen, whilst the proportion of mafic rocks increases.

The Beerenberg stratovolcano was formed in four phases (Fitch, 1964). The first stage was the submarine activity which built the volcano up to sea-level. This led to the formation of the 3000 metre basement on which the subaerially erupted volcano is built. The second phase built a basal shield composed of mainly ankaramitic lava flows. The third phase of activity, which was more explosive, built the current steep-sided cone. Rocks produced during this time were dominated by glomeroporphyritic[10] basalts. The final phase of activity, probably since about 6000 to 7000 years ago, has involved fissure and cinder cone eruptions on the flanks of the volcano.

Since 1600 there have been at least 11 eruptions, with seven eruption since 1970 (Havskov and Atakan, 1991). This skewness in the dates of eruptions is probably due to the permanent settlement on Jan Mayen, but even since 1921 Havskov and Atakan (1991) note that many small unobserved eruptions may have taken place, but were probably hidden by

---

[8] Ankaramites are the most basic of the alkali series and on Jan Mayen have between 10 and 18.5 wt % MgO (Imsland, 1984; Middlemost, 1985).

[9] Tristanites are trachyandesites with a Na_2O/K_2O ratio of less than 1.5 (Middlemost, 1985).

[10] Glomeroporphyritic basalts contain clusters of phenocrysts (Kearey, 1996).

low cloud and fog. It is currently thought that Beerenberg flank eruptions occur at a frequency of about 1 per 100-150 years (Imsland, 1986; Sylvester, 1975). The eruption in 1970 lasted for about four months, about 0.5 km^3 of lava was erupted from a 6 km long fissure which opened at an altitude of about 1000 metres on the north-east slopes of Beerenberg.

Correlation of distal pumice to Jan Mayen

Amongst the scoria cones, scoria mounds and trachytic domes, Imsland (1984) identifies a *dome* of stratified pumice. No analyses of this pumice, however, are presented. Analyses of tristanites published by Imsland (1984) appear to be similar to the analyses of the higher Sr pumice in Boulton and Rhodes (1974). Both of these analyses are presented in Table 5.19.

a)

Svalbard	Rb	Sr	Y	Zr	Nb
mean	71.7	955.0	33.3	455.0	116.7
1σ	5.8	42.7	2.9	34.6	7.6

b)

Jan Mayen	Rb	Sr	Y	Zr
175	100	964	47	415
82	103	966	43	532
37	159	568	51	501

Table 5.19: a) shows the means and standard deviations of the analyses of the non-Icelandic pumice published in Boulton and Rhodes (1974), full data in Table 2.10 (Chapter 2). b) Three analyses of tristanites from Jan Mayen by Imsland (1984).

Table 5.19 and Figure 5.40 show that two of the tristanite analyses are similar to three of the c. 6500 ^{14}C years BP pumice pieces analysed by Boulton and Rhodes (1974). Whilst these analyses were carried out on different types of material, pumice and lava, there sto;; appears to be a close relationship between the two and it is reasonable to state that the c. 6500 ^{14}C year old pumice analysed by Boulton and Rhodes (1974) was most probably erupted by an undated tristanite eruption from Jan Mayen.

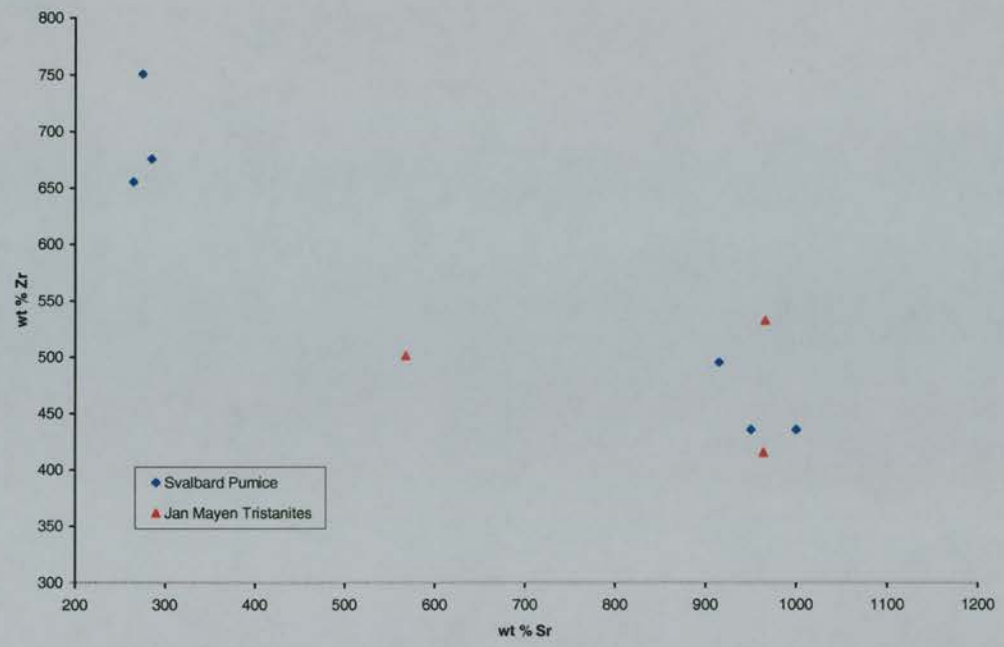

Figure 5.40: Graph (Sr/Zr) to show the similarity between the Jan Mayen tristanites and some of the pumice found on Svalbard.

Summary: Jan Mayen and the ocean-transported pumice

Although there is only limited geochemical data available on Jan Mayen and even less data on the pumice from Svalbard, it seems probable that at least some of the pumice found on the c. 6500 ^{14}C years BP shoreline was produced by an eruption from Jan Mayen. This eruption is undated and Svalbard is the only known place where pumice from Jan Mayen has been found.

5.4 Ocean Transportation

Having established that Iceland and Jan Mayen have probably produced virtually all of the pumice found around the North Atlantic and identified the source volcanoes it is appropriate that the ocean transport pathways discussed in Chapter 2 are reassessed. Chapter 2 noted that Iceland's location in the North Atlantic allows ocean currents to transport pumice which enters the sea to all of the sites where pumice has been found. The identification of Katla and Öræfajökull as the sources of virtually all of the ocean-transported pumice, does not alter this. Figure 5.41 shows that pumice entering the sea from an eruption on the south coast of Iceland is carried by the clockwise currents which encircle Iceland. The pumice which is carried by the Irminger Current either travels northwards along the west coast of

Iceland or south with the East Greenland Current. The northwards floating pumice will be transported along Iceland's north and east coast before reaching the Norwegian Sea, where it will be carried along the north coast of Norway. Eventually this pumice would be carried to Svalbard via the West Spitsbergen Current or the North Cape-Current. Pumice transported southwards by the East Greenland Current will be either carried around the southern tip of Greenland and north into the Davies Strait or southwards to become part of the anticlockwise gyre south of Iceland. The pumice in this gyre may eventually be carried to the west and north of the British Isles. The currents in the Davies Strait will carry the pumice along the west coast of Greenland into Baffin Bay and eventually to Ellesmere and Devon Islands. Westward flowing currents cross the Davies Strait and Baffin Bay and these will carry pumice into the southwards flowing Labrador Current. This pumice would be transported south to eventually join the main North Atlantic Drift and be carried north-westwards towards the British Isles and Scandinavia.

The northerly position of Jan Mayen means that it is less likely that pumice erupted here will be widely distributed by ocean currents around the North Atlantic (Figure 5.41). Pumice would be carried south and become incorporated in the clockwise gyre in the Norwegian Sea. From here it can be carried north by the West Spitsbergen Current along the west and north coasts of Spitsbergen and the north coast of Nordaustlandet. For any pumice to travel south, it would have to be carried by the East Greenland Current.

The patterns of ocean transport described above all follow the most probable routes that modern day surface circulation patterns allow. Pumice rafts, however, as pointed out in Chapter 1, do not always follow these routes and can travel against prevailing currents and faster than the currents that transport them. For example, the larger pumice pieces from the 1962 South Sandwich Island eruption drifted nearly three times faster than most of the smaller pieces, whilst some of the pumice from both the 1883 Krakatau and 1964-69 Tonga eruptions travelled counter to the prevailing currents. There is, therefore, a good chance that some of the pumice found around the North Atlantic did not travel by the circuitous routes shown in Figure 5.41. It is possible, for example, that pumice could have travelled from Iceland to Scotland by a more direct route. For example, a low pressure system to the north of Scotland and the resultant north-westerly winds could possibly results in pumice being carried from Iceland towards the British Isles.

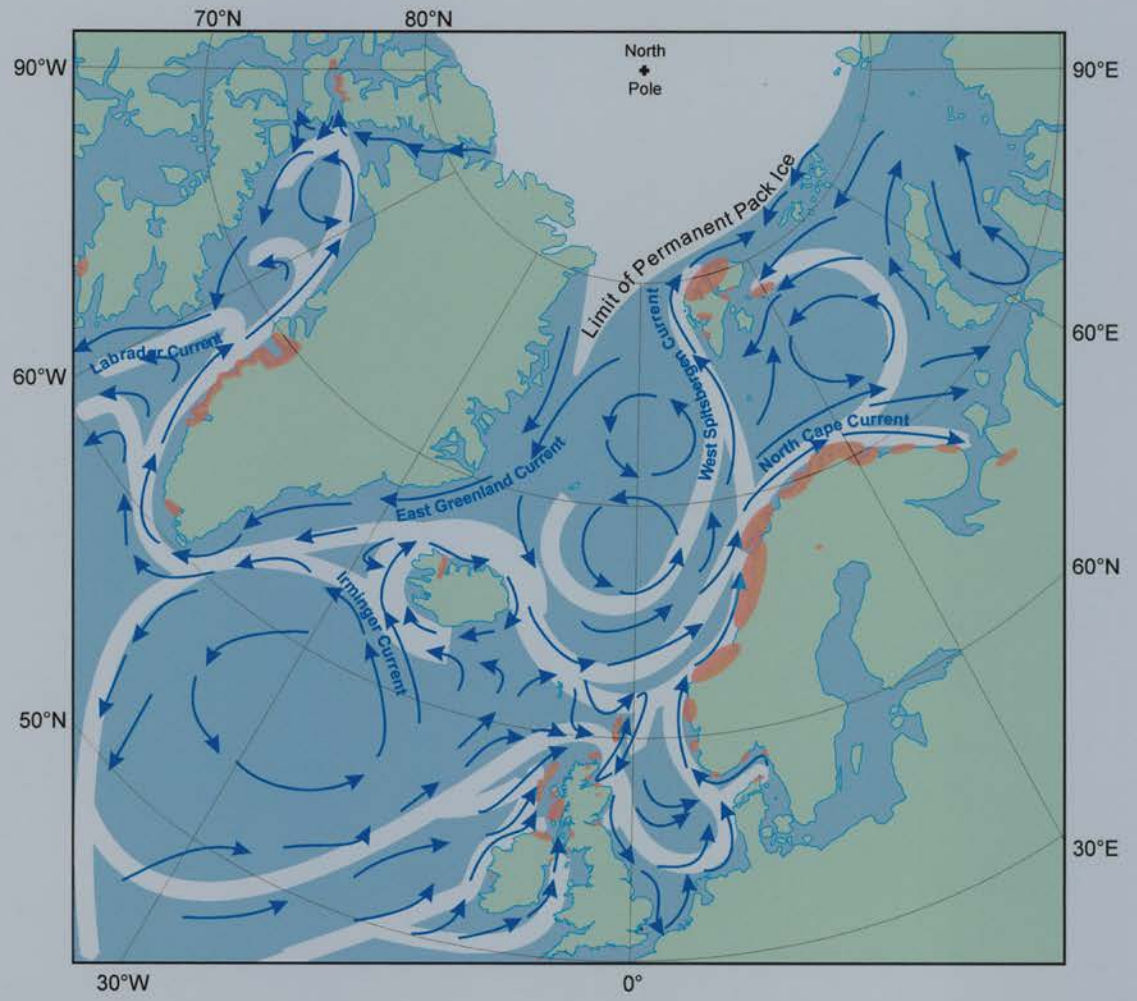

Figure 5.41: Map to show modern day surface currents (arrows) and potential transport pathways (white lines) the pumice may have taken. The location of the pumice deposits is shown by the red shading. K = Katla, Ö = Öræfajökull and J = Jan Mayen. Ocean circulation based on Bearman (1989) Editor (1977), Eggertsson (1994) and Herman (1974).

As all of the pumice deposits found are Holocene, the present day circulation patterns shown in Figure 5.41 are probably a fair representation of the likely transport routes the pumice would have taken. It is possible that pumice was produced by the eruption that produced North Atlantic Ash Zone One and the Vedde Tephra. Any pumice which reached open water during the late-glacial would have been carried south currents south and south-east of Iceland [(Ruddiman and Glover, 1972; Ruddiman and Glover, 1975). Pumice could then have been transported to the British Isles or Scandinavia.

5.5 Summary of Chapter 5

The geochemical analyses presented in this chapter have for the first time identified the sources of the majority of the ocean-transported pumice found around the shores of the North Atlantic region. None of the analysed pumice has been produced by Hekla, the source proposed by several authors.

The majority of the pumice has been produced by a series of eruptions from the Katla Volcanic System, southern Iceland. Evidence of these eruptions in Iceland is provided by distinctive light coloured tephras, the SILK layers. Early Holocene activity produced the pumice found at, at least, one Mesolithic archaeological site in Scotland. These eruptions pre-dated the Hólmsá Fires eruption (c. 6800 ^{14}C years BP), which appears to have resulted in a change in Katla's silicic activity. A series of eruptions between c. 6600 and 1676 ^{14}C years BP produced virtually all of the dacitic pumice found around the North Atlantic. It is probable that the widespread pumice horizons found in Norway were produced by contemporary eruptions and are not the result of reworking of older deposits. It is more difficult to be certain of the age of archaeological pumice due to poor dating control, the small number of pumice pieces found at many sites, and the possibility that people could have found pumice on old beaches or from older settlements. Despite this, it is clear from the geochemical evidence that the post-6000 ^{14}C years BP archaeological pumice is of the same type as the raised beach pumice. Some tentative correlations between archaeological and raised beach pumice can also be made. The silicic volcanic activity from Katla produces tephra and pumice with remarkably consistent geochemical properties. Major, trace and rare earth geochemical variations are small, although it is possible to state that several of the SILK layers were probably not associated with pumice eruptions. A single piece of black basaltic pumice was also found on the 6000 ^{14}C years BP shoreline in Norway and this was also produced by an undated eruption from Katla.

The white rhyolitic pumice found on Shetland was produced by the 1362 AD eruption of Öræfajökull, south-east Iceland. This eruption is known to have produced large quantities of pumice, but pumice has only been found at three sites in Shetland. It is possible that some of this pumice could have reached Shetland by Norse-trading rather than by ocean currents. Pumice from an early Holocene beach in Norway also appears to have been produced by an eruption from Öræfajökull.

Volcanic activity at both Katla and Öræfajökull is associated with jökulhlaups and these provide an efficient mechanism of transporting pumice from the volcano to the sea. Iceland's central North Atlantic position means that present day ocean currents are capable of transporting the pumice to all of the areas where pumice has been found.

Finally, some of the pumice found in Svalbard appears to have been erupted from Jan Mayen. Unfortunately, only limited geochemical data is available for both the Svalbard pumice finds and the products of Jan Mayen. Despite this, it is clear that at least some of the pumice on the c. 6500 ^{14}C years BP shoreline is from Jan Mayen and pumice on the younger beaches is probably from Katla.

The next and final chapter provides a synopsis of the findings of this thesis, discusses the implications of the results and the scope for future research.

Chapter

Conclusions and Implications

6

6.1 Origin and age of the pumice

The new geochemical data presented in this thesis have established that Iceland is the source of the vast majority of the pumice found on raised shorelines and in archaeological sites around the North Atlantic region. Although Iceland was the suspected source of the pumice, until this study little evidence has been presented to support this. An examination of the published data also concludes that some of the pumice present in Svalbard was erupted from Jan Mayen. Although colour has been used in the past as a distinguishing characteristic of the pumice, this study has shown that colour changes are not necessarily significant.

None of the analysed pumice was produced by eruptions from Hekla, despite being identified by previous workers as the most likely source. It appears that none of Hekla's pumice has reached proximal shores, although there are reports of rafts of Hekla pumice being sighted off the Icelandic coast.

6.1.1 Katla Pumice

Virtually all of the pumice analysed during this study was produced by a series of Holocene eruptions from the Katla Volcanic System. Geochemical data obtained from the SILK layers have enabled these to be correlated with the ocean-transported pumice. The dates of the eruptions are shown in chronological order in Table 6.1. Unfortunately, due to the limited geochemical variability between the SILK tephra layers it is not possible to establish precisely which eruption produced the pumice.

Eruption/Tephra	Age of Eruption
Vikurhóll Eruption	> c. 8000
SILK-A12	c. 7200
SILK-A11	c. 7000
SILK-A9	c. 6600
SILK-A8	c. 6400
SILK-A3	c. 5500
SILK-A2	c. 5000
SILK-A1	c. 4600
SILK-N1	c. 4400
SILK-N4	c. 3600
SILK-LN	c. 3139
SILK-MN	c. 2975
SILK-YN	c. 1676

Table 6.1: Table to show the SILK tephra layers which are associated with the ocean-transported pumice deposits. Ages in ^{14}C years BP.

The oldest Katla pumice was found on a Mesolithic archaeological site in Scotland, which is associated with the Vikurhóll pumice and the younger SILK-A11 and A12 tephra layers. The large Hólmsá Fires fissure eruption separates these eruptions from the younger silicic Katla activity. The eruptions which erupted SILK-A9 and SILK-A8 were probably also responsible for producing the pumice deposits which are found on raised shorelines older than about 6000 ^{14}C years BP at many sites along the west coast of Norway. The SILK-A1/N1 and the SILK-LN/MN produced pumices which are found on two younger shorelines along the Norwegian coast. The youngest Norwegian raised shoreline pumice deposits were probably produced by the final SILK eruption, SILK-YN. An eruption sometime before c. 5000 ^{14}C years BP, possibly SILK-A2 or SILK-A3, also produced pumice which has been found in inter-tidal peat deposits in Scotland and on a raised shoreline in North West Iceland. A single piece of basaltic pumice, erupted by Katla, sometime about 6000 ^{14}C years BP, is also found in Norway.

Pumice found at Neolithic and younger archaeological sites in the British Isles must have been produced by an eruption younger than the date of the deposits they are found in. All of this pumice is found, with one exception, in deposits younger than about 4000 ^{14}C years BP. It is probable that much of this pumice was collected from contemporary beaches and most of is likely to have been produced by a recent eruption. This means that the younger SILK layers (SILK-N1 to SILK-YN) are probably associated with this pumice.

All of the dacitic pumice, even from the undated or poorly dated raised shorelines or archaeological sites, was produced by one or more eruptions from Katla between c. 6600 and 1676 ^{14}C years BP.

6.1.2 Öræfajökull Pumice

The white pumice found at three Norse/Medieval to Modern archaeological sites in Shetland can be correlated with the tephra layer produced by the 1362 AD eruption of Öræfajökull. Whilst it is probable that this pumice floated to Shetland on ocean currents, it is also possible that Norse traders and visitors may have brought some or all of it by ship from Iceland.

The white/grey pumice found on a c. 9000 ^{14}C years BP raised shoreline at Trandvikan, Norway was also produced by an eruption from Öræfajökull. If this pumice is *in situ* it appears that two eruptions from Öræfajökull, separated by some 8000 years, produced geochemically identical products.

6.1.3 Jan Mayen Pumice

An examination of the published geochemical data of pumice from Svalbard shows that whilst most of it was probably erupted from Katla, some appears to have been produced by an undated eruption from Jan Mayen. This pumice is found on shorelines dated to c. 6500 ^{14}C years BP.

6.2 Distribution and scale of the pumice

6.2.1 Pumice Sites

Whilst the distribution of pumice finds around the North Atlantic had been established before this study began, this work has shown that pumice also exists on the raised shorelines of Iceland. Previous studies failed to find any records of pumice in Iceland similar to that found elsewhere round the North Atlantic in Iceland. Unfortunately, these shorelines, apart from one site, are poorly dated.

Although it was known that pumice occurred mainly in archaeological sites in the British Isles, this study has been the first for some 30 years to collate all records of pumice finds. The number of sites where pumice has been found has nearly doubled to over 150 and the total number of pumice pieces recovered has increased by 3.5 times. Virtually all of these sites are in Scotland, where pumice occurs at many coastal archaeological sites, especially those in the Western and Northern Isles. Recent finds at Mesolithic archaeological sites include pumice from early Katla eruptions not identified before.

Recent excavations at archaeological sites in Norway have also produced pumice and some of the Mesolithic sites may contain similar pumice to that found in Scotland. Unfortunately none of this pumice has been analysed.

6.2.2 Transportation routes

Pumice from Katla either reached the sea directly through the air or most likely was transported by jökulhlaups triggered by the partial melting of Mýrdalsjökull. These floods form efficient transport mechanisms, and, for example, the AD 1918 jökulhlaup deposited nearly 40% of its pumice into the sea. Eruptions from Öræfajökull also produce jökulhlaups and those produced by the AD 1362 and AD 1727 eruptions are described in contemporary records.

Iceland's central North Atlantic position allows present-day ocean surface currents to distribute any pumice around the North Atlantic. If this pumice is resistant enough not to be broken up and remains afloat, it is capable of reaching all the sites where pumice finds have been reported, even Svalbard, Arctic Canada and Greenland. If the pumice, however, is too fragile (often more silicic) and easily broken up, it is unlikely to remain afloat long enough to reach a distant shoreline. Even if it does survive the journey it is more likely to be broken down by wave action on the beach than the more robust dacitic pumice. This is probably the fate of pumice rafts produced by large Hekla eruptions.

Ocean circulation means that pumice produced by eruptions from Jan Mayen is less likely to be widely distributed and it is probable that it only ever reaches Svalbard.

6.2.3 The scale of the eruptions

Despite the widespread distribution of pumice around the North Atlantic, the Katla eruptions responsible were probably not large. The associated SILK layers have small volumes and it is unlikely than any of these eruptions were large. The thickest SILK layer, SILK-UN, is not associated with any of the analysed pumice pieces. All of the pumice rafts discussed in Chapter 1, with the exception of Krakatau, were also from comparatively small eruptions and these were washed ashore on beaches thousands of kilometres from the source eruptions.

The Öræfajökull AD 1362 eruption was huge, producing over 10 km^3 (uncompacted volume) of acidic tephra. Yet despite being probably two orders of magnitude bigger than

the SILK eruptions, pumice pieces from this event have only been found at three sites in Shetland and it is possible that even these were transported by humans. As with the pumice produced by Hekla, the Öræfajökull pumice is silicic and fragile and was probably more likely to break up and sink than the dacitic Katla pumice.

This thesis has demonstrated that relatively small volcanic eruptions can produce widespread pumice deposits and that pumice produced by large eruptions do not necessarily form widespread distal pumice deposits.

6.3 Methodological conclusions

The geochemical analyses used to correlate pumice deposits and tephra layers were obtained by grain specific analysis, not by bulk analysis. This type of analysis not only identified Katla and Öræfajökull as the sources of the pumice, but provided the evidence to dismiss other potential sources such as Hekla. This shows the value of correlating proximal airfall tephra layers and distal ocean-transported pumice deposits using geochemical analyses.

Whilst grain specific EPMA is now the standard analytical method of characterising the major element geochemistry of tephra layers, most previous analyses of pumice have been by bulk wet chemistry or XRF analysis. The use of these two techniques creates several problems. Firstly, the use of different analytical techniques inevitably results in small errors which can hide the natural geochemical variation between samples. Secondly, bulk analysis of pumice involves the crushing of relatively large samples which can include minerals and contamination within the pores. These are difficult and time consuming to remove. Grain specific analysis allows clear glass to be analysed and areas where phenocrysts are present to be either avoided or noted. Thirdly, the use of bulk technique gives no indication of the geochemical variation within a pumice sample, which can be a distinguishing characteristic. Grain specific analysis of both tephra layers and pumice pieces provides the best means of correlating deposits and identifying source eruptions. The advantages of grain specific analysis applies both to EPMA (major element geochemistry) and SIMS (trace and rare earth geochemistry).

The EPMA and SIMS analyses identified three distinct phases in the Holocene silicic activity of Katla and pumice produced by eruptions in each stage. The geochemical differences between each stage are pronounced, but there is little variability between tephra layers produced during a stage. Indeed the only proximal evidence of the earliest stage of

activity is the presence of pumice deposits on the flanks of Katla, as these eruptions predated Holocene soil formation. It appears that the pumice produced by an eruption shows greater geochemical variation than a tephra layer produced by the same event. This sometimes makes the correlation with a particular eruption difficult. Despite this, the use of dating information, combined with geochemical data about the pumice deposits, allows probable eruptions to be identified.

6.4 Volcanological significance

6.4.1 Atypical Iceland

Most examples of ocean rafted pumice have been produced by island arc volcanism associated with subducting plate boundaries. Iceland is the only site in the world where Mid Ocean Ridge volcanism has produced substantial amounts of dacitic ocean-transported pumice. The subduction zone volcanism described in Chapter 1 occurred at either submarine volcanoes or volcanoes which formed small islands. This enabled pumice to be readily transported to the sea, either directly in submarine eruptions, or either through the air or by pyroclastic flows during subaerial activity. The silicic magma produced in Iceland is associated with a mantle plume and is not typical of spreading plate margins. This makes the pumice produced distinctively Icelandic.

6.4.2 Katla

During the course of this research, an important part of the Holocene volcanic history of Katla has been uncovered. Katla has shown itself to have two apparently unrelated magma systems, one basaltic which feeds the majority of Katla's eruptions and the other silicic, which has produced the SILK layers. Despite being unrelated to the silicic magma chamber, it appears that the huge fissure eruptions at c. 6800 and c. 934 AD had a dramatic impact on Katla's silicic activity. The former eruption coincided with a change to slightly less silicic activity and the later one coincided with an apparent end to 5000 years of SILK activity. The mechanisms which caused these changes are not understood. The homogeneous geochemical composition and size of the majority of the SILK layers suggests that the silicic magma chamber beneath Katla is small and magma does not have time to fractionate before it is erupted. This is different to Hekla, where the magma appears to have a long residence time with the composition of the tephra layers being related to the length of repose.

The late-glacial and early Holocene activity of Katla produced important tephra layers which form components of NAAZO and the Vedde tephra layer. It is now apparent that some of these eruptions also produced pumice, identified so far in a single Mesolithic archaeological site in Scotland. It is possible that unanalysed pumice from other Mesolithic sites in Scotland and Norway and the older pumice pieces identified on early Holocene beaches in Norway, Scotland and Svalbard could have also been produced by this type of activity. The pumice deposits at Vikurhóll suggest that Katla may have experienced several early Holocene eruptions with consistent geochemical characteristics. Indeed it is possible that this type of activity predates the Last Glacial Maximum. This emphasises the fact that distal ocean-rafted pumice deposits can record evidence of volcanic activity which can no longer be found close to the source. The study of these deposits, therefore, can provide an important insight into the activity of a volcano, especially one such as Katla where soil erosion, recent volcanic activity and glaciation has removed evidence of older eruptions.

6.4.3 Dacites, rhyolites and basalts

Chapter 1 showed that dacitic pumice was by far the most common type of pumice which formed large long distance pumice rafts. This thesis has also demonstrated that the majority of the pumice found around the North Atlantic is dacitic. It appears that often pumice from a small dacitic eruption which enters the sea is more likely to reach a distal shoreline than pumice produced by a larger rhyolitic eruption. The physical morphology of dacitic pumice means that it is more liable to remain afloat and not be broken up by either attrition in the pumice raft or whilst being washed ashore. This type of pumice is more likely to be preserved on a raised shoreline. Basaltic pumice is rarer than silicic pumice on distal shorelines. Only a single piece has been found in Norway. The reasons for this are not clear, but it appears that most basaltic pumice is denser than more silicic pumice and is likely to sink before it reaches distant coastlines. The spit formed by the 1918 eruption of Katla, for example, is formed by pumice which sank as soon as it entered the sea.

6.4.4 Jan Mayen

Jan Mayen has produced some pumice, which has been found on at least one raised shoreline in Svalbard. None of the pumice producing eruptions have been dated and it is not possible to say whether such events are common.

6.5 Archaeological Implications

Pumice produced by the dacitic eruptions of Katla are difficult to correlate with specific eruptions and is found in archaeological sites ranging from the Neolithic to modern times. It follows that this type of pumice is an unsuitable dating tool. Furthermore its colour should not be used as a distinguishing characteristic. The absence or presence of pumice at a given archaeological site is partly governed by the skill and experience of the archaeologists. It is likely that pumice will be correctly identified in areas where it has previously been found, but may be overlooked in others. The white Öræfajökull 1362 pumice, however, is very distinctive and this pumice can be used as a dating tool. Any undisturbed deposit containing this pumice must be younger than 1362 AD. The older more silicic Katla pumice found at Staosnaig is also a useful correlative tool. The oldest pumice predates soil formation in Iceland and must have been erupted over 8000 ^{14}C years BP. The younger black pumice was most probably produced by an eruption of Katla c. 7000 ^{14}C years BP.

All of the pumice found in archaeological sites, however, can either have been gathered from a beach a few months after an eruption, or from an older raised shoreline or archaeological site. For this reason, pumice will never be a precise dating tool in archaeology.

6.6 Future Research

Although this thesis has succeeded in its aim of identifying the age and source of the majority of the pumice found around the North Atlantic region, there are several issues which remain to be addressed by future research.

1. During the Late-Glacial and Holocene the Katla Volcanic System has had two separate magma sources, one basaltic and the other silicic. The basaltic one is responsible for the majority of the tephra layers produced. The silicic magma chamber appears to be separate, but has been affected by large basaltic eruptions. Further research is required to understand this complex system. At present, it is not clear whether silicic activity at Katla has finished or will resume, perhaps triggered by a future large fissure eruption. As the silicic eruptive centre appears to be in a different location than the basaltic activity this has important implications for hazard assessment.

2. There is some controversy about the date of the production of the Sólheimar Ignimbrite. The geomorphological evidence points to this being emplaced during an interstadial and then being subjected to full glacial conditions. The Vikurhóll pumice, by contrast, must have been erupted in the early Holocene. There appear to be small geochemical differences between the two deposits, although the number of samples is small. Direct dating of the Sólheimar Ignimbrite provides the only means of resolving its age.

3. Öræfajökull has produced rhyolitic pumice with similar geochemical properties over 8000 years. There is relatively little good quality information about the Holocene activity of Iceland's largest volcano. Future work is hampered by Öræfajökull's location, which means that most tephra layers will be deposited over the sea, not the land. Suitably sited marine cores, away from the jökulhlaup channels, could be used to establish the frequency and nature of eruptions.

4. This thesis has highlighted the lack of good quality geochemical data on pumice found in Arctic Canada, Greenland and Svalbard. It is not clear, for instance, whether the c. 6500 ^{14}C years BP shoreline on Svalbard is the only one to contain pumice from Jan Mayen. Future studies could investigate whether Jan Mayen pumice is more common and whether the widespread use of the pumice as correlative tool is justified.

5. The pumice from Mesolithic archaeological sites in southern Norway provides an opportunity to assess whether the early Holocene activity of Katla produced widespread pumice deposits or whether just a small pumice raft was produced, which only found reached the west coast of Scotland. It is possible that other early Holocene Katla eruptions could be identified by analysing pumice from these sites.

6. The outlet glaciers from Mýrdalsjökull which breach the caldera provide the routeways by which pumice can be carried by jökulhlaups to the sea. This study has not been able to establish precisely which flood routes were used. There is for example, evidence of major floods from Entujökull, although the date of these has not been established.

7. Finally, pumice has recently been recovered from early to mid Holocene inter-tidal beach and peat deposits in Orkney and Shetland. The pumice from Clettnadal was found too late to be included in this study, but its age suggests that it may provide valuable information on the pumice production from Iceland in the early Holocene. Geochemical analysis needs to be undertaken on this pumice to establish the source.

References

Allen, C. C. (1980) Icelandic subglacial volcanism: thermal and physical studies. *Journal of Geology*, **88**, 108-17.

Allen, C. C., Jercinovic, M. J. and Allen, J. S. B. (1982) Subglacial volcanism in north-central British-Columbia and Iceland. *Journal of Geology*, **90**(6), 699-715.

Armit, I. (1988a) Broch landscapes in the Western Isles. *Scottish Archaeological Review*, **5**, 78-86.

Armit, I. (1988b) Excavations at Cnip, west Lewis 1988. *Department of Archaeology, Edinburgh University, Project Paper*, **9**.

Armit, I. (1996) *The archaeology of Skye and the Western Isles*. Edinburgh University Press, Edinburgh, 264 pp.

Bäckström, H. (1890) Über angeschwemmte Bimssteine und Schlacken der nordeuropäischen Küsten. *Bih. t. Kungl. Svenska Vet. Akad. Handl.*, **16**(2-5), 1-43.

Ballantyne, C. and Dawson, A. G. (1997) Geomorphology and landscape change. In: *Scotland: Environment and Archaeology, 8000 BC-AD 1000* (Ed. by K. J. Edwards and I. B. Ralston), pp. 23-44. Wiley & Sons, Chichester.

Ballin Smith, B. (1999) Pumice. In: *The Biggings, Papa Stour, Shetland: the history and archaeology of a royal Norwegian farm* (Ed. by B. E. Crawford and B. Ballin Smith), pp. 177-178. Society of Antiquaries of Scotland Monograph Series No 13, Edinburgh.

Ballin, T. B. and Jensen, O. L. (1995) *Farsundprosjektet - stenalderbopladser på Lista*. Universitetets Oldsaksamling, Olso.

Barber, J. (Forthcoming) *Bronze Age farms and Iron Age farm mounds of the Outer Hebrides*. STAR Monographs, Edinburgh.

Bárðarson, G. G. (1910) Traces of changes of climate and level at Húnaflói, northern Iceland. *Postglaziale Klimaveränderungen*, 347-352.

Bearman, G. (1989) *Ocean circulation*. Pergamon Press, Oxford.

Bennett, K. D., Boreham, S., Sharp, M. J. and Switsur, V. R. (1992) Holocene history of environment, vegetation and human settlement on Catta Ness, Lunnasting, Shetland. *Journal of Ecology*, **80**, 241-273.

Beveridge, E. (1911) *North Uist - its archaeology and topography*. Brown, Edinburgh, 348 pp.

Beveridge, E. (1931) Excavations of an earth-house at Foshigarry and a fort, Dun Thomaidh, in North Uist. *Proceedings of the Societym of Antiquaries of Scotland*, 65, 299-357.

Binns, R. E. (1967a) Drift pumice in northern Europe. *Antiquity*, **49**, 311-312.

Binns, R. E. (1967b) Drift pumice on post-glacial raised shorelines of northern Europe. *Acta Borealia A*, **24**, 1-63.

Binns, R. E. (1971) The distribution and origin of pumice on post-glacial shorelines in northern Europe and the western Arctic (MSc. Thesis), Abersytwyth University.

Binns, R. E. (1972a) Composition and derivation of pumice on post-glaciation strandlines in northern Europe and western Arctic. *Geological Society of America Bulletin*, **83**(8), 2303-2324.

Binns, R. E. (1972b) Drift pumice distribution in the British Isles. *Journal of the Dumfries and Galloway Natural History Antiquaries Society 197?*, **?**, ?

Binns, R. E. (1972c) A Flandrian strandline chronology for the British Isles and the correlation of some European post-glacial strandlines. *Nature*, **235**, 206-210.

Binns, R. E. (1972d) Pumice on post-glacial strandlines and in prehistoric sites in the British Isles. *Scottish Journal of Geology*, **8**(2), 105-114.

Birks, H. H., Gulliksen, S., Halflidason, H., Mangerud, J. and Possnert, G. (1996) New radiocarbon dates for the Vedde Ash and the Saksunarvatn Ash from Norway. *Quaternary Research*, **45**, 119-127.

Bishop, A. H. (1914) An Oronsay shell mound - a Scottish pre-historic site. *Proceedings of the Society of Antiquaries of Scotland*, **48**, 52-108.

Bishop, S. E. (1885) Letter to the editor from S.E. Bishop. *Nature*, **30**, 288-289.

Björnsson, H. (1992) Jökulhlaups in Iceland: prediction, characteristics and simulation. *Annals of Glaciology*, **16**.

Björnsson, H., F., P. and Guðmundsson, M. T. (1993) Mýrdalsjökull: yfirborð, botn og rennslisleiðir Jökulhlaupa. In: *Kölustefna (27-29 March 1993) Rannsóknir á eldvirkni undir Mýrdalsjökuli Veggspajaldasýning í Vík í Mýrdal* (Ed. by G. Larsen), pp. 14-16. Raunvísindasdastofnun Háskólans, Reykjavík.

Blackford, J. J., Edwards, K. J., Dugmore, A. J., Cook, G. T. and Buckland, P. C. (1992) Icelandic volcanic ash and the mid-Holocene Scots Pine (Pinus sylvestris) pollen decline in northern Scotland. *The Holocene*, **2**(3), 260-266.

Blake, W. (1961) Radiocarbon dating of raised beaches in Nordaustlandet, Spitsbergen. In: *Geology of the Arctic* (Ed. by G. O. Raasch), pp. 133-145. University of Toronto Press, Toronto.

Blake, W. (1970) Studies of glacial history in arctic Canada. I. Pumice, radiocarbon dates and differential post-glacial uplift in eastern Queen Elizabeth Island. *Canadian Journal of Earth Sciences*, **7**(2), 634-644.

Blake, W. (1975) Radiocarbon age determinations and post-glacial emergence at Cape Strom, southern Ellesmere Island, arctic Canada. *Geografiska Annaler*, **57A**, 1-71.

Blake, W. (1989) Radiocarbon dating by accelerator mass spectrometry; a contribution to the chronology of Holocene events in Nordaustlandet, Svalbard. *Geografiska Annaler*, **71A**, 59-74.

Bondevik, S., Svendsen, J. I., Johnsen, G., Mangerud, J. and Kaland, P. E. (1997a) The Storegga tsunami along the Norwegian coast, its age and runup. *Boreas*, **26**, 29-53.

Bondevik, S., Svendsen, J. I. and Mangerud, J. (1997b) Tsunami sedimentary facies deposited by the Storegga tsunami in shallow marine basins and coastal lakes, western Norway. *Sedimentology*, **44**, 1115-1131.

Bondevik, S., Svendsen, J. I. and Mangerud, J. (1998) Distinction between the Storegga tsunami and the Holocene marine trangression in coastal basin deposits of western Norway. *Journal of Quaternary Science*, **13**, 529-537.

Boulton, G. S. and Rhodes, M. (1974) Isostatic uplift and glacial history in northern Spitsbergen. *Geology Magazine*, **111**(6), 481-500.

Boygle, J. E. (1994) T*ephra in lake sediments: An unambiguous geochronological marker?* PhD., University of Edinburgh.

Boygle, J.E. (1998) A little goes a long way: discovery of a new mid-Holocene tephra in Sweden. *Boreas*, **27**, 195-199.

Boygle, J.E. (1999) Variability of tephra in lake and catchment sediments, Svínavatn, Iceland. *Global and Planetary Change*, **21**, 129-149.

Branigan, K., Newton, A. J. and Dugmore, A. J. (1995) Pumice. In: *Barra: Archaeological Research on Ben Tangaval* (Ed. by K. Branigan and P. Foster), pp. 144-145. Sheffield Academic Press Ltd.

Bray, W. and Trump, D. (1982) *The Penguin Dictionary of Archaeology*. Penguin, London, 283 pp.

Bryan, W. B. (1968) Low-potash dacite drift pumice from the Coral Sea. *Geological Magazine*, **105**, 431-439.

Bryan, W. B. (1970) Mineralogy of Coral Sea drift pumice. *Carnegie Institute of Washington Year Book*, **68**, 187-190.

Bryan, W. B. (1971) Coral Sea drift pumice stranded on Eua Island, Tonga, in 1969. *Geological Society of America Bulletin*, **82**(10), 2799-2811.

Buckland, P. C., Edwards, K. J., Craigie, R., Mainland, I., Hunter, P. and Whittington, G. (1998) *Archaeological and environmental investigations at Bay of Moaness, Rousay 1997: Interim Report*. Department of Archaeology and Prehistory, University of Sheffield, 29 pp.

Calder, C. S. T. (1937) A Neolithic double chambered cairn of the stalled type and later structures on the Calf of Eday in Orkney. *Proceedings of the Society of Antiquaries of Scotland*, **71**, 115-154.

Calder, C. S. T. (1938) Excavations of three Neolithic chambered cairns....in the islands of Eday and the Calf of Eday in Orkney. *Proceedings of the Society of Antiquaries of Scotland*, **72**, 193-216.

Calder, C. S. T. (1939) Excavations of an Iron Age dwelling on the Calf of Eday in Orkney. *Proceedings of the Society of Antiquaries of Scotland*, **73**, 167-185.

Calder, C. S. T. (1950) Report of the excavation of a Neolithic temple at Stanydale, in the parish of Stansting, Shetland. *Proceedings of the Society of Antiquaries of Scotland*, **84**, 185-205.

Calder, C. S. T. (1952) Report on the partial excavation of a broch at Sae Broch, Esha Ness, in the parish of Northmaven, Shetland. *Proceedings of the Society of Antiquaries of Scotland*, **86**, 178-181.

Calder, C. S. T. (1958) Report on the discovery of numerous Stone Age house sites in Shetland. *Proceedings of the Society of Antiquaries of Scotland*, **86**, 340-346.

Calder, C. S. T. (1961) Excavations in Whalsay, Shetland, 1954-1955. *Proceedings of the Society of Antiquaries of Society*, **94**, 28-45.

Calder, C. S. T. (1962) *Neolithic structures in Shetland. In: The Northern Isles* (Ed. by F. T. Wainwright), pp. 26-43. Nelson, Edinburgh.

Calder, C. S. T. (1965) Cairns, Neolithic houses and burnt mounds in Shetland. *Proceedings of the Society of Antiquaries of Scotland*, **96**, 71.

Callander, J. G. (1921) Report on the excavation of Dun Beag, a broch near Struan, Skye. *Proceedings of the Society of Antiquaries of Scotland*, **55**, 110-131.

Callander, J. G. (1931) Notes on the structures and the relics....pp322-357 in Beveridge E. *Proceedings of the Society of Antiquaries of Scotland*, **65**, 341.

Campbell, E., Smith, A. N. and Sharples, N. (1998) Dating. In: *Scalloway, a broch, late Iron Age settlement and Medieval Cemetary in Shetland* (Ed. by N. M. Sharples), pp. 185-186. Oxbow Monograph 82.

Carter, R. W. G. (1982) Sea-level changes in Northern Ireland. *Proceedings of the Geological Society of London*, **93**, 7-23.

Carter, R. W. G., Devoy, R. J. N. and Shaw, J. (1989) Late Holocene sea levels in Ireland. *Journal of Quaternary Science*, **4**, 7-24.

Carter, S. and Fraser, D. (1996) The Sands of Breckon, Yell, Shetland: archaeological survey and excavation in an area of windblown sand. *Proceedings of the Society of Antiquaries of Scotland*, **126**, 271-301.

Cas, R. A. F. and Wright, J. V. (1991) Subaqueous pyroclastic flows and ignimbrites - an assessment. *Bulletin of Volcanology*, **53**(5), 357-380.

Cashman, K. V. and Fiske, R. (1991) Fallout of pyroclastic debris from submarine volcanic-eruptions. *Science*, **253**(5017), 275-280.

Childe, V. G. (1934) Final report on the excavation of the stone circles at Old Keig, Aberdeenshire. *Proceedings of the Society of Antiquaries of Scotland*, **68**, 372-393.

Childe, V. G. (1952) Re-excavation of the chambered cairn of Quoyness, Sanday. *Proceedings of the Society of Antiquaries of Scotland*, **86**, 121-139.

Childe, V. G. and Grant, W. G. (1939) A Stone Age settlement at the Braes of Rinyo, Rousay, Orkney (1st Report). *Proceedings of the Society of Antiquaries of Scotland*, **73**, 6-31.

Childe, V. G. and Grant, W. G. (1948) A Stone Age settlement at the Braes of Rinyo, Rousay, Orkney (2nd Report). *Proceedings of the Society of Antiquaries of Scotland*, **81**, 16-42.

Clarke, A. (1991) *St Boniface, Papa Westray, Orkney: coarse stone, flint and pumice*. AOC Internal Report, 5 pp.

Clarke, A. (1998a) Miscellaneous pumice. In: *Scalloway, a broch, late Iron Age settlement and Medieval Cemetary in Shetland* (Ed. by N. M. Sharples), Oxbow Monograph 82.

Clarke, A. (1998b) The Pumice. In: *Scalloway, a broch, late Iron Age settlement and Medieval Cemetary in Shetland* (Ed. by N. M. Sharples), pp. 119. Oxbow Monograph 82.

Clarke, A. (1999) The Pumice: The Assemblage. In: *Kebister: the four thousand year old story of one Shetland township* (Ed. by O. Owen and C. Lowe), pp. 167. Society of Antiquaries of Scotland Monograph Series No 13, Edinburgh.

Clarke, A. and Dugmore, A. J. (1990) Pumice. In: *Rhum: Mesolithic and later sites at Kinloch. Excavations 1984-1986, Vol. 7* (Ed. by C. R. Wickham-Jones), pp. 130-131. Society of Antiquaries of Scotland Monograph Series, Edinburgh.

Clarke, A. and Newton, A. J. (in press) Pumice at Dún Aonghasa. In: *The Western Stone Forts Project: The Discovery Programme Monograph Series* (Ed. by C. Cotter), pp. Forthcoming. The Discovery Programme Monograph Series, Dublin.

Cleland, A. M. and Evans, E. E. (1942) Pumice stone and Neolithic sherds from Dundrum, Co. Down. *Ulster Journal of Archaeology*, **3(5)**, 11-13.

Clift, P. D. and Dixon, J. E. (1994) Variations in arc volcanism and sedimentation related to rifting of the Lay Basin (southwest Pacific). *Proceedings of the Ocean Drilling Program, Scientific Results*, **135**, 23-49.

Colgate, S. A. and Sigurgeisson, T. (1973) Dynamic mixing of water and lava. *Nature*, **244**, 552-555.

Coombs, D. S. and Landis, C. A. (1966) Pumice from the South Sandwich eruption of March 1962 reaches New Zealand. *Nature*, **209**, 289-290.

Cotter, C. (1993) Western Stone Fort Project. Interim Report. *Discovery Programme Reports*, **1**, 1-19.

Crawford, B. E. and Ballin Smith, B. (1999) *The Biggings, Papa Stour, Shetland: the history and archaeology of a royal Norwegian farm.* Society of Antiquaries of Scotland Monograph Series No 13, Edinburgh, 270 pp.

Crawford, I. A. (1977) A corbelled Bronze Age burial chamber and beaker evidence from the Rosinish machair, Benbecula. *Proceedings of the Society of Antiquaries of Scotland*, **108**, 94-107.

Crawford, J. (1997) Archaeological collections from sandhill sites in the Isle of Coll, Argyll and Bute. *Proceedings of the Society of Antiquaries of Scotland,* **127**, 467-511.

Cree, J. E. (1924) Account of the excavations on Trapain Law. *Proceedings of the Society of Antiquaries of Scotland*, **58**, 241-284.

Curle, C. S. T. (1933) Account of a further excavation in 1932 of the pre-historic township of Jarlshof, Shetland. *Proceedings of the Society of Antiquaries of Scotland*, **69**, 82-136.

Curle, C. S. T. (1935) An account of the excavation of another pre-historic dwelling (No. V) at Jarlshof, Shetland. *Proceedings of the Society of Antiquaries of Scotland*, **69**, 85-107.

Curle, C. S. T. (1936a) An account of the excavation of a hut-circle with an associated earth-house at Jarlshof, Shetland. *Proceedings of the Society of Antiquaries of Scotland*, **70**, 237-251.

Curle, C. S. T. (1936b) Account of the excavation of an iron smeltry and of an associated dwelling and tumili at Wiltrow in the parish of Dunrossness, near Sumburgh. *Proceedings of the Society of Antiquaries of Scotland*, **70**, 153-169.

Cursiter, I. W. (1886) Notice of a wood-carvers toolbox, with Celtic ornamentation, recently discovered in a peat-moss in the parish of Birasy, Orkney. *Proceedings of the Society of Antiquaries of Scotland*, **20**, 47-50.

de Jongh, W. K. (1973) XRF-analysis using theoretical influence coefficients. *X-ray Spectrometry*, **2**, 151.

Deacon, G. E. R. (1960) The Southern Cold Temperate Zone. *Proceedings of the Royal Society*, **B 152**, 429-677.

Donner, J. J. and West, R. G. (1957) The Quaternary geology of Brageneset, Nordaustlandet, Spitzbergen. *Norsk Polarinstitutts Skrifter*, **109**, 1-29.

Dugmore, A. J. (1987) *Holocene glacier fluctuations around Eyjafjallajökull, Iceland: a tephrochronological study*, Unpublished PhD thesis, University of Aberdeen.

Dugmore, A. J. (1989a) Icelandic volcanic ash in Scotland. *Scottish Geographical Magazine*, **105**(3), 168-172.

Dugmore, A. J. (1989b) Tephrochronological studies of Holocene glacier fluctuations in south Iceland. *Glacier Fluctuations and Climatic Change*, 37-55.

Dugmore, A. J. and Buckland, P. C. (1991) Tephrochronology and late Holocene soil erosion in south Iceland. In: *Environmental Change in Iceland, Past and Present* (Ed. by J. M. Maizels and C. C.), pp. 147-159. Kluwer Academic Publishers, Dordrecht.

Dugmore, A. J. and Newton, A. J. (1992) Thin tephra layers in peat revealed by X-radiography. *Journal of Archaeological Sciences*, **19**, 163-170.

Dugmore, A. J. and Newton, A. J. (1997) Holocene tephra layers in the Faroe Islands. *Fróðskaparrit*, **45**, 141-154.

Dugmore, A. J. and Newton, A. J. (1999a) The Pumice: Origins of the material. In: *Kebister: the four thousand year old story of one Shetland township* (Ed. by O. Owen and C. Lowe), pp. 167-168. Society of Antiquaries of Scotland Monograph Series No 13, Edinburgh.

Dugmore, A. J. and Newton, A. J. (1999b) Tephrochronology at Kebister. In: *Kebister: the four thousand year old story of one Shetland township* (Ed. by O. Owen and C. Lowe), pp. 70-74. Society of Antiquaries of Scotland Monograph Series No 13, Edinburgh.

Dugmore, A. J. and Sugden, D. E. (1991) Do the anomalous fluctuations of Sólheimajokull ice-divide migration. *Boreas*, **20**, 105-113.

Dugmore, A. J., Larsen, G. and Newton, A. J. (1995) Seven tephra isochrones in Scotland. *The Holocene*, **5 (3)**(3), 257-266.

Dugmore, A. J., Larsen, G., Newton, A. J. and Sugden, D. E. (1992) Geochemical stability of fine-grained silicic tephra layers in Iceland and Scotland. *Journal of Quaternary Science*, **7**, 173-183.

Dugmore, A. J., Newton, A. J., Edwards, K. J., Larsen, G., Blackford, J. J. and Cook, G. T. (1996) Long-distance marker horizons from small-scale eruptions: British tephra deposits from AD 1510 eruption of Hekla, Iceland. *Journal of Quaternary Science*, **11(6)**, 511-516.

Dugmore, A. J., Newton, A. J., Larsen, G. and Cook, G. T. (in press) Tephrochronology, environmental change and the Norse settlement of Iceland. *Environmental Archaeology*.

Dugmore, A. J., Shore, J. S., Cook, G. T., Newton, A. J., Edwards, K. J. and Larsen, G. (1994) The radiocarbon dating of Icelandic tephra layers. In: *15th International Radiocarbon Conference Abstracts C-13*.

Dugmore, A. J., Shore, J. S., Cook, G. T., Newton, A. J., Edwards, K. J. and Larsen, G. (1995b) The radiocarbon dating of Icelandic tephra layers in Britain and Ireland. *Radiocarbon*, **37**, 2:286-295.

Editor. (1977) *The Rand McNally Atlas of the Oceans*. Mitchell Beazley Publishers Ltd, London.

Edwards, A. J. H. (1924) Report on the excavations of an earth-house at Galston, Borve, Lewis. *Proceedings of the Society of Antiquaries of Scotland*, **58**, 185-203.

Edwards, K. J. (1996) A Mesolithic of the Western and Northern Isles of Scotland? In: *The Early Prehistory of Scotland* (Ed. by T. Pollard and A. Morrison), pp. 23-38. Edinburgh University Press, Edinburgh.

Edwards, K. J. and Ralston, I. B. M. (1997) Environment and people in prehistoric and early historical times: preliminary considerations. In: *Scotland: Environment and Archaeology* (Ed. by K. J. Edwards and I. B. M. Ralston), pp. 1-10. John Wiley & Sons, Chichester.

Edwards, K. J., Whittington, G. W. and Hirons, K. R. (1995) The relationship between fire and long-tern wet heath development in South Uist, Outer Hebrides, Scotland. In: *Heaths and Moorland: Cultural Landscapes* (Ed. by D. B. A. Thompson, A. J. Hester and M. B. Usher), pp. 240-248. HSMO, Edinburgh.

Eggertsson, O. (1994) Driftwood as an indicator of relative changes of Arctic and Atlantic water into the coastal areas of Svalbard. *Polar Research*, **13**, 209-218.

Einarsson, E. H., Larsen, G. and Thórarinsson, S. (1980) The Solheimar tephra layer and the Katla eruption of ~1357. *Acta Naturalia Islandica*, **28**, 1-24.

Einarsson, P. (1991) Earthquakes and present-day tectonism in Iceland. *Tectonophysics*, **189**, 261-279.

Eiríksson, J., Simonarson, L. A. and Sveinbjörndóttir, A. (1998) Heimsókn ad Bae í Hrutafirdi: Aflaedi og loftslagsbreytingar a nutima og ny timasetning med kolefnisgreiningum og gjoskulagatimatali. Jardfrædafelag Islands. *Vorradstefna 1998. Agrip erinda og veggspjalda*, 20-22.

Fægri, K. (1944) Studies on the Pleistocene of western Norway III. *Bergen Mus. Årb. 1943 Naturvitensk*, **8**, 1-100.

Finlayson, B. and Edwards, K. J. (1997) The Mesolithic in Scotland. In: *Scotland: Environment and Archaeology, 8000BC-AD 1000* (Ed. by K. J. Edwards and I. B. M. Ralston), pp. 109-125. John Wiley & Sons, Chichester.

Firth, C. (1992) Postglacial uplift in Scotland: evidence from shorelines. In: *Noetectonics in North West Scotland: A field guide* (Ed. by C. H. Fenton), pp. 16-20. University of Glasgow, Glasgow.

Fisher, R. V. and Schmincke, H.-U. (1984) *Pyroclastic Rocks*. Springer Verlag, Berlin, 472 pp.

Fitch, F. J. (1964) The development of the Beerenberg volcano. *Proceedings of the Geological Association*, **75**, 135-165.

Fitton, J. G., Saunders, A. D., Larsen, L. M., Hardarsson, B. S. and Norry, M. J. (1998) Volcanic rocks fromthe south-east Greenland margin at 63N: Composition, petrogensis and mantle sources. *Proceedings of Ocean Drilling Program, scientific results*, **152**.

Foster, P. J. (1995) The excavations. In: *Barra: Archaeological Research on Ben Tangaval* (Ed. by K. Branigan and P. Foster), pp. 49-99. Sheffield Academic Press, Sheffield.

Fouquet, Y., von Stackelberg, U., Charlou, J. L., Donval, J. P., Foucher, J. P., Erzinger, J., Herzig, P., Mühe, R., Wiedicke, M., Soakai, S. and Whitechurch, H. (1991) *Geology*, **19**, 303-306.

Fredskild, B. (1967) Palaeobotanical investigations at Sermermiuit, Jakobshavn, West Greenland. *Medd. om Grønland*, **178(4)**, 1-54.

Frick, C. and Kent, C. E. (1984) Drift pumice in the Indian and South Atlantic Oceans. *Transactions Geological Society of South Africa*, **87**(1), 19-33.

Gass, I. G., Harris, P. G. and Holdgate, M. V. (1963) Pumice eruption in the area of the South Sandwich Islands. *Geological Magazine*, **100**, 321-330.

Gilbertson, D. D., Schwenninger, J.-L., Kemp, R. A. and Rhodes, E. J. (1999) Sand-drift and soil formation along an exposed North Atlantic coastline: 14,000 years of diverse geomorphological, climatic and human impacts. *Journal of Archaeological Science*, **26**, 439-469.

Gilbertson, D., Gratton, J. and Pyatt, B. (1996) A reconnaissance of the potential 'coastal-erosion archaeological-hazard' on the islands of Barra, Vatersay, Sandray and Mingulay. In: *The Outer Hebrides: The Last 14,000 Years* (Ed. by D. Gilbertson, M. Kent and J. Grattan). Sheffield Academic Press, Sheffield.

Govindaraju, K. (1994) 1994 compilation of working values and sample description for 383 geostandards. *Geostandards Newsletter : Special Issue*, **18**.

Grant, W. A. (1939) Excavations at Traiversoe, Trumland, Rousay. *Proceedings of the Society of Antiquaries of Scotland*, **73**, 155-166.

Gudmundsson, M. T., Sigmundsson, F. and Björnsson, H. (1997) Ice-volcano interaction of the 1996 Gjálp eruption, Vatnajökull, Iceland. *Nature*, **389**, 954-957.

Gudmundsson, Ó., Brandsdóttir, B., Menke, W. and Sigvaldason, G. E. (1994) The crustal magma chamber of the Katla volcano in south Iceland revealed by 2-D undershooting. *Geophysical Journal International*, **119**, 277-296.

Häggblom, A. (1982) Driftwood as an indicator of sea ice conditions. *Geografiska Annalar*, **64A**, 81-94.

Hald, M. and Vorren, T. O. (1983) A shore displacement curve from the Tromsø district, North Norway. *Norsk Geologisk Tidsskrift*, **63**, 103-110.

Hall, V. A., McVicker, S. J. and Pilcher, J. R. (1994a) Tephra-linked landscape history around 2310 BC of some sites in counties Antrim and Down. *Biology and Environment: Proceedings of the Royal Irish Academy*, **94B 3**, 245-253.

Hall, V. A., Pilcher, J. R. and McCormack, F. G. (1993) Tephra dated lowland landscape history of the north of Ireland, AD 750-1150. *New Phytologist*, **125**, 193-202.

Hall, V. A., Pilcher, J. R. and McCormack, F. G. (1994b) Icelandic volcanic ash and the mid-Holocene Scots pine (Pinus sylvestris) decline in the north of Ireland: No correlation. *The Holocene*, **4**(1), 79-83.

Hall, V. A., Pilcher, J. R. and McVicker, S. J. (1994c) Tephra-linked studies and environmental archaeology, with special reference to Ireland. *Circaea, The Journal of the Association of Environmental Archaeologists*, **11**(1), 17-22.

Hamilton, J. R. C. (1956) Excavations at Jarlshof, Shetland. In: *Ministry of Works Archaeological Report 1*, pp. 228. H.M.S.O.

Hamilton, J. R. C. (1968) *Excavations at Clickhimin, Lerwick, Shetland*. H.M.S.O., 191 pp.

Hansen, A. M. (1915) Den sidste istid. *Naturen*, **39**, 327-340.

Hansen, A. M. (1918) Iosbasesystemet ved slutten av istiden. *Norsk geologisk Tidsskrift*, **4**, 280-287.

Hansom, J. D. and Briggs, D. G. (1991) Sea-level change in Vestirfirdir, north-west Iceland. In: *Environmental Change in Iceland: Past and Present* (Ed. by J. M. Maizels and C. Caseldine), pp. 79-91. Kluwer Academic Publishers, Dordrecht.

Haraldsson, H. (1981) *The Markarfljót sandur area, southern Iceland: sedimentolical, petrographical and stratigraphical studies. Striae, **15***. Societas Upsalienesis Pro Geologia Quaternaria, Upsala, 65 pp.

Havskov, J. and Atakan, K. (1991) Seismicity and volcanism of Jan Mayen Island. *Terra Nova*, **3**, 517-526.

Hedervari, P. (1982) A possible submarine volcano near the central part of Ninetyeast ridge, Indian Ocean. *Journal of Volcanology and Geothermal Research*, **13**, 199-211.

Hencken, H. O. (1932) *The archaeology of Cornwall*. Methuen, London, 322 pp.

Henshall, A. S. (1961) Notes on objects, pp. 40-45 in C.S.T. Calder. *Proceedings of the Society of Antiquaries of Scotland*, **94**, 28-45.

Henshall, A. S. and Wallace, J. C. (1963) The excavation of a chambered cairn at Embo, Sutherland. *Proceedings of the Society of Antiquaries of Scotland*, **96**, 9-36.

Herman, Y. (1974) *Marine geology and oceanography of the Arctic Seas*. Springer-Verlag, New York, 397 pp.

Hinton, R. W. (1995) Ion microprobe analysis in geology. In: *Microprobe techniques in the Earth Sciences* (Ed. by P. J. Potts, J. F. W. Bowles, S. J. B. Reed and M. R. Cave), pp. 235-289. Chapman & Hall, London.

Hjort, C. O., Ingolfsson, O. and Norddahl, H. (1985) Late Quaternary geology and glacial history of Hornstrandir, Northwest Iceland: A Reconnaissance Study. *Jökull*, **35**, 9-29.

Houghton, B. F. and Wilson, C. J. N. (1989) A vesicularity index for pyroclastic deposits. *Bulletin of Volcanology*, **51**, 451-462.

Hunt, J. B. and Hill, P. G. (1996) An inter-laboratory comparison of the electron probe microanalysis of glass geochemistry. *Quaternary International*, **34-36**, 229-241.

Imsland, P. (1978) The geology of the volcanic island Jan Mayen, Arctic Ocean. *Nordic Volcanological Institute Research Reports*, **7812**, 1-74.

Imsland, P. (1984) Petrology, mineralogy and evolution of the Jan Mayen magma system. In: *Vísindafélag Íslendinga, Vol. 43*, pp. 332. Prentsmiðjan Oddi, Reykjavík.

Imsland, P. (1986) The volcanic eruption of Jan Mayen, January 1985: interaction between a volcanic island and a fracture zone. *Journal of Volcanology and Geothermal Research*, **28**, 45-53.

Ingólfsson, Ó. (1991) A review of the Late Weischelian and early Holocene glacial and environmental history of Iceland. In: *Environmental Change in Iceland: Past and Present* (Ed. by J. M. Maizels and C. Caseldine), pp. 13-29. Kluwer Academic Publishers, Dordrecht.

Ingólfsson, Ó. and Norddahl, H. (1994) A review of the environmental history of Iceland, 13000 - 9000 yr BP. *Journal of Quaternary Science*, **9(2)**, 147-150.

Irvine, T. N. and Baragar, W. R. A. (1971) A guide to the classification of the common igneous rocks. *Canadian Journal of Earth Sciences*, **8**, 523-548.

Iyer, S. D. and Karisiddaiah, S. M. (1988) Morphology and petrography of pumice from the Central Indian-Ocean Basin. *Indian Journal of Marine Sciences*, **17**(4), 333-334.

Iyer, S. D. and Sudhakar, M. (1993) Coexistence of pumice and manganese-nodule fields - evidence for submarine silicic volcanism in the Central Indian Basin. *Deep-Sea Research Part I-Oceanographic Research Papers*, **40**(5), 1123-1129.

Jakobsson, S. P. (1979) Petrology of recent basalts of the Eastern Volcanic Zone, Iceland. *Acta Naturalia Islandica*, **26**, 1-103.

Jóhannesson, H., Flores, R. M. and Jónsson, J. (1981) A short account of the Holocene tephrochronology of the Snaesfellsjökull central volcano, Western Iceland. *Jökull*, **31**, 23-30.

John, B. S. (1974) *Northwest Iceland reconnaissance 1973 (Durham University Vestfirðir Project)*. Department of Geography, Durham University Special Publication, 54 pp.

Jokiel, P. L. (1990) Transport of reef corals into the Great Barrier Reef. *Nature*, **347**, 665–667.

Juvigne, E. and Porter, S. C. (1985) Mineralogical variations within two widespread Holocene tephra layers from Cascade Range volcanoes. *Géographie Physique et Quatérnaire*, **39(1)**, 7-12.

Kaland, P. E. (1984) Holocene shore displacement and shorelines in Hordaland, western Norway. *Boreas*, **13**, 203-242.

Kaland, P. E., Kryzwinski, K. and Stabell, B. (1984) Radiocarbon dating of transitions between marine and lacustrine sediments and their relation in the development of lakes. *Boreas*, **13**, 243-258.

Kaldhol, H. (1922) Bidrag til Møre fylkes (Romsdals amt) kvartærgeologi II. *K. norske Vidensk Selsk. Skr.*, **2**, 1-44.

Kaminski, E. and Jaupart, C. (1997) Expansion and quenching of vesicular magma fragments in Plinian eruptions. *Journal of Geophysical Research-Solid Earth*, **102**(B6), 12187-12203.

Kearey, P. (1996) *The New Penguin Dictionary of Geology*. Penguin, London, 366 pp.

Kittleman, L. R. (1979) Geological methods in the studies of Quaternary tephra. In: *Volcanic Activity and Human Ecology* (Ed. by P. D. Sheets and D. K. Grayson), pp. 49-82. Academic Press, London.

Kjemperud, A. (1981) Diatom changes in sediments of basins possessing marine/lacustrine transitions in Frosta, Nord-Trøndlag, Norway. *Boreas*, **10**, 27-38.

Knowles, W. J. (1889) Report on the prehistoric remains from the sandhills of the coast of Ireland. *Proceedings of the Royal Irish Academy*, **3rd Ser. I(2)**, 173-187.

Kokelaar, B. P. and Busby, C. (1992) Subaqueous explosive eruption and welding of pyroclastic deposits. *Science*, **257**(5067), 196-201.

Kokelaar, B. P. and Durant, G. P. (1983) The submarine eruption and erosion of Surtla (Surtsey), Iceland. *Journal of Volcanology and Geothermal Research*, **19**(3-4), 239-246.

Kokelaar, P. (1986) Magma-water interactions in subaqueous and emergent basaltic volcanism. *Bulletin of Volcanology*, **48**, 275-289.

Lacaille, A. D. (1954) The Stone Age of Scotland. Oxford University Press, London, 354 pp.

Lacasse, C., Sigurdsson, H., Johannesson, H., Paterne, M. and Carey, S. (1995) Source of Ash Zone 1 in the North Atlantic. *Bulletin of Volcanology*, **57**, 18-32.

Laidlay, J. W. (1870) Notice of an ancient structure and remains from a "kitchen-midden" on an isolated rock , near Seacliff, East Lothian. *Proceedings of the Society of Antiquaries of Scotland*, **8**, 372-377.

Larsen, G. (1979) Um aldur Eldgjárhrauna (Tephrochronology dating of the Eldgjá lavas in southern Iceland). *Náttúrufræðingurinn*, **49**(1), 1-80.

Larsen, G. (1981) Tephrochronology by microprobe glass analysis. In: *Tephra Studies* (Ed. by S. Self and R. S. J. Sparks), pp. 95-102. D. Reidal, Dordrecht.

Larsen, G. (1982) Gjóskutímatal Jökuldals og nágrennis (Tephrochronology of Jokuldalur and the surrounding areas). In: *Eldur i Nordi* (Ed. by H. Thorarindottir, O. H. Oskarsson, S. Steinthorsson and T. Einarsson), pp. 51-66. Sogufelag, Reykjavik.

Larsen, G. (1984) Recent volcanic history of the Veidivotn fissure swarm, southern Iceland - an approach to volcanic risk assessment. *Journal of Volcanology and Geothermal Research*, **22**, 33-58.

Larsen, G. (1993) Um leiðir Kötluhlaupa og Þróun Mýrdalssands. In: *Kölustefna (27-29 March 1993) Rannsóknir á eldvirkni undir Mýrdalsjökuli Veggspajaldasýning í Vík í Mýrdal* (Ed. by G. Larsen), pp. 8-10. Raunvísindasdastofnun Háskólans, Reykjavík.

Larsen, G. (1994) Súr og basík gjóskulög frá Kötlueldstöðvakerfinu: Hversu dæmigerð er gossaga síðustu 1000 ára? (Silicic and basaltic tephra layers from the Katla System). *Kötlustefna 26 February, Jarðfræðafélag Íslands*, 4-5.

Larsen, G. (1996) Gjóskutímatal og gjóskulög frá tíma norræns landnáms á Íslandi (Tephrochronology and tephra layers from the time of Norse settlement of Iceland). In: *Landnám á Íslandi. Rádstefnurit V* (Ed. by G. Á. Grímsdóttir), pp. 81-106. Vísindafélag Íslendinga, Reykjavík.

Larsen, G. and Ásbjörnsson, S. (1995) Volume of tephra and rock debris deposited by the 1918 jökulhlaups on western Mýrdalssandur, south Iceland. *Abstracts: International Gaciological Society, 20-25 August 1995, Reykjavík.*

Larsen, G. and Thórarinsson, S. (1977) H4 and other acidic Hekla tephra layers. *Jökull*, **27**, 28-46.

Larsen, G., Dugmore, A., J. and Newton, A. J. (1999) Geochemistry of historic silicic tephras in Iceland. *The Holocene*, **9(4)**, 463-471.

Larsen, G., Dugmore, A. and Newton, A. (1995) Íslensk gjóska Í jarðvegi Í Skotlandi, Hjaltlandi, Orkneyjum og Suðureyjum. In: *Jardfraedafelag Islands: Vorrádstefna 1995* (Ed. by M. T. Guðmundsson), pp. 21-23. Haldin I Odda, Reykjavik.

Larsen, G., Gudmundsson, M. T. and Björnsson, H. (1998) Eight centuries of periodic volcanism at the center of the Iceland hotspot revealed by glacier tephrostratigraphy. *Geology*, **26(10)**, 943-946.

Larsen, G., Newton, A. J., Dugmore, A. J. and Vilmundardóttir, E. (in press) Geochemistry, dispersal, volumes and chronology of Holocene silicic tephra layers from the Katla Volcanic System, Iceland. *Journal of Quaternary Science*.

Le Maitre, R. W. (1989) *A classification of igneous rocks and glossary of terms*. Blackwell,, Oxford, 193 pp.

Lethbridge, T. C. (1925) Exploration of a cairn on Canna. *Proceedings of the Society of Antiquaries of Scotland*, **59**, 238-239.

MacDonald, R., McGarvie, D. W., Pinkerton, H., Smith, R. L. and Palacz, Z. A. (1990) Petrogenetic evolution of the Torfajökull Volcanic Complex, Iceland .1. relationship between the magma types. *Journal of Petrology*, **31**, 429-459.

MacGregor, A. (1974) The broch of Burrian, North Ronaldsay, Orkney. *Proceedings of the Society of Antiquaries of Scotland*, **105**, 63-118.

Maizels, J. M. (1991) The origin and evolution of Holocene sandur deposits in the areas of jökulhlaup drainage in Iceland. In: *Environmental Change in Iceland, Past and Present* (Ed. by J. M. Maizels and C. Caseldine), pp. 267-302. Kluwer Academic Publishers, Dordrecht.

Mangerud, J. and Gulliksen, S. (1975) Apparent radiocarbon ages of recent marine shells from Norway, Spitsbergen and Arctic Canada. *Quaternary Research*, **5**, 263-273.

Mangerud, J., Lie, S. E., Furnes, H., Kristiansen, I. L. and Lomo, L. (1984) A Younger Dryas ash bed in western Norway and its possible correlations with tephra in cores from the Norwegian Sea and the North Atlantic. *Quaternary Research*, **21**, 85-104.

Manville, V., White, J. D. L., Houghton, B. F. and Wilson, C. J. N. (1998) The saturation behaviour of pumice and some sedimentological implications. *Sedimentary Geology*, **119**(1-2), 5-16.

Marthinussen, M. (1945) Yngre postglaciale nivåre på Varanger-Halvøya. *Norsk geologisk Tidsskrift*.

Marthinussen, M. (1960) Coast and fjord area of Finmark. In Geology of Norway (Holtedahl O. ed). *Norges Geol. Undersökelse*, **208**, 414-429.

Marthinussen, M. (1962) C14 - datings referring to shore lines, transgressions and glacial substages in northern Norway. *Norges Geol. Undersökelse*, **215**, 37-67.

Martin-Barajas, A., Vallier-Verges, E. and Leclaire, L. (1991) Characteristics of manganese nodules from the Central Pacific Indian Basin: relationship with the sedimentary environment. *Marine Geology*, **101**, 249-265.

May, A. M. (1948) The sandhill cultures of the River Bann estuary, Co. Derry. *Journal of the Royal Society of Antiquaries of Ireland*, **78**, 130-156.

McGarvie, D. W. (1984) Torfajökull: a volcano dominated by magma mixing. *Geology*, **12**, 685-688.

McGarvie, D. W., MacDonald, R., Pinkertonh and Smith, R. L. (1990) Petrogenetic evolution of the Torfajökull Volcanic Complex, Iceland. 2. the role of magma mixing. *Journal of Petrology*, **31**, 461-481.

Meier, P. S., Sigurdsson, H. and Shilling, J. G. (1985) Petrological and geochemical variations along Iceland's neovolcanic axis. *Journal of Geophysical Research*, **90 B12**, 10043-10073.

Mellars, P. A. (1987) *Excavations on Oronsay: Prehistoric human ecology on a small island*. Edinburgh University Press, Edinburgh, 306 pp.

Melson, W. G., Jarosewich, E. and Lundquist, C. A. (1970) Eruption of Metis Shoal, Tonga, 1967–1968: Description and petrology. *Smithsonian Contributions to the Earth Sciences*, **4**, 1-18.

Mercer, J. (1970) A regression-time stone-workers' camp, 33ft OD, Lussa River, Isle of Jura. *Proceedings of the Society of Antiquaries of Scotland*, **103**, 1-33.

Mercer, J. (1972) Microlithic and Bronze Age camps, 75-26ft OD, N Carn, Isle of Jura. *Proceedings of the Society of Antiquaries of Scotland*, **104**, 1-22.

Middlemost, E. A. K. (1985) *Magmas and Magmatic Rocks*. Longman Group Ltd, Harlow, 266 pp.

Miller, J. (1989) The 10th Century eruption of Eldgja, southern Iceland, *Vol. 8903*, pp. 29. Nordic Volcanological Institute, Reykjavik.

Mithen, S. (Forthcoming) *Hunter Gatherer Landscape Archaeology: The Southern Hebrides Mesolithic Project 1988-1998*. McDonald Institute for Archaeological Research, Cambridge, in press pp.

Møllenhus, K. R. (1977) Mesolitiske boplasser pa Møre or Trøndelagskysten. *Det Kgl. Norske Videnskabers Selskab Museet*, **27**.

Møller, J. and Holmeslet, B. (1998) *Program Sealevel Change Ver 3.51 7 Jan 1998*. Universitetet i Tromsø.

Møller, J. J. (1984) Holocene shore displacement at Nappstraumen, Lofoten, north Norway. *Norsk Geologisk Tidsskrift*, **64**, 1-5.

Møller, J. J. (1985) Coastal caves and their relation to early postglacial shore levels in Lofoten and Vesterålen, North Norway. *Nor. geol. unders. Bull*, **400**, 51-65.

Møller, J. J. (1986) Holocene transgression maximum about 6000 years BP at Ramså, Vesterålen, north Norway. *Norsk geografisk Tidsskrift*, **40**, 77-84.

Møller, J. J. (1989) Geometric simulation and mapping of Holocene relative sea-level changes in northern Norway. *Journal of Coastal Research*, **5**(3), 403-417.

Møller, J. J. (1995) Sandy beaches as records of changes in relative sea level and storm frequency. *Journal of Coastal Research Special Issue No 17: Holocene Cycles, sea levels and sedimentation*, **17**, 169-172.

Møller, J. J., Danielsen, T. K. and Fjalstad, A. (1992) Late Weichselian glaical maximum on Andøya, North Norway. *Boreas*, **21**.

Morris, C. D. and Emery, N. (1986) The chapel and enclosure on the Brough of Deerness, Orkney: survey and excavation 1975-1977. *Proceedings of the Society of Antiquaries of Scotland*, **116**, 301-374.

Mudholkar, A. and Fujii, T. (1995) Fresh pumice from the Central Indian Basin: a Krakatau 1883 signature. *Marine Geology*, **125(1-2)**, 143-151.

Newton, A. J. (1995) The Cramp. In: *Two Orcadian cist burials: excavations at Midskaill, Egilsay, and Linga Fiold, Sandwick. Proceedings of the Society of Antiquaries of Scotland, Vol. 125* (Ed. by H. Moore and G. Wilson), pp. 244-245.

Newton, A. J. (1999) Report on the pumice. In: *The Biggings, Papa Stour, Shetland: the history and archaeology of a royal Norwegian farm* (Ed. by B. E. Crawford and B. Ballin Smith), pp. 178. Society of Antiquaries of Scotland Monograph Series No 13, Edinburgh.

Newton, A. J. (Forthcoming-a) Report on pumice found at RUX6 at the Udal, North Uist. In: *The Udal* (Ed. by I. Crawford).

Newton, A.J. (Forthcoming-b) The Pumice. In: *Hunter-Gatherer Landscape Archaeology: The Southern Hebrides Mesolithic Project 1988-1998* (Ed. by S. Mithen), pp. Forthcoming. McDonald Institute for Archaeological Research, Cambridge.

Newton, A. J. (Forthcoming-c) Report on pumice from Cnip 88.

Newton, A. J. and Dugmore, A. J. (1993) Tephrochronology of Core C from Lago Grande di Monticchio. In: *Paleolimnology of European Maar Lakes: Lecture Notes in Earth Sciences, 49* (Ed. by J. F. W. Negendank and B. Zolitschka), pp. 333-348. Springer-Verlag, Berlin.

Newton, A. J. and Dugmore, A. J. (1995) Pumice: Analytical Report. In: *Barra: Archaeological Research on Ben Tangaval* (Ed. by K. Branigan and P. Foster), pp. 145-148. Sheffield Academic Press Ltd, Sheffield.

Newton, A. J. and Dugmore, A. J. (Forthcoming-a) Analysis of pumice from Baleshare. In: *Bronze Age farms and Iron Age farm mounds of the Outer Hebrides* (Ed. by J. Barber). STAR Monographs, Edinburgh.

Newton, A. J. and Dugmore, A. J. (Forthcoming-b) Green Castle Pumice report. In: *Final excavation report of archaeological excavations at Green Castle, Porknockie* (Ed. by I. Ralston).

Newton, A. J. and Metcalfe, S. E. (1999) Tephrochronology of the Toluca Basin, central Mexico. *Quaternary Science Reviews*, **18**, 1039-1059.

Noe-Nygaard, A. (1944) Andesitisk pimpsten fra Julianehaab, Sydgrønland. *Medd. fra dansk geol. Foren*, **10(4)**.

Noe-Nygaard, A. (1951) Sub-fossil Hekla pumice from Denmark. *Medd. fra Dansk Geol. Forening. København.*, **12**, 36-46.

Norddahl, H. and Haflidason, H. (1992) The Skogar Tephra, a Younger Dryas marker in north Iceland. *Boreas*, **21**(1), 23-41.

Ólafsson, M., Imsland, P. and Larsen, G. (1984) Nornahár II (Pelé's hair II. Mode of formation, composition and structure). *Náttúrufræðingurinn*, **53**(3-4), 135-144.

Oldfield, F., Thompson, R., Crooks, P. R. J., Gedye, S. J., Hall, V. A., Harkness, D. D., Housley, R. A., McCormac, F. G., Newton, A. J., Pilcher, J. R., Renberg, I. and Richardson, N. (1997) Radiocarbon dating of a recent high-latitude peat profile: Stor Amyran, northern Sweden. *The Holocene*, **7(3)**, 283-290.

Olsson, I. U. (1980) Content of 14C in marine mammals from northern Europe. *Radiocarbon*, **22**, 662-675.

Orsi, G., Gallo, G., Heiken, G., Wohletz, K., Yu, E. and Bonani, G. (1992) A comprehensive study of pumice formation and dispersal - the Cretaio Tephra of Ischia (Italy). *Journal of Volcanology and Geothermal Research*, **53**(1-4), 329-354.

Ortega-Guerrero, B. and Newton, A. J. (1998) Geochemical characterisation of late Pleistocene-Holocene tephra layers from the Basin of Mexico, central Mexico. *Quaternary Research*, **50(1)**, 90-106.

Owen, N., Kent, M. and Dale, P. (1996) The machair vegetation of the Outer Hebrides: A review. In: *The Outer Hebrides: The Last 14,000 Years* (Ed. by D. Gilbertson, M. Kent and J. Grattan), pp. 123-131. Sheffield Academic Press, Sheffield.

Owen, O. and Lowe, C. (1999) *Kebister: the four thousand year old story of one Shetland township*. Society of Antiquaries of Scotland Monograph Series No 13, Edinburgh, 332 pp.

Persson, C. (1966) Forsok till tefrokronologisk datering av nagra svenska torvmossar tre myrar. *Geoliska Foreningens i Stockholm. Forhandlingar*, **88**, 361-394.

Persson, C. (1967) Forsok till tefrokronologisk datering i tre Norske myrar. *Geoliska Foreningens i Stockholm. Forhandlingar*, **89**, 181-197.

Persson, C. (1968) Forsok till tefrokronologisk datering i tre Faoiska myrar. *Geoliska Foreningens i Stockholm. Forhandlingar*, **90**, 241-266.

Persson, C. (1971) Tephrochronological investigations of peat deposits in Scandinavia and on the Faroe Islands. *Sveriges Geologiska Undersokning Arbok*, **65**(2), 1-34.

Peulvast, J. P. and Dejou, J. (1982) The occurrence of drift pumice on Holocene raised shorelines of the north-east Atlantic - The Petvik Beach (Vestvagøy, Lofoten Islands, North Norway). *Comptes Rendus des Seances de L'Academie des Sciences Serie II - Mecanique Physique Chimie Sciences de L'Universe Sciences de La Terre*, **294**(6), 405-408.

Piggot, S. (1954) *Neolithic cultures of the British Isles*. Cambridge University Press, London, 420 pp.

Pilcher, J. and Hall, V. A. (1992) Towards a tephrochronology for the Holocene for the north of Ireland. *The Holocene*, **2**(3), 255-260.

Pilcher, J. R. and Hall, V. A. (1996) Tephrochronological studies in northern England. *The Holocene*, **6**(1), 100-105.

Pilcher, J. R., Hall, V. A. and McCormac, F. G. (1995) Dates of Holocene Icelandic volcanic eruptions from tephra layers in Irish peats. *The Holocene*, **5**(1), 103-110.

Pilcher, J. R., Hall, V. A. and McCormac, F. G. (1996) An outline tephrochronology for the Holocene of the north of Ireland. *Journal of Quaternary Science*, **11 (6)**, 485-494.

Praeger, R. L. (1895) The raised beaches of Inishowen. *Irish Nat.*, **4**, 278-285.

Prestvik, T. (1980) Petrology of hybrid intermediate and silicic rocks from Öræfajökull, southeast Iceland. *Geologiska Föreningens i Stockholm Förhandlinger*, **101**, 299-308.

Ralston, I. (Forthcoming) *Final excavation report of archaeological excavations at Green Castle, Porknockie*.

Reade, T. M. (1896) Geological observations in Ayrshire. *Proceedings of the Geological Society of Liverpool*, **8**, 104-129.

Reed, S. J. B. (1995) Electron microprobe analysis. In: *Microprobe techniques in the Earth Sciences* (Ed. by P. J. Potts, J. F. W. Bowles, S. J. B. Reed and M. R. Cave), pp. 49-89. Chapman & Hall, London.

Rendall, S. M. (1884) On floating pumice. *Nature*, **30**, 287-288.

Renne, P. R., Sharp, W. D., Deino, A. L., Orsi, G. and Civetta, L. (1997) Ar-40/Ar-39 dating into the historical realm: Calibration against Pliny the Younger. *Science*, **277**(5330), 1279-1280.

Reynolds, R. C. (1963) Matrix corrections in trace element analysis by X-ray fluorescence: estimation of the mass absorption coefficient by Compton scattering. *American Mineralogy*, **48**, 1133-1143.

Richards, A. F. (1958) Transpacific distribution of floating pumice from Isla San Benedicto, Mexico. *Deep-Sea Research*, **5**, 29-35.

Ruddiman, W. F. and Glover, L. K. (1972) Vertical mixing of ice-rafted volcanic ash in North Atlantic. *Geological Society of America Bulletin*, **83**, 2816-2836.

Ruddiman, W. F. and Glover, L. K. (1975) Subpolar North Atlantic circulation at 9300 yr BP: faunal evidence. *Quaternary Research*, **5**, 361-389.

Saemundsson, K. (1979) Outline of the geology of Iceland. *Jökull*, **29**, 7-28.

Salmi, M. (1948) The Hekla ashfalls in Finland. *Suomen Geologinen Seura*, **21**, 87-96.

Salvigsen, O. (1978) Holocene emergence and finds of pumice, whalebones, and driftwood at Svartknausflya, Nordaustlandet. *Norsk Polarinstittot Arbok*, **1977**, 217-228.

Salvigsen, O. (1981) Radiocarbon dated raised beaches in Kong Karls Land, Svalbard and their consequences for the glacial history of the Barents Sea area. *Geografiska Annaler*, **63A**(3-4), 283-291.

Salvigsen, O. (1984a) Occurrence of pumice on raised beaches and the Holocene shoreline displacement in the inner Isfjorden area, Svalbard. *Polar Research*, **2**, 107-113.

Salvigsen, O. (1984b) Two observations of pumice levels from the west coast of Spitsbergen. *Polar Research*, **2**, 115-116.

Salvigsen, O. and Österholm, H. (1982) Radiocarbon dated raised beaches and glacial history of the northern coast of Spitsbergen, Svalbard. *Polar Research*, **1**, 97-115.

Schytt, V., Hoppe, G., Blake, W. and Grosswald, M. G. (1968) The extent of the Würm Glaciation in the European Arctic. *International Association of Scientific Hydrology*, **79**, 207-216.

Scott, W. L. (1932) Rudh' an Dunain chambered cairn, Skye. *Proceedings of the Society of Antiquaries of Scotland*, **66**, 183-213.

Scott, W. L. (1935) The chambered cairn of Clettraval, North Uist. *Proceedings of the Society of Antiquaries of Scotland*, **69**, 480-536.

Scott, W. L. (1948) The chamber tomb at Unival, North Uist. *Proceedings of the Society of Antiquaries of Scotland*, **82**, 1-49.

Scott, W. L. (1951) Eilean an Tighe: a pottery workshop of the Second Millenium B.C. *Proceedings of the Society of Antiquaries of Scotland*, **85**, 1-37.

Self, S. and Rampino, M. R. (1981) The 1883 eruption of Krakatau. *Nature*, **294**, 699-704.

Self, S. and Sparks, R. S. J. (1978) Characteristics of widespread pyroclastic deposits formed by the interaction of silicic magma and water. *Bulletin of Volcanology*, **41-3**, 196-212.

Selkirk, A. and Selkirk, W. (1996) The Udal. *Current Archaeology*, **8(3)**, 84-94.

Shapiro, L. (1975) Rapid analysis of silicate, carbonate and phosphate rocks. *Geological Survey Bulletin*, **1401**, 76 pp.

Sharples, N. M. (1984) Excavations at Pierowall Quarry, Papa Westray, Orkney. *Proceedings of the Society of Antiquaries of Scotland*, **114**, 115-125.

Sharples, N. M. (1998) *Scalloway, a broch, late Iron Age settlement and Medieval Cemetary in Shetland*. Oxbow Monography **82**.

Shaw, J. S. and Carter, W. G. (1994) Coastal peats from northwest Ireland: implications for late-Holocene relative sea-level change and shoreline evolution. *Boreas*, **23**, 74-91.

Shennan, I. (1989) Holocene crustal movements and sea-level changes in Great Britain. *Journal of Quaternary Science*, **4(1)**, 77-89.

Shore, J. S., Cook, G. T. and Dugmore, A. J. (1995) The C-14 content of modern vegetation samples from the flanks of the Katla volcano, southern Iceland. *Radiocarbon*, **37**(2), 525-529.

Sigurdsson, H., Carey, S. and Mandeville, C. (1991) Krakatau. *National Geographic Research and Exploration*, **7**(3), 310-327.

Simkin, T. and Fiske, R. S. (1983) *Krakatau 1883*. Smithsonian Institute, Washington D.C., 455 pp.

Simkin, T., Siebert, L., Blong, R. J. and Russell, J. (1994) *Volcanoes of the world : a regional directory, gazetteer, and chronology of volcanism during the last 10,000 years*. Geoscience Press, Tucson, Arizona, in association with the Smithsonian Institution, 349 pp.

Simpson, D. D. A. (1976) The later neolithic and beaker settlement at Northton, Isle of Harris. In: *Settlement and economy in the Third and Second Millennia BC* (Ed. by C. Burgess and R. Miket), pp. 209-20. British Archaeological Reports, 33, Oxford.

Small, A. (1967) Excavations at Underhall, Unst, Shetland. *Proceedings of the Society of Antiquaries of Scotland*, **98**, 225-248.

Smith, A. N. (Forthcoming-a) Pumice. In: *Pool, Orkney*. Archaeological Science, University of Bradford.

Smith, A. N. (Forthcoming-b) Pumice. In: *Tofts Ness, Orkney*. Archaeological Science, University of Bradford.

Smith, A. N. (Forthcoming-c) Pumice. In: *Eilean Domhnuill*.

Smith, J. (1896) On the occurrence of pumice pebbles in the raised beaches of Ayrshire. *Transactions of the Geological Society of Glasgow*, **10**, 349.

Sparks, R. S. J. and Brazier, S. (1982) New evidence for degassing processes during explosive eruptions. *Nature*, **295**, 218-220.

Stevenson, R. B. K. (1952) A Celtic carved box from Orkney. *Proceedings of the Society of Antiquaries of Scotland*, **86**, 187-190.

Strøm, H. (1762) *Physisk og oeconomisk Beskrivelse af Fogderiet Søndmør, beliggende i Bergens, Sorøe*.

Stuiver, M. and Reimer, P. J. (1993) Extended 14C data base and revised CALIB 3.0 14C age calibration program. *Radiocarbon*, **35**, 215-230.

Sutherland, F. F. (1965) Dispersal of pumice, supposedly from the 1962 South Sandwich Islands eruption, on southern Australian shores. *Nature*, **207**, 1332-1335.

Svendsen, J. I. and Mangerud, J. (1987) Late Weichselian and Holocene sea-level history for a cross-section of western Norway. *Journal of Quaternary Science*, **2**, 113-132.

Svendsen, J. I. and Mangerud, J. (1990) Sea-level changes and pollen stratigraphy on the outer coast of Sunnmøre, western Norway. *Norsk Geologisk Tidskrift*, **70**, 111-134.

Sylvester, A. G. (1975) History and surveillance of volcanic activity on Jan Mayen island. *Bulletin of Volcanology*, **39**, 1-23.

Sylvester, P. J. (1997) New technique using Laser Ablation blasts into geochemical labs. *EOS*, **78(11)**, 117-120.

Symons, G. J. (1888) *The eruption of Krakatau and subsequent phenomena.* Krakatau Committee of the Royal Society, Trubner, London, - pp.

Tauber, H. (1968) Copenhagen Radiocarbon Date IX. *Radiocarbon*, **10**, 295-237.

Thomas, H. H. (1932) Report on pumice, in Scott, W.L., Rudh' an Dunain chambered cairn, Skye. *Proceedings of the Society of Antiquaries of Scotland*, **66**, 212-213.

Thomas, N., Jaupart, C. and Vergniolle, S. (1994) On the vesicularity of pumice. *Journal of Geophysical Research-Solid Earth*, **99**(B8), 15633-15644.

Thomas, R. M. E. and Sparks, R. S. J. (1992) Cooling of tephra during fallout from eruption columns. *Bulletin of Volcanology*, **54**, 542-553.

Thórarinsson, S. (1944) Tefrokronologiska studier på Island. (Tephrochronological studies in Iceland). *Geografiska Annaler*, **26**, 395-398.

Thórarinsson, S. (1954) The tephra fall from Hekla on March 29 1947. *The eruption of Hekla 1947-1948*, **II/3**, 1-68.

Thórarinsson, S. (1955) Nákuðungslögin við Húnaflóa í ljósi nýrra aldursákvarðana (The Nucella shore line at Húnaflói in the light of tephrochronology and radiocarbon dating). *Náttúrufrædingurinn*, **25**, 172-186.

Thórarinsson, S. (1957) The jokulhlaup from the Katla area in 1955 compared with other jökulhlaups in Iceland. *Jökull*, **7**, 21-25.

Thórarinsson, S. (1958) The Öræfajökull eruption of 1362. *Acta Naturalia Islandica*, **2**(2), 1-99.

Thórarinsson, S. (1967) The eruption of Hekla in historical times. A tephrochronological study. *The eruption of Hekla 1947-1948*, **I**, 1-183.

Thórarinsson, S. (1974) The terms tephra and tephrochronology. In: *World Bibliography and Index of Quaternary Tephrochronology* (Ed. by J. A. Westgate and C. M. Gold), pp. 17-19. INQUA/UNESCO, Edmonton, Alberta.

Thórarinsson, S. (1975) Kaltla og annáll Kötlugosa. *Árbók Ferdafélags Íslands*, 124-149.

Thórarinsson, S. (1980) Langleiðir gjósku úr Þremur Kötlugosum (Distant transport of tephra in three Katla eruptions and one Grímsvötn(?) eruption). *Jökull*, **30**, 65-73.

Thórarinsson, S. (1981) Greetings from Iceland - ash-falls and volcanic aerosols in Scandinavia. *Geografiska Annaler Series A*, **63**(3-4), 109-110.

Thórarinsson, S. and Rist, S. (1955) A jökulhlaup in the Skaftá River in Setpember 1955. *Jökull*, **5**, 37-40.

Thors, K. and Helgadóttir, G. (1991) Evidence from south-west Iceland of low sea-level in early Flandrian times. In: *Environmental change in Iceland: Past and Present* (Ed. by J. K. Maizels and C. Caseldine), pp. 93-104. Kluwer Academic Publishers, Dordrecht.

Traill, W. (1885) Notice of excavations at Stenabreck and Howmae in North Ronaldsay, Orkney. *Proceedings of the Society of Antiquaries of Scotland*, **19**, 14-33.

Traill, W. (1890a) Results of excavations at the Broch of Burrian, North Ronaldsay, Orkney. *Archaeol. Scotland*, **5(18)**, 341-364.

Traill, J. (1890b) Notes on the further excavations at Howmae. *Proceedings of the Society of Antiquaries of Scotland*, **24**, 451-461.

Traill, W. and Kirkness, W. (1937) Hower, a prehistoric structure on Papa Westray. *Proceedings of the Society of Antiquaries of Scotland*, **71**, 309-321.

Turney, C. S. M., Harkness, D. D. and Lowe, J. J. (1997) The use of microtephra horizons to correlate Late-Glacial lake sediment successions in Scotland. *Journal of Quaternary Science*, **12 (6)**, 525-531.

Undås, I. (1938) Kvartæstudier i Vestfinnmark og Vesterålen. *Norsk geologisk Tidsskrift*, **19**, 81-217.

Undås, I. (1942) On the late-Quaternary history of Møre and Trøndelag (Norway). *Det KGL Norske Videnskabers Selskabs Skrifter*, **2**, 1-92.

Undås, I. (1945) Drag av Bergensfeltets kvartærgeologi. *Norsk geologisk tidsskrift*, **25**, 433-448.

Undås, I. (1952) Om morener, israndstadier, marine grenser og jordskorpas stining ved den seinglasiale Oslofhord. *Universitet Bergen Årbok Naturvit.*, **1950**, 1-71.

van den Bogaard, C., Dorfler, W., Sandgren, P. and Schmincke, H.-U. (1994) Correlating the Holocene records: Icelandic Tephra found in Schleswig-Holstein (Northern Germany). *Naturwissenschaften*, **81**, 554-556.

Verbeek, R. D. M. (1885) *Krakatau*. Landsdrukkerij, Batavia.

Vilmundardóttir, E. G. and Hjartarson, Á. (1985) Vikurhlaup í Heklugosum. *Náttúrufræðingurinn*, **54 (1)**, 17-30.

von Stackelberg, U. (1987) Pumice and buried manganese nodules form the equatorial North Pacific Ocean. *Geologisches Jahrbuch*, **D87**, 229-285.

Vorren, K. D. and Moe, D. (1986) The early Holocene climate and sea-level changes in Lofoten and Vesterålen, north Norway. *Norsk Geologisk Tidsskrift*, **66**(2), 135-143.

Weidick. (1968) Observations on some Holocene glacier fluctuations in West Greenland. *Arctic*, **15**, 66-73.

Westgate, J. A. (1994) Trace-element analysis of volcanic glass shards by laser ablation inductively coupled palsma spectrometry: application to tephrochronological studies. *Applied Geochemistry*, **9**, 323-335.

Westgate, J. A. and Gorton, M. P. (1981) Correlation techniques in tephra studies. In: *Tephra Studies* (Ed. by S. Self and R. S. J. Sparks), pp. 73-94. D. Reidal, Dordrecht.

Whitham, A. G. and Sparks, R. S. J. (1986) Pumice. *Bulletin of Volcanology*, **48**, 209-223.

Wickham-Jones, C. R. (1990) *Rhum: Mesolithic and later sites at Kinloch. Excavations 1984-1986*. Society of Antiquaries of Scotland Monograph Series, Edinburgh, 183 pp.

Wilson, J. (1973) Mantle plumes and plate motions. *Tectonophysics*, **19**, 149-164.

Wilson, L. (1976) Explosive volcanic eruptions - III. Plinian eruption columns. *Geophysical Journal of the Royal Astronomical Society*, **45**, 453-556.

Wilson, L., Sparks, R. S. J. and Walker, G. P. L. (1980) Explosive volcanic eruption, IV, the control of magma properties and conduit geometry on eruption column behaviour. *Geophysical Journal of the Royal Astronomical Society*, **63**, 117-148.

Wohletz, K. H. (1983) Mechanisms of hydrovolcanic pyroclast formation: grain-size, scanning electron microscopy, and experiment studies. *Journal of Volcanology and Geothermal Research*, **17**, 31-63.

Wohletz, K. H. (1986) Explosive magma-water interactions: thermodynamics, explosion mechanisms, and field studies. *Bulletin of Volcanology*, **48**, 245-264.

Wolfe, C. J., Bjarnason, I. T., VanDecar, J. C. and Soloman, S. C. (1997) Seismic structure of the Iceland mantle plume. *Nature*, **385**, 245-247.

Wood, R. M. (1990) Designer Volcanoes. *Terra Nova*, 496-498.

Woodham, A. A. and Mackenzie, S. (1957) Two cists at Golspie, Sutherland. *Proceedings of the Society of Antiquaries of Scotland*, **90**, 234-238.

Young, A. N. (1953) An aisled framhouse at the Allasdale, Isle of Barra. *Proceedings of the Society of Antiquaries of Scotland*, **87**, 80-105.

Young, A. N. (1956) Excavations at Dun Cuier, Isle of Barra. *Proceedings of the Society of Antiquaries of Scotland*, **89**, 290-327.

Young, A. N. and Richardson, K. M. (1960) A Cheardach Mhor, Drimore, South Uist. *Proceedings of the Society of Antiquaries of Scotland*, **93**, 135-173.

Zhang, Y. X. (1998) Experimental simulations of gas-driven eruptions: kinetics of bubble growth and effect of geometry. *Bulletin of Volcanology*, **59 (4)**, 281-290.

Zielinski, G. A., Germani, M. S., Larsen, G., Baillie, M. G. L., Whitlow, S., Twicker, M. S. and Taylor, K. (1995) Evidence of the Eldgjá (Iceland) eruption in the GISP2 Greenland ice core: relationship to eruption processes and climatic conditions in the tenth century. *The Holocene*, **5/2**, 129-140.

Appendix

1

Pumice from sites in the British Isles

Appendix 1 contains a complete list of all of the sites in the British Isles where pumice has been found. The sites are arranged by country. The sites in Northern Ireland and Ireland are ordered by county. The sites in Scotland are arranged by regions as described in Chapter 2 and then by island or council area. Publications are given where available. No. column refers to the numbers used on the maps in Chapters 2 and 4. The Grid Ref. column refers to Ordnance Survey British National Grid in Britain and the Ordnance Survey Irish Grid in the island of Ireland. NMS 1 and NMS 2 refer to codes for pumice stored at the National Museum of Scotland. RCAHMS refers to details of pumice retrieved from CANMORE, but no further details were available. PSAS refers to donations listed in the Proceedings of the Society of Antiquaries of Scotland. This list of sites builds on the one originally presented in Binns (1971).

England

St Marys, Isles of Scilly, Cornwall

No.	Site	Grid Ref.	Description	Pumice	Context	Age	NMS 1	NMS 2	Publication
1	Porth Hellick Down	SU 928 105	1 small brown piece	1	Passage grave (Bronze Age)	c. 4000 14C years BP			Scott (1932), Hencken (1932)

Wales

Sully Island, Glamorgan

No.	Site	Grid Ref.	Description	Pumice	Context	Age	NMS 1	NMS 2	Publication
144	Sully Island	ST 166 670	2 pieces of grey/greyish pumice	2	Present storm beach	modern			Binns (1971)

Northern Ireland

County Antrim

No.	Site	Grid Ref.	Description	Pumice	Context	Age	NMS 1	NMS 2	Publication
5	Portstewart-Grangemore	C 81 38	several		Sandhill sites on PG raised beach (E. Bronze Age)	c. 3450 14C years BP			Knowles (1889)
146	River Bann (mouth of)	C 79 37	many pieces		Main post-glacial and later Holocene raised beaches	c. 6500 14C years BP			Smith (1896)
6	River Bann (mouth of)	C 79 37	many dark brown to black		Sandhill on PG shoreline (E. Bronze Age)	c. 3450 14C years BP			May (1948)
7	Whitepark	J 01 44	2 small brown	2	Sandhill on PG shoreline				Binns (1971)

County Down

No.	Site	Grid Ref.	Description	Pumice	Context	Age	NMS 1	NMS 2	Publication
4	Dundrum	J 40 30	1 medium brown	1	Sand dunes on PG (early Bronze Age)	c. 3450 14C years BP			Cleland and Evans (1942)

Ireland

County Donegal

No.	Site	Grid Ref.	Description	Pumice	Context	Age	NMS 1	NMS 2	Publication
2	Portstewart	C 89 44	several pieces of pumice		raised shoreline	c. 6400 14C years BP			Praeger (1895), Carter (1982)

County Galway
Inis Mór, Aran Islands

No.	Site	Grid Ref.	Description	Pumice	Context	Age	NMS 1	NMS 2	Publication
3	Dún Aonghasa	L 823 098	mainly brown with small vesicles	179	Late Bronze Age hillfort	c. 2900-2600 14C years BP			Clarke and Newton (2001)

Scotland - Inner Islands

Arran

No.	Site	Grid Ref.	Description	Pumice	Context	Age	NMS 1	NMS 2	Publication
42	Glensurig	NR 994 369	half a pumice bead or ring	1	n/a	n/a			Gorman et al (1993) RCAHMS

Canna

No.	Site	Grid Ref.	Description	Pumice	Context	Age	NMS 1	NMS 2	Publication
39	An t-Oban, Sanday	NG 282 041	at least one piece of pumice 2 medium	3	Cairns (Iron Age)	2500-1200 14C years BP			IO613 Lethbridge (1925)

Coll

No.	Site	Grid Ref.	Description	Pumice	Context	Age	NMS 1	NMS 2	Publication
25	Cornaigmore	NM 24 63	18 pieces	18	Sandhill sites - chaotic Norse and younger	Younger than about c. 900 AD			Crawford (1997)
26	Feall	NM 14 55	5 pieces of pumice	5	Sandhill sites -	n/a			Crawford (1997)
27	Gallanach	NM 21 61	3 pieces of pumice	3	Sandhill sites from various periods	n/a			Crawford (1997)
28	Grishipoll	NM 19 59	7 pieces of pumice	7	Sandhill sites	n/a			Crawford (1997)
29	Sorisdale	NM 27 63	65 pieces of pumice	65	Sandhill sites - Mesolithic, Late Neolithic, Bronze Age	pre 5200 to 4200-2500 14C years BP			Crawford (1997), Close-Brooks (1978)
30	Torastan	NM 22 62	1 piece of pumice	1	Sandhill sites from middens and old land surfaces	n/a			Crawford (1997)
31	Tràigh Hogh	NM 172 578	6 pieces of pumice	6	Sandhill sites - below possible dun, include mesolithic	some older than 5200 14C years BP			Crawford (1997)

Colonsay

No.	Site	Grid Ref.	Description	Pumice	Context	Age	NMS 1	NMS 2	Publication
10	Staosnaig	NR 397 934	23 pieces of pumice light brown and black	23	Mesolithic	7900-7000 14C years BP			Newton (Forthcoming-b)

Iona

No.	Site	Grid Ref.	Description	Pumice	Context	Age	NMS 1	NMS 2	Publication
16	Dùn Cùl Bhuirg	NM 264 246	One piece of pumice (PSAS 1978-80)	1	n/a	n/a	HHD 98	1979.43	n/a

Coll

No.	Site	Grid Ref.	Description	Pumice	Context	Age	NMS 1	NMS 2	Publication
13	Lussa River	NR 644 873	dark brown pumice	1	Obanian early Neolithic site	4700-4400 14C years BP			Binns (1971), Mercer (1970)
14	Lussa Wood I	NR 644 873	black and brown		Mesolithic - Neolithic modern	6950 50 BP			Binns (1971)
15	North Carn	NR 685 939	1 piece of dark grey pumice	1	Mesolithic radiocarbon dated trench in a platform	7414±80 14C years BP			Mercer (1972)

Oronsay

No.	Site	Grid Ref.	Description	Pumice	Context	Age	NMS 1	NMS 2	Publication
9	Cnoc Sligeach	NR 372 880	several		Midden (Mesolithic)	5426±190 14C years BP			Bishop (1914), Lacaille (1954), Mellars (1987)
11	Unknown	n/a	Rounded piece of pumice from refuse tips	1	Probably a Mesolithic midden	c. 5400 14C years BP	HP 704	1972.228	n/a
12	Unknown	n/a	Small fragment of pumice from refuse heaps	1	Probably a Mesolithic midden	c. 5400 14C years BP	HP 715	1972.239	n/a

Rum

No.	Site	Grid Ref.	Description	Pumice	Context	Age	NMS 1	NMS 2	Publication
37	Kinloch Farm	NM 403 998	11 pieces of pumice	11	Mesolithic/Neolithic site	8590 ± 50 14C years BP* to 3890 ± 65 14C years BP			Clarke and Dugmore (1990)

*the Mesolithic pumice may be mainly industrial slag.

Skye

No.	Site	Grid Ref.	Description	Pumice	Context	Age	NMS 1	NMS 2	Publication
23	Broch of Dùn Beag (Struan)	NG 339 386	Brown pumice rubbing stone	1	Broch (Iron Age or later)	probably post 100 AD (post 1900 14C years BP)	GA 1040	VIII.20. 15	Callander (1921)
			Brown rubbing stone	1			GA 1041	VIII.20. 16	Callander (1921)
			Piece of pumice with narrow grooves Several more	1			GA 1052	VIII.20. 14	Callander (1921)
151	Dùn Ardtreck	NG 33 35	single piece of brown/grey pumice	1	Iron Age Broch (2nd to 3rd Century AD)	c. 1900-1750 14C years BP			Mackay (pers comm., 1999)
24	Rudh' an Dùnain	NG 399 162	2 pieces of pumice	2	Cave (Beaker, early Bronze Age)	c. 3650 14C years BP			Scott (1932), Thomas (1932)

Tiree

No.	Site	Grid Ref.	Description	Pumice	Context	Age	NMS 1	NMS 2	Publication
150	Dun Mór Vaul	NM 04 49	single piece of brown pumice	1	Iron Age Broch (2nd to 3rd Century AD)	c. 1900-1750 14C years BP			Mackay (pers. comm., 1999)

Scotland - Orkney

Calf of Eday

No.	Site	Grid Ref.	Description	Pumice	Context	Age	NMS 1	NMS 2	Publication
50	Calf of Eday	HY 579 386	Piece from potter's workshop	1	Round Houses (early Iron Age)	2500-2000 14C years BP	HD 615	1937.2 36	Calder (1937; 1938; 1939)
			1 large, 1 medium 29 others	32					
			Piece from potter's workshop	1			HD 614	1937.2 35	

Eday

No.	Site	Grid Ref.	Description	Pumice	Context	Age	NMS 1	NMS 2	Publication
51	Huntersquoy	HY 562 377	Piece of pumice from chambered cairn	1	Chambered Cairn (late Neolithic)	older than 4000 14C years BP	EO 740	1938.1 035	Calder (1939)

Mainland

No.	Site	Grid Ref.	Description	Pumice	Context	Age	NMS 1	NMS 2	Publication
44	Beachview	HY 247 275	pumice		Norse	younger than about 900 AD			Morris and Emery (1986)
45	Brough of Birsay	HY 239 285	One perforated piece of rounded pumice –	1	Norse/Pictish	late first millennium	HB 601 B		
66	Hawell	HY 512 065	Worked pumice piece from burnt mound		Burnt Mound	n/a	BG 322	1935.4 83	IO613
46	Howe, Birsay	HY 246 270	Piece of smoothed pumice from leather workers toolbox	1	Leather workers tool box (early Christian)	post 6th Century AD	FC 262.25	1952.3 86.25	Cursiter (1886), Callander (1931), Stevenson (1952)
65	Skara Brae, Skaill	HY 231 187	70 pieces of pumice	70					Ritchie and Clarke (1972)
			Two pieces of pumice, one smoothed	2	Neollithic village	c. 4500 14C years BP	HA 687	ND	

North Ronaldsay

No.	Site	Grid Ref.	Description	Pumice	Context	Age	NMS 1	NMS 2	Publication
47	Broch of Burrian	HY 762 513	Pumice, abraded from use as rubber	1	Broch (Iron Age or later)	Younger than 2000 14C years BP	GB 17 B	1872	Traill (1890a), Callander (1931)
			Pumice, abraded from use as rubber	1			GB 16 A	1872	
			Pumice, abraded from use as rubber	1			GB 15 A	1872	
			Pumice, abraded from use as rubber	1			GB 15 B	1872	
			Pumice, abraded from use as rubber	1			GB 18	1872	
			Pumice, abraded from use as rubber	1			GB 17 A	1872	
			Pumice, abraded from use as rubber	1			GB 16 B	1872	
			Pumice, abraded from use as rubber	1			GB 14	1872	MacGregor (1974)
			Pumice, abraded from use as rubber	1			GB 19	1872	
48	Hollandstoun (Hollandstown)	HY 751 538	n/a		n/a	n/a			Nat. Museum Collection (Binns, 1971)
49	Howe Mae (Howmae Brae)	HY 758 522	One piece grooved – dark brown	1	early Iron Age	2500-2000 14C years BP	GO 93	1884	Traill (1890b; 1885), Callander (1931)
			One piece grooved – dark brown	1			GO 92	1884	
			One piece grooved –	1			GO 91	1884	

No.	Site	Grid Ref.	Description	Pumice	Context	Age	NMS 1	NMS 2	Publication
			dark brown						
			One piece grooved – dark brown	1			GO 90	1884	
			One piece grooved – dark brown	1			GO 89	1884	
			One piece grooved dark brown	1			GO 87	1884	
			One piece grooved – dark brown	1			GO 88	1884	

Papa Westray

No.	Site	Grid Ref.	Description	Pumice	Context	Age	NMS 1	NMS 2	Publication
55	Hower	HY 49 54	One piece of pumice - brown	1	House (L Bronze-E. Iron Age)	2500-2000 14C years BP	HD 637	1937.291	Trail and Kirkness (1937)
			One piece of pumice - black	1			HD 636	1937.29	
			One piece of pumice - brown	1			HD 635	1937.289	
56	Knap of Howar	HY 483 518	13 pieces of pumice	13	Neolithic settlement	c. 4500 14C years BP	HD 2029	1975.192	
57	St Boniface	HY 488 526	22 pieces of pumice, one third grooved	22	Broch - Iron Age	c. 2000 14C years BP			Clarke (1991)

Rousay

No.	Site	Grid Ref.	Description	Pumice	Context	Age	NMS 1	NMS 2	Publication
58	Bay of Moaness	HY 378 292	14 pieces of pumice 1-5 cm in diameter	14	Inter-tidal deposits (-0.6 m OD)	older than 5000 BP			Buckland (1998)
59	Brinian House	HY 443 278	pumice	1	Unstratified deposit	n/a			RCAHMS
60	Gripps, Frotoft	HY 405 272	4 pieces of pumice	4	Souterrain (Iron Age)	2500-1200 14C years BP			Grant (1939)
61	Karston Farm	HY 443 296	pumice		Unstratified deposit	n/a			RCAHMS
62	Rinyo	HY 439 322	many		Late Neolithic	4300-4000 14C years BP			Childe and Grant (1939; 1948)
			Four pieces of rubbed pumice	4			HDA 286	1947.747	
			One piece, smoothed with grooves	1			HDA 157	1939.542	
			One piece, smoothed with grooves	1			HDA 151	1939.536	
			One piece, smoothed with grooves	1			HDA 150	1939.535	
			One piece, smoothed	1			HDA	1939.5	

No.	Site	Grid Ref.	Description	Pumice	Context	Age	NMS 1	NMS 2	Publication
			with grooves				148	33	
			One piece, smoothed with grooves	1			HDA 149	1939.5 34	
63	Taversoe Tuick, Trumland	HY 425 276	One small brown pendant	1	Chambered Cairn (late Neolithic)	4300-4000 14C years BP	EO 752	1938.1 96	Grant (1939), Henshall (1972)
64	Westness	HY 38 29	Four pieces of pumice Norse	4	Norse	Younger than about 900 AD	IL 741 B	1966.2 02 B	
			at least 2 pieces	2					Morris and Emery (1986)

Sanday

No.	Site	Grid Ref.	Description	Pumice	Context	Age	NMS 1	NMS 2	Publication
52	Pool	HY 619 378	164 pieces of pumice	164	Late Neolithic, Iron Age and Norse	c. 4000, 2500-1200 14C years BP			Smith (Forthcoming-c)
53	Quoyness, Els Ness	HY 676 378	One piece of medium grooved	1	Chambered Cairn (late Neolithic)	4300-4000 14C years BP	EO 947	1953.1 103	Childe (1952)
54	Tofts Ness	HY 760 470	256 pumice pieces	256					Smith (Forthcoming-a)
			1 piece of pumice	1	Broch? (Iron Age)	c. 2000 14C years BP			IO613 Cursitor (1885)

Stronsay

No.	Site	Grid Ref.	Description	Pumice	Context	Age	NMS 1	NMS 2	Publication
67	Huip	HY 636 304	1 pumice fragment	1	Settlement - age not known	n/a			RCAHMS

Westray

No.	Site	Grid Ref.	Description	Pumice	Context	Age	NMS 1	NMS 2	Publication
68	Pierowall Quarry	HY 43 48	7 pieces of pumice	7	mainly L Neolithic	4300-4000 14C years BP			Sharples (1984)

Unknown

No.	Site	Grid Ref.	Description	Pumice	Context	Age	NMS 1	NMS 2	Publication
69	Hirta souterrain	?	Three pumice pieces/ash	3	Iron Age souterrain	Younger than about 2200 14C years BP	HD 2080	1978.4 05	P.R. Richie (1974)
70	Unknown	?	Three pumice pieces/ash	3	n/a	n/a	HD 2068	1978.3 93	P.R. Richie (1974)

Scotland – Shetland

Fetlar

No.	Site	Grid Ref.	Description	Pumice	Context	Age	NMS 1	NMS 2	Publication
74	Kirkhouse Point and Still Farm	HU 659 911	One piece of pumice (Muirskirk)	1	n/a	n/a	HD 1923	1968	n/a

Foula

No.	Site	Grid Ref.	Description	Pumice	Context	Age	NMS 1	NMS 2	Publication
93	Churchyard (North Harrier?)	HT 957 404	Piece of perforated pumice	1	n/a	n/a	HR 1123	1956.4 11	n/a

Mainland

No.	Site	Grid Ref.	Description	Pumice	Context	Age	NMS 1	NMS 2	Publication
76	Clickhimin	HU 464 408	many various sizes, mainly brown		Broch (Iron Age)	younger than 2200 14C years BP			Hamilton (1968)
82	Gruting (Ness of)	HU 277 484	2 pieces of pumice one grooved	2			HD 1021	1952.4 92	
			1 piece of grooved and smoothed pumice	1	House (L. Neolithic - E. Bronze)	4300-3500 14C years BP	HD 900	1951.8 38	Calder (1958; 1962)
			2 pieces of pumice one grooved	2			HD 1022	1952.4 93	
			Piece of pumice smoothed	1			HD 1512	1953.9 22	
			One piece of pumice	1			HD 1543	1953.1	
			One piece of pumice	1			HD 1544	1953.1	
			One piece of grooved pumice	1			HD 1545	1953.1	
			One piece of grooved pumice	1			HD 1546	1953.1	
71	Ireland Wick	HU 374 213	pumice		Iron Age midden	2500-1200 14C years BP			RCAHMS
78	Islesburgh	HU 333 684	Two medium brown pumice pieces	2	House (L. Neolithic - E. Bronze)	4300-3500 14C years BP	HD 1824	1959.7 6	Calder (1965)
78	Islesburgh	HU 333 684	Utilised large black pumice piece	1			HD 1825	1959.7 7	
72	Jarlshof	HU 398 095	many, mainly brown		Early Neol., early Iron Age + Norse	4300-4000. c 2500, 1200 14C years BP			Curle (1933; 1935; 1936a) Hamilton (1956)
			Small piece of burnt	1			HSA	1973.1	

No.	Site	Grid Ref.	Description	Pumice	Context	Age	NMS 1	NMS 2	Publication
			pumice				1394	7	
			Piece of grooved pumice	1			HSA 3246	1964.6 26	
			Piece of grooved pumice	1			HSA 3430	1964.8 18	
			Box of pieces of pumice				HSA 3436	1964.8 24	
85	Kebister, Dales Voe	HU 457 455	60 pieces of pumice, 2/3 of which show wear.	60	Multi-period site (Bronze Age to post-medieval). Most pumice found in Iron Age and later contexts	younger than 3600 14C years BP			Dugmore and Newton (1999); Clark (1999)
86	Outnabreck (Scord Quarry)	HU 414 400	2 pieces of worked pumice	2	Ruined cairn	?			MacSween (unpublished)
79	Punds Water	HU 322 714	1 piece of dark brown pumice	1			HD 1816	1959.6 8	
			3 pieces of pumice	3	House (L. Neolithic, Bronze, Iron Age)	4300-1200 14C years BP			(Binns, 1971)
			1 piece of grey pumice	1			HD 1815	1959.6 7	
			1 piece of grooved, smoothed pumice	1			HD 1817	1959.6 9	
			1 piece of brown grooved pumice?	1			HD 1814	1959.6 6	
80	Sae Breck, Esha Ness	HU 210 780	3 medium brown and black	3	Broch (Iron Age)	Younger than 2200 14C years BP	GA 1229	1950.4 62	Calder (1952)
87	Scalloway	HU 40 40	at least 2 large black pieces of pumice and a white piece	2	Norse-Medieval	Younger than 900 AD			Biglow (unpublished)
83	Silwick	HU 290 426			Chambered cairn (Neolithic?)	5200-4000 14C years BP			
84	Stanydale	HU 285 502	1 brown pumice grooved	1	Earth houses, hut circles		HD 1094	1952.5 65	
			Brown oval pumice piece	1	Chambered cairns, House (Late Neol - E Bronze)	4300-3500 14C years BP	EO 805	1950.4 27	Calder (1950; 1958)
			1 brown pumice pendant	1			EO 791	1950.4 13	
81	The Cumlins, Olnefirth	HU 308 769	2 small pieces of pumice, well worn, 1 grooved	2			HD 741	1947.1 8	
88	Upper Scalloway	HU 406 399	347 pieces of pumice	347	Late Iron Age Broch (1st to 8th Century AD)	2030±40 - 1330 ± 70 14C years BP			Sharples (1998)

No.	Site	Grid Ref.	Description	Pumice	Context	Age	NMS 1	NMS 2	Publication
89	Weisdale Voe, Heglabister	HU 395 534	Piece of pumice from a burnt mound	1	Burnt mound		BN 150	1932.38	
73	Wiltrow, South Voe	HU 395 145	several		House (Bronze Age)	4000-2500 14C years BP			Curle (1936b)

Papa Stour

No.	Site	Grid Ref.	Description	Pumice	Context	Age	NMS 1	NMS 2	Publication
92	The Biggings, Papa Stour	HU 175 604	6 pieces of white/grey pumice, 15 brown pumice - some worked	21	Mainly Norse farm site and younger to 19th Century	11 Century to 19th Century, including 1362 AD Öræfajökull pumice			Newton (1999)

Unst

No.	Site	Grid Ref.	Description	Pumice	Context	Age	NMS 1	NMS 2	Publication
90	Clugan	HP 644 064	At least one piece of pumice	1	Iron Age - post broch age	younger than 2000 14C years BP			IO613 Small (1970)
91	Underhoull	HP 573 043	many in both levels - black		Early Iron Age to Norse	2500 to less than 1000 14C years BP			Small (1967)

West Burra

No.	Site	Grid Ref.	Description	Pumice	Context	Age	NMS 1	NMS 2	Publication
75	Brough	HU 378 349	One piece of grooved pumice	1			HR 1136	1956	
			One piece of grooved pumice	1	Refuse tips, broch nearby (probably Iron Age)	Younger than about 2200 14C years BP	HR 1135	1956	
149	Clettnadal	HU 357 299	1 piece of dark grey angular pumice 2cm long 1 cm across (Sample 2 (10-15cm) = 229-234	1	Inter-tidal peat deposit	9170±45 14C years BP			Buckland (pers. comm.)

Whalsay

No.	Site	Grid Ref.	Description	Pumice	Context	Age	NMS 1	NMS 2	Publication
77	The Bennie Hoose (Bunyie Hoose), Pettigarsfield	HU 586 652	Piece of grooved pumice	1			HD 861	1950.6 89	
			many dark brown		L. Neolithic, Bronze, Iron Age	3000-1200 14C years BP			Calder (1961), Henshall (1961)
			Pumice with two grooves	1			HD 1728	1955.2 95	

Yell

No.	Site	Grid Ref.	Description	Pumice	Context	Age	NMS 1	NMS 2	Publication
94	Breckon	HP 530 054	pumice		unstratified possibly iron age, eroding out of sand dunes	n/a			RCAHMS
95	Sands of Breckon	HP 53 05	75 small pieces of pumice	75	sand dunes				Carter and Fraser (1996)
			19 Brown and 1 white (O1362) pumice	20	Deflation surface of settlement site in sand dunes. Norse/Medieval	c. 14th Century, including 1362 AD Öræfajökull pumice			Buckland (pers. comm.)

Scotland – Western Isles

Barra

No.	Site	Grid Ref.	Description	Pumice	Context	Age	NMS 1	NMS 2	Publication
96	Allt Chrisal	NL 642 977	57 pieces of brown pumice, 21 worked	57	Neolithic-Beaker, Iron Age and Modern	4470 ± 60 14C years BP, 2500-1200 14C years BP, post 18th Century AD			Newton and Dugmore (1995)
97	Dùn Cuier	NF 664 034	1 medium grooved piece of pumice several more pieces	1	Roundhouse (Dun early Christian 4-7th C AD)	first millennium BC to pre-Norse roundhouse	GU 390	ND	Young (1956); Armit (1988)
99	Tigh Talamhanta, Allasdale	NF 676 022	Worked piece of pumice	2	Aisled longhouse (Iron Age)	2500-1200 14C years BP	GU 124	1958.3 29	Young (1953)
100	Vaslain	NF 693 057	1 piece of pumice	1	Hearths (Bronze Age?)	4000-2500 14C years BP			IO613 (Davies, 1973)

Benbecula

No.	Site	Grid Ref.	Description	Pumice	Context	Age	NMS 1	NMS 2	Publication
138	Roisinish	NF 872 538	Rectangular pumice pendant	1	unstratified in Machair	n/a	GR 82	1975.1 41	Crawford (1977)

Ensay

No.	Site	Grid Ref.	Description	Pumice	Context	Age	NMS 1	NMS 2	Publication
107	Ensay	NF 973 867	pumice		Beaker midden (Early Bronse Age)	c. 3650 14C years BP			RCAHMS

Harris

No.	Site	Grid Ref.	Description	Pumice	Context	Age	NMS 1	NMS 2	Publication
108	Northton	NF 98 90	ca. 180 pieces mainly brown	180	Middens (Neolithic, Beaker, Iron Age)	c. 4530-4300, c. 3690-3570, c. 2500-1200 14C years BP			Binns (1971); Simpson (1976)

Lewis

No.	Site	Grid Ref.	Description	Pumice	Context	Age	NMS 1	NMS 2	Publication
101	Barvas Machair 1	NB 348 516	36 pieces of pumice, many worked	36	Late Bronze/Early Iron Age late 2nd/early 1st mill. BC	3000-2500 14C years BP			Cowie (unpublished)
102	Barvas Machair 2	NB 351 519	5 pieces of pumice, two pieces worked	5	Norse site	10-11th Century AD			Cowie (unpublished)
145	Barvas Machair 3	NB 349 518	3 pieces of pumice	3	Beaker burial (Early Bronze Age)	c. 3650 14C years BP			Cowie (unpublished)
140	Cleit na h-Uamha, Loch Tealasavay	NB 037 183	One piece of pumice	1	Cave	not known	HR 988	1949.303	PSAS (1948-9) IO613
141	Cnip, Bhaltos	NB 099 364	3 pieces of pumice	3	Iron Age wheelhouse	c. 2000-1850 14C years BP			Newton (Forthcoming-c)
139	Eilean nan Caorach, Holm	NB 460 306	Piece of unworked pumice	1	n/a	n/a	HRC 64	1980.772	IO613 PSAS (1982)
103	Galson, Borve	NB 437 594	2 pieces of pumice	2	Middens (early Christian)	c. 1500-1100 14C years BP			Edwards (1924)
104	High Borve	NB 420 555	1 pumice disk with hole drilled - float	1	n/a	n/a			IO613 DES (1983)
105	Mol a' Chladaich, Arnol	NB 303 483	One large piece of pumice	1	n/a	n/a	HR 1338	1973.201	n/a
106	Swainbost (Suaincbost), Ness	NB 506 640	some pumice		Iron Age surface samples - uncertain age	2500-1200 14C years BP			Cowie, unpublished

South Uist

No.	Site	Grid Ref.	Description	Pumice	Context	Age	NMS 1	NMS 2	Publication
109	Bac Mhic Connain	NF 769 761	11 pieces of pumice	11	Wheelhouse (Iron Age)				Callander (1931), Beveridge (1931)
			Fragment of pumice stone	1		c. 2100-1850 14C BP	GNA 117	1921.125	

No.	Site	Grid Ref.	Description	Pumice	Context	Age	NMS 1	NMS 2	Publication
110	Buaile, Risary	NF 766 729	5 small	5	Dun (Iron Age - early Christian)	2000-1000 14C years BP			Beveridge (1911)
111	Caerdach Rudh, Baleshare (Baile Sear)	NF 776 615	Two pieces of grooved pumice	2			GT 1268	1975.176	
			44 pieces of brown and black pumice	44	Bronze Age - Iron Age	c. 3400 to 2050 14C years BP			Newton and Dugmore (Forthcoming-a)
112	Clettraval (Cleitreabhal)	NF 749 713	One brown piece, one side worn flat	1	Chambered cairn (L. Neo-beaker), Aisled round house (Iron Age)	c. 4500-3600, and 2450-1550 14C BP	EO 503	1935.249	Scott (1935)
			One half a whorl of pumice	1			HD 1331	1953.646	
			One half a whorl of pumice	1			HD 1332	1953.647	
113	Cnoc a' Comhdalach, Grimnish (Grìminis)	NF 770 741	1 medium brown pumice	1	Aisled round house (Iron Age)	2500-1200 14C years BP			Beveridge (1931), Callander (1931)
114	Dùn Aonghuis	NF 856 738			Dun (Iron Age or later)	younger than c. 2500 14C years BP			Beveridge (1911)
115	Dùn Cnon A' Comdhalalch	?	One piece ground on one side	1	Iron Age, either Atlantic roundhouse or wheelhouse	c. 2100-1850 14C BP or possibly older	GT 30	1912 p.340	Armit (1996)
116	Dùn na Dise, Eilean nan Carnan	NF 807 617	shaped pumice	1					IO613
			1 medium piece of pumice	1	Dun (Iron Age early Christian)	2500-1100 14C years BP	GT 561	1963.42	Beveridge (1911)
117	Dùn Thomaidh, Vallay Sound	NF 759 758			Dun with later structures	Younger than 2500 14C years BP			Beveridge (1931), Callander (1931)
118	Eilean an Tighe, Loch nan Geirann	NF 842 731	Pumice piece	1			EOA 457	1953 p.506	
			1 piece of pumice	1					IO613
			22 pieces of pumice	22					Scott (1951)
			7 pieces of grooved pumice	7	Neolithic Settlement	c. 4000-2500 14C years BP	EOA 456	1953 p.505	Beveridge (1911, 1931), Callander (1931), Scott (1951)
119	Eilean Domhnuill, Loch Olabhat (Eilean Olavat)	NF 749 752	116 pieces of pumice	116	Neolithic	c. 4500-4380 14C years BP			Smith (Forthcoming-b)
120	Eileann Maleit	NF 774 738			Aisled round house (Iron - E. Christian)	c. 2500-1200 14C years BP			Beveridge (1911)
121	Foshigarry	NF 742 764	46 pieces of small, medium brown pumice, many showing evidence of rubbing	46	Aisled round and wheelhouses (Iron Age)	c. 2100-1850 14C years BP	GNA 307	1921 p.307	Beveridge (1931), Callander (1931), Armit (1996)
122	Garry Iochdrach, Vallay	NF 772 742	One pumice pendant	1	Aisled round house (Iron - E. Christian)	c. 2100-1200 14C years BP	GT 516	1962.474	Beveridge (1931)

No.	Site	Grid Ref.	Description	Pumice	Context	Age	NMS 1	NMS 2	Publication
123	Geirisclett, Vallay Sound	NF 767 753	Oval piece of pumice	1	Iron Age	c. 2500-1200 14C years BP	GT 674	1963.16	Beveridge (1911)
124	Machair Leathann	NF 822 775	Piece of pumice [(appor NF822755) F Ack 1978/17	1	n/a	n/a	GT 1355	1978.143	n/a
125	Old Cattle Fold, (prob. Lombaidh) Vallay	NF 761 756	1 medium brown pumice	1	Iron Age - early Christian	2500-1200 14C years BP	GT 367	1934.3	Beveridge (1911)
126	Rudh' an Duin, Vallay	NF 786 761	Piece of pumice	1	Dun (early Christian)	Younger than 1500 14C years BP	GT 784	1963.27	Beveridge (1911)
127	The Udal	NF 824 784	1 medium piece	1	Midden in sandhills (E Christian)	Younger than c. 1500 14C years BP			Beveridge (1911)
			138 pieces of pumice	138	E Neolithic Age - Bronze Age - Modern	5200-4500 and 4100 - 2500 BP 14C years BP			Newton (Forthcoming-a)
128	Unival	NF 800 668	Pendant of pumice	1	Chambered cairn (Late Neolithic)	c.4100 14C years BP	EO 870	1951.44	Scott (1948), Calder (1950), Piggot (1954), Henshall (1972)
129	Unknown	?	3 pieces of pumice	3	archaeological	n/a	GT 897	1963.384	n/a

Pabbay

No.	Site	Grid Ref.	Description	Pumice	Context	Age	NMS 1	NMS 2	Publication
98	Pabbay (Pabaigh)	NL 60 87	3 pieces of light brown pumice, elongated vesicles - smoothed and grooved	3	?				Branigan (unpublished)

South Uist

No.	Site	Grid Ref.	Description	Pumice	Context	Age	NMS 1	NMS 2	Publication
130	A' Cheardach Mhor, Drimore	NF 756 412	6 pieces	6	Wheelhouse (Iron Age)	c. 2200-1800 14C years BP	GSA 364 A	1976.219	Young and Richardson (1960)
			One piece (1 of 4)	1			GSA 365	1976.219	
			One piece (1 of 4)	1			GSA 366	1976.219	
			One piece (1 of 4)	1			GSA 367	1976.219	
			2 small (black and brown). 28 in total	2					
			One piece (1 of 11)	1			GSA 363	1976.219	
			One piece (1 of 4)	1			GSA 368	1976.219	

No.	Site	Grid Ref.	Description	Pumice	Context	Age	NMS 1	NMS 2	Publication
			One piece (1 of 11)	1			GSA 361	1976.2 19	
			One piece (1 of 11)	1			GSA 360	1976.2 19	
			One piece (1 of 11)	1			GSA 359	1976.2 19	
			One piece (1 of 11)	1			GSA 358	1976.2 19	
			One piece (1 of 11)	1			GSA 357	1976.2 19	
			One piece (1 of 11)	1			GSA 356	1976.2 19	
			One piece (1 of 11)	1			GSA 355	1976.2 19	
			One piece (1 of 11)	1			GSA 354	1976.2 19	
			One piece (1 of 11)	1			GSA 362	1976.2 19	
			One piece (1 of 11)	1			GSA 353	1976.2 19	
			One large piece	1			GSA 364	1976.2 19	
131	Bruthach a Sithean (Kilpheder)	NF 733 202	2 pieces facetted by rubbing	2	Aisled wheelhouse	c. 2200-1800 14C years BP	GS 138	1958 p.669	
			2 pieces of grooved pumice	2			GS 161	1958 p.692	
			2 pieces facetted by rubbing	2			GS 139	1958 p.670	
							GS 140		
132	Cill Donain (Kildonan)	NF 28 72	At least 41 pieces of pumice, mainly brown with some black	41	Iron Age midden	c. 1900-1600 14C years BP			Newton (unpublished)
133	Cille Pheadair (Kilpheder)	NF 733 702	A least one piece of pumice	1	Iron Age wheelhouse	c. 2200-1800 14C years BP			Newton (unpublished), Mike Parker Pearson (pers. comm.)
134	Cladh Hallan, Daliburgh	NF 729 221	A few pieces of black pumice		Shell midden	n/a			RCAHMS
135	Daliburgh	NF 73 22	One piece of brown pumice	1			GS 236	1970 p.181	
136	Gorton	NF 804 143	pumice fragments		Midden - beaker shards	c. 3650 14C years BP			
137	Loch Hallan, Daliburgh	NF 73 21	1 piece of pumice	1	Middens	n/a			IO613 PSAS 1915-6, 14-5, 47-8

Scotland – Mainland sites

Aberdenshire

No.	Site	Grid Ref.	Description	Pumice	Context	Age	NMS 1	NMS 2	Publication
8	Old Keig	NJ 596 193	n/a		Stone circle (L. Neolithic - Bronze)	4500-3000 14C years BP			Childe (1934)

Dumfries and Galloway

No.	Site	Grid Ref.	Description	Pumice	Context	Age	NMS 1	NMS 2	Publication
17	Glenluce Sands	NX 17 56	Rounded pumice from beach in 1960	1	Modern beach	Modern	BH 9207	1962.2 2	
18	Mid Torrs, Glen Luce	NX 12 53	2 small - black/dark brown	2	Sand dunes on PG shoreline	5700-3900 BP			Binns (1967)

East Lothian

No.	Site	Grid Ref.	Description	Pumice	Context	Age	NMS 1	NMS 2	Publication
21	Ghegan, Seacliff	NT 603 848	1 piece	1	Midden (Iron Age)	c 2500-1200 14C years BP			Laidlay (1870), Callander (1931)
20	Longniddry	NT 42 75	many small – brown		Post-glacial raised shoreline (3-4 m)	4100-2400 14C years BP			Binns (1971)
19	Traprain Law	NT 580 747	Pumice used as a rubber, 3 medium - dk grey/brown to brown	3	Iron Age	2500-1200 14C years BP	GV 1308	1924.2 1	Cree (1924)

Highland

No.	Site	Grid Ref.	Description	Pumice	Context	Age	NMS 1	NMS 2	Publication
32	Embo - chambered cairn	NH 817 926	1 medium sized piece	1	Chambered cairn (L. Neolithic)	4500-4100 14C years BP			Henshall and Wallace (1963)
33	Embo - raised shoreline	NH 81 93			6.8 m shoreline				Binns (1972)
35	Golspie	NL 834 003	Trapeze shaped pumice pendant	1	Cist (Iron Age - Dark Age)	2500-1200 14C years BP	EQ 628	1960.6 3	Woodham and Mackenzie (1957), IO613
147	Golspie	check	6 small pieces of black/brown pumice	6	Raised beach				Newton (unpublished)
148	Ord North, Lairg	NC 573 056			Chambered Cairn (Neolithic	4260±60 (GU-1168) and 4665±70 (GU1169)			Sharples, N. (1981) PSAS 111
22	Risga, Loch Sunart	NM 611 599	n/a		Mesolithic midden	older than 5200 14C years BP			Hunterian Museum Collection
36	Rubha'n Achaidh Mhóir/Beinn an	NM 65 94	Nine piece of pumice from a small bay	9	n/a	n/a	HR 1652	1980.7	n/a

	Achaidh Mhóir		between two sites						
34	Strathnaver	NC 73 52	n/a		unknown - donation	n/a			IO613 PSAS (1886)

Moray

No.	Site	Grid Ref.	Description	Pumice	Context	Age	NMS 1	NMS 2	Publication
40	Green Castle, Portknockie	NJ 488 687	8 pieces of pumice	8	L Bronze Age - Pictish	first millennium BC to the first millennium AD			Newton and Dugmore (Forthcoming-b)

North Ayrshire

No.	Site	Grid Ref.	Description	Pumice	Context	Age	NMS 1	NMS 2	Publication
43	Ardeer	NS 27 42	many - brown		Post-glacial raised shoreline	4100-2400 BP			Smith (1896), Binns (1971; 1972)
41	Shewalton Moor	NS 33 36	many small or medium - brown		Post-glacial raised shoreline	5700-5500 BP			Smith (1896), Reade (1896), Binns (1971; 1972)

Appendix

2

Published geochemical data on pumice from the North Atlantic Region

Location	Sample	SiO_2	TiO_2	Al_2O_3	FeO	MnO	MgO	CaO	Na_2O	K_2O	Total	Reference
Canada												
C.Storm, Ellesmere Island	243	60.85	1.21	15.30	5.97	0.19	1.40	3.70	4.90	2.60	97.90	Blake (1970)
C.Storm, Ellesmere Island	244	60.78	1.18	19.10	5.60	0.19	1.10	3.10	4.90	2.50	100.00	Blake (1970)
C.Storm, Ellesmere Island	245	59.88	1.18	14.70	5.68	0.20	1.60	3.20	4.70	2.60	96.70	Blake (1970)
C.Storm, Ellesmere Island	246	62.17	1.18	14.90	5.60	0.18	1.60	3.10	4.80	2.60	99.00	Blake (1970)
C.Storm, Ellesmere Island	247	62.16	1.26	15.30	5.72	0.19	1.70	3.40	5.00	2.60	99.00	Blake (1970)
C.Storm, Ellesmere Island	248	61.47	1.21	16.50	5.68	0.19	1.40	3.60	4.90	2.60	99.40	Blake (1970)
C. Hawes, Devon	249	60.91	1.18	16.30	5.50	0.18	1.90	3.50	4.90	2.60	99.40	Blake (1970)
C. Hawes, Devon	250	61.44	1.18	15.40	5.60	0.19	1.50	3.50	5.00	2.60	98.60	Blake (1970)
Greenland												
Julianhaab	3	63.53	1.05	13.72	6.25	0.18	1.22	3.90	5.39	2.35	99.59	Noe-Nygaard (1951)
Svalbard												
V. Tvillingneset	235	64.82	1.16	15.60	5.41	0.18	1.60	3.10	5.10	2.70	100.70	Blake (1970)
Jaderinfjorden	236	65.27	1.16	15.20	5.59	0.18	1.90	3.00	5.00	2.70	101.00	Blake (1970)
Planiusbukta	237	65.05	1.15	15.70	5.59	0.18	1.00	3.10	5.10	2.70	100.60	Blake (1970)
Ripfjorden W	238	64.29	1.13	15.00	5.49	0.18	1.30	2.90	5.00	2.70	99.60	Blake (1970)
Ripfjorden W	239	63.78	1.09	17.00	5.28	0.18	1.10	2.80	5.00	2.70	100.20	Blake (1970)
Ripfjorden SE	240	65.60	1.05	15.10	5.27	0.18	1.10	2.70	5.10	2.80	99.70	Blake (1970)
Zordrargerfjorden	241	63.81	1.28	15.50	6.23	0.19	1.30	3.30	4.90	2.60	100.40	Blake (1970)
Zordrargerfjorden	242	52.82	1.58	20.40	7.05	1.20	0.23	2.20	4.30	3.10	99.70	Blake (1970)
Bohemanneset	48	64.20	1.25	14.40	5.70	0.18	1.29	3.44	4.20	1.90	97.43	Binns (1971)
Brageneset	49	62.70	2.82	13.60	7.95	0.16	2.32	9.31	3.80	3.00	103.84	Binns (1971)

Location	Sample	SiO_2	TiO_2	Al_2O_3	FeO	MnO	MgO	CaO	Na_2O	K_2O	Total	Reference
Tempelfjorden	51	53.59	3.26	17.96	6.96	0.68	2.55	6.53	4.54	3.18	100.03	Binns (1971)
Langgrunnodden	50	64.39	0.54	13.96	6.22	-	1.34	3.58	5.16	2.88	98.76	Bäckström (1890)
Scandinavia												
Revsbotn, Norway	13	64.40	1.08	14.60	5.91	0.20	-	3.07	5.20	1.70	97.03	Binns (1971)
Revsbotn, Norway	14	51.80	2.41	17.50	8.18	0.22	3.79	6.41	4.16	1.90	97.81	Binns (1971)
Revsbotn, Norway	16	64.00	1.18	14.80	6.07	0.20	-	3.50	5.00	1.90	97.52	Binns (1971)
Girsavaguoppe, Norway	22	64.00	1.17	14.70	5.84	0.19	-	3.01	5.00	1.80	96.55	Binns (1971)
Girsavaguoppe, Norway	24	63.90	1.10	14.20	5.29	0.18	-	2.89	4.90	1.70	94.91	Binns (1971)
Øra, Kornfjord, Norway	27	65.80	1.20	14.60	5.88	0.20	1.34	2.89	4.90	1.80	99.45	Binns (1971)
Bleik, Andøya, Norway	35	69.00	0.12	14.80	1.96	0.08	0.27	1.44	4.40	2.60	95.04	Binns (1971)
Nordmjele, Norway	37	65.10	0.33	13.60	3.45	0.11	0.05	1.10	6.00	4.00	94.42	Binns (1971)
Vearoy, Norway	42	63.20	1.22	14.40	5.70	0.19	1.22	3.34	4.50	1.90	96.55	Binns (1971)
Blomøy, Norway	2	62.33	0.97	14.25	6.01	0.17	1.06	4.04	5.61	2.40	99.61	Noe-Nygaard (1951)
Petvik, Norway	1	63.90	1.40	14.40	5.76	0.19	1.30	3.10	5.10	2.80	99.60	Peulvast and Dejou (1982)
Sovkrog, Denmark	1	63.16	0.87	13.84	6.03	0.13	1.06	4.03	5.58	2.40	99.57	Noe-Nygaard (1951)
Scotland												
Northton, Harris	2	63.80	1.25	14.60	5.97	0.19	1.41	3.29	4.95	1.80	98.10	Binns (1971)
Northton, Harris	4	64.00	1.19	14.60	5.92	0.19	1.40	3.35	4.90	1.80	98.21	Binns (1971)
Northton, Harris	5	63.00	1.16	14.60	5.94	0.19	-	3.70	5.10	1.70	96.26	Binns (1971)
Shewalton Moor, Ayrshire	7	64.40	1.25	14.60	5.79	0.18	1.38	3.06	4.90	1.90	98.30	Binns (1971)
Shewalton Moor, Ayrshire	8	61.30	1.45	14.60	6.02	0.18	1.46	3.21	4.30	1.70	95.08	Binns (1971)
Burrian, Orkney	9	63.70	1.22	14.70	6.18	0.21	-	3.21	4.70	1.80	96.58	Binns (1971)
Silwick, Shetland	10	53.70	2.12	17.80	4.02	0.21	2.94	6.48	3.90	2.20	94.42	Binns (1971)

Appendix

3

New geochemical data on pumice from the North Atlantic

Appendix 3A: Norwegian Pumice EPMA Data

Site	Pumice	SiO_2	TiO_2	Al_2O_3	FeO	MnO	MgO	CaO	Na_2O	K_2O	Total
Brandsvik	**BV 1**	66.61	1.27	14.12	5.39	0.14	0.98	2.78	4.49	2.90	98.68
	BV 1	66.53	1.21	14.13	5.21	0.11	1.09	2.91	4.58	3.08	98.85
	BV 1	66.09	1.16	14.23	5.61	0.13	1.16	2.80	4.60	3.01	98.79
	BV 1	65.65	1.01	14.17	5.41	0.13	1.06	2.98	4.60	2.78	97.79
	BV 1	65.50	1.24	13.79	5.21	0.19	1.05	2.79	4.88	2.90	97.56
	BV 1	65.45	1.15	14.07	5.15	0.10	1.27	3.03	4.70	2.83	97.75
	BV 1	65.12	1.12	13.79	5.27	0.17	1.04	2.90	4.42	2.63	96.46
	BV 1	64.99	1.10	13.33	5.56	0.23	1.06	2.66	4.51	3.03	96.48
	BV 1	64.94	1.13	13.85	4.98	0.22	0.99	2.73	4.39	2.89	96.14
	BV 1	63.90	1.16	13.49	5.30	0.19	1.12	2.73	4.64	2.89	95.42
	BV 2	66.62	1.06	13.88	5.03	0.16	1.08	2.82	4.81	2.92	98.38
	BV 2	66.35	1.12	13.93	5.02	0.12	1.12	2.85	4.59	2.87	97.97
	BV 2	65.91	1.22	14.01	5.32	0.18	1.05	3.16	4.71	2.88	98.44
	BV 2	65.86	1.04	13.73	4.65	0.17	0.96	2.97	4.59	2.84	96.82
	BV 2	65.83	1.21	14.05	5.32	0.16	1.15	2.83	4.64	2.92	98.11
	BV 2	65.05	1.14	13.86	5.08	0.13	1.09	2.77	4.57	2.89	96.57
	BV 2	64.74	1.07	13.76	4.78	0.12	1.17	3.06	4.66	2.72	96.10
	BV 2	64.61	1.14	14.11	5.22	0.16	1.05	2.78	4.68	3.04	96.80
	BV 2	64.48	1.14	13.86	4.86	0.12	1.11	2.81	4.44	2.87	95.71
	BV 2	63.54	1.13	14.04	5.22	0.19	1.05	2.65	4.66	3.17	95.65
	BV 3	66.42	1.02	14.04	4.99	0.09	1.13	2.87	4.71	3.00	98.27
	BV 3	66.28	1.16	14.04	5.26	0.22	1.07	2.94	4.77	2.89	98.63
	BV 3	65.91	1.07	14.10	5.61	0.15	1.22	3.18	4.59	2.88	98.71
	BV 3	65.49	1.18	14.12	5.30	0.08	0.94	2.97	4.43	2.84	97.35
	BV 3	65.35	1.17	14.04	5.42	0.14	1.13	3.05	4.77	2.94	98.01
	BV 3	65.20	1.15	13.89	5.27	0.12	1.13	2.92	4.55	2.86	97.10
	BV 3	64.90	1.22	13.66	5.05	0.17	1.16	3.38	4.56	2.78	96.87
	BV 3	64.79	1.17	13.52	5.36	0.16	1.13	3.11	4.73	2.74	96.72
	BV 3	64.31	1.13	13.72	5.23	0.15	1.03	2.96	4.53	2.81	95.88
	BV 3	64.09	1.08	13.58	5.21	0.14	1.13	2.94	4.85	2.69	95.70
	BV 4	66.18	1.24	13.92	5.40	0.18	1.23	3.00	4.23	2.91	98.29
	BV 4	65.74	1.25	13.78	5.27	0.12	1.19	3.00	4.36	2.97	97.68
	BV 4	65.69	1.16	13.76	5.52	0.19	1.15	3.10	4.25	2.84	97.66
	BV 4	65.36	1.24	13.72	4.60	0.13	1.17	2.98	4.62	2.90	96.72
	BV 4	65.27	1.07	14.28	5.43	0.15	1.10	3.11	4.47	2.66	97.54
	BV 4	65.25	1.07	13.95	5.43	0.13	1.14	3.04	4.55	2.91	97.47
	BV 4	65.03	1.17	14.04	5.36	0.18	1.08	3.28	4.72	2.84	97.70
	BV 4	64.98	1.14	14.04	5.06	0.16	1.13	3.11	4.73	2.94	97.29
	BV 4	64.94	1.10	13.96	5.55	0.18	1.14	2.97	4.50	2.82	97.16
	BV 4	64.71	1.10	14.00	5.01	0.12	1.21	3.01	4.69	2.87	96.72

Site	Pumice	SiO_2	TiO_2	Al_2O_3	FeO	MnO	MgO	CaO	Na_2O	K_2O	Total
Gjøsund U	**GJU 1**	66.82	1.09	14.29	5.57	0.16	1.09	3.03	4.86	2.96	99.87
	GJU 1	66.54	1.11	14.01	5.58	0.16	1.18	3.23	4.45	2.69	98.95
	GJU 1	66.30	1.19	13.96	5.52	0.16	1.19	3.33	4.75	2.65	99.05
	GJU 1	66.04	1.19	13.95	5.75	0.20	1.24	3.21	4.58	2.85	99.01
	GJU 1	65.77	1.11	14.14	5.26	0.21	1.15	3.03	4.65	2.84	98.16
	GJU 1	65.72	1.23	14.23	5.60	0.23	1.21	3.34	4.67	2.83	99.06
	GJU 1	65.57	1.19	13.66	5.75	0.21	1.26	3.23	4.65	2.65	98.17
	GJU 1	65.48	1.14	13.99	5.41	0.17	1.18	3.28	4.61	2.88	98.14
	GJU 1	65.41	1.07	14.00	5.71	0.17	1.17	3.33	4.61	2.75	98.22
	GJU 1	65.30	1.27	13.77	5.80	0.22	1.19	3.36	4.58	2.63	98.12
	GJU 2	65.87	1.08	14.21	5.19	0.24	1.08	2.86	4.56	2.96	98.05
	GJU 2	65.78	1.11	13.94	5.21	0.20	1.08	2.96	4.51	3.33	98.12
	GJU 2	65.52	1.21	13.90	5.45	0.16	1.09	2.85	4.69	2.89	97.76
	GJU 2	65.39	1.17	14.37	5.43	0.20	1.11	3.13	4.59	2.96	98.35
	GJU 2	65.37	1.03	13.72	5.03	0.11	1.11	2.82	4.33	2.98	96.50
	GJU 2	65.34	1.06	13.79	5.16	0.18	1.04	2.87	4.65	2.83	96.92
	GJU 2	65.01	1.11	14.07	5.29	0.20	1.03	3.09	4.52	3.09	97.41
	GJU 2	64.88	1.10	14.12	5.48	0.21	1.11	3.03	4.64	2.87	97.44
	GJU 2	64.72	1.18	13.53	5.61	0.17	1.07	2.65	4.84	3.18	96.95
	GJU 3	66.83	1.20	13.42	5.32	0.16	0.90	2.36	4.38	2.92	97.49
	GJU 3	66.18	1.03	14.20	5.27	0.12	1.14	2.82	4.64	2.78	98.18
	GJU 3	65.81	1.15	14.41	5.02	0.18	1.08	2.87	4.45	2.70	97.67
	GJU 3	65.75	1.24	13.40	5.28	0.16	1.11	2.65	4.77	2.93	97.29
	GJU 3	65.68	1.04	14.48	5.24	0.20	1.03	2.91	4.64	2.84	98.06
	GJU 3	65.67	1.07	14.51	5.37	0.18	1.07	2.73	4.71	2.82	98.13
	GJU 3	65.52	1.10	14.57	5.50	0.21	1.12	2.97	4.79	3.00	98.78
	GJU 3	65.34	1.16	14.13	5.05	0.20	1.02	2.83	4.57	2.87	97.17
	GJU 3	64.88	1.19	14.28	5.30	0.25	1.01	2.91	4.59	2.72	97.13
	GJU 3	64.62	1.20	13.97	5.51	0.18	1.06	2.87	4.66	2.88	96.95
	GJU 4	65.98	1.14	14.03	5.42	0.17	1.10	3.25	4.92	2.77	98.78
	GJU 4	65.44	1.13	14.67	5.79	0.17	1.13	3.01	4.59	2.68	98.61
	GJU 4	65.24	1.21	14.11	5.49	0.12	1.18	3.09	4.51	2.69	97.64
	GJU 4	65.20	1.09	13.93	5.41	0.19	1.13	2.97	4.66	2.77	97.35
	GJU 4	65.16	1.16	14.11	5.70	0.19	1.13	3.09	4.60	2.78	97.92
	GJU 4	65.00	1.13	14.06	5.59	0.18	1.10	3.10	4.84	2.81	97.81
	GJU 4	64.68	0.93	13.38	5.69	0.18	1.20	3.30	4.87	2.88	97.11
	GJU 4	64.67	1.18	13.59	5.70	0.20	1.15	3.30	4.74	2.74	97.27
	GJU 4	64.49	1.00	14.28	5.67	0.17	1.15	3.00	4.89	2.91	97.56
Gjøsund U	**GJL 1**	66.56	1.37	13.92	5.77	0.19	1.10	3.12	4.80	2.81	99.64
	GJL 1	66.11	1.22	13.98	5.77	0.16	1.14	3.34	2.85	2.71	97.28
	GJL 1	66.01	1.29	13.98	5.59	0.17	1.11	3.14	4.68	2.82	98.79
	GJL 1	65.86	1.28	14.01	5.91	0.16	1.28	3.13	4.65	2.68	98.96
	GJL 1	65.22	1.32	13.98	5.82	0.14	1.01	3.01	4.50	2.81	97.81
	GJL 1	65.13	1.37	13.94	5.81	0.13	1.10	3.22	4.69	2.90	98.29
	GJL 1	64.90	1.27	13.93	5.75	0.19	1.21	3.12	4.94	2.17	97.48
	GJL 1	64.83	1.29	13.73	5.92	0.14	1.18	3.06	4.59	2.80	97.54
	GJL 1	64.79	1.20	14.06	5.45	0.17	1.06	2.72	4.59	2.84	96.88
	GJL 1	64.48	1.26	12.66	5.77	0.13	1.17	2.96	4.75	2.90	96.08
	GJL 1	64.36	1.18	13.69	6.12	0.16	1.16	2.95	4.71	2.87	97.20
	GJL 2	65.26	1.20	13.63	5.76	0.18	1.12	3.07	2.45	2.78	95.45

Site	Pumice	SiO_2	TiO_2	Al_2O_3	FeO	MnO	MgO	CaO	Na_2O	K_2O	Total
	GJL 2	65.05	1.28	13.78	5.78	0.19	1.07	3.13	4.60	2.76	97.64
	GJL 2	64.87	1.23	13.76	5.68	0.17	1.16	3.15	4.73	2.86	97.61
	GJL 2	64.85	1.35	13.69	5.65	0.17	1.10	3.03	4.57	2.84	97.25
	GJL 2	64.79	1.18	13.79	5.88	0.14	1.10	3.15	4.50	2.63	97.16
	GJL 2	64.78	1.15	13.40	5.85	0.16	1.13	3.12	4.72	2.77	97.08
	GJL 2	64.71	1.44	13.60	5.79	0.20	1.14	3.13	4.52	2.82	97.35
	GJL 2	64.49	1.23	13.70	5.58	0.19	1.12	3.11	4.33	2.93	96.68
	GJL 2	64.45	1.26	13.62	5.88	0.17	1.13	3.07	4.46	2.75	96.79
	GJL 2	64.26	1.22	13.51	5.55	0.18	1.23	2.97	4.72	2.79	96.43
	GJL 3	66.85	1.21	14.28	5.27	0.18	1.04	2.82	4.67	2.93	99.25
	GJL 3	66.03	1.22	14.04	5.09	0.10	0.91	2.83	4.72	2.85	97.79
	GJL 3	65.61	1.22	14.02	5.79	0.17	1.28	3.24	4.81	2.98	99.12
	GJL 3	65.53	1.07	14.26	5.63	0.14	1.14	3.33	4.71	2.85	98.66
	GJL 3	65.51	1.28	13.90	5.68	0.16	1.17	3.14	4.46	2.80	98.10
	GJL 3	65.48	1.26	13.96	5.95	0.18	1.15	3.17	4.63	2.73	98.51
	GJL 3	65.43	1.16	13.96	5.59	0.18	1.15	2.99	4.88	2.88	98.22
	GJL 3	65.24	1.18	13.98	5.77	0.14	1.10	3.17	4.66	2.83	98.07
	GJL 3	64.92	1.17	14.44	5.21	0.14	1.10	2.88	4.57	2.80	97.23
	GJL 3	64.55	1.12	13.38	5.76	0.14	1.20	3.14	4.55	2.83	96.67
	GJL 4	66.76	1.14	14.10	5.02	0.19	1.11	2.36	4.94	3.20	98.82
	GJL 4	66.11	1.28	14.19	5.65	0.19	1.15	3.13	4.57	2.91	99.18
	GJL 4	65.98	1.15	14.15	5.68	0.16	1.15	3.11	4.94	2.83	99.15
	GJL 4	65.81	1.19	14.19	5.38	0.15	1.18	3.33	4.70	2.96	98.89
	GJL 4	65.81	1.12	14.17	5.52	0.15	1.23	3.11	4.82	2.84	98.77
	GJL 4	65.72	1.27	14.03	5.85	0.22	1.16	2.78	5.04	2.51	98.58
	GJL 4	65.72	1.31	13.95	5.17	0.09	1.16	3.37	4.50	3.17	98.44
	GJL 4	65.65	1.08	14.21	4.77	0.14	1.02	2.85	4.80	2.65	97.17
	GJL 4	65.58	1.35	14.16	5.73	0.18	1.15	3.20	4.87	2.99	99.21
	GJL 4	65.54	1.24	13.94	5.36	0.15	1.11	3.14	4.92	2.97	98.37
	GJL 4	65.52	1.31	13.80	5.77	0.16	1.14	2.93	4.25	3.95	98.83
	GJL 4	65.30	1.12	13.75	5.72	0.05	1.13	3.04	4.69	2.88	97.68
	GJL 4	65.28	1.21	13.61	5.57	0.10	1.12	3.15	4.51	3.39	97.94
	GJL 4	65.27	1.27	14.18	5.46	0.16	1.22	3.29	4.88	2.79	98.52
	GJL 4	65.21	1.23	13.69	5.67	0.15	1.15	3.15	4.81	2.99	98.05
	GJL 4	65.18	1.21	14.03	5.37	0.19	1.07	3.05	4.75	3.21	98.06
	GJL 4	65.05	1.14	14.07	5.67	0.23	1.15	2.87	4.55	2.92	97.65
	GJL 4	65.05	1.30	13.82	5.41	0.16	1.24	2.93	4.77	2.67	97.35
	GJL 4	65.03	1.20	13.69	5.77	0.15	1.14	2.96	4.72	3.11	97.77
	GJL 4	64.72	1.21	13.89	5.70	0.11	1.15	3.05	4.44	2.87	97.14
	GJL 4	64.64	1.29	14.01	5.60	0.23	1.19	2.99	4.83	2.80	97.58
	GJL 4	64.24	1.20	14.15	5.73	0.14	1.12	3.00	4.34	3.87	97.79
Kobbvika L	**KVL 1**	67.60	1.28	12.83	5.23	0.15	0.56	1.93	4.46	3.24	97.28
	KVL 1	67.59	1.29	12.91	5.64	0.20	0.65	2.26	4.83	3.17	98.54
	KVL 1	67.58	1.04	14.79	3.80	0.12	0.41	2.69	5.70	2.65	98.78
	KVL 1	67.24	1.18	13.65	4.80	0.13	0.51	2.11	4.85	3.15	97.62
	KVL 1	67.06	1.17	13.58	4.97	0.20	0.62	2.54	4.67	2.94	97.75
	KVL 1	66.65	1.20	13.89	5.54	0.15	0.52	2.89	5.23	3.02	99.09
	KVL 1	64.92	0.78	16.74	3.48	0.09	0.78	3.61	5.92	2.07	98.39
	KVL 1	64.64	1.11	13.64	5.20	0.22	1.70	4.02	5.03	2.10	97.66
	KVL 1	64.35	1.38	14.70	6.99	0.27	1.09	3.53	5.10	2.36	99.77

Site	Pumice	SiO_2	TiO_2	Al_2O_3	FeO	MnO	MgO	CaO	Na_2O	K_2O	Total
	KVL 2	65.55	1.12	13.76	5.62	0.19	1.18	2.93	4.41	2.85	97.61
	KVL 2	65.52	1.28	13.86	5.54	0.20	1.10	2.92	4.58	3.04	98.04
	KVL 2	65.41	1.12	13.81	5.53	0.20	1.06	2.66	4.83	2.92	97.54
	KVL 2	65.34	1.20	13.65	5.55	0.17	1.18	3.00	4.29	3.28	97.66
	KVL 2	65.16	1.03	12.51	5.47	0.23	1.04	3.03	4.47	3.76	96.70
	KVL 2	64.45	1.12	13.36	5.70	0.11	1.18	2.68	4.26	3.87	96.73
	KVL 2	64.27	1.28	13.92	5.72	0.22	1.13	3.25	5.47	2.28	97.54
	KVL 3	67.44	1.28	12.79	5.40	0.25	0.87	2.38	4.55	3.14	98.10
	KVL 3	67.15	1.21	13.53	5.17	0.21	0.91	2.59	4.56	3.02	98.35
	KVL 3	66.51	1.18	13.95	5.03	0.18	0.81	2.71	4.66	2.77	97.80
	KVL 3	66.51	1.23	13.68	5.06	0.19	0.71	2.60	4.62	3.01	97.61
	KVL 3	66.38	1.15	14.62	4.58	0.17	0.74	2.80	5.18	2.88	98.50
	KVL 3	66.12	1.39	12.11	5.93	0.24	0.89	2.36	4.60	3.04	96.68
	KVL 3	65.90	1.31	12.87	5.77	0.23	1.07	2.54	4.28	2.81	96.78
	KVL 3	64.75	0.76	16.39	3.82	0.11	0.60	3.65	5.61	2.15	97.84
	KVL 3	64.02	0.97	16.16	4.53	0.20	0.75	3.64	5.51	2.11	97.89
	KVL 4	67.96	1.14	13.36	5.16	0.20	0.73	2.60	4.31	3.03	98.49
	KVL 4	67.49	1.11	13.60	4.92	0.18	0.69	2.62	4.59	3.05	98.25
	KVL 4	67.46	1.30	12.95	5.19	0.19	0.71	2.48	4.41	3.26	97.95
	KVL 4	67.24	1.13	13.14	5.06	0.24	0.86	2.18	4.45	3.20	97.50
	KVL 4	66.59	1.20	12.19	6.97	0.31	1.96	2.49	4.08	3.20	98.99
	KVL 4	66.55	1.19	13.86	4.92	0.14	0.63	2.67	5.06	2.73	97.75
	KVL 4	66.14	1.13	14.37	4.59	0.13	0.67	3.19	5.42	2.50	98.14
	KVL 4	65.97	1.33	12.79	6.02	0.25	0.97	2.30	4.06	3.21	96.90
	KVL 4	65.76	1.29	14.48	5.58	0.20	0.67	2.67	4.77	2.75	98.17
	KVL 4	65.57	1.48	12.74	6.13	0.27	1.71	2.80	4.26	3.07	98.03
	KVL 5	67.59	1.08	13.28	5.35	0.21	1.07	2.47	4.44	3.02	98.52
	KVL 5	67.35	1.27	13.73	5.38	0.19	0.83	2.72	4.42	2.90	98.79
	KVL 5	66.46	0.97	13.46	5.59	0.18	0.97	2.81	4.41	2.91	97.99
	KVL 5	66.38	1.08	12.94	5.26	0.20	0.61	2.28	4.97	2.85	96.57
	KVL 5	66.34	1.25	11.89	6.05	0.26	1.06	2.46	4.98	3.00	97.32
	KVL 5	66.17	1.08	14.49	4.89	0.13	1.00	3.27	4.79	2.45	98.28
	KVL 5	65.41	1.19	13.66	4.60	0.23	0.68	3.56	4.34	3.18	96.84
	KVL 5	65.35	1.00	14.12	5.29	0.20	1.26	3.26	4.84	2.69	98.12
	KVL 5	64.62	1.35	13.22	4.75	0.18	1.44	2.94	4.05	3.05	95.60
	KVL 5	64.23	0.98	16.49	4.25	0.17	0.77	2.95	4.72	2.88	97.47
Kobbvika L	**KVM 1**	66.41	1.42	13.92	5.70	0.27	1.29	3.19	2.54	2.66	97.40
	KVM 1	66.22	1.22	14.05	5.36	0.23	1.13	2.84	4.62	2.75	98.42
	KVM 1	65.98	1.10	14.02	5.65	0.21	1.12	2.92	4.74	2.62	98.36
	KVM 1	65.84	1.30	14.05	5.71	0.22	1.25	2.78	4.55	2.73	98.43
	KVM 1	65.79	1.30	13.72	5.77	0.19	1.20	3.00	4.60	2.60	98.17
	KVM 1	65.49	1.22	14.02	5.91	0.20	1.28	3.17	4.75	2.74	98.78
	KVM 1	65.05	1.39	13.83	5.40	0.21	1.20	2.95	4.36	2.88	97.27
	KVM 1	64.83	1.20	14.00	5.79	0.18	1.19	3.11	4.41	2.87	97.58
	KVM 1	64.81	1.22	13.97	6.40	0.24	1.23	3.27	4.59	2.71	98.44
	KVM 1	64.60	1.32	13.64	5.96	0.21	1.21	3.00	4.52	2.76	97.22
	KVM 2	66.00	1.37	13.94	5.34	0.20	1.05	2.69	4.54	2.75	97.88
	KVM 2	65.98	1.24	13.96	5.47	0.16	1.11	2.82	4.67	2.97	98.38
	KVM 2	65.55	1.23	13.65	5.78	0.18	1.15	3.08	4.49	2.70	97.81
	KVM 2	65.38	1.33	14.06	5.89	0.19	1.13	3.05	4.51	2.70	98.24

Site	Pumice	SiO_2	TiO_2	Al_2O_3	FeO	MnO	MgO	CaO	Na_2O	K_2O	Total
	KVM 2	65.35	1.18	14.45	5.77	0.23	1.19	3.11	4.56	2.72	98.56
	KVM 2	65.14	1.24	13.89	5.81	0.28	1.19	3.11	4.66	2.72	98.04
	KVM 2	65.04	1.20	14.03	5.55	0.25	1.23	3.05	4.69	2.68	97.72
	KVM 2	64.78	1.19	13.46	5.38	0.18	1.09	2.93	4.52	2.83	96.36
	KVM 2	64.40	1.14	12.86	5.79	0.24	1.10	2.93	4.71	2.55	95.72
	KVM 2	64.39	1.23	13.83	5.63	0.20	1.06	3.08	4.49	2.71	96.62
	KVM 3	66.47	1.30	13.77	5.61	0.18	1.14	2.91	4.29	2.86	98.53
	KVM 3	66.40	1.42	13.85	5.81	0.20	1.13	2.95	4.55	2.78	99.09
	KVM 3	66.17	1.23	13.47	5.78	0.17	1.05	2.92	4.55	2.85	98.19
	KVM 3	66.13	1.14	14.04	5.90	0.18	1.14	2.90	4.72	2.89	99.04
	KVM 3	65.78	1.26	13.88	5.79	0.22	1.11	2.99	4.57	2.86	98.46
	KVM 3	65.61	1.29	13.57	5.48	0.23	1.10	2.75	4.43	3.25	97.71
	KVM 3	65.57	1.27	14.27	5.77	0.19	1.11	2.96	4.65	2.73	98.52
	KVM 3	65.43	1.29	13.78	5.77	0.22	1.00	3.04	4.46	2.94	97.93
	KVM 3	65.27	1.31	13.90	5.40	0.21	1.05	2.97	4.48	2.81	97.40
	KVM 3	65.26	1.29	13.79	5.97	0.19	1.05	2.90	4.66	2.85	97.96
	KVM 4	65.87	1.21	13.74	5.73	0.21	1.01	2.77	4.43	2.79	97.76
	KVM 4	65.80	1.15	13.58	5.79	0.15	1.03	2.62	4.43	2.98	97.53
	KVM 4	65.66	1.23	13.83	5.78	0.20	1.07	2.81	4.52	2.76	97.86
	KVM 4	65.56	1.24	13.86	5.52	0.17	1.11	2.82	4.43	2.89	97.60
	KVM 4	65.51	1.22	12.98	5.23	0.17	0.97	2.57	4.30	2.82	95.77
	KVM 4	65.36	1.23	13.98	5.65	0.20	1.09	2.70	4.55	2.80	97.56
	KVM 4	65.24	1.21	13.65	5.57	0.17	1.05	2.71	4.34	2.75	96.69
	KVM 4	65.21	1.31	13.93	5.56	0.19	1.07	2.73	4.54	2.92	97.46
	KVM 4	65.12	1.33	13.68	5.54	0.23	1.05	3.05	4.35	2.75	97.10
	KVM 4	65.11	1.28	13.80	5.70	0.19	1.07	2.83	4.33	2.89	97.20
	KVM 5	66.80	1.23	14.03	5.73	0.22	1.22	3.04	4.50	2.70	99.47
	KVM 5	66.65	1.17	13.89	5.50	0.16	1.17	3.07	4.43	2.72	98.75
	KVM 5	66.30	1.24	13.90	5.47	0.17	1.18	2.96	4.45	2.86	98.55
	KVM 5	65.91	1.17	13.79	5.67	0.16	1.18	3.85	4.37	2.72	98.76
	KVM 5	65.81	1.23	14.02	5.81	0.16	1.21	3.20	3.96	2.80	98.21
	KVM 5	65.71	1.16	13.94	5.65	0.20	1.20	3.22	4.22	2.74	98.05
	KVM 5	65.59	1.15	14.14	5.15	0.20	1.12	3.28	4.37	2.80	97.80
	KVM 5	65.45	1.25	13.62	5.65	0.24	1.04	2.98	4.52	2.88	97.62
	KVM 5	65.37	1.17	13.90	5.58	0.18	1.21	3.23	4.19	2.73	97.57
	KVM 5	64.64	1.19	13.76	5.61	0.21	1.16	3.18	4.45	2.76	96.97
Kobbvika U	**KVU 1**	66.65	1.12	13.96	5.27	0.15	1.11	2.90	4.66	2.79	98.61
	KVU 1	66.40	1.13	13.91	4.49	0.12	1.02	2.72	4.66	3.03	97.48
	KVU 1	65.98	1.22	14.19	5.30	0.15	1.22	3.09	4.89	2.90	98.94
	KVU 1	65.73	1.13	14.12	5.47	0.19	1.13	3.14	4.44	2.66	98.01
	KVU 1	65.73	1.25	14.01	5.41	0.15	1.11	3.19	4.66	2.97	98.48
	KVU 1	65.70	1.11	14.00	5.14	0.15	1.20	3.02	4.68	2.89	97.89
	KVU 1	65.52	1.24	13.59	5.78	0.16	1.27	3.18	4.48	2.78	98.00
	KVU 1	65.20	1.19	13.80	5.60	0.17	1.24	3.16	4.57	2.66	97.59
	KVU 1	65.11	1.24	13.81	5.68	0.19	1.30	3.10	4.61	2.67	97.71
	KVU 1	65.08	1.23	13.87	5.73	0.17	1.25	3.39	4.83	2.81	98.36
	KVU 1	65.04	1.21	14.27	5.56	0.19	1.08	2.95	4.65	2.68	97.63
	KVU 1	64.83	1.22	14.01	5.58	0.15	1.20	3.20	4.58	2.83	97.60
	KVU 2	65.79	1.28	14.07	5.47	0.22	1.21	3.06	4.51	2.72	98.33
	KVU 2	65.56	1.25	13.82	5.55	0.24	1.31	3.30	4.29	2.67	97.99

Site	Pumice	SiO_2	TiO_2	Al_2O_3	FeO	MnO	MgO	CaO	Na_2O	K_2O	Total
	KVU 2	65.18	1.24	13.89	5.95	0.20	1.25	3.33	4.51	2.67	98.22
	KVU 2	65.17	1.34	13.86	5.42	0.21	1.26	3.15	4.57	2.60	97.58
	KVU 2	65.03	1.15	14.08	5.08	0.16	1.12	3.13	4.51	2.91	97.17
	KVU 2	64.99	1.21	14.37	5.32	0.18	1.14	3.23	4.60	2.83	97.87
	KVU 2	64.88	1.22	13.84	5.85	0.21	1.31	3.32	4.33	2.74	97.70
	KVU 2	64.81	1.23	13.85	5.32	0.21	1.17	3.16	4.73	2.86	97.34
	KVU 2	64.66	1.23	13.89	5.48	0.13	1.33	3.14	4.57	2.86	97.29
	KVU 2	64.58	1.30	14.23	5.68	0.20	1.20	3.23	4.53	2.90	97.85
	KVU 3	67.02	1.07	13.81	5.11	0.18	0.97	2.55	4.67	2.88	98.26
	KVU 3	66.67	1.17	13.99	5.35	0.19	1.17	3.12	4.45	2.76	98.87
	KVU 3	65.71	1.23	13.97	5.00	0.13	1.07	2.96	4.59	2.95	97.61
	KVU 3	65.64	1.26	14.10	5.51	0.20	1.20	3.12	4.65	2.74	98.42
	KVU 3	65.51	1.12	14.22	5.28	0.19	1.21	2.94	4.47	2.96	97.90
	KVU 3	65.51	1.15	13.70	5.51	0.21	1.13	3.11	4.52	2.83	97.67
	KVU 3	64.93	1.15	13.75	5.58	0.37	1.09	3.18	4.72	2.97	97.74
	KVU 3	64.58	1.11	13.95	5.46	0.14	1.11	2.87	4.69	2.98	96.89
	KVU 3	64.02	1.28	14.04	5.77	0.10	1.26	3.11	4.63	2.85	97.06
	KVU 3	63.85	1.25	13.57	5.54	0.18	1.17	2.91	4.72	2.72	95.91
	KVU 4	65.87	1.26	14.18	5.26	0.14	1.23	3.08	4.46	2.75	98.23
	KVU 4	65.60	1.15	14.06	5.99	0.20	1.17	3.07	4.52	2.65	98.41
	KVU 4	65.45	1.18	14.00	5.57	0.18	1.18	2.95	4.61	2.72	97.84
	KVU 4	65.12	1.16	13.69	5.60	0.22	1.22	2.97	4.45	2.68	97.11
	KVU 4	64.85	1.26	13.94	5.57	0.15	1.25	3.31	4.64	2.70	97.67
	KVU 4	64.74	1.25	13.93	5.30	0.14	1.08	3.05	4.70	2.93	97.12
	KVU 4	65.07	1.28	14.02	5.38	0.17	1.15	3.08	4.75	2.87	97.77
	KVU 4	65.12	1.17	14.17	5.43	0.17	1.17	3.09	4.51	2.81	97.64
	KVU 4	64.86	1.18	13.98	5.55	0.14	1.21	3.19	4.67	2.73	97.51
	KVU 4	65.05	1.22	13.88	5.48	0.22	1.19	3.15	4.66	2.87	97.72
	KVU 5	46.12	4.56	12.42	14.37	0.20	4.97	9.47	3.23	0.75	96.09
	KVU 5	46.19	4.77	12.40	14.53	0.22	4.98	9.54	3.21	0.79	96.63
	KVU 5	46.79	4.64	12.33	14.27	0.26	4.95	9.50	3.26	0.77	96.78
	KVU 5	46.09	4.63	12.47	14.38	0.23	4.99	9.38	3.29	0.72	96.20
	KVU 5	46.65	4.48	12.32	14.40	0.23	4.91	9.52	3.23	0.78	96.53
	KVU 6	66.16	1.20	14.25	5.62	0.21	1.20	3.24	4.69	2.57	98.78
	KVU 6	66.12	1.19	13.63	5.46	0.15	1.20	3.24	4.69	2.86	98.55
	KVU 6	65.99	1.21	13.85	5.82	0.20	1.01	3.18	4.59	2.80	98.62
	KVU 6	65.61	1.29	14.10	5.34	0.18	1.12	3.20	4.38	2.80	98.02
	KVU 6	65.17	1.17	14.01	5.32	0.24	1.21	3.16	4.55	2.81	97.64
	KVU 7	66.33	1.34	13.77	5.45	0.18	1.17	3.04	4.48	2.98	98.75
	KVU 7	65.30	1.27	13.95	5.39	0.16	1.16	3.26	4.50	2.90	97.88
	KVU 7	65.71	1.24	13.71	5.26	0.19	1.21	3.26	4.75	2.74	98.09
	KVU 7	66.14	1.28	13.67	5.76	0.16	1.19	3.10	4.49	2.80	98.58
	KVU 7	66.12	1.24	13.80	5.47	0.17	1.10	3.17	4.73	2.71	98.50
	KVU 8	67.19	1.15	13.73	4.77	0.14	0.83	2.59	4.61	2.98	98.99
	KVU 8	66.16	1.01	13.66	4.89	0.12	0.89	2.50	4.64	3.11	96.98
	KVU 8	67.54	1.11	13.80	4.93	0.17	0.92	2.44	4.37	2.99	98.28
	KVU 8	67.98	1.00	13.70	4.97	0.09	0.75	2.41	4.51	3.02	98.42
	KVU 8	67.07	1.15	13.89	4.73	0.16	0.87	2.42	4.64	3.04	97.97
	KVU 9	66.01	1.21	14.00	5.58	0.13	1.24	3.00	4.63	2.78	98.57
	KVU 9	66.42	1.11	14.02	5.31	0.21	1.02	2.86	4.56	2.76	98.32

Site	Pumice	SiO_2	TiO_2	Al_2O_3	FeO	MnO	MgO	CaO	Na_2O	K_2O	Total
	KVU 9	66.07	1.10	13.61	5.77	0.19	1.15	3.25	4.48	2.79	98.42
	KVU 9	65.04	1.21	13.98	5.80	0.14	1.13	3.10	4.51	2.89	97.82
	KVU 10	65.70	1.12	13.86	5.13	0.14	1.01	2.88	4.54	2.75	97.13
	KVU 10	66.94	1.09	13.72	5.27	0.09	0.99	2.86	4.59	2.89	98.43
	KVU 10	66.51	1.02	13.83	4.90	0.20	1.01	2.74	4.79	2.81	97.82
	KVU 11	66.25	1.33	13.69	5.58	0.16	1.24	3.12	4.73	2.79	98.89
	KVU 11	66.53	1.22	13.83	5.31	0.16	1.05	3.06	4.56	2.92	98.63
	KVU 11	64.44	1.17	13.57	5.58	0.19	1.26	3.08	4.53	2.83	96.64
	KVU 12	64.18	1.21	13.83	5.77	0.17	0.95	3.05	4.71	2.80	96.66
	KVU 12	65.86	1.26	13.51	5.80	0.17	1.21	3.30	4.58	2.83	98.52
	KVU 12	66.16	1.21	13.87	5.26	0.23	1.23	3.21	4.50	2.97	98.63
	KVU 13	66.67	1.10	13.92	5.22	0.17	1.15	3.11	4.46	2.81	98.62
	KVU 13	66.10	1.14	13.73	5.30	0.15	1.06	2.82	4.64	2.86	97.79
	KVU 13	65.95	1.05	13.83	5.20	0.18	1.11	3.14	4.76	2.73	97.97
Ramså	**R 1**	67.06	1.19	14.14	5.32	0.13	1.06	2.94	5.04	2.70	99.58
	R 1	66.63	1.25	13.96	5.36	0.16	1.10	3.21	5.18	2.62	99.47
	R 1	66.58	1.14	14.26	5.57	0.14	1.20	2.78	5.25	2.79	99.71
	R 1	66.47	1.19	14.07	5.27	0.16	1.14	2.98	5.40	2.74	99.42
	R 1	66.10	1.25	13.95	5.45	0.22	1.09	2.92	5.07	2.74	98.79
	R 1	66.05	1.10	13.95	5.39	0.23	1.09	2.91	5.21	2.96	98.89
	R 1	65.99	1.19	13.71	5.35	0.19	1.10	3.10	5.01	2.98	98.62
	R 1	65.91	1.07	14.12	5.50	0.15	1.07	2.94	5.02	2.61	98.39
	R 1	65.88	1.22	14.28	5.33	0.17	1.14	3.04	4.88	2.67	98.61
	R 1	65.77	1.22	14.28	5.43	0.17	1.07	2.90	5.29	2.68	98.81
	R 2	66.32	1.15	14.07	5.46	0.21	1.05	2.66	5.15	2.81	98.88
	R 2	66.31	1.25	14.32	5.21	0.15	1.03	2.66	5.04	2.74	98.71
	R 2	66.21	1.08	13.98	5.84	0.24	1.13	2.73	5.01	2.59	98.81
	R 2	65.70	1.21	13.73	5.73	0.19	1.12	2.82	5.29	2.68	98.47
	R 2	65.63	1.11	13.92	5.66	0.14	1.14	2.77	5.03	2.81	98.21
	R 2	65.32	1.22	14.16	5.28	0.16	1.00	2.72	5.18	2.71	97.75
	R 2	65.29	1.27	14.01	5.62	0.15	1.13	2.81	5.18	2.90	98.36
	R 2	65.16	1.06	14.04	5.84	0.18	1.14	2.67	4.98	2.72	97.79
	R 2	65.14	1.19	13.85	5.81	0.21	1.16	2.69	5.13	2.63	97.81
	R 2	65.10	1.06	14.04	5.53	0.18	1.16	2.95	5.35	2.82	98.19
	R 3	66.20	1.11	14.05	5.64	0.16	1.14	2.79	4.54	2.74	98.37
	R 3	66.03	1.09	14.11	5.95	0.20	1.18	3.11	4.52	2.62	98.81
	R 3	65.84	1.16	14.20	5.45	0.16	1.13	2.80	4.98	2.79	98.51
	R 3	65.72	1.16	14.23	5.83	0.21	1.27	2.90	4.62	2.72	98.66
	R 3	65.37	1.23	13.76	5.12	0.23	1.18	2.85	4.68	2.74	97.16
	R 3	65.37	1.14	13.79	5.59	0.19	1.07	2.91	4.78	2.79	97.63
	R 3	65.15	1.22	13.93	5.70	0.23	1.09	3.13	4.83	2.70	97.98
	R 3	65.14	1.28	14.15	5.65	0.18	1.22	2.95	4.57	2.68	97.82
	R 3	64.95	1.16	14.12	5.46	0.19	1.09	3.20	4.74	2.95	97.86
	R 3	64.69	1.15	14.18	5.60	0.16	1.14	2.91	4.57	2.65	97.05
	R 4	65.72	1.20	13.96	5.53	0.19	1.13	2.92	4.70	2.88	98.23
	R 4	65.59	1.25	14.12	5.75	0.15	1.18	2.98	4.60	2.78	98.40
	R 4	65.55	1.32	14.26	5.39	0.14	1.05	2.96	4.77	2.81	98.25
	R 4	65.54	1.18	14.18	5.78	0.20	1.12	2.89	4.48	2.82	98.19
	R 4	65.23	1.20	14.33	5.65	0.15	1.16	2.93	4.33	2.85	97.83
	R 4	64.96	1.21	14.20	5.81	0.14	1.13	2.99	4.54	2.72	97.70

Site	Pumice	SiO_2	TiO_2	Al_2O_3	FeO	MnO	MgO	CaO	Na_2O	K_2O	Total
	R 4	64.81	1.19	13.94	5.67	0.19	1.16	2.98	4.60	2.74	97.28
	R 4	64.77	1.26	13.89	5.20	0.22	1.16	2.92	4.61	2.76	96.79
	R 4	64.74	1.26	14.12	5.79	0.17	1.08	2.85	4.72	2.70	97.43
	R 4	64.71	1.25	13.70	5.91	0.17	1.15	3.16	4.39	2.67	97.11
Storvik	ST 1	68.23	1.34	12.75	5.58	0.14	0.63	2.12	4.54	3.32	98.65
	ST 1	67.19	1.30	13.06	5.60	0.21	0.84	2.33	4.42	3.28	98.23
	ST 1	67.12	1.00	14.31	4.81	0.17	0.53	2.65	5.42	2.83	98.83
	ST 1	66.66	1.19	13.18	6.12	0.18	1.57	2.91	4.76	2.96	99.53
	ST 1	64.86	1.14	14.64	5.95	0.26	1.29	3.53	5.55	2.37	99.59
	ST 2	66.95	1.16	14.03	5.03	0.16	1.05	2.86	4.72	2.66	98.62
	ST 2	66.86	1.23	13.90	5.40	0.20	1.16	2.89	4.51	2.65	98.80
	ST 2	66.28	1.19	13.96	5.66	0.17	1.13	3.03	4.80	2.68	98.90
	ST 2	66.20	1.12	13.86	5.16	0.15	1.09	2.87	4.69	2.98	98.12
	ST 2	65.58	1.26	14.13	5.62	0.23	1.17	3.04	4.89	2.69	98.61
	ST 2	65.40	1.11	14.03	5.81	0.19	1.20	2.98	5.25	2.83	98.80
	ST 2	65.17	1.19	14.11	5.51	0.23	1.18	2.88	4.79	2.72	97.78
	ST 2	64.86	1.29	13.70	5.62	0.18	1.22	2.89	4.78	2.72	97.26
	ST 2	64.72	1.30	13.95	5.57	0.18	1.20	3.08	4.91	2.76	97.67
	ST 2	64.49	1.22	14.18	5.74	0.20	1.14	3.13	4.75	2.74	97.59
	ST 3	67.11	1.15	13.79	5.29	0.21	1.01	2.94	4.57	2.79	98.86
	ST 3	66.74	1.36	14.11	5.40	0.21	1.13	3.06	4.74	2.66	99.41
	ST 3	66.73	1.30	14.25	5.55	0.19	1.13	3.10	4.68	2.59	99.52
	ST 3	66.33	1.24	14.13	5.68	0.15	1.11	2.79	4.77	2.71	98.91
	ST 3	66.28	1.20	13.85	5.39	0.22	1.10	3.04	4.63	2.78	98.49
	ST 3	66.20	1.29	14.20	5.44	0.20	1.05	2.96	4.67	2.69	98.70
	ST 3	66.19	1.15	14.14	5.34	0.19	1.10	2.91	5.03	2.71	98.76
	ST 3	65.48	1.20	13.86	5.80	0.20	1.11	3.04	4.49	2.68	97.86
	ST 3	65.32	1.19	14.10	5.58	0.21	1.13	2.82	4.60	2.75	97.70
	ST 3	65.00	1.17	14.19	5.52	0.25	1.16	2.92	4.77	2.70	97.68
	ST 4	66.61	1.24	14.63	5.85	0.18	1.14	3.15	2.34	2.84	97.98
	ST 4	66.29	1.38	14.13	5.94	0.19	1.14	3.04	4.53	2.95	99.59
	ST 4	66.25	1.10	14.08	5.49	0.21	1.16	2.87	4.72	2.82	98.70
	ST 4	66.19	1.28	13.91	5.44	0.16	1.14	2.99	4.79	2.57	98.47
	ST 4	65.99	1.14	14.10	5.64	0.19	1.16	3.03	4.60	2.60	98.45
	ST 4	65.88	1.13	14.15	5.70	0.15	1.12	3.05	4.51	2.65	98.34
	ST 4	64.88	1.15	13.48	5.46	0.20	1.03	3.04	4.34	2.74	96.32
	ST 4	64.82	1.30	14.30	5.60	0.17	1.19	3.07	4.56	2.65	97.66
	ST 4	64.79	1.22	13.86	5.76	0.20	1.14	3.23	4.39	2.67	97.26
Trandvikan	T 1	72.25	0.19	13.49	3.21	0.14	0.02	1.01	4.95	3.64	98.90
	T 1	72.03	0.27	13.68	3.21	0.10	0.04	0.97	5.28	3.54	99.12
	T 1	71.97	0.19	13.21	3.38	0.06	0.06	1.03	4.42	3.43	97.75
	T 1	71.67	0.22	13.52	3.27	0.13	0.07	0.95	5.08	3.57	98.48
	T 1	71.58	0.18	13.51	3.30	0.08	0.04	0.96	5.04	3.60	98.29
	T 1	71.48	0.23	13.29	3.40	0.08	0.02	1.00	3.86	3.67	97.03
	T 1	71.40	0.26	13.84	3.29	0.12	0.05	1.07	5.58	3.37	98.98
	T 1	71.33	0.16	13.16	3.18	0.13	0.03	1.10	4.71	3.55	97.35
	T 1	71.19	0.19	12.88	3.17	0.08	0.03	0.99	4.68	3.43	96.64
	T 1	70.63	0.18	13.03	3.39	0.13	0.02	0.89	4.91	3.30	96.48

Appendix 3B: Norwegian Raised Beach Pumice SIMS Data

Site	Pumice	Ti	Rb	Sr	Y	Zr	Nb	Ba	La	Ce
Kobbvika	**KVU 3**	5804	42.9	236.0	54.4	731.5	90.5	484.2	63.9	138.3
	KVU 3	5727	41.2	226.5	54.4	725.0	91.2	463.1	61.6	134.5
	KVU 3	5575	43.0	217.8	53.6	739.4	93.1	480.2	63.5	134.2
	KVU 3	5857	43.2	235.6	55.0	746.1	92.9	492.7	64.4	138.0
	KVU 3	5720	41.7	230.8	53.0	718.0	89.1	475.6	62.7	132.6
	KVU 3	5384	33.8	328.1	50.6	672.9	82.4	470.0	62.3	130.6
	KVU 3	5793	42.0	233.5	54.1	731.9	90.6	480.9	63.9	133.7
	KVM 1	5961	41.7	230.0	53.1	731.2	90.4	466.6	61.0	130.3
	KVM 1	6156	42.4	243.3	57.9	774.6	98.4	511.0	69.0	148.2
	KVM 1	6123	42.7	253.9	58.6	779.4	97.8	513.3	69.5	149.3
	KVM 1	6135	43.5	231.0	56.5	764.2	98.9	485.0	66.6	143.6
	KVM 1	6022	45.3	229.0	53.1	759.6	99.9	488.5	63.0	136.0
	KVM 1	6037	43.5	240.4	55.6	760.4	95.2	495.3	65.6	139.3
	KVL 1	6654	49.5	170.1	60.1	872.6	108.9	518.4	72.8	157.5
	KVL 1	5856	42.3	228.3	55.9	802.8	98.3	491.8	67.9	142.9
	KVL 1	5816	41.5	302.7	53.2	772.2	95.2	524.8	66.3	139.8
	KVL 1	6394	39.7	283.6	54.1	767.6	93.7	495.2	65.9	142.0
	KVL 1	6576	43.0	219.7	54.4	788.0	97.0	491.1	66.0	140.0
	KVL 1	6065	49.8	143.3	58.6	850.4	104.7	478.3	66.6	143.3
	KVL 1	5514	46.5	222.2	54.0	804.4	98.5	509.3	64.9	139.5
	KVL 1	5805	51.6	170.1	60.7	866.4	105.4	526.8	70.5	149.6
	KVL 1	6301	50.7	129.9	58.0	848.0	104.9	490.4	66.7	143.3
	KVL 1	5587	45.4	247.3	53.8	782.8	95.4	496.3	64.8	137.2
Gjøsund	**GJU 1**	5655	43.0	227.8	53.9	729.9	94.7	476.9	64.0	134.6
	GJU 1	5628	43.0	225.1	54.7	730.3	94.1	472.3	62.8	134.5
	GJU 1	5612	43.2	233.9	56.0	756.9	98.7	503.4	66.3	140.0
	GJU 1	5647	42.4	224.5	55.0	733.5	93.0	477.9	64.8	134.9
	GJU 1	5711	42.6	239.0	56.1	749.6	95.7	500.0	65.9	141.5
	GJU 1	5683	40.0	224.2	55.3	751.0	93.4	477.7	64.3	136.6
	GJU 1	5740	40.8	241.9	57.4	762.5	93.8	499.2	67.4	144.8
	GJL 2	5874	40.5	249.7	55.0	748.5	93.1	493.4	65.3	140.0
	GJL 2	5863	41.8	250.3	55.2	748.6	93.1	492.7	65.6	141.1
	GJL 2	5933	42.1	254.1	55.7	758.0	94.5	500.6	67.8	145.5
	GJL 2	5875	41.7	249.7	52.7	719.4	89.7	472.8	63.1	133.9
	GJL 2	5847	41.2	242.7	53.9	734.4	91.3	476.5	64.3	137.4
	GJL 2	5755	41.7	244.6	52.0	732.9	90.2	478.7	62.9	135.7
	GJL 2	5902	37.6	248.9	55.5	748.6	89.9	481.9	66.1	141.0
	GJL 2	5902	37.5	245.4	54.9	740.6	90.2	473.3	64.7	137.4
	GJL 2	5975	37.3	245.0	56.7	755.6	92.3	469.9	68.1	143.7

Appendix 3C: Icelandic Raised Beach Pumice EPMA Data

Site	Pumice	SiO_2	TiO_2	Al_2O_3	FeO	MnO	MgO	CaO	Na_2O	K_2O	Total
Bær	BR 1	67.61	1.21	13.98	5.04	0.16	0.94	2.50	5.01	3.08	99.53
	BR 1	67.48	1.21	14.03	5.06	0.18	1.01	2.69	4.80	2.83	99.29
	BR 1	67.21	1.21	14.27	5.13	0.34	0.96	2.46	5.02	2.77	99.37
	BR 1	67.01	1.15	13.84	5.35	0.16	1.02	2.70	5.02	2.87	99.12
	BR 1	65.97	1.24	14.06	5.41	0.09	1.06	2.73	4.94	2.92	98.42
	BR 1	65.92	1.04	14.05	5.30	0.18	0.93	3.03	5.27	2.69	98.41
	BR 1	65.82	1.16	14.08	5.36	0.14	1.09	2.73	5.07	2.89	98.34
	BR 1	65.72	1.08	14.14	4.95	0.14	0.96	2.79	5.17	2.90	97.85
	BR 1	65.66	1.11	13.99	5.67	0.20	1.15	2.72	5.01	2.72	98.23
	BR 1	65.63	1.13	14.04	5.22	0.19	1.08	2.62	5.08	2.89	97.88
	BR 1	64.24	1.08	14.31	4.84	0.14	0.94	2.55	5.07	2.97	96.14
	BR 2	67.17	1.22	14.24	5.18	0.12	1.10	2.84	4.93	2.73	99.53
	BR 2	67.03	1.24	14.33	5.06	0.13	1.12	2.80	5.16	2.80	99.67
	BR 2	66.52	1.14	13.82	5.83	0.16	1.16	3.03	5.06	2.80	99.52
	BR 2	66.46	1.20	14.47	5.59	0.19	1.14	2.96	4.91	2.74	99.66
	BR 2	66.42	1.23	14.39	5.52	0.16	1.14	3.03	5.18	2.52	99.59
	BR 2	66.22	1.15	14.19	5.39	0.21	1.20	2.95	4.79	2.62	98.72
	BR 2	66.09	1.15	14.25	5.45	0.20	1.24	2.90	4.90	2.78	98.96
	BR 2	65.98	1.24	14.07	5.38	0.15	1.18	2.96	5.09	2.82	98.87
	BR 2	65.97	1.12	14.21	5.24	0.18	1.18	2.96	5.06	2.74	98.66
	BR 2	65.53	1.20	14.32	5.40	0.21	1.15	2.80	5.22	2.72	98.55
	BR 3	66.53	1.08	14.19	5.08	0.12	1.07	2.73	4.60	2.88	98.28
	BR 3	66.31	1.20	14.21	5.46	0.14	1.15	2.76	4.37	2.93	98.53
	BR 3	66.18	1.17	13.96	5.56	0.10	1.04	2.64	4.83	2.96	98.44
	BR 3	66.14	1.16	13.86	5.12	0.15	1.06	2.80	2.62	2.77	95.68
	BR 3	65.70	1.20	14.00	5.69	0.16	1.07	2.86	4.56	3.08	98.32
	BR 3	65.58	1.21	13.90	5.46	0.16	1.08	2.79	4.65	2.84	97.67
	BR 3	65.45	1.15	14.03	5.24	0.19	1.10	2.82	4.48	3.01	97.47
	BR 3	65.39	1.16	14.02	5.47	0.14	1.07	2.76	4.63	3.02	97.66
	BR 3	65.24	1.10	13.46	5.19	0.12	1.03	2.75	4.36	2.93	96.18
	BR 3	64.85	1.24	14.18	5.08	0.16	1.01	2.51	4.81	3.03	96.87
	BR 4	67.05	1.27	14.32	4.83	0.08	0.87	2.47	4.69	3.21	98.79
	BR 4	66.93	1.06	14.37	5.23	0.17	0.94	2.51	4.63	2.88	98.72
	BR 4	66.25	1.13	14.02	5.02	0.20	0.88	2.60	4.58	3.10	97.78
	BR 4	66.02	1.13	13.90	4.78	0.19	0.99	2.45	4.77	2.99	97.22
	BR 4	65.82	1.08	13.83	5.49	0.20	1.05	2.67	4.61	2.79	97.54
	BR 4	65.81	1.06	13.63	5.48	0.20	1.02	2.83	4.59	2.91	97.53
	BR 4	65.76	1.16	13.85	5.14	0.15	0.93	2.56	4.59	2.92	97.06
	BR 4	65.58	1.19	13.94	5.29	0.17	0.99	2.64	4.49	3.04	97.33
	BR 4	65.58	1.08	14.00	5.35	0.15	1.07	2.56	4.64	2.72	97.15
	BR 4	65.28	1.18	13.91	5.32	0.15	1.00	2.67	4.77	2.82	97.10
Eyvindar-fjörður	E 1	66.96	1.13	14.10	5.58	0.19	1.13	3.31	4.51	3.08	99.99
	E 1	66.61	1.23	14.24	5.69	0.17	1.15	3.25	4.60	2.89	99.83
	E 1	66.44	1.20	14.47	5.37	0.13	1.28	3.22	4.58	2.94	99.62
	E 1	66.25	1.24	13.93	5.27	0.22	1.15	3.25	4.80	2.79	98.90
	E 1	66.11	1.19	14.08	5.75	0.20	1.15	3.21	4.60	2.90	99.20
	E 1	66.02	1.24	14.06	5.57	0.20	1.22	3.29	4.78	2.98	99.36
	E 1	66.01	1.29	14.03	5.39	0.18	1.22	3.17	5.10	2.91	99.30
	E 1	65.60	1.27	13.88	5.77	0.14	1.10	3.20	4.56	2.86	98.69
	E 1	65.54	1.28	13.62	5.40	0.13	1.27	3.25	4.77	2.85	99.11

Site	Pumice	SiO_2	TiO_2	Al_2O_3	FeO	MnO	MgO	CaO	Na_2O	K_2O	Total
	E 1	64.70	1.20	14.52	5.45	0.13	1.29	3.54	4.77	3.02	98.61
	E 1	64.13	1.22	13.84	5.63	0.20	1.19	3.10	4.49	2.99	96.79
Hrútafjörður	HF 1	65.51	1.13	14.30	5.56	0.20	1.14	3.02	4.94	2.82	98.60
	HF 1	67.03	1.17	14.07	5.08	0.21	1.10	2.73	4.95	2.97	99.31
	HF 1	65.92	1.10	13.71	5.57	0.19	1.09	3.03	4.90	2.85	98.37
	HF 1	67.62	1.31	13.97	4.93	0.13	0.97	2.84	4.94	2.98	99.70
Ófeigs-fjörður S8L	OF8L 1	71.70	1.22	15.89	2.43	0.03	1.79	0.29	1.37	4.34	99.06
	OF8L 1	72.09	0.88	15.34	2.51	0.03	1.85	0.33	1.53	4.46	99.02
	OF8L 1	71.33	0.80	16.13	1.84	0.01	1.58	0.27	1.36	4.25	97.57
	OF8L 1	70.13	1.53	17.23	2.65	0.39	1.78	0.37	1.43	4.03	99.54
	OF8L 2	67.02	1.22	14.16	5.71	0.20	1.16	3.16	4.65	2.71	99.99
	OF8L 2	66.79	1.08	14.02	5.89	0.16	1.18	3.04	4.77	2.78	99.71
	OF8L 2	66.36	1.11	13.57	5.59	0.14	1.11	3.11	4.51	2.95	98.45
	OF8L 2	66.35	1.26	13.69	5.74	0.19	1.10	3.04	4.47	2.77	98.61
	OF8L 2	66.01	1.21	13.88	5.73	0.14	1.11	3.06	4.72	2.73	98.59
	OF8L 2	65.73	1.29	13.92	5.47	0.21	1.07	3.09	4.67	2.88	98.33
	OF8L 2	65.38	1.30	13.95	5.75	0.17	1.12	3.04	4.79	2.89	98.39
	OF8L 2	64.70	1.18	13.91	5.45	0.20	1.10	2.95	4.78	2.82	97.09
	OF8L 2	64.41	1.24	13.76	5.57	0.16	1.12	2.83	4.54	2.85	96.48
	OF8L 3	67.67	1.22	13.94	5.27	0.15	1.11	2.87	4.51	2.76	99.50
	OF8L 3	66.60	1.32	14.10	5.88	0.11	1.13	3.09	4.67	2.86	99.76
	OF8L 3	66.57	1.14	13.80	5.25	0.20	1.09	3.05	4.69	2.89	98.68
	OF8L 3	66.45	1.04	13.92	5.77	0.26	1.17	2.81	4.80	2.78	99.00
	OF8L 3	66.42	1.08	14.22	5.76	0.13	1.06	2.93	4.82	2.81	99.23
	OF8L 3	65.86	1.24	14.28	5.98	0.21	1.14	3.09	4.61	2.79	99.20
	OF8L 3	65.84	1.30	13.96	5.54	0.14	1.09	3.15	4.71	3.03	98.76
	OF8L 3	65.80	1.07	14.06	5.54	0.20	1.17	2.94	4.29	2.80	97.87
	OF8L 3	65.76	1.26	13.86	5.67	0.18	1.18	3.01	4.64	3.02	98.58
	OF8L 3	65.65	1.31	13.96	5.59	0.19	1.10	2.92	4.48	2.82	98.02
	OF8L 4	66.04	1.21	14.06	5.70	0.22	1.15	3.15	4.43	2.96	98.92
	OF8L 4	65.89	1.28	14.13	5.47	0.19	1.18	3.14	4.39	3.08	98.75
	OF8L 4	65.83	1.33	13.48	5.45	0.18	1.21	3.33	5.76	1.40	97.97
	OF8L 4	65.80	1.18	13.96	5.19	0.16	1.16	3.00	4.19	3.90	98.54
	OF8L 4	65.76	1.25	14.13	5.39	0.22	1.15	3.14	4.38	2.99	98.41
	OF8L 4	65.75	1.12	14.40	4.93	0.15	0.90	3.68	5.83	1.35	98.11
	OF8L 4	65.70	1.12	13.38	5.46	0.17	1.15	3.17	4.73	2.96	97.84
	OF8L 4	65.67	1.31	13.93	5.41	0.17	1.15	3.29	4.61	3.05	98.59
	OF8L 4	65.54	1.29	13.99	5.52	0.19	1.16	3.04	4.62	3.03	98.38
	OF8L 4	65.34	1.12	13.28	5.50	0.20	1.16	2.83	4.13	4.28	97.84
Ófeigs-fjörður S8U	OF8U 1	66.36	1.25	14.05	5.48	0.17	1.22	2.96	4.86	2.69	99.04
	OF8U 1	66.11	1.25	14.05	5.40	0.19	1.15	2.98	4.82	2.86	98.81
	OF8U 1	65.70	1.22	14.18	5.28	0.16	1.16	3.02	4.84	2.65	98.21
	OF8U 1	65.19	1.39	13.86	5.55	0.15	1.16	3.15	5.00	2.71	98.16
	OF8U 1	65.17	1.32	14.17	5.60	0.16	1.22	3.21	4.77	2.74	98.36
	OF8U 1	64.86	1.30	14.12	5.82	0.22	1.09	3.21	4.64	3.01	98.27
	OF8U 1	64.58	1.10	14.21	5.68	0.16	1.13	3.00	5.03	2.80	97.69
	OF8U 1	64.56	1.20	13.62	5.42	0.13	1.11	3.06	4.58	2.78	96.46
	OF8U 1	64.40	1.16	13.66	5.36	0.13	1.08	3.08	4.73	2.79	96.39
	OF8U 2	66.50	1.25	13.63	5.38	0.19	1.01	2.94	4.61	2.85	98.36
	OF8U 2	66.46	1.26	13.75	5.65	0.19	1.12	3.08	4.59	2.80	98.90
	OF8U 2	66.18	1.19	13.81	5.93	0.17	1.22	3.18	4.40	2.68	98.76
	OF8U 2	65.99	1.28	13.84	5.95	0.14	1.15	3.08	4.51	2.73	98.67
	OF8U 2	65.87	1.25	13.80	5.60	0.19	1.13	3.04	4.52	2.73	98.13
	OF8U 2	65.85	1.17	13.88	5.63	0.20	1.03	2.90	4.49	2.74	97.89

Site	Pumice	SiO_2	TiO_2	Al_2O_3	FeO	MnO	MgO	CaO	Na_2O	K_2O	Total
	OF8U 2	65.68	1.21	13.96	5.83	0.19	1.23	3.10	4.52	2.81	98.53
	OF8U 2	65.61	1.10	13.84	5.67	0.19	1.13	3.19	4.61	2.66	98.00
	OF8U 2	65.40	1.26	13.69	5.67	0.20	1.15	3.14	4.24	2.95	97.70
	OF8U 2	65.31	1.07	13.83	5.75	0.24	1.15	2.99	4.50	2.73	97.57
	OF8U 3	66.43	1.20	13.78	5.82	0.15	1.10	3.14	4.68	3.23	99.53
	OF8U 3	66.35	1.30	13.80	5.61	0.16	1.13	3.08	4.71	2.93	99.07
	OF8U 3	66.25	1.19	13.94	5.85	0.18	1.20	2.88	4.52	3.05	99.06
	OF8U 3	66.13	1.19	14.12	5.62	0.21	1.17	3.07	4.37	3.00	98.88
	OF8U 3	66.11	1.16	13.52	5.69	0.18	1.06	3.00	4.38	3.10	98.20
	OF8U 3	66.03	1.29	13.91	5.60	0.20	1.23	2.96	4.52	2.79	98.53
	OF8U 3	65.95	1.16	13.89	5.28	0.14	1.17	2.94	4.61	3.02	98.16
	OF8U 3	65.67	1.24	13.91	5.67	0.26	1.21	3.15	4.56	2.91	98.58
	OF8U 3	65.27	1.16	13.40	5.63	0.15	1.06	2.97	4.51	2.87	97.02
	OF8U 3	64.53	1.18	13.80	5.71	0.18	1.15	3.04	4.53	3.23	97.35
	OF8U 4	66.76	1.26	13.80	5.41	0.19	1.15	2.98	4.78	2.73	99.06
	OF8U 4	66.65	1.15	13.93	5.25	0.19	1.11	2.93	4.75	2.86	98.82
	OF8U 4	66.27	1.11	13.84	5.63	0.22	1.16	2.96	4.64	2.72	98.55
	OF8U 4	66.18	1.15	13.82	5.45	0.21	1.12	3.07	4.79	2.77	98.56
	OF8U 4	66.07	1.33	13.84	5.94	0.12	1.20	3.13	5.05	2.90	99.58
	OF8U 4	66.00	1.24	13.98	5.70	0.17	1.12	2.98	4.59	2.87	98.65
	OF8U 4	65.80	1.23	13.93	5.49	0.16	1.12	3.15	4.81	2.76	98.45
	OF8U 4	65.80	1.24	13.82	5.74	0.17	1.11	3.20	4.85	2.88	98.81
	OF8U 4	65.61	1.20	14.00	5.98	0.16	1.19	3.01	4.71	2.72	98.58
	OF8U 4	65.55	1.18	13.87	5.61	0.21	1.10	3.12	4.90	2.74	98.28
Ófeigs-fjörður S6C	**OF6C 1**	67.06	1.32	13.96	5.50	0.16	1.03	3.07	4.67	2.81	99.58
	OF6C 1	67.04	1.28	14.24	5.45	0.17	1.04	2.96	4.74	2.78	99.70
	OF6C 1	66.31	1.23	13.97	5.71	0.25	1.11	3.01	4.86	2.85	99.30
	OF6C 1	66.25	1.30	13.94	5.65	0.25	1.10	3.18	4.28	2.77	98.72
	OF6C 1	66.17	1.24	14.36	5.69	0.13	1.20	3.17	4.82	2.87	99.65
	OF6C 1	66.01	1.24	13.80	5.61	0.17	1.17	2.99	4.58	2.74	98.31
	OF6C 1	65.98	1.26	14.10	5.71	0.17	1.10	3.10	4.62	2.83	98.87
	OF6C 1	65.98	1.19	13.73	6.37	0.16	1.25	3.16	4.57	2.74	99.15
	OF6C 1	65.86	1.24	13.96	5.85	0.18	1.10	2.97	4.81	2.87	98.84
	OF6C 1	65.75	1.30	13.96	5.87	0.19	1.22	3.15	4.49	2.92	98.85
	OF6C 2	67.74	1.08	13.77	5.44	0.17	0.97	2.76	4.79	2.91	99.63
	OF6C 2	67.32	1.17	14.11	5.34	0.23	1.10	2.92	4.59	2.86	99.64
	OF6C 2	66.66	1.25	14.00	5.50	0.21	1.06	2.91	4.50	2.95	99.04
	OF6C 2	66.59	1.20	13.91	4.80	0.27	1.18	3.41	4.69	3.09	99.14
	OF6C 2	66.11	1.18	13.98	6.00	0.14	1.18	3.13	4.56	2.83	99.11
	OF6C 2	65.92	1.28	14.17	5.49	0.19	1.18	3.05	4.45	3.33	99.06
	OF6C 2	65.90	1.26	14.00	5.85	0.22	1.16	2.88	5.47	2.71	99.45
	OF6C 2	65.77	1.23	13.76	5.39	0.19	1.04	2.91	4.49	3.51	98.29
	OF6C 2	65.60	1.30	13.71	5.08	0.14	1.18	3.00	4.34	3.95	98.30
	OF6C 2	65.50	1.20	13.88	5.68	0.20	1.06	3.07	4.53	2.75	97.87
	OF6C 3	67.14	1.17	13.91	5.29	0.14	1.11	3.18	4.91	2.80	99.65
	OF6C 3	67.06	1.21	13.99	5.49	0.13	1.06	2.93	4.65	2.88	99.40
	OF6C 3	66.71	1.22	13.95	5.31	0.16	1.07	3.03	4.85	2.93	99.23
	OF6C 3	66.61	1.22	13.93	5.47	0.18	1.21	2.98	4.72	2.67	98.99
	OF6C 3	66.59	1.23	13.99	5.64	0.25	1.13	3.18	4.81	3.00	99.82
	OF6C 3	66.46	1.31	13.55	5.68	0.15	1.02	3.05	4.69	2.75	98.66
	OF6C 3	66.39	1.18	13.94	5.55	0.16	1.06	3.00	4.67	2.92	98.87
	OF6C 3	66.25	1.15	13.85	5.43	0.12	1.08	2.96	4.72	2.76	98.32
	OF6C 3	65.99	1.11	13.97	5.86	0.17	1.15	3.06	4.76	2.78	98.85
	OF6C 3	65.36	1.11	13.94	5.70	0.17	1.12	3.00	4.69	3.00	98.09
	OF6C 4	66.81	1.13	13.40	5.01	0.20	1.10	3.13	4.36	3.17	98.31

Site	Pumice	SiO_2	TiO_2	Al_2O_3	FeO	MnO	MgO	CaO	Na_2O	K_2O	Total
	OF6C 4	66.54	1.25	13.73	5.90	0.20	1.11	3.01	4.17	4.04	99.95
	OF6C 4	66.50	1.28	13.74	5.74	0.19	1.12	3.16	6.13	1.70	99.56
	OF6C 4	66.48	1.27	13.76	5.62	0.14	1.06	3.80	5.80	1.40	99.33
	OF6C 4	66.40	1.20	13.96	5.41	0.19	1.14	2.97	4.51	3.40	99.18
	OF6C 4	66.34	1.26	13.82	5.75	0.20	1.12	2.73	6.16	1.74	99.12
	OF6C 4	66.22	1.19	13.81	5.01	0.16	1.03	3.99	5.66	1.38	98.45
	OF6C 4	66.19	1.19	13.73	5.42	0.22	1.03	2.92	5.78	2.27	98.75
	OF6C 4	66.03	1.19	13.68	5.49	0.20	1.12	3.06	4.07	3.85	98.69
	OF6C 4	65.89	1.13	13.78	5.18	0.18	1.14	2.99	4.42	3.47	98.18
Ófeigs-fjörður S6D	**OF6D 1**	67.29	1.12	13.87	5.34	0.22	0.95	2.59	4.78	2.91	99.07
	OF6D 1	67.19	1.14	14.10	5.67	0.24	0.91	2.41	4.75	3.04	99.45
	OF6D 1	67.08	1.19	13.95	5.42	0.19	0.89	2.60	4.58	3.08	98.98
	OF6D 1	66.82	1.27	14.07	5.14	0.23	0.83	2.41	4.87	3.12	98.76
	OF6D 1	66.47	1.11	13.65	5.36	0.23	0.78	2.38	4.70	2.97	97.65
	OF6D 1	66.39	1.25	14.07	5.22	0.20	0.99	2.62	4.83	2.69	98.26
	OF6D 1	66.30	1.23	14.02	4.78	0.17	0.83	2.56	4.55	2.89	97.33
	OF6D 1	66.24	1.11	14.06	5.14	0.19	0.77	2.34	4.66	3.06	97.57
	OF6D 1	65.98	1.12	13.61	5.42	0.19	0.95	2.77	4.55	3.01	97.60
	OF6D 1	65.83	1.14	14.01	5.36	0.19	0.82	2.58	4.65	2.85	97.43
	OF6D 2	66.70	1.00	13.62	5.39	0.18	1.16	3.10	4.64	2.95	98.74
	OF6D 2	66.66	1.18	14.07	5.40	0.18	1.09	3.24	4.82	2.81	99.45
	OF6D 2	66.63	1.14	13.88	5.49	0.14	1.21	3.10	4.88	2.95	99.42
	OF6D 2	66.59	1.10	14.22	5.47	0.19	1.16	3.06	4.76	2.80	99.35
	OF6D 2	66.46	1.11	14.01	5.13	0.14	1.07	3.00	4.74	2.90	98.56
	OF6D 2	66.37	1.15	13.83	5.75	0.16	1.15	3.02	4.77	2.66	98.86
	OF6D 2	66.10	1.12	14.01	5.66	0.11	1.12	2.92	4.74	2.87	98.65
	OF6D 2	66.06	0.99	14.04	5.47	0.17	1.14	2.95	4.80	2.80	98.42
	OF6D 2	65.36	1.19	13.73	5.29	0.15	1.16	3.06	4.77	2.80	97.51
	OF6D 2	64.84	1.14	13.84	5.61	0.20	1.22	3.03	4.68	2.96	97.52
	OF6D 3	67.08	1.18	14.28	5.14	0.19	1.04	2.79	4.64	3.10	99.44
	OF6D 3	66.89	1.25	13.81	5.23	0.16	1.13	3.05	4.57	2.78	98.87
	OF6D 3	66.76	1.28	14.09	5.24	0.15	1.07	2.57	4.54	2.95	98.65
	OF6D 3	66.73	1.13	14.00	5.33	0.17	1.18	2.93	4.37	2.79	98.63
	OF6D 3	66.58	1.20	13.85	5.67	0.21	1.22	3.06	4.37	2.76	98.92
	OF6D 3	66.36	1.29	14.03	5.39	0.19	1.11	2.99	4.31	2.84	98.51
	OF6D 3	66.22	1.21	14.06	5.19	0.18	1.09	2.92	4.77	2.91	98.55
	OF6D 3	65.89	1.93	14.33	5.66	0.18	1.10	2.93	4.41	2.70	99.13
	OF6D 3	65.86	1.16	13.99	5.69	0.16	1.22	3.08	4.32	2.64	98.12
	OF6D 3	65.60	1.19	14.02	5.60	0.18	1.22	3.04	4.52	2.79	98.16
	OF6D 4	67.09	1.25	13.94	5.57	0.17	1.08	2.82	2.42	3.53	97.87
	OF6D 4	66.67	1.17	13.86	5.46	0.16	1.06	2.90	4.59	2.97	98.84
	OF6D 4	66.45	1.12	13.99	5.17	0.19	1.00	2.80	4.41	3.08	98.21
	OF6D 4	66.44	1.10	13.85	5.27	0.11	1.10	2.79	4.44	2.95	98.05
	OF6D 4	66.33	1.08	13.70	5.73	0.16	1.08	3.14	5.21	2.60	99.03
	OF6D 4	66.29	1.26	13.95	5.41	0.19	1.05	2.85	4.14	3.13	98.27
	OF6D 4	66.21	1.12	14.12	5.71	0.12	1.09	2.87	4.62	2.97	98.83
	OF6D 4	65.83	1.38	13.96	5.53	0.15	1.20	2.87	4.51	3.64	99.07
	OF6D 4	65.68	1.34	13.52	5.43	0.12	1.14	2.83	4.51	3.03	97.60
	OF6D 4	65.47	1.15	13.93	5.55	0.18	1.07	2.81	4.47	3.03	97.66
	OF6D 5	67.39	1.16	13.86	5.59	0.17	1.00	2.72	4.67	2.83	99.39
	OF6D 5	67.29	1.29	13.78	5.16	0.13	0.98	2.57	4.63	3.03	98.86
	OF6D 5	67.23	1.32	13.75	5.30	0.16	0.92	2.57	4.53	3.23	99.01
	OF6D 5	67.16	1.25	13.57	4.33	0.16	0.89	2.86	4.46	3.09	97.77
	OF6D 5	67.11	1.24	13.68	5.33	0.15	0.94	2.90	4.59	3.00	98.94
	OF6D 5	67.10	1.19	13.60	5.41	0.19	0.98	2.60	4.60	2.91	98.58

Site	Pumice	SiO_2	TiO_2	Al_2O_3	FeO	MnO	MgO	CaO	Na_2O	K_2O	Total
	OF6D 5	66.79	1.23	13.73	5.75	0.13	1.02	2.66	4.36	3.05	98.72
	OF6D 5	66.70	1.17	13.53	5.07	0.15	0.98	2.58	4.46	3.11	97.75
	OF6D 5	66.39	1.21	13.77	5.75	0.17	1.07	2.85	4.54	2.76	98.51
Reykjarnes	RJ 1	65.64	1.23	13.41	5.67	0.18	1.13	3.00	4.89	3.08	98.23
	RJ 1	65.06	1.27	13.44	5.50	0.22	1.09	2.92	5.00	2.92	97.42
	RJ 1	64.75	1.37	13.72	5.34	0.20	1.14	2.76	4.87	2.95	97.11
	RJ 1	64.27	1.27	13.55	5.77	0.20	1.11	3.11	5.11	3.18	97.57
	RJ 1	64.19	1.21	13.42	5.60	0.24	1.11	3.00	5.34	2.83	97.04
	RJ 1	63.75	1.27	13.91	5.73	0.22	1.13	3.06	4.76	3.04	96.86
	RJ 1	63.66	1.16	13.96	5.63	0.14	1.23	3.08	4.96	3.15	97.00
	RJ 1	63.61	1.08	13.77	5.83	0.15	1.05	2.78	5.31	3.08	96.65
	RJ 1	63.57	1.26	13.52	5.44	0.19	1.11	2.88	4.77	2.95	95.69
	RJ 1	63.56	1.16	13.67	5.45	0.19	1.12	2.82	4.85	2.98	95.81

Appendix 3D: Icelandic Raised Beach Pumice SIMS Data

Site	Pumice	Ti	Rb	Sr	Y	Zr	Nb	Ba	La	Ce
Bær	BR 1	5593	44.4	194.2	53.9	800.8	101.8	487.6	65.2	140.3
		5531	43.6	197.6	54.1	797.4	102.0	488.0	66.4	142.3
		5920	44.9	207.6	58.1	805.8	102.8	519.8	69.9	150.6
		5753	42.3	216.9	56.0	785.6	99.6	497.5	68.3	146.5
		5696	41.8	228.7	55.9	765.6	97.4	493.4	68.7	146.2
		5573	46.1	218.8	57.0	807.0	101.6	523.9	70.1	146.9
		5829	46.0	209.6	54.1	778.0	100.1	490.7	64.0	135.3
		5842	43.5	217.6	54.7	765.0	98.2	490.7	65.6	137.2
		5763	44.8	235.9	55.0	755.9	96.2	494.6	66.2	141.3
		5731	44.7	226.4	56.2	785.2	100.8	509.4	67.4	143.9

Appendix 3E: Scottish Raised Beach Pumice EPMA Data

Site	Pumice	SiO_2	TiO_2	Al_2O_3	FeO	MnO	MgO	CaO	Na_2O	K_2O	Total
Bay of Moaness	BM 1	66.89	1.24	13.84	5.47	0.15	1.15	2.75	4.55	2.71	98.75
	BM 1	66.77	1.15	14.11	5.71	0.20	1.16	3.13	4.77	2.71	99.71
	BM 1	66.62	1.16	13.64	5.63	0.19	1.13	2.99	4.85	2.76	98.97
	BM 1	66.23	1.13	13.63	5.68	0.21	1.08	3.21	4.93	2.84	98.94
	BM 1	66.11	1.23	13.81	5.61	0.17	1.22	2.90	4.76	2.64	98.45
	BM 1	66.01	1.14	13.86	5.85	0.27	1.12	3.02	4.95	2.68	98.90
	BM 1	65.89	1.17	13.83	5.45	0.17	1.05	3.05	4.59	2.63	97.83
	BM 1	65.55	1.30	13.82	5.41	0.19	1.18	2.93	4.87	2.81	98.06
	BM 1	65.47	1.16	13.98	5.69	0.19	1.22	2.93	4.83	2.79	98.26
	BM 1	65.34	1.18	12.72	5.75	0.19	1.26	3.11	4.72	2.56	96.83
	BM 2	66.32	1.11	14.08	5.75	0.23	1.24	3.22	4.71	2.72	99.38
	BM 2	66.08	1.08	13.64	5.56	0.18	1.14	2.98	4.94	2.89	98.49
	BM 2	66.01	1.09	13.82	5.44	0.22	1.05	3.05	4.72	2.91	98.31
	BM 2	65.96	1.17	13.81	5.52	0.19	1.21	3.12	4.57	2.85	98.40
	BM 2	65.83	1.28	14.05	5.55	0.19	1.15	2.77	4.88	2.93	98.63
	BM 2	65.76	1.25	13.99	5.84	0.22	1.18	3.18	4.86	2.76	99.04
	BM 2	65.69	1.18	13.85	5.60	0.23	1.13	3.13	4.55	2.83	98.19
	BM 2	65.60	1.20	13.89	5.06	0.19	1.01	3.21	4.88	2.87	97.91
	BM 2	65.31	1.11	13.25	5.67	0.17	1.10	3.01	4.84	2.81	97.27
	BM 2	64.30	1.15	13.70	5.44	0.13	1.11	3.00	4.61	2.83	96.27

Site	Pumice	SiO_2	TiO_2	Al_2O_3	FeO	MnO	MgO	CaO	Na_2O	K_2O	Total
	BM 3	67.65	1.14	13.92	5.23	0.21	1.11	2.72	4.70	2.93	99.61
	BM 3	67.37	1.02	13.84	5.44	0.25	1.00	2.68	4.52	2.88	99.00
	BM 3	67.06	1.12	13.77	4.84	0.28	1.04	2.62	4.83	2.93	98.49
	BM 3	66.91	1.02	14.00	5.17	0.22	1.08	2.83	4.82	2.81	98.86
	BM 3	66.86	1.11	13.62	5.14	0.21	1.02	2.75	3.09	2.85	96.65
	BM 3	66.82	1.06	13.74	5.30	0.18	0.95	2.89	5.08	2.83	98.85
	BM 3	66.43	1.22	13.61	5.12	0.22	1.13	2.95	4.90	2.67	98.25
	BM 3	66.26	1.08	14.07	5.40	0.14	1.08	2.79	4.82	2.75	98.39
	BM 3	66.23	1.18	13.64	5.46	0.21	1.03	2.75	4.94	2.93	98.37
	BM 3	65.40	0.96	13.53	5.11	0.22	1.00	2.80	4.71	3.00	96.73
	BM 4	67.51	1.21	12.82	5.99	0.21	0.95	2.59	4.46	3.16	98.90
	BM 4	67.34	1.19	12.92	5.50	0.19	1.04	2.75	4.91	3.08	98.92
	BM 4	67.19	1.12	13.22	5.54	0.22	0.93	2.59	4.35	2.79	97.95
	BM 4	66.89	1.23	12.73	5.52	0.21	0.80	2.31	4.64	3.18	97.51
	BM 4	66.01	1.07	13.89	4.44	0.21	1.01	2.90	5.12	2.75	97.40
	BM 4	65.79	1.44	12.62	6.48	0.19	0.81	2.36	3.88	3.17	96.74

Appendix 3F: Scottish Raised Beach Pumice SIMS Data

Site	Pumice	Ti	Rb	Sr	Y	Zr	Nb	Ba	La	Ce
Bay of Moaness	**BM 4**	6478	48.1	151.8	59.5	866.0	109.3	491.5	68.9	148.0
		5803	43.7	258.6	53.2	770.6	98.3	509.1	64.2	135.5
		5869	44.0	243.6	56.1	789.9	98.6	508.7	66.1	139.4
		5800	42.2	250.8	56.3	794.3	99.0	511.5	66.4	140.2
		6118	45.7	188.0	56.3	811.8	101.0	491.5	66.4	142.3
		5749	46.4	231.7	55.2	805.7	98.1	504.2	65.9	140.5
		5628	45.3	220.8	57.1	805.6	101.7	506.0	68.4	143.2

Appendix 3G: Scottish Archaeological Pumice EPMA Data

Site	Code	SiO_2	TiO_2	Al_2O_3	FeO	MnO	MgO	CaO	Na_2O	K_2O	Total
Allt Chrisal	**AC 1**	67.31	1.11	13.80	4.50	0.17	0.91	2.56	4.53	2.81	97.70
	AC 1	67.23	1.14	13.73	4.59	0.24	1.00	2.70	4.52	2.96	98.10
	AC 1	66.74	1.08	13.83	4.94	0.21	0.97	2.86	4.70	3.09	98.42
	AC 1	66.53	1.08	13.88	4.75	0.23	0.95	2.71	4.71	2.87	97.69
	AC 1	65.90	1.06	13.81	4.53	0.22	0.87	2.42	4.85	2.83	96.51
	AC 1	65.85	1.10	13.77	4.88	0.19	1.00	2.60	4.64	3.04	97.07
	AC 1	65.78	1.07	13.72	4.91	0.22	1.03	2.68	4.67	2.98	97.06
	AC 1	65.21	1.12	13.98	5.13	0.22	1.05	2.79	4.60	2.98	97.08
	AC 2	66.51	1.24	13.63	4.84	0.18	1.16	3.08	4.29	2.86	97.80
	AC 2	65.12	1.16	13.76	5.24	0.15	1.17	2.91	4.41	2.73	96.66
	AC 2	64.88	1.23	13.46	5.57	0.20	1.14	3.16	4.48	2.70	96.81
	AC 2	64.65	1.13	13.77	5.46	0.24	1.12	3.02	4.35	2.80	96.53
	AC 2	64.64	1.28	13.79	5.52	0.22	1.04	2.99	4.40	2.65	96.53
	AC 3	66.28	1.32	13.85	5.39	0.15	1.11	3.22	4.68	2.74	98.74
	AC 3	65.26	1.19	13.22	4.94	0.19	1.06	2.81	4.60	2.96	96.23
	AC 3	65.16	1.17	13.65	5.36	0.15	1.04	2.97	4.65	2.88	97.03
	AC 3	64.99	1.21	14.17	5.46	0.18	1.18	3.03	4.60	2.82	97.64
	AC 3	63.91	1.24	13.82	5.84	0.26	1.33	3.13	4.56	2.65	96.75

Site	Code	SiO_2	TiO_2	Al_2O_3	FeO	MnO	MgO	CaO	Na_2O	K_2O	Total
	AC 4	65.21	1.20	13.78	5.69	0.17	0.91	2.87	4.66	2.83	97.32
	AC 4	65.19	1.21	13.79	4.89	0.11	1.09	3.23	4.60	2.92	97.04
	AC 4	64.41	1.25	13.98	5.26	0.20	1.27	3.06	4.67	2.79	96.89
	AC 4	64.10	1.11	13.57	5.56	0.12	1.19	3.32	4.66	2.77	96.41
	AC 4	63.99	1.19	13.50	5.47	0.18	1.15	2.85	4.63	2.78	95.74
	AC 4	63.87	1.13	13.10	5.14	0.16	1.17	3.07	4.66	2.88	95.17
	AC 4	63.54	1.22	13.56	5.42	0.12	1.14	3.24	4.43	2.76	95.44
Ceardach Rudh	CR 1	65.86	1.26	13.95	6.10	0.14	1.15	3.01	5.03	2.71	99.20
	CR 1	65.85	1.16	14.02	5.75	0.22	1.14	3.04	4.85	2.71	98.75
	CR 1	65.28	1.21	14.25	5.73	0.22	1.19	3.12	4.91	2.65	98.67
	CR 1	64.57	1.20	13.89	5.63	0.20	1.18	3.23	4.81	2.81	97.53
	CR 1	64.17	1.28	13.76	5.86	0.16	1.18	3.00	5.16	2.58	97.16
	CR 2	67.04	1.15	13.96	5.55	0.13	1.03	2.96	4.67	2.59	99.08
	CR 2	66.45	1.29	14.02	5.89	0.15	1.13	3.05	4.33	2.82	99.12
	CR 2	66.19	1.17	13.85	5.61	0.20	1.16	3.06	4.81	2.70	98.76
	CR 2	66.13	1.27	14.17	5.99	0.20	1.15	3.27	4.89	2.80	99.87
	CR 2	65.88	1.29	14.28	5.68	0.18	1.12	3.14	4.71	2.66	98.23
	CR 2	65.83	1.24	14.12	5.57	0.18	1.17	3.07	4.79	2.75	98.70
	CR 2	65.25	1.25	13.92	5.61	0.24	1.10	3.07	4.72	2.77	97.91
	CR 2	64.83	1.21	14.22	5.76	0.19	1.11	3.27	4.73	2.70	98.02
	CR 2	64.63	1.22	14.01	5.99	0.17	1.11	3.11	4.80	2.71	97.75
	CR 2	63.68	1.13	13.98	5.34	0.15	1.05	2.89	4.64	2.54	95.39
	CR 3	65.96	1.21	14.15	5.76	0.23	1.12	2.97	4.82	2.65	98.87
	CR 3	65.59	1.27	14.19	6.07	0.17	1.13	3.27	4.68	2.62	98.99
	CR 3	64.88	1.20	14.04	5.77	0.27	1.18	3.28	4.73	2.56	97.91
	CR 3	64.76	1.34	13.76	5.44	0.17	1.18	2.87	4.87	2.87	97.28
	CR 3	64.25	1.15	13.82	6.11	0.25	1.19	3.38	4.77	2.57	97.50
	CR 4	67.40	1.01	14.46	5.04	0.11	1.04	2.74	4.70	3.19	99.69
	CR 4	67.35	1.09	13.57	4.17	0.14	1.02	3.06	4.55	2.96	97.91
	CR 4	67.05	1.16	14.14	4.73	0.13	0.87	2.83	4.69	2.86	98.46
	CR 4	66.82	1.02	13.79	5.31	0.13	0.84	2.84	4.85	2.81	98.41
	CR 4	66.56	1.06	13.85	5.00	0.18	0.91	2.63	5.00	3.15	98.33
	CR 4	66.38	1.13	14.32	5.43	0.11	0.93	2.78	4.70	2.77	98.55
	CR 4	66.21	1.03	13.50	5.14	0.13	1.07	2.76	4.80	2.85	97.51
	CR 4	66.16	1.06	13.83	5.12	0.14	1.06	2.98	4.76	2.76	97.87
	CR 4	65.43	1.08	13.99	4.92	0.17	0.94	2.64	4.80	2.85	96.82
	CR 5	66.90	1.23	14.31	5.38	0.18	1.17	3.33	4.54	2.71	99.74
	CR 5	66.51	1.23	14.11	5.49	0.17	1.10	3.08	3.19	2.50	97.39
	CR 5	66.34	1.19	14.35	5.35	0.18	1.12	3.14	4.86	2.74	99.27
	CR 5	66.05	1.26	13.96	5.56	0.14	1.08	3.18	4.59	2.57	98.39
	CR 5	65.87	1.19	14.32	5.61	0.11	1.12	2.98	4.85	2.68	98.74
	CR 5	65.81	1.03	14.00	5.25	0.14	1.09	2.98	4.52	2.71	97.54
	CR 5	65.68	1.35	13.98	5.44	0.17	1.09	3.11	4.55	2.66	98.04
	CR 5	65.30	1.14	13.86	5.32	0.22	1.20	3.19	4.68	2.63	97.54
	CR 5	64.97	1.13	14.24	5.39	0.15	1.18	3.23	4.75	2.66	97.70
	CR 6	65.73	1.21	13.87	5.46	0.21	1.26	2.93	5.12	2.71	98.51
	CR 6	65.49	1.20	14.00	5.88	0.13	1.12	2.93	5.03	2.82	98.59
	CR 6	65.01	1.20	13.71	5.79	0.19	1.12	3.04	5.14	2.78	97.97
	CR 6	64.39	1.18	13.80	5.89	0.22	1.16	3.17	4.78	2.77	97.38
	CR 7	66.48	1.15	13.84	6.03	0.20	1.04	2.58	4.86	3.73	99.90
	CR 7	65.77	1.21	13.62	5.31	0.19	0.99	2.52	4.60	3.73	97.94
	CR 7	65.64	1.20	13.73	5.64	0.18	0.90	2.60	4.74	2.90	97.53

Site	Code	SiO_2	TiO_2	Al_2O_3	FeO	MnO	MgO	CaO	Na_2O	K_2O	Total
	CR 7	65.08	1.17	13.99	5.37	0.09	1.03	2.51	4.29	3.49	97.01
	CR 7	64.78	1.18	14.12	5.06	0.14	0.96	3.14	5.65	1.91	96.94
Cill Donain	CD 1	66.76	1.13	14.06	5.75	0.16	1.10	3.17	4.76	2.73	99.60
	CD 1	66.29	1.22	13.90	5.42	0.21	1.12	2.54	4.80	2.79	98.29
	CD 1	66.13	1.21	14.32	5.04	0.11	1.06	2.73	4.55	2.80	97.95
	CD 1	65.89	1.11	14.15	5.80	0.21	1.27	3.17	4.28	2.68	98.56
	CD 1	65.71	1.22	13.92	5.82	0.17	1.17	3.10	4.54	2.85	98.50
	CD 1	65.59	1.28	14.25	5.54	0.17	1.22	2.97	4.38	2.75	98.15
	CD 1	65.46	1.13	14.02	5.20	0.18	1.16	3.16	4.25	2.77	97.33
	CD 1	65.10	1.19	14.04	5.56	0.14	1.07	2.94	4.50	2.78	97.32
	CD 1	65.04	1.13	14.07	5.50	0.17	1.20	3.06	4.54	2.66	97.37
	CD 1	65.00	1.20	14.04	5.50	0.20	1.09	2.98	4.59	2.74	97.34
	CD 1	64.98	1.15	14.26	5.49	0.24	1.24	2.93	4.44	2.76	97.49
	CD 1	64.52	1.22	14.21	5.59	0.20	1.18	3.06	4.54	2.87	97.39
	CD 1	64.45	1.13	14.09	5.44	0.18	1.25	3.07	4.40	2.71	96.72
	CD 2	66.87	1.16	13.65	5.54	0.18	1.11	3.04	4.63	2.85	99.03
	CD 2	65.95	1.19	14.03	5.89	0.17	1.06	2.90	4.60	2.84	98.63
	CD 2	65.83	1.19	14.21	5.41	0.15	1.08	3.00	4.50	2.73	98.10
	CD 2	65.78	1.15	13.77	5.43	0.18	1.12	3.07	4.47	2.68	97.66
	CD 2	65.68	1.27	14.06	6.56	0.21	1.06	3.03	4.45	2.72	99.04
	CD 2	65.68	1.25	14.28	5.68	0.21	1.18	2.99	4.60	2.89	98.76
	CD 2	65.54	1.15	14.14	5.53	0.18	1.20	2.99	4.59	2.77	98.09
	CD 2	65.40	1.24	14.25	5.76	0.20	1.14	2.97	4.59	2.68	98.23
	CD 2	65.27	1.27	13.84	5.74	0.16	1.06	2.83	4.49	2.74	97.39
	CD 2	65.22	1.15	14.12	5.57	0.24	1.09	2.86	4.82	2.78	97.85
	CD 2	65.06	1.30	13.96	5.89	0.14	1.15	3.12	4.34	2.66	97.62
	CD 2	64.73	1.33	13.85	5.59	0.13	1.12	2.83	4.66	2.85	97.09
	CD 2	64.31	1.24	13.99	5.74	0.17	1.08	3.03	4.43	2.74	96.73
	CD 3	66.90	1.31	14.22	5.53	0.19	1.13	3.04	2.23	2.73	97.28
	CD 3	66.13	1.14	14.05	5.36	0.20	1.16	2.94	4.50	2.70	98.18
	CD 3	65.90	1.22	13.90	5.44	0.20	1.09	3.10	4.58	2.76	98.18
	CD 3	65.75	1.22	14.35	5.37	0.16	1.20	2.99	4.46	2.72	98.22
	CD 3	65.69	1.21	13.94	5.40	0.19	1.12	2.98	4.46	2.88	97.87
	CD 3	65.66	1.19	14.35	5.72	0.19	1.19	3.05	4.37	2.70	98.42
	CD 3	65.64	1.23	14.13	5.31	0.21	1.10	2.91	4.49	2.69	97.71
	CD 3	65.49	1.20	14.33	5.37	0.19	1.12	3.05	4.56	2.65	97.96
	CD 3	65.45	1.14	14.53	5.60	0.13	1.09	3.18	4.50	2.60	98.22
	CD 3	65.23	1.14	14.36	5.25	0.16	1.15	2.91	4.52	2.74	97.46
	CD 3	64.80	1.15	13.81	5.53	0.16	1.13	3.49	4.26	2.83	97.16
	CD 3	64.66	1.28	14.07	5.50	0.12	1.22	3.18	4.45	2.64	97.12
	CD 3	64.40	1.13	14.12	5.54	0.18	1.20	3.07	4.51	2.77	96.92
	CD 4	66.85	1.34	14.22	5.01	0.17	1.15	2.81	4.49	2.88	98.92
	CD 4	66.48	1.12	14.45	5.42	0.15	1.03	2.80	4.66	2.70	98.81
	CD 4	66.02	1.21	14.01	5.56	0.19	1.17	3.16	4.35	2.47	98.14
	CD 4	65.76	1.23	14.18	5.29	0.13	1.25	2.93	4.01	2.47	97.25
	CD 4	65.58	1.29	14.25	5.44	0.18	1.15	3.19	4.41	2.71	98.20
	CD 4	65.57	1.22	13.77	5.07	0.21	1.20	3.00	4.53	2.85	97.42
	CD 4	65.51	1.30	14.11	5.45	0.14	1.13	3.06	4.50	2.81	98.01
	CD 4	65.38	1.14	13.61	5.62	0.23	1.12	3.19	4.21	2.55	97.04
	CD 4	65.28	1.23	14.33	5.75	0.24	1.20	3.13	4.31	2.76	98.23
	CD 4	65.13	1.31	14.31	5.73	0.22	1.18	3.32	4.43	2.69	98.32
	CD 4	65.12	1.26	14.37	5.67	0.18	1.14	3.25	4.40	2.55	97.94
	CD 4	64.60	1.28	14.20	5.67	0.23	1.20	3.03	4.69	2.66	97.56

Site	Code	SiO_2	TiO_2	Al_2O_3	FeO	MnO	MgO	CaO	Na_2O	K_2O	Total
	CD 5	66.72	1.31	13.64	5.27	0.21	1.13	3.14	4.63	2.95	99.01
	CD 5	66.39	1.05	13.57	5.27	0.16	1.14	3.03	4.37	2.74	97.72
	CD 5	66.32	1.26	14.32	5.26	0.16	1.10	3.05	4.42	2.73	98.62
	CD 5	66.10	1.13	14.13	5.59	0.13	1.13	3.21	4.52	2.61	98.55
	CD 5	66.08	1.02	14.29	5.21	0.22	1.14	3.15	4.40	2.77	98.28
	CD 5	66.07	1.23	14.17	5.31	0.19	1.15	3.03	4.37	2.78	98.30
	CD 5	65.79	1.14	14.05	5.32	0.16	1.13	3.15	4.45	2.80	97.99
	CD 5	65.61	1.15	14.09	5.10	0.09	1.05	3.05	4.34	3.01	97.49
	CD 5	65.36	1.08	14.16	5.59	0.13	1.11	2.93	4.44	2.63	97.43
	CD 5	65.34	1.08	14.09	5.51	0.15	1.09	3.00	4.21	2.84	97.31
	CD 5	65.01	1.22	13.95	5.33	0.15	1.21	3.23	4.35	2.81	97.26
	CD 5	64.86	1.00	13.72	5.50	0.17	1.07	2.93	4.33	2.82	96.40
	CD 5	64.65	1.17	14.01	5.44	0.23	1.13	3.10	4.59	2.78	97.10
	CD 6	66.83	1.12	14.19	5.25	0.15	1.14	3.02	4.06	2.90	98.66
	CD 6	66.79	1.12	14.24	5.34	0.18	1.07	2.94	4.22	2.76	98.66
	CD 6	66.50	1.04	14.05	5.34	0.18	1.13	3.16	4.35	2.76	98.51
	CD 6	66.04	1.23	13.94	5.15	0.19	1.00	3.11	4.72	2.88	98.25
	CD 6	65.96	1.07	13.89	5.44	0.19	1.09	3.09	4.38	2.77	97.88
	CD 6	65.95	1.22	14.32	5.71	0.15	1.13	3.16	4.42	2.84	98.90
	CD 6	65.95	1.28	14.20	5.48	0.14	1.15	2.88	4.43	2.73	98.24
	CD 6	65.81	1.07	14.07	4.98	0.15	1.14	3.00	4.17	2.87	97.26
	CD 6	65.53	1.14	14.03	5.60	0.18	1.05	2.86	4.66	2.83	97.88
	CD 6	65.48	1.32	13.86	5.31	0.16	1.08	2.81	4.72	2.54	97.28
	CD 6	65.34	1.16	13.99	5.40	0.12	1.13	2.96	4.56	2.74	97.40
	CD 6	64.79	1.16	13.83	5.50	0.25	1.10	3.20	4.58	2.73	97.14
	CD 6	64.22	1.25	13.89	5.54	0.25	1.16	3.05	4.53	2.82	96.69
	CD 7	66.32	1.07	14.28	5.32	0.19	1.15	2.88	4.55	2.84	98.60
	CD 7	66.29	1.13	14.08	5.41	0.21	1.10	3.06	4.23	3.01	98.52
	CD 7	66.24	1.03	14.08	5.58	0.19	1.15	3.16	4.23	2.80	98.46
	CD 7	66.12	1.32	14.10	4.97	0.19	0.88	2.97	4.81	2.86	98.22
	CD 7	66.10	1.19	14.09	5.51	0.18	1.11	3.15	4.85	2.81	98.99
	CD 7	66.00	1.10	14.07	5.40	0.14	1.14	3.14	4.31	2.73	98.03
	CD 7	65.88	1.09	14.04	5.49	0.25	1.13	2.99	4.38	2.85	98.10
	CD 7	65.48	1.09	13.93	5.27	0.14	1.11	2.96	4.18	2.76	96.92
	CD 7	65.32	1.16	13.97	5.30	0.13	1.09	2.84	4.40	2.54	96.75
	CD 7	64.56	1.15	13.82	5.35	0.17	1.22	3.09	4.56	2.75	96.67
	CD 7	63.92	1.11	13.81	5.17	0.15	1.04	2.76	4.51	2.78	95.25
	CD 7	63.84	1.19	13.96	5.25	0.22	1.11	2.96	4.59	2.65	95.77
	CD 7	63.44	1.25	14.14	5.21	0.20	1.29	3.18	4.78	2.91	96.40
	CD 8	67.83	1.23	14.14	4.47	0.11	1.04	2.52	4.41	3.02	98.77
	CD 8	67.77	1.09	14.19	4.84	0.16	0.93	2.69	4.56	2.74	98.97
	CD 8	67.06	1.20	14.10	5.34	0.17	1.17	3.14	4.89	2.79	99.86
	CD 8	66.90	1.12	14.07	4.99	0.21	1.05	2.94	4.51	2.75	98.54
	CD 8	66.90	1.23	14.10	5.11	0.17	1.09	2.73	4.60	2.84	98.77
	CD 8	66.26	1.31	14.11	5.46	0.18	1.08	2.91	4.63	2.56	98.50
	CD 8	66.19	1.27	13.87	5.43	0.15	1.14	3.20	4.71	2.66	98.63
	CD 8	66.19	1.20	13.94	5.54	0.20	1.13	2.87	4.53	2.66	98.26
	CD 8	66.04	1.26	14.17	5.56	0.14	1.16	2.90	4.61	2.71	98.55
	CD 8	65.51	1.22	14.26	5.61	0.19	1.04	2.94	4.51	2.94	98.21
	CD 8	65.46	1.21	14.15	5.55	0.17	1.19	3.20	4.52	2.77	98.22
	CD 8	65.30	1.12	14.13	5.98	0.23	1.27	3.16	4.82	2.78	98.79
	CD 8	64.93	1.21	14.08	5.91	0.16	1.12	2.97	4.69	2.69	97.76
Cille	CP 1	68.78	1.42	12.51	5.73	0.27	0.87	2.16	4.48	3.44	99.66

Site	Code	SiO_2	TiO_2	Al_2O_3	FeO	MnO	MgO	CaO	Na_2O	K_2O	Total
Pheadair											
	CP 1	68.19	1.19	13.23	4.71	0.15	0.65	2.27	4.83	3.47	98.69
	CP 1	67.63	1.29	13.55	4.91	0.16	0.46	2.29	5.36	2.88	98.53
	CP 1	67.54	1.40	12.67	5.42	0.19	0.66	2.15	5.09	3.10	98.21
	CP 1	66.51	1.10	13.19	5.41	0.18	1.29	2.89	4.75	2.73	98.06
	CP 1	66.47	1.29	12.86	5.27	0.23	1.19	3.01	4.67	2.99	97.98
	CP 1	65.68	1.53	14.09	5.70	0.18	0.85	2.74	5.22	3.14	99.12
Cnip	**C 1**	66.23	1.28	14.00	5.74	0.14	1.19	3.03	4.97	2.76	99.34
	C 1	66.07	1.32	14.36	5.58	0.19	1.11	3.05	4.81	2.74	99.23
	C 1	66.04	1.22	14.33	5.68	0.18	1.15	3.10	4.88	2.63	99.21
	C 1	65.99	1.20	14.12	5.83	0.24	1.12	3.10	5.00	2.61	99.21
	C 1	65.66	1.31	14.03	5.88	0.20	1.23	2.98	4.77	2.75	98.81
	C 1	65.63	1.26	14.12	5.94	0.14	1.11	3.07	4.77	2.71	98.75
	C 1	65.61	1.12	13.85	5.75	0.17	1.14	3.03	4.76	2.62	98.05
	C 1	65.54	1.18	14.05	5.79	0.24	1.18	3.07	4.82	2.76	98.63
	C 1	65.34	1.23	14.12	5.79	0.22	1.21	3.10	4.75	2.46	98.22
	C 1	65.06	1.22	14.10	5.81	0.16	1.13	3.10	4.95	2.75	98.28
	C 2	66.42	1.25	14.04	5.69	0.15	1.12	2.97	4.65	2.94	99.23
	C 2	66.20	1.33	14.29	5.47	0.20	1.17	3.01	4.74	2.80	99.21
	C 2	65.99	1.24	14.00	5.80	0.16	1.19	3.15	4.69	2.89	99.11
	C 2	65.97	1.29	13.95	5.77	0.16	1.14	3.12	4.69	2.74	98.83
	C 2	65.96	1.13	14.26	5.63	0.23	1.12	3.00	4.67	2.80	98.80
	C 2	65.72	1.14	13.90	5.79	0.15	1.17	3.15	4.79	2.72	98.53
	C 2	65.72	1.23	13.82	5.62	0.16	1.19	3.16	4.64	2.84	98.38
	C 2	65.58	1.24	14.09	5.99	0.25	1.17	3.09	4.61	2.72	98.74
	C 2	65.38	1.15	14.04	5.71	0.14	1.07	3.04	4.64	2.66	97.83
	C 2	65.11	1.30	14.07	5.92	0.18	1.08	3.23	4.54	2.83	98.26
	C 3	67.70	1.15	13.45	4.04	0.13	0.83	2.14	5.42	2.39	97.25
	C 3	66.91	1.07	14.01	4.87	0.11	0.68	2.55	5.12	2.80	98.12
	C 3	66.81	1.14	15.04	4.84	0.16	0.83	3.21	5.11	2.74	99.88
	C 3	66.61	1.03	15.02	4.06	0.13	0.58	3.12	5.26	2.42	98.23
	C 3	66.36	1.43	12.87	5.91	0.13	0.92	2.13	4.57	3.26	97.58
	C 3	66.27	1.14	12.98	4.85	0.13	0.82	3.06	5.96	3.15	98.36
	C 3	66.08	1.15	13.14	6.16	0.17	0.84	2.78	4.61	3.37	98.30
	C 3	66.03	1.33	14.34	5.51	0.12	1.13	3.29	4.63	2.71	99.09
	C 3	66.01	1.09	11.66	7.56	0.29	2.34	2.77	4.15	2.75	98.62
	C 3	65.65	1.58	11.43	6.73	0.24	1.96	3.51	4.02	3.00	98.12
Dún Aonghasa	**D 1**	67.01	1.21	13.74	4.78	0.17	1.17	3.38	4.66	2.68	98.80
	D 1	66.69	1.27	13.98	5.23	0.22	1.12	3.23	4.75	2.58	99.08
	D 1	66.38	1.28	13.95	5.83	0.18	1.29	3.16	4.96	2.71	99.74
	D 1	66.24	1.04	13.89	5.38	0.18	1.20	3.16	4.81	2.77	98.67
	D 1	65.82	1.28	13.88	5.77	0.18	1.26	3.24	4.56	2.61	98.61
	D 1	65.29	1.22	13.77	5.34	0.15	1.17	3.09	4.85	2.67	97.57
	D 1	65.29	1.15	13.88	5.85	0.12	1.12	3.15	4.73	2.79	98.09
	D 1	65.13	1.16	14.03	5.79	0.08	1.17	3.21	4.82	2.83	98.20
	D 1	64.99	1.24	14.06	5.37	0.18	1.19	3.29	4.52	2.60	97.43
	D 1	64.44	1.14	14.01	5.51	0.17	1.10	3.20	4.75	2.78	97.10
	D 2	67.06	1.19	13.72	4.88	0.20	1.03	2.90	4.66	2.78	98.42
	D 2	66.98	1.23	13.87	5.41	0.15	1.00	3.06	4.59	2.69	98.99
	D 2	66.49	1.19	13.98	5.51	0.22	1.04	3.00	4.75	2.65	98.84
	D 2	66.45	1.24	13.73	5.46	0.17	1.06	2.77	4.80	2.74	98.41
	D 2	66.24	1.17	13.86	5.28	0.12	1.16	3.09	4.82	2.80	98.54

Site	Code	SiO_2	TiO_2	Al_2O_3	FeO	MnO	MgO	CaO	Na_2O	K_2O	Total
	D 2	66.20	1.17	13.73	5.17	0.19	1.12	2.91	4.74	2.64	97.89
	D 2	66.10	1.26	13.61	5.35	0.18	0.98	2.30	4.55	2.78	97.81
	D 2	65.96	1.21	13.82	5.11	0.19	1.02	3.02	4.57	2.78	97.69
	D 2	65.65	1.21	13.82	5.53	0.18	1.05	3.18	4.82	2.82	98.25
	D 2	65.11	1.16	14.01	5.32	0.18	1.05	2.97	4.70	2.69	97.19
	D 3	66.88	1.25	13.99	4.78	0.15	1.16	3.26	4.64	2.88	99.01
	D 3	66.16	1.34	14.01	5.33	0.12	1.36	3.36	4.96	2.79	99.43
	D 3	66.13	1.32	14.14	5.43	0.19	1.18	3.18	4.85	2.81	99.24
	D 3	65.80	1.26	13.84	5.56	0.15	1.17	3.37	5.05	2.81	99.01
	D 3	65.76	1.33	14.70	5.49	0.14	1.12	3.23	4.78	2.76	99.30
	D 3	65.66	1.15	14.06	5.40	0.13	1.19	3.35	4.62	2.59	98.15
	D 3	65.54	1.25	14.09	5.34	0.12	1.18	3.30	4.88	2.84	98.48
	D 3	65.29	1.24	13.98	5.14	0.15	1.23	3.27	4.84	2.86	97.99
	D 3	65.12	1.29	14.10	5.42	0.19	1.13	3.18	4.62	2.69	97.71
Green Castle	GC 1	66.25	1.25	13.97	5.37	0.20	1.05	2.72	4.90	2.88	98.60
	GC 1	65.53	1.17	14.01	5.81	0.20	1.14	3.04	4.56	2.86	98.32
	GC 1	65.42	1.21	13.80	5.59	0.25	1.19	3.15	4.85	2.77	98.24
	GC 1	65.37	1.25	14.26	5.48	0.22	1.19	3.11	4.76	2.82	98.47
	GC 1	64.97	1.17	13.87	5.55	0.23	1.05	2.97	4.91	2.75	97.47
	GC 2	66.92	1.28	14.09	5.64	0.20	1.13	2.90	4.79	2.88	99.82
	GC 2	66.24	1.17	13.84	5.47	0.20	1.00	2.84	4.78	2.80	98.34
	GC 2	65.67	1.20	14.01	5.48	0.18	1.06	2.98	4.61	2.77	97.96
	GC 2	65.52	1.20	14.06	5.44	0.17	1.15	2.88	4.75	2.69	97.86
	GC 2	65.30	1.32	14.04	5.64	0.21	1.01	3.03	4.84	2.81	98.19
	GC 2	65.27	1.25	13.95	5.23	0.20	1.17	2.95	4.96	2.73	97.72
	GC 2	65.23	1.20	13.81	5.67	0.17	1.10	2.92	4.78	2.99	97.85
	GC 2	65.17	1.14	14.12	5.75	0.20	1.15	2.94	4.82	2.65	97.94
	GC 3	67.04	1.30	12.89	5.54	0.17	0.91	2.20	4.64	3.14	97.83
	GC 3	64.01	1.09	12.09	6.32	0.32	0.66	3.66	5.20	2.84	96.19
	GC 4	66.58	1.07	13.89	5.69	0.19	1.18	2.98	4.81	2.69	99.09
	GC 4	66.57	1.08	14.15	5.37	0.22	1.16	3.01	4.92	2.67	99.13
	GC 4	66.56	1.25	14.45	5.44	0.19	1.08	2.95	4.91	2.80	99.63
	GC 4	66.04	1.18	14.25	5.50	0.14	1.14	2.77	4.37	3.14	98.51
	GC 5	66.80	1.11	14.01	5.70	0.21	1.22	3.04	4.81	2.53	99.43
	GC 5	66.78	1.13	14.39	5.53	0.19	1.14	2.91	4.70	2.65	99.41
	GC 5	66.52	1.16	14.71	5.41	0.21	1.11	2.96	4.88	2.70	99.67
	GC 5	66.49	1.22	13.61	5.25	0.20	1.09	3.00	4.89	2.66	98.41
	GC 5	66.37	1.24	14.32	5.40	0.20	1.10	2.94	4.93	2.64	99.15
	GC 5	66.14	1.25	14.21	5.54	0.15	0.89	2.82	5.06	2.86	98.91
	GC 5	66.10	1.05	14.20	5.32	0.22	1.01	2.94	4.61	3.29	98.75
	GC 5	65.87	1.22	14.03	4.93	0.22	1.10	2.76	4.89	2.90	97.92
	GC 5	65.76	1.14	14.22	5.77	0.15	1.04	3.09	4.97	2.73	98.88
	GC 5	65.72	1.30	14.10	5.62	0.17	1.15	2.99	5.10	2.78	98.92
	GC 5	64.93	1.18	13.72	5.35	0.21	1.17	2.91	4.76	2.63	96.86
	GC 5	64.74	1.21	14.01	5.51	0.14	1.12	3.10	4.75	2.87	97.45
Kebister	K 1	66.81	1.30	13.44	5.22	0.15	1.05	2.95	5.00	2.95	98.85
	K 1	66.74	1.24	13.92	5.53	0.13	1.17	2.83	4.81	2.78	99.15
	K 1	65.79	1.17	13.72	5.27	0.10	1.06	3.09	4.88	2.66	97.74
	K 1	65.68	1.03	13.91	5.44	0.18	1.21	3.18	5.02	2.85	98.51
	K 1	65.59	1.14	13.85	5.35	0.15	1.15	3.17	4.96	2.75	97.11
	K 1	65.46	1.18	13.53	6.10	0.22	1.18	3.32	5.03	2.56	98.57
	K 1	65.41	1.30	14.04	5.57	0.18	1.12	3.19	5.15	2.67	98.64

Site	Code	SiO_2	TiO_2	Al_2O_3	FeO	MnO	MgO	CaO	Na_2O	K_2O	Total
	K 1	65.30	1.09	13.79	5.45	0.14	1.19	3.03	5.01	2.60	97.60
	K 1	65.29	1.11	13.69	5.78	0.17	1.21	3.00	5.01	2.65	97.90
	K 1	64.65	1.22	13.64	5.44	0.17	1.11	2.93	4.82	2.81	96.80
The Biggings	TB 1	72.58	0.34	13.38	3.46	0.07	0.09	1.06	4.62	3.23	98.83
	TB 1	72.48	0.27	13.18	3.67	0.09	0.04	1.20	4.83	3.09	98.85
	TB 1	72.12	0.23	13.33	3.38	0.06	0.09	1.19	4.66	3.33	98.39
	TB 1	72.02	0.31	13.05	3.32	0.10	0.02	0.97	4.40	3.23	97.42
	TB 1	71.54	0.39	13.71	3.82	0.10	0.08	1.29	4.70	3.15	98.78
	TB 1	71.53	0.25	13.02	3.20	0.10	0.05	1.13	4.91	3.27	97.46
	TB 1	71.35	0.36	13.83	4.21	0.12	0.13	1.47	4.95	3.19	99.61
	TB 1	71.14	0.36	13.40	3.83	0.21	0.10	1.28	4.49	3.17	97.98
	TB 1	70.47	0.21	12.75	3.50	0.12	0.04	1.06	4.72	3.31	96.18
	TB 1	69.92	0.44	13.24	4.44	0.16	0.22	1.66	4.70	3.04	97.82
	TB 2	73.34	0.28	13.11	3.08	0.10	0.04	0.95	4.96	3.81	99.67
	TB 2	72.49	0.23	12.80	3.06	0.10	0.03	0.88	4.85	3.59	98.03
	TB 2	72.40	0.28	12.83	3.16	0.11	0.01	0.88	5.38	3.59	98.64
	TB 2	72.24	0.25	12.67	3.03	0.12	0.06	0.88	4.67	3.54	97.46
	TB 2	71.67	0.28	13.50	2.87	0.04	0.02	0.93	5.32	3.85	98.48
	TB 2	71.45	0.26	12.30	2.88	0.07	0.03	0.87	4.49	3.04	95.39
	TB 2	71.37	0.20	12.65	3.25	0.07	0.01	0.89	5.28	3.57	97.29
	TB 2	71.30	0.20	12.32	3.17	0.13	0.03	0.87	5.97	3.14	97.13
	TB 2	71.30	0.23	12.62	3.07	0.13	0.03	0.93	4.94	3.37	96.62
	TB 2	70.01	0.26	13.06	2.98	0.12	0.06	0.96	4.94	3.41	95.80
	TB 3	72.93	0.21	13.34	3.28	0.11	0.01	0.97	5.26	3.72	99.83
	TB 3	72.93	0.29	13.48	3.26	0.12	0.01	1.05	5.03	3.68	99.85
	TB 3	72.82	0.26	13.20	3.11	0.05	0.04	0.99	5.06	3.58	99.11
	TB 3	72.76	0.23	12.87	2.98	0.10	0.04	0.96	4.91	3.58	98.43
	TB 3	72.63	0.21	13.11	3.08	0.05	0.07	0.94	4.74	3.43	98.26
	TB 3	72.43	0.22	13.34	3.19	0.12	0.04	0.98	5.13	3.74	99.19
	TB 3	72.37	0.20	13.16	3.20	0.07	0.03	0.91	3.64	3.59	97.17
	TB 3	72.06	0.24	13.39	3.18	0.12	0.03	1.01	5.00	3.43	98.46
	TB 3	70.80	0.21	13.26	3.19	0.08	0.01	0.94	5.04	3.45	96.98
	TB 3	70.79	0.21	13.31	3.20	0.08	0.05	0.97	4.79	3.32	96.72
	TB 4	73.81	0.21	12.99	3.26	0.10	0.05	1.01	4.71	3.39	99.53
	TB 4	73.70	0.22	13.20	3.20	0.09	0.01	0.94	4.92	3.51	99.79
	TB 4	73.20	0.27	13.58	3.27	0.05	0.03	1.02	4.99	3.52	99.93
	TB 4	73.17	0.26	13.03	3.16	0.07	0.04	1.02	4.60	3.56	98.91
	TB 4	73.09	0.17	13.23	3.25	0.10	0.04	1.18	4.57	3.55	99.18
	TB 4	73.02	0.23	13.25	3.16	0.13	0.02	1.01	4.79	3.33	98.94
	TB 4	72.42	0.22	13.24	3.30	0.10	0.03	1.04	5.07	3.30	98.72
	TB 4	72.09	0.20	12.72	3.19	0.13	0.02	1.02	4.59	3.39	97.35
	TB 4	71.22	0.26	13.30	3.34	0.12	0.03	0.89	4.89	3.54	97.59
	TB 4	71.20	0.16	12.82	3.21	0.12	0.05	0.95	4.65	3.21	96.37
Sands of Breakon	SB 1	72.36	0.21	13.60	3.16	0.12	0.05	0.95	5.73	3.31	99.49
	SB 1	72.07	0.22	13.43	3.26	0.19	0.01	1.05	5.46	3.52	99.21
	SB 1	71.87	0.16	13.49	3.28	0.10	0.02	0.99	5.61	3.44	98.96
	SB 1	71.85	0.22	13.37	3.25	0.09	0.05	0.90	5.30	3.43	98.47
	SB 1	71.18	0.21	13.25	3.02	0.07	0.05	1.09	5.55	3.54	97.96
	SB 1	71.04	0.25	13.26	3.05	0.12	0.01	1.04	5.42	3.46	97.66
	SB 1	71.02	0.22	13.22	3.07	0.08	0.04	0.96	5.40	3.18	97.18
	SB 1	70.62	0.22	12.92	3.09	0.07	0.03	0.93	5.54	3.44	96.86

Site	Code	SiO_2	TiO_2	Al_2O_3	FeO	MnO	MgO	CaO	Na_2O	K_2O	Total
	SB 1	70.48	0.18	12.91	2.98	0.08	0.02	0.98	5.58	3.21	96.41
	SB 1	70.33	0.24	12.95	3.19	0.14	0.02	1.00	5.23	3.60	96.69
	SB 2	66.89	1.25	12.33	5.94	0.26	1.55	2.50	4.53	3.11	98.34
	SB 2	66.76	1.12	13.19	5.03	0.20	0.80	2.54	4.91	3.04	97.59
	SB 2	66.19	1.12	14.93	4.51	0.14	0.61	3.16	5.39	2.64	98.69
	SB 2	66.08	1.33	12.99	5.74	0.19	0.96	2.64	4.72	3.12	97.77
	SB 2	65.94	1.27	12.18	6.70	0.30	2.19	3.02	4.43	2.97	99.00
	SB 2	65.92	1.20	13.66	5.18	0.20	0.96	2.85	5.18	2.75	97.92
	SB 2	65.80	1.32	13.00	5.83	0.26	1.14	2.60	4.53	3.08	97.57
	SB 2	65.51	0.98	14.76	5.59	0.14	0.79	3.43	5.73	2.69	98.61
	SB 2	65.49	0.95	15.46	4.07	0.14	0.76	3.71	5.54	2.30	98.44
	SB 2	65.40	1.41	13.60	5.73	0.23	0.89	2.86	4.99	2.82	97.96
Scalloway	S 1	66.12	1.31	14.01	5.38	0.21	1.01	3.03	4.75	3.02	98.84
	S 1	66.09	1.29	14.14	5.58	0.16	1.04	3.11	4.68	3.36	99.44
	S 1	65.38	1.25	14.10	5.58	0.09	1.14	3.03	4.73	2.88	98.19
	S 1	65.30	1.31	13.98	5.50	0.22	1.04	2.85	4.59	3.14	97.95
	S 1	65.15	1.30	13.70	5.97	0.14	1.14	2.95	4.64	2.85	97.83
	S 1	65.06	1.25	13.94	5.38	0.11	1.14	3.07	4.94	2.78	97.67
	S 1	65.03	1.23	13.54	5.62	0.18	1.18	3.02	4.77	2.85	97.43
	S 1	64.89	1.20	14.15	5.48	0.18	1.14	2.98	4.52	3.11	97.64
	S 1	64.77	1.21	14.04	5.64	0.18	1.14	2.91	4.87	2.93	97.69
	S 2	73.48	0.30	13.04	3.37	0.06	0.01	1.00	4.89	3.50	99.67
	S 2	73.34	0.22	13.32	3.33	0.09	0.00	0.87	4.77	3.56	99.50
	S 2	73.08	0.21	13.41	3.31	0.09	0.03	0.97	5.05	3.62	99.76
	S 2	73.00	0.23	13.26	3.23	0.03	0.03	0.94	4.50	3.53	98.74
	S 2	72.90	0.29	13.18	3.28	0.08	0.01	0.96	5.16	3.45	99.31
	S 2	72.62	0.27	13.13	3.26	0.11	0.03	1.05	4.99	3.48	98.92
	S 2	72.59	0.16	13.25	3.31	0.09	0.01	0.99	5.30	3.50	99.19
	S 2	72.56	0.24	13.26	3.25	0.11	0.02	0.97	5.06	3.40	98.87
	S 2	72.40	0.25	13.29	3.25	0.07	0.05	1.01	5.14	3.46	98.92
	S 2	72.19	0.24	13.12	3.32	0.06	0.01	1.01	4.83	3.52	98.30
Staosnaig	SG 1	70.35	0.23	13.19	3.64	0.14	0.20	1.35	5.34	3.17	97.61
	SG 1	69.84	0.28	13.19	3.91	0.09	0.20	1.33	5.30	3.41	97.55
	SG 1	69.77	0.26	13.17	3.91	0.15	0.20	1.35	5.36	3.47	97.64
	SG 1	69.64	0.30	13.13	3.67	0.11	0.21	1.34	5.30	3.62	97.32
	SG 1	69.60	0.28	12.87	3.58	0.09	0.19	1.28	5.40	3.55	96.84
	SG 1	69.48	0.27	13.18	3.79	0.14	0.20	1.35	5.35	3.62	97.38
	SG 1	69.48	0.19	12.95	3.84	0.10	0.21	1.36	5.26	3.53	96.92
	SG 1	69.29	0.28	13.10	3.75	0.15	0.22	1.30	5.41	3.47	96.97
	SG 1	68.91	0.28	13.17	4.02	0.17	0.22	1.38	5.32	3.40	96.87
	SG 1	68.48	0.30	13.15	3.67	0.16	0.17	1.21	5.33	3.61	96.08
	SG 2	68.16	0.88	13.84	4.17	0.10	0.73	2.00	5.15	3.08	98.11
	SG 2	68.01	0.78	13.71	3.82	0.10	0.70	1.98	5.23	3.22	97.55
	SG 2	67.78	0.77	13.70	4.02	0.14	0.71	1.92	5.23	3.16	97.43
	SG 2	67.65	0.86	13.66	4.07	0.13	0.78	2.19	5.44	3.26	98.04
	SG 2	67.49	0.88	13.52	4.13	0.16	0.73	2.24	5.26	3.15	97.56
	SG 2	67.32	0.85	13.67	4.32	0.11	0.82	2.14	5.21	3.26	97.70
	SG 2	67.31	0.83	13.41	4.43	0.13	0.74	2.13	5.06	3.02	97.06
	SG 2	67.27	0.72	13.83	4.27	0.15	0.74	2.07	5.19	3.08	97.32
	SG 2	66.80	0.90	13.63	3.83	0.10	0.58	1.90	5.20	3.13	96.07
	SG 2	66.47	0.84	13.23	4.28	0.10	0.75	2.02	5.05	3.08	95.82
	SG 3	69.07	0.88	13.83	3.52	0.14	0.61	1.83	5.02	3.24	98.14
	SG 3	69.00	0.73	13.76	4.13	0.21	0.72	1.95	4.54	3.17	98.21

Site	Code	SiO_2	TiO_2	Al_2O_3	FeO	MnO	MgO	CaO	Na_2O	K_2O	Total
	SG 3	68.73	0.86	13.55	3.84	0.10	0.68	1.81	4.95	3.15	97.67
	SG 3	68.21	0.76	13.42	3.73	0.20	0.75	2.08	4.99	3.02	97.16
	SG 3	68.16	0.88	13.58	4.11	0.09	0.76	2.02	5.25	3.21	98.06
	SG 3	68.04	0.77	13.61	3.68	0.13	0.62	1.74	5.02	3.29	96.90
	SG 3	67.82	0.82	13.81	4.28	0.10	0.74	1.93	5.29	3.04	97.83
	SG 3	67.78	0.79	13.28	3.90	0.14	0.67	1.95	4.92	3.10	96.53
	SG 3	67.28	0.92	13.42	4.11	0.16	0.68	2.24	5.14	3.27	97.22
	SG 3	66.52	0.85	13.62	4.03	0.17	0.75	1.96	5.01	3.02	95.93
	SG 4	71.34	0.25	12.96	3.51	0.13	0.21	1.42	5.13	3.45	98.40
	SG 4	70.41	0.25	13.13	3.81	0.17	0.21	1.31	5.27	3.48	98.04
	SG 4	70.31	0.21	12.78	3.67	0.11	0.20	1.26	5.38	3.60	97.52
	SG 4	69.75	0.37	12.88	3.78	0.11	0.21	1.24	5.45	3.43	97.22
	SG 4	69.73	0.19	12.82	4.06	0.14	0.22	1.44	5.16	3.49	97.25
	SG 4	69.70	0.30	13.16	3.89	0.14	0.21	1.35	5.54	3.58	97.87
	SG 4	69.69	0.33	13.18	3.74	0.16	0.21	1.33	5.40	3.52	97.56
	SG 4	69.61	0.26	12.28	3.89	0.09	0.22	1.52	5.49	3.62	96.98
	SG 4	69.60	0.23	13.14	3.63	0.17	0.22	1.26	5.00	3.53	96.78
The Udal	U 1	66.78	1.19	13.99	5.41	0.16	0.93	2.63	4.48	2.85	98.42
	U 1	66.63	1.33	13.81	5.02	0.20	0.91	3.03	4.54	2.90	98.37
	U 1	66.46	1.22	14.43	5.08	0.18	0.89	2.36	4.64	3.02	98.28
	U 1	66.24	1.18	13.51	5.42	0.18	0.97	2.59	4.56	2.92	97.57
	U 1	65.62	1.14	15.06	5.16	0.17	0.83	3.16	4.99	2.64	98.77
	U 2	66.62	1.19	14.23	5.56	0.22	1.05	3.01	4.43	2.82	99.13
	U 2	66.02	1.16	14.43	5.35	0.21	1.02	2.75	4.97	2.69	98.60
	U 2	65.97	1.31	14.33	5.19	0.17	0.96	2.78	4.83	3.03	98.57
	U 2	65.58	1.28	14.05	5.26	0.21	1.11	2.93	4.78	2.88	98.08
	U 2	65.39	1.24	14.20	5.44	0.28	1.11	2.79	4.72	2.76	97.93
	U 3	67.01	1.26	14.07	4.83	0.16	0.93	2.61	4.91	3.09	98.87
	U 3	66.18	1.16	13.96	5.18	0.15	1.06	3.09	4.89	2.82	98.49
	U 3	65.65	1.28	14.40	5.66	0.18	1.16	3.20	4.85	2.87	99.25
	U 3	64.97	1.19	14.06	5.50	0.21	1.22	3.29	4.94	2.92	98.30
	U 3	64.60	1.39	14.08	5.65	0.26	1.21	3.18	4.78	2.86	98.01
	U 4	66.37	1.33	14.25	5.55	0.23	1.04	2.98	4.58	2.64	98.97
	U 4	66.33	1.19	14.33	5.43	0.22	1.18	3.11	4.80	2.80	99.39
	U 4	66.28	1.24	14.45	5.63	0.21	1.18	3.04	4.80	2.76	99.59
	U 4	65.79	1.26	14.26	5.33	0.20	1.19	3.27	4.62	2.75	98.67
	U 4	65.47	1.23	14.41	5.23	0.29	1.11	3.04	4.87	2.86	98.51
	U 5	64.94	1.14	13.71	5.57	0.22	0.82	3.04	4.43	2.67	96.54
	U 5	64.90	1.17	13.59	5.53	0.23	0.91	2.97	4.36	2.90	96.56
	U 5	64.86	1.12	13.76	5.48	0.17	0.89	3.16	4.50	2.62	96.56
	U 5	64.75	1.28	13.54	5.39	0.16	0.91	3.02	4.37	2.69	96.11
	U 5	64.70	1.17	13.80	5.72	0.24	0.77	3.41	4.63	2.80	97.24
	U 5	64.57	1.10	13.56	5.54	0.20	0.83	3.12	4.83	2.75	96.50
	U 5	63.63	1.06	13.79	5.19	0.19	0.81	2.96	4.67	2.78	95.08
Upper Scalloway	US 1	65.89	0.84	15.84	2.69	0.06	0.20	3.14	5.98	2.54	97.17
	US 1	64.52	1.00	15.63	4.52	0.21	1.23	3.99	5.31	2.41	98.81
	US 1	62.92	0.86	16.88	4.93	0.20	1.34	4.67	5.67	1.89	99.37
	US 2	67.75	1.23	13.14	5.36	0.20	0.71	2.32	4.80	3.13	98.66
	US 2	67.18	1.14	15.78	4.20	0.07	0.75	3.28	5.16	2.33	99.89
	US 2	66.61	1.12	12.54	6.44	0.29	2.07	3.21	4.71	2.95	99.94
	US 2	65.67	1.19	12.26	6.48	0.30	2.09	2.70	3.91	2.97	97.58

Appendix 3H: Hekla HSv Pumice EPMA Data

Site	Pumice	SiO_2	TiO_2	Al_2O_3	FeO	MnO	MgO	CaO	Na_2O	K_2O	Total
Selsund	HSV1	75.74	0.11	12.55	1.24	0.07	0.05	1.11	4.62	2.82	98.31
	HSV1	71.95	0.21	13.49	3.00	0.07	0.13	1.87	4.35	2.61	97.68
	HSV1	70.95	0.19	13.52	3.10	0.13	0.18	1.90	4.58	2.22	96.77
	HSV1	70.67	0.15	13.23	2.88	0.10	0.14	1.88	4.43	2.36	95.84
	HSV1	70.06	0.21	13.43	2.83	0.08	0.16	1.81	4.55	2.51	95.64
	HSV1	65.40	1.31	13.48	5.20	0.18	1.08	2.96	4.58	2.79	96.98
	HSV1	57.59	1.59	13.36	10.29	0.17	2.21	5.28	4.02	1.55	96.06
	HSV1	57.10	1.58	13.74	9.80	0.33	1.91	5.36	4.19	1.55	95.56
	HSV1	56.07	2.03	13.68	9.13	0.35	2.18	6.17	4.05	1.45	95.11
	HSV2	75.04	0.08	12.57	1.81	0.14	0.04	1.30	4.40	2.70	98.08
	HSV2	70.82	0.22	13.57	2.92	0.13	0.17	1.75	4.85	2.42	96.85
	HSV2	69.93	0.21	13.41	2.81	0.16	0.15	1.83	4.61	2.39	95.50
	HSV2	67.24	0.35	14.44	4.76	0.17	0.37	2.81	4.59	2.14	96.87
	HSV2	67.22	0.36	14.25	4.80	0.14	0.44	2.78	4.45	2.12	96.56
	HSV2	55.78	2.13	13.05	11.26	0.31	2.44	5.73	4.11	1.40	96.21
	HSV2	55.34	2.06	13.14	10.89	0.33	2.40	5.93	4.14	1.35	95.58
	HSV2	55.07	2.09	12.77	11.16	0.42	2.41	5.60	4.07	1.53	95.12
	HSV2	54.57	2.08	13.31	11.04	0.26	2.71	5.80	4.06	1.29	95.12
	HSV3	73.17	0.20	13.78	2.83	0.12	0.17	1.96	4.71	2.61	99.55
	HSV3	72.95	0.22	13.85	3.24	0.08	0.17	1.94	4.76	2.69	99.90
	HSV3	72.90	0.23	13.65	2.81	0.16	0.20	1.97	4.66	2.57	99.15
	HSV3	72.71	0.21	13.72	2.97	0.11	0.21	1.87	4.76	2.60	99.16
	HSV3	72.48	0.23	13.82	2.93	0.11	0.18	1.91	4.88	2.56	99.10
	HSV3	72.39	0.17	13.75	2.99	0.10	0.19	1.85	4.48	2.44	98.36
	HSV3	72.09	0.17	13.82	2.78	0.12	0.20	1.89	4.59	2.59	98.25
	HSV3	71.92	0.16	13.90	2.86	0.16	0.18	1.75	5.00	2.47	98.40
	HSV3	71.66	0.22	13.86	3.06	0.0	0.16	2.01	4.54	2.60	98.21
	HSV3	70.88	0.22	13.87	2.95	0.14	0.17	1.85	4.81	2.62	97.51
	HSV4	69.63	0.34	14.10	3.88	0.16	0.27	2.51	4.44	2.41	97.74
	HSV4	69.41	0.14	14.90	3.07	0.18	0.17	2.99	4.94	2.30	98.10
	HSV4	68.64	0.34	14.57	4.75	0.16	0.35	2.77	4.38	2.36	98.32
	HSV4	66.83	0.41	14.47	5.16	0.20	0.42	3.18	4.52	2.04	97.23
	HSV4	59.06	1.55	13.37	10.29	0.61	2.30	5.55	4.12	1.36	98.21
	HSV4	57.73	1.49	14.18	10.12	0.33	2.38	5.61	3.94	1.37	97.15
	HSV4	57.17	1.74	14.55	9.90	0.34	2.44	5.65	4.00	1.42	97.21
	HSV4	56.80	2.28	13.27	11.50	0.27	2.41	6.01	3.70	1.45	97.69
	HSV4	56.49	2.03	13.02	10.70	0.34	2.45	5.85	4.00	1.41	96.29
	HSV4	55.38	2.20	12.34	11.21	0.39	2.79	5.73	3.88	1.55	95.47

Appendix 3I: Katla Silicic Pumice EPMA Data

Site	Pumice	SiO_2	TiO_2	Al_2O_3	FeO	MnO	MgO	CaO	Na_2O	K_2O	Total
Vikurhóll	VH 1	70.66	0.36	13.48	3.77	0.18	0.22	1.27	5.14	3.57	98.65
	VH 1	70.26	0.34	13.28	3.79	0.13	0.23	1.36	5.36	3.43	98.18
	VH 1	70.24	0.33	13.40	3.83	0.16	0.23	1.36	5.09	3.47	98.11
	VH 1	70.21	0.28	13.66	3.82	0.16	0.22	1.34	5.32	3.52	98.53
	VH 1	69.92	0.31	13.52	3.67	0.19	0.20	1.25	5.08	3.70	97.84
	VH 1	69.88	0.31	13.27	3.83	0.14	0.24	1.39	5.43	3.43	97.92
	VH 1	69.81	0.33	13.04	3.88	0.08	0.24	1.28	5.13	3.56	97.35
	VH 1	69.80	0.35	13.05	3.72	0.13	0.19	1.48	5.03	3.36	97.11
	VH 1	68.97	0.28	13.23	3.78	0.12	0.23	1.46	5.12	3.52	96.71
	VH 1	68.47	0.31	13.74	3.57	0.14	0.19	1.39	5.72	3.29	96.82
	VH 2	71.64	0.27	12.98	3.89	0.11	0.20	1.28	5.05	3.68	99.10
	VH 2	71.48	0.29	13.09	3.57	0.15	0.19	1.22	5.15	3.53	98.67
	VH 2	71.41	0.27	13.05	3.77	0.14	0.23	1.33	5.38	3.43	99.01
	VH 2	71.06	0.32	13.15	3.68	0.15	0.22	1.27	5.15	3.20	98.20
	VH 2	70.96	0.27	13.23	3.77	0.14	0.25	1.26	5.37	3.49	98.74
	VH 2	70.73	0.29	12.85	3.82	0.21	0.24	1.16	5.14	3.52	97.96
	VH 2	70.23	0.32	13.25	3.89	0.24	0.23	1.23	5.11	3.21	97.71
	VH 2	69.72	0.27	13.13	3.46	0.20	0.21	1.17	5.22	3.43	96.81
	VH 2	68.73	0.31	13.29	3.94	0.14	0.24	1.36	5.16	3.45	96.62
	VH 2	68.59	0.29	12.93	3.81	0.17	0.26	1.27	5.05	3.37	95.74
	VH 2	68.34	0.30	13.23	3.58	0.13	0.23	1.15	5.25	3.40	95.61
	VH 3	70.72	0.35	13.72	3.55	0.12	0.21	1.21	5.00	3.35	98.23
	VH 3	69.92	0.30	13.35	3.74	0.21	0.24	1.35	5.37	3.42	97.90
	VH 3	69.43	0.33	13.32	3.79	0.17	0.24	1.24	5.28	3.37	97.17
	VH 3	69.42	0.30	13.46	3.87	0.12	0.20	1.26	5.29	3.33	97.25
	VH 3	69.16	0.32	13.16	3.64	0.15	0.27	1.41	5.09	3.60	96.80
	VH 3	68.99	0.31	13.31	3.62	0.15	0.20	1.33	5.22	3.63	96.76
	VH 3	68.81	0.30	13.11	3.89	0.10	0.25	1.30	5.13	3.53	96.42
	VH 3	68.77	0.29	13.27	3.45	0.21	0.23	1.28	5.47	3.62	96.59
	VH 3	68.69	0.29	13.23	3.77	0.13	0.26	1.39	5.12	3.42	96.30
	VH 3	68.22	0.32	13.33	3.73	0.16	0.21	1.24	5.20	3.59	96.00
Sólheimar	SI 1	68.38	0.29	13.13	3.70	0.15	0.22	1.28	5.06	3.49	95.70
	SI 1	68.51	0.39	13.17	3.85	0.16	0.20	1.26	4.94	3.58	96.06
	SI 1	67.71	0.28	13.73	3.89	0.08	0.19	1.39	4.80	3.39	95.46
	SI 1	68.14	0.33	12.96	3.40	0.16	0.21	1.41	4.63	3.43	94.67
	SI 1	69.70	0.29	13.03	3.68	0.12	0.17	1.28	4.96	3.36	96.59
	SI 1	69.27	0.30	13.13	3.90	0.13	0.22	1.40	4.82	3.49	96.66
	SI 1	69.58	0.35	13.15	3.76	0.15	0.17	1.35	4.80	3.57	96.88
	SI 1	68.50	0.27	12.89	3.70	0.15	0.21	1.36	4.63	3.49	95.20
	SI 2	68.64	0.26	13.25	3.54	0.13	0.22	1.45	4.64	3.55	95.68
	SI 2	68.78	0.38	13.53	3.69	0.17	0.17	1.34	4.79	3.42	96.27
	SI 2	67.88	0.36	13.10	3.70	0.15	0.17	1.64	4.84	3.49	95.33
	SI 2	68.14	0.30	13.05	3.46	0.11	0.17	1.46	4.88	3.44	95.01
	SI 2	68.92	0.33	13.24	3.68	0.11	0.21	1.32	4.72	3.39	95.92
	SI 2	70.14	0.32	13.17	3.72	0.20	0.22	1.44	4.49	3.41	97.11
	SI 2	69.59	0.23	13.08	3.74	0.12	0.23	1.49	4.64	3.66	96.78
	SI 2	68.49	0.31	13.23	3.54	0.16	0.22	1.40	4.82	3.30	95.47
	SI 2	69.83	0.30	13.31	3.87	0.13	0.20	1.30	4.76	3.44	97.14

Site	Pumice	SiO_2	TiO_2	Al_2O_3	FeO	MnO	MgO	CaO	Na_2O	K_2O	Total
	SI 2	69.81	0.29	12.99	3.80	0.16	0.23	1.37	4.85	3.61	97.11
	SI 3	69.34	0.29	13.61	3.84	0.11	0.23	1.43	5.06	3.62	97.53
	SI 3	69.16	0.27	13.26	3.79	0.10	0.21	1.43	5.20	3.43	96.85
	SI 3	69.00	0.26	13.35	3.75	0.11	0.19	1.39	5.02	3.49	96.56
	SI 3	68.83	0.28	13.16	3.68	0.14	0.23	1.41	4.85	3.50	96.08
	SI 3	69.12	0.29	13.26	3.82	0.14	0.19	1.39	5.00	3.69	96.90
	SI 3	68.77	0.35	12.99	3.61	0.10	0.20	1.48	4.81	3.54	95.85
	SI 3	68.98	0.26	13.45	3.74	0.11	0.20	1.39	5.01	3.55	96.69
	SI 3	69.47	0.20	13.41	3.75	0.12	0.20	1.46	5.00	3.61	97.22
	SI 3	68.60	0.27	13.11	3.98	0.15	0.26	1.52	4.88	3.43	96.20
	SI 3	68.41	0.27	13.19	3.63	0.10	0.17	1.53	4.95	3.46	95.71
	SI 4	69.55	0.29	13.35	3.97	0.18	0.23	1.42	5.13	3.36	97.48
	SI 4	68.79	0.27	13.27	3.65	0.15	0.24	1.35	4.92	3.48	96.12
	SI 4	69.30	0.29	13.30	3.64	0.10	0.18	1.29	4.91	3.51	96.52
	SI 4	68.88	0.27	13.53	3.73	0.15	0.23	1.33	5.06	3.41	96.59
	SI 4	68.23	0.26	13.31	3.91	0.10	0.19	1.43	4.96	3.29	95.68

Appendix

4

Geochemical data: SILK Tephra Layers

Appendix 4A: EPMA Geochemical Data

SILK Layer	Local	SiO_2	TiO_2	Al_2O_3	FeO	MnO	MgO	CaO	Na_2O	K_2O	Total
SILK-YN	N8	66.39	0.98	14.07	5.52	0.18	0.84	2.38	4.78	3.00	98.14
		65.90	1.27	14.01	6.17	0.21	1.07	2.86	4.37	2.63	98.49
		65.64	1.10	14.46	6.16	0.15	1.02	2.97	4.24	2.58	98.32
		65.61	1.19	14.33	5.99	0.16	1.11	3.09	4.51	2.73	98.72
		65.50	1.24	14.40	5.71	0.19	0.96	2.90	4.66	2.72	98.28
		65.50	1.11	14.10	6.18	0.18	1.10	2.95	4.66	2.71	98.49
		64.78	1.28	13.99	6.20	0.19	1.10	3.00	4.76	2.54	97.84
		64.66	1.25	13.94	6.16	0.19	1.23	3.25	4.66	2.74	98.08
		64.54	1.31	14.04	6.13	0.25	1.09	3.02	4.67	2.72	97.77
		64.53	1.19	14.16	6.14	0.17	1.11	2.97	4.18	2.60	97.05
	YN	67.09	0.98	13.91	5.18	0.17	0.82	2.72	4.42	2.93	98.22
		66.97	0.96	13.91	5.38	0.19	0.88	2.62	4.28	2.86	98.05
		66.53	1.12	13.90	5.80	0.15	0.93	2.75	3.92	2.89	97.99
		66.38	1.05	13.66	5.60	0.18	0.96	2.69	3.92	2.82	97.26
		66.17	1.19	14.02	5.71	0.19	1.00	3.04	4.42	2.67	98.41
		66.08	1.18	13.95	6.04	0.23	1.07	3.26	4.60	2.48	98.89
		65.76	1.25	14.13	5.71	0.19	1.11	3.07	3.94	2.74	97.90
		65.72	1.06	14.20	6.06	0.20	1.15	3.05	4.45	2.72	98.61
		65.69	1.27	14.10	6.25	0.14	1.18	3.10	4.57	2.70	99.00
		65.42	1.18	14.16	6.06	0.18	1.05	3.08	4.24	2.67	98.04
		65.20	1.12	13.99	6.04	0.16	1.03	3.10	4.34	2.66	97.64
		65.04	1.13	14.10	5.91	0.20	1.06	3.25	4.04	2.63	97.36
		64.98	1.16	13.95	5.89	0.21	1.13	3.13	4.09	2.70	97.24
		64.74	1.02	13.72	5.86	0.14	1.01	2.94	4.02	2.87	96.32
		64.73	1.16	13.77	6.11	0.19	1.19	3.21	4.37	2.76	97.49
		64.58	1.10	13.84	6.28	0.21	1.08	3.17	4.06	2.61	96.93
		64.31	1.25	14.06	6.02	0.22	1.07	3.10	3.93	2.78	96.74
		64.24	1.09	13.99	6.06	0.17	1.14	3.14	4.02	2.77	96.62
		63.76	1.20	13.89	5.98	0.23	1.05	3.10	4.03	2.86	96.10
SILK-UN	N7	64.97	1.40	14.05	5.81	0.19	1.34	3.43	4.11	2.65	97.95
		64.55	1.37	13.83	5.96	0.22	1.40	3.31	4.54	2.30	97.48
		64.36	1.31	14.36	5.85	0.18	1.47	3.62	4.13	2.62	97.90
		64.22	1.43	14.01	5.67	0.16	1.29	3.50	4.49	2.63	97.40
		64.21	1.27	13.89	6.19	0.17	1.32	3.34	4.10	2.60	97.09
		64.09	1.38	14.11	6.04	0.19	1.36	3.38	4.54	2.57	97.66
		64.02	1.28	13.98	5.24	0.20	1.19	3.17	4.53	2.70	96.31
		63.93	1.26	13.92	6.14	0.20	1.47	3.50	4.64	2.58	97.64
		63.66	1.29	13.43	6.25	0.25	1.36	3.44	4.35	2.68	96.71
		63.59	1.32	13.93	6.25	0.23	1.36	3.28	4.30	2.60	96.86
SILK-MN	N6	66.43	1.05	14.30	5.38	0.17	1.08	2.86	4.01	2.44	97.72

SILK Layer	Local	SiO_2	TiO_2	Al_2O_3	FeO	MnO	MgO	CaO	Na_2O	K_2O	Total
		65.82	1.16	14.33	5.63	0.27	1.11	3.03	4.53	2.50	98.38
		65.72	1.16	14.34	5.47	0.21	1.19	3.06	4.05	2.69	97.89
		65.45	1.25	13.96	5.58	0.23	1.22	2.98	4.24	2.70	97.61
		65.13	1.24	14.20	5.82	0.20	1.20	2.88	4.35	2.82	97.84
		64.92	1.22	14.07	5.51	0.18	1.09	2.89	4.48	2.58	96.94
		64.85	1.25	14.47	5.50	0.21	1.11	3.09	4.01	2.49	96.98
		64.77	1.20	13.97	5.43	0.22	1.06	2.92	4.10	2.78	96.45
SILK-MN	**MNL**	67.35	1.20	13.86	5.62	0.15	1.07	3.15	4.49	2.80	99.70
		67.25	1.15	14.38	5.60	0.15	1.11	3.03	4.40	2.92	99.99
		67.18	1.15	14.22	5.72	0.23	1.14	3.23	3.91	2.87	99.65
		66.70	1.11	14.45	5.26	0.17	1.07	2.89	4.13	2.82	98.60
		66.56	1.29	14.04	5.70	0.16	1.15	2.83	4.38	2.99	99.12
		66.38	1.16	13.76	5.55	0.20	1.13	3.12	4.63	2.86	98.79
		66.03	1.21	14.02	5.47	0.20	1.15	2.99	4.19	2.87	98.11
		65.60	1.30	13.84	5.36	0.17	1.07	2.87	4.13	2.85	97.19
		65.09	1.23	14.20	5.82	0.23	1.22	3.15	4.64	2.65	98.22
		64.71	1.15	14.08	5.76	0.15	1.20	2.86	4.63	2.55	97.10
	Eng 1 10	67.79	1.17	13.94	5.61	0.19	0.90	2.93	4.39	2.84	99.96
		67.68	1.30	14.26	5.35	0.15	1.05	2.93	4.40	2.70	99.82
		67.65	1.28	13.90	5.57	0.19	1.15	2.98	4.22	2.73	99.69
		67.20	1.23	13.96	5.57	0.18	1.15	2.97	4.68	2.74	99.68
		67.02	1.21	14.08	5.41	0.18	1.10	3.07	4.52	2.74	99.32
		66.99	1.30	14.34	5.84	0.19	1.13	2.97	4.36	2.73	99.86
		66.90	1.21	14.47	5.74	0.14	1.13	2.92	4.48	2.94	99.92
		66.66	1.24	14.37	5.49	0.14	1.13	3.06	4.34	2.63	99.07
		65.97	1.16	13.93	5.51	0.17	1.11	3.12	4.32	2.67	97.96
	Eng 62A 48	67.05	1.24	14.28	5.57	0.20	1.14	2.94	4.40	2.83	99.65
		66.80	1.27	14.16	5.47	0.16	1.10	2.97	4.04	2.68	98.65
		66.16	1.15	14.06	5.60	0.18	1.10	2.97	4.44	2.79	98.45
		66.06	1.32	13.90	5.69	0.22	1.09	3.15	4.44	2.63	98.50
		65.94	1.24	14.51	5.70	0.26	1.15	2.99	4.38	2.70	98.87
		65.85	1.34	13.92	5.64	0.19	1.09	2.85	4.29	2.77	97.94
		65.54	1.37	14.08	5.69	0.18	1.15	2.98	4.40	2.74	98.13
		65.33	1.25	14.23	5.57	0.17	1.11	3.02	4.42	2.59	97.69
		65.33	1.20	14.18	5.72	0.23	1.15	2.89	4.51	2.65	97.86
		64.68	1.21	13.90	5.78	0.17	1.18	3.01	4.18	2.70	96.83
SILK-LN	**N5**	65.93	1.25	14.32	5.83	0.20	1.12	3.06	4.51	2.91	99.13
		65.84	1.26	14.34	5.80	0.18	1.09	3.15	4.45	2.83	98.94
		65.63	1.27	14.09	5.48	0.20	1.09	3.02	4.54	2.86	98.18
		65.58	1.12	14.38	5.73	0.23	1.18	2.95	4.40	2.74	98.31
		65.34	1.24	14.29	5.69	0.10	1.14	3.06	4.51	2.76	98.13
		65.30	1.20	14.19	5.38	0.15	1.12	3.08	4.28	2.79	97.49
		65.01	1.23	14.45	5.42	0.18	1.19	2.90	4.09	2.64	97.11
		64.73	1.24	13.92	5.41	0.22	1.06	2.81	3.91	2.59	95.89
		64.28	1.14	14.03	5.65	0.20	1.08	3.03	4.49	2.60	96.50
		64.12	1.22	14.13	5.60	0.25	1.11	2.92	4.54	2.71	96.60
	LNL	66.73	1.26	14.14	5.65	0.19	1.15	2.99	4.68	2.78	99.56
		66.60	1.17	14.04	5.88	0.17	1.10	3.05	4.58	2.69	99.20
		66.59	1.29	14.35	5.71	0.17	1.13	3.08	4.28	2.61	99.27

SILK Layer	Local	SiO_2	TiO_2	Al_2O_3	FeO	MnO	MgO	CaO	Na_2O	K_2O	Total
		66.42	1.21	13.65	5.66	0.15	1.09	3.02	4.43	2.66	98.83
		66.41	1.26	13.79	5.68	0.19	1.11	2.98	4.63	2.80	98.74
		66.39	1.22	13.62	5.53	0.18	1.11	3.07	4.45	2.68	98.25
		66.36	1.18	13.17	5.63	0.18	1.06	2.94	4.93	2.60	98.04
		66.32	1.15	14.50	5.64	0.12	1.15	2.90	4.88	2.76	99.43
		65.91	1.22	13.57	5.65	0.20	1.11	3.02	4.56	2.64	97.88
		65.78	1.21	14.02	5.67	0.22	1.16	2.92	4.53	2.71	98.22
		63.75	1.21	13.46	5.62	0.21	1.03	3.02	4.40	2.66	95.36
	Eng 1 15	67.35	1.22	14.32	5.61	0.21	1.12	2.90	4.21	2.79	99.72
		67.24	1.25	14.18	5.80	0.22	1.07	3.06	4.47	2.67	99.96
		66.83	1.19	14.02	5.74	0.22	1.11	2.97	4.46	2.86	99.40
		66.66	1.25	13.98	5.88	0.18	1.02	3.01	4.56	2.71	99.24
		66.37	1.19	14.05	5.73	0.17	1.12	3.09	4.75	2.87	99.34
		66.03	1.16	14.48	5.98	0.18	1.10	3.14	4.47	2.75	99.28
		66.01	1.14	13.74	5.76	0.13	1.11	3.01	4.71	2.85	98.47
	Eng62A 53	66.76	1.11	14.01	5.83	0.18	1.16	2.96	3.51	2.71	98.23
		66.71	1.18	14.36	6.20	0.12	1.21	3.26	4.15	2.74	99.93
		66.59	1.18	14.59	5.53	0.13	1.16	2.95	4.04	2.63	98.80
		66.39	1.18	14.47	5.45	0.18	1.07	2.93	4.28	2.82	98.79
		66.03	1.18	14.00	5.77	0.20	1.15	3.10	4.59	2.68	98.70
		65.99	1.21	14.26	5.52	0.13	1.15	3.14	4.29	2.77	98.45
		65.97	1.20	14.41	5.54	0.15	1.04	2.96	4.56	2.69	98.53
		65.62	1.24	14.58	5.54	0.15	1.26	2.93	4.17	2.59	98.07
		65.32	1.28	14.49	5.33	0.13	1.08	2.92	3.89	2.76	97.20
		65.12	1.25	14.83	5.63	0.22	1.25	3.08	4.34	2.89	98.61
SILK-N4	**N4**	67.25	1.19	14.20	4.96	0.18	1.03	2.71	4.57	2.95	99.04
		66.66	1.30	14.10	5.98	0.17	1.07	3.07	4.23	2.79	99.37
		66.62	1.32	14.13	5.35	0.19	1.12	2.79	4.42	2.81	98.75
		66.39	1.22	13.98	5.94	0.17	1.12	2.92	4.63	2.79	99.16
		66.18	1.26	14.08	5.58	0.16	1.19	2.83	4.69	2.80	98.77
		66.12	1.19	14.25	5.72	0.20	1.13	2.95	4.41	2.73	98.70
		65.84	1.12	14.08	5.55	0.20	1.05	2.93	4.40	2.67	97.84
		65.70	1.22	14.15	5.60	0.17	1.15	2.91	4.29	2.87	98.06
		65.61	1.28	14.13	5.45	0.13	1.41	2.81	4.64	2.83	98.29
		65.57	1.23	13.87	5.55	0.22	1.13	3.08	4.73	2.74	98.12
SILK-N3	**N3**	65.50	1.37	14.32	5.96	0.18	1.33	3.51	4.35	2.55	99.07
		65.39	1.45	14.07	6.03	0.18	1.33	3.26	4.36	2.63	98.70
		65.17	1.47	14.30	5.84	0.23	1.33	3.45	4.35	2.50	98.64
		65.02	1.53	14.03	6.09	0.24	1.39	3.43	3.94	2.62	98.29
		64.91	1.50	14.06	4.74	0.15	1.30	3.38	4.31	2.68	97.03
		64.67	1.48	14.43	6.12	0.25	1.38	3.33	4.30	2.49	98.45
		64.40	1.35	14.17	6.03	0.21	1.40	3.37	4.25	2.71	97.89
		64.18	1.58	13.96	6.02	0.20	1.39	3.23	4.17	2.62	97.35
		63.84	1.49	14.08	6.07	0.23	1.38	3.27	4.07	2.58	97.01
		63.77	1.59	14.06	6.66	0.15	1.28	3.24	4.42	2.64	97.81
SILK-N2	**N2**	64.31	1.50	14.07	6.23	0.23	1.35	3.53	4.39	2.52	98.13
		64.26	1.49	13.98	6.24	0.21	1.46	3.79	4.36	2.72	98.51
		63.95	1.49	14.14	6.47	0.25	1.35	3.58	4.57	2.47	98.27
		63.72	1.51	13.98	6.17	0.23	1.50	3.51	4.01	2.54	97.17

SILK Layer	Local	SiO_2	TiO_2	Al_2O_3	FeO	MnO	MgO	CaO	Na_2O	K_2O	Total
		63.63	1.67	14.03	6.16	0.14	1.44	3.47	4.23	2.55	97.32
		63.51	1.53	13.97	6.20	0.24	1.36	3.51	4.44	2.51	97.27
		63.41	1.36	13.79	6.44	0.19	1.47	3.61	4.21	2.44	96.92
		63.36	1.49	13.75	6.51	0.20	1.55	3.87	4.67	2.55	97.95
		63.26	1.50	13.70	6.50	0.19	1.37	3.53	4.30	2.56	96.91
		62.49	1.63	13.95	6.61	0.20	1.52	3.56	4.04	2.46	96.46
SILK-N1	N1	66.08	1.30	13.71	5.30	0.21	1.04	2.76	4.27	2.75	97.42
		65.73	1.37	13.79	5.71	0.18	1.15	3.02	4.07	2.72	97.74
		65.65	1.33	13.54	5.79	0.18	1.19	3.14	4.56	2.70	98.08
		65.49	1.44	13.45	5.81	0.18	1.17	2.97	4.65	2.83	97.99
		65.31	1.42	13.81	5.47	0.18	1.25	3.17	4.43	2.58	97.62
		65.22	1.36	13.87	5.92	0.13	1.23	3.05	4.49	2.94	98.21
		65.20	1.40	13.97	5.85	0.18	1.18	2.92	4.53	2.94	98.17
		65.08	1.32	13.60	6.12	0.28	1.22	3.03	4.75	2.80	98.20
		64.73	1.39	13.65	6.13	0.22	1.22	3.46	4.70	2.82	98.32
		64.69	1.35	13.26	5.66	0.18	1.22	2.82	4.70	2.71	96.59
SILK-A1	TYN9	66.36	1.34	13.84	5.85	0.19	1.12	2.85	4.14	2.91	98.60
		65.74	1.41	13.42	5.93	0.21	1.19	2.89	3.68	2.79	97.26
		65.70	1.34	13.61	6.04	0.20	1.07	2.73	3.90	2.74	97.33
		65.45	1.46	13.66	5.92	0.22	1.17	3.05	4.65	2.79	98.37
		65.43	1.36	13.25	6.12	0.18	1.15	3.17	4.02	2.73	97.41
		65.37	1.40	13.41	5.87	0.20	1.16	2.98	4.37	2.88	97.64
		65.36	1.43	13.53	5.86	0.17	1.19	2.95	4.22	2.74	97.45
		65.32	1.37	13.35	6.15	0.21	1.23	3.10	4.54	2.66	97.93
		65.27	1.33	13.53	5.52	0.16	1.10	2.83	4.23	2.77	96.74
		65.04	1.37	13.32	5.82	0.16	1.17	3.09	4.41	2.68	97.06
		64.99	1.40	13.31	5.81	0.19	1.14	2.92	4.57	3.00	97.33
		64.92	1.41	13.64	5.78	0.16	1.09	2.99	4.20	2.84	97.03
		64.77	1.24	13.25	5.69	0.17	1.05	2.99	4.49	2.62	96.27
		64.75	1.40	13.41	6.43	0.27	1.25	2.99	4.31	2.79	97.60
		64.55	1.30	13.50	6.12	0.17	1.13	3.10	4.03	2.55	96.45
		64.53	1.43	13.71	6.13	0.23	1.30	3.08	4.33	2.68	97.42
		64.49	1.40	13.41	6.19	0.17	1.27	3.05	4.29	2.67	96.94
		64.33	1.35	13.70	5.46	0.18	1.17	2.99	4.11	2.82	96.11
		64.10	1.30	13.57	5.92	0.21	1.21	2.91	4.45	2.83	96.50
		63.93	1.50	13.40	5.61	0.20	1.19	2.92	4.50	2.72	95.97
SILK-A5	MBH-3	65.14	1.40	14.28	5.96	0.17	1.26	3.35	4.30	2.58	98.44
		64.93	1.24	13.85	5.90	0.21	1.24	3.35	4.28	2.57	97.57
		64.80	1.26	14.19	5.81	0.18	1.25	3.25	4.11	2.73	97.58
		64.56	1.30	14.06	6.16	0.20	1.31	3.30	4.30	2.82	98.01
		64.51	1.38	13.82	5.93	0.20	1.32	3.40	4.22	2.71	97.49
		64.45	1.26	14.18	6.33	0.18	1.36	3.49	4.54	2.78	98.57
		64.32	1.43	13.84	6.34	0.19	1.37	3.39	4.37	2.56	97.81
		64.18	1.48	13.85	6.29	0.17	1.41	3.52	4.01	2.56	97.47
		64.17	1.32	14.05	5.91	0.21	1.37	3.41	4.41	2.69	97.54
		63.79	1.30	13.96	5.91	0.23	1.24	3.50	4.50	2.62	97.05
SILK-A7	TYN3	66.13	1.08	14.04	5.19	0.18	0.95	2.76	4.54	2.89	97.76
		65.38	1.29	14.24	5.81	0.15	1.22	3.19	4.67	2.61	98.56
		65.12	1.10	13.42	5.82	0.14	1.18	3.42	4.59	2.74	97.53
		64.47	1.20	14.25	5.56	0.23	1.20	3.36	4.61	2.49	97.37

SILK Layer	Local	SiO_2	TiO_2	Al_2O_3	FeO	MnO	MgO	CaO	Na_2O	K_2O	Total
		64.39	1.26	13.95	5.86	0.19	1.30	3.33	4.73	2.70	97.71
		64.23	1.24	13.97	5.91	0.14	1.22	3.29	4.50	2.67	97.17
		63.88	1.32	14.22	6.07	0.18	1.32	3.54	4.68	2.43	97.64
		63.75	1.29	13.89	5.88	0.19	1.31	3.64	4.68	2.65	97.28
		63.56	1.31	13.84	5.72	0.19	1.23	3.34	4.76	2.59	96.54
		63.44	1.44	14.13	5.95	0.15	1.34	3.53	4.34	2.75	97.07
	MBH-2	65.54	1.22	14.18	4.87	0.17	1.18	3.16	4.46	2.91	97.69
		65.40	1.15	14.00	5.27	0.19	1.08	3.16	4.60	2.81	97.66
		65.16	1.17	13.91	5.49	0.20	1.22	3.15	4.50	2.86	97.66
		65.00	1.32	13.75	5.70	0.22	1.33	3.31	4.45	2.69	97.77
		65.00	1.22	13.94	5.62	0.17	1.16	3.05	4.38	2.59	97.13
		64.82	1.39	14.01	5.74	0.20	1.19	3.47	4.55	2.83	98.20
		64.69	1.20	14.07	5.56	0.20	1.24	3.21	4.22	2.76	97.15
		64.56	1.34	13.80	5.79	0.20	1.16	3.40	4.56	2.59	97.40
		64.16	1.29	14.00	5.58	0.17	1.14	3.41	4.56	2.71	97.02
		63.95	1.38	13.73	5.60	0.16	1.25	3.38	4.48	2.75	96.68
SILK-A8	**MBH-1**	65.50	1.16	13.79	4.95	0.20	1.09	2.92	4.56	2.83	97.00
		65.48	1.17	13.72	5.57	0.17	1.18	3.12	4.38	2.73	97.52
		65.16	1.19	14.02	5.64	0.13	1.16	3.34	4.41	2.81	97.86
		65.10	1.15	14.00	4.97	0.12	1.10	3.10	4.37	2.72	96.63
		65.02	1.18	14.03	5.64	0.17	1.13	3.05	4.33	2.66	97.21
		64.96	1.26	13.87	5.40	0.15	1.09	3.26	4.39	2.74	97.12
		64.94	1.12	14.03	5.33	0.21	1.14	3.13	4.32	2.74	96.96
		64.91	1.25	13.73	5.45	0.14	1.13	3.06	4.43	2.70	96.80
		64.90	1.17	13.83	5.37	0.13	1.13	3.18	4.53	2.82	97.06
		64.68	1.17	13.87	5.45	0.20	1.06	3.10	4.56	2.90	96.99
SILK-A9	**TYN-2**	65.73	1.08	14.05	5.30	0.12	1.14	2.84	4.54	2.65	97.45
		65.54	1.22	14.39	5.53	0.21	1.17	3.19	4.44	2.72	98.41
		65.47	1.19	14.09	5.56	0.23	1.16	3.22	4.44	2.65	98.01
		65.07	1.05	13.85	5.59	0.18	1.11	3.19	4.66	2.70	97.40
		64.89	1.14	14.04	5.33	0.16	1.15	3.26	4.46	2.70	97.13
		64.63	1.10	13.83	5.45	0.16	1.13	3.07	4.55	2.81	96.73
		64.54	1.20	14.04	5.48	0.16	1.16	3.15	4.75	2.68	97.16
		64.22	1.20	13.87	5.52	0.16	1.16	2.91	4.83	2.62	96.49
		63.86	1.12	13.74	5.27	0.15	1.09	3.08	4.72	2.75	95.78
SILK-A11	**A11**	69.48	0.83	13.98	4.26	0.21	0.80	2.14	4.43	3.23	99.36
		69.08	0.92	13.76	4.18	0.17	0.73	2.00	4.59	3.19	98.62
		68.92	0.98	13.77	4.14	0.11	0.76	2.08	4.71	3.15	98.62
		68.62	0.91	13.81	4.53	0.14	0.71	2.18	3.94	3.02	97.86
		68.59	0.89	13.60	3.97	0.11	0.75	1.97	4.46	3.15	97.49
		68.48	0.85	13.59	3.99	0.14	0.69	1.98	4.28	3.22	97.22
		68.35	0.88	13.60	4.15	0.15	0.69	2.07	4.30	3.12	97.31
		68.16	0.94	13.81	4.02	0.17	0.72	1.90	4.23	3.23	97.18
		67.08	0.95	13.74	4.11	0.13	0.69	1.89	4.27	3.13	95.99
		66.96	0.81	13.77	4.00	0.15	0.75	2.00	4.27	3.26	95.97
SILK-A12	**A12**	68.82	0.85	13.87	3.91	0.14	0.70	2.06	4.57	3.08	98.00
		68.45	0.94	13.71	4.28	0.16	0.83	2.21	4.55	3.19	98.32
		68.33	0.78	13.44	4.16	0.14	0.74	2.32	4.35	3.31	97.57
		68.31	0.89	13.81	3.92	0.18	0.69	2.03	4.53	3.27	97.63
		68.10	0.81	13.67	4.31	0.12	0.74	2.03	4.67	3.02	97.47

SILK Layer	Local	SiO_2	TiO_2	Al_2O_3	FeO	MnO	MgO	CaO	Na_2O	K_2O	Total
		68.09	0.89	13.92	4.24	0.19	0.79	2.27	4.30	3.19	97.88
		67.91	0.88	13.48	4.34	0.15	0.71	2.19	4.44	3.04	97.14
		67.87	0.90	13.87	4.34	0.11	0.72	2.25	4.49	2.99	97.54
		67.48	0.90	13.75	4.29	0.15	0.76	2.08	4.66	3.04	97.11
		66.65	0.87	13.96	4.26	0.15	0.76	2.03	4.75	3.03	96.46

Appendix 4B: SIMS Geochemical Data

Sample	Local	Ti	Rb	Sr	Y	Zr	Nb	Ba	La	Ce
SILK-YN	N8	5901	44.7	266.3	57.6	799.6	95.6	539.7	68.1	147.5
		5803	44.0	256.4	54.8	774.7	92.1	512.4	64.5	139.3
		5757	42.4	261.4	56.0	773.6	93.4	517.7	65.6	139.4
		5667	44.3	265.5	56.8	776.7	91.8	535.2	69.0	143.6
		5597	46.8	253.0	54.1	781.7	90.0	513.5	63.8	137.4
		5456	44.3	269.8	52.8	745.9	89.4	524.3	63.4	132.4
SILK-UN	N7	6401	44.3	294.6	56.3	741.1	91.3	534.6	67.1	143.0
		6429	52.5	251.2	57.4	739.9	90.8	530.5	67.8	145.5
		6744	43.8	288.2	59.2	759.9	94.6	536.1	71.0	154.0
		6144	53.2	221.7	51.0	797.2	91.4	478.0	48.6	106.2
		6497	44.6	276.7	55.6	749.2	96.2	523.3	65.9	150.7
		5743	42.5	314.9	52.4	739.9	93.0	507.1	65.6	138.4
		6636	45.0	272.1	55.4	749.0	95.2	521.9	67.4	143.1
		6547	44.6	264.0	54.6	740.2	93.7	507.8	64.6	135.7
SILK-MN	N6	5847	45.2	256.9	55.4	768.6	96.6	523.9	67.3	145.9
		5825	42.8	255.1	54.9	751.0	94.4	510.8	65.7	140.6
		5932	45.7	260.7	55.3	765.7	98.2	530.8	68.1	146.1
		6080	49.3	269.0	57.6	815.8	101.0	551.4	69.9	148.7
		5763	36.9	235.0	73.0	725.2	86.4	412.7	56.5	124.9
SILK-LN	N5	5511	46.3	242.4	53.8	777.0	93.7	542.5	65.7	141.3
		5810	44.0	244.0	54.2	756.4	95.0	508.6	65.6	138.0
		5415	49.3	241.0	56.1	813.0	101.4	556.1	69.6	149.1
		5522	49.3	239.2	55.4	784.2	99.1	543.3	68.0	145.8
		5875	47.1	253.8	55.7	769.6	98.1	539.2	67.8	145.3
		5910	49.1	249.5	56.0	782.2	98.8	539.5	68.6	147.2
SILK-N4	N4	5865	45.7	261.0	55.8	771.0	98.0	533.5	68.4	143.9
		6046	46.3	264.1	56.9	784.1	99.6	534.6	68.9	147.1
		5991	46.3	261.7	56.4	778.9	97.7	546.7	69.0	145.7
		5856	45.8	261.5	56.3	764.2	96.7	528.0	67.7	145.5
		6025	46.7	260.7	56.1	774.6	98.9	529.5	68.4	144.8
		6003	43.9	254.1	55.0	752.8	104.1	495.7	67.2	144.3
		6026	42.9	253.6	55.3	746.6	103.9	484.8	66.2	141.5
		6046	44.3	258.4	56.3	774.6	107.2	511.3	69.7	149.5
		6053	43.6	255.1	56.1	749.7	104.2	494.0	67.2	144.1
		6042	43.4	257.4	55.1	748.3	104.1	496.2	66.3	143.0
SILK-N3	N3	7319	45.5	279.4	57.2	757.0	97.3	523.5	69.1	149.3
		7095	43.0	255.7	53.1	720.4	91.9	486.1	63.2	135.7
		7232	42.8	271.6	56.4	740.9	94.7	501.8	67.6	145.0
		7176	44.4	274.8	57.3	762.7	97.6	522.1	69.1	146.9

Sample	Local	Ti	Rb	Sr	Y	Zr	Nb	Ba	La	Ce
SILK-N1	N1	6405	47.8	260.5	56.1	766.1	99.3	547.3	68.0	143.4
		6156	48.1	221.1	54.5	766.2	98.3	515.6	65.0	137.1
		6294	46.1	230.2	57.5	798.5	97.0	532.1	67.7	144.7
		6559	48.9	242.6	58.1	803.4	102.8	549.7	70.9	151.5
		6376	44.4	231.6	56.7	771.4	98.9	526.8	67.3	143.9
		6530	44.8	241.6	59.5	786.7	98.2	533.2	69.3	150.6
		6606	50.0	245.9	60.3	825.2	105.6	567.1	72.9	156.8
		6654	48.3	238.8	58.2	798.1	100.6	550.1	70.4	150.0
		6514	47.8	242.2	60.0	819.8	103.2	564.8	72.4	153.4
		6533	48.3	244.6	59.1	809.6	102.5	556.5	71.6	150.6
SILK-A5	MBH3	6546	40.6	283.2	54.2	672.3	82.0	470.7	59.1	129.5
		6252	43.3	257.0	53.5	730.0	92.6	505.2	64.7	136.8
		6224	44.4	255.0	54.9	739.3	92.9	507.1	64.9	138.1
		6089	44.0	261.3	53.8	724.8	93.1	513.6	65.4	137.6
		6133	45.7	253.6	55.4	736.7	94.3	514.0	64.2	139.2
		6206	46.0	259.1	56.6	758.2	96.9	532.1	68.3	144.6
		6096	44.9	254.1	55.2	725.7	93.0	513.9	66.2	138.5
		6527	45.9	268.5	56.9	758.1	96.8	530.7	68.0	146.4
		6229	47.2	269.2	56.5	754.8	98.8	538.3	67.9	144.0
		6050	45.6	257.2	55.9	748.1	96.4	522.8	65.8	144.1
SILK-A8	MBH1	5698	48.7	242.9	57.4	774.6	100.0	549.6	68.4	146.7
		5686	47.8	240.9	56.4	761.2	99.7	530.2	68.9	145.9
		5444	48.2	234.4	55.4	758.3	98.4	530.0	66.5	142.2
		5553	48.3	217.2	56.8	779.2	100.7	528.1	69.3	148.8
		5606	47.8	239.9	55.5	748.2	96.9	528.3	67.0	144.0
		5382	45.9	239.1	54.3	741.0	95.9	520.7	66.5	139.8
		5525	46.3	237.9	54.8	742.7	96.1	523.7	66.6	138.9
		5619	48.1	241.6	55.9	749.0	98.2	529.2	66.6	144.7
		5585	45.9	242.8	56.8	759.5	97.2	533.5	66.7	143.4
SILK-A9	TYN-2	5748	43.4	235.7	56.7	768.2	101.9	517.6	70.6	151.9
		5689	43.8	234.8	56.8	763.2	98.9	512.3	68.8	150.1
		5470	42.9	230.3	55.2	734.5	93.7	487.5	66.4	142.0
		5831	45.5	229.3	56.3	771.9	103.5	502.4	69.2	147.6
		5555	43.6	232.2	55.2	739.9	94.8	500.7	66.1	140.6
		5441	44.1	228.6	53.7	717.3	90.2	485.0	64.5	137.9
		5576	43.1	228.6	54.2	731.3	94.0	491.3	65.7	140.5
		5866	44.4	240.0	55.8	746.2	96.6	511.4	67.4	144.8
		5708	47.3	241.4	57.1	766.9	98.3	521.0	68.8	149.1
		5568	43.3	239.3	57.3	748.0	102.3	495.5	66.8	142.1
		5619	42.7	246.4	58.3	753.3	103.6	509.4	68.8	147.0
		5596	43.0	232.6	55.7	732.3	101.6	488.0	66.6	140.2
		5586	41.7	233.1	56.0	722.0	100.0	474.7	65.9	140.4
		5413	42.8	233.1	55.3	710.9	93.6	480.1	65.4	138.4
SILK-A11	A11	3986	52.5	170.0	55.6	799.8	106.1	532.0	67.1	143.1
		4037	50.2	170.7	55.2	813.3	105.1	539.6	68.2	143.6
		4008	50.9	165.2	53.8	783.1	104.1	524.8	66.3	141.8
		4131	51.0	168.4	55.4	813.0	108.1	543.9	67.9	145.8
		4010	48.2	166.5	54.3	794.6	103.4	530.9	66.7	140.4
		3962	48.9	165.9	54.2	806.5	102.0	527.3	66.5	136.5
		4016	49.3	164.3	55.4	808.5	103.7	525.7	67.3	140.6
		4066	51.9	173.3	56.5	831.3	108.3	558.4	71.5	150.7

Sample	Local	Ti	Rb	Sr	Y	Zr	Nb	Ba	La	Ce
		4116	51.1	175.3	57.5	845.5	109.4	568.3	73.6	157.0
SILK-A12	**A12**	4100	49.0	169.9	56.8	821.1	104.7	536.9	70.4	144.6
		4130	52.4	179.0	56.9	830.9	109.5	562.3	73.0	153.0
		4090	47.9	183.7	57.0	824.5	107.7	547.3	69.1	145.8
		4149	48.4	176.9	57.7	816.6	107.4	549.8	70.2	146.2
		4066	52.0	173.8	55.9	815.9	106.0	536.0	67.9	145.8
		4124	46.1	177.8	57.2	819.0	103.1	536.5	69.5	141.9
		4097	46.5	174.8	56.4	817.9	103.2	538.0	69.0	142.9
		4143	47.1	178.2	56.7	830.2	105.3	542.0	69.5	145.8
		4138	45.6	178.2	57.4	826.4	102.6	535.4	68.7	143.1
		4154	46.9	185.1	55.8	812.6	101.6	534.8	68.0	139.3

Appendix

References published 1993-1999

5

Branigan, K., Newton, A. J. and Dugmore, A. J. (1995) Pumice. In: *Barra: Archaeological Research on Ben Tangaval* (Ed. by K. Branigan and P. Foster), pp. 144-145. Sheffield Academic Press Ltd.

Clarke, A. and Newton, A. J. (2001) Pumice at Dún Aonghasa. In: *The Western Stone Forts Project: The Discovery Programme Monograph Series* (Ed. by C. Cotter), pp. Forthcoming. The Discovery Programme Monograph Series, Dublin.

Dugmore, A. J., Larsen, G. and Newton, A. J. (1995a) Seven tephra isochrones in Scotland. *The Holocene*, **5 (3)**(3), 257-266.

Dugmore, A. J. and Newton, A. J. (1996) Ideas and evidence from studies of tephra. In: *The Outer Hebrides: The Last 14,000 Years* (Ed. by D. Gilbertson, M. Kent and J. Grattan), pp. 45-50. Sheffield Academic Press, Sheffield.

Dugmore, A. J. and Newton, A. J. (1997) Holocene tephra layers in the Faroe Islands. *Fróðskaparrit*, **45**, 141-154.

Dugmore, A. J. and Newton, A. J. (1999a) The Pumice: Origins of the material. In: *Kebister: the four thousand year old story of one Shetland township* (Ed. by O. Owen and C. Lowe), pp. 167-168. Society of Antiquaries of Scotland Monograph Series No 13, Edinburgh.

Dugmore, A. J. and Newton, A. J. (1999b) Tephrochronology at Kebister. In: *Kebister: the four thousand year old story of one Shetland township* (Ed. by O. Owen and C. Lowe), pp. 70-74. Society of Antiquaries of Scotland Monograph Series No 13, Edinburgh.

Dugmore, A. J., Newton, A. J., Edwards, K. J., Larsen, G., Blackford, J. J. and Cook, G. T. (1996) Long-distance marker horizons from small-scale eruptions: Bristish tephra deposits from AD 1510 eruption of Hekla, Iceland. *Journal of Quaternary Science*, **11(6)**, 511-516.

Dugmore, A. J., Newton, A. J., Larsen, G. and Cook, G. T. (in press) Tephrochronology, environmental change and the Norse settlement of Iceland. *Environmental Archaeology*.

Dugmore, A. J., Shore, J. S., Cook, G. T., Newton, A. J., Edwards, K. J. and Larsen, G. (1994) The radiocarbon dating of Icelandic tephra layers. In: *15th International Radiocarbon Conference Abstracts C-13*.

Dugmore, A. J., Shore, J. S., Cook, G. T., Newton, A. J., Edwards, K. J. and Larsen, G. (1995b) The radiocarbon dating of Icelandic tephra layers in Britain and Ireland. *Radiocarbon*, **37**, 2:286-295.

Larsen, G., Dugmore, A. and Newton, A. (1995) Íslensk gjóska Í jarðvegi Í Skotlandi, Hjaltlandi, Orkneyjum og Suðureyjum. In: *Jardfraedafelag Islands: Vorrádstefna 1995* (Ed. by M. T. Guðmundsson), pp. 21-23. Haldin I Odda, Reykjavik.

Larsen, G., Dugmore, A., J. and Newton, A. J. (1999) Geochemistry of historic silicic tephras in Iceland. *The Holocene*, **9(4)**, 463-471.

Larsen, G., Newton, A. J., Dugmore, A. J. and Vilmundardóttir, E. (in press) Geochemistry, dispersal, volumes and chronology of Holocene silicic tephra layers from the Katla Volcanic System, Iceland. *Journal of Quaternary Science*.

Newton, A. J. (1995) The Cramp. In: *Two Orcadian cist burials: excavations at Midskaill, Egilsay, and Linga Fiold, Sandwick. Proceedings of the Society of Antiquaries of Scotland, Vol. 125* (Ed. by H. Moore and G. Wilson), pp. 244-245.

Newton, A. J. (1996) Tephrabase: A Tephrochronological Database. *Quaternary Newsletter*, **78**, 8-13.

Newton, A. J. (1999) Report on the pumice. In: *The Biggings, Papa Stour, Shetland: the history and archaeology of a royal Norwegian farm* (Ed. by B. E. Crawford and B. Ballin Smith), pp. 178. Society of Antiquaries of Scotland Monograph Series No 13, Edinburgh.

Newton, A. J. (Forthcoming-a) The Pumice. In: *Hunter-Gatherer Landscape Archaeology: The Southern Hebrides Mesolithic Project 1988-1998* (Ed. by S. Mithen), pp. Forthcoming. McDonald Institute for Archaeological Research, Cambridge.

Newton, A. J. (Forthcoming-b) Report on pumice found at RUX6 at the Udal, North Uist. In: *The Udal* (Ed. by I. Crawford).

Newton, A. J. (Forthcoming-c) Report on pumice from Cnip 88.

Newton, A. J. and Dugmore, A. J. (1993) Tephrochronology of Core C from Lago Grande di Monticchio. In: *Paleolimnology of European Maar Lakes: Lecture Notes in Earth Sciences, 49* (Ed. by J. F. W. Negendank and B. Zolitschka), pp. 333-348. Springer-Verlag, Berlin.

Newton, A. J. and Dugmore, A. J. (1995) Pumice: Analytical Report. In: *Barra: Archaeological Research on Ben Tangaval* (Ed. by K. Branigan and P. Foster), pp. 145-148. Sheffield Academic Press Ltd, Sheffield.

Newton, A. J. and Dugmore, A. J. (Forthcoming-a) Analysis of pumice from Baleshare. In: *Bronze Age farms and Iron Age farm mounds of the Outer Hebrides* (Ed. by J. Barber). STAR Monographs, Edinburgh.

Newton, A. J. and Dugmore, A. J. (Forthcoming-b) Green Castle Pumice report. In: *Final excavation report of archaeological excavations at Green Castle, Porknockie* (Ed. by I. Ralston).

Newton, A. J., Gittings, B. and Stuart, N. (1997) Designing a scientific database Query Server using the World Wide Web: The example of Tephrabase. In: *Inovations in GIS 4* (Ed. by K. Kemp), pp. 251-266. Taylor & Francis, London.

Newton, A. J. and Metcalfe, S. E. (1999) Tephrochronology of the Toluca Basin, central Mexico. *Quaternary Science Reviews*, **18**, 1039-1059.

Oldfield, F., Thompson, R., Crooks, P. R. J., Gedye, S. J., Hall, V. A., Harkness, D. D., Housley, R. A., McCormac, F. G., Newton, A. J., Pilcher, J. R., Renberg, I. and Richardson, N. (1997) Radiocarbon dating of a recent high-latitude peat profile: Stor Amyran, northern Sweden. *The Holocene*, **7(3)**, 283-290.

Ortega-Guerrero, B. and Newton, A. J. (1998) Geochemical characterisation of late Pleistocene-Holocene tephra layers from the Basin of Mexico, central Mexico. *Quaternary Research*, **50(1)**, 90-106.